

Topics in Heterocyclic Chemistry 56

Series Editors: Bert Maes · Janine Cossy · Slovenko Polanc

Upendra K. Sharma

Erik V. Van der Eycken *Editors*

Flow Chemistry for the Synthesis of Heterocycles



Springer

56

Topics in Heterocyclic Chemistry

Series Editors:

Bert Maes, Antwerp, Belgium
Janine Cossy, Paris, France
Slovenko Polanc, Ljubljana, Slovenia

Editorial Board:

D. Enders, Aachen, Germany
S.V. Ley, Cambridge, UK
G. Mehta, Bangalore, India
R. Noyori, Nagoya, Japan
L.E. Overman, Irvine, CA, USA
A. Padwa, Atlanta, GA, USA

Aims and Scope

The series Topics in Heterocyclic Chemistry presents critical reviews on present and future trends in the research of heterocyclic compounds. Overall the scope is to cover topics dealing with all areas within heterocyclic chemistry, both experimental and theoretical, of interest to the general heterocyclic chemistry community.

The series consists of topic related volumes edited by renowned editors with contributions of experts in the field. All chapters from Topics in Heterocyclic Chemistry are published OnlineFirst with an individual DOI. In references, Topics in Heterocyclic Chemistry is abbreviated as Top Heterocycl Chem and cited as a journal.

More information about this series at <http://www.springer.com/series/7081>

Upendra K. Sharma • Erik V. Van der Eycken
Editors

Flow Chemistry for the Synthesis of Heterocycles

With contributions by

M. Baumann • I. R. Baxendale • V. Bieliūnas • A. R. Bogdan •
W. M. De Borggraeve • R. O. M. A. de Souza • J. Demaerel •
R. Gérardy • T. Glasnov • J.-C. M. Monbaliu • S. G. Newman •
M. G. Organ • M. T. Rahman • R. J. Sullivan •
S. Van Mileghem • C. Veryser • T. Wirth

 Springer

Editors

Upendra K. Sharma
Department of Chemistry
University of Leuven (KU Leuven)
Leuven, Belgium

Erik V. Van der Eycken
Department of Chemistry
University of Leuven (KU Leuven)
Leuven, Belgium

ISSN 1861-9282

ISSN 1861-9290 (electronic)

Topics in Heterocyclic Chemistry

ISBN 978-3-319-94327-5

ISBN 978-3-319-94328-2 (eBook)

<https://doi.org/10.1007/978-3-319-94328-2>

Library of Congress Control Number: 2018946687

© Springer International Publishing AG, part of Springer Nature 2018

This work is subject to copyright. All rights are reserved by the Publisher, whether the whole or part of the material is concerned, specifically the rights of translation, reprinting, reuse of illustrations, recitation, broadcasting, reproduction on microfilms or in any other physical way, and transmission or information storage and retrieval, electronic adaptation, computer software, or by similar or dissimilar methodology now known or hereafter developed.

The use of general descriptive names, registered names, trademarks, service marks, etc. in this publication does not imply, even in the absence of a specific statement, that such names are exempt from the relevant protective laws and regulations and therefore free for general use.

The publisher, the authors and the editors are safe to assume that the advice and information in this book are believed to be true and accurate at the date of publication. Neither the publisher nor the authors or the editors give a warranty, express or implied, with respect to the material contained herein or for any errors or omissions that may have been made. The publisher remains neutral with regard to jurisdictional claims in published maps and institutional affiliations.

Printed on acid-free paper

This Springer imprint is published by the registered company Springer International Publishing AG part of Springer Nature.

The registered company address is: Gewerbestrasse 11, 6330 Cham, Switzerland

Preface

The heterocyclic ring is the most prevalent structural motif in the majority of natural products, pharmaceuticals as well as agrochemicals and shows tuneable interactions with biological targets besides conferring a degree of structural and metabolic stability. Heterocyclic chemistry can be regarded as an inexhaustible source of novel compounds due to the vast number of possible combinations of carbon, hydrogen and heteroatoms. Due to increased environmental concern and the impact of their work, synthetic chemists are actively responding to the so-called green agenda. In recent times, flow chemistry has heralded a paradigm shift in organic synthesis as it offers several unique advantages over conventional methods such as drastic acceleration of sluggish transformations, enhanced yields, cleaner reactions and safe handling of hazardous and obnoxious materials. Such recent technological developments to alleviate the labour-intensive practices in chemical industry encouraged us to compile a volume especially towards the application of flow chemistry in heterocyclic synthesis. Given the importance of heterocycles in natural products, medicinal chemistry and pharmaceuticals, an update to its predecessor (*Organometallic flow chemistry*) was well warranted.

We anticipate that this volume *Flow Chemistry for the Synthesis of Heterocycles*, which offers a versatile overview of the topic alongside discussing the recent progress in the flourishing area of flow chemistry in relevance to heterocyclic chemistry, will help researchers to better understand the chemistry behind these reactions. This would, in turn, provide a platform for future discoveries towards the designing of novel transformations under continuous flow. The contribution from leading research groups in the field assures the success of this book to achieve the above-mentioned objectives. This volume mainly focuses on recent developments in the synthesis and functionalization of heterocycles in flow with different outlooks, safety aspects and most importantly industrial applications. Besides, the potential of new applications combined with other modern methods in organic synthesis is also highlighted wherever applicable.

The first chapter specifically focuses on the synthesis of heterocyclic active pharmaceutical ingredients in a multistep continuous-flow manner highlighting the opportunities as well as problems arising during these chemical processes.

Moreover, the combination of multistep chemical sequences along with purifications or in-line analysis is also discussed in detail. The second chapter highlights the application of photo-flow technology towards heterocyclic synthesis, bringing the future of organic synthesis to the continuous-flow platform.

Chapter “Flow-Assisted Synthesis of Heterocycles via Multicomponent Reactions” highlights how proficiently multicomponent chemistry for heterocycle synthesis has been brought to continuous-flow regimes, mostly in one operational step to generate a vast library of compounds followed by another chapter on functionalizations of heteroarenes. Also the application of flow chemistry towards the synthesis of saturated heterocycles is nicely covered. This is followed by a chapter on flow-assisted synthesis of heterocycles at high temperature (200–450°C) which previously seemed unreasonable or even impossible. Then the applications of flow chemistry from the medicinal chemistry perspective are highlighted, therefore rendering it as an important drug discovery tool for future discoveries.

Chapter “Safe Use of Hazardous Chemicals in Flow” in this book deals with an important aspect in organic synthesis, i.e. safe use of hazardous chemicals as well as fast and furious chemical processes. How flow chemistry can tackle safety hazards and cryogenic, inert and special reaction conditions has been covered in depth. Due to small reaction volumes and excellent heat and mass transfer capabilities, microflow platforms minimize the explosion risks. Moreover, over-reactive intermediates can be made to react in a subsequent reaction within a sub-second or millisecond time regime. Any undesirable isomerization, decomposition or side reactions can be minimized and avoided. The final chapter of this book sheds some light on industrial approaches developed or already being used towards the continuous production of APIs at different scales, though not many examples are published in this direction. However, with the rapid developments in this field, more such examples are expected in the coming years.

Finally, we are very grateful to all authors for their contribution to this volume. We firmly believe that it will be of great help to both the novices in the field and experts in academia and industry for future innovations.

Leuven, Belgium
30 March 2018

Upendra K. Sharma
Erik V. Van der Eycken

Contents

Multistep Continuous-Flow Processes for the Preparation of Heterocyclic Active Pharmaceutical Ingredients	1
Romaric Gérardy and Jean-Christophe M. Monbaliu	
Photochemical Synthesis of Heterocycles: Merging Flow Processing and Metal-Catalyzed Visible Light Photoredox Transformations	103
Toma Glasnov	
Flow-Assisted Synthesis of Heterocycles via Multicomponent Reactions	133
Seger Van Mileghem, Cedrick Veryser, and Wim M. De Borggraeve	
Flow-Assisted Synthesis of Heterocycles at High Temperatures	161
Ryan J. Sullivan and Stephen G. Newman	
Flow Chemistry Approaches Applied to the Synthesis of Saturated Heterocycles	187
Marcus Baumann and Ian R. Baxendale	
Functionalization of Heteroarenes Under Continuous Flow	237
Joachim Demaerel, Vidmantas Bieliūnas, and Wim M. De Borggraeve	
Flow Chemistry as a Drug Discovery Tool: A Medicinal Chemistry Perspective	319
Andrew R. Bogdan and Michael G. Organ	
Safe Use of Hazardous Chemicals in Flow	343
Md Taifur Rahman and Thomas Wirth	
Industrial Approaches Toward API Synthesis Under Continuous-Flow Conditions	375
Rodrigo O. M. A. de Souza	
Index	391

Multistep Continuous-Flow Processes for the Preparation of Heterocyclic Active Pharmaceutical Ingredients



Romarc Gérardy and Jean-Christophe M. Monbaliu

Contents

1	Introduction	2
2	Multistep Continuous-Flow Processes Toward Heterocyclic Active Pharmaceutical Compounds	3
2.1	Chemotherapeutic Agents	4
2.2	Antiviral Active Compounds	12
2.3	Antiparasitic and Antibiotic Pharmaceuticals	15
2.4	Central Nervous System and Related Conditions	24
2.5	Hypertension and Cardiovascular Diseases	38
2.6	Anesthetics and Analgesics	39
2.7	Allergy	42
2.8	Inflammation	43
2.9	Miscellaneous	48
3	Multistep Continuous-Flow Processes Toward Advanced Heterocyclic Intermediates for API Manufacturing	49
3.1	Chemotherapeutic Agents	49
3.2	Antiviral Active Compounds	57
3.3	Antiparasitic and Antibiotic Pharmaceuticals	63
3.4	Central Nervous System and Related Conditions	67
3.5	Hypertension and Cardiovascular Diseases	74
3.6	Anesthetics and Analgesics	75
3.7	Inflammation	78
3.8	Miscellaneous	80
4	Miscellaneous	82
4.1	Biologically Active Compounds Inspired from Natural Compounds	82
4.2	Derivatives of Known APIs	88
4.3	Libraries of Highly Potent Molecules	90
	References	99

R. Gérardy and J.-C. M. Monbaliu (✉)
Center for Integrated Technology and Organic Synthesis, Department of Chemistry,
University of Liège, Liège, Belgium
e-mail: jc.monbaliu@ulg.ac.be

Abstract Flow chemistry has many fascinating facets, among which the most challenging is arguably the implementation of complex multistep processes within one uninterrupted fluidic network. This document provides a thorough overview of some of the most representative examples of multistep continuous-flow strategies in the specific context of preparing heterocyclic active pharmaceuticals. Selected examples emphasizing the implementation of multistep sequences, including various combinations of chemical transformations, purifications, or in-line analysis, are discussed.

Keywords Flow chemistry · Heterocyclic APIs · Multistep continuous processes

1 Introduction

Continuous-flow chemistry has changed many facets of preparative organic chemistry. Its status has evolved over the last decade from lab curiosity to must-have in the chemistry toolkit. Flow chemistry unquestionably provides new tools to tackle with complex chemical processes. The most prominent assets of flow chemistry, including safer and cleaner chemical processes, are deeply rooted into the inherent properties of flow reactors. Most notably, flow chemistry enables the exploration of new process windows and drastically reduces the time and space footprints for chemical processes. The possibility to perform multiple steps without manual intervention or isolation of intermediates, i.e. reaction telescoping, by streamlining individual process steps within an uninterrupted reactor network is arguably one of the most fascinating aspects of flow chemistry. A full picture of the main assets of flow chemistry would not be complete without mentioning the fast transition from lab scale to production scale under continuous-flow conditions. Obviously, flow chemistry is not just a simple transposition of batch procedures into chips and tubes. It takes more than that, and requires a thorough redesign of conventional chemical processes.

This review aims at illustrating the most representative examples of multistep continuous-flow strategies in the specific context of preparing heterocyclic active pharmaceuticals (Fig. 1). Selected examples emphasize the implementation of multistep sequences (at least two), including various combinations of chemical transformations, purifications, or in-line analysis. The examples are presented according to three main subsections: (a) multistep continuous-flow procedures for the preparation of heterocyclic active pharmaceutical ingredients (APIs); (b) multistep continuous-flow procedures for the preparation of advanced fragments for the preparation of heterocyclic APIs; and (c) multistep continuous-flow procedures for preparation of biologically active molecules and libraries of highly potent molecules. The APIs are classified according to their main biological activities/pharmaceutical applications.

Heterocyclic APIs (total synthesis or fragments)	Highly potent scaffolds and libraries	
<p>Chemotherapeutics Akt kinase inhibitor (frag., 3.1) ATR kinase inhibitor (total, 2.1) Bendamustine (fragment, 3.1) Brivanib alaninate (frag., 3.1) Capecitabine (total, 2.1) Eribulin (fragment, 3.1) Galocitabine (total, 2.1) Gemcitabine (total, 2.1) Imatinib (total, 2.1) JAK2 kinase inhibitor (frag., 3.1) Osimertinib (total, 2.1) Oxomaritidine (total, 2.1) PARP-1 inhibitor (fragment, 3.1) Prexasertib (fragment, 3.1) Ribociclib (total, 2.1) Antiviral compounds AS-136A (total, 2.2.2) Atazanavir (fragment, 3.2.1) Daclatasvir (fragment, 3.2.2) Darunavir (fragment, 3.2.1) Doravirine (fragment, 3.2.1) Efavirenz (total, 2.2.1; frag., 3.2.1) Edoxudine (total, 2.2.2) Lamivudine (fragment, 3.2.1) Nevirapine (fragment, 3.2.1) Antiparasitics and antibiotics Artemisinin & deriv. (total, 2.3.1) Borrerine (total, 2.3.1) Bassianolide (total, 2.3.2) Boscalid (fragment, 3.3.2) Ciprofloxacin (total, 2.3.2) Linezolid (fragment, 3.3.3) Mur ligase inhibitor (total, 2.3.2) OZ439 (fragment, 3.3.1) Pyrazine-2-carboxamide (total, 2.3.2) CNS-related compounds 5HT1B antagonist (total, 2.4.3) Alpidem (total, 2.4.2) AR-A2 (3.4.5)</p>	<p>CNS-related compounds (continued) Cariprazine (total, 2.4.1) DAO inhibitor (fragment, 3.4.1) Diazepam (total, 2.4.2) δ-opioid receptor agonist (total, 2.4.3) lloperidone (total, 2.4.1) Levomilnacipran (fragment, 3.4.3) LY2886721 (total, 2.4.5) Meclizertant (fragment, 3.4.3) Methylphenidate (total, 2.4.6) NBI-75043 (fragment, 3.4.3) Olanzapine (total, 2.4.1) Rufinamide (total, 2.4.4; frag. 3.4.4) Zolpidem (total, 2.4.2) Cardiovascular conditions Rosuvastatin (fragment, 3.5) Telmisartan (total, 2.5) Anesthetics and analgesics Bupivacaine (total, 2.6.1) Hydrocodone (fragment, 3.6.1) Mepivacaine (total, 2.6.1) Noroxymorphone (total, 2.6.2; frag., 3.6.1) Ropivacaine (total, 2.6.1) Anti-allergy drugs Buclizine (total, 2.7) Cinnarizine (total, 2.7) Cyclizine (total, 2.7) Inflammation CCR1 antagonist (fragment, 3.7) Etodolac (fragment, 3.7) Fanetizole (total, 2.8) Grossamide (total, 2.8) Rolipram (total, 2.8) Miscellaneous Atropine (total, 2.9) Canagliflozin (fragment, 3.8) Dantrolene (fragment, 3.8) Vildagliptin (fragment, 3.8)</p>	<p>Natural products Dumetorine (frag., 4.1) Histronicotoxins (frag., 4.1) Siphonazole (frag., 4.1) API derivatives Amoxapine (deriv., 4.2) Fenofibrate (deriv., 4.2) Nucleosides (deriv., 4.2) Libraries BCP modulators (libr., 4.3) Benzothiazoles (libr., 4.3) CCR8 ligands (libr., 4.3) CKI (libr., 4.3) Coumarin & deriv. (libr., 4.3) DHPM (libr., 4.3) HCVT inhibitors (libr., 4.3) Pyrazoles (libr., 4.3)</p>

Fig. 1 Glossary of heterocyclic APIs, fragments of heterocyclic APIs and highly potent molecules prepared according to multistep continuous-flow strategies

2 Multistep Continuous-Flow Processes Toward Heterocyclic Active Pharmaceutical Compounds

This section regroups the most representative examples of multistep continuous-flow procedures for the preparation of heterocyclic active pharmaceutical compounds. Examples illustrating single step procedures, even sequential, are deliberately excluded from this review. Heterocyclic active pharmaceutical ingredients are arranged according to their main pharmaceutical activity in the following subsections.

2.1 Chemotherapeutic Agents

[ATR kinase inhibitor] Kappe and colleagues reported the development of a continuous-flow sulfoxide imidation protocol for the preparation of pharmaceutically active ingredients endowed with ATR kinase inhibitor properties [1]. Reaction conditions involved pumping an advanced sulfoxide intermediate **1** with NaN_3 or TMSN_3 in the presence of fuming sulfuric acid, affording the target sulfoximine **2** with a selectivity of $\sim 90\%$ after a residence time of only 10–15 min at 50°C (Fig. 2). The authors found that the starting sulfoxide was not very stable in concentrated sulfuric acid, and developed an alternative biphasic imidation process. TMSN_3 was used as the imidation reagent, and $\text{CH}_2\text{Cl}_2/\text{H}_2\text{SO}_4$ biphasic conditions were successfully implemented in a PFA coil flow reactor. A large amount of gas (N_2) was formed upon reaction, and a residence time of 14 min was necessary to reach reaction completion within 7 bar of counter-pressure. The mixture was subsequently quenched in-line with H_2O . Phase separation, neutralization, and re-extraction with an organic solvent furnished the product in excellent purity (96%, HPLC) and good yield, although loss of chirality was noticed.

[Capecitabine] Jamison and Shen devised a continuous-flow procedure for the preparation of capecitabine (**7**) [2], a 5'-deoxyribonucleoside derivative used in the treatment of breast and colorectal cancer. The authors used a microfluidic assembly constructed from PFA capillaries (Fig. 3). The first step involved the glycosylation of silylated nitrogenous bases such as **4** with 5'-deoxyribose derivatives, in the presence of pyridinium triflate **3** as a catalyst. It was observed that the reaction was compatible with several bases, affording the target compounds in excellent 86–99% yields ($>98:2$ d.r.). Subsequent removal of acetyl protecting groups was effected by mixing the reactor effluent with sodium hydroxide in water/MeOH. Such solvent combination was critical to keep fully homogeneous conditions and avoid reactor clogging.

A critical aspect of the process toward **7** is the instability of intermediate **6**, the preparation of which was fully integrated in the telescoped process. The carbamate

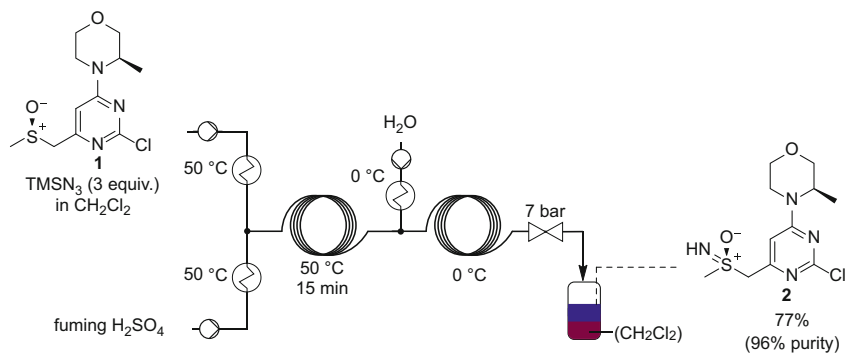


Fig. 2 Preparation of ATR kinase inhibitor **2** [1]

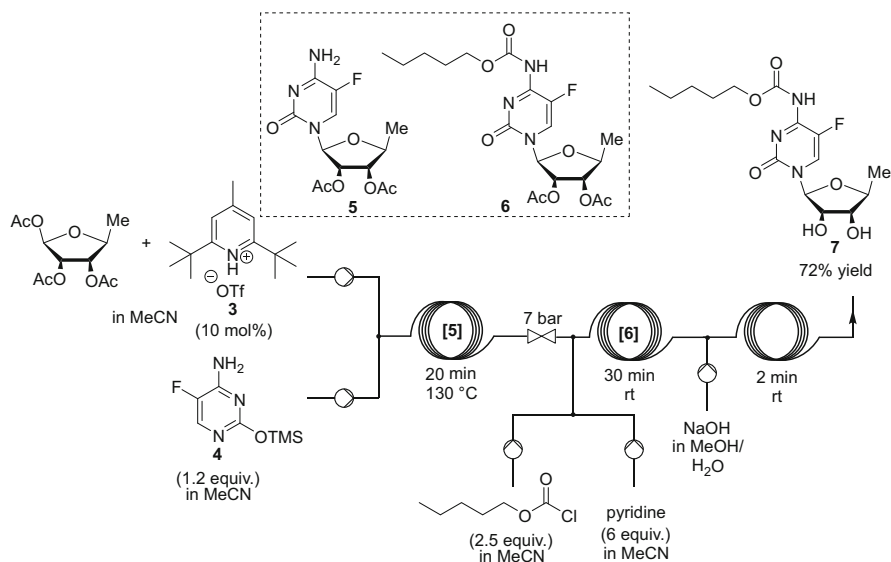


Fig. 3 Telescoped process toward capecitabine (7) [2]

moiety on **6** was thus installed between the glycosylation and the deprotection steps. Pyridine and pentyl chloroformate were injected at 0 °C to avoid premature decomposition, and capecitabine (**7**) was generated in 72% yield.

[Galocitabine] The procedure reported by Jamison and Shen for capecitabine (**7**) was simplified for the preparation of galocitabine (**10**) [2], an orally available 5-fluorouracil prodrug with antineoplastic activity. Unlike carbamate **6** utilized for the preparation of capecitabine, intermediate **8** was stable and could be utilized directly in a feed solution. A 2-step sequence was successfully applied to the preparation of the drug galocitabine (**10**), where starting material **8** was first prepared in batch and directly utilized in the flow setup, affording the target API in 89% yield (Fig. 4).

[Gemcitabine monophosphate] Ying and colleagues reported a continuous-flow procedure using a mesofluidic reactor for the synthesis of natural and non-natural 5'-nucleotides and deoxynucleotides, including the preparation of gemcitabine monophosphate (Gemzar, **13**) [3]. Gemzar is an antineoplastic drug. The procedure is conceptually simple and relies on a two-step reaction (phosphorylation/hydrolysis) with, comparatively to standard batch procedures, a significantly reduced excess of phosphorylating reagent, and no handling of chemical intermediates. Additives and solvent effects were examined to optimize the process. The authors found that the presence of a base had a drastic impact on the reaction, and proton sponge (*N,N,N',N'*-tetramethyl-1,8-naphthalenediamine) was found to be the most effective, with up to 85% yield within 15 min of residence time. The reaction output was also very dependent on the mixing efficiency, and a slit plant micromixer LH25 operating according to the principle of multilamination was utilized. The internal diameter of

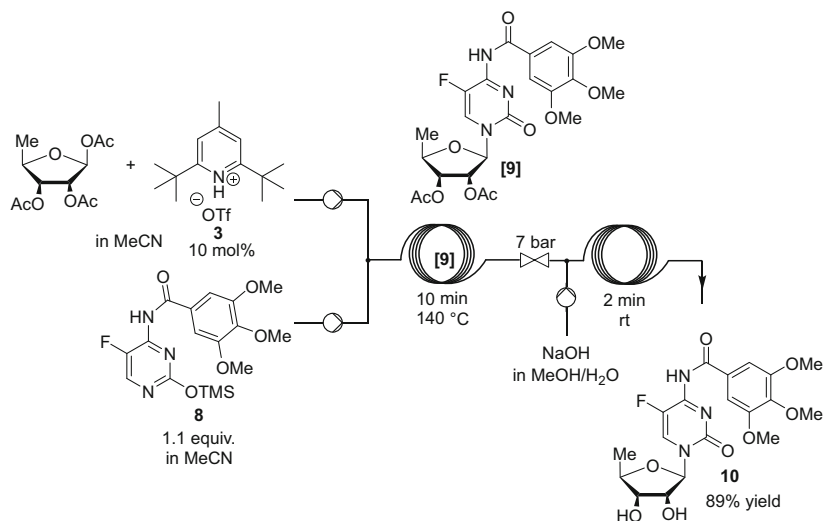


Fig. 4 Telescoped process toward galocitabine (10) [2]

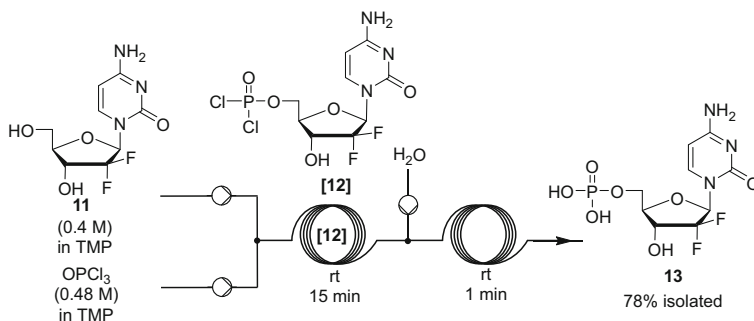


Fig. 5 Gemcitabine monophosphate [3]

the PFA coil was also critical. The optimized parameters were next applied to a variety of nucleotides, and excellent chemoselectivity was reported, without the formation of noticeable side products. The continuous-flow procedure was next extended to the preparation of deoxyribonucleotides, affording very high yields and selectivities as well. Finally, the authors tested the procedure for the preparation of gemcitabine monophosphate (2'-deoxy-2',2'-difluoro-5'-cytidylic acid, 13). Under the optimized conditions, the reaction proceeded efficiently and gemcitabine monophosphate was obtained in 78% isolated yield (Fig. 5). A typical procedure is illustrated below. Two feed solutions including difluoro compound 11 (0.4 M in trimethyl phosphate), optionally in the presence of proton sponge, and POCl₃ (0.48 M in trimethyl phosphate) were mixed through a static mixer and sent to a first PFA coil, and the reaction was completed within 15 min of residence at room

temperature. The reactor effluent was next mixed with a stream of water and reacted for 1 min of residence time in a second PFA coil (4 mL internal volume). The crude was collected and purified by HPLC (78% yield).

[Imatinib] Imatinib (Gleevec, **19**) is a tyrosine kinase inhibitor developed by Novartis AG with use for the treatment of chronic myeloid leukemia. The continuous-flow preparation of imatinib has attracted a great deal of attention [4–7]. Ley and colleagues pioneered its continuous-flow preparation [5]. The authors devised a simple flow assembly constructed from tubular flow coils and cartridges packed with reagents or scavengers for in-line purification and/or specific chemical transformation (Fig. 6). The assembly also featured an in-line solvent switching procedure. The fluids were managed using HPLC pumps, injection valves, and sample loops. The first stage aimed at the preparation of intermediate amide **16**. The sequence started with the reaction of a polystyrene-supported DMAP (PS-DMAP) resin contained in a glass column with acid chloride **14**. The latter was thus trapped in an activated form on the resin. Then, a stream containing aniline **15** (0.2 M, 1 equiv. in CH_2Cl_2) was passed through the column, thereby reacting with activated **14** and releasing amide **16**. The reactor effluent was next passed through another column packed with polymer-supported dimethylamine (QP-DMA) to scavenge any acidic side-products. Amide **16** was directly isolated after off-line processing in 78% yield (>95% purity). Dispersion effects precluded the direct telescoping of stage 1 with the following steps. Instead, the authors inserted a UV-spectrometer and a fraction

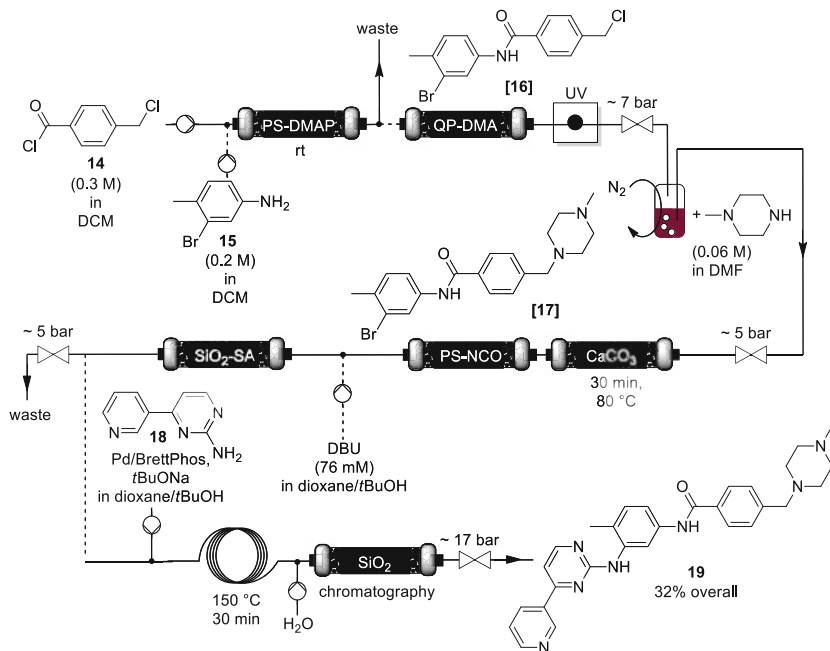


Fig. 6 Multistep preparation of imatinib [5]

collector to monitor reaction progress. Amide **16** was collected in a solution of 1-methylpiperazine (0.06 M, 2 equiv., in DMF), thus forming a homogeneous solution that could be injected in the next stage of the synthesis. A system comprising a flow of nitrogen and a condenser was devised to evaporate CH_2Cl_2 , as it was demonstrated that it affected the conversion in the following step. It involved a $\text{S}_{\text{N}}2$ displacement by reaction of **16** with 1-methylpiperazine in a column packed with CaCO_3 and operated at 80°C (counter-pressure of 100 psi). The reactor effluent was next directed to a cartridge containing polystyrene-supported isocyanate (PS-NCO) to scavenge any unreacted 1-methylpiperazine, resulting in 70% conversion. The stream containing intermediate **17** was then directed into a column containing silica-supported sulfonic acid (SiO_2 -SA) to perform a catch-and-release purification. The column was rinsed with MeOH, and product **17** was then released by flushing the column with a solution of DBU in 1,4-dioxane/*t*BuOH (76 mM). The desired product **17** was obtained in 80% isolated yield (>95% purity). No further purification was required. The final stage relied on a Buchwald–Hartwig coupling between bromide **17** and compound **18** using a BrettPhos Pd precatalyst in the presence of *t*BuONa at 150°C within 30 min of residence time. The addition of a stream of water was necessary at the end of the reactor to dissolve the accumulating NaBr. The reactor effluent was subjected to chromatography on silica gel (Biotage SP1 purification system), to give the final product **19** in 69% yield (32% overall, 95% purity).

The same group reported an updated procedure a few years later [6]. Alternative routes were considered, and reaction conditions were optimized to circumvent the insolubility of several intermediates. In-line UV-reaction monitoring was implemented at pivotal locations in the reactor, and the process was extended to various biologically active analogs of imatinib. Buchwald reported a general and efficient method for *C-N* cross-coupling using *N,N*-dimethyloctanamide (DMO) as a catalytic co-solvent for biphasic continuous-flow applications [7]. The method was amenable to the preparation of a variety of biaryl amines and was integrated into a two-step sequence, converting phenols into biaryl amines, including imatinib, via either triflates or tosylates. All feeds were handled with syringe pumps (Fig. 7). The first step, which involved the coupling of 4-chloromethylbenzoyl chloride (**14**) with

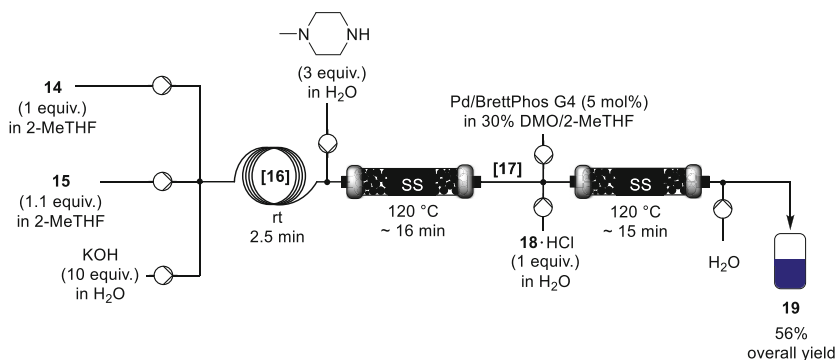


Fig. 7 Continuous-flow preparation of imatinib (**19**) [7]

3-bromo-4-methylaniline (**15**), was performed under 2-MeTHF/H₂O biphasic conditions in the presence of KOH. Complete conversion to form amide **16** was achieved within 3 min of residence time at room temperature (87% yield) in a PFA coil. The next step involved the nucleophilic substitution of benzylic chloride **16** with 1-methylpiperazine, and was implemented by directly using the reactor effluent of the first step. 1-Methylpiperazine was injected as an aqueous solution, and the mixture was next passed through a SS column packed with SS powder and operated at 120°C. Reaction completion was attained within 15 min of residence time (84% yield). The last step involved the C-N cross-coupling of intermediate **17** with 2-aminopyrimidine hydrochloride **18**·HCl using 5 mol% of BrettPhos G4 precatalyst (in 30% *N,N*-dimethyloctanamide/2-MeTHF). The latter was directly injected in the reactor effluent of step 2, with the concomitant injection of **18**·HCl (1 equiv.) in water through a cross junction. Because of the high selectivity of BrettPhos for the coupling of primary amines, removal of 1-methylpiperazine in excess was not mandatory. The reaction was sent to a SS packed-bed reactor (packing material: SS powder) for maximal mixing efficiency of the two phases. The residence time in the last reactor was of 15 min, and imatinib was isolated in 56% overall yield after a batchwise downstream process step.

[Osimertinib] AZD9291, a.k.a. osimertinib (Tagrisso, **21**), is an irreversible epidermal growth factor receptor kinase inhibitor. The last step of its synthesis, an amide-bond formation followed by an elimination, was reported in a PTFE coil flow reactor with the implementation of on-line HPLC analysis and a self-optimization algorithm [8]. The algorithm included a feedback control loop that utilized HPLC data from previous runs to generate new sets of reaction conditions. Preliminary optimization using 2,4-dimethoxyaniline as a model substrate furnished useful reaction information without wasting high value-added material. The continuous-flow procedure was next applied to the synthesis of **21**, which was obtained with 89% yield after 42 experimental points generated in 26 h, and only 10 g of starting material utilized (Fig. 8).

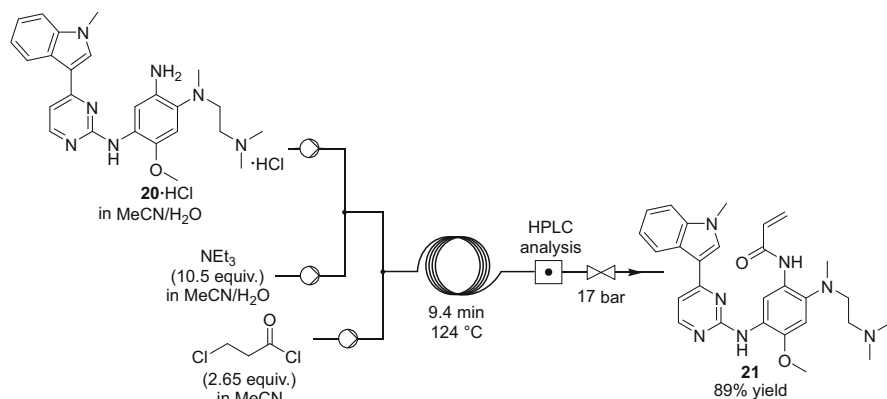


Fig. 8 Self-optimizing continuous-flow preparation of osimertinib (**21**) [8]

[Oxomaritidine] (±)-Oxomaritidine (**31**) is a cytotoxic alkaloid commonly found in plants from the Amaryllidaceae family. Ley and coworkers reported a multistep flow process for the synthesis of alkaloid **31** [9]. It relied on microfluidic pumping systems and various packed columns containing immobilized reagents, catalysts, and scavengers assembled according to seven stages (Fig. 9). The first stage involved reacting a stream of 4-(2-bromoethyl)phenol **22** (MeCN/THF 1:1) in a glass column with an azide exchange resin (PS-N₃) at 70 °C in a Syrris AFRICA flow system. Bromide **22** was quantitatively converted into the corresponding azide **23**. The reactor effluent was next passed through a second column containing a polymer-supported phosphine (PS-PR₂), thus trapping intermediate azide **23** as the corresponding aza-Wittig intermediate **24**. The oxidation of commercially available benzyl alcohol **25** was carried out in parallel using a column packed with tetra-*N*-alkylammonium perruthenate (PS-RuO₄). The reactor effluent containing the corresponding aldehyde **26** was redirected through the column containing aza-Wittig intermediate **24**, producing imine **27** in THF. Imine **27** was next subjected to hydrogenation in a ThalesNano H-Cube equipped with a 10% Pd/C cartridge. The reactor effluent containing benzylamine derivative **28** was next processed in a Vapourtec V-10 solvent evaporator, and eventually dissolved in CH₂Cl₂. The next

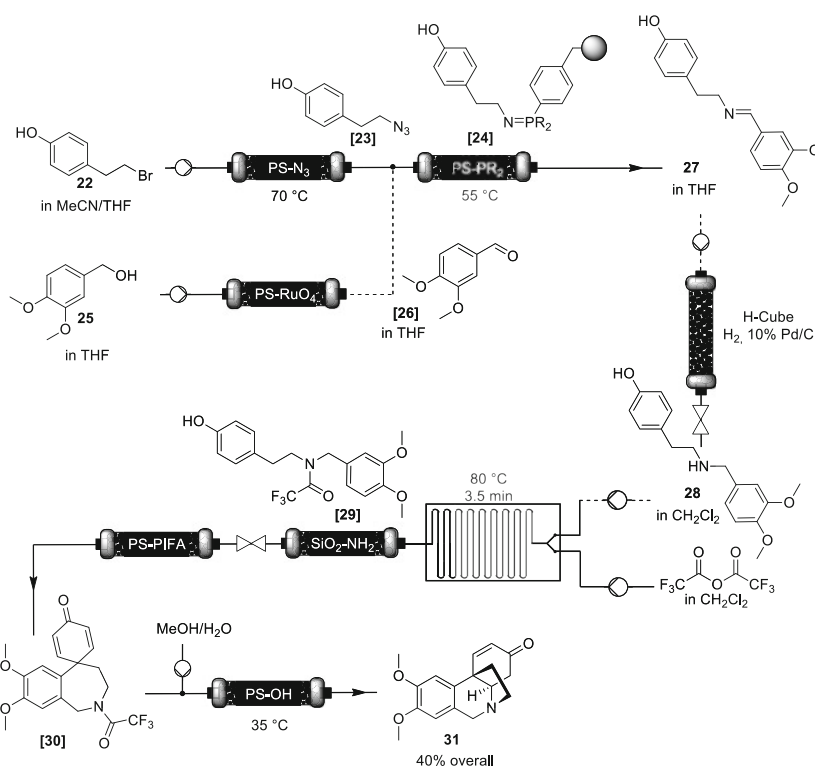


Fig. 9 Multistep continuous-flow preparation of oxomaritidine (**31**) [9]

stage implied reacting amine **28** with trifluoroacetic anhydride in a glass microfluidic chip operated at 80°C (3.5 min of residence time), yielding trifluoroacetamide **29**. The reactor effluent was next passed through a short scavenging column containing a silica-supported primary amine (SiO₂-NH₂) for removing TFAA in excess or residual trifluoroacetic acid. A back-pressure regulator was inserted downstream for allowing superheated conditions in CH₂Cl₂. The purified effluent was then redirected to a column packed with polymer-supported (ditrifluoroacetoxi) benzene (PS-PIFA), and amide **29** underwent an oxidative phenolic coupling toward 7-membered tricyclic intermediate **30**. The reaction stream was next passed through another column packed with a hydroxide exchange resin (PS-OH) for hydrolyzing the amide, and promoting an intramolecular Michael addition toward oxomaritidine (**31**). The reactor effluent was next processed off-line, and the desired compound was recovered in 40% overall yield (90% purity). A comprehensive study of each individual step indicated that the phenolic coupling bottlenecked the entire process with a mere 50% yield.

[Ribociclib] A team with Novartis Pharma AG reported the continuous-flow synthesis of ribociclib (**35**), which is a CDK4/CDK6 inhibitor endowed with potential activity for the treatment of breast cancers and pediatric solid tumors [10]. The two last reactions of the sequence, namely an amination and a subsequent Boc-deprotection, were optimized in batch and then transposed in a PFA continuous-flow reactor (Fig. 10). The original amination step relied on a Buchwald-Hartwig Pd-catalyzed reaction, but the authors opted for a metal-free alternative to lower production costs. After a preliminary screening of bases and solvents, LiHMDS in THF was identified as the best combination to promote the amination. Next, the deprotection step of intermediate **34** with aqueous HCl was telescoped. Two in-line purification steps were inserted downstream. It consisted in a liquid-liquid

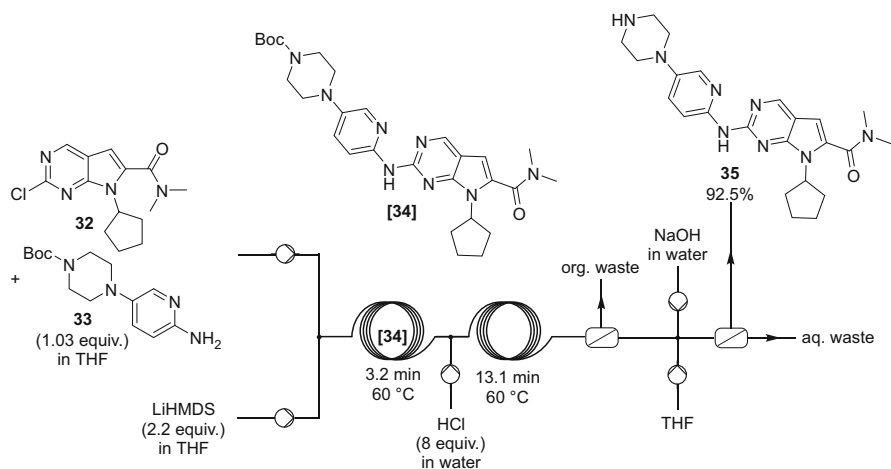


Fig. 10 Continuous-flow preparation of ribociclib (**35**) [10]

separation followed by alkaline pH adjustment to release **35** as a free base. Ribociclib (**35**) was obtained in 92.5% overall yield, with 95% purity and a productivity of 51 g h⁻¹.

2.2 Antiviral Active Compounds

2.2.1 HIV/AIDS Medications

[Efavirenz] McQuade and Seeberger developed a semi-continuous process that provides the HIV treatment drug *rac*-efavirenz (**40**) with an overall yield of 45% [11, 12]. By contrast to the conventional industrial routes developed in industry (Merck, five-step production method from *p*-chloroaniline; Lonza, four-step synthesis from 1,4-dichlorobenzene), the authors developed a much more direct and efficient strategy using less toxic and more effective reagents (Figs. 11 and 12). The method relies on a pivotal one-step copper-catalyzed installation/cyclization of the carbamate ring of efavirenz. Three different stages were developed in separated flow modules. A Vapourtec E-Series System was utilized for pumping the chemicals, and the coil reactors were constructed with standard HPLC fittings, PTFE tubing, and ETFE static mixers. The authors argued that the most efficient method to synthesize the propargylic alcohol precursor **39** would utilize two *n*BuLi-mediated lithiation steps, which are known to be very sensitive to local stoichiometry and heat management. The first step involved an ortho-lithiation of 1,4-dichlorobenzene and a subsequent trifluoroacylation reaction of intermediate **36** with trifluoroacetylmorpholine (Fig. 11). A packed-bed reactor containing anhydrous silica (SiliCycle silica) was inserted downstream to quench the reactor effluent at -10°C. The optimized conditions led to 87% yield within a total residence time of 17.3 min (4 min in loop 1 and 13.3 min in loop 2) at -45°C.

The second step involved the nucleophilic addition of lithium cyclopropylacetylide to crude intermediate trifluoroketone **37** (Fig. 12). The reaction was extremely efficient, and 92% conversion was achieved in less than 2 min of residence time at -20°C using a 0.5 M solution of cyclopropylacetylene (in THF)

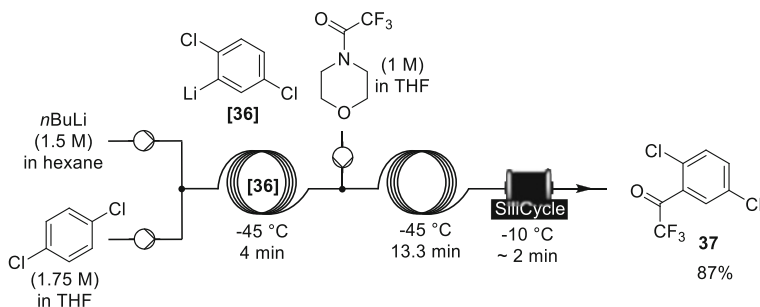


Fig. 11 Multistep preparation of intermediate **37** en route toward *rac*-efavirenz (**40**) [11]

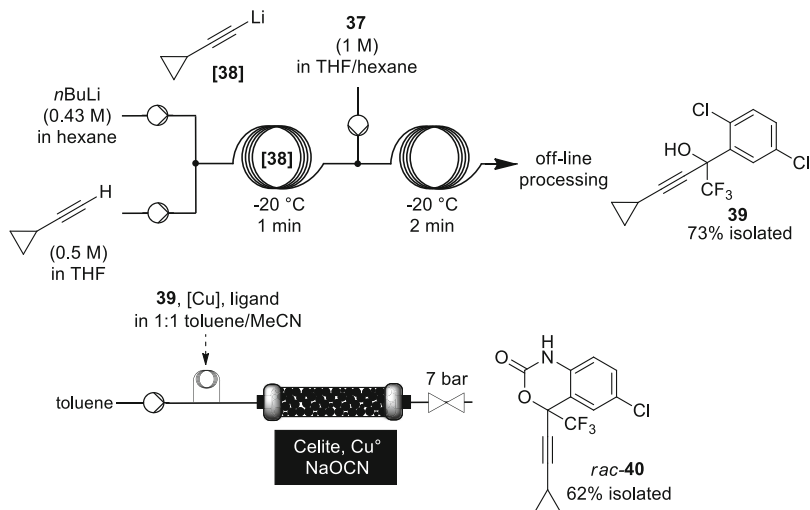


Fig. 12 Multistep preparation of *rac*-efavirenz (40) [11, 12]

and a 0.43 M solution of *n*BuLi (in hexane). The presence of unreacted alkyne as well as small amounts of other by-products imposed an off-line purification and quaternary propargylic alcohol **39** was isolated in 73% yield overall. The last step utilized a column packed with Celite, NaOCN, and Cu⁺ (0.5 equiv.). An injection loop was inserted upstream the column and was utilized for the injection of a solution of purified alcohol **39** (0.2 M), a Cu(II) salt such as Cu(OTf)₂ (typ. 5 mol%) and a ligand such as *trans*-*N,N'*-dimethyl-1,2-cyclohexanediamine in a 1:1 toluene/acetonitrile mixture (Fig. 12). Very high conversion of alcohol **39** was observed (60 min residence time), with isolated yields of 62% in *rac*-efavirenz (**40**) after off-line processing.

2.2.2 Antiviral Pharmaceuticals

[AS-136A] Jamison reported a continuous-flow system enabling the modular synthesis of highly functionalized fluorinated pyrazoles and pyrazolines, including measles therapeutic AS-136A (**45**) [13]. The system relied on transforming fluorinated amines into diazoalkane derivatives and the subsequent [3 + 2] cycloadditions with alkenes or alkynes. The corresponding intermediates bearing an azole scaffold were then sequentially modified through additional reactor modules performing various steps, including *N*-alkylation and arylation, deprotection, and amidation. The authors reported an impressive molecular diversity, including agrochemical and pharmaceutical compounds. The setup relied entirely on PFA microfluidic coils. The paper also showcased the telescoped preparation of AS-136A (**45**), according to a four-step sequence, with a total residence time of 31.7 min and an output of 1.76 g h⁻¹ (Fig. 13). The process began with the optimization of the formation of

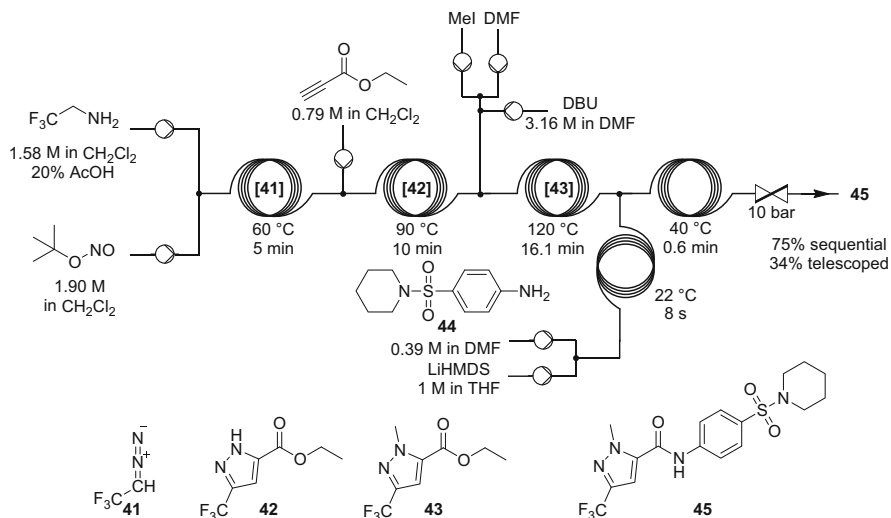


Fig. 13 Multistep continuous-flow preparation of measles therapeutic AS-136A **45** [13]

2,2,2-trifluoromethyl diazomethane (**41**) from the reaction of 2,2,2-trifluoroethylamine (1.6 M in CH₂Cl₂ in the presence of 0.32 M of AcOH) and *t*BuONO (1.9 M in CH₂Cl₂) at 60 °C in a first module. The formation of **41** was next telescoped to a [3 + 2] cycloaddition with ethyl propiolate in a second module at 90 °C. The formation of **41** required only 5 min at 60 °C, and the [3 + 2] cycloaddition only 10 min of residence time at 90 °C to quantitatively yield **42**. The combination of both steps in the same microfluidic element at 90 °C led to a significant decrease in yield, most likely as a consequence of the thermal instability of **41**. The next module took care of the methylation of 3-trifluoromethyl pyrazole **42**. Further optimization revealed that DBU and MeI at 120 °C for 16 min provided the most suitable conditions to form alkylated compound **43**. The last module performed the direct amidation of **43** by combining a 1 M LiHMDS solution with 4-(piperidin-1-ylsulfonyl)aniline (**44**, 0.39 M, in DMF) with **43** at 40 °C within less than 1 min of residence time. The system could be entirely telescoped, although lower yield were obtained (34%). The sequential strategy, with each module operated independently, led to an overall yield of 75%.

[Edoxudine] Deoxynucleosides are a class of compounds featuring unique biological features such as antitumoral and antiviral activities. In particular, edoxudine (**51**) is a deoxynucleoside-based antiviral drug. It is an analog of thymidine, and has shown effectiveness against herpes simplex virus. Jamison and Shen prepared 2'-deoxy- and 2',3'-dideoxynucleosides in a continuous-flow reactor [14, 15]. The reaction sequence is based on a previously reported batch strategy, and involves the derivatization of the C2' alcohol of a protected ribose into *m*-CF₃-benzoate **46**, followed by coupling with a TMS-protected nitrogenous base **47**. The trifluoromethylbenzoate moiety favors a high diastereoselectivity toward **48**, and is

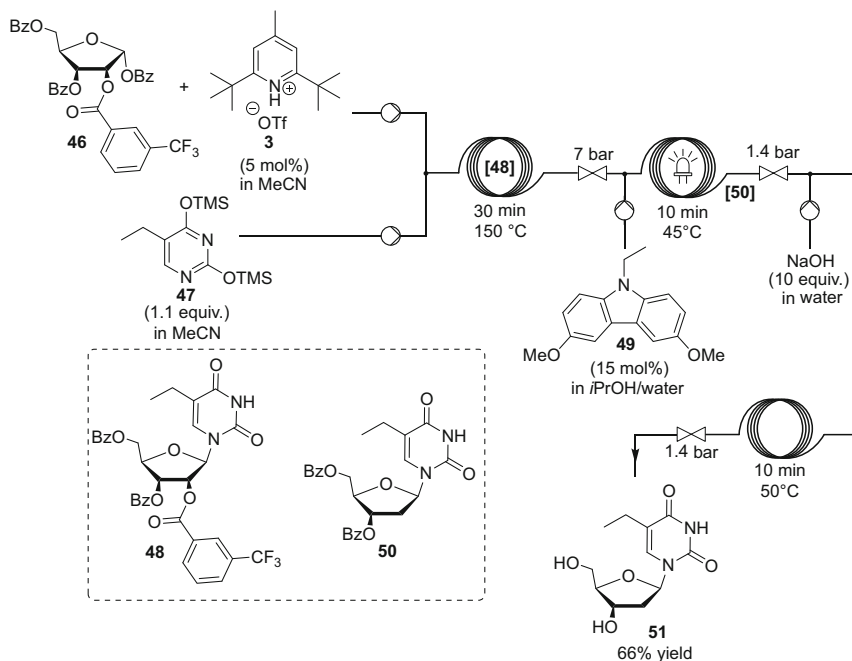


Fig. 14 Telescoped multistep continuous-flow synthesis of edoxudine (**51**) [15]

then removed through a photosensitized electron-transfer, which is followed by chemically triggered removal of the other protecting groups (Fig. 14). The photochemical reaction was studied in a continuous-flow photoreactor combining a medium pressure Hg lamp equipped with a Pyrex sleeve (280 nm cutoff) and a quartz coil wrapped around the lamp. Various photosensitizers were evaluated on a model reaction, and 3,6-dimethoxy-9-ethylcarbazole **49** was identified as the most efficient for producing intermediate **50**.

After extension of the substrate scope, an alternative setup was designed where a stream of aqueous NaOH was inserted after the photochemical reactor to trigger the removal of the remaining Bz protecting groups. Additionally, condensation of the nitrogenous base with the protected ribose was also implemented upstream the photochemical reactor, and this three-stage continuous-flow setup proved efficient for the preparation of the drug edoxudine (**51**) in 66% yield.

2.3 Antiparasitic and Antibiotic Pharmaceuticals

2.3.1 Malaria

[Artemisinin and derivatives] Antimalaria drugs have attracted considerable attention from the scientific community, and in particular the development of efficient, yet

affordable, processes thereof. Artemisinin is a sesquiterpene endoperoxide that is nowadays part of the standard treatment for malaria. Artemisinin and its derivatives are the most studied antimalaria compounds in continuous-flow chemistry. The first attempt to prepare dihydroartemisinin (**53**) from artemisinin (**52**) dates back to 2012. Dihydroartemisinin is used in Artemisinin Combination Therapies for the treatment of malaria. Lapkin and colleagues demonstrated the reduction of artemisinin (**52**) into dihydroartemisinin (**53**) in a glass chip continuous-flow reactor [16]. Since batch scaling-up is notoriously tedious and possibly hazardous with unstable compounds such as peroxides, the authors considered flow chemistry as a promising alternative. Despite the challenges associated with the handling of solid reducing agents under flow conditions, NaBH_4 , $\text{LiAlH}(\text{O}t\text{Bu})_3$, $\text{NaAlH}_2(\text{OCH}_2\text{CH}_2\text{OMe})_2$, and LiBHET_3 were assessed as potential reductants. LiBHET_3 was identified as the most promising, providing enhanced yield, shorter reaction times and a wider temperature tolerance. The reaction was then translated to continuous-flow, where THF and then biosourced 2-MeTHF were used as solvents (Fig. 15). Acetic acid was injected downstream the reactor to quench the remaining reducing agent. In 2-MeTHF, 94% yield could be obtained at 25°C and 20 s residence time, which represents a significant improvement of the current batch procedures. The authors next developed a continuous-flow etherification of **53** toward the preparation of artemether (**54**) [17], which is also used in Artemisinin Combination Therapies for the treatment of malaria. At first, batch optimization was performed using Amberlyst-15 and QuadraSil as acidic catalysts, hence enhancing considerably the reaction rate. Additionally, no leaching and deactivation was noticed for QuadraSil, by opposition to Amberlyst-15. Similar catalytic behaviors were observed under continuous-flow conditions. However, the reduction and the etherification steps were not telescoped, and an intermediate off-line purification was necessary.

Seeberger and colleagues devised a multistep process for the preparation of artemisinin (**52**) [18]. Their original report described the implementation of the three-step process for the conversion of dihydroartemisinic acid (**55**) into artemisinin (Fig. 16). The procedure combined a photooxidation with singlet oxygen, an acid-mediated Hock cleavage, and triplet oxygen oxidation, and the procedure was further optimized in follow-up papers [19, 20]. The first stage involved the

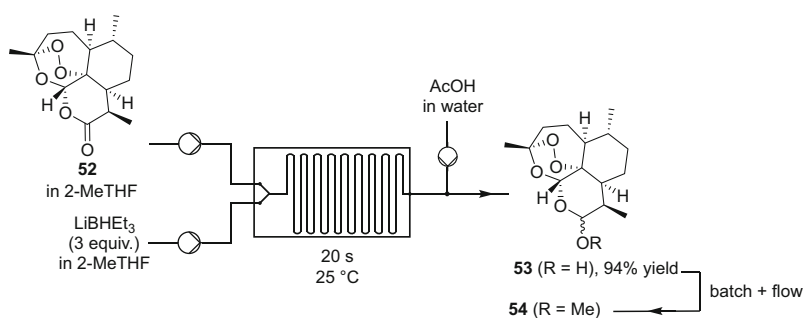


Fig. 15 Reduction of artemisinin toward dihydroartemisinin (**53**) [16, 17]

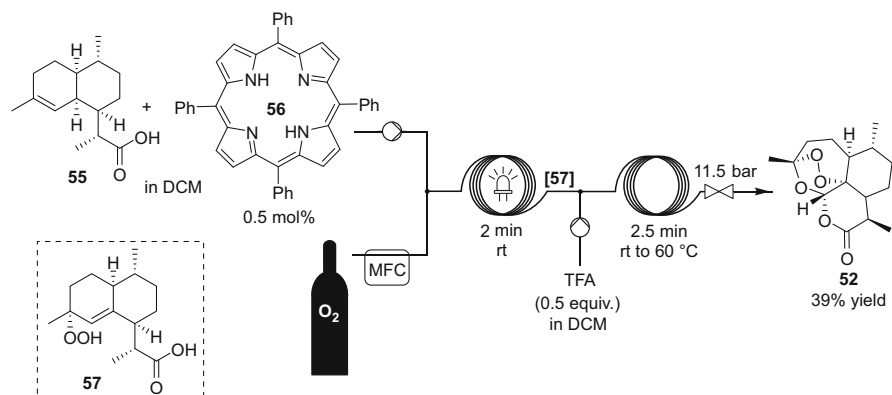


Fig. 16 Continuous-flow preparation of artemisinin [18]

photooxidation of **55**, and was optimized in a continuous-flow reactor that consisted in a FEP tubing wrapped around a medium-pressure mercury lamp. Oxygen was delivered using a mass-flow controller and mixed with the solution of the starting material and the photosensitizer.

DCM was selected as solvent owing to its non-flammable nature and tetraphenylporphyrin (**56**) as photosensitizer, due to its resistance toward photobleaching and its high quantum yield. The intermediate allyl hydroperoxide **57** was obtained in 75% yield. Next, Hock cleavage and subsequent triplet oxygen oxidation were first optimized in a batch setup. Several Lewis and Brønsted acids were evaluated in the presence of oxygen, and TFA gave the best results, affording 50% yield of **52**. The reaction was then translated to continuous-flow conditions, and full telescoping was attempted. The solution of **56** decreased its efficiency as photosensitizer. Artemisinin was obtained in 39% yield overall, with a productivity of 200 g day⁻¹.

The same authors reported later some improvements of their original procedure [19]: (a) toluene was selected as solvent instead of dichloromethane, which improved the yield; (b) 9,10-dicyanoanthracene (9,10-DCA, **58**) was utilized as photosensitizer (9,10-DCA is non-protonable, and therefore TFA could be added to the photosensitizer and substrate feed before the photooxidation step), resulting in the utilization of a single feed stock; (c) 420 nm LED were utilized instead of a medium-pressure Hg lamp; and (d) the photooxidation temperature was changed to -20°C, which increased the selectivity. The modified setup improved the yield from 39 to 65%.

Another paper from Seeberger and coworkers illustrated their final effort to integrate in-line IR analyses and in-line purifications to the continuous-flow preparation of artemisinin and derivatives (Fig. 17) [20]. At first, the three-step one-pot process, involving a sequence of photooxidation with singlet oxygen, TFA-mediated acidic Hock cleavage, and triplet oxygen oxidation on **55** toward artemisinin was conducted as reported in [18, 19]. The setup was then telescoped to a column packed

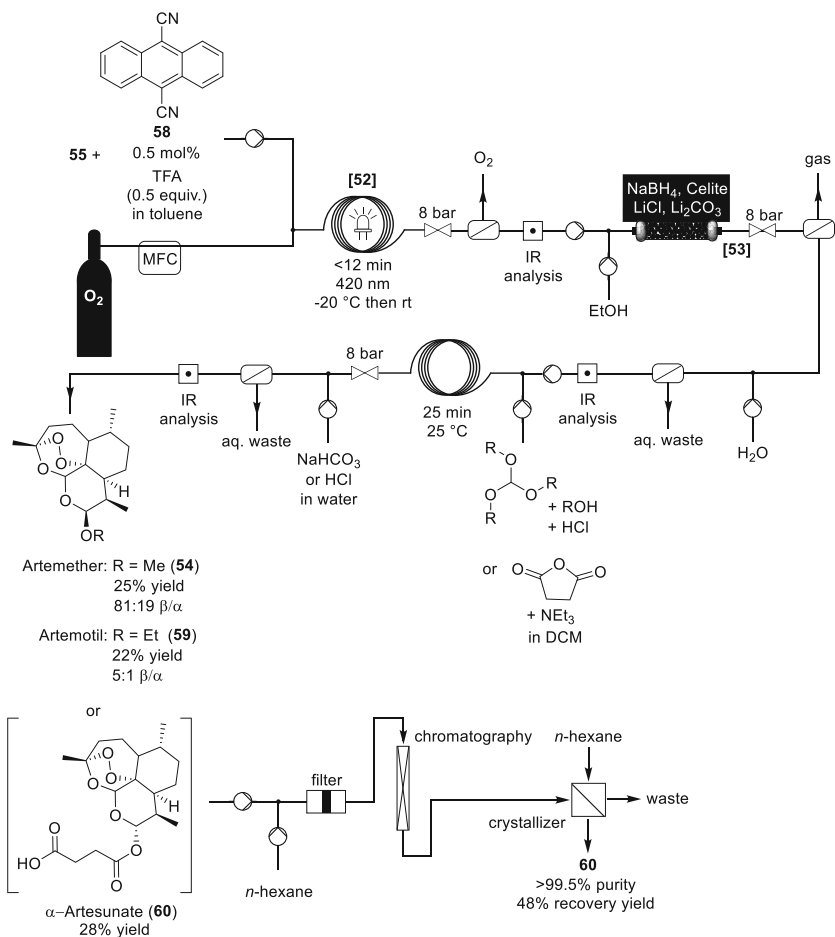


Fig. 17 Artemisinin and derivatives [20]

with NaBH₄/celite to perform the reduction of the ester moiety of **52** into the corresponding hemiketal **53**. The authors reported that clogging occurred in many cases, and further optimization was necessary. It was found that mixing NaBH₄ and celite with LiCl and Li₂CO₃ accelerated the reduction (in situ formation of LiBH₄), and buffered the TFA present in the reaction stream, respectively. Additionally, ethanol as a co-solvent enabled prolonged operation without clogging. The effluent of the reactor was then degassed, washed with water to cleave the alkoxyborane formed upon reduction, and then combined with a stream of MeOH/trimethyl orthoformate/HCl to form artemether (**54**) in the third module. The reactor effluent was mixed with a stream of aqueous NaHCO₃, and subjected to in-line liquid–liquid extraction. The desired β-diastereomer of artemether (**54**) was obtained in 25% yield with a 81:19 β/α ratio. Similarly, combination of the second module effluent with a

stream of ethanol, triethyl orthoformate and HCl afforded artemotil (**59**) in 22% yield with a 5:1 β/α ratio.

Alternatively, the injection of succinic anhydride and NEt_3 gave artesunate (**60**) in 28% yield with the exclusive formation of the α -diastereomer, after neutralization with aqueous HCl and in-line liquid–liquid extraction. An in-line purification process, including filtration, column chromatography, and recrystallization was finally implemented and applied to **60**. At first, hexane was injected to precipitate impurities, and the solution was passed through alternating filters allowing continuous filtration. The soluble material was then directed toward a system comprising of five alternating chromatography columns, also enabling continuous purification using five elution steps. The fraction containing **60** was finally directed toward a continuous crystallizer using hexane as antisolvent. The purification strategy gave a purity of >99.5%, meeting the USP standards, with 48% recovery yield of the API **60**.

Kappe and colleagues developed a continuous-flow procedure to enable the selective reduction of artemisinic acid (**61**) toward dihydroartemisinic acid (**55**), which is the key precursor for the synthesis of artemisinin [21]. The authors considered a metal-free reduction procedure based upon the formation of diimide from hydrazine hydrate under aerobic conditions. General operating conditions were optimized on various olefins, and then transposed to the case of artemisinic acid (**61**). The authors used four consecutive liquid feeds of hydrazine hydrate and residence time units (PFA coils) to improve the reduction of **61** toward **55**. Artemisinic acid (**61**) and hydrazine hydrate (2 equiv.) were dissolved in *n*PrOH and injected through a sample loop into a main stream of *n*PrOH (Fig. 18).

The latter was mixed with oxygen through a static T-mixer, and next reacted in a first 10 mL PFA coil operated at 60°C. The reactor effluent was subsequently mixed with fresh hydrazine hydrate (3.33 M in *n*PrOH), and then reacted in a 10 mL PFA coil, the entire process being repeated three times without interruption of the flow. The effluent of the last coil was cooled, and collected after a back-pressure regulator set at 20 bar. After off-line processing, including solvent evaporation under reduced pressure, the product **55** was obtained in high yield (>93%) and purity (>95%) within approximately 40 min at 60°C and under 20 bar of O_2 .

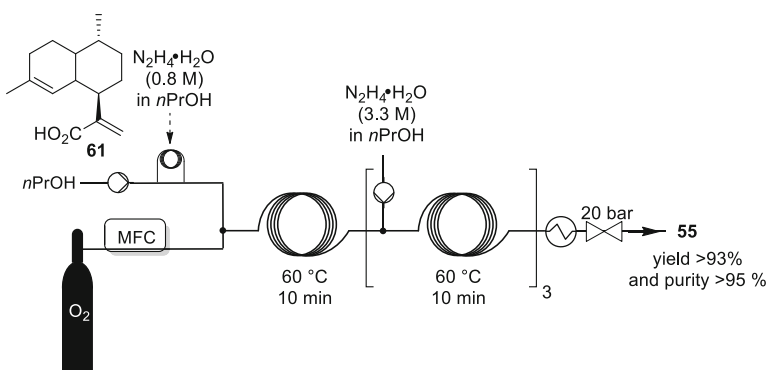


Fig. 18 Reduction of artemisinic acid toward dihydroartemisinic acid [21]

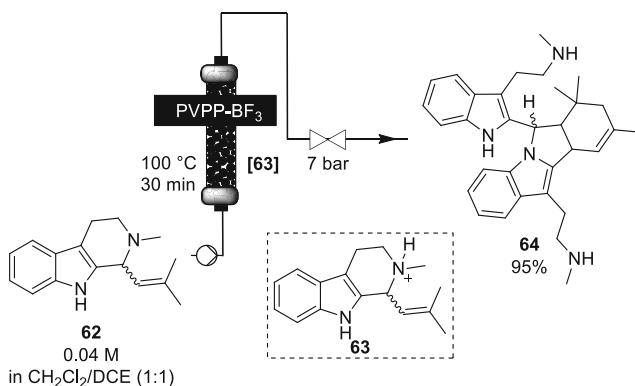


Fig. 19 Continuous-flow preparation of isoborreverine [22]

[Borrerine] Ley and Kamptmann reported a flow procedure for the preparation of antimalarial borrerine derivatives using a biomimetic approach [22]. Borreverine and isoborreverine (**64**) are bisindole alkaloids that can be directly derived from the dimerization of the naturally occurring indole alkaloid borrerine (**62**). Flow chemistry was implemented to overcome the inherent batch limitations for handling reactive intermediates. For instance, the preparation of isoborreverine (**64**) followed a Diels-Alder strategy with the intermediate ring opening of borrerine (**62**) (Fig. 19). Isoborreverine (**64**) is typically obtained by an acid-promoted one-step procedure from **62**. The authors screened different solid-supported Lewis acids among which the most successful was PVPP- BF_3 . Using a 1:1 CH_2Cl_2 /1,2-dichloroethane solvent mixture, **64** was formed essentially free of side products. Off-line work-up including a basic wash of the reaction mixture delivered isoborreverine free base (**64**) in 95% yield.

2.3.2 Antibiotics

[Bassianolide] A team at the University of Cambridge reported a flow chemistry protocol for the coupling and macrocyclization of linear peptide fragments for the rapid synthesis of both natural and unnatural depsipeptides in high yields [23]. The authors applied the method for the preparation of a series of cyclooligomeric depsipeptides of three different ring sizes including the natural products beauvericin, bassianolide (**69**), and enniatin C (Fig. 20). The flow synthesis of the depsipeptides began with preliminary optimizations for the deprotection and the intermolecular couplings to give the necessary linear precursors for macrocyclization. The partners were deprotected either by flow hydrogenation using a ThalesNano H-Cube equipped with a 10% Pd/C CatCart to afford acid **66**, or by batch removal of the Boc group with anhydrous HCl in dioxane to afford hydrochloride **67**. The crude products were then processed in batch, and readied for the coupling under flow

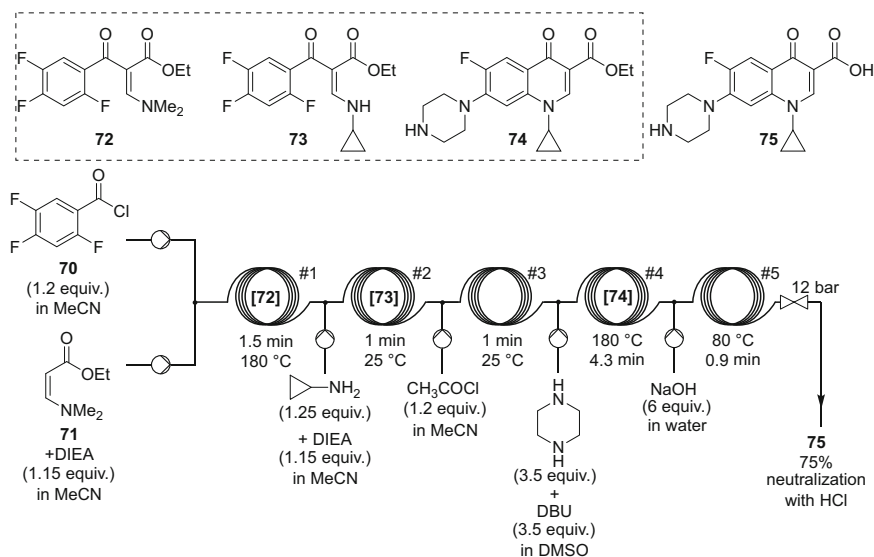


Fig. 21 Multistep continuous-flow preparation of ciprofloxacin [24]

piperazine/DBU solution was injected before reactor #4, which was operated at 180°C, and two S_NAr reactions were triggered: a cyclization in the *ortho*-position of the acyl moiety and the amination with piperazine in the *para*-position, affording **74**. The last step, namely, hydrolysis, was implemented downstream by injection of aqueous sodium hydroxide. The hydrolysis was performed in the fifth reactor operated at 80°C. The crude sodium salt of **75** was then converted in its acid form by off-line addition of aqueous HCl. Crude ciprofloxacin (**75**) was obtained in 75% yield over the six steps. Further off-line purification by reactive crystallization, filtration, and washing afforded analytical samples in 60% overall isolated yield.

[Mur ligase inhibitor] Cosford and colleagues reported a continuous-flow procedure for the preparation of imidazo[1,2-*a*]pyridine-2-carboxylic acids directly from 2-aminopyridines and bromopyruvic acid using an AFRICA system from Syrris [25]. The process was amenable to the multistep synthesis of imidazo[1,2-*a*]pyridine-2-carboxamides, including a Mur ligase inhibitor **77** endowed with potential antibacterial activity. It relied on the telescoping of various steps within two microreactors (Fig. 22). The authors reported that the continuous-flow procedure was superior to its batch analog. The first microreactor chip was dedicated to the installation of the imidazo scaffold through the condensation of 2-aminopyridin-3-ol (1.0 equiv.) and bromopyruvic acid (1.2 equiv.) in dimethylformamide (DMF) at 125°C, in the presence of a catalytic amount of *p*-toluenesulfonic acid (PTSA) (0.25 equiv.). Full conversion was obtained within 10 min of residence time at 125°C and 4 bar of counter-pressure. The next microreactor was utilized for accessing imidazo [1,2-*a*]pyridine-2-carboxamides by direct telescoping of an amidation step with the imidazo[1,2-*a*]pyridine-2-carboxylic acid scaffold. Upon optimization, the best

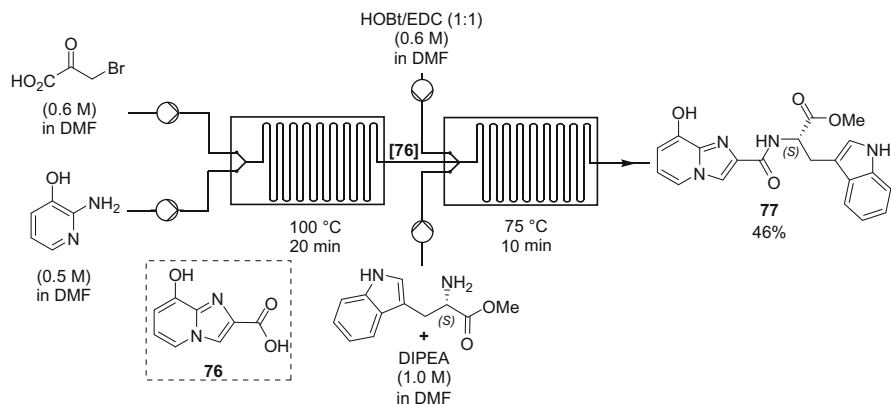


Fig. 22 Two-step telescoped preparation of mur ligase inhibitor **77** [25]

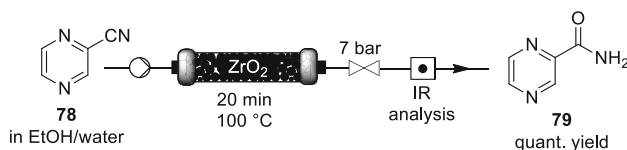


Fig. 23 Preparation of pyrazine-2-carboxamide (**79**) featuring in-line analysis and automated processing of the reactor effluent [26]

conditions for the amidation step required a combination of EDC/HOBt/DIPEA and a residence time of 10 min at 75°C (complete conversion). Reaction telescoping required minor adjustments in the first reaction, since PTSA was deleterious to the second step. The authors decided to remove PTSA, and to increase the residence time within the first microreactor to 20 min at 100°C. The reactor effluent containing imidazo[1,2-a]pyridine-2-carboxylic acid **76** was next combined with a stream of EDC/HOBt and with a stream of tryptophan methyl ester/DIPEA, and reacted in a second microreactor at 75°C for 10 min. The procedure was successfully applied to Mur ligase inhibitor **77**. The batch procedure, relying on manual intervention and isolation of the intermediate **76**, proceeded with 16.4% overall yield, while the continuous-flow procedure gave a much improved 46% overall yield.

[Pyrazine-2-carboxamide] Pyrazine-2-carboxamide (**79**) is used in the treatment of tuberculosis. Ley and colleagues used an open-source software and a low-power computer for the real-time control of several continuous-flow chemistry elements and sensors, and utilized the setup for the preparation of **79** from the hydration of the corresponding nitrile **78** [26]. Nitrile hydration was optimized using several solvents and heterogeneous catalysts, and the combination of ZrO₂ as catalyst and ethanol as solvent afforded quantitative yield in the target amide **79** (Fig. 23).

The monitoring software was next connected to the setup as well to an IR analysis flow cell mounted after the catalytic bed. Under such conditions, the algorithm ensured that predefined values of column temperature and pressure as well as IR

absorption were met during a predefined equilibration time, before collection of the reactor effluent. If these parameter values were not met or lost at some point, the system automatically switched to disposal. The procedure was amenable to the fully automated preparation of **79**.

2.4 Central Nervous System and Related Conditions

2.4.1 Schizophrenia

[Cariprazine] Greiner and colleagues devised a microfluidic continuous-flow setup for the preparation of libraries of non-symmetrical urea derivatives, including active pharmaceutical ingredient cariprazine (**82**, US: Fraylar, EU: Reagila) [27]. Cariprazine is an atypical antipsychotic used in the treatment of schizophrenia and bipolar mania; it acts as a dopamine D2 and D3 receptor partial agonist. The method relied on a previously reported batch procedure, where *tert*-butoxycarbonyl protected amines were treated with trifluoromethanesulfonic anhydride (Tf₂O) in the presence of 2-chloropyridine as a base to form an intermediate isocyanate upon elimination of the *tert*-butoxy group. Subsequent addition of primary or secondary amines eventually led to the desired urea derivatives. Greiner translated and optimized the original conditions for an implementation under continuous-flow. The corresponding microfluidic assembly consisted in a first glass microreactor for the formation of unstable isocyanate intermediate, which was next mixed with a secondary amine and sent to a second PTFE coil microreactor to yield the desired urea (Fig. 24). Since Tf₂O is a very corrosive reagent, glass and PTFE were mandatory for the construction of the microfluidic assembly. The feed solution containing Tf₂O was injected in the reactor through a glass/PTFE syringe pump, while the feed solution containing the starting carbamate was injected through a classical HPLC pump. The author also included in-line Fourier transform infrared (FT-IR)

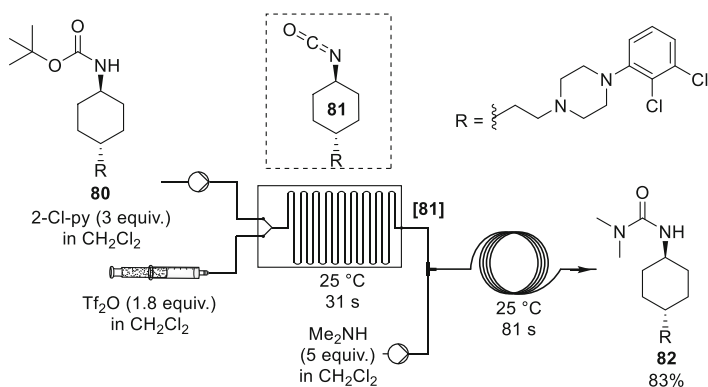


Fig. 24 Continuous-flow preparation of cariprazine [27]

spectroscopy to monitor the reaction. The conditions were amenable to the generation of a variety of urea derivatives, and minor adjustments were necessary for the preparation of cariprazine starting from an advanced carbamate **80**. Feed 1 consisted in a premixed solution of **80** and 2-chloropyridine (3 equiv.) in dichloromethane, which was injected in a 250 μL first glass microchip at 25°C in the presence of Feed 2 (Ti_2O , 1.8 equiv. in CH_2Cl_2). Total conversion was attained within 31 s of residence time. Intermediate isocyanate **81** was not isolated, but its preparation was telescoped to the formation of **82** by the injection of a feed of dimethylamine in DCM. Cariprazine (**82**) was isolated in 83% yield after a 81 s residence time at 25°C, with an output of 320 mg h^{-1} . The most obvious advantage of this continuous-flow procedure is to alleviate the isolation and handling of an unstable isocyanate.

[Iloperidone] Iloperidone (**87**) is an antipsychotic drug used in the treatment of schizophrenia. Kirschning and Hartwig developed a steel continuous-flow reactor featuring inductive heating with an external magnetic field, internal temperature monitoring, and feedback control to adjust heating [28]. The preparation of **87** was demonstrated in such an innovative inductive heating flow reactor (Fig. 25), using a sequential flow strategy with four independent stages. The first stage involved a Fries rearrangement on 2-methoxyphenyl acetate, and was conducted in superheated CH_2Cl_2 in a PEEK column packed with SS beads. Acetophenone **83** was obtained in 75% yield after rearrangement in the presence of methanesulfonic acid. During stage 2, ketone **84** was transformed into oxime **85** using hydroxylamine. The reaction was performed in a steel coil reactor, and oxime **85** was obtained in 87% yield. The cyclization and *N*-alkylation of **85** toward isoxazole **86** were then simultaneously performed in a steel flow reactor, in the presence of 1-bromo-3-chloropropane and LiOH within stage 3. A second passage of the reactor effluent in the SS coil reactor under the same conditions was necessary since full conversion was not attained. Stage 4 consisted in the coupling of compounds **83** and **86**. A final purification (not shown) using a column filled with silica was implemented, yielding compound **87** in 67% yield.

[Olanzapine] Kirschning and colleagues reported a continuous multistep flow synthesis for the preparation of atypical neurolepticum olanzapine (**92**, Zyprexa), an antipsychotic medication used to treat schizophrenia and bipolar disorder, using an advanced heating method [29]. A high-frequency inductor that could be accommodated to various types of flow reactors including packed-bed reactors (glass, PEEK or ceramic) or coil reactors made of Hastelloy C-steel was developed. The authors utilized a high-frequency inductor for rapid heating within short residence times. The individual steps were independently optimized, and telescoping was attempted later (Fig. 26). The first reactor module was dedicated to the preparation of nitro compound **89** starting from the Buchwald coupling of 1-iodo-2-nitrobenzene and thiophene **88** in the presence of a Pd catalyst. The reactor effluent was subjected to in-line liquid–liquid extraction, and an additional purification module consisting of a cartridge filled with silica to remove traces of Pd was inserted downstream the extractor. The extractor consisted in a vertically oriented tube filled with D.I. water. High yield in nitro **89** was obtained (90%). The next step involved a Pd-catalyzed reduction of the nitro group on compound **89**, giving aniline **90**: the

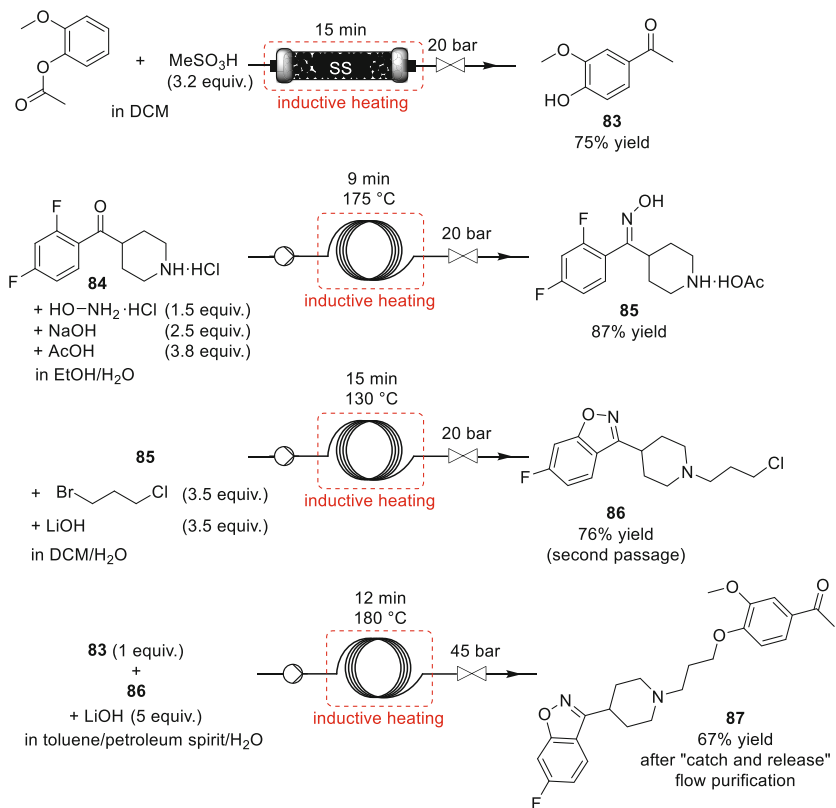


Fig. 25 Sequential continuous-flow synthesis of iloperidone (87) [28]

purified effluent from the first reaction module was mixed with triethylsilane and reacted in a column packed with cotton-wool and Pd/C (10%). The reduction proceeded extremely well with 97% yield in ethyl acetate within a residence time of ~ 40 min. The catalyst could be used for more than 250 h without loss of activity. The reactor effluent was collected in a surge to vent the remaining hydrogen gas. A stream of HCl in MeOH (0.6 M) was added and the resulting solution was injected into a metal tubular flow reactor at 140°C . The complete reactor setup was operated continuously for 30 h, providing 313 mg (88% overall yield) of thieno[1,5]-benzodiazepine **91**. The final step was performed in an additional reactor packed with a supported $\text{Ti}(\text{O}i\text{Pr})_4$, yielding olanzapine (**92**) in 83% within 45 min of residence time at 85°C .

2.4.2 Sedatives and Anxiolytics

[Alpidem, Zolpidem] Ley and Baxendale reported the development of a multistep continuous-flow, computer-controlled platform for the preparation of imidazo[1,2-a]

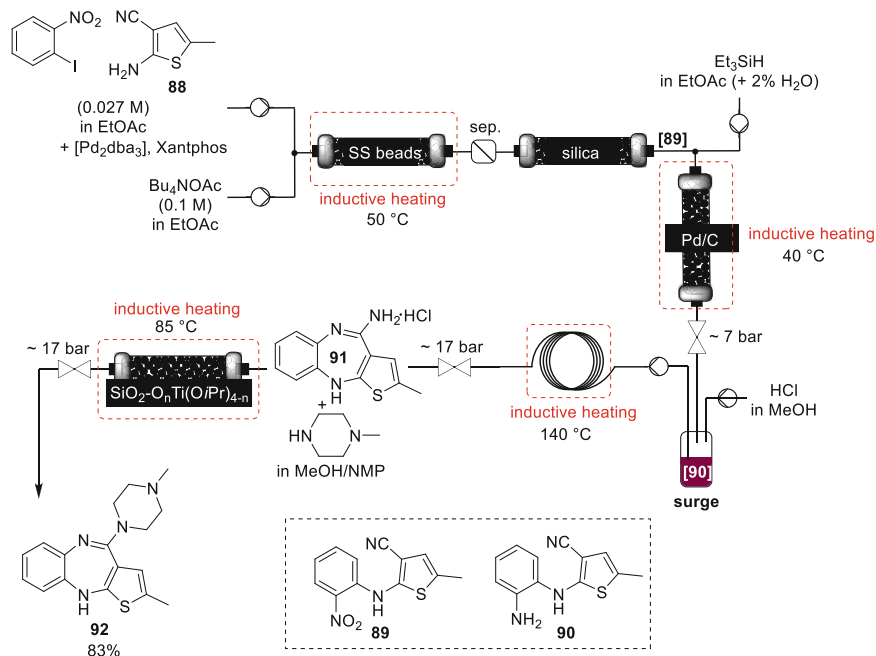


Fig. 26 Multistep continuous-flow preparation of olanzapine [29]

pyridines, including zolpidem and alpidem [30]. Zolpidem (**95**, Ambien) and alpidem (Ananxyl) are short-acting non-benzodiazepine agonists of GABAA receptors belonging to the imidazopyridine class, endowed with mild sedative and anxiolytic properties. The continuous-flow strategy is illustrated below (Fig. 27) for the preparation of zolpidem (**95**), and all steps were amenable to multigram scale. The reagents were injected through sample loops. The first step involved the acid-catalyzed condensation between ethyl glyoxylate (in excess) and 1-(p-tolyl) ethanone, leading to unsaturated ketone intermediate **93**. The reaction occurred in column reactors packed with polymer-supported sulfonic acid resin (QP-SA) within 25 min of residence time at 120 °C. A column packed with a supported benzyl amine (QP-BZA) was inserted downstream to scavenge the excess ethyl glyoxylate, thus leaving a stream of virtually pure enone **93** (85% yield). Crude **93** was collected and transferred to the next step without additional purification step. The following sequence of steps aimed at installing the imidazopyridine scaffold. It first involved the condensation of 5-methylpyridin-2-amine (slight excess) and enone **93** (cat. $HBF_4 \cdot Et_2O$) in a column packed with $MgSO_4$ at 50 °C to promote the formation of an intermediate ketimine, which was subsequently transferred to a 14 mL internal volume coil reactor operated at 120 °C to induce 5-exo cyclization toward compound **94**. A back pressure regulator (100 psi) was inserted downstream to enable superheated conditions and therefore shorter reaction times (4 h) than under conventional heating (24 h). The effluent was passed through a cartridge containing a supported

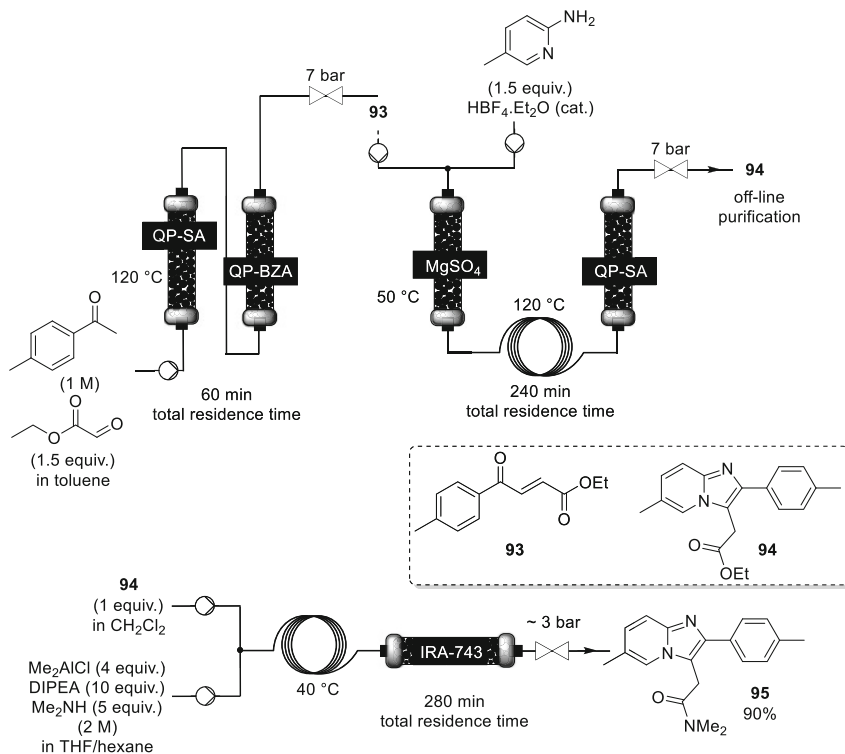


Fig. 27 Multistep continuous-flow preparation of zolpidem (**95**) [30]

acid resin (QP-SA) to capture the excess of 5-methylpyridin-2-amine (that could be later recovered according to a catch-and-release strategy). Compound **94** was obtained in moderate yield and purity, and required off-line purification (30% after column chromatography). The last reaction aimed at converting the ester moiety of **94** to the corresponding amide using dimethyl aluminum chloride. The reaction was carried out at 40 °C within 280 min of residence time. The reactor effluent was next passed through a column packed with IRA-743 and a plug of silica for removing the aluminum salts and the excess of base, affording zolpidem (**95**) in 90% yield. The continuous-flow reactor was connected downstream with a Frontal Affinity Chromatography screening assay to investigate their interaction with Human Serum Albumin (HSA).

[Diazepam] A team led by Jensen, Jamison, and Myerson at MIT designed a compact and reconfigurable system that enabled the fully continuous-flow production of pharmaceuticals [31]. Among the API targets, diazepam (**98**, Valium) was successfully synthesized according to a three-step telescoped continuous-flow process (Fig. 28). Diazepam belongs to the benzodiazepine family that typically produces a calming effect. Upstream reaction module feeding was operated by three HPLC pumps and one dual glass syringe pump. The downstream extraction module

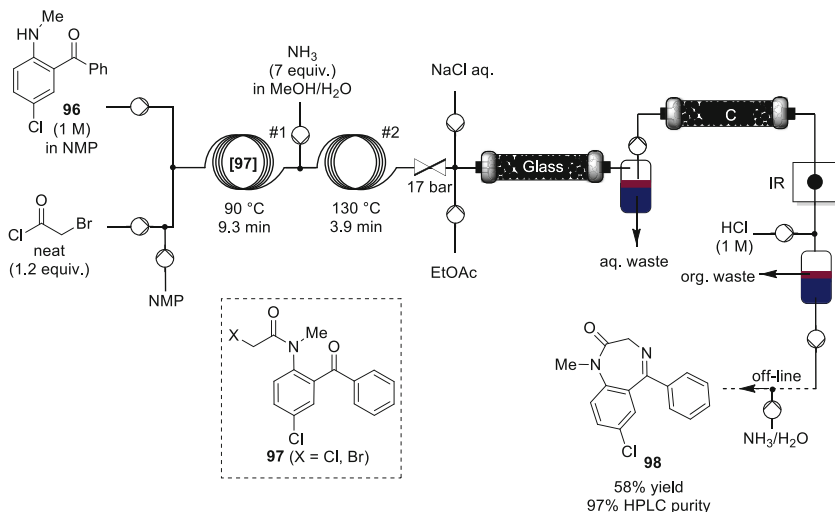


Fig. 28 Three-step, two-stage synthesis of diazepam (**98**) [31]

was fed by three HPLC pumps and a diaphragm pump for diazepam. Fluids were conveyed to the reaction modules through PFA tubing (1/16 and 1/8") and PEEK static T-mixers. The reaction module was composed of easily interchangeable coil mesofluidic reactors of 10 mL internal volume. Each coil reactor consisted of PFA tubing embedded in an aluminum shell for mechanical strength and thermal conductivity, and was associated with an independent heat dispenser and control unit. Temperature, pressure, flow, and level sensors were included at strategic positions in the reactor setup. The last component of the reaction module was connected to a customized chemically resistant back pressure regulator (set at ~17 bar). After the BPR, a cross junction allowed for the treatment of reactor effluents with extraction fluids and led to the extraction unit. After a short stainless steel packed-bed column filled with borosilicate beads ($\phi = 0.1$ mm) for improved mass transfer, the biphasic effluents were collected and handled in an automated gravity-operated liquid–liquid separator. Further downstream processing including crystallization and formulation was included as well, using semi-continuous protocols. The synthesis designed for the production of diazepam involved a three-step continuous chemical reaction (Fig. 28). Chloroacetyl bromide enabled highly efficient amination/intramolecular imine formation at low water ratio (MeOH:Water = 9:1) without causing reactor clogging. Intermediate **97**, obtained as a mixture of the chloro and bromo-analogs, was next converted into diazepam (**98**) through reaction with ammonia in the second PFA coil. Reaction temperature, residence time as well as the concentration and equivalent of ammonia were all crucial parameters to ensure high conversion and efficiency. Under optimal conditions, conversion of intermediate **97** reached 97–98%, affording diazepam (**98**) in 78% yield (HPLC). Analysis of the crude mixture revealed several side products including 5-chloro-2-(methylamino)benzophenone (**96**), hydrolysis products, very small amount of unreacted **97**, dimers/

trimers of **97** as well as cyclohexenone derivatives. The following continuous purification setup, a two-stage sequential extraction sequence together with a charcoal filtration column, was designed for removing all the side products and impurities and delivering diazepam (**98**) in high purity. The first stage of the extraction sequence consisted of the concomitant injection of aqueous sodium chloride (20 wt.-%, 2.5 mL min⁻¹) and ethyl acetate (5 mL min⁻¹) in the reactor effluent through a cross junction. This extraction served to remove all the organic and inorganic salts generated in the reactions as well as highly water soluble impurities. After separation, carried out by a continuous liquid–liquid extractor, the organic stream was passed through a cartridge loaded with activated charcoal to remove dark colored by-products. At this point, an in-line silicon IR probe was inserted for real-time monitoring, prior to the second extraction with aqueous HCl. Upon removal of non-basic organic impurities, the aqueous diazepam solution was then collected in 100 mL fractions. Neutralization and isolation of diazepam free base was carried out off-line by slow addition of aqueous ammonium hydroxide (28 wt.-%), giving diazepam as a pale yellow solid in 58% yield (97% HPLC purity).

The procedure for producing diazepam was further optimized by Jamison in a follow-up paper, and in particular, the E-factor associated with the process was greatly improved [32]. The E-factor associated with the original diazepam flow synthesis [31] was drastically reduced from 36 to 9. The utilization of 2-MeTHF in the first step instead of NMP strongly contributed to this reduction since it enabled both reaction and extraction. Chloroacetyl bromide was changed to chloroacetyl chloride, and the second reactor was operated at 100°C (130°C in the original report). Also, the MeOH/H₂O solution of NH₃, injected before the second reactor, was replaced by a NH₄Cl aqueous solution (injected under sonication). Diazepam (**98**) was isolated in 51% yield after the second step, which is by contrast much lower than in the original report (78%).

Cooks and colleagues also reported on the continuous-flow preparation of diazepam [33]. The authors studied the preparation of **98** in a glass chip continuous-flow reactor. The individual reactions were screened in electrospray and Leidenfrost droplets, and analyzed by ESI-MS, enabling fast optimization. The authors reported that bromoacetyl chloride was more efficient than chloroacetyl chloride for the first step, as reported in the original procedure [31], affording diazepam in quantitative yield over two steps.

2.4.3 Depression

[5HT1B antagonist] Ley and colleagues reported the continuous-flow synthesis of carboxamide **104**, a potent 5HT1B antagonist with antidepressant activity developed by AstraZeneca [34]. The authors used a complex, sequential flow strategy relying on the use of a catch-and-release strategy and supported reagents (Figs. 29, 30, 31, and 32). The process started with the preparation of aniline derivative **100** (Fig. 29). A stream of 3-fluoro-4-nitroanisole (0.5 M in ethanol) and a stream of 1-methylhomopiperazine (0.5 M, 1 equiv., in ethanol) were mixed through a static

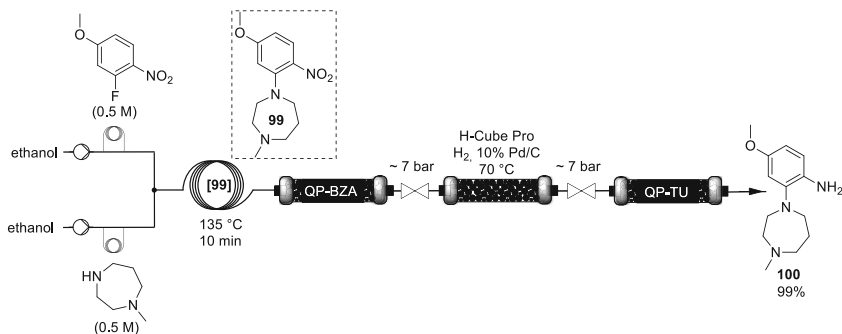


Fig. 29 First stage of the continuous-flow process toward 5HT1B antagonist **104** [34]

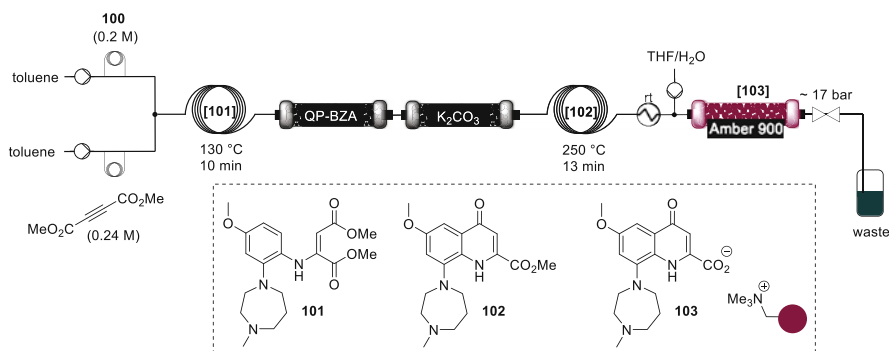


Fig. 30 Second stage of the continuous-flow process toward 5HT1B antagonist **104** [34]

T-mixer and reacted in a heated (135°C) PFA coil (10 mL internal volume) with a residence time of 10 min. The reactor effluent was next passed through a glass column packed with Quadrapure benzylamine (QP-BZA) for scavenging the hydrofluoric acid released during the S_NAr reaction. The reaction mixture was next redirected to a continuous-flow hydrogenator (ThalesNano H-Cube) equipped with a 10% Pd/C cartridge and operated at 70°C. The reactor effluent was then passed through an additional glass column filled with Quadrapure thiourea (QP-TU) to scavenge any leached metal catalyst. The desired aniline **100** was obtained in nearly quantitative yield, and processed off-line.

The second stage (Fig. 30) implied mixing a stream of **100** (0.2 M in toluene) and dimethyl acetylenedicarboxylate (0.24 M, 1.2 equiv., in toluene) through a static T-mixer. The mixture was next reacted in a heated (130°C) PFA coil (10 mL internal volume) with a residence time of ~10 min. The reactor effluent was then passed through a column of QP-BZA to scavenge any residual dimethyl acetylenedicarboxylate, before entering a second column filled with anhydrous potassium carbonate to dry the reaction mixture. Intermediate **101** was next subjected to a high temperature cyclocondensation reaction in a stainless steel flow coil (11 mL internal volume) operated at 250°C for a residence time of 13 min to

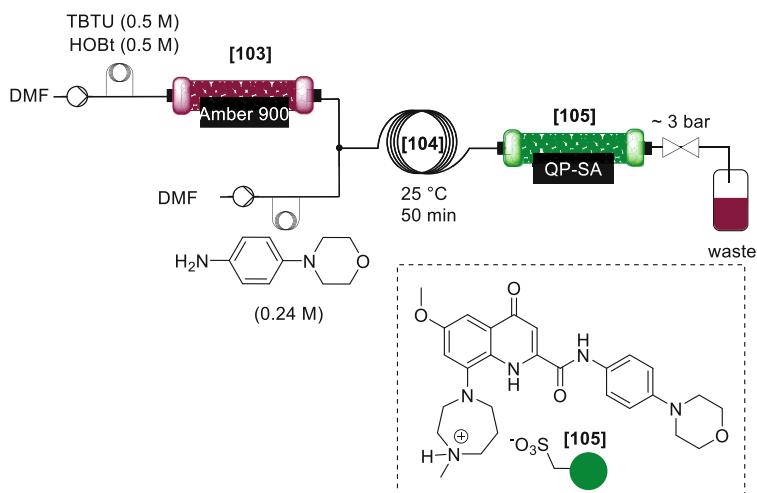


Fig. 31 Third stage of the continuous-flow process toward 5HT1B antagonist **104** [34]

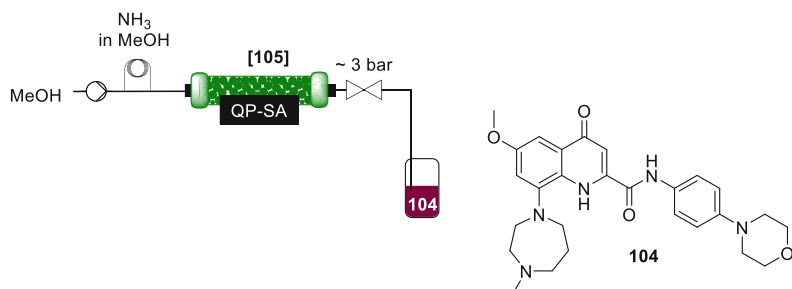


Fig. 32 Fourth stage of the continuous-flow process toward 5HT1B antagonist **104** [34]

afford methyl ester **102**. The reactor effluent was next cooled to room temperature, and mixed with a stream of THF-H₂O (30:1). The resulting combined stream was then passed through a glass column packed with Ambersep 900 hydroxide form for ester hydrolysis. The resulting carboxylate **103** was retained within the basic resin column. The entire reactor setup was operated with a downstream counter-pressure of ~17 bar.

The loaded Ambersep 900 hydroxide cartridge was next inserted in last stage setup (Fig. 31), which involved an amide coupling using TBTU as coupling reagent, and featured a “catch-and-release” purification. A feed solution containing *O*-(benzotriazol-1-yl)-*N,N,N',N'*-tetramethyluronium tetrafluoroborate (TBTU; 0.5 M, 2.5 equiv.) and 1-hydroxybenzotriazole (HOBt; 0.5 M, 2.5 equiv.) in DMF was pumped through the column containing carboxylate **103**. The procedure led to both activation and release of carboxylate **103**, and the effluent was directly mixed with a second stream of 4-morpholinoaniline in DMF (0.24 M, 1.2 equiv.). The mixture was reacted in a PFA coil reactor (10 mL volume) operated at room temperature with

a residence time of 50 min. The reactor effluent was next passed through a glass column loaded with Quadrapure-sulfonic acid (QP-SA) that scavenged the desired product **104** (Fig. 31).

Compound **104** was finally released in a final step by passing a methanolic solution of ammonia (2.0 M), and collected in a batch vessel (Fig. 32). Further downstream processing involved concentrated under vacuum and recrystallization, yielding **104** in an 18% overall yield (98% purity).

[δ -opioid receptor agonist] Ley and colleagues reported a continuous-flow synthesis of *N,N*-diethyl-4-(3-fluorophenyl)piperidin-4-ylidenemethyl)benzamide (**111**), a potent δ -opioid receptor agonist developed by AstraZeneca [35]. The process relied on a sequence of flow-based microreactors, with integrated purification and analytical protocols (Fig. 33). The four stage continuous-flow sequence was implemented in a commercial Vapourtec R2+/R4 reactor. Reactions were first optimized individually, and an incremental complexity through reaction telescoping was next envisioned.

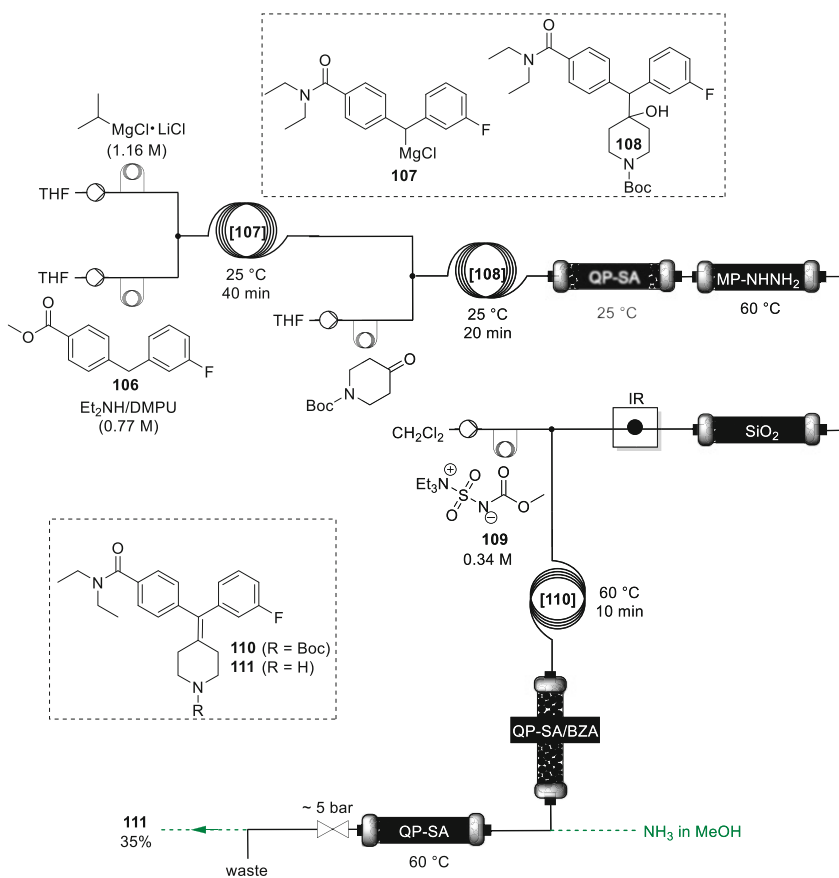


Fig. 33 Continuous-flow preparation of δ -opioid receptor agonist **111** [35]

The first stage involved mixing a stream of *i*PrMgCl·LiCl (1.16 M, 2.0 equiv., in THF) and a stream containing a mixture of diethylamine (2.5 equiv.) and ester **106** (0.77 M, 1.0 equiv. in THF with 1,3-dimethyl-3,4,5,6-tetrahydro-2(1H)-pyrimidinone as co-solvent) through a static T-mixer. The resulting mixture was then reacted in a PFA coil (10 mL internal volume) operated at 25°C and with 40 min of residence time. The reaction mixture was next reacted with a stream of 1-Boc-4-piperidone (1.2 equiv.) for 20 min at room temperature in a second PFA coil (10 mL internal volume). The reactor effluent was redirected through a series of three glass columns, packed with Quadrapure-sulfonic acid (QP-SA), polystyrene sulfonyl hydrazide resin (MP-TsNHNH₂, operated at 60°C) and silica, respectively, to combine both quench and work-up of the reactor effluent. Compound **108** could be obtained in 50% after purification by column chromatography. In the fully telescoped flow assembly, an in-line IR spectrometer (ReactIR) was strategically inserted just between the first and the second stage. The second stage involved the dehydration of intermediate **108** using Burgess' reagent (**109**). The reactor effluent of the previous step was mixed with a stream containing Burgess' reagent (0.34 M, 6.0 equiv.) in CH₂Cl₂ and a stream containing intermediate **108** (0.5 M, 1.0 equiv.) through a static T-mixer, and then reacted in a PFA coil (10 mL internal volume) operated at 60°C. The reactor effluent was next passed through a column loaded with a mixture of QP-SA and Quadrapure-benzylamine (QP-BZA) to scavenge the excess reagent **109** and its by-products, providing alkene **110** (99% yield after evaporation of the solvent). The reactor effluent containing **110** was next passed through a heated column (60°C) of QP-SA for the final Boc-deprotection. Amine **111** was released from the acid resin by elution with a solution of ammonia in MeOH (2.0 M) at room temperature in the fourth stage. The desired product **111** was obtained in 92% yield after off-line processing.

2.4.4 Anti-seizure Compounds

[Rufinamide] Jamison reported a convergent continuous procedure for the preparation of anti-seizure medication rufinamide (**114**, Banzel or Inovelon) [36]. The authors used a pivotal copper-catalyzed [3 + 2] cycloaddition of azide **112** and propiolamide (**113**), the preparation of which was fully integrated without isolation of either intermediates (Fig. 34). The starting reagents, including 2-(bromomethyl)-1,3-difluorobenzene and methyl propiolate, are commercially available. Each of the individual steps was optimized independently, and then fully telescoped. The microfluidic setup was constructed from PFA capillaries, copper tubing and standard HPLC connectors. The first step involved the synthesis of 2,6-difluorobenzylazide (**112**) through a S_N2 substitution of 2-(bromomethyl)-1,3-difluorobenzene with sodium azide in DMSO. The reaction reached completion within 1 min of residence time at room temperature. The other upstream branch of the convergent process concerned the preparation of propiolamide (**113**) from methyl propiolate and aqueous ammonia. The reaction reached 95% conversion with 6 equiv. of ammonia at 0°C within 5 min of residence time. Both flows containing **112** and **113** were

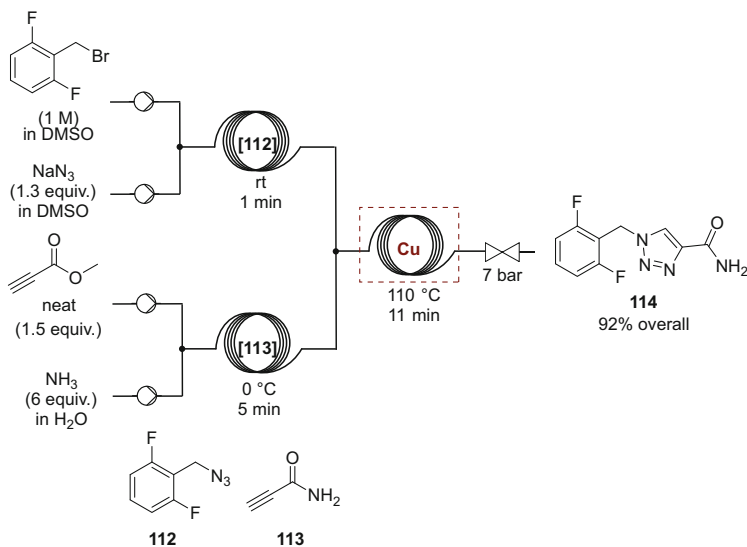


Fig. 34 Telescoped continuous-flow process for rufinamide (**114**) [36]

combined through a static T-mixer, and reacted at elevated temperature (110 °C) in a copper coil reactor for a residence time of 11 min (100 psi). Rufinamide (**114**) was obtained accordingly in 92% overall yield.

2.4.5 Neurodegenerative Diseases

[LY2886721] Researchers with Eli Lilly reported the implementation of a pilot-scale continuous amide bond formation and reactive crystallization to afford LY2886721 (**117**) [37]. LY2886721 is a potent and selective inhibitor of beta-amyloid cleaving enzyme (BACE), with potential applications as treatment for Alzheimer's disease, but the clinical development of LY2886721 was halted in Phase 2 due to its toxicity. Acid chloride **115** is unstable and challenging to isolate; the authors therefore opted for its in situ preparation under continuous-flow conditions (Fig. 35). The preparation of **115** involved the reaction of 5-fluoropicolinic acid with oxalyl chloride in the presence of DMF; while alternative amide coupling strategies were tested, the oxalyl chloride/DMF procedure remained the most efficient. Two alternative addition procedures were tested. The addition of oxalyl chloride to a slurry of 5-fluoropicolinic acid in the presence of DMF_{cat} proceeded with high conversion and selectivity, but the authors noticed coloration of the feed solution upon extended storage. As an alternative, a reverse addition procedure was envisioned: the stoichiometric generation of Vilsmeier's reagent (VR), followed by addition of 5-fluoropicolinic acid gave reaction mixtures with less colored impurities that were stable at 0 °C for several weeks without substantial decrease in potency. However, despite promising results,

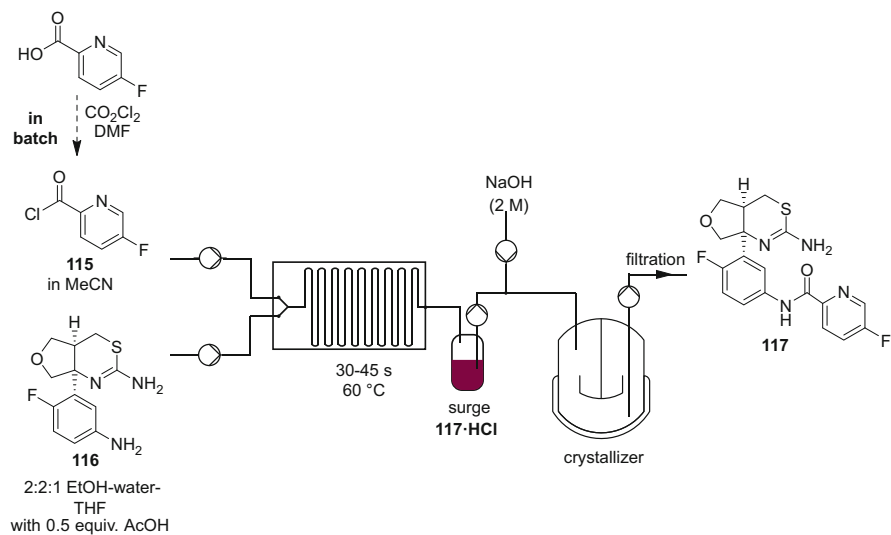


Fig. 35 Continuous-flow preparation of LY2886721 [37]

the poor solubility of 5-fluoropicolinic acid precluded the direct implementation of its activation under continuous-flow conditions.

Acyl chloride **115** was prepared in batch in acetonitrile, and the crude solution was used as a feed for coupling with diamine **116** under continuous-flow. The authors considered a glass microfluidic chip for the preliminary optimization phase. A critical aspect of the research inherently came from the low solubility of **117·HCl** in the reactor effluent, which would eventually crystallize and clog the chip. Attempts to improve the solubility of the salt through additional solvent failed, while an increase in temperature succeeded: above 60 °C, **117·HCl** was fully soluble. The optimum for the residence time was established at 30–45 s to ensure both high conversion and avoid product crystallization. Careful selection of the pumps, reactors, and auxiliaries with resistant wetted inner parts was mandatory to avoid corrosion upon exposure to both the reagents and products. The authors next studied the direct recrystallization of the reactor effluent in a CSTR-type setup. Since the bioavailability was impacted by the particle size, much development was focused on providing non-agglomerated crystals with a size less than 200 μm . The process was then progressively scaled up to production rates of 1 and 10 kg day^{-1} .

2.4.6 Stimulants

[Methylphenidate] A joint research program between the University of Liège and Corning Reactor Technologies aimed at demonstrating the continuous-flow preparation of methylphenidate (**124**, Ritalin), the most widely prescribed stimulant medication for the treatment of attention deficit hyperactivity disorder (ADHD)

[38]. Two strategies were implemented and telescoped, and both relied on the generation and consumption of hazardous diazo compounds (Figs. 36 and 37). The first strategy, namely, the intermolecular strategy, involved the generation of a hazardous organic azide, which was consumed in a diazo transfer reaction with methyl 2-phenylacetate to generate methyl phenyldiazoacetate (**119**). Compound **119** was then utilized in a Rh(II)-catalyzed C-H insertion reaction with *N*-Boc piperidine to generate *N*-Boc methylphenidate (**120**). At first, the critical diazo transfer reaction was optimized in batch, and the combination of tosyl azide (**118**) as diazo donor, DBU as base and NMP as solvent afforded the best results. The reaction was then implemented in a continuous-flow reactor. Then, the preparation

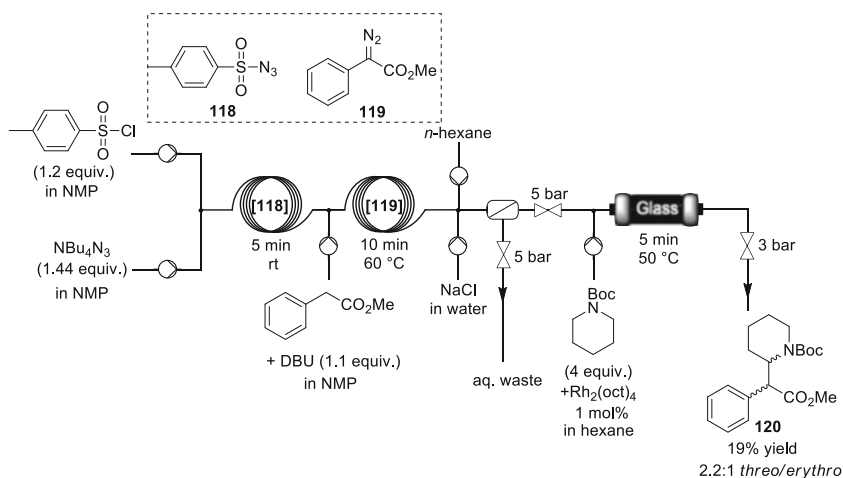


Fig. 36 Telescoped intermolecular continuous-flow strategy toward methylphenidate [38]

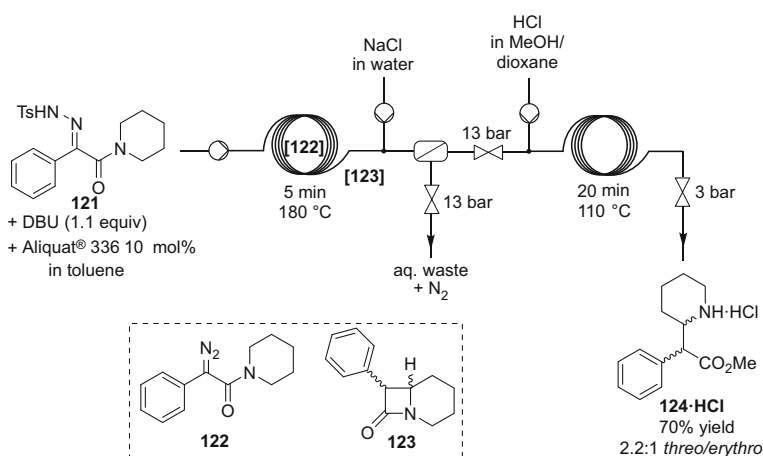


Fig. 37 Telescoped intramolecular continuous-flow strategy toward methylphenidate [38]

of tosyl azide (**118**) from tosyl chloride and tetrabutylammonium azide was implemented in a flow reactor, and telescoped to the continuous diazo transfer reaction. Crude diazo **119** was extracted from NMP by concomitant injection of *n*-hexane and an aqueous NaCl solution downstream the reactor, and the biphasic mixture was directed toward an in-line liquid–liquid extraction device. The target diazo compound **119** was obtained with 77% yield and 88% purity. Several catalysts were screened in batch for the C-H insertion of **119** into *N*-protected piperidine, and $\text{Rh}_2(\text{oct})_4$ afforded the best results. The C-H insertion step was implemented under continuous-flow-conditions using a column packed with glass beads, and *N*-Boc methylphenidate (**120**) was obtained in 38% yield, with a 2.2:1 d.r. in favor of the *threo*-isomers. The continuous C-H insertion was ultimately telescoped to the previous steps and afforded **120** in 19% isolated yield. The material finally underwent deprotection into **124**·HCl either in batch or under continuous-flow conditions, with full retention of stereochemistry and in quantitative yield (not shown).

An alternative strategy, namely, the intramolecular route, involved the thermal or photochemical decomposition of tosylhydrazone **121**, leading to transient diazo species **122** (Fig. 37). Compound **122** then underwent intramolecular C-H insertion to afford **123**. β -lactam **123** was then methanolized under acidic conditions to afford methylphenidate hydrochloride (**124**·HCl). One of the main challenges of the intramolecular route was to prepare a homogeneous feed solution of tosylhydrazone **121** due to its low solubility in most organic solvents. After a preliminary screening of several bases and solvents, it appeared that DBU and toluene were the most efficient to prepare a homogeneous concentrated feed of **121**, using Aliquat[®] 336 as stabilizing agent. The solution of **121** was then either thermolyzed or photolyzed in a PFA coil. The thermal process afforded β -lactam intermediate **123** within 5 min of residence time at 180°C, while the continuous photoreaction required 60 min to reach completion. An in-line membrane separator was implemented downstream to remove water-soluble impurities and nitrogen gas, and the crude material was then methanolized in the presence of HCl in a second PFA coil at 110°C. Methylphenidate hydrochloride was obtained in 70% yield overall, with a 2.2:1 *threo/erythro* ratio. A simple recrystallization in batch (off-line) enabled to selectively recover *threo*-**124**·HCl. The microfluidic process sustained a daily productivity of ~1,400 doses of *threo*-methylphenidate hydrochloride. The critical thermal intramolecular C-H insertion reaction was next implemented in a pilot-scale continuous-flow reactor (36 mL internal volume), which sustained a daily productivity of 4.25 kg for intermediate **123**.

2.5 Hypertension and Cardiovascular Diseases

[Telmisartan] Gupton and colleagues reported a continuous-flow synthesis for the preparation of telmisartan (**128**), the active ingredient in the antihypertensive drug Micardis [39]. The authors developed a convergent strategy that required neither

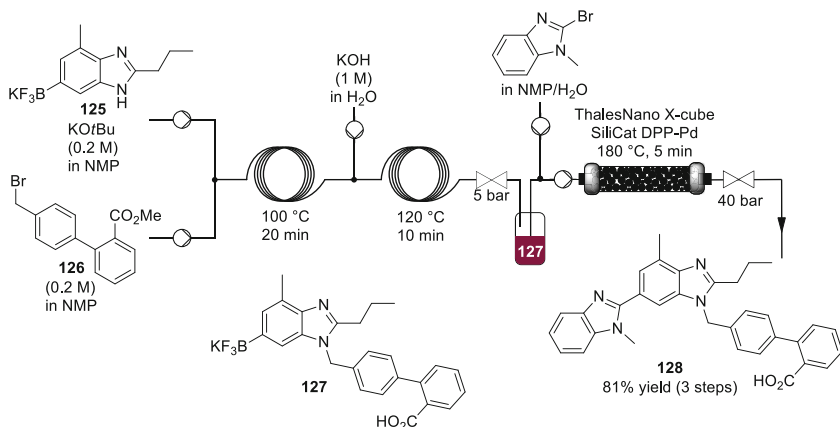


Fig. 38 Continuous-flow preparation of telmisartan (**128**) [39]

intermediate purifications nor solvent exchanges. It relied on a Suzuki cross-coupling reaction between two functionalized benzimidazoles catalyzed by a solid-supported Pd catalyst. The sequence combined an alkylation and an ester hydrolysis that were performed in a Vapourtec E-Series system with two 10 mL TFA reactor coils (Fig. 38). In the first reactor coil, benzimidazole **125** was reacted with benzyl bromide **126** in the presence of potassium tert-butoxide in NMP, at 100 °C for a residence time of 20 min. The reactor effluent was next mixed with potassium hydroxide in water (excess) and reacted into the second reactor coil at 120 °C for a residence time of 10 min under 5 bar of counter-pressure, resulting in complete hydrolysis of the methyl ester. A total conversion of 97% was noticed for these two reactions, and the reactor effluent was collected in a surge. The raw reactor effluent was mixed with a solution containing 1.2 equivalents of 2-bromo-1-methylbenzimidazole in 1:1 NMP- H_2O , and the reaction mixture was sent to a ThalesNano X-Cube flow reactor, equipped with a SiliCat[®] DPP-Pd CatCart. The optimized conditions involved a residence time of 5 min under 180 °C and 40 bar of pressure. Telmisartan (**128**) was isolated in 81% yield.

2.6 Anesthetics and Analgesics

2.6.1 Anesthetics

[Bupivacaine, mepivacaine, ropivacaine] Kappe et al. reported a convenient, fast and high-yielding method for the generation of the racemic amide anesthetics bupivacaine (**130**, Marcaine), mepivacaine (**131**, Carbocaine), and ropivacaine (**132**, Naropin) [40]. The preparation of the key intermediate 2',6'-picolinoylidide (**129**) was carried out in a closed MW vessel. The latter was subsequently engaged into a continuous-flow high-pressure hydrogenator (H-Cube Pro[™]) in the presence

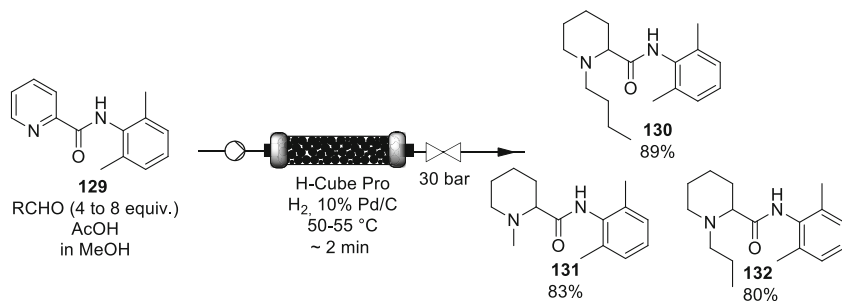


Fig. 39 Continuous-flow preparation of bupivacaine, mepivacaine, and ropivacaine [40]

of an aldehyde. Both the hydrogenation of the pyridine ring and a reductive amination were carried out, providing a robust continuous-flow integrated procedure for the preparation of the final amide anesthetics as racemic mixtures (Fig. 39). The authors first studied the hydrogenation of **129** (feed solution in methanol) with a 70 mm cartridge containing 10% Pd/C as a catalyst. Complete reduction was noticed at 50°C under 50 bar of H₂, although competitive methylation occurred to a certain extent (up to 37% mepivacaine (**131**) as contaminant). Upon optimization, the authors telescoped the reduction of the pyridine ring to the reductive amination of the newly formed piperidyl fragment. A feed solution containing **129** (0.01 M) as well as formaldehyde, propanal or butanal (4–8 equiv.) in methanol/AcOH 3:1 was pumped into the hydrogenation reactor. In the presence of formaldehyde, the authors were confronted to a rapid catalyst deactivation, and further optimization revealed that decreasing the amount of AcOH to 1 M at a reaction temperature of 50°C increased the catalyst stability (as well as the selectivity to *rac*-mepivacaine (**131**), up to 97%). The reaction conditions were then applied to the synthesis of *rac*-ropivacaine (**132**, with propanal, 92% selectivity) and to *rac*-bupivacaine (**130**, with butanal, 75% selectivity). Increasing the temperature to 55°C finally increased the selectivity toward bupivacaine to 95%. Leaching of palladium from the catalyst bed remained negligible, even after 8 h of operation.

2.6.2 Analgesics

[Noroxymorphone] Noroxymorphone (**136**) is an important intermediate in the synthesis of several opioid antagonists and a potent agonist of the μ -opioid receptor that has minimal analgesic activity. Kappe and coworkers studied the transformation of 14-hydroxymorphinone (**133**) into **136** in a continuous-flow reactor [41, 42]. The sequence of reactions involved subsequent *N*-demethylation and alkene hydrogenation reactions starting from **133** (Fig. 40). *N*-Methyl group removal was first optimized in batch in the presence of a Pd⁰ or Pt⁰ catalyst and molecular oxygen as oxidant. Under such conditions, *N*-methyl oxidation of the substrate afforded the corresponding 1,3-oxazolidine **134** in high yield, in particular when the reaction was

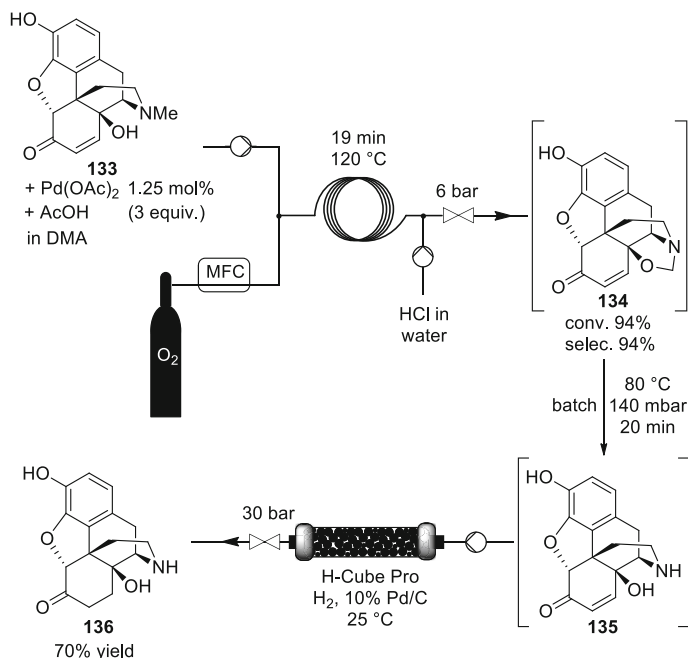


Fig. 40 Continuous-flow preparation of noroxymorphone (**136**) [41]

conducted in aprotic polar solvents such as DMA or DMSO. Similar results were obtained when Pd⁰ nanoparticles were generated in situ by heating a solution of Pd(OAc)₂ in DMA/AcOH. Direct hydrogenation of the alkene moiety was attempted by replacing the O₂ supply with a H₂ supply mounted on the batch reactor. However, instead of C=C reduction, hydrogenolysis of the oxazolidine ring occurred, leading back to **133**.

The authors therefore performed the hydrolysis of the oxazolidine ring prior to the alkene reduction, and a straightforward one-pot subsequent oxidation/hydrolysis was implemented. The hydrolysis was conducted by diluting the reaction medium with HCl and heating the whole mixture at 80 °C under reduced pressure (140 mbar). This procedure accordingly afforded the hydrolysis product **135** in high yield. Finally, noroxymorphone (**136**) was obtained in 70% yield by injecting the crude obtained from the oxidation/hydrolysis one-pot process into a Thales H-Cube Pro continuous-flow reactor equipped with a catalyst cartridge packed with 10% Pd/C and operated at 25 °C and 30 bar in the presence of H₂. The procedure was next transposed under continuous-flow conditions. Preliminary optimization of the methyl oxidation step in the presence of O₂ over Pt/C or Pd/Al₂O₃ packed in a column indicated leaching of the catalyst, and thus poor stability, as well as poor carbon balance. In an alternative procedure, a feed solution containing **133** and Pd(OAc)₂ in AcOH/DMA was mixed with oxygen and reacted in a FEP pressurized tube flow reactor. HCl was injected downstream the reactor before entering the BPR

to avoid precipitation of **134** within the BPR. Excellent selectivity (94%) and conversion (94%) were obtained. Despite numerous attempts, the hydrolysis of **134** had to be conducted in batch. The final reduction was performed as described above. The target noroxymorphone (**136**) was obtained in 70% yield.

Another strategy was also considered, involving a sequence of (a) hydrogenation, (b) methyl oxidation, and (c) hydrolysis. Alkene reduction on **133** was effectively conducted over supported Pd/C under continuous-flow conditions. Then Pd⁰ species were generated in a second packed-bed continuous-flow reactor after the pretreatment of a supported Pd²⁺ catalyst with ethylene glycol, and the corresponding material was used for the subsequent oxidation step. However, leaching of Pd was again evidenced, despite elevated conversion and selectivity (>95%). Pd⁰ species were then generated in situ from Pd(OAc)₂ upon heating, as previously, and used in a batch H₂-mediated reduction of **133**. Then, the crude mixture of reduced substrate and Pd⁰ species was directly reacted with O₂ in a pressurized FEP tube reactor. A moderate selectivity was observed.

2.7 Allergy

[Buclizine, cinnarizine, cyclizine] Noël and Hessel developed a four-step continuous process for the preparation of antihistamines, including buclizine (**137**), cinnarizine (**139**), and cyclizine (**138**), starting from bulk alcohols (Fig. 41) [43]. Intermediate chlorides were generated under continuous-flow by reacting alcohols and HCl (3 equiv.), within short reaction time (15 min, 120°C) and excellent yields. The microfluidic assembly was constructed from PFA capillaries and standard HPLC connectors (Fig. 42). The appropriate intermediate chloride was next reacted with piperazine. For instance, the preparation of cyclizine involved a linear two-step continuous-flow process with the chlorination of diphenylmethanol (100°C, 10 min), followed by a nucleophilic substitution with *N*-methylpiperazine (100°C, 45 min), yielding cyclizine (**138**) in 94% yield. The preparation of cinnarizine (**139**) is detailed below. Very much alike for the preparation of cyclizine, 1-diphenylmethyl piperazine (**142**) was prepared in the first section of microfluidic assembly. The first step involved the chlorination of diphenylmethanol (3.1 M in acetone) at 100°C (~7 bar), yielding chlorodiphenylmethane (**140**) in 97% with 10 min of residence time. The reactor

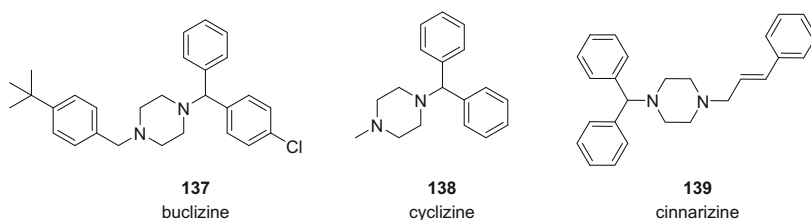


Fig. 41 Structures of buclizine, cinnarizine, and cyclizine

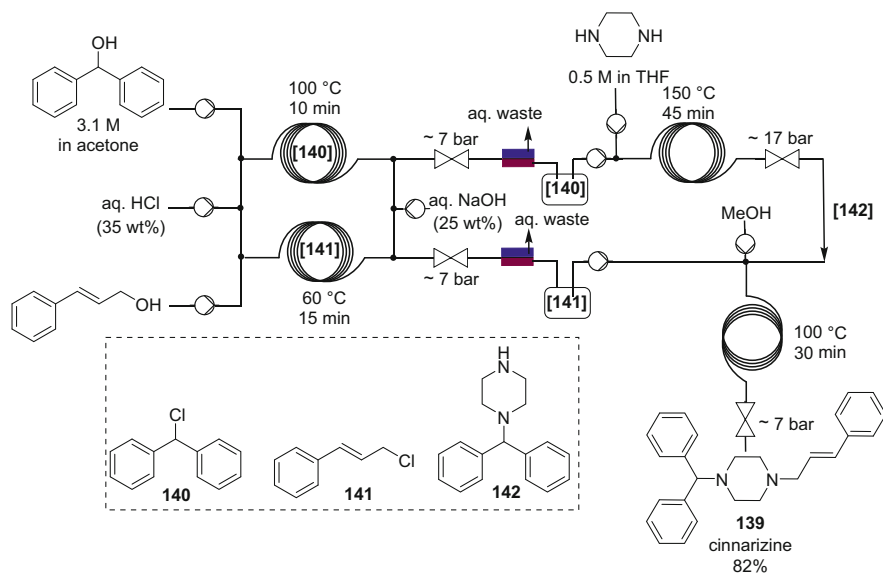


Fig. 42 Telescoped continuous-flow preparation of cinnarizine (**139**) [43]

effluent was neutralized with aqueous sodium hydroxide, and the biphasic mixture was separated through a liquid–liquid membrane separator. The organic stream was redirected to a surge, and then reinjected for reaction with piperazine. Full conversion with 92% selectivity toward 1-(diphenylmethyl)piperazine (**142**) was observed at 150 °C with 45 min of residence time and 1.5 equivalents of piperazine.

At this point, intermediate **142** was redirected to the convergent section of the microfluidic assembly, and was mixed with methanol and with cinnamyl chloride (**141**). Cinnamyl chloride was prepared upstream, in another linear microfluidic assembly starting from cinnamyl alcohol. At 100 °C and 30 min of residence time, full conversion of **142** was observed. MeOH was used for the recrystallization of cinnarizine (off-line, batch). Overall isolated yields for cinnarizine, cyclizine, and a buclizine derivative are 82%, 94%, and 87%, respectively. The total residence time for the four steps is 90 min with a productivity of 2 mmol h⁻¹.

2.8 Inflammation

[Fanetizole] Reactor setups based in the semipermeable Teflon AF-2400 membrane (copolymer of tetrafluoroethene and perfluorodimethyldioxolane) have been successfully utilized under continuous-flow conditions with several commonly used reactive gases (O₃, O₂, H₂, CO, CO₂, C₂H₄). A typical tube-in-tube reactor setup consists of two concentric capillaries: an inner Teflon AF-2400 tubing embedded in a larger PTFE outer tube. Two operation modes are usually reported: (a) the carrier

solvent is circulated in the larger PTFE tube, while the gaseous reagent is circulated in the porous inner Teflon AF-2400 tubing, or, the opposite, (b) with the gaseous reagent in the PTFE tubing and the liquid stream in the inner Teflon AF-2400 tubing. Report was made by Ley and coworkers for the development of a tube-in-tube reactor based on a semipermeable polymer membrane for the transfer of ammonia gas into liquid flow streams [44]. The setup was conveniently utilized for the preparation and scaling-up process affording alkyl thioureas, including the preparation of anti-inflammatory agent fanetizole (**144**, Fig. 43). The procedure was amenable on a multigram scale. The authors first optimized the delivery of ammonia, and succeeded in developing a system sustaining a stable and reproducible concentration of ammonia over long production campaigns. The authors started to optimize the addition of ammonia to 2-phenylethyl isothiocyanate for the preparation of the corresponding thiourea **143**. The feed solution containing 2-phenylethyl isothiocyanate was fed with ammonia gas through a tube-in-tube reactor setup at 0°C. The gassed liquid stream was next sent to an additional reactor coil (PFA, 10 mL) at 100°C. A BPR (6 bar) was placed downstream to keep ammonia in solution. Full conversion to the corresponding thiourea **143** was obtained with an isothiocyanate concentration of up to 1.2 M in DME and 1.6 M in MeOH. Upon optimization, the authors used the procedure for the preparation of fanetizole (**144**). The reactor effluent from the first reactor containing thiourea **143** was combined through a static Y-mixer with a stream of 3-bromoacetophenone (3:1:1 DME/water/DMF), and reacted at 100°C in another PFA coil. Fanetizole (**144**) co-precipitated with its hydrobromide (**144**·HBr) from the crude reactor effluent in the collection flask upon cooling, affording 99% combined yield (output 10 g h⁻¹).

[Grossamide] Grossamide (**148**) is a natural product belonging to the lignanamide family, a class of compounds that regulates biological functions in plants and microorganisms. Grossamide has also potential anti-inflammatory properties. Ley and coworkers prepared grossamide using a continuous-flow reactor featuring solid-

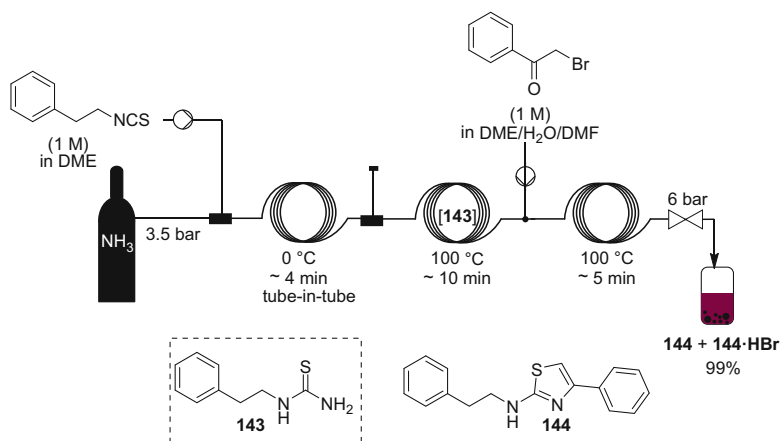


Fig. 43 Continuous-flow preparation of fanetizole (**144**) [44]

supported reagents [45]. A solution of ferrulic acid (**145**) in the presence of PyBroP and DIPEA was injected into a column packed with PS-supported hydroxybenzotriazole (PS-BtOH), to immobilize the corresponding activated ester (Fig. 44). Then, injection of tyramine (**146**) in THF eluted the corresponding amide after coupling, and the reaction was monitored by in-line UV-Vis. The reactor effluent containing amide **147** was next passed through a column packed with PS-supported sulfonic acid (PS-SA) to scavenge the excess tyramine. Most notably, multiple columns were utilized in parallel, to enable simultaneous activation of the carboxylic acid while the ester is consumed by tyramine, and to regenerate sulfonic acid with TEA while the excess tyramine is scavenged. This configuration enabled continuous processing without the usual interruption to regenerate the supported reagents. The effluent was then mixed with a stream of H₂O₂ and urea (phosphate buffer, pH 4.5), and finally eluted through a column packed with an immobilized horseradish peroxidase (HP). Oxidative dimerization and intramolecular cyclization occurred accordingly, affording **148**. The reaction was monitored by automatic sampling and LC-MS analysis.

[Rolipram] Kobayashi and colleagues reported the continuous-flow synthesis of (*R*)- and (*S*)-rolipram (**153**), an anti-inflammatory drug and one of the family of γ -aminobutyric acid (GABA) derivatives [46]. The authors designed a conceptually simple, yet very efficient, system using only columns packed with heterogeneous catalysts (Fig. 45). Commercially available starting materials were successively passed through four columns containing achiral and chiral heterogeneous catalysts to produce either (*S*)- or (*R*)-**153**. Eight-step steps in total were conducted without isolation of any intermediates and without the separation of any catalysts, co-products, by-products, and excess reagents. The various reactions were first

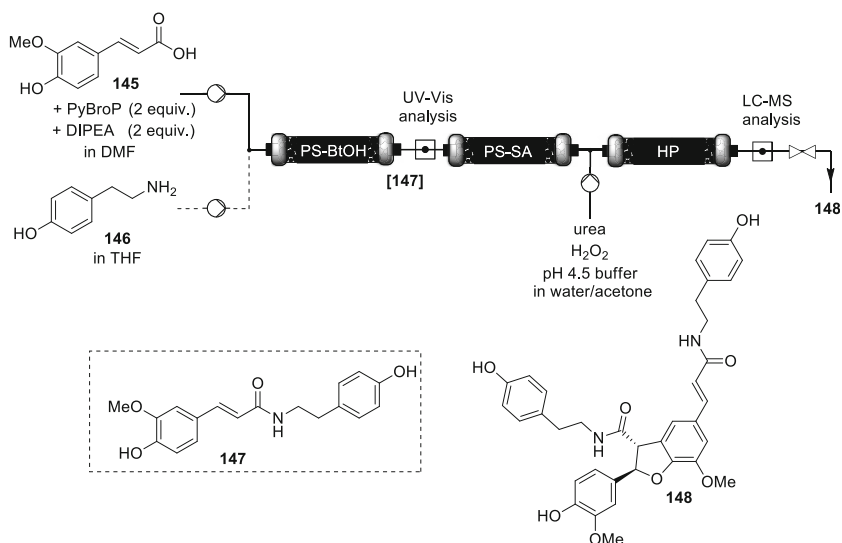


Fig. 44 Continuous-flow preparation of grossamide [45]

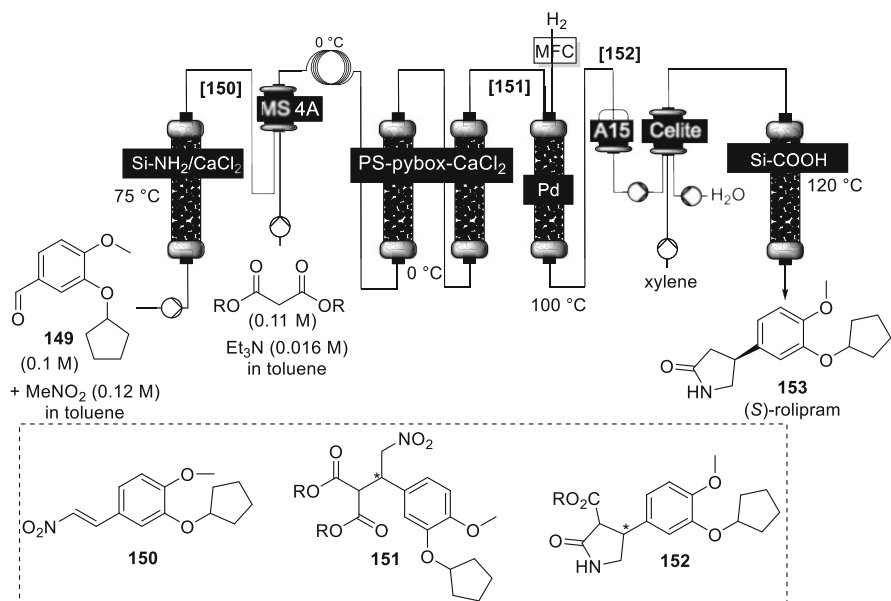


Fig. 45 Multistep continuous-flow process toward rolipram [46]

optimized individually, and next telescoped within an uninterrupted reactor network that consisted of four different modules fluidically connected in series with multiway valves. These modules were dedicated to specific chemical operations: (a) preparation of nitroalkene intermediate **150**, (b) asymmetric 1,4-addition system to **151**, (c) reduction of **151** toward **152**, and (d) decarboxylation of **152** toward **153**. The authors first optimized the preparation of nitroolefin **150** from advanced intermediate **149** and nitromethane in toluene. The best results (90% yield) were obtained with silica-supported amine mixed with anhydrous calcium chloride and packed in a SS column operated at 50–75 °C. The next step involved the asymmetric 1,4-addition of dimethyl malonate to **150** using a chiral heterogeneous catalyst. The reaction mixture entering the second module was precooled at 0 °C using a loop, then entered two columns fluidically connected in series and each packed with PS-(S)-pybox, CaCl₂·2H₂O and Celite. The crude reactor effluent after module 2 contained mainly intermediate **151** as well as small amounts of nitromethane, dimethyl malonate, and triethylamine. During the optimization phase, the crude was quenched with ammonium chloride, and processed in batch, yielding nitroester **151** in 84% yield (94% ee).

The procedure was amenable to other aldehydes than **149**. The next step involved the reduction of the nitro group. Hydrogen gas was mixed with a solution of **151** in toluene, and the heterogeneous mixture was passed through a column packed with a polysilane supported palladium/carbon heterogeneous catalyst mixed with celite. At 100 °C under atmospheric pressure, the reduction proceeded well and afforded γ -lactam **152** with 74% yield (94% e.e.). The reactor effluent from the third module was passed through a small column packed with Amberlyst 15Dry, then combined

with *o*-xylene and water and passed through a column packed with Celite, before entering the last module.

The last step involved the hydrolysis and decarboxylation of **152** that proceeded upon contact with a silica-supported carboxylic acid (Si-COOH) at 120°C. (*S*)-Rolipram was obtained in 50% yield from **149** after preparative thin layer chromatography (~1 g day⁻¹ output, 96% e.e.). The flow system could be operated for at least 1 week. Further recrystallization from water/methyl alcohol gave optically pure (*S*)-rolipram. (*R*)-Rolipram was obtained similarly, by simply changing PS-(*S*)-pybox-calcium chloride with its PS-(*R*)-pybox-calcium chloride enantiomer. A similar productivity was achieved, and (*R*)-rolipram was obtained in 50% yield (96% e.e.) from intermediate **149**, and the product contained negligible traces of Pd (>0.01 ppm). The system was also successfully tested for the preparation of other GABA derivatives.

The same year, Seeberger and coworkers designed a chemical assembly system that incorporated five interchangeable modules for the continuous-flow multistep manufacturing of biologically relevant compounds, including rolipram (**153**, Fig. 46) [47].

The specific setup for the preparation of **153** is detailed here above. Module 1 performed a biphasic TEMPO/bleach-mediated oxidation of **154** toward aldehyde **149**, with subsequent in-line liquid–liquid separation. Module 2 was dedicated to an olefination reaction. For accessing **153**, a Horner-Wadsworth-Emmons reaction was implemented to transform aldehyde **149** into olefin **155**. Module 2 also included an

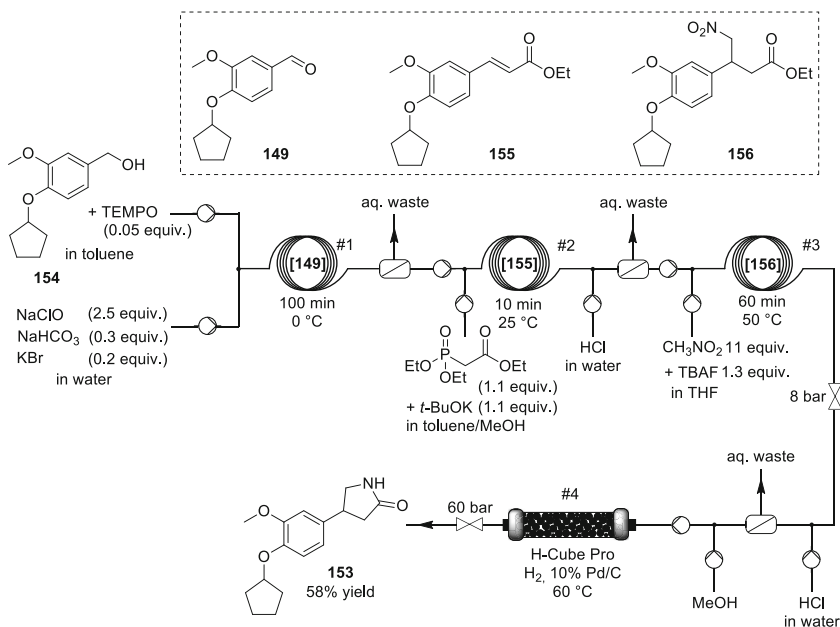


Fig. 46 Multistep continuous-flow process toward rolipram [47]

acidic aqueous quench, followed by in-line liquid–liquid extraction. Module 3 was dedicated to the TBAF-mediated Michael addition of nitromethane onto **155**, giving nitro ester **156**. Again, it included acidic in-line work-up and extraction for the removal of water-soluble impurities. Lastly, a catalytic hydrogenation was implemented in Module 4, which actually consisted in flowing a solution of **156** through a commercially available continuous-flow hydrogenator (H-Cube) equipped with a cartridge packed with 10% Pd/C and operated at 60°C (60 bar). Rolipram was obtained in 58% yield with a productivity of 11.8 g day⁻¹. Additional modules were available, and various combinations made the procedure amenable to β - and γ -amino acids as well as γ -lactams.

2.9 Miscellaneous

[Atropine] Jamison and colleagues reported the multistep synthesis and purification of atropine (**159**) in a continuous-flow reactor (Fig. 47) [48]. Atropine is mostly utilized as an antidote to certain types of nerve agent and pesticide poisonings, as well as to treat some cardiac conditions. The authors first assessed the phenylacetyl chloride esterification of tropine (**157**) under batch conditions, and realized that both the alcohol and the tertiary amine of **157** were reactive toward phenylacetyl chloride. To alleviate this issue, utilization of tropine hydrochloride (**157**·HCl) was considered, and the esterification step could be efficiently implemented in flow. Next, various formaldehyde sources and bases were screened for the hydroxymethylation step, and aqueous CH₂O (37%) in the presence of NaOH were identified as the most efficient reagents for the transformation toward **159**. Careful continuous-flow optimization of the conditions was performed to minimize elimination of the alcohol into

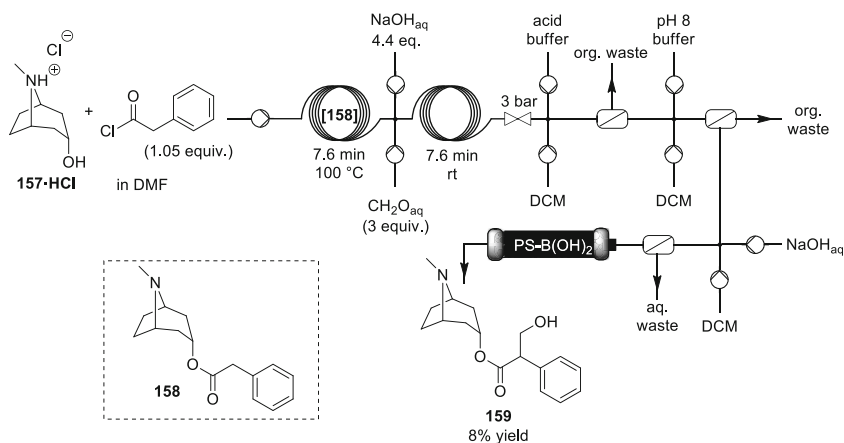


Fig. 47 Continuous-flow preparation of atropine, featuring a complex in-line extraction sequence [48]

the corresponding alkene. The esterification and hydroxymethylation steps were then telescoped, but the authors identified several by-products structurally similar to atropine (omitted for clarity). An advanced in-line purification process, based on pKa difference of impurities, was studied to selectively extract atropine. Aqueous acid buffer and DCM were injected downstream the reactor, and the biphasic mixture was subjected to in-line liquid–liquid extraction.

The pH of the aqueous effluent of the first separator, containing atropine hydrochloride (**159**·HCl), was adjusted to pH 8 and extracted with DCM. The resulting biphasic mixture was subjected to another in-line liquid–liquid extraction. The aqueous effluent of the second separator, containing atropine hydrochloride (**159**·HCl), was then combined with a stream of DCM and aqueous NaOH, and again subjected to in-line liquid–liquid extraction. Atropine free base (**159**) and other minor organic impurities were recovered in the organic stream. A final in-line purification consisted in passing the organic stream coming out the third separator through a column packed with a boronic acid resin. Atropine was isolated with an excellent purity (>98%), but a mere 8% overall yield.

The authors then reported an improvement of their original report [32], and the E-factor was accordingly dramatically reduced from 2,245 to 24, with an increase of 8–22% isolated yield. Most notably, utilization of two separated feedstocks in the first step enabled the utilization of neat phenylacetyl chloride and of a concentrated solution of tropine free base (**157**) in DMF. A decrease of the number of NaOH equivalents, injected before the second reactor, from 4.4 to 1.2 was also possible. Finally, the optimization of the purification steps using computational modelling revealed that DCM, used in the original report, was not the best option as extraction solvent. Atropine was isolated from its by-products by liquid–liquid extraction and phase separation based on pH adjustment, where toluene and an aqueous solution basified at pH 11 were conveyed to the setup, and **159** was recovered in the organic phase in 22% yield, with only 10% of impurities observed by NMR.

3 Multistep Continuous-Flow Processes Toward Advanced Heterocyclic Intermediates for API Manufacturing

This section gathers representative examples dealing with multistep continuous-flow preparation of advanced scaffolds that are pivotal intermediates for the preparation of heterocyclic active pharmaceutical compounds.

3.1 Chemotherapeutic Agents

[Akt kinase inhibitor] A research team with Merck developed a 17-step process toward allosteric Akt kinase inhibitor **163**, among which an early key transformation

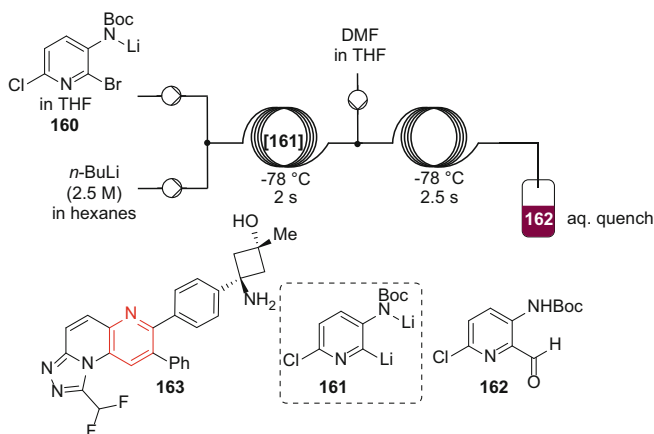


Fig. 48 Continuous-flow preparation of intermediate **162** (fragment of Akt kinase inhibitor **163**) [49]

toward pivotal intermediate **162** was developed under continuous-flow conditions (Fig. 48) [49]. It consisted of the formylation of dianion **161** derived by deprotonation and subsequent lithium-halogen exchange from 2-bromo-3-aminopyridine precursor **160**. The authors noted a much improved reaction yield and practicality under flow conditions by comparison with the batch process. The reaction was amenable on kilogram scale.

A feed solution containing a preformed anion **160** was mixed with *n*BuLi (2.5 M in hexanes) through a static T-mixer, and then reacted in SS coil reactor operated at $-78\text{ }^{\circ}\text{C}$ (2 s of residence time). The authors used peristaltic pumps with pressure gauges (PI) and polytetrafluoroethylene (PTFE) tubing for the feed lines. The reactor effluent containing dianion **161** was immediately mixed with a solution of DMF in THF through another static T-mixer, and reacted at $-78\text{ }^{\circ}\text{C}$ in another SS coil reactor (2.5 s of residence time). The reactor effluent was next transferred through PTFE tubing into an aqueous quench solution (acetic acid/*tert*-butyl methyl ether/water) in a glass batch vessel for quench. A yield of 85% for aldehyde **162** was reported, and lower amounts of side products were detected by comparison with the batch process.

[Bendamustine] Bendamustine (**167**, Treanda) was approved for the treatment of chronic lymphocytic leukemia (CLL) and indolent B-cell non-Hodgkin's lymphoma. A key step for its synthesis involves the formation of benzimidazole **166** through reduction of two aromatic nitro moieties of **164**, followed by subsequent nucleophilic addition of the *ortho*-amine onto the amide carbonyl. Finally, dehydration of intermediate **165** under acidic conditions led to **166**. The authors noted safety concerns upon scale-up, as well as the emergence of by-products due to poor mass and heat transfer in conventional batch reactors. Chen and colleagues studied the implementation of these key steps in a H-Cube continuous-flow hydrogenator. Upon optimization, the process was implemented in a pilot scale H-Cube midi flow reactor (Fig. 49) [50]. Catalyst optimization revealed that the Raney Ni performed better

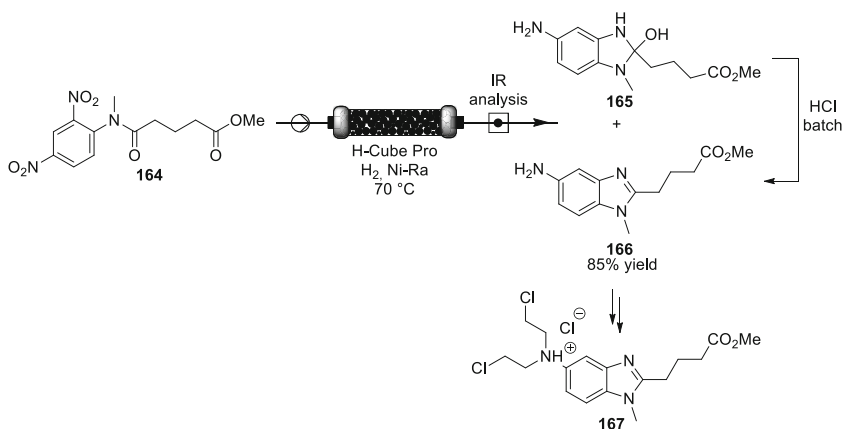


Fig. 49 Preparation of fragment **166** en route to bendamustine [50]

than Pd/C for the reduction of **164**. MeOH was selected as reaction solvent, despite the poor solubility of the substrate. Other solvents such as THF, methyl acetate and ethyl acetate triggered side-reactions. A two-level fractional factorial design was utilized to identify the best combination of parameters to reach the highest reaction yield possible. A mixture containing mainly alcohol **165** and traces of benzimidazole **166** was obtained in almost quantitative yield, and the reaction was then scaled up in a H-cube midi reactor. In-line IR analysis was implemented downstream for additional process control. Excellent results were obtained on the pilot scale as well, with 85% isolated yield after subsequent batch dehydration.

[Brivanib alaninate] The identification of a potential chemical runaway in the batch process triggered the development of a continuous-flow process to produce an important intermediate in the preparation of brivanib alaninate (**171**), an anti-tumorigenic drug for oral administration. The incriminated reaction is the exothermic conversion of a tertiary alcohol **168** to hydroxypyrrrolotriazine intermediate **170**. Without proper heat management, this transformation that requires hydrogen peroxide and a catalyst (hydrochloric acid in the preliminary experiments, or methanesulfonic acid in the optimized flow process) could eventually lead to a runaway upon scale-up. Laporte and colleagues with Bristol-Myers Squibb designed and engineered a continuous-flow reactor that enabled safer operation upon scale-up [51]. Reactor and process engineering were supported by a thorough mechanistic investigation. The sequence of reaction is complex, and involves the formation of intermediate hydroperoxide **169**, and its further rearrangement under acidic conditions. A lab scale continuous plug-flow reactor featuring two temperature operating regimes was developed, and designed both keeping in mind reaction heat and fast kinetics to minimize total reaction time (Fig. 50). The first section of the reactor, where the reaction produced the most heat, was operated below 0 °C. The second section of the reaction was operated at 12–15 °C to increase the reaction rate and

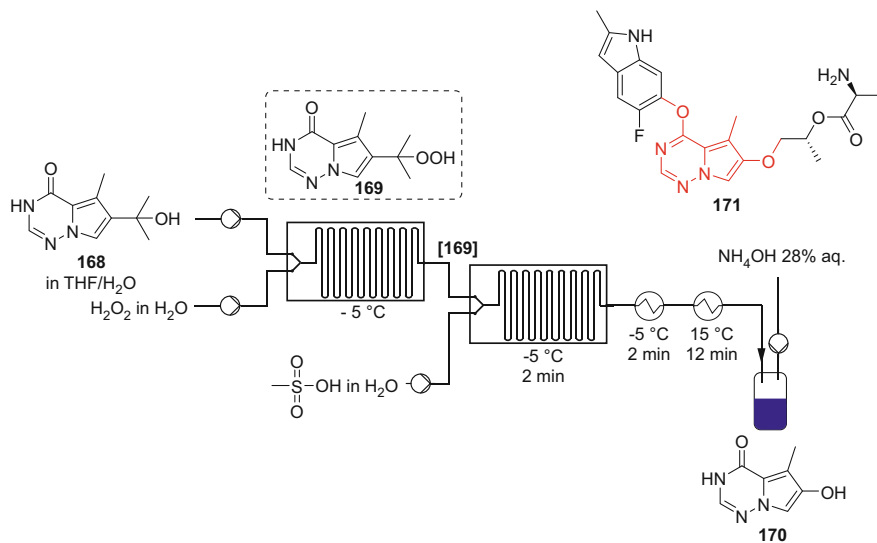


Fig. 50 Continuous-flow preparation of hydroxypyrrrolotriazine intermediate **170**, an important fragment for brivanib alaninate [51]

allow the reaction to reach completion. Three feed solutions were prepared, and maintained at rt.: (a) tertiary alcohol **168** in solution in THF/water, (b) hydrogen peroxide in water and (c) methanesulfonic acid in water. Feeds (a) and (b) were premixed in a first glass microreactor (Mikroglas, single T-mixer, ~1 mL internal volume) at -5°C , and the reactor effluent was next mixed with feed (c) and reacted in a second glass microreactor (Mikroglas, single T-mixer, ~1 mL internal volume) at -5°C . The reaction mixture was next passed through two successive heat exchangers operated at -5°C and 15°C , respectively, and finally collected in a batch tank with concomitant addition of 28% aqueous ammonium hydroxide under vigorous stirring. Upon optimization, the process was successively implemented under continuous-flow conditions in a kilo lab reactor (5.6 kg day^{-1} of starting material), then in a pilot plant reactor (22.4 kg day^{-1} of starting material) and eventually in a commercial reactor (44.8 kg day^{-1} of starting material). The process was demonstrated for up to 33 days of continuous operation.

[Eribulin mesylate] Eribulin mesylate (**176**) is an inhibitor of microtubule dynamics, used for the treatment of breast cancer. Tagami and colleagues evaluated the batch to continuous-flow translation of two key steps for the preparation of **176** [52]. These two steps included a DIBAL-H reduction of ester **172**, leading to aldehyde **173**, followed by coupling of aldehyde **173** with sulfone **174** in the presence of *n*BuLi.

These reactions are typically conducted at -70°C in the batch process to avoid overreduction of substrate **172**. The authors used a continuous-flow reactor constructed from SS316 tubing with micromixers. The enhanced mass and heat transfer enabled extremely short reaction times at -50°C (Fig. 51). The setup was

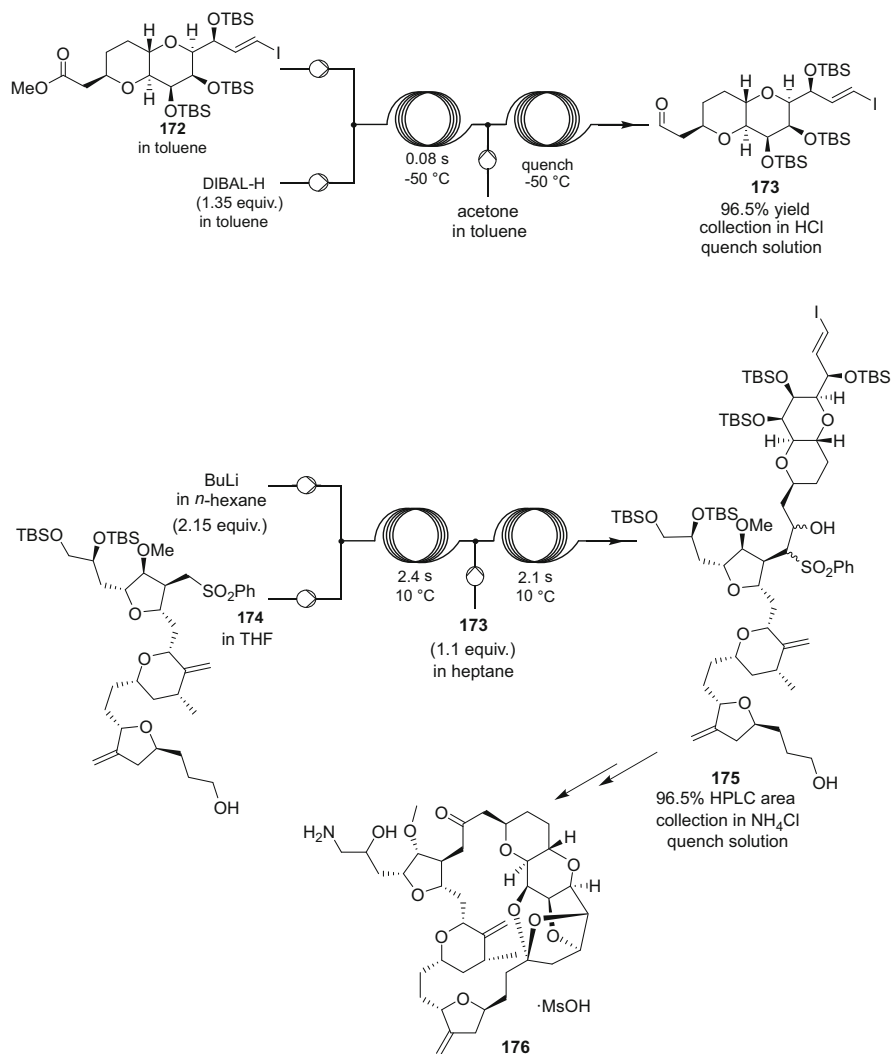


Fig. 51 Continuous-flow preparation of important intermediates toward eribulin mesylate [52]

operated for 87 min, and 306 g of aldehyde **173** was obtained. The *n*BuLi-mediated coupling reaction was also improved under continuous-flow conditions, using a PTFE coil reactor. The reaction temperature could be increased to 10 °C, yet affording a higher conversion by comparison to the batch process.

[JAK2 kinase inhibitor] Poliakoff and colleagues demonstrated the scale-out from gram to kilogram scale of an asymmetric hydrogenation under continuous-flow conditions toward JAK2 kinase inhibitor **179** [53]. The synthesis of key intermediate **178** for the preparation of this API was demonstrated through an enantioselective hydrogenation of enamide **177** (Fig. 52).

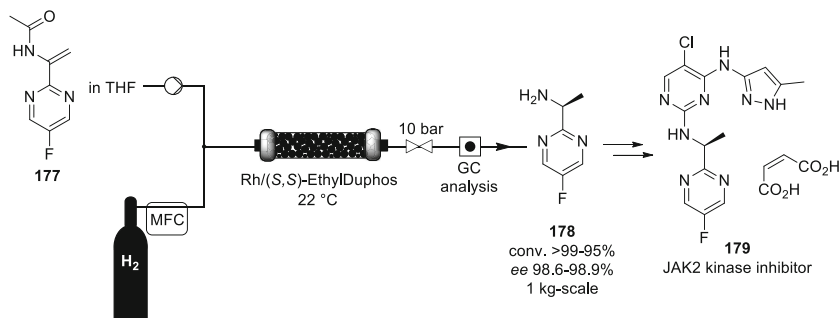


Fig. 52 Preparation of intermediate **178** toward JAK2 kinase inhibitor **179** [53]

Commercial Rh/(*S,S*)-EthylDuphos catalyst was immobilized through ionic interactions on a modified aluminum oxide material. Catalyst anchoring and reaction solvents were optimized on the microscale, demonstrating the necessity for oxygen- and water-free conditions, as well as the superiority of THF. The process was then transposed to kg-scale, and on-line GC analysis was implemented to monitor product quality (conversion and e.e.). The setup consisted of two 150 mL internal volume packed-bed reactors that could be alternated, in case of catalyst failure. On-line GC analysis enabled automatic feedback and correction actions switching through valves. The setup was operated continuously for 18 h. Conversion and e.e. ranged from 95 to >99%, and from 98.6% to 98.9%, respectively. Minimal catalyst leaching was detected in the final product (<1 ppm). By comparison to the batch procedure, the flow process required a reduced amount of catalyst, was less prone to Rh contamination and benefited from a dramatic space-time yield improvement.

[PARP-1 inhibitor] PARP-1 inhibitors are compounds displaying a broad range of biological activities, including promising anticancer activity. Thieno[2,3-*c*]isoquinolin-5(4H)-one (**183**) is highly potent, and an important intermediate for other advanced PARP-1 inhibitors. The classical batch procedure for accessing **183** relies on hazardous reagents, tedious reactions and purifications, and proceeds with a moderate overall yield. To address these issues, Gioiello and colleagues considered the implementation of the process under continuous-flow conditions in PTFE coils, featuring in-line UV reaction monitoring [54]. Several solvents and bases were screened under batch conditions to evaluate the best combination for the first Suzuki coupling of **180** with phenylboronic acid. Sodium hydroxide and water/THF/PEG-400 performed best. The conditions were next transposed under continuous-flow. Temperature and flow rates were optimized using a central composite design under continuous-flow conditions, and >90% yield was achieved upon optimization (Fig. 53).

The original batch strategy for the second step involved the derivatization of carboxylic acid **181** into the corresponding acyl azide **182** through the intermediate formation of an acyl chloride and its reaction with sodium azide. The conditions were adjusted for the flow application, and acyl azide **182** was obtained in 84% yield by directly reacting **181** with diphenylphosphoryl azide in the presence of NEt_3 . The

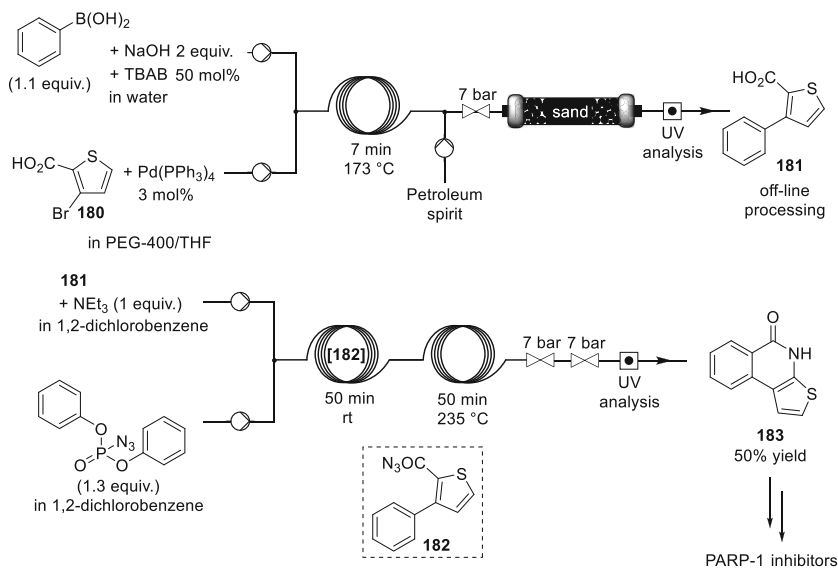


Fig. 53 Preparation of fragment **183** toward PARP-1 inhibitors [54]

reactor effluent was next reacted at 235 °C for 50 min, and the final Curtius rearrangement proceeded with 70% conversion. The whole reaction sequence was then telescoped with, however, off-line liquid–liquid separation and filtration after the Suzuki coupling step. Petroleum spirit was injected downstream the first reactor and flowed through a column packed with sand to improve mass transfer. The resulting biphasic mixture was then directed toward a separation funnel and processed off-line, and readied for the azide formation/Curtius rearrangement sequence. Compound **183** was obtained in 50% overall yield (33% overall yield in batch) accordingly.

[Prexasertib monolactate monohydrate] A multidisciplinary research team with Eli Lilly developed a multistep continuous-flow cGMP process with an output of 3 kg day⁻¹ of prexasertib monolactate monohydrate (**188**), an inhibitor of checkpoint kinase 1 (CHK1) [55]. Prexasertib is currently being assessed in phase 1b and 2 clinical trials in combination with cytotoxic chemotherapy. Prexasertib was originally synthesized according to a nine-step sequential batch strategy. The authors reported here a seven-step strategy amenable to continuous manufacturing. Various continuous unit operations were telescoped according to four main steps to produce the target at ~3 kg per day using small continuous reactors, extractors, evaporators, crystallizers, and filters. Online process analytical technology (PAT) was implemented to monitor and characterize the processes including online HPLC and refractive index measurement, as well as temperature, pressure, and mass flow rates. Stage 1 (Fig. 54) started from advanced nitrile **184** that was prepared according to a sequential batch procedure. It involved the condensation of **184** with hydrazine to form pyrazole **185**. This reaction is notoriously slow under batch conditions, and

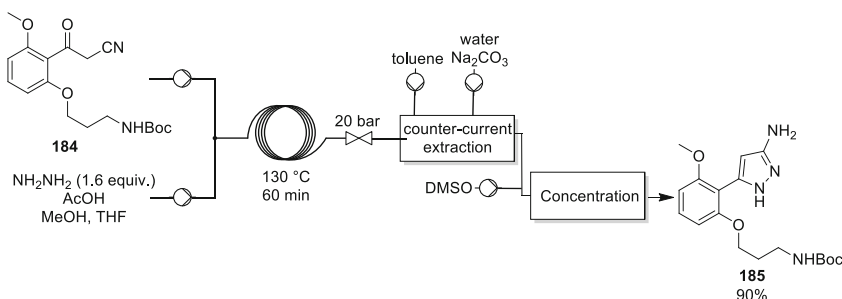


Fig. 54 Stage 1 for the preparation of a synthetic intermediate toward prexasertib monolactate monohydrate [55]

was significantly accelerated under continuous-flow conditions using superheated THF. The authors performed the reaction in a SS PFR of 3.2 mL internal volume. The optimized conditions involved 130°C and 20 bar of counter-pressure to obtain pyrazole **185** in high yield (90%) within 60 min of residence time, with a 1.6 equiv. excess of hydrazine. The reaction was next scaled in 1.4 L internal volume SS PFR, giving a productivity of 3.4 kg day⁻¹. The process also came with a significantly improved inherent safety, since only 20 g of hydrazine was present at any time in the PFR. The reactor effluent next underwent a sequence of purification steps including a liquid–liquid extraction and a solvent swap. A three-stage continuous countercurrent extraction was developed to minimize product loss. Each stage consisted of a mixing tank for rapid mass transfer between layers and a static gravity decanter separation. Toluene was injected to facilitate phase separation. The extraction process was very efficient, and residual hydrazine levels were below 2 ppm and the other impurities dropped below 5% (HPLC) after extraction. The extracted product was next directed to a surge vessel feeding a solvent exchange device that enabled fully automated continuous operation. Toluene and other volatile compounds were removed and DMSO was added during the concentration process. The DMSO concentrate was next typically stored, but could be immediately transferred to the next operation, therefore avoiding isolation and operational exposure.

Stage 2 involved a S_NAr reaction between pyrazole **185** and pyrazine **186**, and provided intermediate **187** with good yield and selectivity (Fig. 55). Optimized conditions implied the presence of a base to neutralize any acid that could induce premature Boc-deprotection on **187**. *N*-Ethylmorpholine was selected since it was soluble in DMSO and not reactive with starting pyrazine **186**. The flow reactor was constructed from PFA tubing. A narrow section at the upstream part of the coil provided fast diffusional mixing between the static T-mixer and the main reactor. The conditions were next scaled in a 2.8 L internal volume reactor (91 m of 6.31 mm internal diameter PFA tubing) immersed in a thermostated bath, affording intermediate **187** in 90% purity (HPLC). The next stages were dedicated to purification of **187**. A continuous antisolvent (methanol) crystallization process was implemented. It relied on two mixed-suspension, mixed-product removal vessels (MSMPR) fluidically connected in series. The recrystallization step afforded 99.8% purity

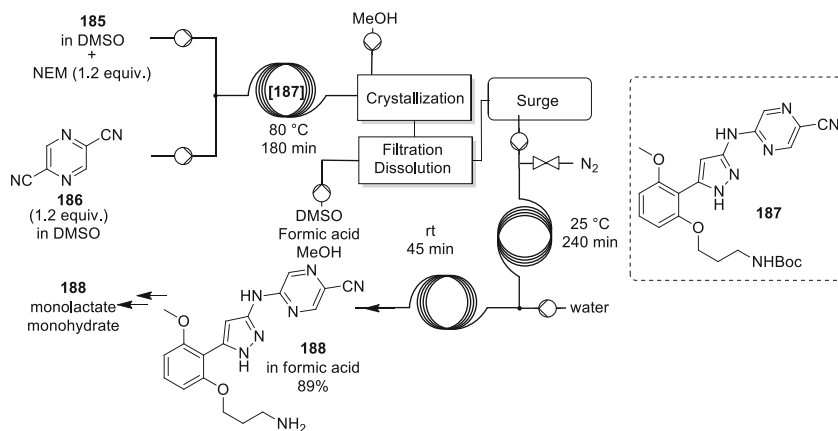


Fig. 55 Stages 2–3 for the preparation of a synthetic intermediate toward prexasertib monolactate monohydrate [55]

(HPLC). The crystallization slurry was transferred through a custom-built intermittent flow transfer zone, and intermittently filtered on automated and agitated single-plate filters. The latter were designed to filter, wash, partially dry (nitrogen flux) the solids, automatically, without any intervention. Recrystallized **187** was dissolved in formic acid and transferred to a cooled surge vessel that decoupled the recrystallization process from the deprotection, thus enabling intervention and maintenance on the reactors without shutting down the entire process. Exposure to formic also promoted Boc-deprotection. The Boc-deprotection step was performed in a vertically oriented coil reactor (PFA tubing with 15.9 mm internal diameter) operated under gas–liquid segmented regime.

The authors noticed that the impurity profile was much improved when the gaseous side-products isobutene and carbon dioxide were removed in situ, which was achieved by the concomitant injection of nitrogen gas in a 1:1 ratio with the liquid phase. The residence time for the liquid phase was of 4 h, and the deprotection was carried out at 25 °C. The reactor effluent was next diluted with water and collected. Stage 3 consisted mainly in removing formic acid in the presence of lactic acid to enable the isolation of prexasertib monolactate monohydrate. A large excess (8 equiv.) of lactic acid was combined with a continuous concentration step, followed by a dilution with THF. The resulting mixture was transferred to a surge vessel, and next transferred to an antisolvent (THF) crystallization step.

3.2 Antiviral Active Compounds

3.2.1 HIV/AIDS Medications

[Atazanavir] Kappe and de Souza groups reported the multistep continuous-flow synthesis of the biaryl hydrazine unit of Atazanavir (**192**, Reyataz) in a SS

continuous-flow reactor [56]. Atazanavir is a typical API used for the treatment of HIV. The synthesis involves a Suzuki cross coupling of 4-formylphenylboronic acid with 2-bromopyridine toward intermediate **189**, followed by condensation with Boc-hydrazine and hydrogenation (Fig. 56) toward biaryl hydrazine **191**. At first, the biphasic cross coupling reaction was optimized under microwave batch conditions, and the best results were obtained with K_3PO_4 as a base. The conditions were then translated to continuous-flow, and compound **189** was obtained with 95% conversion. The crude reaction mixture was directly utilized for a preliminary set of optimizations for the formation of hydrazone **190** under microwave batch conditions. Trimethylsilyl triflate was identified as a promising Lewis acid catalyst. The reaction was also transposed to continuous-flow conditions, where a three-feed system consisting in feed stocks of crude biaryl aldehyde **189**, *tert*-butyl carbazate, and the catalyst was considered. Hydrazone **190** was obtained in 99% conversion.

The final hydrogenation was directly optimized in a commercial continuous-flow hydrogenator (H-Cube Pro) equipped with a 10% Pd/C catalyst cartridge. Quantitative conversion was obtained with a purified feed of **190**, but direct use of the reactor effluent led to catalyst poisoning. An intermediate in-line purification step was therefore implemented to neutralize the reactor effluent containing hydrazine **190** (injection of aqueous K_2CO_3 and in-line liquid–liquid extraction prior to injection in the hydrogenation setup). Under such conditions, almost quantitative conversion to **191** was obtained. The entire setup was finally telescoped, although manual phase separation was still performed after the Suzuki coupling reaction. Compound **191** was obtained in 74% yield (53% in batch).

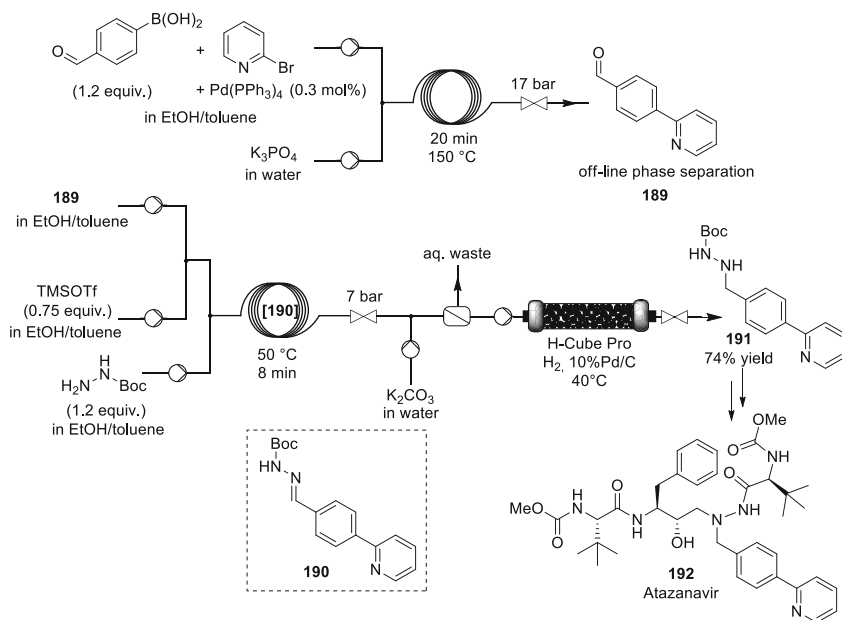


Fig. 56 Preparation of hydrazide fragment **191** toward atazanavir [56]

The same group reported later the preparation of α -haloketones intermediates, which are important building blocks for the preparation of HIV protease inhibitors, such as atazanavir (**192**) and darunavir (**193**) [57]. In the process, mixed anhydride **194** was generated under continuous-flow conditions from the corresponding *N*-protected amino acid, tributylamine and ethyl chloroformate (Fig. 57).

It then reacted with anhydrous diazomethane generated in a tube-in-tube reactor. The tube-in-tube reactor consists in a gas-permeable Teflon AF-2400 inner tubing embedded in an impermeable PTFE outer tubing. CH_2N_2 was generated from reaction between Diazald and KOH in aqueous phase inside the inner permeable tubing of the tube-in-tube reactor. After crossing the permeable polymer, it reacted with anhydride **194** in the outer chamber of the reactor, generating α -diazoketone **195**. The preparation of **195** was directly telescoped with the next step, and the injection of aqueous HCl led to α -haloketone **196** in 87% yield, with a 1.25 mmol h^{-1} productivity. Most notably, the procedure came with complete retention of the stereochemistry. One year later, de Souza and colleagues reported an alternative continuous-flow procedure for an important fragment of darunavir (**193**) [58].

[Doravirine] Doravirine (**201**) is a non-nucleoside reverse transcriptase inhibitor, and a clinical candidate for the treatment of AIDS. Gauthier and colleagues designed an original sequence for its synthesis, where a key fragment is pyridone **200**

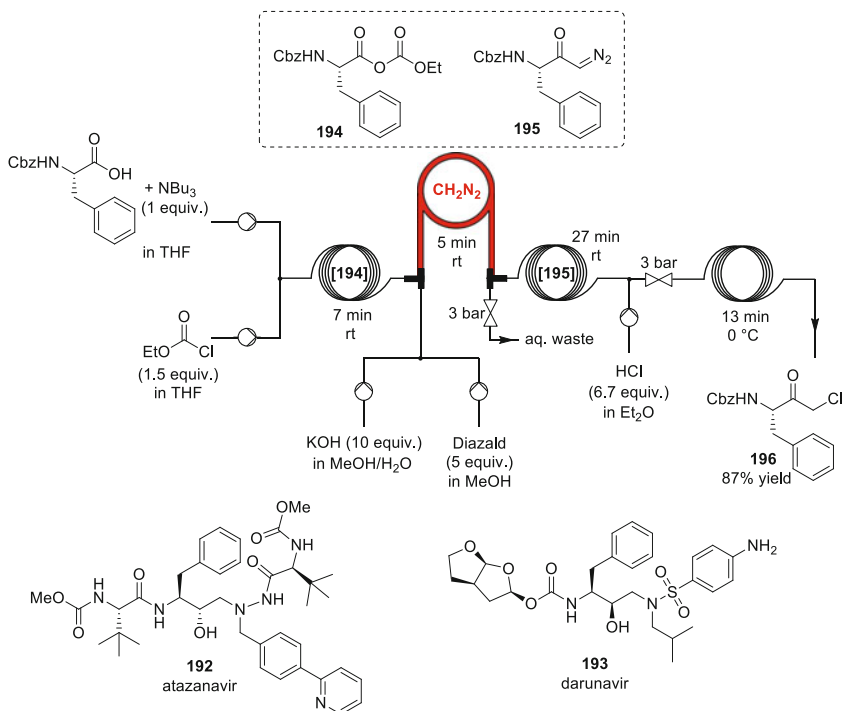


Fig. 57 Preparation of pivotal chloroketone **196** toward atazanavir [57]

[59]. The latter was prepared from an aldol reaction, followed by dehydration of corresponding alcohol adduct **199** and cyclization with ammonia (Fig. 58).

The condensation of ethyl ester **197** and trifluoromethyl ketone **198** was first optimized in batch, and potassium *tert*-amyloxide in toluene was identified as the most efficient combination for the reaction. The conditions were then transposed under continuous-flow conditions in a SS coil reactor, and adduct **199** was obtained in 85% yield after in-line quench (65% in batch). Due to solubility issues, the subsequent cyclization steps could not be performed under continuous-flow conditions.

[Efavirenz] Efavirenz (**40**) is used for the treatment of AIDS (see also Sect. 2.2.1), and the group of Watts implemented two key steps, for the preparation of this API, in a glass plate-type continuous-flow reactor (Fig. 59) [60]. The *ortho*-lithiation of *N*-Boc-4-chloroaniline was mediated using *n*BuLi, and next telescoped to a trifluoracylation step, affording intermediate **202** (total residence time of 516 s).

The reactor effluent was then quenched in a column packed with SiO₂. A dramatically higher yield was obtained under continuous-flow conditions (70%) by comparison to the conventional batch process (28%). Additionally, the procedure

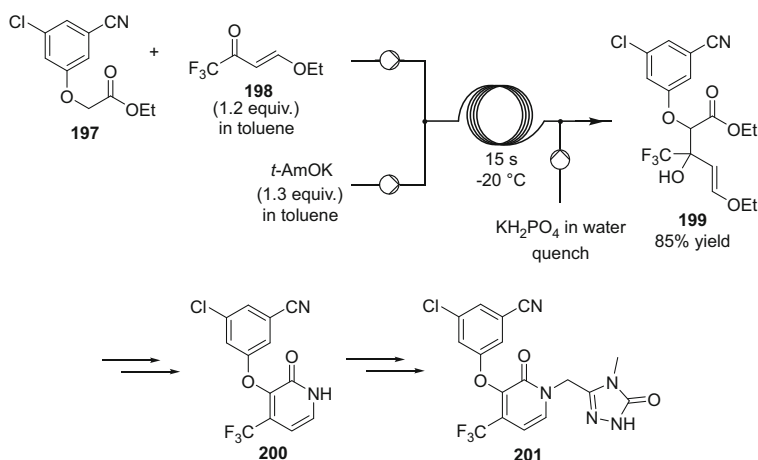


Fig. 58 Preparation of an important pyridone fragment of doravirine [59]

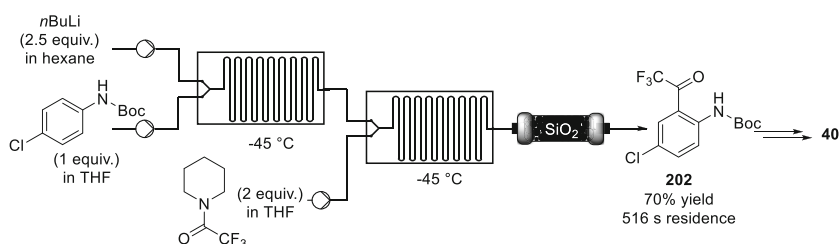


Fig. 59 Multistep continuous-flow preparation of fragment **202** toward efavirenz [60]

alleviates the use of tetramethylethylenediamine (TMEDA), which is typically used as a complexing agent, therefore increasing cost-efficiency. Besides, the reaction is typically conducted in the presence of *sec*- or *tert*-BuLi in the literature, and Watts' procedure represented the first example of the *n*BuLi-mediated *ortho*-lithiation.

[Lamivudine] Watts et al. reported a semi continuous-flow preparation of lamivudine (**206**), an antiretroviral drug used in the treatment of HIV/AIDS and hepatitis B (T3C) [61]. The preparation of a key intermediate, namely 5-acetoxy oxathiolane **205** was carried out by an integrated two-step continuous-flow process from L-menthyl glyoxalate (**203**) in high yield (Fig. 60).

Feed solutions (acetonitrile) of menthyl glyoxalate hydrate (**203**, 0.43 M) and 1,4-dithiane-2,5-diol (**204**, 0.22 M) were injected into a 2 mL glass reactor (at 90°C). The outlet of the first reactor was connected to a glass fluidic element for intense mixing (LTF-MX, 0.2 mL, rt) of the reactor effluent with acetic anhydride in acetonitrile (1.73 M). The resulting mixture was next redirected to the last glass fluidic element for increasing the residence time (LTF-V, 1.7 mL, rt). Reaction parameters such as the residence time, temperature, and concentration were subsequently optimized to increase the efficiency of the process. After optimization, 5-acetoxy oxathiolane **205** was obtained in 95% yield after 9.7 min of residence time. Such results are definitively a considerable improvement of the original batch conditions that required a much longer reaction time (12 h) at a higher temperature (110°C).

[Nevirapine] Nevirapine (**210**) is a widely prescribed non-nucleosidic reverse transcriptase inhibitor for the treatment of HIV. McQuade et al. reported a continuous-flow procedure for the preparation of 2-bromo-4-methylnicotinonitrile (**209**), a pivotal building block for the preparation of nevirapine [62]. The authors developed a process starting from inexpensive, acyclic commodity-based raw materials that could potentially decrease the production costs of nevirapine (Fig. 61).

The process started from acetone and malonitrile, which were reacted through a column packed with solid Al₂O₃ and MS (3 Å) within minutes, leading to

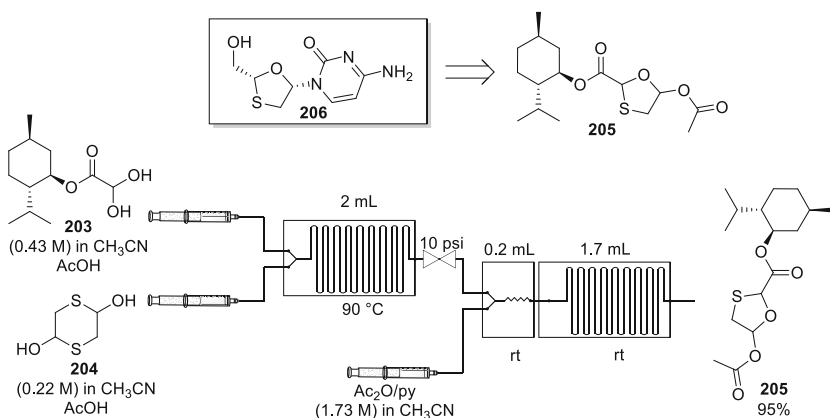


Fig. 60 Preparation of 5-acetoxy oxathiolane **205** en route toward lamivudine [61]

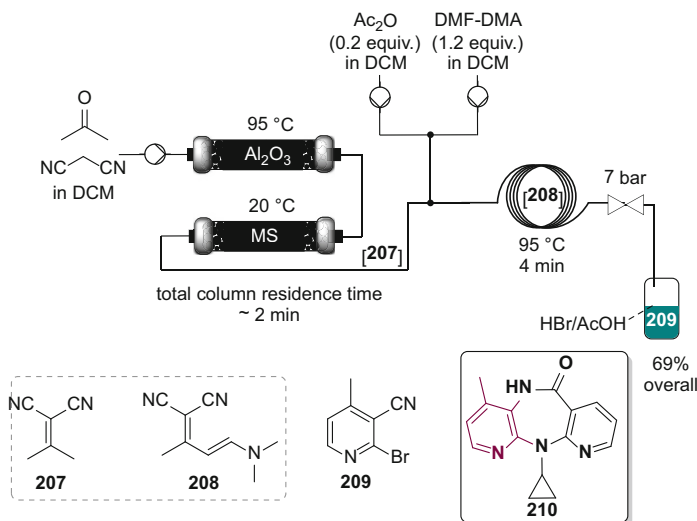


Fig. 61 Continuous-flow preparation of 2-bromo-4-methylnicotinonitrile [62]

intermediate alkydene malononitrile **207**. The incorporation of MS (3 Å) was mandatory because of the deleterious presence of water for the next step. The stream containing compound **207** was next reacted in the presence of acetic anhydride with *N,N*-dimethylformamide dimethylacetal (DMF-DMA, 1.2 equiv.) to yield enamine **208** under superheated conditions (95°C). Despite promising results with the successful telescoping of a Knoevenagel reaction and an enamine formation, the method suffers from a limited operation time, down to 24 min depending on the concentration. The reactor effluent was collected in a batch vessel where it was allowed to react with HBr in the presence of AcOH, giving 2-bromo-4-methylnicotinonitrile (**209**) in an overall yield of 69%. A final crystallization in batch was necessary to obtain a high purity.

3.2.2 Other Antiviral Pharmaceuticals

[Daclatasvir] Daclatasvir (**213**) is an inhibitor of the viral phosphoprotein NS5A, used in the treatment of hepatitis C. Kappe and coworkers designed a continuous-flow protocol for the preparation of pivotal intermediate **212** bearing the phenyl imidazole core of daclatasvir. Compound **212** was obtained from α -bromoacetophenone and *N*-Boc-protected proline (Fig. 62) [63]. The condensation between α -bromoacetophenone and acetic acid was first evaluated as a model reaction in microwave batch reactor, and proceeded smoothly in the presence of NEt_3 . The cyclization of the resulting acyloxy ketone, in the presence of ammonia and acetic acid, was also optimized under microwave batch conditions. The target imidazole could be obtained with an excellent selectivity (95%) under optimized

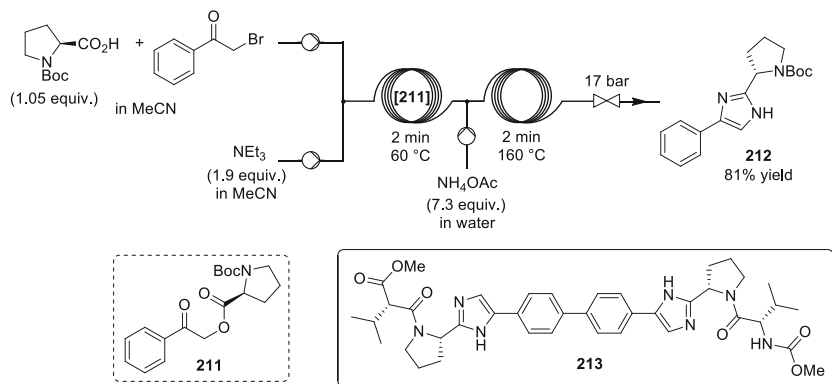


Fig. 62 Continuous preparation of fragment **211** toward daclatasvir [63]

conditions, with the corresponding oxazole being the only minor by-product. However, when the reaction was attempted with *N*-Boc proline, other by-products resulting from Boc deprotection and *N*-acylation were also detected, decreasing the selectivity toward imidazole **212**. 70% yield could be obtained with an equimolar amount of NH_3 and acetic acid. NH_4OAc was therefore directly used for optimization under continuous-flow conditions. The two steps were then separately transposed to continuous-flow conditions.

The preparation of acyloxy ketone **211** was conducted in a PFA coil reactor, while the installation of the imidazole core was conducted in a SS coil. A dramatic improvement of the selectivity toward **212** was obtained by comparison to the MW batch process, with Boc-deprotection and oxazole formation being inhibited as a consequence of the fast heating and short residence time under continuous-flow conditions. The two steps were then telescoped, and compound **212** was obtained in 81% yield, with full retention of stereochemistry. The scope of the flow procedure was also extended to other bromoketones and carboxylic acids. However, the symmetric biphenyl bisbromoketone, necessary for preparation of the central core of daclatasvir, was not soluble in MeCN, and the corresponding acyloxy ketone was therefore prepared in batch. It was then subjected to cyclization into imidazole using the previously established continuous-flow conditions, and the target compound was obtained in 71% yield.

3.3 Antiparasitic and Antibiotic Pharmaceuticals

3.3.1 Malaria

[OZ439] Ley and colleagues reported a sequential flow route toward antimalarial drug candidate OZ439 (**218**) featuring a quite unique trioxolane scaffold. Despite the promising antimalarial profile of drug candidate OZ439, its classical preparation

relies on the use of a commercial, yet very expensive starting material (4-(4-hydroxyphenyl)cyclohexan-1-one, **214**) and uses large amounts of pentane [64]. The authors started first by developing a very convenient flow procedure for the preparation of **214** from readily available and affordable bisphenol, through a selective reduction under continuous-flow conditions (Fig. 63). The authors used the HEL FlowCat platform, and the optimized conditions involved a solution of bisphenol in EtOH/H₂O (1:1 v/v, 0.05 M) that was passed through a bed reactor (3 mL internal volume; 20% Pd/C) within 3 min of residence time under 5 bar of counter-pressure. Compound **214** was isolated in 58% after off-line recrystallization from the reaction mixture (>95% NMR purity). With an unrestricted on-demand supply of **214**, the authors next developed a method for its continuous acetylation (using either a Vapourtec R2+/R4 module or a Uniqsis Flowsyn module). A solution of acetic anhydride (1.5 equiv) in CH₂Cl₂ and a solution of phenol **214**, DMAP (5 mol%), and Et₃N (4.5 equiv) were combined through a static T-mixer and reacted for ~12 min of residence time in a 10 mL PFA coil reactor. Off-line filtration through silica and evaporation of the reactor output gave intermediate **215**. The next step involved the co-ozonolysis reaction between ketone **215** and an oxime **216**, a reaction known as Griesbaum ozonolysis and used for the preparation of 1,2,4-trioxolanes. The authors first optimized the reaction conditions starting from readily available 4-phenylcyclohexanone as a model substrate. A solution containing the oxime **216** and the ketone in EtOAc was reacted with a stream of ozone. To ensure long operation without clogging, the concentration of oxime **216** was set at 0.2 M

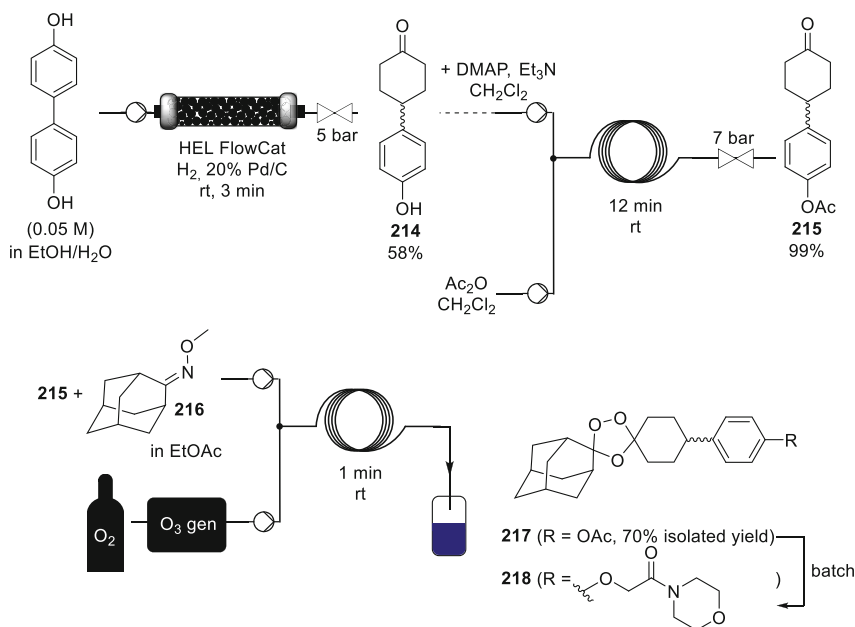
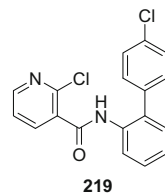


Fig. 63 Preparation of an advanced fragment toward OZ43 [64]

Fig. 64 Boscalid [64]

and the concentration of ketone was set at 0.1 M. Both the liquid and gaseous flow rates were set at 1 mL min^{-1} and 1 L min^{-1} , respectively. Under these diluted conditions, the reactor was operated for over 3 h, and the model product was isolated in 78% with a calculated throughput of 1.6 g h^{-1} . These reaction conditions were next applied to ketone **215**, and the desired 1,2,4-trioxolane **217** was isolated in 70% yield (9:1 *cis* – *trans* selectivity; output 45.6 g day^{-1}). Further steps in batch provided OZ439 (**218**) in 86% isolated yield.

3.3.2 Fungicides

[Boscalid] Boscalid (**219**, Fig. 64) is a fungicide, and several reports were published for the production of pivotal chemical intermediates for its preparation [65–67]. Kappe and coworkers generated and used Fe_3O_4 nanocrystals for the continuous-flow reduction of nitroaromatics into aniline precursors of APIs including boscalid [68]. At first, iron oxide particles generation and utilization in the model nitrobenzene reduction were studied in MW batch conditions. $\text{Fe}(\text{acac})_3$ was selected as precursor with only 0.25 mol% employed, and hydrazine hydrate as reducing agent with only 20% stoichiometric excess, although other iron species such as FeCl_2 , FeCl_3 , and $\text{Fe}(\text{OAc})_2$ were also efficient. The one-pot process was suitable for the reduction of numerous nitroaromatics, containing other reducible functionalities, in excellent yields (95–99%) and with short reaction times (2–8 min). The Fe_3O_4 nanocrystals were efficiently eliminated from the reaction medium by simple magnetic trapping, and could be recycled for further batches. However, the utilization of hydrazine in an exothermic reaction on large scale raises safety concerns, and the process was translated in stainless steel continuous-flow reactor. 4-Chloro-2'-nitrobiphenyl, an intermediate in the preparation of **219**, was accordingly reduced in 97% yield with 1.5 min residence time and a 60 g h^{-1} productivity. See also Sect. 3.3.3 for a similar procedure.

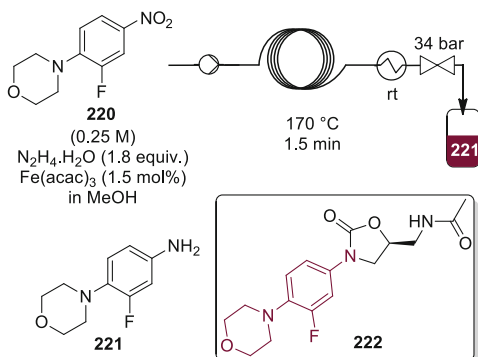
3.3.3 Antibiotics

[Linezolid] Kappe and colleagues studied the applicability of iron oxide as catalyst for the reduction of nitroarenes to anilines in the presence of hydrazine hydrate [66, 67]. Of particular interest was aniline **221**, since it is a direct precursor of

linezolid **222**, a potent oxazolidinone-based antibiotic developed by Pfizer. The catalyst was generated in situ from an inexpensive and readily available iron source ($\text{Fe}(\text{acac})_3$). This versatile procedure is chemoselective, avoids the use of precious metals and can be applied for the reduction of aliphatic nitro compounds and azides as well. Although preliminary trials were carried out in batch and microwave reactors, the authors next studied its implementation under continuous-flow conditions (Fig. 65). The main rationale for the implementation under continuous-flow conditions was to temper the exothermicity of hydrazine-based high-temperature reductions. Since the catalyst is generated in a colloidal form, its implementation under continuous-flow conditions was straightforward. The authors used a commercial flow system (FlowSyn reactor, Uniqsis) equipped with a stainless steel coil reactor (1.0 mm internal diameter, 25 m length, 20 mL internal volume) heated at 150–180°C and with a 25–34 bar back pressure regulator. The reaction released nitrogen gas, and a rather high counter-pressure was mandatory to control the residence time within the reaction loop. The reaction conditions were optimized with nitrobenzene as a model substrate, but the authors turned their attention to more challenging substrates. The authors studied the reduction of 3-fluoro-4-morpholinylnitrobenzene (**220**) toward the continuous-flow preparation of 3-fluoro-4-morpholinylaniline (**221**), an important intermediate for linezolid **222**. A 40°C preheated solution containing **220** (~0.25 M), hydrazine hydrate and 1.5 mol% of the iron precursor was reacted under continuous-flow conditions at 170°C within 1.5 min of residence time, yielding the desired aniline **221** in 95% (output: 30 g h⁻¹).

The authors noted that the nanocrystals could be recovered and recycled for other runs, although a decrease in catalytic activity was reported. In a follow-up paper, the authors studied the same reaction using a heterogeneous catalyst with a ThalesNano X-Cube reactor [67]. The heterogeneous catalyst consisted of a dispersion of Fe_3O_4 nanocrystals in Al_2O_3 and was packed in a SS column (CatCart).

Fig. 65 Continuous-flow preparation of a fragment toward linezolid [66]



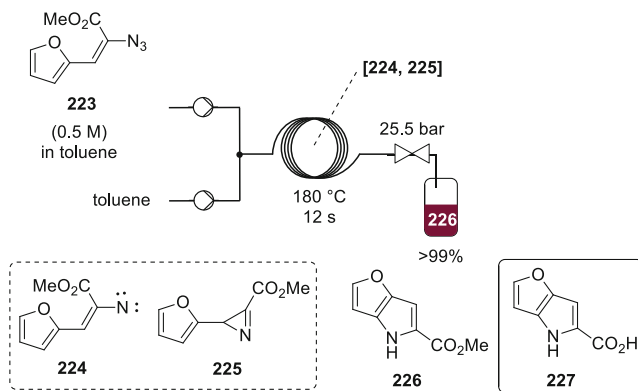


Fig. 66 Continuous-flow preparation of DA00 inhibitor intermediate **226** [69]

3.4 Central Nervous System and Related Conditions

3.4.1 Schizophrenia

[DA00 inhibitor] Seeberger reported an efficient, safe, and scalable procedure for the continuous-flow thermolysis of azidoacrylates toward indole derivatives, through the formation of intermediate nitrene transient species **224**, including advanced pharmaceutical intermediates for the treatment of schizophrenia such as DA00 inhibitor 4H-furo[3,2-b]pyrrole-5-carboxylic acid (**227**) [69]. The scalability of the process was demonstrated in the continuous-flow synthesis of precursor **226** (Fig. 66). The cyclization of azide **223** (0.5 M in the feed solution) was performed at 180 °C within a residence time of 12 s in a SS coil reactor, leading to 8.5 g of **226** in excellent purity and yield within 21 min of operation. The reaction most likely involved transient intermediates **224** and **225**.

3.4.2 Depression

[Levomilnacipran] Levomilnacipran (**230**) is a serotonin-norepinephrine reuptake inhibitor used in the treatment of fibromyalgia and depression. Wirth and coworkers translated a known batch strategy for the preparation of intermediate **229** for the synthesis of API **230** [70]. The procedure relies on an intramolecular cyclopropanation using diazo compound **228** in the presence of a Rh catalyst (Fig. 67). A diazo transfer reaction was first optimized on allyl phenylacetate under continuous-flow conditions using IR in-line spectroscopy, with DBU as base and 4-acetamidobenzenesulfonyl azide (*p*-ABSA) as diazo donor, affording the target diazo **228** with a 93% conversion. The cyclopropanation was then optimized under continuous-flow conditions, using purified allyl phenyldiazoacetate (**228**) and Rh catalyst as separated feeds. Rh₂(oct)₄ gave the best results in toluene,

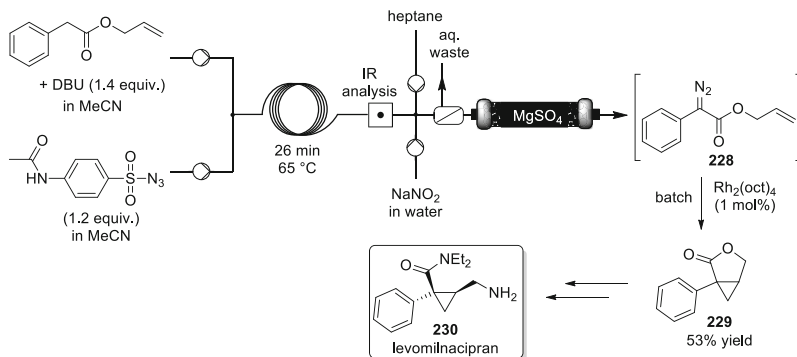


Fig. 67 Continuous-flow process for the preparation of levomilnacipran precursor **229** [70]

yielding compound **229** in 82%, despite low solubility of the catalyst. The two steps were next telescoped according to a semi-continuous-flow process. Diazo transfer was first conducted in a coil reactor, including various downstream operations (in-line IR analysis, in-line azide quench and extraction). The organic outlet from the liquid–liquid separator was then conveyed to a batch reactor containing the catalyst and *n*-heptane. However, the presence of MeCN and traces of water resulting from the diazo transfer and liquid/liquid extraction steps triggered various side-reactions, and significantly affected the yield (30%). The organic outlet containing diazo species **228** was therefore passed through a column packed with MgSO_4 before its injection into the catalyst solution, which was kept under Ar atmosphere over molecular sieves. Lactone **229** was obtained in 53% yield overall.

[Meclinertant] Meclinertant (**241**, SR48692), developed by Sanofi–Aventis, is a non-peptide neurotensin receptor-1 antagonist (NTS1) endowed with anxiolytic, anti-addictive, and memory-impairing properties. Ley and colleagues developed a flow-chemistry alternative to the conventional batch procedure for accessing advanced fragment **240** [71]. The procedure uses columns packed with supported reagents and scavengers, and relies on an eight-stage sequence of flow reactors (Figs. 68, 69, 70, 71, and 72). The authors started with the preparation of one of the key intermediates, ketone **234**, starting from cheap and readily available compounds. The first stage (Fig. 68) started with the *O*-acylation of cyclohexa-1,3-dione, which is an exothermic reaction potentially difficult to scale up. The diketone in solution was simply mixed with acetyl chloride in the presence of DIPEA in a 10 mL internal volume coil at 40°C under 7 bar of counter-pressure. A filtering column was inserted before the pressure regulator. Intermediate **231** was obtained in 93% yield accordingly. Although CH_2Cl_2 was utilized in the first trials, the authors shifted to toluene to enable direct telescoping with the second reaction (see below). The next step of stage 1 consisted of the rearrangement of intermediate **231** into triketone **232** (Fig. 68). Such a rearrangement can be triggered in the presence of DMAP, and the authors argued that the use of heterogeneously supported DMAP would be an elegant option. The authors tested various options (such PS-DMAP), but the best results and productivity were obtained with the use of a DMAP monolith packed

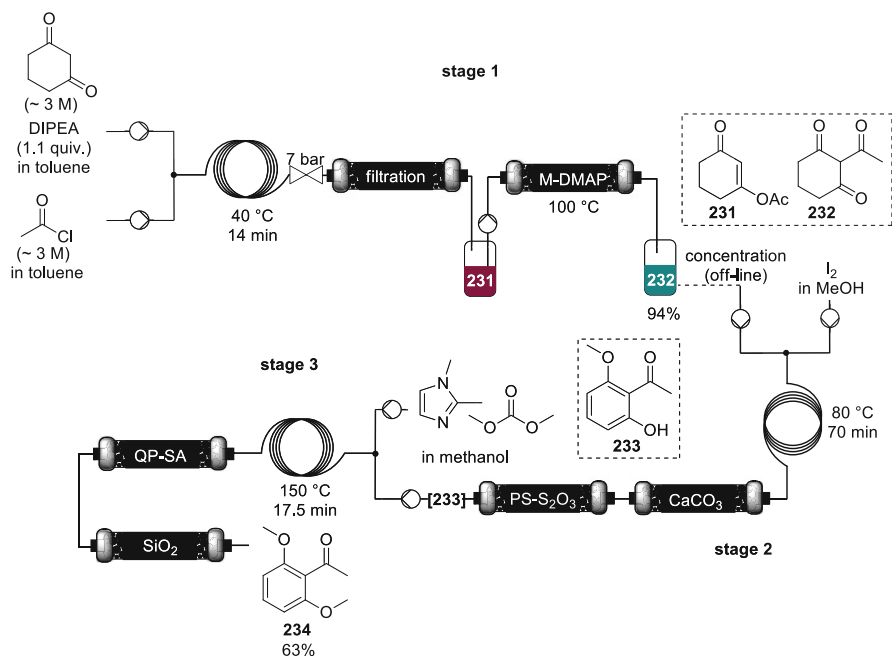


Fig. 68 Stages 1–3 for the preparation of advanced intermediate **240** toward meclizolant [71]

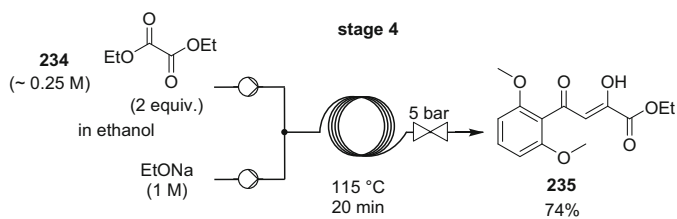


Fig. 69 Stage 4 for the preparation of advanced intermediate **240** toward meclizolant [71]

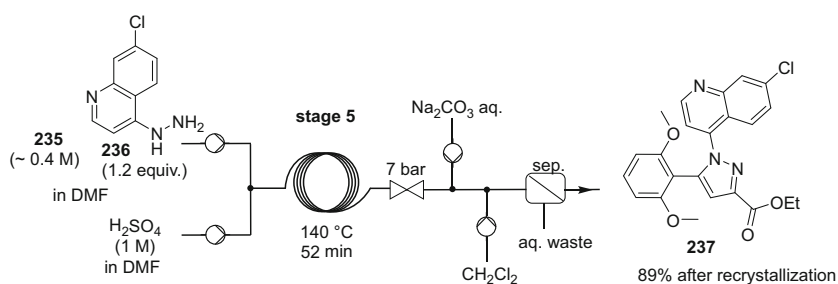


Fig. 70 Stage 5 for the preparation of advanced intermediate **240** toward meclizolant [71]

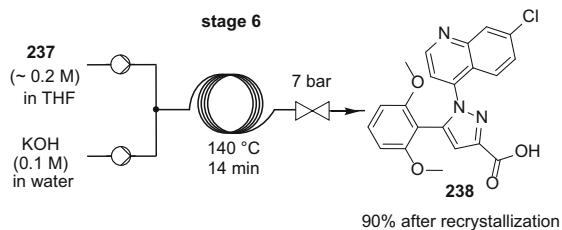


Fig. 71 Stage 6 for the preparation of advanced intermediate **240** toward meclintant [71]

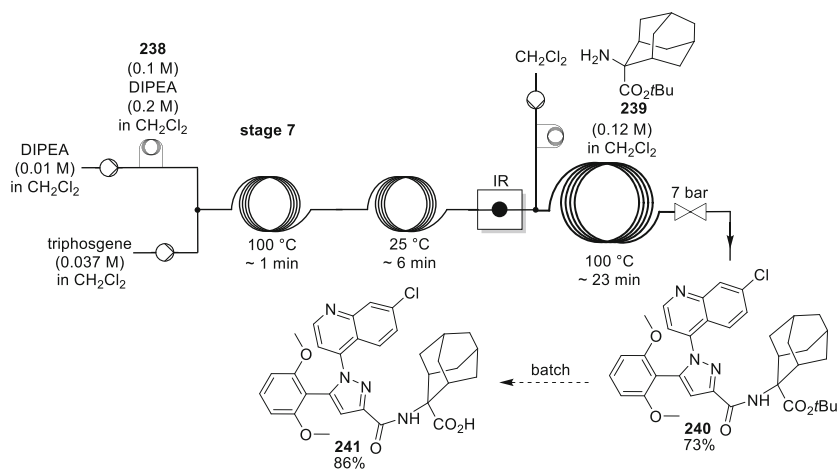


Fig. 72 Stage 7 for the preparation of advanced intermediate **240** toward meclintant [71]

inside a glass column at 100 °C. The rearrangement proceeded well in toluene (95% yield), and could therefore be directly telescoped to the first step (94% overall). The reactor effluent was concentrated off-line and readied for the next stage. Stage 2 relied on the iodine oxidation of triketone **232** to form methoxyacetophenone **233** (Fig. 68). The reaction was sensitive to the scale, and a variety of side products were observed upon scaling-up. Upon optimization, a stream of substrate **232** in methanol was mixed with a stream of iodine and reacted in a tubular reactor at 80 °C for 70 min of residence time. The reactor effluent was passed through a glass column packed with CaCO₃ to scavenge hydroiodic acid, then redirected to a column packed with PS-thiosulfate beads dispersed in celite to capture the excess iodine. The final reactor effluent was collected and concentrated to yield **233** in 68% yield (99% purity).

Stage 3 aimed at a final methylation step using dimethyl carbonate and 1,2-dimethylimidazole to give desired dimethoxy acetophenone **234** (Fig. 68). A stream of acetophenone **233** in methanol was combined with a stream of dimethylcarbonate (DMC) and 1,2-dimethylimidazole (DMI) in methanol through

a static T-mixer and reacted into a PFA tubular flow coil (14 mL) operated at 150°C under 7 bar. The reactor effluent was passed through an immobilized acid scavenger (QP-SA) for scavenging DMI and destroying the excess DMC, giving compound **234** in quantitative yield (95% isolated yield). Upon optimization, the last two steps were telescoped into one uninterrupted reactor network, affording acetophenone **234** in 63% yield from intermediate **232**.

In stage 4, acetophenone **234** was reacted with diethyl oxalate in the presence of sodium ethoxide (Fig. 69). The implementation of this reaction under continuous-flow conditions was troublesome since precipitation occurred. The authors opted for a PFA coil with a wider internal diameter (1/8") operated at 115°C (5 bar), and used a specific back-pressure regulator with a design compatible with slurries. Intermediate **235** was obtained in 74% yield. Stages 5 and 6 involved the installation of the core pyrazole scaffold and the hydrolysis of an ester (Figs. 70 and 71). The Knorr pyrazole condensation in flow was straightforward: compound **235** in DMF was reacted with hydrazine **236** in a PFA coil (1/8") at 140°C (7 bar). The corresponding pyrazole ester **237** was isolated in 89% yield after extraction and concentration of the reactor effluent. The authors also implemented an in-line liquid–liquid extraction to enable direct, in-line effluent processing. The reactor effluent containing **237** was mixed with aqueous sodium carbonate and dichloromethane, and the resulting biphasic mixture was next sent to a semipermeable membrane separator, enabling in-line extraction and liquid–liquid separation. Compound **237** was obtained in 89% yield after recrystallization.

Next, a flow protocol for the hydrolysis of ester **237** was devised. Reaction completion was obtained after a residence time of 14 min at 140°C by mixing a stream of ester **237** (in THF) with a stream of KOH in water in a PFA coil (7 bar). The reactor effluent was collected, and processed in batch, affording acid **238** in 90%.

Stage 7 aimed at the amide coupling of acid **238** with adamantane amino acid **239** (Fig. 72). A solution of pyrazole carboxylic acid **238** and DIPEA (0.2 M) in dichloromethane was injected through a sample loop into a DIPEA/dichloromethane flow stream in the presence of triphosgene (0.037 M). The reactive solution was then passed through a 0.5 mL SS loop at 100°C to trigger the in-situ formation of phosgene. The reaction mixture was next passed through a 2.5 mL SS coil reactor to complete the formation of the acid chloride. An in-line IR spectrometer was inserted for reaction monitoring and to ensure complete consumption of acid **238**. A stream of Boc-protected amino acid **239** in CH₂Cl₂ (0.12 M) was injected downstream, and the resulting mixture was reacted in a 14 mL coil operated at 100°C. A back pressure regulator set at 7 bar was inserted downstream. The reactor effluent was collected in a flask containing an aqueous saturated solution of ammonium chloride to quench the reaction. A simple extraction with EtOAc and subsequent filtration through a pad of silica gel afforded fragment **240** in 73% yield. Compound **240** was next dissolved in CH₂Cl₂, and the corresponding solution was left overnight in a batch reactor in the presence of Quadrapure sulfonic acid (QP-SA) to deprotect the *t*-butyl protecting group, and afford meclizertant (**241**, 86%).

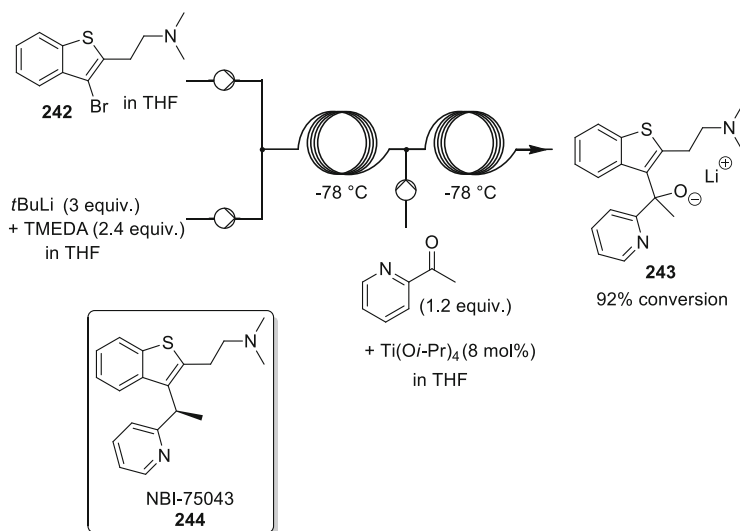


Fig. 73 Continuous-flow preparation of an intermediate toward NBI-75043 [72]

[NBI-75043] NBI-75043 (**244**) is an antagonist of the histamine receptor H1, for the treatment of insomnia. A key step for the preparation of this compound involved the lithiation of bromobenzothiophene **242**, followed with its addition to 2-acetylpyridine to form intermediate **243**. Gross and colleagues studied the preparation of compound **243** under continuous-flow conditions [72]. However, issues were encountered upon scaling-up, as the exothermic nature of the lithiation caused selectivity concerns, and prolonged reaction times under diluted conditions were required. The lithiation and alkoxide formation were therefore optimized in stainless steel continuous-flow reactors and telescoped. Precise control of the temperature, reagent stoichiometry, and residence time afforded improved results by comparison to the batch procedure, where 92% conversion of the starting material into the target product was obtained (Fig. 73).

3.4.3 Anti-seizure Compounds

[Rufinamide]. Based upon preliminary results [73], Hessel and Noël demonstrated the telescoped preparation of a rufinamide precursor in ETFE capillary and Hastelloy continuous-flow reactors, where the last amidation step would be conducted batchwise (Fig. 74) [74]. The process involved only neat reactants, with MeOH as the sole organic solvent utilized for the final crystallization. The sequence started with the preparation of 2,6-difluorobenzyl chloride (**246**), which was generated from gaseous HCl and the corresponding neat alcohol **245**. The next step, which involved the reaction of benzylic chloride **246** with aqueous sodium azide toward compound **112**, was challenging since sodium azide reacts with acids to form toxic and

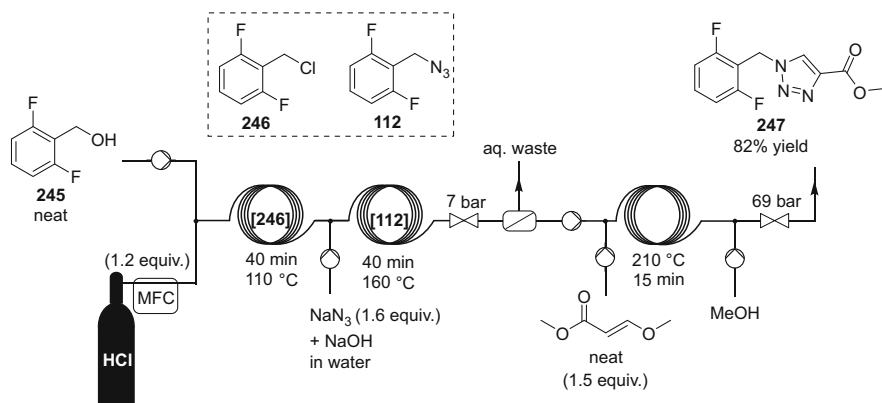


Fig. 74 Continuous-flow preparation of an advanced fragment toward rufinamide [74]

explosive hydrazoic acid. To the feed solution of NaN_3 , was thus added NaOH to neutralize HCl . A segmented regime was formed and the corresponding phases were separated through an in-line liquid–liquid separator positioned downstream the second reactor, as **112** is liquid at room temperature. Azide **112** was collected and directly mixed with neat (*E*)-methyl 3-methoxyacrylate, and reacted into a Hastelloy flow reactor, leading to **247** through 1,3-dipolar cycloaddition. (*E*)-methyl 3-methoxyacrylate is a convenient dipolarophile since it is affordable and safe by contrast with other common dipolarophiles used for preparing rufinamide (**114**). Finally, methanol was injected, and **247** crystallized in 82% yield (95 min total residence time), with a 9 g h^{-1} productivity.

3.4.4 Miscellaneous

[AR-A2] Meadows and colleagues reported a continuous Buchwald–Hartwig process using the bulky *N*-heterocyclic carbene (NHC) precatalyst $[\text{Pd}(\text{IPr}^*)(\text{cin})\text{Cl}]$ for the synthesis of a key intermediate in the preparation of AR-A2 (**250**), a drug candidate previously under development at AstraZeneca for CNS disorders [75, 76]. One of the most challenging features associated with the development of continuous-flow processes for the Buchwald–Hartwig reaction is related to the formation of salts. Various approaches were described in the literature, including the use of ultrasonic inducers coupled to continuous-flow setups. The authors first optimized the reaction at the microscale before attempting progressive implementation at the lab scale and then at the meso (pilot) scale. The microfluidic setup consisted of a T-mixer linked to a SS tube (internal diameter of 2 mm). The static mixer and the tubular reactor were immersed in a thermoregulatory bath. Reagents were conveyed to the reactor via two syringe pumps, one containing the catalyst (in toluene) and the other containing the substrates and base, i.e. arylbromide **248**, *N*-methylpiperazine and potassium *tert*-amylate in toluene solution. A first round of

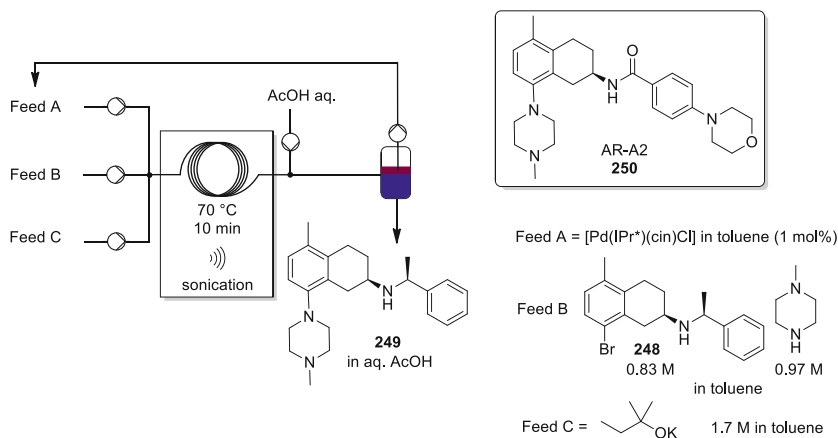


Fig. 75 Continuous-flow preparation of intermediate **249** toward AR-A2 [75, 76]

optimization indicated that full conversion was reached with 1 mol% of catalyst (corresponding to a ~0.001 M overall concentration in the reactor) at 50°C after a residence time of 45 min. The conditions were next translated to a lab scale tubular reactor made of PTFE coils (10 mL internal volume, 1.5 mm internal diameter) submerged in an ultrasonic bath at 70°C to avoid clogging. Three separate streams were employed, to segregate the catalyst from the other reagents. Feed A consisted of a solution of the catalyst ([Pd(IPr*)(cin)Cl], 1 mol%) in toluene. Bromide **248** (1 equiv.) and *N*-methylpiperazine (1.15 equiv.) were dissolved in toluene (Feed B). Feed C consisted of a 1.7 M solution of potassium *tert*-amylate kept under inert conditions (Fig. 75).

The authors also implemented a postreaction quench with aqueous acetic acid (pH 5.5) and phase separation to enable recycling of the catalyst (organic phase) from the product **249** (in aqueous phase as an acetate). After phase separation, the organic phase was redirected to Feed A. The authors reported complete conversion within a residence time of 10 min. After 30 min of operation, the conversion remained at 100%, but then dropped to 30% after 50 min of operation as a consequence of both the dilution of Feed A and the accumulation of water in Feed A, that would ultimately deactivate the catalyst. Samples of crude **249** were subjected to ICP-OES analysis, and passed with no notable amount of palladium detected. The process was next translated to mesoscale, using a cascade of CSTR reactors.

3.5 Hypertension and Cardiovascular Diseases

[Rosuvastatin] Rosuvastatin (**253**, Crestor) is a member of the superstatin family, which are among the most valued pharmaceuticals within the cardiovascular therapeutic category (cholesterol management). Scientists with Lek pharmaceuticals

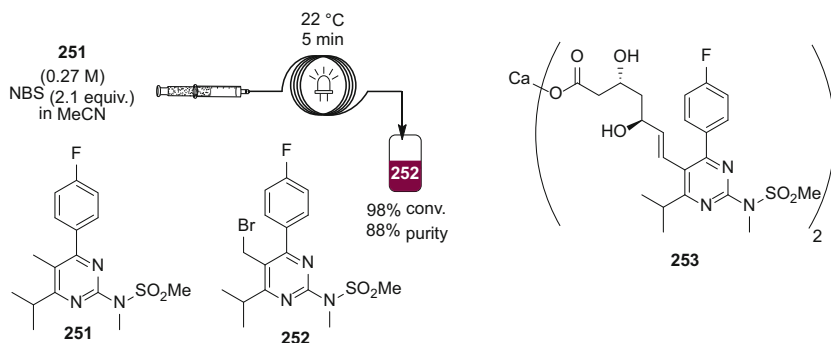


Fig. 76 Preparation of an important intermediate of rosuvastatin [77]

considered 5-methylpyrimidine **251** as a potential starting material for accessing **252** through bromination, although competitive bromination reactions at other sites are very likely to occur [77]. In order to decrease the likelihood of side reactions by overexposure, and enable large scale production, the authors developed a flow photochemical bromination of a 5-methyl-substituted pyrimidine precursor **251**. The flow reactor consisted of FEP coils (0.8 mm inner diameter, 36 m length) wrapped around a quartz cooling jacket support holding the 150 W medium-pressure Hg lamp (Fig. 76).

The feed solution containing the substrate **251** (0.27 M) and NBS (2.1 equiv.) in acetonitrile was handled by a standard syringe pump. With residence time ranging from 10 to 30 min at 22 °C, the reaction performed with high conversion (>99.8%, HPLC) and with comparable purity (~89%), very much alike the preliminary batch trials, though the productivity was up to 3.6 times higher under flow conditions. With a shorter residence time of 5 min, the conversion decreased to 98% (purity 88%). The crude reactor effluent was collected and precipitated upon addition of water. After recrystallization, compound **252** was obtained in 86% yield (93% purity).

3.6 Anesthetics and Analgesics

3.6.1 Analgesics

[Hydrocodone] Hydrocodone (or dihydrocodeinone, **256**) is a semi-synthetic opioid synthesized from codeine. It is a narcotic analgesic used orally for relief of moderate to severe pain. Kappe and coworkers reported a continuous-flow process for producing hydrocodone from thebaine (**254**) [78]. The authors developed a selective olefin reduction forming 8,14-dihydrothebaine (**255**), which was next hydrolyzed to yield hydrocodone. The reduction of olefin **254** was carried out under continuous-flow conditions using in situ generated diimide, while the hydrolysis was carried out under batch conditions (Fig. 77). The authors tested two alternative strategies for the

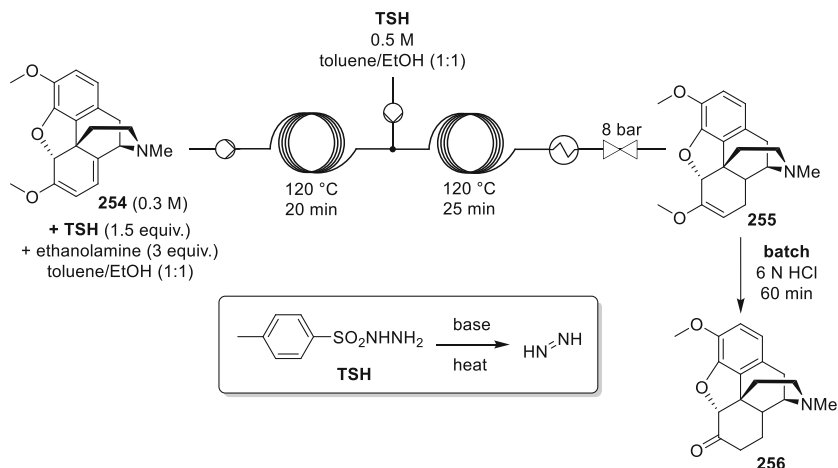


Fig. 77 Continuous-flow preparation of hydrocodone from thebaine [78]

generation of diimide: (a) the first method relied on the oxidation of hydrazine hydrate with oxygen, and (b) the second method used a rather conventional procedure using *p*-toluenesulfonyl hydrazide and a base. The first method was a priori the most atom-economic, but the authors faced unexpected side-reactions such as the competitive *N*-oxidation of thebaine (**254**) and of 8,14-dihydrothebaine (**255**). The initial experiments were carried out by a standard gas/liquid continuous-flow setup. The liquid stream was pumped via a HPLC pump and mixed with oxygen through a static T-mixer. A mass-flow controller was utilized to deliver the flow of oxygen. The gas-liquid segmented flow was next passed through a heated coil to increase the residence time. A heat exchanger and a back-pressure regulator were inserted downstream. Different materials were tested for the residence coil, such as PFA and SS. The authors noted that SS coil led to discrepancy in the results, and privileged PFA as reactor material. An additive such as dimethylsulfide or trimethylamine was necessary to decrease the competitive *N*-oxidation. Reaction parameters such as reagents ratio, temperature, pressure, residence time, and the presence of additives were thoroughly optimized, and the authors came to the conclusion that only a multi-injection of hydrazine hydrate would enable high conversion and selectivity. Although promising, the continuous-flow multi addition strategy resulted in $\geq 95\%$ conversion using up to 12 equiv. of the diimide with four liquid feeds (120 °C, 10 bar) in the presence of dimethyl sulfide. The crude reactor effluent was collected, but the remaining thebaine could not be separated from the desired 8,14-dihydrothebaine. The authors proceeded with a batch hydrolysis (6 N HCl), and obtained quantitative conversion of 8,14-dihydrothebaine (**255**) into hydrocodone (**256**), while other impurities and thebaine (**254**) remained unchanged. The second method using *p*-toluenesulfonyl hydrazide (TSH) was next investigated in the presence of ethanolamine as a base. A simple continuous-flow system was utilized at first, simply by pumping a simple feed of the reaction mixture through a

heated residence time unit (PFA). After some optimization, the conversion reached 94% conversion within 40 min at 120°C (8 bar). A multi-injection strategy involving a second feed of *p*-toluenesulfonyl hydrazide (1.5 equiv.) led to quantitative reaction within 45 min of residence time. Off-line crystallization gave pure 8,14-dihydrothebaine (**255**) in 86% as a colorless solid.

[Noroxymorphone] Kappe et al. reported a Pd-catalyzed *N*-demethylation of opioid alkaloids to form their nor-derivatives, and in particular toward noroxymorphone (**136**) (Fig. 78) [79]. **136** is a potent agonist of the μ -opioid receptor that has minimal analgesic activity (poor ability to cross BBB). Colloidal Pd(0) particles were obtained upon heating of Pd(II) acetate in *N,N*-dimethylacetamide, and were very effective catalysts for the aerobic *N*-demethylation of selected opiate alkaloids. The demethylation of 14-hydroxymorphinone 3,14-diacetate (**257**) with pure oxygen as oxidant in a continuous-flow reactor provided the demethylated product with excellent selectivity after residence times of up to 20 min (2.5–5 mol% Pd(II) acetate) on a laboratory scale. The reaction mixture containing the substrate and Pd(II) acetate in *N,N*-dimethylacetamide was pumped by a HPLC pump into a mixing unit at room temperature, where the liquid feed encountered the gas feed. The gas–liquid stream then went through a residence tube, which was heated to the desired temperature in a GC-oven. The reactor effluent was cooled in a short residence tube in a water bath and left the reactor through a back-

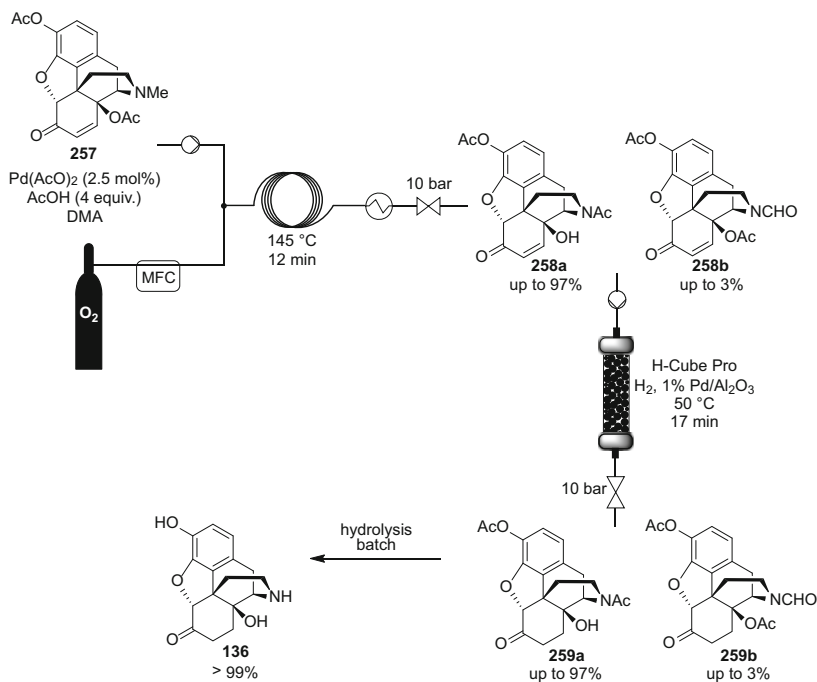


Fig. 78 Continuous-flow preparation of intermediates toward noroxymorphone [79]

pressure regulator (BPR). The reaction was improved with AcOH as additive, since it stabilizes the colloidal Pd(0) and prevents its precipitation. With 4 equiv. of AcOH, the catalyst loading was reduced to 2.5 mol% yet providing ~95% conversion of the hydroxymorphinone **257** after a 12 min residence time at 145°C (1.7 equiv. of O₂). The formation of the main side product, i.e. the *N*-formyl derivative **258b** was suppressed in the presence of AcOH. In the next step, the authors studied the implementation of the hydrogenation of 14-hydroxynormorphinone derivative **258a** toward noroxymorphone derivative **259a**. The crude mixture, dissolved in 80 mL of DMA, was pumped through a ThalesNano H-Cube Pro (1% Pd/Al₂O₃, 10 bar H₂, 50°C, 17 min residence time), 14-Hydroxynormorphinone derivative **258a** was reduced to noroxymorphone derivative **259a** (>99% conversion). Although the two steps (demethylation and hydrogenation) were not formally telescoped during the lab scale optimization, the raw effluent of the demethylation step could be directly utilized in the hydrogenation step. The process was next translated to kg-scale, and the sequential oxidation and hydrogenation in flow as well as a final hydrolysis in batch afforded noroxymorphone (**136**) in high quality and good yield.

3.7 Inflammation

[CCR1 antagonist] A research team with Boehringer Ingelheim Pharmaceuticals reported a convergent, robust, and concise synthesis of an important intermediate en route toward potent CCR1 antagonist **264** using continuous-flow technology [80]. **264** is an investigational active pharmaceutical ingredient (API) in development as an oral, efficacious treatment option for rheumatoid arthritis. The strategy relied on a sequence of acyl azide formation and Curtius rearrangement for the preparation of intermediate isocyanate **262**, which would eventually be quenched with an alcohol to form carbamate **263**. The authors studied other potential routes as well. A Uniqsis coil flow reactor was utilized for the optimization of important process parameters such as relative flow rates, residence time, and temperature for the formation of intermediate acyl azide **261** (Fig. 79). The optimized conditions involved two feed solutions: (a) DPPA in toluene and (b) a solution containing carboxylic acid **260**, triethylamine and *p*-methoxybenzyl alcohol (PMBOH) in toluene.

A kinetic and mechanistic study emphasized that the capture of the intermediate isocyanate **262** with PMBOH was actually faster than the Curtius rearrangement at 135°C in superheated toluene. Carbamate **263** was obtained in 90% yield after a residence time of 3 min. In-line FTIR monitoring was utilized for real-time monitoring of the flow process, and it was successfully utilized on a multi-kg scale. Carbamate **263** was next processed to form CCR1 antagonist **264**. The authors also envisioned an alternative semi-continuous synthesis of **264** wherein the intermediate isocyanate **262** generated under flow conditions would flow directly into a batch

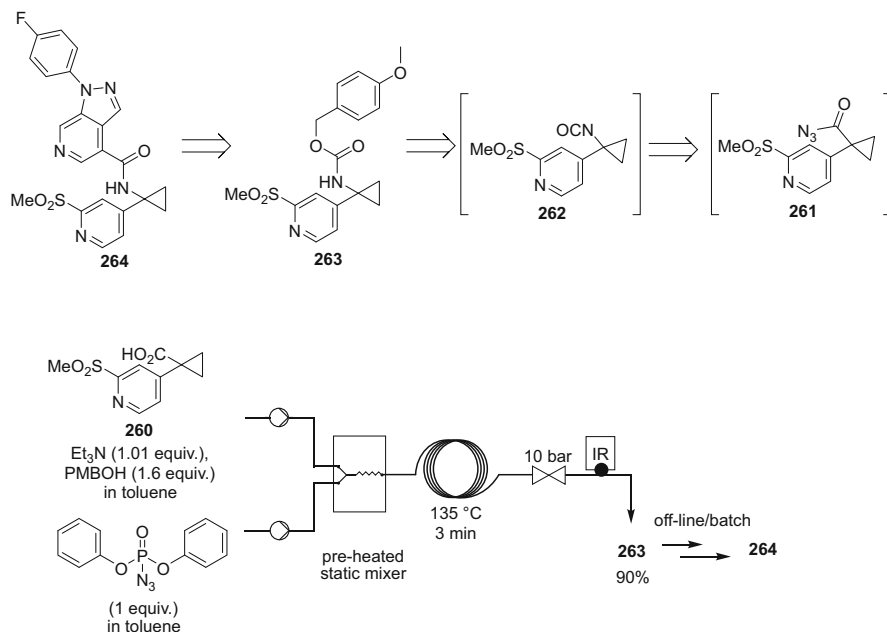


Fig. 79 Preparation of an intermediate toward CCR1 antagonist **264** [80]

vessel containing a mixture of acid precursor and NEt_3 to promote the direct coupling. Amide **264** was obtained in 76% accordingly.

[Etodolac] 7-Ethyltryptophol (**267**) is a pivotal intermediate for the synthesis of the clinically effective analgesic and anti-inflammatory drug etodolac (**268**). Etodolac (**268**) has an outstanding safety profile with respect to the gastrointestinal and renal tract, and also retards the progression of skeletal changes in rheumatoid arthritis. Based upon a thorough mechanistic study and reaction optimization, Su and colleagues developed an efficient telescoped process toward 7-ethyltryptophol (**267**) (Fig. 80) [81]. The process implies the formation of a hydrazone intermediate **266** and a subsequent [3 + 3] sigmatropic rearrangement. A feed solution of intermediate **265** in ethylene glycol/water (5:2) was mixed with a stream of 4-hydroxybutyraldehyde (1 equiv.) in ethylene glycol/water (5:2), and reacted for 20 s at $115\text{ }^\circ\text{C}$ within the first reaction loop (Hastelloy tube, 7 mm o.d., 6 mm i.d.), immediately followed by the introduction of 50% aqueous sulfuric acid and reaction into the next reaction loop for 4 min of residence time at $115\text{ }^\circ\text{C}$ (Hastelloy tube, 7 mm o.d., 6 mm i.d.). The reactor effluent was next cooled by passing through a cooling loop, and the reaction was quenched by collecting the reactor effluent in a batch vessel containing 30% aqueous NaOH. Further batch processing included removal of ethylene glycol by extraction into water, and **267** was extracted by MTBE. 7-Ethyltryptophol (**267**) was isolated in 75% yield (98% purity). Yield and purity were much improved under continuous-flow conditions by comparison with the batch process, and key to success was the accurate temperature control.

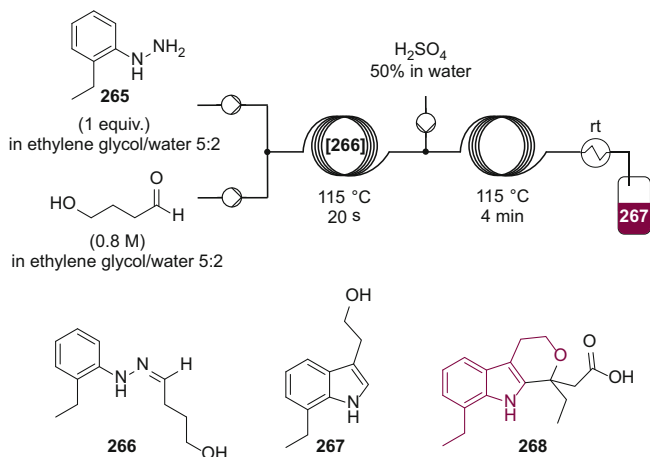


Fig. 80 Preparation of 7-ethyltryptophol as an intermediate toward etodolac [81]

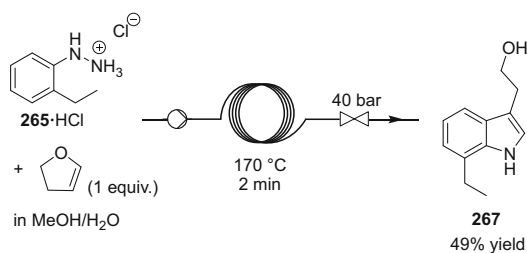


Fig. 81 Preparation of 7-ethyltryptophol as an intermediate toward etodolac [82]

Kappe and coworkers also studied the preparation of 7-ethyltryptophol (**267**) under continuous-flow conditions (Fig. 81) [82]. The reaction proceeds through opening of 2,3-dihydrofuran into 4-hydroxybutyraldehyde, which undergoes Fischer indolization with 2-ethylphenylhydrazine (**265**). The impact of different parameters, such as the presence or absence of an acid or base catalyst, as well as the effect of temperature and reaction time, was studied. It was found that the yield could never exceed about 50%, but the reaction was implemented in environmentally-friendly solvents, under catalyst-free conditions and in a simple Hastelloy tubing. Most notably, by-products were eliminated after a straightforward process. A mechanistic rationalization, based on the identification of by-products and computational investigation, was proposed.

3.8 Miscellaneous

[Dantrolene] Kappe and colleagues reported a photochemical methodology for the C-H arylation of (hetero)arenes. The method was amenable to the preparation of intermediates for the synthesis of dantrolene (**272**, Dantrium), a muscle relaxant, and

for the synthesis of canagliflozin (**270**), a drug used in the treatment of diabetes [83]. Anilines were converted into the corresponding nitrosamines from treatment with *tert*-butylnitrite, and these species were in a dimerization equilibrium with their diazo anhydrides. The latter were decomposed by UV light into the corresponding aryl radicals, which finally reacted with (hetero)arenes to yield the target bis (hetero) aryls (Fig. 82).

At first, the reaction between thiophene and *p*-chloroaniline was studied in batch and it was shown that neither a photocatalyst nor a Lewis acid catalyst was necessary for the reaction to occur. The reaction was then transposed to continuous-flow conditions, using FEP tubing wrapped around a medium-pressure Hg lamp equipped with a wavelength filter. The substrate scope was extended to other substituted anilines and (hetero)arenes. Most notably, the preparation of 2-(4-fluorophenyl) thiophene (**269**), an important intermediate in the synthesis of canagliflozin (**270**), was demonstrated with 74% yield. Similarly, the preparation of 2-(4-nitrophenyl) furaldehyde (**271**), which is an intermediate for dantrolene (**272**) preparation, was demonstrated with 56% yield.

[Vildagliptin] Vildagliptin (**276**) is an antihyperglycemic drug used in the treatment of diabetes. A key step involves the dehydration of amide **273** into nitrile **274**, mediated by Vilsmeier's reagent (VR). However, the latter is highly reactive and moisture sensitive, precluding applications in large-scale batch processes. Sedelmeier and Pellagetti optimized the preparation and use of VR in a telescoped continuous-flow process to avoid handling of this hazardous material [84]. The flow reactors were constructed from PFA coils, suitable to handle the low pH medium related to the preparation of VR (Fig. 83).

VR preparation was initially studied under batch conditions using various agents such as $(\text{COCl})_2$, SOCl_2 or POCl_3 , and the latter was selected for further flow optimization. The continuous-flow preparation of VR was then telescoped with the dehydration of amide **273**, which was conducted in a tube reactor packed with glass

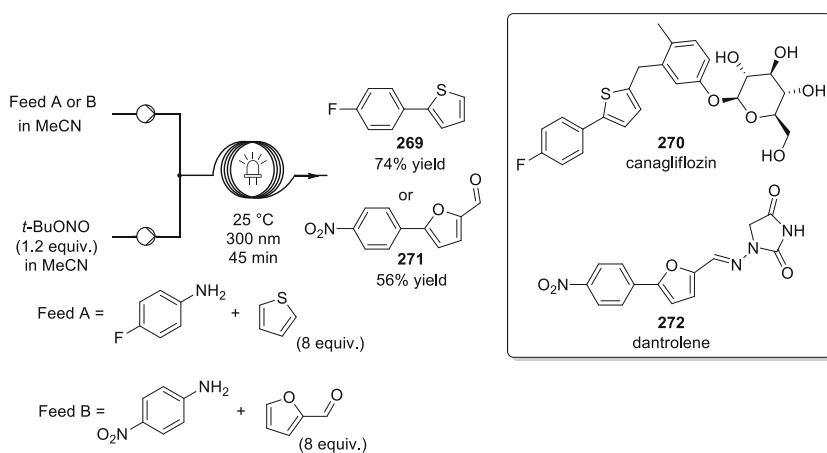


Fig. 82 Intermediates for the preparation of canagliflozin and dantrolene [83]

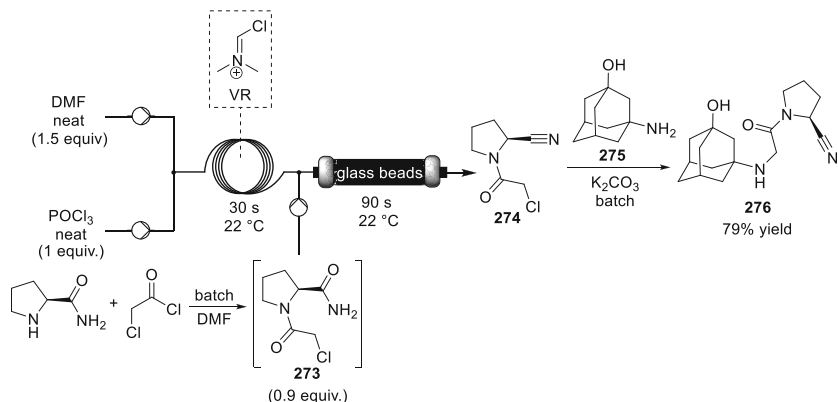


Fig. 83 Preparation of an advanced fragment of vildagliptin [84]

beads to improve mixing efficiency. The crude substrate undergoing dehydration was prepared from L-proline amide and chloroacetyl chloride in batch. The two-step telescoped process afforded the target nitrile **274** in 79% yield (99% purity after off-line crystallization). Vildagliptin (**276**) was finally obtained by reacting **274** with adamantane **275** under batch mode, with 79% yield starting from L-proline amide.

4 Miscellaneous

This section gathers representative examples dealing with the total synthesis of biologically active compounds inspired from natural compounds, the preparation of derivatives of known APIs or libraries of highly potent molecules using multistep continuous-flow procedures.

4.1 Biologically Active Compounds Inspired from Natural Compounds

[Histrionicotoxins] Histrionicotoxins are a class of toxins found in poison frogs, which are non-competitive inhibitors of the neuromuscular, ganglionic and nicotinic acetylcholine receptors. Brasholz and colleagues prepared tricyclic dinitrile precursor **279** of these toxins under continuous-flow conditions, using a previously reported batch procedure [85]. The first step aimed at converting dicyano ketone **277** into the corresponding oxime in the presence of hydroxylamine, which directly underwent Michael addition and 1,3-dipolar cycloaddition to give 6,5,5-tricyclic intermediate **278**. Compound **278** was next subjected to thermal 1,3-dipolar cycloreversion-cycloaddition, affording 6,6,5-dinitrile precursor **279**. At an early

stage of their study, the authors developed a batch strategy for the gram-scale preparation of ketone **277** (Fig. 84) [85]. The preparation of **278** was then implemented under continuous-flow conditions, by injecting and heating at 50°C a solution containing ketone **277**, hydroxylamine hydrochloride and sodium acetate. Compound **278** was obtained in 67% yield. The purified material was then subjected to thermal rearrangement at 180°C in a home-made MW-heated continuous-flow reactor, and **279** was obtained in 72% yield. Telescoping of the two steps was then implemented. At first, a two-stage process was investigated, implementing a 150°C heated reactor positioned after a packed bed of supported DMAP, which served as substitute for sodium acetate. However, **279** was obtained in about 15% yield, highlighting epimerization triggered by the excess of hydroxylamine and degradation. To alleviate this issue, a sequential 4-stage telescoped process was considered, where the solution was subsequently flowed over supported-DMAP, heated at 50°C, flowed over supported acetoacetate as scavenger for hydroxylamine, and finally heated at 160°C. This modified procedure improved the yield up to 31%. However, the best results were obtained when a lower excess of hydroxylamine was utilized in the presence of sodium acetate, and when the solution was heated in a two-stage telescoped process without packed bed reactors (Fig. 84). Precursor **279** was obtained in 48% yield accordingly.

The same authors designed a batch and flow total synthesis of (–)-perhydrohistrionicotoxin (**288**), another representative of the histrionicotoxin class [86]. The *n*-pentyl-substituted 6,6,5-tricyclic isoxazolidine precursor **287** was prepared under batch conditions using an eight-step synthesis. Several steps were implemented in continuous-flow reactors to improve the methodology (Fig. 85). Lithiation of starting alkyne **280** with *n*BuLi was performed in the first reactor at 0°C, while –78°C was required in batch. More than 30 min was required for the reaction to reach completion. The reactor effluent containing the lithiated alkyne was mixed with a stream of racemic 6-pentyltetrahydropyran-2-one, which underwent ring opening, and alcohol **281** was obtained using standard batch work-up. Next, total hydrogenation of **281** into **282** was conducted in a H-Cube reactor equipped with a cartridge packed with Pd(OH)₂ supported on carbon, in the presence of

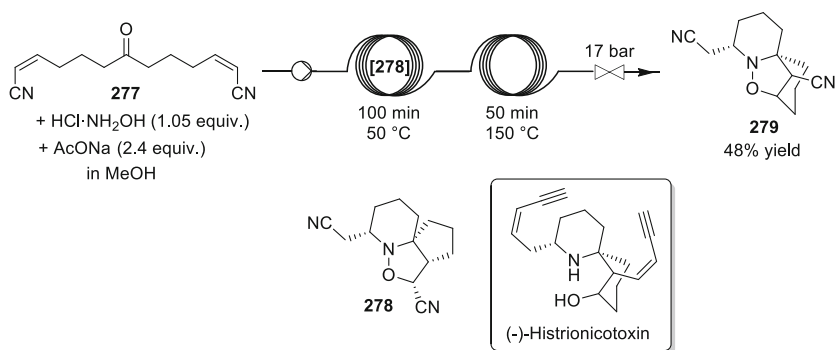


Fig. 84 Continuous-flow preparation of a precursor of histrionicotoxins [85]

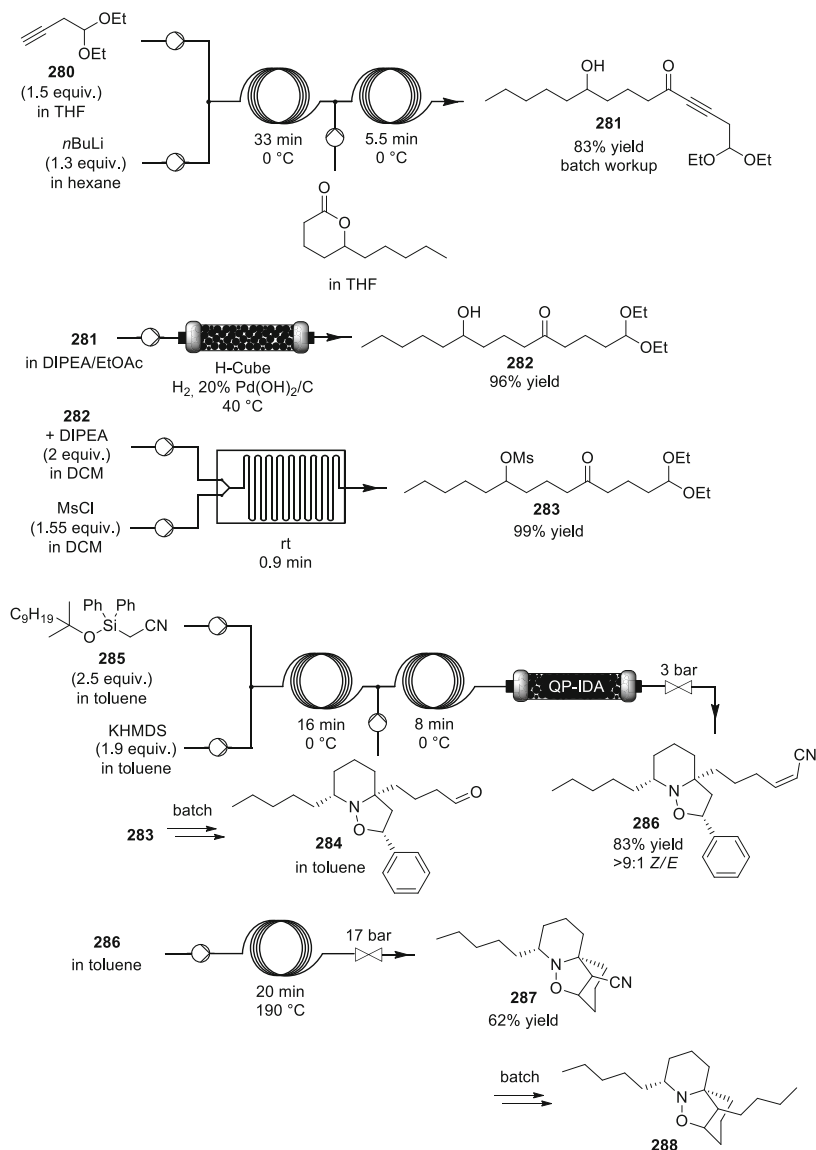


Fig. 85 Sequential, semi-continuous preparation of an advanced intermediate toward histrionicotoxin [86]

DIPEA. As the continuous hydrogenation was relatively unaffected by impurities, it was telescoped to the lactone ring-opening step. However, clogging occurred at some point due to precipitation of LiOH. LDA was considered as an alternative to *n*BuLi and, while it alleviated the clogging issue, it led to incomplete lactone

conversion (60%). Therefore, the sequential process was preferred for the preparation of **282**.

The next step involved mesylation of alcohol **282**, in the presence of DIPEA, which took place within 1 min of residence time in a glass fluidic chip. The subsequent transformation of **283** through oxime formation, intramolecular nucleophilic displacement of the mesylate, and 1,3-dipolar cycloaddition with styrene was conducted in a one-pot MW batch process, affording the target acetal precursor of **284**. After acetal cleavage under classical batch conditions, aldehyde **284** underwent Peterson olefination within a telescoped continuous-flow reactor. By comparison to the batch procedure, the silylated reagent was modified to simplify the next step involving purification by column chromatography, and the reaction was conducted with KHMDS in toluene to avoid clogging. The silylated reagent **285** was mixed in a first reactor with a stream of KHMDS, and **284** was injected before the second reactor, where the coupling reaction occurred. The reactor effluent was quenched by passing through a column packed with supported dicarboxylic acid, affording **286** in 83% yield and >9:1 *Z/E* ratio. Purified **286** was then injected in a stainless steel coil reactor, where it underwent thermal cycloreversion-cycloaddition toward racemic precursor **287**. After separation of the enantiomers of **287**, the last three steps of the synthesis, namely, DIBAL reduction, Wittig olefination, and hydrogenation, were conducted in batch, affording (–)-perhydrohistrionicotoxin (**288**).

[Siphonazole] Ley and coworkers designed a combined batch and flow synthesis of *O*-methyl siphonazole (**297**) (Fig. 86), a natural product with a potentially interesting biological activity profile [87]. The first step concerned the coupling of dimethoxycinnamic acid (**289**) with threonine *tert*-butyl ester hydrochloride under continuous-flow conditions in the presence of CDI. The reactor effluent containing compound **290** was then mixed with a stream of diethylaminosulfur trifluoride, and reacted in a second reactor to cyclize into oxazoline **291**. The effluent was passed through a column packed with supported scavengers, such as a sulfonic acid, a tertiary amine, CaCO₃ and SiO₂, which sequestered triethylamine, imidazole, the unreacted protected threonine, the unreacted acid, DAST and HF, respectively. Compound **291** was obtained in 90% yield (>95% purity). Solvent swap from DCM to MeCN was performed off-line, and **291** was oxidized into the corresponding oxazole **292** in another continuous-flow reactor in the presence of DBU and BrCCl₃. The reactor effluent was then directly passed through a heated column packed with supported sulfonic acid to induce cleavage of the *t*-Bu ester protecting group.

Carboxylic acid **293** was obtained in 90% yield, and could be converted into the corresponding acyl chloride **294** under standard batch conditions. Precursors of the oxazole central fragment were also prepared under batch conditions, and were coupled with **294** through a Claisen condensation both under batch and continuous-flow conditions. For instance, **294** was coupled with oxazole nitrile **295** using a supported phosphazene base, and LiBr was added to the feed to avoid scavenging of the enolate, creating a strongly chelated and soluble lithium enolate **296**. The last steps of the process were eventually all conducted in batch. Although the resulting nitrile adduct from the Claisen condensation underwent smooth

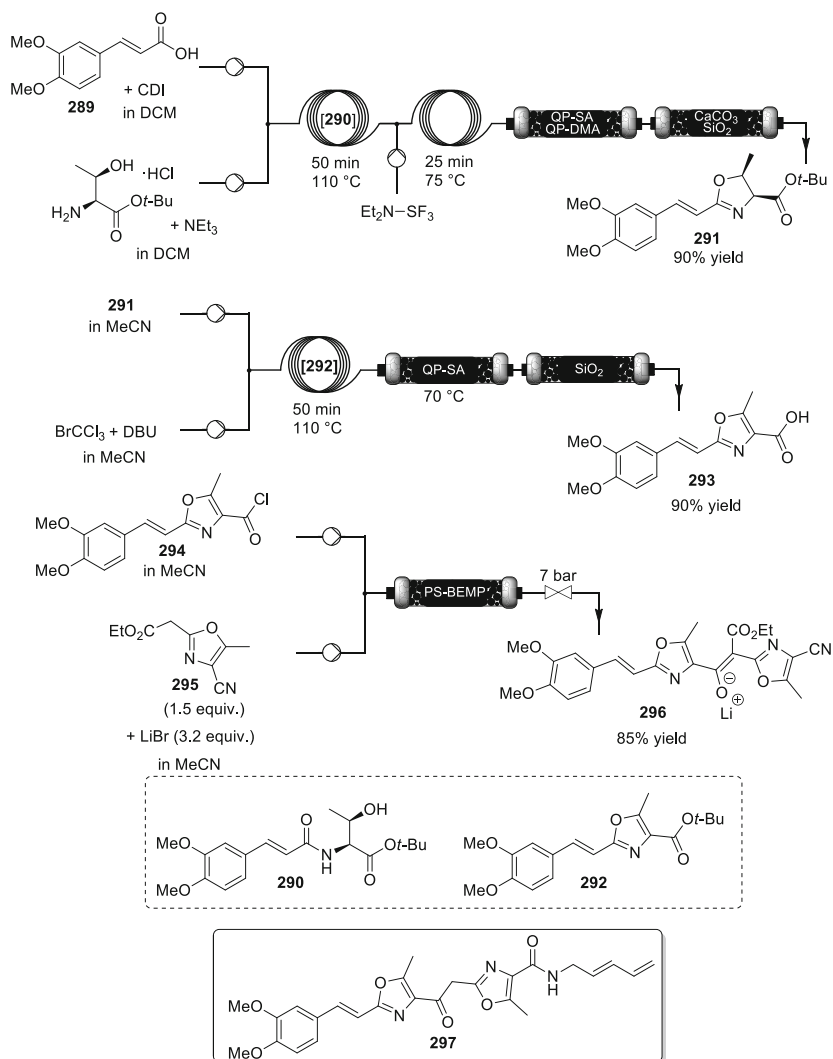


Fig. 86 Sequential, semi-continuous preparation of an advanced intermediate toward siphonazole [87]

decarboxylation with 73% yield over two steps, the hydrolysis of the nitrile function into the corresponding carboxylic acid failed. Alternatively, the corresponding phenyl ester adduct gave a lower 40% yield after decarboxylation. The hydrolysis into the acid, followed by the coupling with pentadienyl amine in the presence of TBTU afforded the target *O*-methyl siphonazole (**297**) in 47% yield (two steps).

[Dumetorine] (+)-Dumetorine (**303**) is a natural product with an interesting biological activity. Martinelli and colleagues designed a sequential continuous-flow protocol for the preparation of **303** (Fig. 87) [88]. At first, *N*-Boc-(*S*)-2-

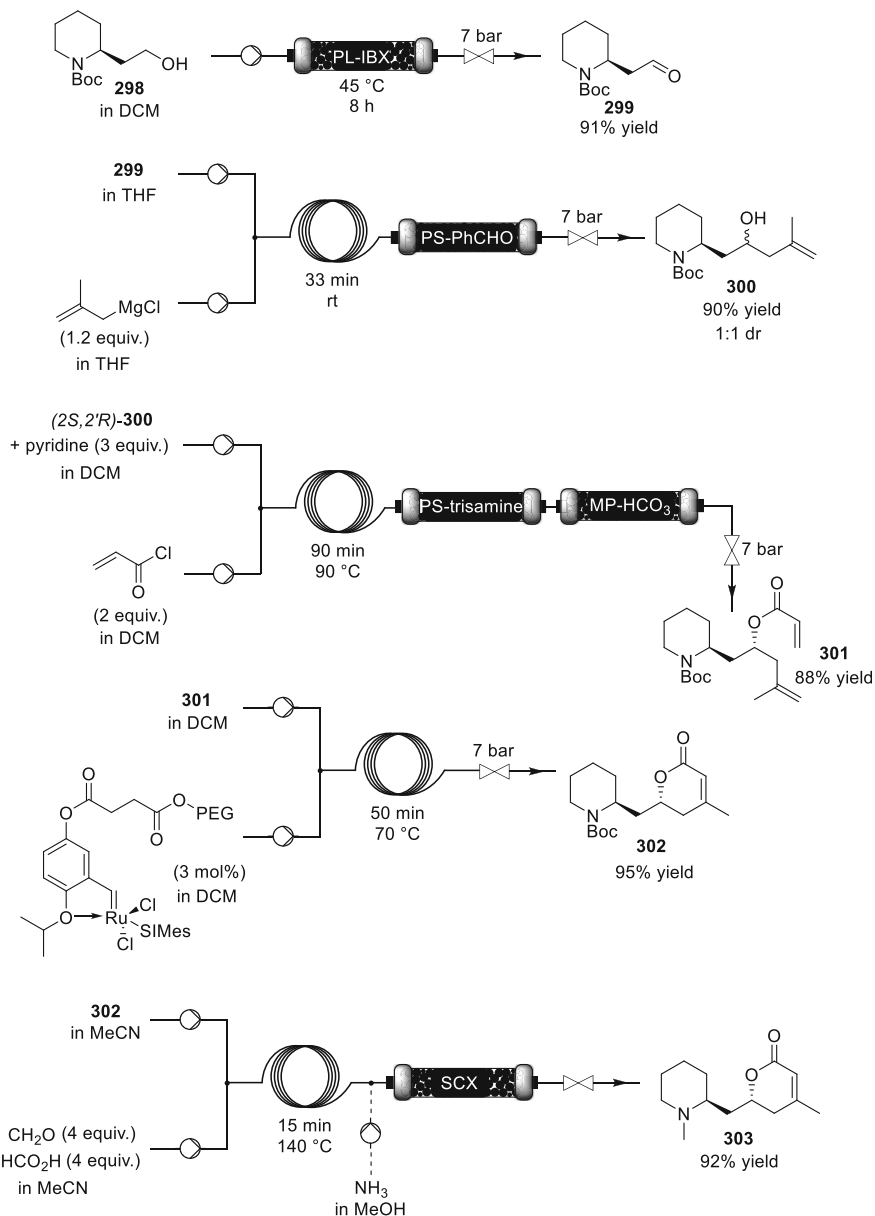


Fig. 87 Sequential, continuous-flow protocol toward dumetorine [88]

(piperidin-2-yl)ethanol (**298**) was oxidized into aldehyde **299** using supported PL-IBX amide in a packed-bed reactor. The feed was cycled for 8 h at 45 °C until complete conversion was achieved, affording **299** in 91% yield. Then, addition of 2-methylallylmagnesium chloride on **299** was efficiently conducted at room

temperature. A column packed with PS-supported benzaldehyde was inserted downstream the reactor to quench excess of Grignard reagent, and **300** was obtained in 90% combined yield with approximately a 1:1 ratio of diastereomers. The (2*S*,2'*R*) isomer of **300** was isolated by chromatography and injected in the subsequent setup, where it was acylated with acryloyl chloride. The exiting stream was passed through a column packed with PS-supported trisamine as scavenger for the excess acryloyl chloride, and through a bed of supported bicarbonate to quench pyridinium chloride. Pure **301** was obtained accordingly in 88% yield, and was then subjected to ring closing metathesis toward **302**. The RCM step was conducted by injecting and mixing solutions of **301** and of a PEG-supported Hoveyda catalyst. The catalyst was recyclable up to six times before minor deactivation was observed, by straightforward precipitation and filtration cycles. Finally, the *N*-Boc protecting group of **302** was cleaved, and alkylation of the free amine through Eschweiler–Clarke reaction took place in the last continuous step, where the target (+)-dumetorine (**303**) was then trapped over silica-supported sulfonic acid. The column was washed with MeOH, and **303** was released while eluting with NH₃/MeOH.

This “catch-and-release” procedure afforded **303** in 92% yield (>98% purity). Overall, the procedure afforded (+)-dumetorine (**303**) in 29% yield, while only 1% yield was obtained using batch conditions.

4.2 Derivatives of Known APIs

[Amoxapine and fenofibrate derivatives] Roesner and Buchwald developed a continuous-flow process for the preparation of fluorobiaryls using PFA capillary reactors (Fig. 88) [89].

Substituted fluoro- and trifluoromethylbenzenes first underwent regioselective lithiation in the presence of *n*BuLi and *t*BuOK at –40°C. The corresponding lithiated intermediates were then subjected to transmetalation by injection of ZnCl₂ in the second telescoped reactor, which was also operated at –40°C. Finally, Negishi coupling with arylbromides, in the presence of Pd XPhos G3 precatalyst was performed in the third telescoped reactor. Sonication was implemented in this final stage to avoid precipitation of inorganic species and clogging. Upon optimization, the total residence time in the fully telescoped setup was only of 15 min. Fluoropyridine substrates were also considered, which required system reoptimization. Indeed, although fluoropyridines could be efficiently lithiated with LDA in the absence of *t*BuOK at 0°C, clogging occurred after zinc chloride injection, and the solvent was thus switched to THF instead of 2-MeTHF. The modified setup also involved shorter total residence times (5–11 min). The substrate scope included fenofibrate (**304**), a cholesterol level-modulating drug and amoxapine (**305**), an antidepressant, which were coupled with 2,5-difluoropyridine to afford **306** and **307** in 95% and 72% isolated yields, respectively.

[Nucleosides] Nucleosides and their analogs are a well-established and important class of highly potent antiviral and anticancer agents. Jamison and coworkers

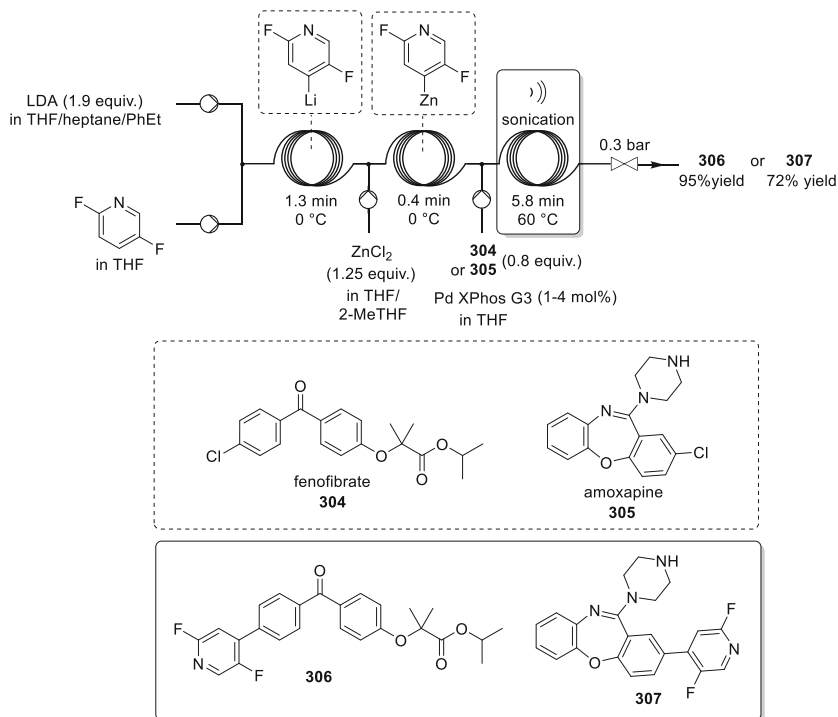


Fig. 88 Continuous-flow preparation of derivatives of fenofibrate and amoxapine [89]

reported a telescoped continuous-flow procedure with high product yield and short reaction time, using pyridinium triflate derivative **3** as catalyst [90] (see also Sects. 2.1 and 2.2). The conditions involved reacting readily available ribofuranose derivatives and silyl-protected nucleobases, in the presence of 2,6-di-tert-butyl-4-methylpyridinium triflate (**3**), at temperatures ranging from 100 to 150 °C within minutes of residence time and ~7 bar of counter-pressure (Fig. 89).

The procedure was amenable to the preparation of small libraries of nucleoside analogs. Preliminary trials and optimization were carried out in PFA capillary coils (500 μm internal diameter). Scalability of the reaction was demonstrated by transferring the optimized conditions to a commercially available flow system (Vapourtec), and a productivity of up to 7.4 g h⁻¹ was obtained accordingly. The authors next turned their attention to the development of a telescoped multistep process for the preparation of fully deprotected nucleosides. The deprotection step was carried out using methanolic NaOMe (0.15 M), affording high yields of deprotected nucleosides (up to 95%) within 8 min. The continuous-flow process is illustrated above for the preparation of adenosine (**308**).

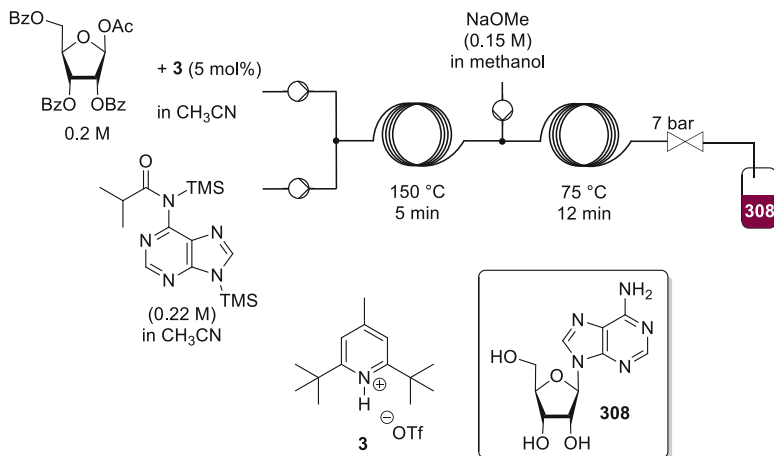


Fig. 89 Preparation of nucleosides under telescoped continuous-flow conditions [90]

4.3 Libraries of Highly Potent Molecules

[CKI] Imidazo[1,2-*b*]pyridazine derivatives **312** are inhibitors of casein kinase I- ϵ , and have therefore the potential to treat mood disorders and modulate sleep. Ley and coworkers prepared 20 compounds belonging to this class, using sequential continuous-flow synthesis (Fig. 90) [91]. The procedure was optimized for the preparation of four chloro-substituted precursors **311**, and these were then functionalized with various amines by S_NAr, leading to a library of 20 derivatives bearing general structure **312**. The reaction sequence started with the addition of an organolithium reagent to an ester for the preparation of the corresponding ketones **309**. These reactions required a strict temperature control to avoid side reactions and hot spots. A dual sample injection loop system was devised, which enabled the injection of a continuous and steady stream of the lithium base to the reactor under cryogenic conditions. Using this delivery system, a 0 °C solution of LiHMDS was mixed with a stream of the ethyl ester and 4-methylpyridine or 4-methylpyrimidine, affording ketones **309** in 79–94% yield. The reaction failed when 2-methylpyridine was processed, most likely as a consequence of a competitive nucleophilic addition. To address this issue, a –78 °C solution of *n*BuLi was employed, resulting in an efficient transformation toward the desired material. The next step concerned the α -bromination of ketones **309** using a column packed with PS-supported pyridine hydrobromide perbromide. Accurate control of the residence time inhibited the competitive formation of dibrominated species, and derivatives **310** were obtained in quantitative yield. Next, **310** were reacted with 3-amino-6-chloropyridazine under continuous-flow toward imidazopyridazines **311**. The reactor effluent was next passed through a column packed with K₂CO₃.

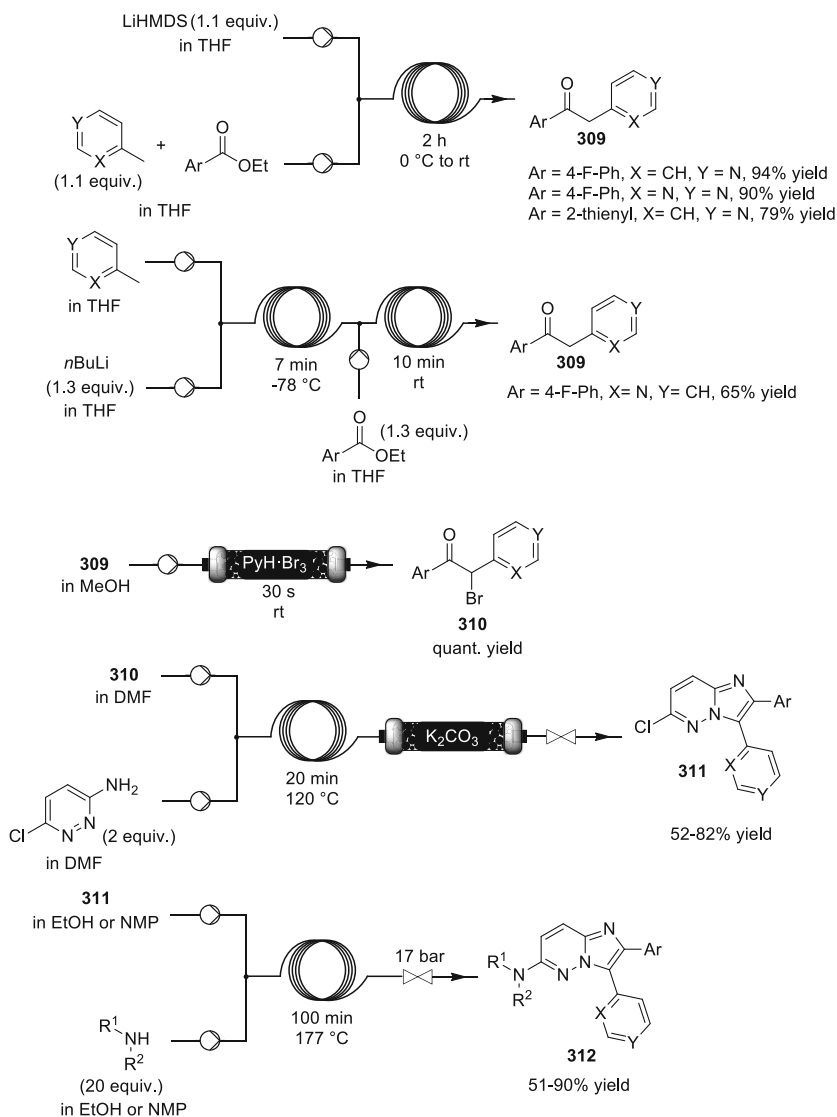


Fig. 90 Sequential continuous-flow preparation of a library of casein kinase I- ϵ inhibitors [91]

The last step concerned the functionalization of **311** by reaction with various amines, giving compounds **312** in 51–90% yield. The setup for the final step was fully automated, including an autosampler and a fraction collector.

[BCP modulators] Researchers at the University of Durham reported a continuous-flow process for the preparation of a library of key building blocks for the synthesis of Bromodomain-containing proteins (BCP) modulator libraries

[92]. BCPs are considered as relevant therapeutic targets with potential applications in oncology and the treatment of neurological as well as inflammatory diseases. The process relied on dynamically mixed flow reactors, a technology that enables processing of slurries and suspensions while maintaining high productivity (Fig. 91). The authors used an AM Technology Cofflore[®] ATR equipped with ten interconnected tubes (internal volume of 1 L) and an internal dynamic mixer generating a turbulent flow stream through lateral shacking. Intermediate **313** was obtained through a sulfuric acid-promoted deacylation of dehydroacetic acid. Compound **313** was isolated and next reacted with diazonium species **314** within a telescoped convergent process. There are several challenges that are inherently related to this reaction. The initial diazo coupling reaction is strongly exothermic, and, besides, some diazonium salts are unstable, thus affecting the impurity profile. Additional issues were related to the formation of CO₂ and the insolubility of some materials. The details of the flow process are given below. Diazonium compound **314** was obtained in a first coil by mixing an aqueous solution of NaNO₂ (0.4 M) and 4-bromoaniline (0.33 M in aqueous HCl) through a static T-mixer. **314** was obtained in quantitative conversion, and the reactor effluent was fed through a secondary input into a series of dynamically mixed flow reactors. In the first section, diazonium salt **314** was coupled with intermediate **313** in the presence of a substoichiometric quantity of K₂CO₃ (0.65 equiv.) Intermediate **313** could be easily processed within 10 min of residence time. The subsequent intramolecular cyclization involved the successive injection of aqueous K₂CO₃ (1.5 M) to promote the conversion of hydrazone **315** to the final pyridazone **316**. A total residence time of 53 min at

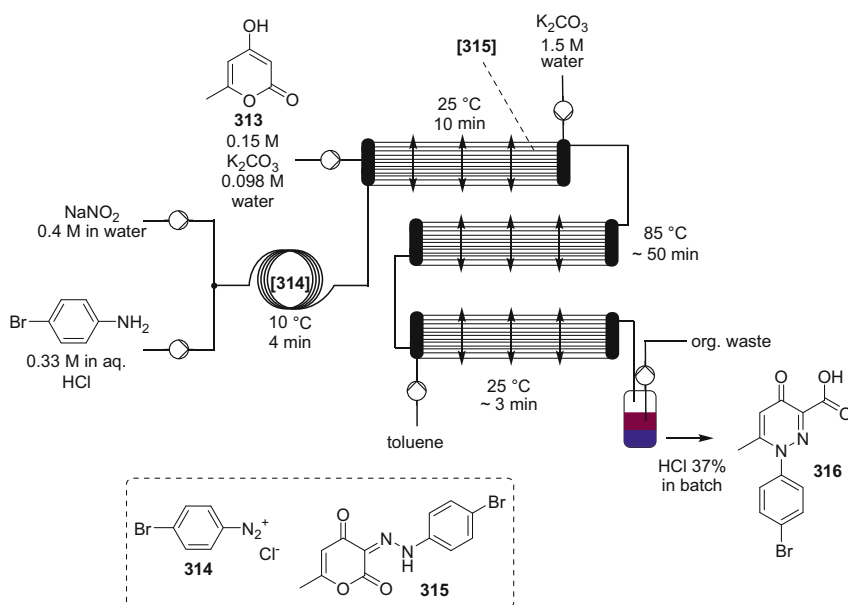


Fig. 91 Preparation of a library of BCP modulators [92]

85°C was necessary. Downstream processing was carried out in batch, affording compound **316** in 73% isolated yield. The scope was then extended to the preparation of other derivatives.

[Library of ligands for chemokine receptor CCR8] Ulven and colleagues designed multistep continuous-flow processes for the preparation of a chemical library of ligands for chemokine receptor CCR8 with anti-inflammatory potency (Fig. 92) [93, 94]. In an earlier attempt, a continuous-flow setup featuring supported scavengers was considered [94]. The first stage of the setup aimed at coupling a monoprotected diamine with an isocyanate to form ureas of general structure **317**. The excess isocyanate was subsequently trapped on PS-supported trisamine packed in a column downstream the reactor. *N*-Cbz-deprotection was attempted on **317** using a H-Cube flow reactor equipped with a cartridge packed with Pd/C to afford **318**. The effluent of the hydrogenation reactor was then mixed with a stream of benzyl bromides **319** in the presence of supported *N*-methylmorpholine. Finally, the reactor effluent was passed through a column packed with PS-supported trisamine for scavenging the excess **319**, affording **320**. However, although good results were obtained for the preparation of the target compounds **320**, the productivity was hampered by the inherent properties of supported scavengers. Indeed, at some point, they became saturated, and the system required manual intervention to replace the packing materials. Utilization of larger columns did not solve this issue as a chromatographic effect was observed, decreasing even further the efficiency of the system. The setup was modified accordingly, and the packed columns were removed. A stoichiometric amount of the isocyanate material was loaded in the first feed to eliminate the necessity for scavenging the excess. Also, the packed bed of supported *N*-methylmorpholine was replaced by a more cost-effective Na₂CO₃/sand bed, and the final trisamine column was removed as **320** were anyway purified by column chromatography. A library of compounds **320** was obtained accordingly, with moderate to excellent 49–94% yields. Besides, the process was highly flexible and versatile.

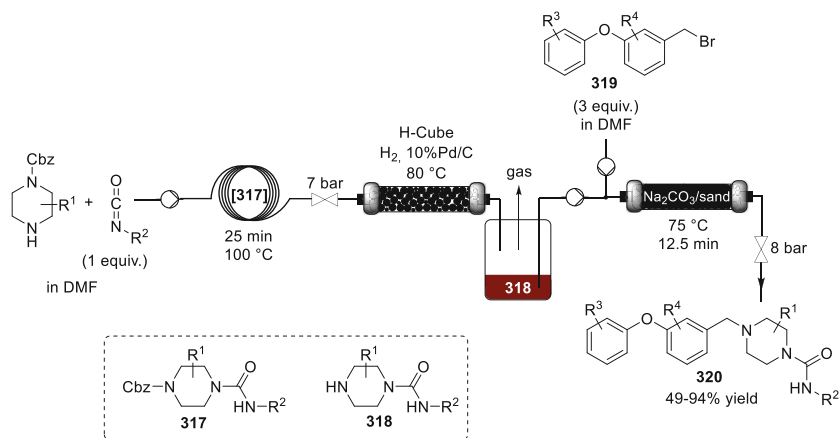


Fig. 92 Continuous preparation of a library of ligands for chemokine receptor CCR8 [93]

[Hepatitis C virus translation inhibitor] Kappe and coworkers generated BrCN, a highly toxic yet versatile reagent, under continuous-flow conditions and subsequently used it in the telescoped preparation of cyclic guanidines and 2-aminobenzoxazoles (Fig. 93) [95]. BrCN was first generated by reacting an aqueous solution of Br₂ with an aqueous solution of KCN. It was then extracted by injection of DCM, and the organic phase was separated from the aqueous phase using a membrane-based liquid–liquid separator. In-line IR spectroscopy monitored the generation of BrCN, that was then reacted with the substrate. The substrate was injected as MeOH solution to avoid precipitation of the hydrobromide salt upon consumption of BrCN. The methodology was most notably applied to the preparation of the hydrobromide salt of a potential hepatitis C virus translation (HCVT) inhibitor **322** using diamine **321** as a substrate. **322** was obtained in 87% yield using 1.16 equiv. of BrCN. The generation of Br₂ was also implemented and telescoped upstream, but not applied to the preparation of the API.

[DHPM] Cosford and colleagues used a microfluidic assembly for the preparation of a small library of dihydropyrimidinone (DHPM) derivatives **326**, which have been reported to be active against HIV [96, 97]. The authors utilized a Syrris AFRICA continuous-flow synthesis station. The process relied on a three-step reaction (thiazole formation/deprotection/Biginelli reaction), two-chip sequence (Fig. 94). Two feed solutions containing thioamide **323** (typically 0.45 M in DMF) and α -bromoketones (typically 0.45 M in DMF), respectively, were injected in a 250 μ L microfluidic reactor operated at 150°C with a residence time of about 4 min. The reactor effluent, which contained compounds **324** with a ketothiazole scaffold, was next mixed with a third stream containing 3-hydroxybenzaldehyde and ureas **325** (0.54 M in DMF), and the corresponding mixture was reacted in a 1,000 μ L internal volume microreactor operated at 200°C (10 min residence time).

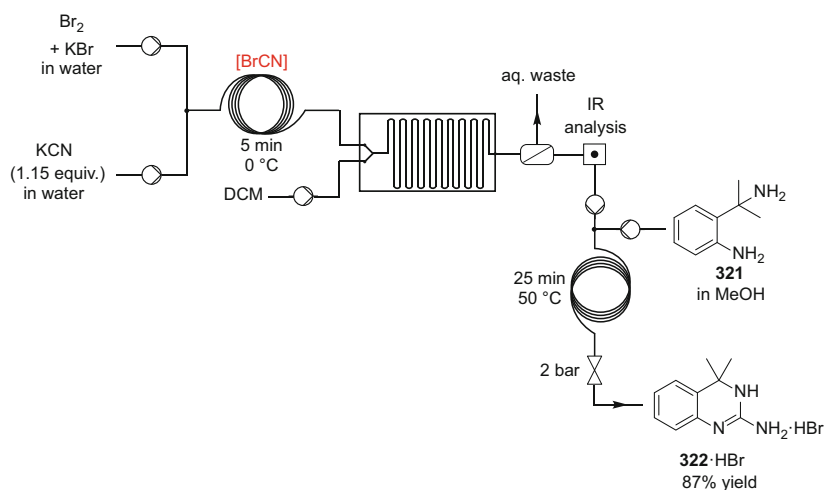


Fig. 93 In situ generation of BrCN and preparation of a hepatitis C virus translation inhibitor [95]

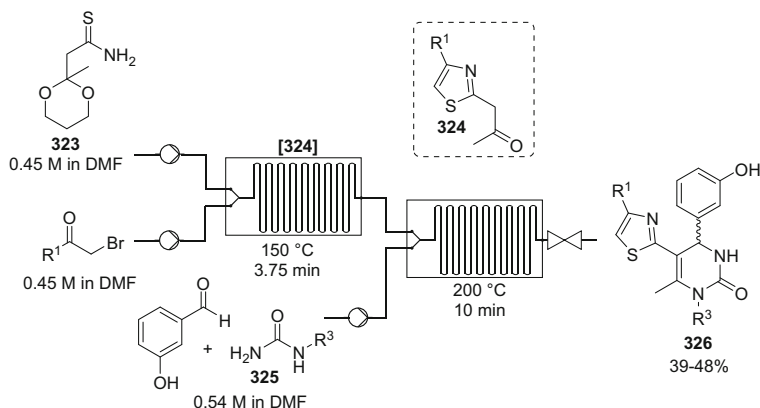


Fig. 94 Preparation of a library of DHPM derivatives using a three-step two-chip sequence [96]

Identical flow rates were used on each entry. Minor adjustments were necessary for some specific compounds, but, overall, the two-chip microfluidic sequence required less than 1 h for completion from start to finish, and the chemistry proceeded with isolated yields ranging from 39 to 48% for compounds **326**.

[Benzothiazoles] Benzothiazoles are *S*- and *N*-containing heterocyclic scaffolds that are encountered in several biologically active molecules. Túróš and colleagues developed a flow protocol for the preparation of fused benzothiazoles **335** [98]. Different routes were first studied in batch to identify the most suitable pathway. The best reaction sequence was then transposed in glass chip continuous-flow reactors (Fig. 95). The first step concerned the condensation of various nitrophenols **327** with ethyl bromoacetate in the presence of DIPEA, to yield phenylethers **328**. Compounds **328** were then isolated off-line, and subjected to cyclization in another glass chip continuous-flow reactor toward benzofurans **329**. The procedure required the presence of a catalytic amount of Verkade's base. The methodology could be extended to the preparation of benzothiophenes **331** through a one-pot continuous-flow process by condensation of fluoronitrobenzenes **330** and ethyl thioglycolate, followed by direct cyclization in the same reactor. In the following step, the nitro moiety on benzofurans **329** and benzothiophenes **331**, as well as on commercially available indoles **332**, was reduced, giving primary amines **333**. The reaction was implemented in a H-Cube continuous-flow reactor equipped with a column packed with 10% Pd/C. Almost quantitative yields were obtained for all compounds. During the final step, furo-, thieno-, and pyrrolo[2,3-*g*][1,3]benzothiazoles **335** were prepared by reacting amines **333** in the presence of ammonium thiocyanate, followed by a bromine-mediated cyclization. Compounds **335** were isolated in moderate to good yield.

The last part of the reaction sequence, including the hydrogenation of the nitro group and cyclization into benzothiazole, was telescoped using nitroindole **332a** as a model compound (Fig. 96). The reaction conditions required some adjustment, and the target benzothiazole **335a** was eventually obtained with 33% yield (three steps).

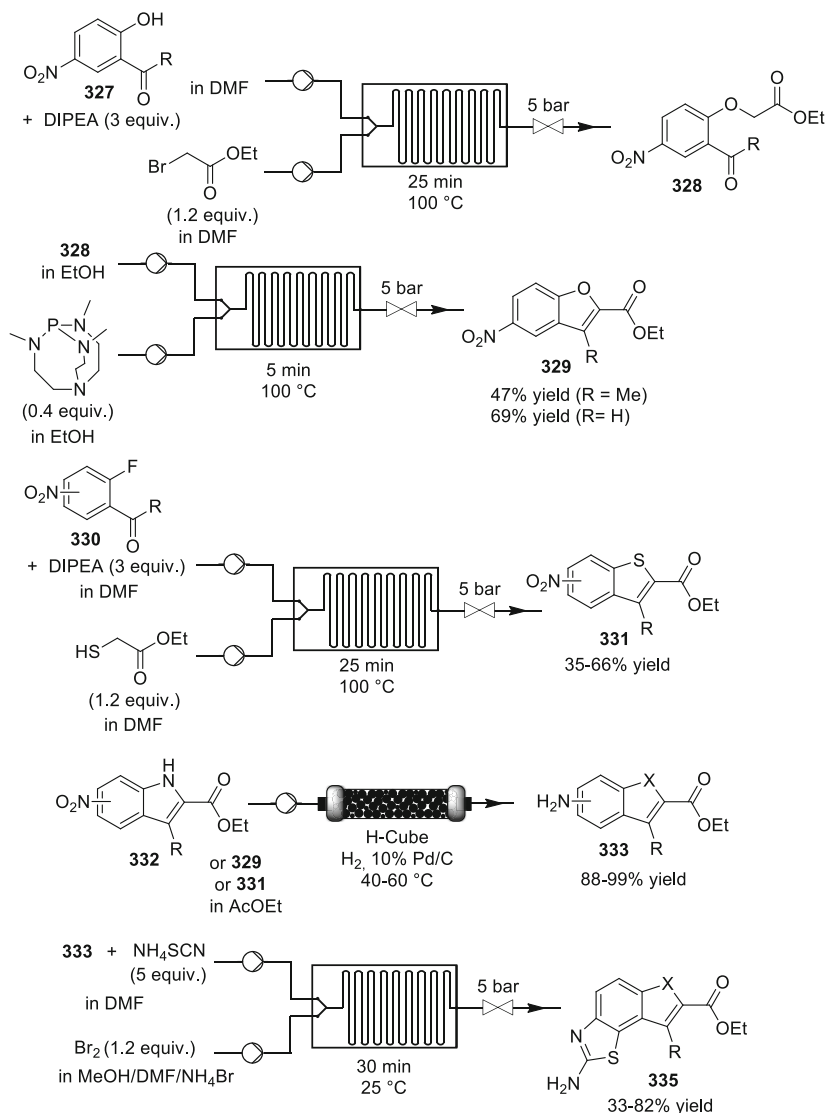


Fig. 95 Sequential, multistep continuous-flow preparation of benzothiazole scaffolds [98]

The process was characterized by a low productivity (24 mg h^{-1}) as a consequence of both the extended residence time and the high dilution of the nitroindole feed.

[Pyrazole] The pyrazole core is an important chemical entity found in many blockbuster drugs, such as in celecoxib, rimonabant, pyrazofurin, sildenafil, and crizotinib. Li and colleagues translated a batch strategy for the preparation of *N*-aryl pyrazole **338** to continuous-flow conditions (Fig. 97) within the frame of a research

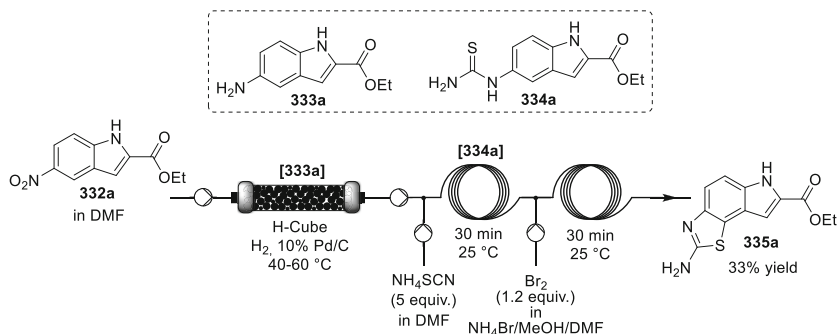


Fig. 96 Sequential, multistep continuous-flow preparation of benzothiazole scaffolds [98]

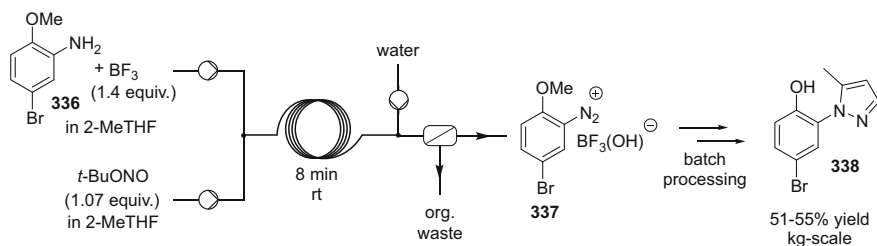


Fig. 97 Preparation of pyrazole through a continuous-flow diazotization [99]

program with Pfizer [99]. The batch process came with major safety concerns since the sequence involved the diazotization of an aniline, followed by a SnCl_2 -mediated reduction into the corresponding hydrazine, which finally would undergo a cyclocondensation with a ketoenamine. In the preliminary stage of the research program, the reactions were studied in batch. Anisole derivative **336** was considered as a starting material instead of the free phenol, providing a more robust process. The diazotization was next implemented under continuous-flow conditions, and diazonium **337** was collected in a flask containing SnCl_2 and the ketoenamine. The reduction and cyclocondensation steps proceeded in the collection batch vessel with moderate overall 35–40% yield. The authors argued that the reduced yield resulted from organic impurities formed during the diazotization step, and they successfully implemented in-line liquid–liquid extraction to separate the water-soluble diazonium salt **337** from the organic-soluble impurities. The modified setup consisted in a 400 mL internal volume PTFE tubing (1/8" i.d.) for the diazotization, telescoped to a CSTR in which the reactor stream was mixed with water before entering the in-line standpipe decanter, where phase separation occurred. The batch reactions were also slightly reoptimized to improve the yield, which reached 51–55% on a kg-scale, without any purification. The process could be operated for 8 h without interruption, despite the formation of solid diazonium salt **337** within the continuous reactor.

The preparation of other common scaffolds such as imidazoles and pyrrolidines was studied as well under continuous-flow [100, 101].

[Coumarin] Coumarin (**340**) and derivatives are very common scaffolds for active pharmaceuticals, such as warfarin. The continuous-flow synthesis of coumarin (**340**) was realized using a two-step continuous-flow setup consisting of two reaction coils operated at different temperatures (Vapourtec R4/R2+ flow reactor) (Fig. 98) [102]. The first coil was operated at an optimal 150 °C for the preliminary *O*-acetylation of salicylaldehyde in the presence of acetic anhydride (1.1 equiv.), acetic acid (0.26 equiv.), and potassium acetate (0.01 equiv.). A residence time of 22.5 min afforded a high conversion (>95%).

Longer residence times had a deleterious effect on the conversion of salicylaldehyde to **339**. The reactor effluent was directly engaged in the next step consisting in an intramolecular aldol-type condensation. The second step required a higher temperature (250 °C) to proceed with a high conversion within a residence time of 22.5 min. Coumarin (**340**) was obtained accordingly in 91% yield, with much less side reactions than in conventional batch procedures.

Khosropour and Zamani prepared 3-aminohexahydrocoumarin derivatives **344**, a class of compounds with important biological activities, using a telescoped two-step process. The reactor was constructed from glass-tubing, and the reactions were conducted using a deep eutectic solvent (DES) (Fig. 99) [103]. The first step of the sequence involved the condensation of *p*-methylbenzaldehyde, hippuric acid, and acetic anhydride, followed by the addition of dimedone (**343**) to the resulting material (**342**). Reaction conditions were first optimized in batch, and choline chloride/urea was identified as a promising reaction medium/catalyst. The reaction was transposed to continuous-flow conditions, and 94% yield were achieved upon optimization. Moreover, after off-line addition of water, phase separation and drying, the DES could be recycled for up to 5 runs, with only a minor decrease in yield (from 94 to 79%). The scope of the reaction was then extended to 1,3-cyclohexadione, as well as other aromatic aldehydes and hippuric acid derivatives **341**, with the presence of EDG, EWG, or even heteroaromatics. The reaction was applied to the preparation of a library of 40 compounds with a general structure of **344** with excellent isolated yields (80–97%).

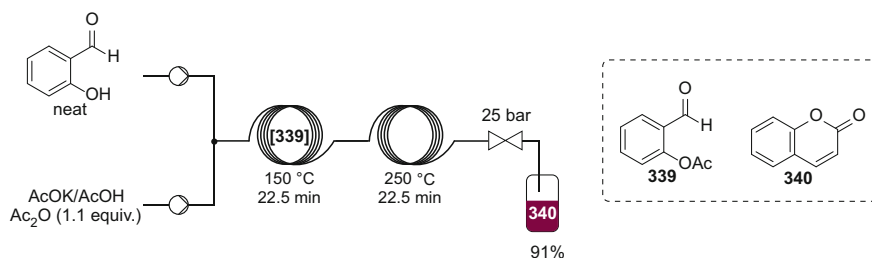


Fig. 98 Two-step continuous-flow preparation of coumarin [102]

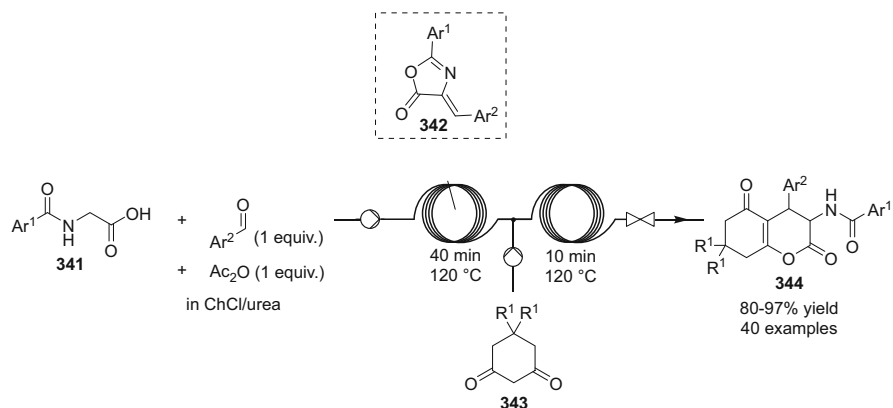


Fig. 99 Multistep continuous-flow preparation of 3-aminohexahydrocoumarin derivatives [103]

References

- Gutmann B, Elsner P, O’Kearney-McMullan A, Goundry W, Roberge DM, Kappe CO (2015) *Org Process Res Dev* 19:1062
- Shen B, Jamison TF (2012) *Org Lett* 14:3348
- Zhu C, Tang C, Cao Z, He W, Chen Y, Chen X, Guo K, Ying H (2014) *Org Process Res Dev* 18:1575
- Lee DS, Amara Z, Poliakoff M, Harman T, Reid G, Rhodes B, Brough S, McNally T, Woodward S (2015) *Org Process Res Dev* 19:831
- Hopkin MD, Baxendale IR, Ley SV (2010) *Chem Commun* 46:2450
- Hopkin MD, Baxendale IR, Ley SV (2013) *Org Biomol Chem* 11:1822
- Yang JC, Niu D, Karsten BP, Lima F, Buchwald SL (2016) *Angew Chem Int Ed* 55:2531
- Holmes N, Akien GR, Blacker AJ, Woodward RL, Meadows RE, Bourne RA (2016) *React Chem Eng* 1:366
- Baxendale IR, Deeley J, Griffiths-Jones CM, Ley SV, Saaby S, Tranmer GK (2006) *Chem Commun* 24:2566
- Pellegatti L, Hafner A, Sedelmeier J (2016) *J Flow Chem* 6:198
- Correia CA, Gilmore K, McQuade DT, Seeberger PH (2015) *Angew Chem Int Ed* 54:4945
- Correia CA, McQuade DT, Seeberger PH (2013) *Adv Synth Catal* 355:3517
- Britton J, Jamison TF (2017) *Angew Chem Int Ed* 56:8823
- Shen B, Bedore MW, Sniady A, Jamison TF (2012) *Chem Commun* 48:7444
- Shen B, Jamison TF (2013) *Aust J Chem* 66:157
- Fan X, Sans V, Yaseneva P, Plaza DD, Williams J, Lapkin A (2012) *Org Process Res Dev* 16:1039
- Yaseneva P, Plaza D, Fan X, Loponov K, Lapkin A (2015) *Catal Today* 239:90
- Lévesque F, Seeberger PH (2012) *Angew Chem Int Ed* 51:1706
- Kopetzki D, Lévesque F, Seeberger PH (2013) *Chem Eur J* 19:5450
- Gilmore K, Kopetzki D, Lee JW, Horváth Z, McQuade DT, Seidel-Morgenstern A, Seeberger PH (2014) *Chem Commun* 50:12652
- Pieber B, Glasnov T, Kappe CO (2015) *Chem Eur J* 21:4368
- Kamptmann SB, Ley SV (2015) *Aust J Chem* 68:693
- Lücke D, Dalton T, Ley SV, Wilson ZE (2016) *Chem Eur J* 22:4206
- Lin H, Dai C, Jamison TF, Jensen KF (2017) *Angew Chem Int Ed* 56:8870

25. Herath A, Dahl R, Cosford NDP (2010) *Org Lett* 12:412
26. Ingham RJ, Battilocchio C, Hawkins JM, Ley SV (2014) *Beilstein J Org Chem* 10:641
27. Bana P, Lakó Á, Kiss NZ, Béni Z, Szigetvári Á, Kóti J, Túrós GI, Éles J, Greiner I (2017) *Org Process Res Dev* 21:611
28. Hartwig J, Kirschning A (2016) *Chem Eur J* 22:3044
29. Hartwig J, Ceylan S, Kupracz L, Coutable L, Kirschning A (2013) *Angew Chem Int Ed* 52:9813
30. Guetzoyan L, Nikbin N, Baxendale IR, Ley SV (2013) *Chem Sci* 4:764
31. Adamo A, Beingessner RL, Behnam M, Chen J, Jamison TF, Jensen KF, Monbaliu J-CM, Myerson AS, Revalor EM, Snead DR, Stelzer T, Weeranoppanant N, Wong SY, Zhang P (2016) *Science* 352:61
32. Bédard AC, Longstreet AR, Britton J, Wang Y, Moriguchi H, Hicklin RW, Green WH, Jamison TF (2017) *Bioorg Med Chem* 25:6233
33. Ewan HS, Iyer K, Hyun S-H, Wlekinski M, Cooks RG, Thompson DH (2017) *Org Process Res Dev* 21:1566
34. Qian Z, Baxendale IR, Ley SV (2010) *Synlett* 505
35. Qian Z, Baxendale IR, Ley SV (2010) *Chem Eur J* 16:12342
36. Zhang P, Russell MG, Jamison TF (2014) *Org Process Res Dev* 18:1567
37. Polster CS, Cole KP, Burcham CL, Campbell BM, Frederick AL, Hansen MM, Harding M, Heller MR, Miller MT, Phillips JL, Pollock PM, Zaborenko N (2014) *Org Process Res Dev* 18:1295
38. Gérardy R, Winter M, Vizza A, Monbaliu J-CM (2017) *React Chem Eng* 2:149
39. Martin AD, Siamaki AR, Belecki K, Gupton F (2015) *J Flow Chem* 5:145
40. Suveges NS, de Souza ROMA, Gutmann B, Kappe CO (2017) *Eur J Org Chem* 24:6511
41. Gutmann B, Cantillo D, Weigl U, Cox DP, Kappe CO (2017) *Eur J Org Chem* 914
42. Gutmann B, Weigl U, Cox DP, Kappe CO (2016) *Chem Eur J* 22:10393
43. Borukhova S, Noël T, Hessel V (2016) *ChemSusChem* 9:67
44. Pastre JC, Browne DL, O'Brien M, Ley SV (2013) *Org Process Res Dev* 17:1183
45. Baxendale IR, Griffiths-Jones CM, Ley SV, Tranmer GK (2006) *Synlett* 3:427
46. Tsubogo T, Oyamada H, Kobayashi S (2015) *Nature* 520:329
47. Ghislieri D, Gilmore K, Seeberger PH (2015) *Angew Chem Int Ed* 54:678
48. Dai C, Snead DR, Zhang P, Jamison TF (2015) *J Flow Chem* 5:133
49. Grongsaard P, Bulger PG, Wallace DJ, Tan L, Chen Q, Dolman SJ, Nyrop J, Hoerner RS, Weisel M, Arredondo J, Itoh T, Xie C, Wen X, Zhao D, Muzzio DJ, Bassan EM, Shultz CS (2012) *Org Process Res Dev* 16:1069
50. Chen J, Przyuski K, Roemmele R, Bakale RP (2014) *Org Process Res Dev* 18:1427
51. LaPorte TL, Spangler L, Hamedí M, Lobben P, Chan SH, Muslehiddinoglu J, Wang SSY (2014) *Org Process Res Dev* 18:1492
52. Fukuyama T, Chiba H, Kuroda H, Takigawa T, Kayano A, Tagami K (2016) *Org Process Res Dev* 20:503
53. Amara Z, Poliakoff M, Duque R, Geier D, Franciò G, Gordon CM, Meadows RE, Woodward R, Leitner W (2016) *Org Process Res Dev* 20:1321
54. Filippini P, Ostacolo C, Novellino E, Pellicciari R, Gioiello A (2014) *Org Process Res Dev* 18:1345
55. Cole KP, McClary Groh J, Johnson MD, Burcham CL, Campbell BM, Diseroad WD, Heller MR, Howell JR, Kallman NJ, Koenig TM, May SA, Miller RD, Mitchell D, Myers DP, Myers SS, Phillips JL, Polster CS, White TD, Cashman J, Hurley D, Moylan R, Sheehan P, Spencer RD, Desmond K, Desmond P, Gowran O (2017) *Science* 356:1144
56. Dalla-Vechia L, Reichart B, Glasnov T, Miranda LSM, Kappe CO, de Souza ROMA (2013) *Org Biomol Chem* 11:6806
57. Pinho VD, Gutmann B, Miranda LSM, de Souza ROMA, Kappe CO (2014) *J Org Chem* 79:1555

58. Leão RAC, de Lopes RO, de Bezerra MAM, Muniz MN, Casanova BB, Gnoatto SCB, Gosmann G, Kocsis L, de Souza ROMA, de Miranda LSM (2015) *J Flow Chem* 5:216
59. Gauthier DR, Sherry BD, Cao Y, Journet M, Humphrey G, Itoh T, Mangion I, Tschäen DM (2015) *Org Lett* 17:1353
60. Chada S, Mandala D, Watts P (2017) *J Flow Chem* 7:37
61. Mandala D, Chada S, Watts P (2017) *Org Biomol Chem* 15:3444
62. Longstreet AR, Opalka SM, Campbell BS, Gupton BF, McQuade DT (2013) *Beilstein J Org Chem* 9:2570
63. Carneiro PF, Gutmann B, de Souza ROMA, Kappe CO (2015) *ACS Sustain Chem Eng* 3:3445
64. Lau S-H, Galván A, Merchant RR, Battilocchio C, Souto JA, Berry MB, Ley SV (2015) *Org Lett* 17:3218
65. Glasnov TN, Kappe CO (2010) *Adv Synth Catal* 352:3089
66. Cantillo D, Moghaddam MM, Kappe CO (2013) *J Org Chem* 78:4530
67. Moghaddam MM, Pieber B, Glasnov T, Kappe CO (2014) *ChemSusChem* 7:3122
68. Cantillo D, Baghbanzadeh M, Kappe CO (2012) *Angew Chem Int Ed* 51:10190
69. O'Brien AG, Lévesque F, Seeberger PH (2011) *Chem Commun* 47:2688
70. Müller STR, Murat A, Hellier P, Wirth T (2016) *Org Process Res Dev* 20:495
71. Battilocchio C, Deadman BJ, Nikbin N, Kitching MO, Baxendale IR, Ley SV (2013) *Chem Eur J* 19:7917
72. Gross TD, Chou S, Bonneville D, Gross RS, Wang P, Campopiano O, Ouellette MA, Zook SE, Reddy JP, Moree WJ, Jovic F, Chopade S (2008) *Org Process Res Dev* 12:929
73. Borukhova S, Noël T, Metten B, de Vos E, Hessel V (2013) *ChemSusChem* 6:2220
74. Borukhova S, Noël T, Metten B, de Vos E, Hessel V (2016) *Green Chem* 18:4947
75. Chartoire A, Claver C, Corpet M, Krinsky J, Mayen J, Nelson D, Nolan SP, Peñafiel I, Woodward R, Meadows RE (2016) *Org Process Res Dev* 20:551
76. Falb S, Tomaiuolo G, Perazzo A, Hodgson P, Yaseneva P, Zakrzewski J, Guido S, Lapkin A, Woodward R, Meadows RE (2016) *Org Process Res Dev* 20:558
77. Šterk D, Jukić M, Časar Z (2013) *Org Process Res Dev* 17:145
78. Pieber B, Cox DP, Kappe CO (2016) *Org Process Res Dev* 20:376
79. Gutmann B, Elsner P, Cox DP, Weigl U, Roberge DM, Kappe CO (2016) *ACS Sustain Chem Eng* 4:6048
80. Marsini MA, Buono FG, Lorenz JC, Yang B-S, Reeves JT, Sidhu K, Sarvestani M, Tan Z, Zhang Y, Li N, Lee H, Brazzillo J, Nummy LJ, Chung JC, Luvaga IK, Narayanan BA, Wei X, Song JJ, Roschangar F, Yee NK, Senanayake CH (2017) *Green Chem* 19:1454
81. Lv Y, Yu Z, Su W (2011) *Org Process Res Dev* 15:471
82. Gutmann B, Gottsponer M, Elsner P, Cantillo D, Roberge DM, Kappe CO (2013) *Org Process Res Dev* 17:294
83. Cantillo D, Mateos C, Rincon JA, De Frutos O, Kappe CO (2015) *Chem Eur J* 21:12894
84. Pellegatti L, Sedelmeier J (2015) *Org Process Res Dev* 19:551
85. Brasholz M, Johnson BA, Macdonald JM, Polyzos A, Tsanaktsidis J, Saubern S, Holmes AB, Ryan JH (2010) *Tetrahedron* 66:6445
86. Brasholz M, MacDonald JM, Saubern S, Ryan JH, Holmes AB (2010) *Chem Eur J* 16:11471
87. Baumann M, Baxendale IR, Brasholz M, Hayward JJ, Ley SV, Nikbin N (2011) *Synlett* 10:1375
88. Riva E, Rencurosi A, Gagliardi S, Passarella D, Martinelli M (2011) *Chem Eur J* 17:6221
89. Roesner S, Buchwald SL (2016) *Angew Chem Int Ed* 55:10463
90. Sniaady A, Bedore MW, Jamison TF (2011) *Angew Chem Int Ed* 50:2155
91. Venturoni F, Nikbin N, Ley SV, Baxendale IR (2010) *Org Biomol Chem* 8:1798
92. Filippini P, Baxendale IR (2016) *Eur J Org Chem* 2000
93. Petersen TP, Mirsharghi S, Rummel PC, Thiele S, Rosenkilde MM, Ritzén A, Ulven T (2013) *Chem Eur J* 19:9343
94. Petersen TP, Ritzén A, Ulven T (2009) *Org Lett* 11:5134

95. Glotz G, Lebl R, Dallinger D, Kappe CO (2017) *Angew Chem Int Ed*. <https://doi.org/10.1002/anie.201708533>
96. Pagano N, Teriete P, Mattmann ME, Yang L, Snyder BA, Cai Z, Heil ML, Cosford NDP (2017) *Bioorg Med Chem*. <https://doi.org/10.1016/j.bmc.2017.03.061>
97. Pagano N, Herath A, Cosford NDP (2011) *J Flow Chem* 1:28
98. Lövei K, Greiner I, Éles J, Szigetvári Á, Dékány M, Lévai S, Novák Z, Túrós GI (2015) *J Flow Chem* 5:74
99. Li B, Widlicka D, Boucher S, Hayward C, Lucas J, Murray JC, O'Neil BT, Pfisterer D, Samp L, Van Alsten J, Xiang Y, Young J (2012) *Org Process Res Dev* 16:2031
100. May SA, Johnson MD, Braden TM, Calvin JR, Haeberle BD, Jines AR, Miller RD, Plocharczyk EF, Renner GA, Richey RN, Schmid CR, Vaid RK, Yu H (2012) *Org Process Res Dev* 16:982
101. Baumann M, Baxendale IR, Kuratli C, Ley SV, Martin RE, Schneider J (2011) *ACS Comb Sci* 13:405
102. Li X, Chen A, Zhou Y, Huang L, Fang Z, Gan H, Guo K (2015) *J Flow Chem* 5:82
103. Zamani P, Khosropour AR (2016) *Green Chem* 18:6450

Photochemical Synthesis of Heterocycles: Merging Flow Processing and Metal-Catalyzed Visible Light Photoredox Transformations



Toma Glasnov

Contents

1	Introduction	104
2	Equipment and Light Sources	105
3	Visible Light Photoredox Catalysis: General Aspects	108
4	Visible Light Photoredox Synthesis of Heterocycles	110
4.1	Cyclization Reactions	110
4.2	Oxygenations and Aerobic Oxidation Reactions	112
4.3	Cycloadditions	115
4.4	Miscellaneous	116
5	Further Photochemical Transformations for the Synthesis of Heterocycles	118
5.1	Cyclization Reactions	119
5.2	Oxygenations and Aerobic Oxidation Reactions	121
5.3	Cycloadditions	121
5.4	Rearrangements	124
6	Visible Light Photoredox Decoration of Heterocyclic Scaffolds	125
7	Conclusions	129
	References	129

Abstract The ubiquitous presence of heterocyclic moieties in everyday life justifies the ongoing intensive research within the synthetic community to discover effective methodologies for their construction. As the social concern regarding environmental protection gains importance, the use of light as the ultimate green promoter for chemical reactions has been revived in the scientific community. Specifically, visible-light photoredox processes based on metal- and organic photosensitizer are attracting significant attention and have seen an exceptional advance recently.

Additionally, continuous-flow processing has enabled a safer and more efficient generation of various heterocycles, whilst allowing their syntheses in a scalable

T. Glasnov (✉)
Institute of Chemistry, University of Graz, Graz, Austria
e-mail: toma.glasnov@uni-graz.at

manner. In this chapter, recent achievements in the area of continuous-flow aided photoredox synthesis are covered, including some general remarks on instrumentation, theoretical background and selected flow UV-photochemistry examples.

Keywords Continuous flow · Flow reactor · Heterocycles · Light source · Metal photosensitizers · Organic photosensitizers · Photoredox catalysis · Visible and UV light

Abbreviations

Cu(Xantphos)(dmp)BF ₄	Copper (I) (2,9-dimethyl-1,10-phenanthroline-kN1, kN10)[1,1'-(9,9-dimethyl-9H-xanthene-4,5-diyl)bis[1,1-diphenylphosphine-kP]](T-4) tetrafluoroborate
DIY	Do it yourself
DMAP	<i>N,N</i> -dimethylaminopyridine
<i>fac</i> -Ir(ppy) ₃	<i>fac</i> -Tris(2-phenylpyridine)iridium (III)
Fe(phen) ₃ (NTf ₂) ₂	Iron (II) tris(1,10-phenanthroline-kN1,kN10)-(OC-6-11) di(1,1,1-trifluoro- <i>N</i> -[(trifluoromethyl)sulfonyl]methanesulfonamide)
Ir(dF(CF ₃)ppy) ₂ (dtbbpy)PF ₆	[4,4'-Bis(1,1-dimethylethyl)-2,2'-bipyridine- <i>N</i> ₁ , <i>N</i> ₁ ']bis[3,5-difluoro-2-[5-(trifluoromethyl)-2-pyridinyl- <i>N</i>]phenyl-C]Iridium(III) hexafluorophosphate
[Ir(dtbbpy)(ppy) ₂]PF ₆	4,4'-Bis(1,1-dimethylethyl)-2,2'-bipyridine- <i>N</i> ₁ , <i>N</i> ₁ '] bis[2-(2-pyridinyl- <i>N</i>)phenyl-C]iridium(III) hexafluorophosphate
LEDs	Light-emitting diodes
<i>N</i> -Boc	<i>N</i> -tert-Butyloxycarbonyl
Ru(bpy) ₃ (PF ₆) ₂	Tris(2,2'-bipyridine)ruthenium (II) hexafluorophosphate
Ru(bpy) ₃ Cl ₂	Tris(bipyridyl)ruthenium(II) dichloride
<i>tert</i> -BuOOH	<i>tert</i> -Butyl hydroperoxide
TMSCN	Trimethylsilyl cyanide
TrocN ₃	2,2,2-Trichloroethyl azidoformate

1 Introduction

The ubiquitous presence of heterocyclic moieties in everyday life justifies the ongoing intensive research within the synthetic community to discover new and effective methodologies for their construction [1–3]. Intriguingly, many functionalized heterocycles can be produced using photochemical synthesis. More

specifically, visible light photoredox synthesis in continuous flow regime, reported at the end of the last decade, has become an intriguing technique that offers a variety of synthetic options for the modern organic chemist and has attracted a considerable attention in recent years [4–15].

Initially utilizing the inherent photocatalytic activity of iridium(III) and ruthenium(II) complexes, different strategies for heterocyclic synthesis have recently surfaced. Among these are cycloadditions, radical cyclizations, or radical processes mediated by molecular oxygen. These have proven to be of significant value for expanding the heterocyclic space. As will be demonstrated in this chapter, visible light photoredox continuous flow synthesis of heterocycles so far predominantly relies on the use of soluble iridium and ruthenium complexes as well as continuous flow techniques to impart high levels of efficacy. Generally, due to enhanced mass-transport (mixing) properties, small intrinsic reactor volumes, and improved light utilization, flow photoreactors represent one-of-a-kind alternative to batch setups, frequently intended to provide scale-up options aiming at straightforward industrial implementation [16, 17]. In several scenarios, copper or iron complexes as well as organic dyes in the role of photosensitizers to trigger radical formation for the successive heterocyclic formation have successfully replaced the iridium and ruthenium complexes.

Owing to the large diversity and considerable recent advances in visible light photochemical transformations, this chapter is focused on continuous flow processes and visible light chemistry to prepare heterocyclic moieties and is organized to cover literature examples published between January 2010 and May 2017. Selected “classical” UV photochemistry examples are treated briefly in the second part of the chapter. Early examples of “classical” UV photochemistry in flow (before 2010) as well as visible light photoredox examples not involving heterocycles have been largely omitted and have been already covered previously [16, 18, 19]. In addition, a small number of selected examples treating the functionalization of heterocyclic scaffolds can be found at the end of the chapter.

2 Equipment and Light Sources

First pioneering experiments in continuous flow organic photosynthesis were carried out in DIY devices [19]. However, due to common issues with proper engineering, reaction control, and reproducibility, the use of tailored commercial available systems is conceivably more straightforward and less time-consuming. Despite the persistence of the DIY trend in device manufacturing, the use of dedicated instruments for chemical photosynthesis is undoubtedly on the rise with new devices emerging on the market. In a typical batch photoreactor (immersion well, “Rayonet”), the irradiation power and thus the reaction progress are generally determined by the characteristics of the light source, the used cutoff filters (if any), and the reactor overall architecture. In general, these arguments also apply for flow photoreactors. It is very important to understand that due to high absorption loss as

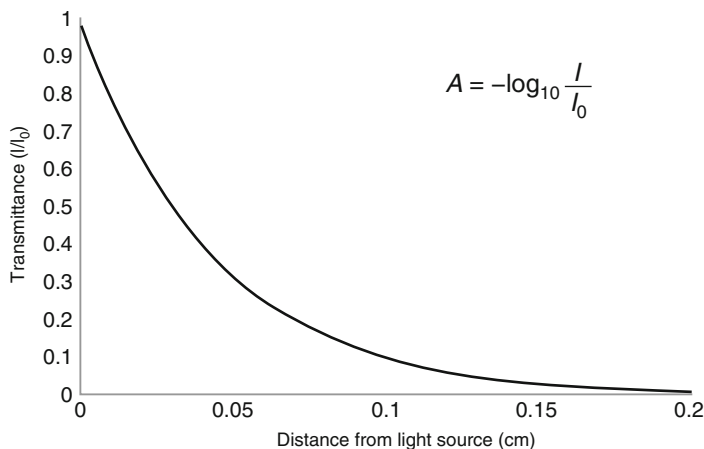


Fig. 1 Bouguer-Lambert-Beer law in photoreactions. At roughly 0.2 cm layer thickness, all of the light is already absorbed

described by the Bouguer-Lambert-Beer law (Fig. 1), the step from several gram scale to larger scale is complicated by the exponential decrease of light intensity with penetration depth. Essentially, at a depth of 0.01–0.15 cm, almost all of the light is absorbed by the reaction solution. This disadvantage, combined with the harsh UV light produced by the mercury-discharge lamps and the lack of safety controls (radical generation, explosive potential), means that alternative techniques are highly desirable.

The introduction of continuous flow reaction techniques in organic synthesis has been received with large hopes with respect to the plethora of obstacles inherent to traditional batch synthesis techniques, including the described challenges of photochemical syntheses [20, 21]. Today's commercially available dedicated flow photoreactors for synthesis feature easily exchangeable light sources with variable power and narrowband tunable wavelengths (± 10 nm), precise temperature control over a wide range (-5 to -80°C , Vapourtec[®] UV150), and software that enables constant online control of the overall flow process (Fig. 2) (<https://www.corning.com/worldwide/en/innovation/corning-emerging-innovations/advanced-flow-reactors.html>; <http://futurechemistry.com/products-and-services/flow-chemistry-instruments/>; <https://www.vapourtec.com/products/flow-reactors/photochemistry-uv-150-photochemical-reactor-features/>; <https://ymc.de/keychem-lumino.html>). Two different principles dominate the present flow photoreactor design: chip-based and tube-based reactors (Fig. 2). Both DIY and commercial devices follow these two architectures. In the chip-based instruments (conceptually close to a falling film reactor), the reaction mixture is processed through channels within the micro- or meso-scale milled or etched Quartz or Pyrex glass channels. The light source is placed above, below or on both sides and in very close proximity to the chip to ensure maximal photon input. In the much more common tube-based reactors, the reaction mixture is directed through UV-transparent fluoropolymer HPLC tubing

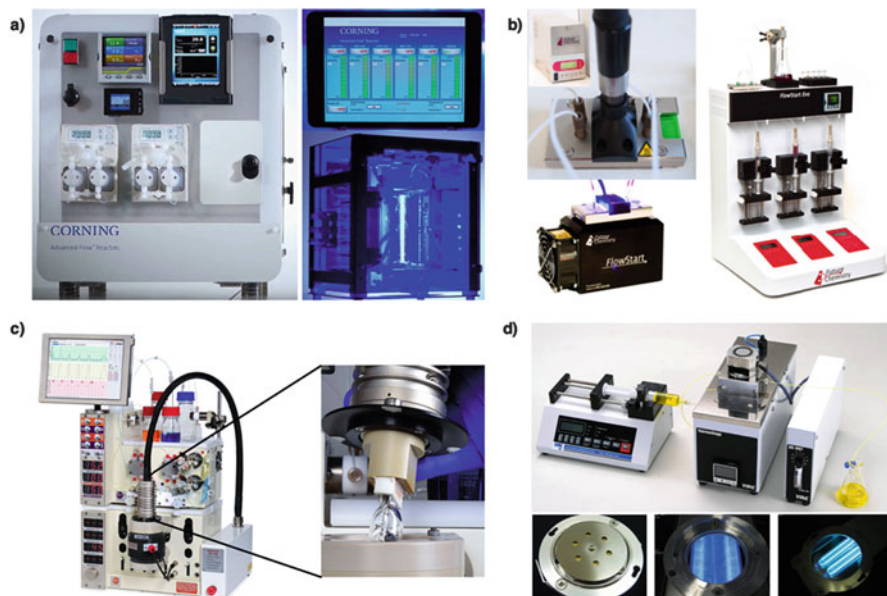


Fig. 2 Commercial continuous flow photoreactors for laboratory research: (a) Corning Lab Reactor with photoreaction module and wireless controller switch for six different wavelengths (chip-based); (b) Future Chemistry FlowStart Evo[®] with deep UV module (<300 nm) and LED module (365 and 470 nm) (chip-based); (c) Vapourtec UV-150 photoreactor with metal halide lamp (tube-based); (d) KeyChem-Lumino with three exchangeable light sources – LEDs (365 nm), excimer lamp (308 nm), and low-pressure Hg lamp (254 nm) (chip-based)

(up to 1 mm internal diameter) wrapped around a Quartz or Pyrex cylinder and in a close proximity to the light radiation source mounted inside the cylinder, thus delivering a consistent photon flux throughout the reaction zone.

As light sources generate and emit heat, an important detail of the reactor design is the heat dissipation unit – excess heat can be removed by active or passive dissipation using fan (air), liquid cooling, or active cooling with Peltier elements. Higher throughput (scale-up) can be usually achieved by the “numbering-up” principle using multiple devices in parallel. Principally, instrument companies offer a variety of options in terms of automation, pumping modules, safety features, and temperature and pressure control in addition to light sources with variable wavelengths. Currently dedicated commercial photoflow instruments can generally process unlimited reaction volumes through a reactor zone of only few mL internal volume, thus allowing the preparation of even kilograms of very valuable and often unique photoreaction products. Still, the formation of solids during the reaction remains a major issue for every flow reactor as it can lead to clogging of the device. Thus, careful reaction optimization, typically in batch, is required. Chip-based reactor designs are more prone to failure and high-cost replacement, while tube-based designs allow replacement of clogged reactor sections in a “quick-fix” fashion by a comparably inexpensive replacement of the fluoropolymer tubing.

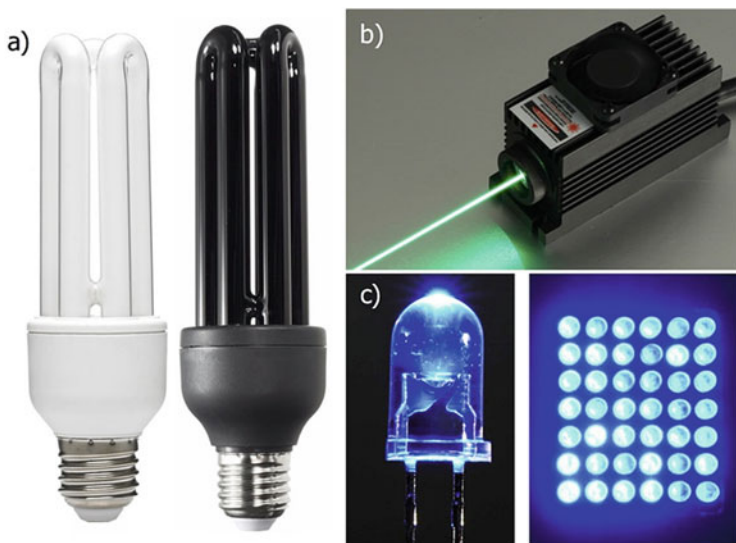
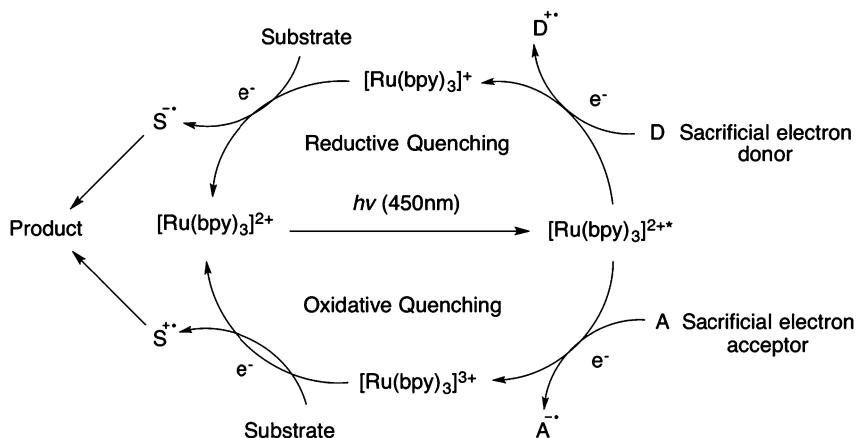


Fig. 3 Common light sources used in flow photosynthesis: (a) household energy saving lamps – white light and “black” (UV, 365 nm) light bulbs; (b) laser; (c) LEDs, single blue-light-emitting LED and an array of 6×7 LEDs

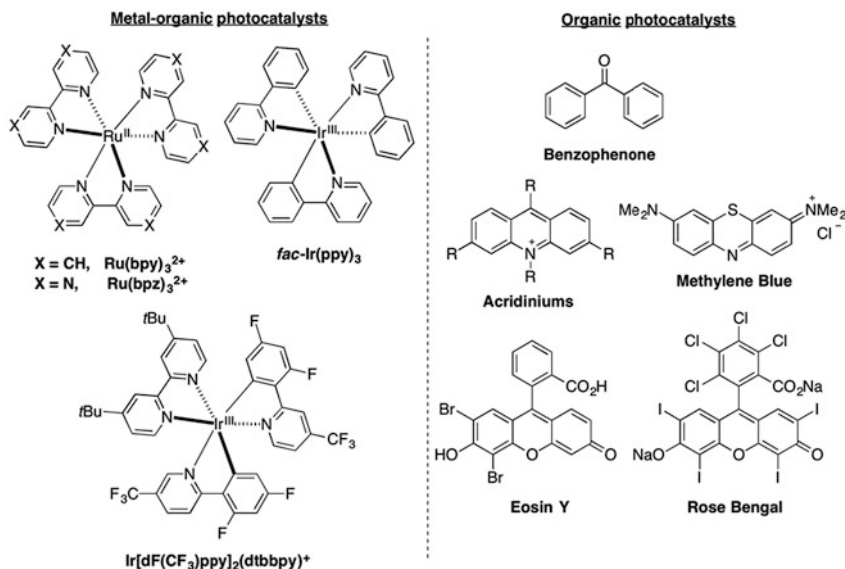
The most common sources for traditional photochemical transformations requiring UV light remain commercial metal (mercury, sodium) discharge lamps – low-, medium-, or high-pressure types. These provide UV light with wavelengths below 365 nm – covering the UVA, UVB, and UVC regions (365–190 nm). However, to fulfill the needs of visible light photoredox synthesis, light sources of different type (high power household lamps, lasers, or light-emitting diodes – Fig. 3) covering the 390–700 nm wavelength regions are used. Most notable among these are the light-emitting diodes. Currently, LEDs are considered an almost ideal light emitter with long life (up to 100,000 h), low heat generation, high light intensity, and narrowband light emission. Accordingly, LEDs have become indispensable not only for various industrial and domestic applications, but they are also currently revolutionizing the field of photochemistry. In particular arrays or matrices of LEDs covering various wavelengths are of special interest, allowing the use of specific wavelengths without the need to change the light source.

3 Visible Light Photoredox Catalysis: General Aspects

The first report of using $[\text{Ru}(\text{bpy})_3]^{2+}$ as a photocatalyst dates back to 1978 [22]. Nevertheless, it took several decades before photoredox catalysis grew into a thriving field of synthetic organic chemistry. The simultaneous reports by the groups of MacMillan and Yoon in 2008 paved the way for the now ever-growing number of



Scheme 1 Typical visible light-induced photoredox cycle with Ru(II) catalysts



Scheme 2 Some common photoredox catalysts employed in flow photochemical syntheses

research articles on visible light photoredox catalysts for various organic transformations [23, 24].

Theoretically, a photosensitizer or photocatalysts are excited by visible light via discrete single-electron transfer events. Subsequent photo-relaxation involving intermolecular reductive or oxidative quenching provides the mechanistic rationalization for photoredox catalysis (Scheme 1, shown for $[\text{Ru}(\text{bpy})_3]^{2+}$) [25–30].

Numerous stable complexes of Ru(II) and Ir(III) have been demonstrated as effective photoredox catalysts (Scheme 2) [31]. Due to their high levels of visible

light absorption, they are capable of easy, efficient, and selective photoexcitation relative to the reaction substrates for most scenarios. More recently, the ability of several organic chromophores (Scheme 2) to participate in photoinduced single electron transfer (PSET) processes has been considered in photoredox continuous flow syntheses as an alternative to transition metal complexes [8, 31, 32].

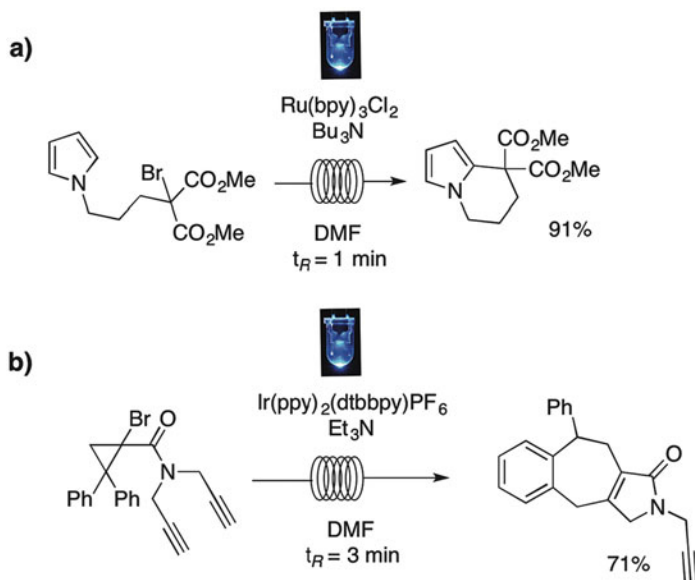
4 Visible Light Photoredox Synthesis of Heterocycles

Heterocycles are an extended class of structural motifs that are widely spread in nature as well as in synthetic agrochemicals and, further, in compounds with biological activity and pharmaceutical applications [1–3]. Thus, a major trend in contemporary synthetic chemistry is the continuous search for strategies and novel reactivity toward heterocycle synthesis. Additionally, as the social concern regarding environmental protection gains importance, the use of light as the ultimate green promoter for chemical reactions has been revived in the scientific community. Specifically, visible light photoredox processes are attracting significant attention and have seen an exceptional advance recently [33–35]. Many of these research studies have focused on catalytic strategies relying predominantly on iridium and ruthenium metal complexes, but also organocatalysts (see above) have been employed. These endeavors have resulted in numerous structurally diverse heterocycles synthesized with the aid of light under usually very mild conditions [36]. Unlike conventional batch setups, continuous flow processing has enabled a safer and more efficient generation of various heterocycles while allowing their syntheses in a scalable manner [9].

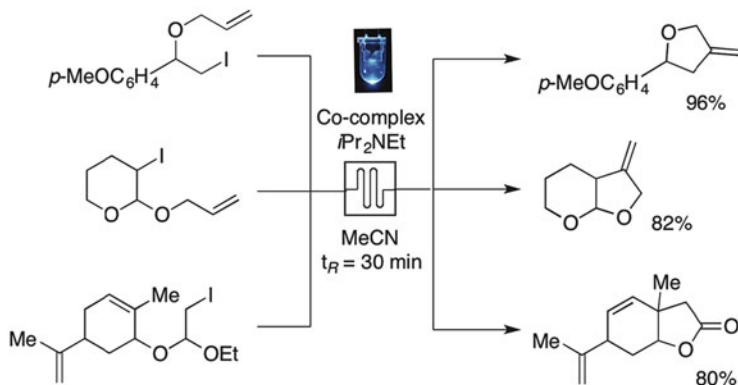
4.1 Cyclization Reactions

Radical cyclization reactions are often used to rapidly assemble valuable five- or six-membered carbo- or heterocycles with good selectivity. Consequently, some of these early and methodologically elegant synthetic examples were reported by Stephenson and co-workers in 2012 under continuous flow conditions [37]. Conducted in a DIY reactor of only 459 μL internal volume under irradiation with seven blue LEDs, both a radical cyclization onto a heteroaromatic ring and on a terminal olefin were catalyzed by $\text{Ru}(\text{bpy})_3\text{Cl}_2$ as the photosensitizer of choice.

A substituted 5,6,7,8-tetrahydroindolizine was formed in 91% yield from the corresponding substituted pyrrole after only 1 min of residence time (t_R) in the chosen tube-based reactor design (Scheme 3a). Likewise, blue-light irradiation during 3 min residence time in the reactor coil and in the presence of $[\text{Ir}(\text{dtbbpy})(\text{ppy})_2]\text{PF}_6$ as the photosensitizer promoted a tandem radical cyclization/Cope rearrangement sequence to afford a substituted 3,4,9,10-tetrahydrobenzo[4,5]cyclohepta[1,2-c]pyrrol-1(2H)-one in 71% yield (Scheme 3b). Noteworthy was



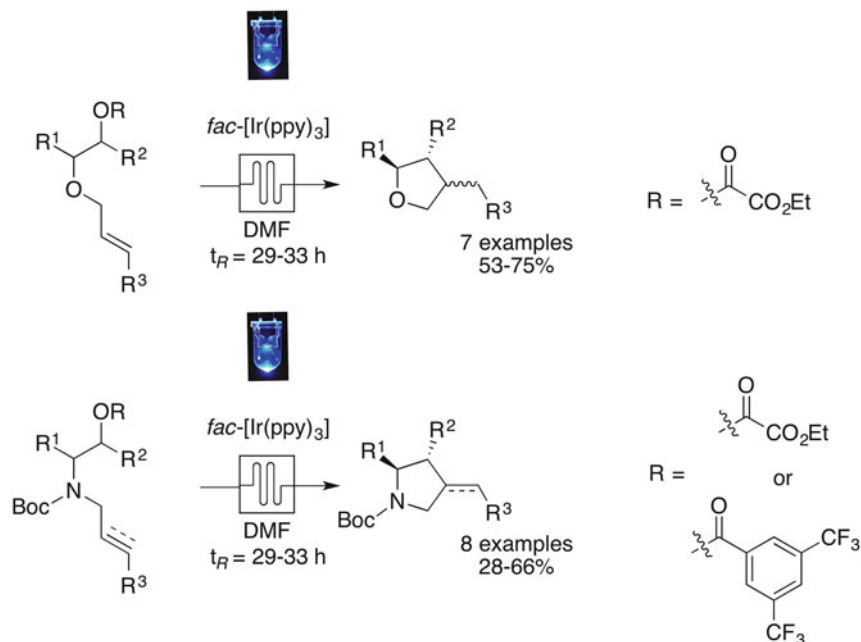
Scheme 3 Photoredox radical cyclization and radical cyclization/Cope rearrangement sequence



Scheme 4 Cobalt-catalyzed radical cyclization toward tetrahydrofuran-related heterocycles

the efficiency of this reaction under flow conditions which could not be duplicated in a comparative batch experiment.

In a similar fashion, the synthesis of a number of tetrahydrofuran-related heterocycles was achieved in a DIY flow photoreactor using a chip-based design approach (Scheme 4) [38]. An array of 42 LEDs in total was employed to provide an estimated 37 W of radiant flux. Interestingly, in this particular case, batch control experiments did not reveal any significant differences in terms of yields, as compared to the outcome of the flow approach. However, the flow synthesis required only 30 min, while the batch synthesis required 24 h to reach completion.

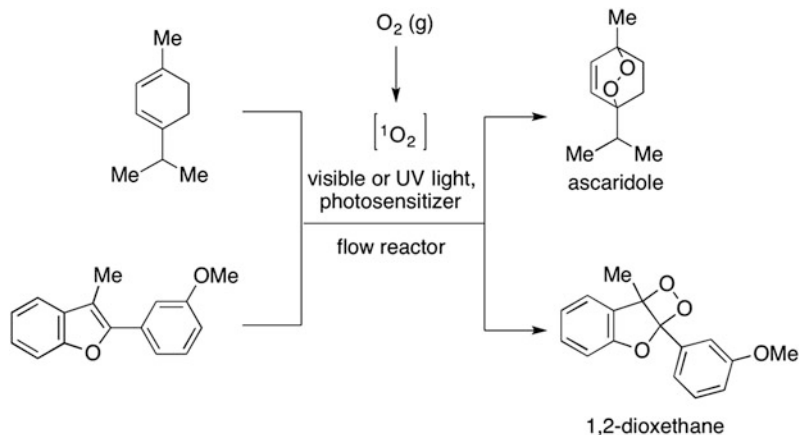


Scheme 5 Photoredox synthesis of tetrahydrofurans and pyrrolidines

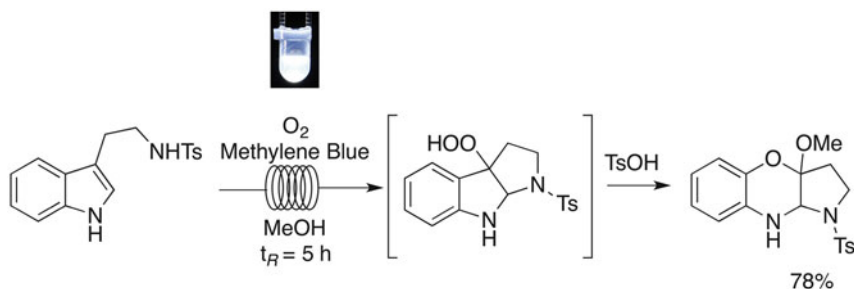
Recently, Reiser and co-workers investigated the reactivity of several oxalates in order to generate diversely substituted tetrahydrofurans and pyrrolidines via a photoredox flow process [39]. Initially developed as an electrochemical deoxygenation process, the reaction protocol was further advanced to involve a subsequent intramolecular cyclization. Optimization experiments under batch conditions led to identification of *fac*-Ir(ppy)₃ as the photocatalyst of choice. These preliminary batch experiments required additional heating and extended reaction times (days) and made evident the potential benefit of a continuous flow process. As anticipated, reaction times were significantly shortened from 7 days to 29–33 h, and a significantly improved yield was obtained. Seven further closely related examples were reported in the original article. Finally, a switch from 1,2-diols to the corresponding 1,2-aminoalcohols expanded the scope to a number of substituted pyrrolidines (Scheme 5).

4.2 Oxygenations and Aerobic Oxidation Reactions

Singlet oxygen (¹O₂) is a highly reactive short-lived metastable species that can be easily generated in a photochemical process to enable the formation of new carbon-oxygen or heteroatom-oxygen bonds [40]. Nevertheless, a large photon flux and an efficient mass transfer of O₂(g) are needed to ensure efficient reaction progress and



Scheme 6 Photoredox singlet oxygen generation and utilization in the flow synthesis of oxygen-containing heterocycles

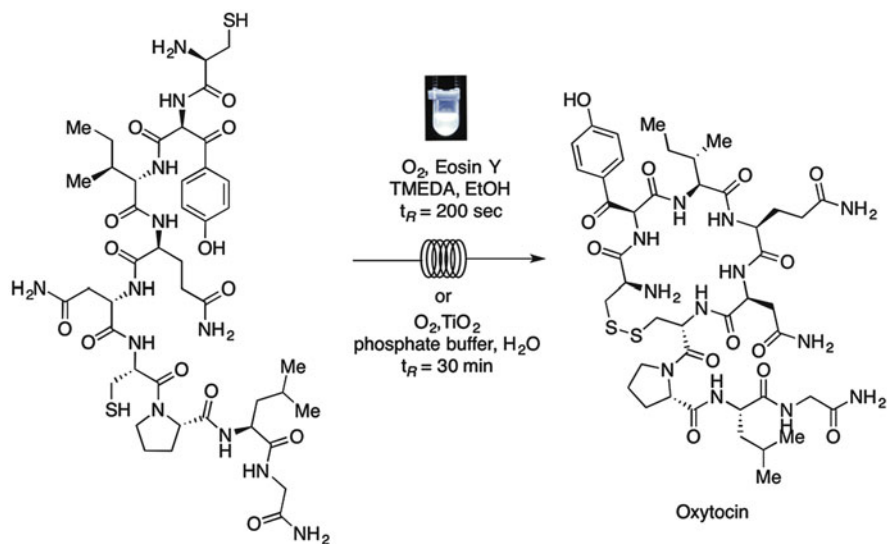


Scheme 7 Tricyclo-1,4-benzoxazine photoredox flow synthesis

acceptable reaction rate. The synthesis of ascaridole (a heterocyclic peroxide) via the near-instantaneous [4 + 2] addition of 1O_2 to α -terpinene has been utilized as a test reaction for the evaluation of various flow reactor concepts for sensitized photochemical oxidations (Scheme 6) [41–44]. Common organic compounds such as methylene blue, tetraphenylporphyrin, or rose bengal are utilized as photosensitizers. Another recent reaction example of this kind is the [2 + 2] addition of 1O_2 to 2-(3-methoxyphenyl)-3-methyl-1-benzofuran to afford the corresponding dioxethane (Scheme 6). In this particular case, recirculation of the reaction mixture for 5 h was required to achieve a 97% conversion [44].

Similar reaction conditions – $O_2(g)$, methylene blue, white LEDs, and continuous flow in recirculation mode – were also used by Chen and co-workers for the generation of tricyclic-1,4-benzoxazines from indoles (Scheme 7) [45].

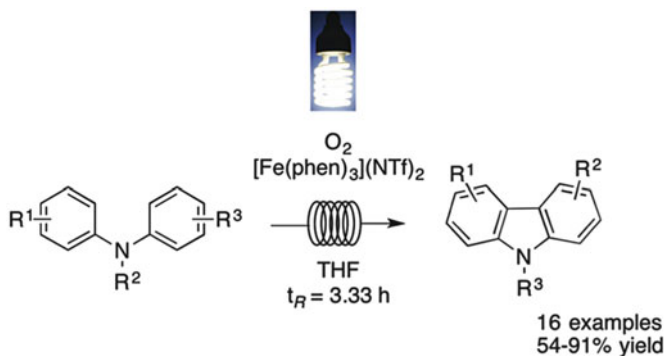
Another synthetically useful application of oxygen is the synthesis of disulfides under mild conditions. Disulfides are a valuable motif with various applications [46]. Noël and co-workers have demonstrated that a protocol employing



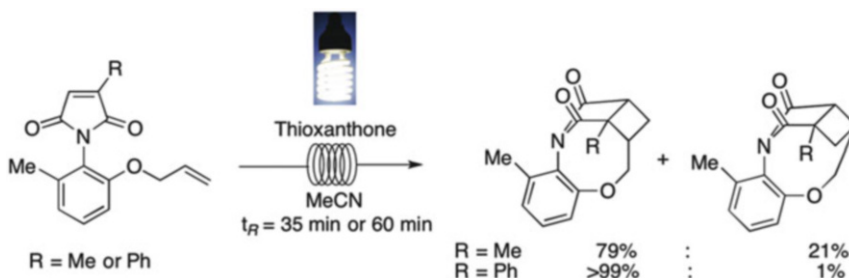
Scheme 8 Oxidative photosynthesis of oxytocin

flow processing and gaseous oxygen as a green and cheap oxidant is an excellent approach to the preparation of various disulfides, including oxytocin (a macrocyclic hormonal neuromodulator in mammalian brains), with very short residence times (Scheme 8) [47]. For this reaction, both organic and inorganic photosensitizers (Eosin Y or TiO_2) are applicable in combination with white LEDs as a light source [47, 48].

Carbazoles represent another class of valuable heterocyclic core structures provoking continued synthetic research [49–51]. Recently, a photochemical synthesis involving a combination of an iron complex as the photosensitizer and molecular oxygen as the oxidant was demonstrated [52]. Among the tested photosensitizers, $Ru(bpy)_3(PF_6)_2$, $Ir(ppy)_3$, Eosin Y, $Cu(Xantphos)(dmp)BF_4$ [53], and various iron complexes, the iron complex $Fe(phen)_3(NTf_2)_2$ provided superior yields and consequently was chosen as the photosensitizer. In a second step, boosting the dissolution of molecular oxygen in the reaction mixture decreased the initial reaction time from almost 7 h. For this purpose, a DIY tube-based flow reactor was assembled, allowing reducing the required reaction time to only 3.33 h. With the aid of this optimized flow setup, a library of 16 carbazoles was successfully prepared (Scheme 9). Noteworthy, a practical example of the “numbering-up” strategy for scaling-up of the reaction was also demonstrated. The same group previously reported a similar protocol, where a Cu-based photosensitizer was used in combination with molecular iodine as the oxidant with similar result, however requiring 20 h of reaction time. A number of carbazole-like heterocycles were prepared in similar manner [54].



Scheme 9 Oxidative photosynthesis of carbazoles



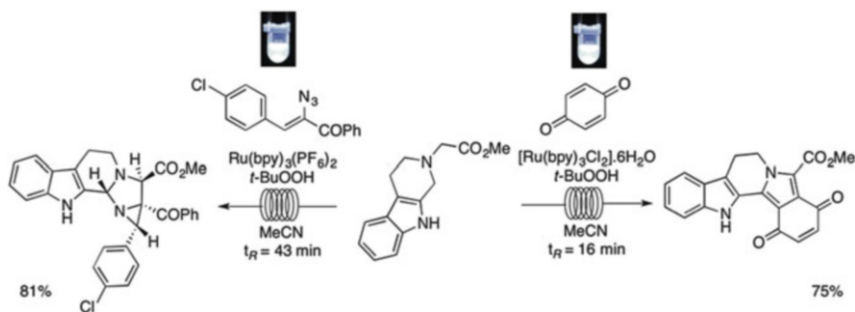
Scheme 10 [2 + 2] Photocycloaddition catalyzed by thioxanthone using visible light irradiation

4.3 Cycloadditions

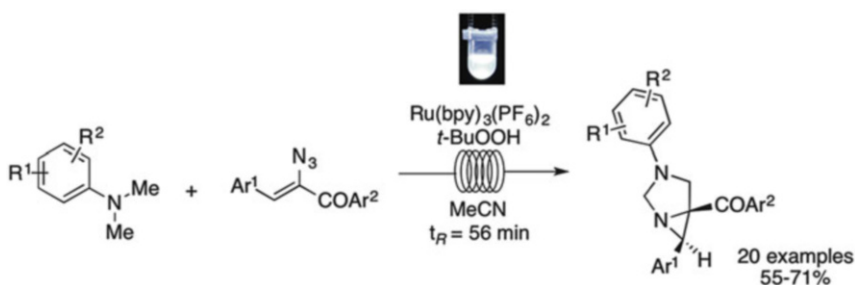
Cycloaddition reactions provide an array of opportunities to access different carbo- and heterocycles and are described in a vast amount of publications [55]. With the recent progress of photochemistry and flow synthesis, a significant number of visible light photoredox cycloadditions aiming at the preparation of heterocycles were published.

The group of Sivaguru developed an intramolecular [2 + 2] cycloaddition process utilizing substituted atropisomeric maleimides to generate various seven-membered heterocycles [56]. Striving to increase efficiency and scalability, a simple DIY flow device was assembled. Using a 40 W compact fluorescent lamp and thioxanthone as organic photosensitizer, complete conversion of the corresponding maleimides in 35/60 min was accomplished (Scheme 10).

In 2015, Maurya and co-workers described a photoredox-mediated oxidation/[3 + 2] cycloaddition/re-aromatization three-step cascade to obtain fused β -carboline (Scheme 11) [57]. After initial batch optimization, continuous flow experiments were performed in a DIY tube-based assembly. The best results were obtained using MeCN as the solvent in the presence of $\text{Ru}(\text{bpy})_3\text{Cl}_2$ as



Scheme 11 A photocascade involving [3 + 2] cycloaddition toward fused β -carboline



Scheme 12 A photocascade involving [3 + 2] cycloaddition toward diazabicyclo[3.1.0]hexanes

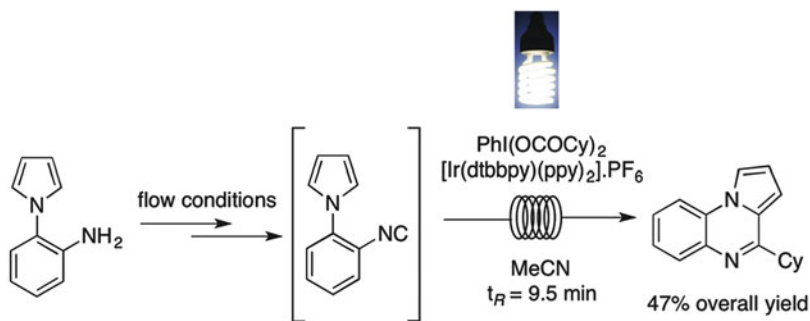
photosensitizer and *tert*-BuOOH as the oxidant. The procedure proved to be superior in terms of reaction time and yield as compared to a batch experiment.

The same group also reported an interesting modification of this protocol enabling the flow-photoredox cascade depicted in Scheme 11 to be carried out with α -azido chalcones instead of benzophenone. A different class of fused β -carbolines was obtained in 81% yield and excellent region and diastereoselectivity [58]. The extension of the general reaction cascade to *N,N*-dimethylanilines utilizing the same reactor setup was published very recently [59]. A small library of richly substituted diazabicyclo[3.1.0]hexanes was easily generated in 55–71% yield under photoflow conditions (Scheme 12).

Structurally diverse imidazoles were alternatively obtained by the visible light/ $\text{Ru}(\text{bpy})_3(\text{PF}_6)_2$ -mediated coupling of vinyl azides and secondary amines [60].

4.4 Miscellaneous

The thriving popularity of visible light photoredox chemistry and the increased number of reported synthetic flow processes have attracted a steadily growing attention both from industry and academia. Apparently, numerous photochemical



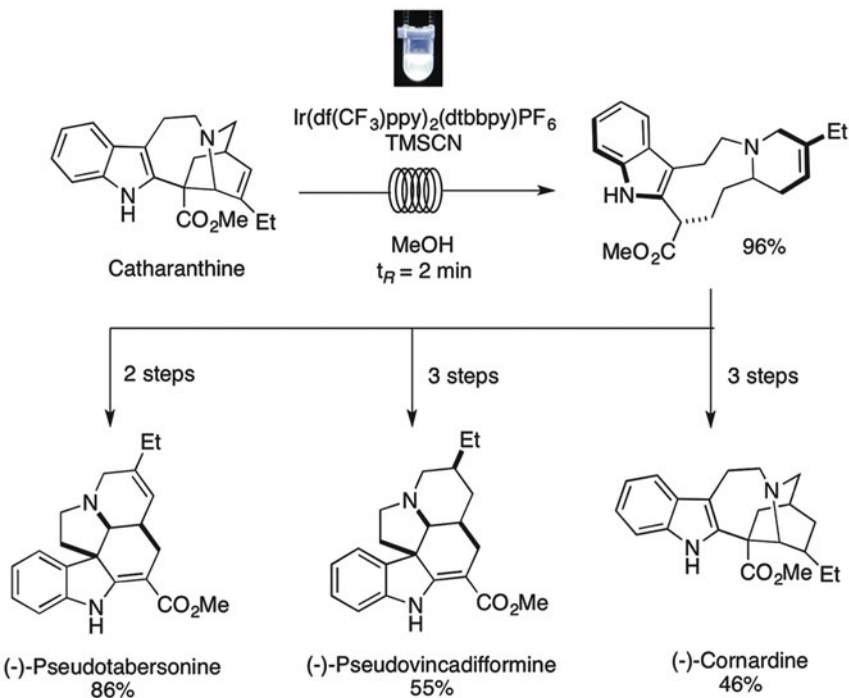
Scheme 13 Photoredox flow synthesis of 4-cyclohexylpyrrolo[1,2-*a*]quinoxaline

transformations can be carried out under predominantly homogeneous flow conditions including heterocyclic syntheses.

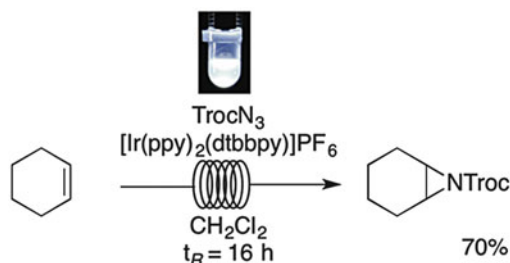
Jamison and co-workers have described a mild method for preparing highly functionalized nitrogen-rich quinoxaline derivatives [61]. A visible light decarboxylative coupling of 1-(2-isocyanophenyl)-1*H*-pyrrole with radicals generated from phenyliodine(III) dicyclohexanecarboxylate catalyzed by [Ir(dtbbpy)(ppy)₂].PF₆ was demonstrated under flow conditions. The overall flow process involves a telescoped three-step in situ preparation of corresponding isocyanide from an aromatic amine, followed by a photoredox reaction in a DIY reactor (Scheme 13) requiring only a short residence time (<15 min) at room temperature.

Searching for a suitable chemoselective approach to several natural alkaloids, Beatty and Stephenson have utilized a photoredox fragmentation reaction in continuous flow for the synthesis of (+)-catharanthine to open up high-yielding synthetic pathways toward (–)-pseudotabersonine (86%, two steps), (–)-pseudovincadifformine (55%, three steps), and (+)-coronaridine (46%, three steps; Scheme 14) [62]. A flow experiment conducted on a 2 g scale using Ir(dF(CF₃)ppy)₂(dtbbpy)PF₆ as a photosensitizer provided a comparable yield to a control batch experiment – 96% vs. 93%.

Aziridines are another class of valuable nitrogen-containing heterocycles with various applications in organic synthesis and are also featured in numerous natural products [63, 64]. The photoredox synthesis of aziridines has been studied in detail by the research group of Scholz et al. [65]. 2,2,2-Trichloroethyl azidoformate was carefully selected as an excellent precursor since it is less prone to Curtius-type rearrangements and less easily reduced than acyl azides, thus to partake in undesired photoreductive reaction pathways, and is thermodynamically feasible with the use of Ir complexes as photosensitizers. After optimizing and demonstrating the usefulness of the designed method for the synthesis of a small library of aziridines, a continuous flow study using a DIY reactor was conducted to investigate the scalability of the protocol. A reaction mixture containing cyclohexene, 2 equiv. of TrocN₃, and 2.5 mol% of [Ir(dtbbpy)(ppy)₂].PF₆ as the photocatalyst in dichloromethane as the solvent was processed for 16 h while being irradiated by visible light to generate 785 mg (70%) of the pure product (Scheme 15).



Scheme 14 Photoredox-assisted synthesis of natural products



Scheme 15 Cyclohexene photoaziridination with TrocN_3 in flow

5 Further Photochemical Transformations for the Synthesis of Heterocycles

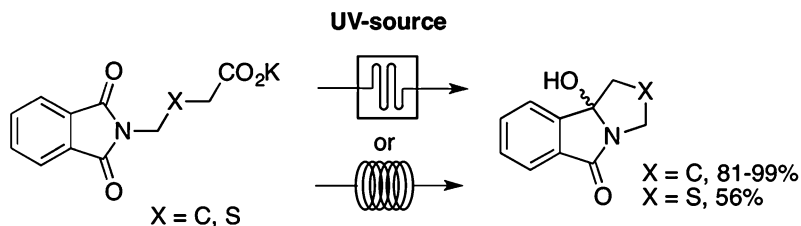
A general requirement for a photochemical reaction is that the photons must provide “just the right” energy. It is evident that visible light photons (400–800 nm) are less energetic (70–40 kcal/mol) as compared to UV light photons (150–70 kcal/mol). Thus, until recently, ultraviolet light has been mostly used to induce photochemical reactions. Alternatively, sunlight has been employed since the early days of organic photochemistry by Trommsdorf [66], Ciamician [67], and Nasini et al. [68]. Most of

the early reported examples of flow-assisted photosynthesis were performed using such traditional light sources – UV lamps or direct sunlight [19, 69]. To explore the opportunities of flow processing, common batch UV-promoted reactions have been typically translated to flow protocols [19]. Therefore, only a short selection of recent examples is presented.

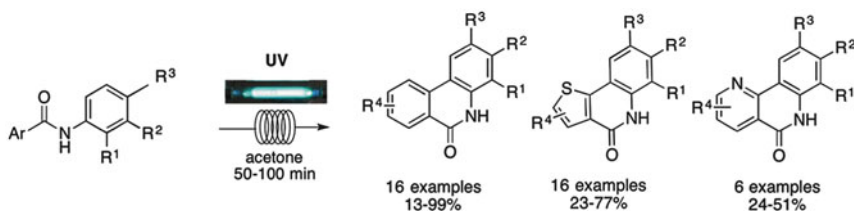
5.1 Cyclization Reactions

An interesting intramolecular decarboxylative radical cyclization reaction of phthalimides was recently reevaluated in flow by Shvydkiv et al. [70] and Josland et al. [71]. Processing a solution of the corresponding phthalimide in either a DIY chip or a commercially available capillary coil flow photoreactor under UV light irradiation granted access to valuable tricyclic heterocycles (Scheme 16). When working with UV-LEDs (UV-A), 4,4'-dimethoxybenzophenone was used as a photocatalyst. Additionally, Poliakoff and co-workers used the same reaction to illustrate the application of interchangeable narrowband excimer lamps as an alternative light source for photoflow processing [72].

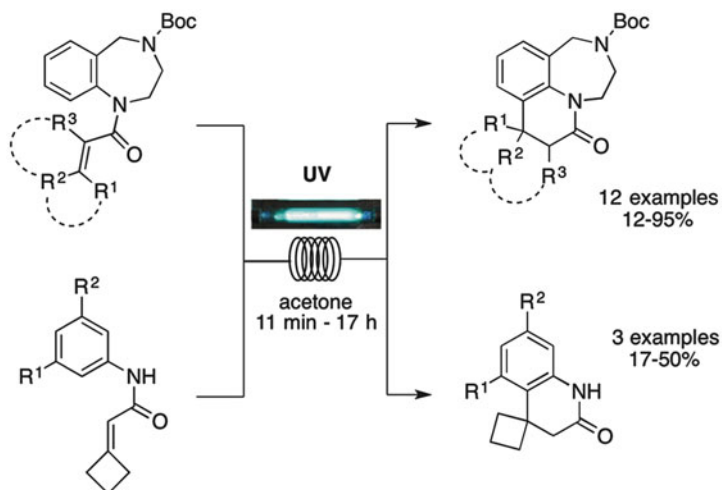
Several thieno[3,2-*c*]quinolin-4(5*H*)-ones, benzo[*h*]-1,6-naphthyridine-5(6*H*)-ones, and 6(5*H*)-phenanthridinones have been synthesized for use in a medicinal chemistry program (Scheme 17) [73, 74]. The photocyclization reactions were conducted in a commercially available tube-based reactor equipped with a medium pressure mercury lamp. Interestingly, the synthesis of benzo[*h*]-1,6-naphthyridine-



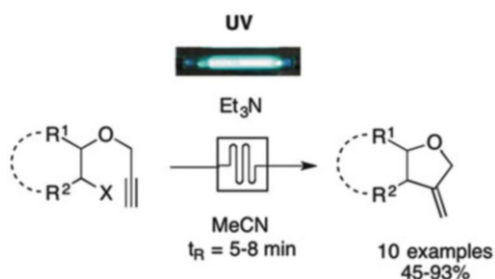
Scheme 16 Photodecarboxylative cyclization reaction of phthalimides



Scheme 17 Flow synthesis of various fused heterocycles using a commercially available UV photoreactor



Scheme 18 Photoflow [6 π]-acrylanilide cyclization toward tetrahydroquinolines

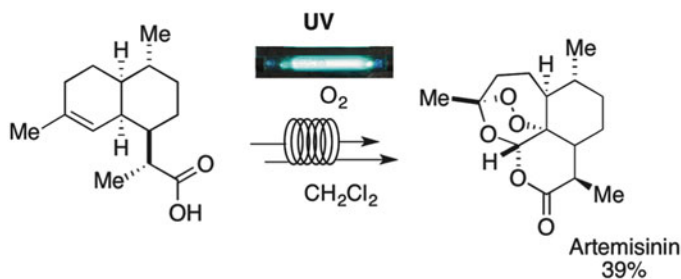


Scheme 19 Photosynthesis of fused tetrahydrofurans under flow conditions

5(6*H*)-ones was more demanding and required the addition of Ru(bpy)₃(PF₆)₂. The authors assume that its chelation to the pyridine nitrogen or amide functionalities contributes to the observed improved yields and not its photoredox activity. Purification issues could rationalize the lower isolated yields in the other case.

In a conceptually similar reaction, Koolman and co-workers presented the photoflow synthesis of 4,4'-disubstituted and spiro-tetrahydroquinolines via a [6 π]-acrylanilide cyclization (Scheme 18). Various flow conditions (residence times, reactor types, and mercury lamps) were required to generate the desired cyclization products in yields of 12–95% [75].

A novel approach to the intriguing 5-*exo-dig* photocyclization of organohalides onto a C–C triple bond under photoflow conditions to prepare fused tetrahydrofurans was reported by Fukuyama et al. [76]. After initial optimization, reaction times in the range of 5–8 min and yields in the range of 45–93% were achieved (Scheme 19). Additional deuterium-labeling experiments supported the proposed reaction mechanism proposed by the authors.



Scheme 20 Photochemical oxidation cascade for the synthesis of artemisinin from dihydroartemisinic acid

5.2 Oxygenations and Aerobic Oxidation Reactions

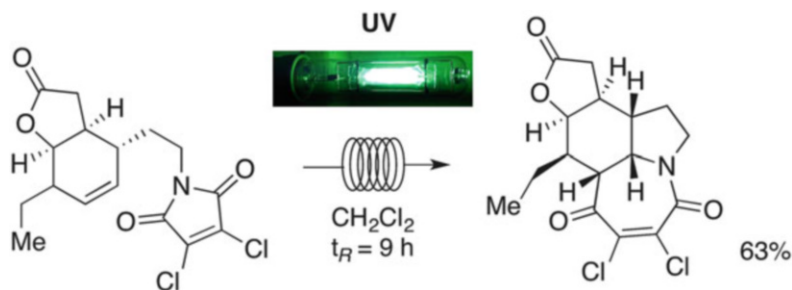
The synthesis of ascaridole (a heterocyclic peroxide) via the almost instantaneous [4 + 2] addition of $^1\text{O}_2$ to α -terpinene has often been employed as a benchmark reaction to evaluate and compare various flow reactor concepts for photochemical oxidations since the early days of photoflow synthesis [77–79].

Another remarkable oxygenation process is the synthesis of the sesquiterpene endoperoxide artemisinin – a first-line drug against multiresistant *Plasmodium* species in malaria treatment. Artemisinic acid is an abundant natural precursor and ideal starting point for the synthesis of artemisinin that involves a singlet oxygen-induced ene reaction and the addition of triplet oxygen to trigger the incorporation of the endoperoxide group essential for the biological activity. Levesque and Seeberger recently established a photoinduced and photosensitized (tetraphenylporphyrin) photoflow process delivering up to 200 g/day of artemisinin (Scheme 20) [80, 81].

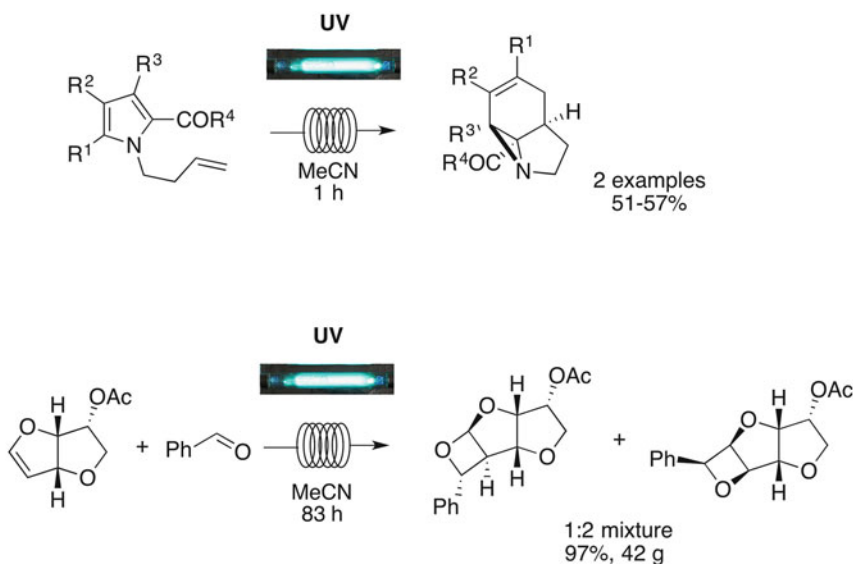
5.3 Cycloadditions

One of the first photoreactions able to generate complex naturally occurring heterocycles under flow conditions was reported by Booker-Milburn and co-workers at the University of Bristol back in 2008 [82]. Employing a [5 + 2] photocycloaddition of maleimide, an important part of the molecular skeleton of (\pm)-neostenine was accessed. The DIY tube-based flow photoreactor proved capable of producing >500 g/day (63% yield) of the desired pyrrolo[1,2-*a*]azepine core using a standard 400 W medium pressure mercury UV lamp (Scheme 21). Ultimately, the desired natural product could be obtained in 14 synthetic steps from the corresponding furan without using protecting groups.

The same group recently reported another interesting [2 + 2]/rearrangement sequence for the preparation of tricyclic aziridines from pyrroles using the same DIY flow reactor approach (Scheme 22a) [82]. After improving of the initial experimental setup, a direct batch-to-flow comparison was conducted. The study clearly demonstrated that unless careful precautions are taken to assure comparable



Scheme 21 Photoflow preparation of a key intermediate in the synthesis of (±)-neosteine

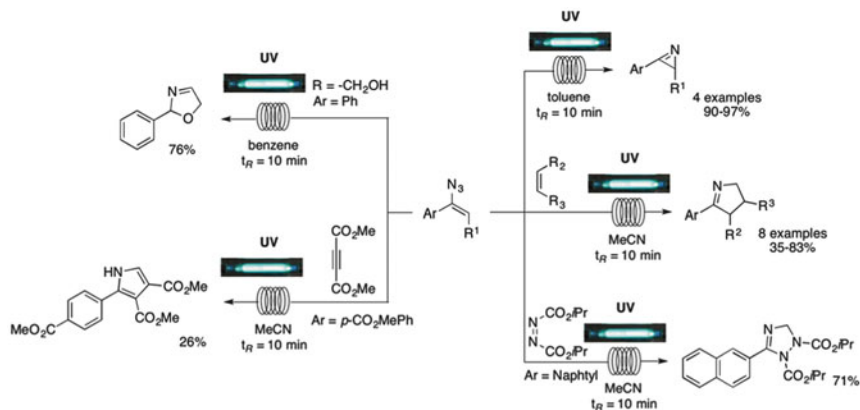


Scheme 22 [2 + 2] Cycloaddition approach to selected heterocyclic backbones

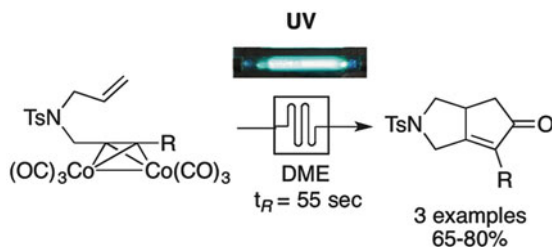
processing conditions, it is very difficult to decide whether batch or flow performs better. Interestingly, the obtained results clearly demonstrate that for the investigated type of photochemical reaction protocol, a carefully designed batch equipment is able to deliver results comparable to a flow process ($\pm 20\%$ yield difference) [83]. Another work published in 2016 on a Paterno-Büchi [2 + 2] photoflow cycloaddition depicts the preparation of an intermediate for the synthesis of the naturally occurring cytotoxic lactone (+)-goniofufrone on a >40 g scale (Scheme 22b) [84].

Rutjes and co-workers have synthesized a tricyclic nitrogen-containing scaffold via a [2 + 2] photoflow cycloaddition on a gram scale in a similarly constructed DIY flow photoreactor setup [85].

Kirschning and co-workers have used the [3 + 2] photocycloadditions of vinyl azides with selected 1,3-dipolarophiles to generate various nitrogen-containing



Scheme 23 Vinyl azides as substrates in [3 + 2] photocycloadditions under flow conditions



Scheme 24 Photoflow Pauson-Khand reaction

heterocycles [86]. Under thermal or photochemical conditions, vinyl azides lose nitrogen and transform into *2H*-azirines, which, if reacted further, yield nitrile ylides in situ able to further react with 1,3-dipolarophiles. For the *2H*-azirine syntheses, shown in Scheme 23, both thermal and photochemical generation under flow conditions were compared. Depending on the starting vinyl azide, differences in terms of isolated yields of up to 53% were observed, clearly demonstrating the mildness and general superiority of the photochemical flow approach.

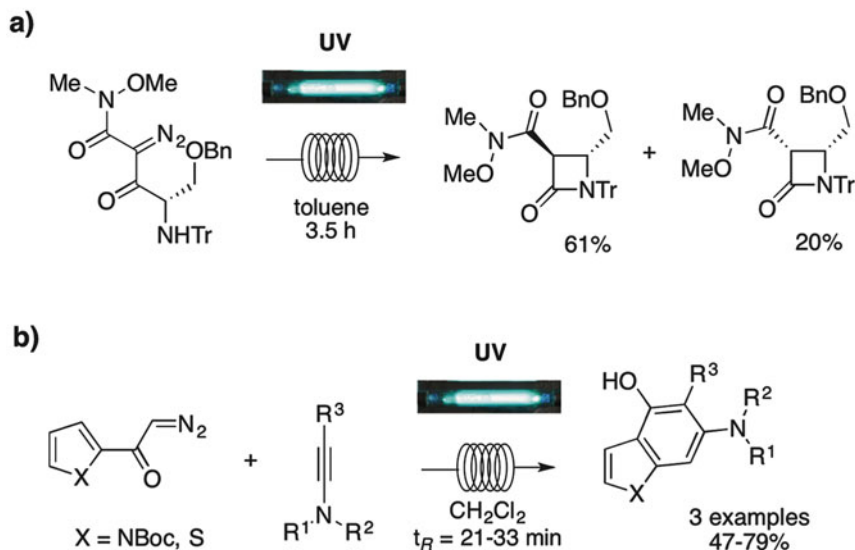
The Pauson–Khand [2 + 2 + 1] cycloaddition of an alkene, an alkyne, and a carbon monoxide is among the most preferred methods for the construction of complex cyclopentenone frameworks. Yoshida and co-workers have demonstrated that such Pauson–Khand reactions can be carried out very efficiently under photoflow conditions (Scheme 24) [87]. Under carefully optimized reaction conditions, a 0.05 M solution of the preformed cobalt complexes in 1,2-dimethoxyethane was processed under UV irradiation for only 55 s to accomplish the intramolecular Pauson–Khand transformation to the desired cycloadducts in good yields [87].

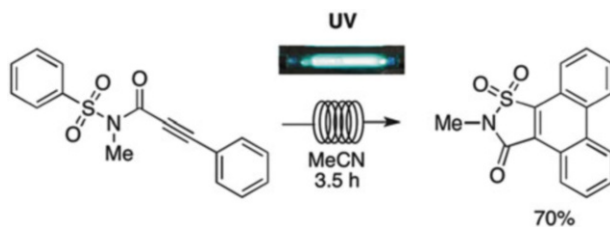
5.4 Rearrangements

The UV-reactivity profile of diazoketones has been utilized to trigger a Wolff rearrangement reaction [88, 89]. Aiming at improving throughput capacity, the Wolff rearrangement of a selected α -diazo- β -ketoamide was realized on 1 g scale. The reaction was complete after 3.5 h and afforded 81% of a 3:1 separable *trans/cis* mixture of the corresponding β -lactam (Scheme 25a). A benzannulation reaction was achieved via a pericyclic cascade mechanism triggered by a photochemical Wolff rearrangement of a diazoketone and followed by a cyclization with a corresponding ynamide to prepare a small number of indoles and benzothiophenes (Scheme 25b). Nearly identical yields were obtained in a batch vs. flow comparison study.

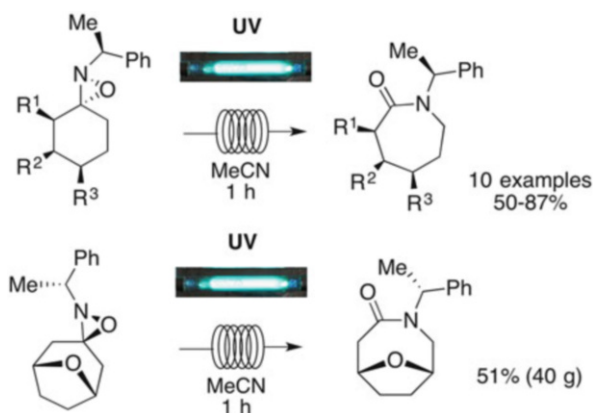
Xia and co-workers recently explored a novel photochemical approach for the synthesis of heterocyclic phenanthrene derivatives [90]. Starting from the linear 3-aryl-*N*-(arylsulfonyl)propiolamides, a tandem radical Smiles rearrangement/C-S bonding/Mallory reaction sequence was developed. To demonstrate the scalability of the synthetic protocol, a photoflow protocol with the optimal reaction conditions (UV-A light, 10 mM solution in acetonitrile) was successfully established (Scheme 26).

As a part of a medicinal chemistry efforts at Vertex Pharmaceuticals, a photoflow rearrangement toward chiral bicyclic lactams was evaluated [91]. As an alternative to the Schmidt and Beckmann rearrangements toward lactams, readily obtainable oxaziridines were subjected to UV irradiation in a DIY photoflow reactor in the form of a 0.1 M acetonitrile solution. After 26 min of processing, the desired chiral bicyclic products could be isolated in 50–87% yield (Scheme 27).





Scheme 26 Photoflow synthesis of phenanthrene derivatives



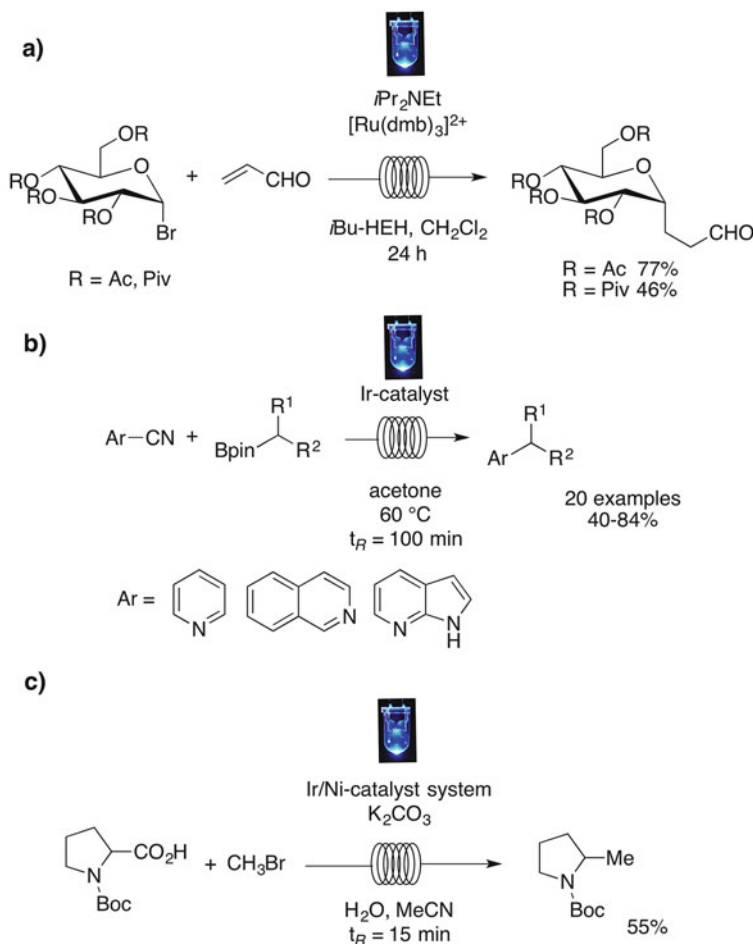
Scheme 27 Photoflow rearrangement of oxaziridines into lactams

6 Visible Light Photoredox Decoration of Heterocyclic Scaffolds

Highly functionalized heterocyclic moieties are of great importance for medicinal chemists to introduce further molecular diversity on selected lead structures. Following this line of thoughts, visible light photoredox synthesis offers a plethora of opportunities [23, 26]. In addition, an adequate combination with a well-designed flow process allows easy generation of gram quantities of the API for early stage pharmacological screenings. Numerous recent reports have documented successful examples of visible light photoflow functionalization of a variety of heterocyclic scaffolds. Since the aim of this chapter is to highlight heterocyclic synthesis, only the most recent trends in the area of scaffold decoration will be presented in the form of selected examples from 2012 to 2017. Further examples can be found in earlier review articles and books [16, 26].

Homogeneous transition metal-catalyzed cross-coupling reactions are of high importance to organic chemists in both academia and industry [92]. In this field, visible light photoredox reactions have turned out to be valuable complementary options or alternatives in several cases [93]. A recently published photoredox example mimicking a Heck vinylic substitution involves the coupling of aryl

aldehydes with brominated sugars [94]. Using a Ru-based photosensitizer and blue LEDs, scale-up study was performed, delivering multigram quantities of the glycoconjugates as starting point for the synthesis of glycopeptides. In an extended 24 h run, more than 97% conversion and up to 77% yield of the desired glycoconjugate were achieved (Scheme 28a). In 2016 Steven Ley and co-workers reported the visible light activation of boronic esters for efficient photoredox C–C couplings in a flow regime [95]. The dual iridium- and nickel-catalyzed photoflow process circumvents the known solubility issues associated with the use of potassium tetrafluoroborates. Importantly, the addition of a pyridine-derived base (DMAP) was found to be critical for the progress of the reaction. Based on this observation and additionally studies, the method was developed so that various cyanopyridines were coupled with corresponding boronic esters circumventing the need for DMAP (Scheme 28b). A similar concept of synergistic iridium and nickel



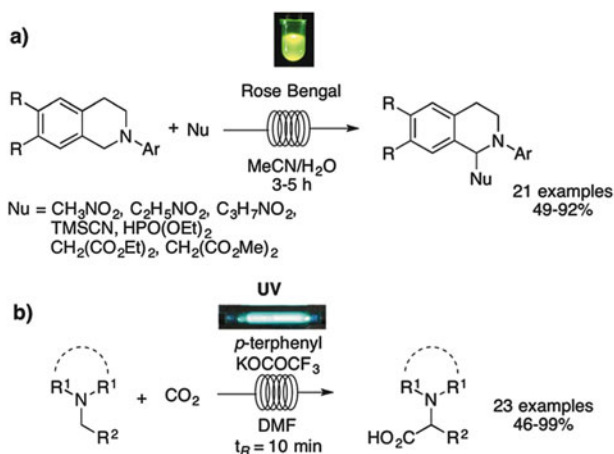
Scheme 28 Selected examples of C–C/C–H photoredox decoration of heterocyclic scaffolds

catalysis was used for the development of a $C(sp^3)-C(sp^3)$ coupling process upon visible light exposure to couple abundant carboxylic acids and alkyl halides [96]. Within the broad spectrum of published examples, the flow methylation of *N*-Boc proline with bromomethane in acetonitrile and in the presence of Ir/Ni-catalytic system deserves mentioning. Employing a Vapourtec E-series photoflow reactor, a 55% yield of the corresponding coupling product was obtained within 15 min residence time (Scheme 28c).

More recent selected C–C and C–H coupling examples include the use of alkyl trifluoroborates in a $C(sp^3)-C(sp^2)$ photoredox coupling [97, 98], the application of acridinium salts as organic alternative to iridium and ruthenium complexes [99], synergistic iridium/palladium photoredox catalysis [100], and tungsten salts [101] or titanium oxide [102] as photoredox catalysts.

Another commonly studied C–C coupling process relies on the photoredox generation of reactive amine radical cations and their interception by carbon nucleophiles [103]. Not surprisingly, a number of recent reports have documented the application of flow processing techniques to carry out such transformations. In 2013, the group of Rueping identified rose bengal as a beneficial organic photosensitizer for the α -functionalization of tertiary amines with several C- and P-nucleophiles [104]. Exposing a reaction mixture containing a tertiary amine, rose bengal, and a nucleophile (CH_3NO_2 , $CH_2(CO_2Et)_2$, TMSCN, $HPO(OEt)_2$, etc.) to green light provided the corresponding C–C and C–P adducts in good yields (Scheme 29a). A similar process was investigated by Opatz and co-workers in 2017 [105]. A sunlight-driven α -cyanation of tertiary amines to access the corresponding α -aminonitriles of several model substrates was used to evaluate the efficiency of a DIY flow reactor setup.

Apart from transformations based on the more traditional two-electron mechanisms for CO_2 activation, Jamison and co-workers established the α -carboxylation of tertiary amines with CO_2 as one-carbon building block in a green photoredox flow

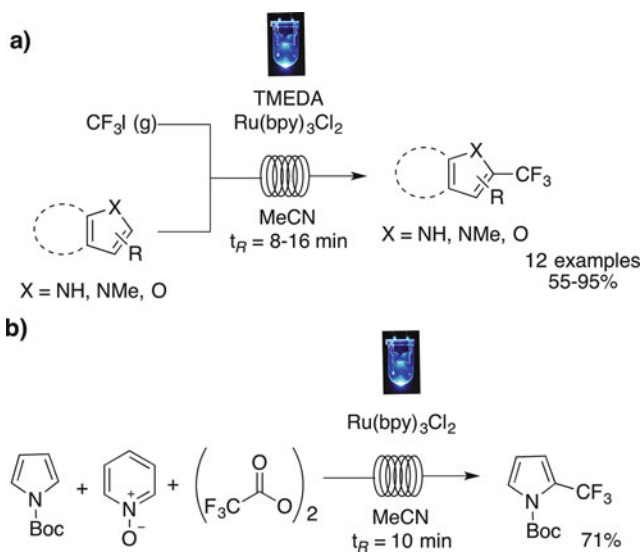


Scheme 29 Photoredox α -functionalization of tertiary amines

process. Using *p*-terphenyl as photosensitizer, KOCOCF_3 as base, and a UV light source, a small library of racemic amino acids was rapidly generated (Scheme 29b) [106].

Fluorine-containing heterocycles are important building blocks in pharmaceutical, agrochemical, and fine chemical industries. The incorporation of fluorinated functional groups often leads to overall improved chemical and pharmacological properties of drug candidates [107–109]. This has stimulated the development and improvement of novel methodologies to introduce fluorine-containing substituents [110]. Recently, several efforts to affect visible light photoredox-mediated trifluoromethylation of heterocyclic scaffolds in a flow regime have been reported.

In 2014 Noël and co-workers were arguably the first to present a photoredox flow trifluoromethylation of various five-membered heterocycles [111]. Using 1 mol% of $[\text{Ru}(\text{bpy})_3]\text{Cl}_2$ as a photosensitizer in the presence of an organic base and employing gaseous CF_3I and a short optimization in a DIY flow device, various CF_3 -substituted heterocycles were obtained within only 8–16 min residence time and 55–95% yield (Scheme 30a). The same procedure was further applied in the generation of several perfluoroalkylated indoles. Stephenson's group dedicated considerable efforts in the investigation of novel methodologies to introduce CF_3 substituents. In a scalable trifluoromethylation process, trifluoroacetic acid and its anhydride have been exploited as an attractive and alternative low-cost source of CF_3 radicals [112]. Pyridine *N*-oxide was used as sacrificial redox auxiliary to generate an adduct that could be easily decomposed by light irradiation to generate a CF_3 radical and pyridine, thus omitting the addition of exogenous base. In a scale-up study, gram amounts of trifluoromethylated *N*-Boc pyrrole were successfully generated (Scheme 30b). A follow-up study by the same group includes an extended scope of generated heterocycles and a scale increased to nearly 1 kg [113].



Scheme 30 Photoredox trifluoromethylation of heterocyclic scaffolds

Further examples of flow-assisted photoredox functionalizations on heterocyclic scaffolds include examples of reductive dehalogenation, deoxygenation, decarboxylation, and numerous other types of reaction types which have been reviewed elsewhere [114–117].

7 Conclusions

The selection of examples summarized in this chapter is clear evidence that many types of visible light photoredox and more traditional UV light-promoted transformations for the preparation of heterocyclic scaffolds can be carried out successfully under continuous flow conditions. Although dramatic rate enhancement compared to many classical batch processes have been observed in a majority of cases, many of those comparisons are difficult to interpret, since they all suffer from the evident difficulty to design experiments allowing valid conclusions on the methodical performance of batch and flow techniques employing reactor setups, and processing principles are very different from each other. Nevertheless, continuous flow technology offers a powerful although currently rather costly option for transferring small-scale laboratory protocols to industrial process scale. Although this main hurdle for implementing photochemistry into chemical industry has yet to be overcome, it has already become common practice to employ the continuous flow approach to demonstrate a scale-up option for a specific photochemical process.

Additionally, the high price of commercially available continuous flow photoreactor systems keeps the design and usage of DIY reaction equipment attractive and may be the main reason for the high number of publications with such DIY devices.

Visible light photoredox synthesis of heterocycles offers a valuable alternative to more conventional syntheses (e.g., Suzuki or Heck C–C coupling reactions) and is able to provide alternative disconnection patterns, establishing new and divergent synthetic routes. The portfolio of disclosed photoredox-catalyzed reactions underlines the diversity of photoredox methodologies and their potential scope. The remaining challenges (light intensity/penetration depth issues, efficient mixing) can be conquered with the help of continuous flow processing to feature reproducibility and scalability.

References

1. Pozharskii AF, Soldatenkov A, Katritzky AR (2011) *Heterocycles in life and society: an introduction to heterocyclic chemistry, biochemistry and applications*. 2nd edn. Wiley, New York
2. Alvarez-Builla J, Vaquero JJ, Barluenga J (eds) (2011) *Modern heterocyclic chemistry*, vol 1–4. Wiley VCH, Weinheim
3. Eicher T, Hauptmann S, Speicher A (2012) *The chemistry of heterocycles: structures, reactions, synthesis and applications*. 3rd edn. Wiley-VCH, Weinheim

4. Su Y, Straathof NJW, Hessel V, Noël T (2014) *Chem Eur J* 20:10562
5. Garlets ZJ, Nguyen JD, Stephenson CRJ (2014) *Isr J Chem* 54:351
6. Schuster EM, Wipf P (2014) *Isr J Chem* 54:361
7. Staveness D, Bosque I, Stephenson CRJ (2016) *Acc Chem Res* 49:2295
8. Romero NA, Nicewicz DA (2016) *Chem Rev* 116:10075
9. Cambie D, Bottecchia C, Straathof NJW, Hessel V, Noël T (2016) *Chem Rev* 116:10276
10. Zhou L, Hossain ML, Xiao T (2016) *Chem Rec* 16:319
11. Shaw MH, Twilton J, MacMillan DWC (2016) *J Org Chem* 81:6898
12. Mizuno K, Nishiyama Y, Ogaki T, Terao K, Ikeda H, Kakiuchi K (2016) *J Photochem Photobiol C Photochem Rev* 29:107
13. Ciriminna R, Delisi R, Xu Y-J, Pagliaro M (2016) *Org Process Res Dev* 20:403
14. Douglas JJ, Sevrin MJ, Stephenson CRJ (2016) *Org Process Res Dev* 20:1134
15. Morse PD, Beingessner RL, Jamison TF (2017) *Isr J Chem*. <https://doi.org/10.1002/ijch.201600095>
16. Noël T (ed) (2017) *Photochemical processes in continuous-flow reactors: from engineering principles to chemical applications*. World Scientific Publishing, London
17. Glasnov T (2016) *Continuous-flow chemistry in the research laboratory: modern organic chemistry in dedicated reactors at the dawn of the 21st century*. Springer, Heidelberg
18. Matsushita Y, Ichimura T, Ohba N, Kumada S, Sakeda K, Suzuki T, Tanibata H, Murata T (2007) *Pure Appl Chem* 79:1959
19. Knowles JP, Elliot LD, Booker-Milburn KI (2012) *Beilstein J Org Chem* 8:2025
20. Wirth T (ed) (2013) *Microreactors in organic chemistry and catalysis*. 2nd edn. Wiley-VCH, Weinheim
21. Hessel V, Kralish D, Kockmann N (2015) *Novel process windows – innovative gates to intensified and sustainable chemical processes*. Wiley-VCH, Weinheim
22. Hedstrand DM, Kruizinga WH, Kellogg RM (1978) *Tetrahedron Lett* 19:1255
23. Nicewicz DA, MacMillan DWC (2008) *Science* 322:77
24. Ischay MA, Anzovino ME, Du J, Yoon TP (2008) *J Am Chem Soc* 130:12886
25. Tucker JW, Stephenson CRJ (2012) *J Org Chem* 77:1617
26. Prier CK, Rankic DA, MacMillan DWC (2013) *Chem Rev* 113:5322
27. Piter SP, McTiernan CD, Scaiano JC (2016) *Acc Chem Res* 49:1320
28. Arias-Rotondo DM, McCusker JK (2016) *Chem Soc Rev* 45:5803
29. Corrigan N, Shanmugam S, Xu J, Boyer C (2016) *Chem Soc Rev* 45:6165
30. Hoffmann N (2017) *Eur J Org Chem* 2017:1982
31. Lerch S, Unkel L-N, Wienefeld P, Brasholz M (2014) *Synlett* 25:2673
32. Teegardin K, Day JJ, Chan J, Weaver J (2016) *Org Process Res Dev* 20:1156
33. Naranyanam JM, Stephenson CRJ (2011) *Chem Soc Rev* 40:102
34. Boubertakh O, Goddard JP (2017) *Eur J Org Chem* 2017:2072
35. Chen J-R, Hu X-Q, Lu L-Q, Xiao W-J (2016) *Acc Chem Res* 49:1911
36. Kärkäs MD, Porco Jr JA, Stephenson CRJ (2016) *Chem Rev* 116:9683
37. Tucker JW, Zhang Y, Jamison TF, Stephenson CRJ (2012) *Angew Chem Int Ed* 51:4144
38. Kreis LM, Krautwald S, Pfeiffer N, Martin RE, Carreira EM (2013) *Org Lett* 15:1634
39. Rackl D, Kais V, Lutsker E, Reiser O (2017) *Eur J Org Chem* 2017:2130
40. Ghogare AA, Greer A (2016) *Chem Rev* 116:9994
41. Maurya RA, Park CP, Kim D-P (2011) *Beilstein J Org Chem* 7:1158
42. Park CP, Maurya RA, Lee JH, Kim D-P (2011) *Lab Chip* 11:1941
43. Yavorsky A, Shvydkiv O, Limburg C, Nolan K, Delaure YMC, Oelgemöller M (2012) *Green Chem* 14:888
44. Ziegenbalg D, Kreisel G, Weiß D, Kralisch D (2014) *Photochem Photobiol Sci* 13:1005
45. Wu G, Lv T, Mo W, Yang X, Gao Y, Chen H (2017) *Tetrahedron Lett* 58:1395
46. Cremlyn RJ (1996) *An introduction to organosulfur chemistry*. Wiley-VCH, New York
47. Talla A, Driessen B, Straathof NJW, Milroy L-G, Brunsveld L, Hesel V, Noël T (2015) *Adv Synth Catal* 357:2180

48. Bottecchia C, Erdmann N, Tjjssem PMA, Milroy L-G, Brunsveld L, Hessel V, Noël T (2016) *ChemSusChem* 9:1781
49. Thevissen K, Marchand A, Chaltin P, Meert EMK, Cammue BPA (2009) *Curr Med Chem* 16:2205
50. Roy J, Jana AK, Mal D (2012) *Tetrahedron* 68:6099
51. Bashir M, Afifa B, Subhan A (2015) *Molecules* 20:13496
52. Parisien-Collette S, Hernandez-Perez AC, Collins SK (2016) *Org Lett* 18:4994
53. Hernandez-Perez AC, Collins SK (2013) *Angew Chem Int Ed* 52:12696
54. Hernandez-Perez AC, Caron A, Collins SK (2015) *Chem Eur J* 21:16673
55. Poplata S, Tröster A, Zou Y-Q, Bach T (2016) *Chem Rev* 116:9748
56. Kumarasamy E, Raghunathan R, Jockusch S, Ugrinov A, Sivaguru S (2014) *J Am Chem Soc* 136:8729
57. Chandrasekhar D, Borra S, Kapure JS, Shailendra Shivaji GS, Srinivasulu G, Maurya RA (2015) *Org Chem Front* 2:1308
58. Chandrasekhar D, Borra S, Nanubolu JB, Maurya RA (2016) *Org Lett* 18:2974
59. Borra S, Chandrasekhar D, Adhikary S, Rasala S, Gokulnath S, Maurya RA (2017) *J Org Chem* 82:2249
60. Tiwari DK, Maurya RA, Nanubolu JB (2016) *Chem Eur J* 22:526
61. He Z, Bae M, Wu J, Jamison TF (2014) *Angew Chem Int Ed* 53:14451
62. Beatty JW, Stephenson CRJ (2014) *J Am Chem Soc* 136:10270
63. Huang C-Y, Doyle AG (2014) *Chem Rev* 114:8153
64. Yudin AK (ed) (2006) *Aziridines and epoxides in organic synthesis*. Wiley-VCH, Weinheim
65. Scholz SO, Farney EP, Kim S, Bates DM, Yoon TP (2016) *Angew Chem Int Ed* 55:2239
66. Trommsdorf H (1834) *Ann Chem Pharm* 11:190
67. Ciamician G (1912) *Science* 36:385
68. Nasini R, Brown R, Ree A, Miller WL, Hewitt JT, Dawson HM, Knecht E (1926) *J Chem Soc* 129:993
69. Oelgemöller M (2016) *Chem Rev* 116:9664
70. Shvydkiv O, Nolan K, Oelgemöller M (2011) *Beilstein J Org Chem* 7:1055
71. Josland S, Mumatz S, Oelgemöller M (2016) *Chem Eng Technol* 39:81
72. DeLaney EN, Lee DS, Elliott LD, Jin J, Booker-Milburn KI, Poliakoff M, George MW (2017) *Green Chem* 19:1431
73. Fang Y, Tranmer GK (2016) *Org Biomol Chem* 14:10799
74. Fang Y, Tranmer GK (2016) *Med Chem Commun* 7:720
75. Koolman HF, Braje WM, Haupt A (2016) *Synlett* 27:2561
76. Fukuyama T, Fujita Y, Rashid MA, Ryu I (2016) *Org Lett* 18:5444
77. Bourne RA, Han X, Chapman AO, Arrowsmith NJ, Kawanami H, Poliakoff M, George MW (2008) *Chem Commun*:4457
78. Levesque F, Seeberger PH (2011) *Org Lett* 13:5008
79. Han X, Bourne RA, Poliakoff M, George MW (2011) *Chem Sci* 2:1059
80. Levesque F, Seeberger PH (2012) *Angew Chem Int Ed* 51:1706
81. Lainchbury MD, Medley MI, Taylor PM, Hirst P, Dohle W, Booker-Milburn KI (2008) *J Org Chem* 73:6497
82. Maskill KG, Knowles JP, Elliott LD, Alder RW, Booker-Milburn KI (2013) *Angew Chem Int Ed* 52:1499
83. Elliott LD, Knowles JP, Koovits PJ, Maskill KG, Ralph MJ, Lejeune G, Edwards LJ, Robinson RI, Clemens IR, Cox B, Pascoe DD, Koch G, Eberle M, Berry MB, Booker-Milburn KI (2014) *Chem Eur J* 53:15226
84. Ralph M, Ng S, Booker-Milburn KI (2016) *Org Lett* 18:968
85. Blanco-Ania D, Gawade SA, Zwinkels LJJ, Maartense L, Bolster MG, Benningshof JCI, Rutjes FPJ (2015) *Org Process Res Dev* 20:409
86. Cludius-Brandt S, Kupracz L, Kirschning A (2013) *Beilstein J Org Chem* 9:1745
87. Asano K, Uesugi Y, Yoshida J-I (2013) *Org Lett* 15:2398

88. Vaske YSM, Mahoney ME, Konopelski JP, Rogow DL, McDonald WJ (2010) *J Am Chem Soc* 132:11379
89. Willumstad TP, Haze O, Mak XY, Lam TY, Wang Y-P, Danheiser RL (2013) *J Org Chem* 78:11450
90. Chen M, Yang Y, Wang Y, Li D, Xia W (2016) *Org Lett* 18:2280
91. Cochran JE, Waal N (2016) *Org Process Res Dev* 20:1533
92. De Meijere A, Bräse S, Oestreich M (eds) (2014) *Metal catalyzed cross-coupling reactions and more*. Wiley-VCH, Weinheim
93. Ravelli D, Protti S, Fagnoni M (2016) *Chem Rev* 116:9859
94. Andrews RS, Becker JJ, Gagne MR (2012) *Angew Chem Int Ed* 51:4140
95. Lima FL, Kabeschov MA, Tran DN, Battilocchio C, Sedelmeier J, Sedelmeier G, Schenkel B, Ley SV (2016) *Angew Chem Int Ed* 55:14085
96. Johnston CP, Smith RT, Allmendinger S, MacMillan DWC (2016) *Nature* 536:322
97. DeLano TJ, Bandarage UK, Palaychuk N, Green J, Boyd MJ (2016) *J Org Chem* 81:12525
98. Palaychuk N, DeLano TJ, Boyd MJ, Green J, Bandarage UK (2016) *Org Lett* 18:6180
99. Joshi-Pangu A, Levesque F, Roth HG, Oliver SF, Campeau L-C, Nicewicz D, DiRocco DA (2016) *J Org Chem* 81:7244
100. Sharma UK, Gemoets HPL, Schröder F, Noël T, van der Eycken EV (2017) *ACS Catal* 7:3818
101. Capaldo L, Fagnoni M, Ravelli D (2017) *Chem Eur J* 23:6527
102. Fabry DC, Ho YA, Tremel W, Panthöfer M, Rueping M, Rehm TH (2017) *Green Chem* 19:1911
103. Hu J, Wang J, Nguyen TH, Zheng N (2013) *Beilstein J Org Chem* 9:1977
104. Rueping M, Vila C, Bootwicha T (2013) *ACS Catal* 3:1676
105. Nauth AM, Lipp A, Lipp B, Opatz T (2017) *Eur J Org Chem* 2017:2099
106. Seo H, Katcher MH, Jamison TF (2017) *Nat Chem* 9:453
107. Kirsch P (2004) *Modern fluoroorganic chemistry: synthesis, reactivity, applications*. Wiley-VCH, Weinheim
108. Begue JP, Bonnet-Delpon F (2008) *Bioorganic and medicinal chemistry of fluorine*. Wiley-VCH, Weinheim
109. Rehm TH (2016) *Chem Eng Technol* 39:66
110. Chatterjee T, Iqbal N, You Y, Cho EJ (2016) *Acc Chem Res* 49:2284
111. Straathof NJW, Gemoets HPL, Wang X, Schouten JC, Hessel V, Noël T (2014) *ChemSusChem* 7:1612
112. Beatty JW, Douglas JJ, Cole KP, Stephenson CRJ (2015) *Nat Commun* 6:7919
113. Beatty JW, Douglas JJ, Miller R, McAtee RC, Cole KP, Stephenson CRJ (2016) *Chem* 1:456
114. Nguyen JD, Reiss B, Dai C, Stephenson CRJ (2013) *Chem Commun* 49:4352
115. Weaver JD (2014) *Synlett* 25:1946
116. Perkowski AJ, Cruz CL, Nicewicz DA (2015) *J Am Chem Soc* 137:15684
117. Roslin S, Odell R (2017) *Eur J Org Chem* 2017:1993

Flow-Assisted Synthesis of Heterocycles via Multicomponent Reactions



Seger Van Mileghem, Cedrick Veryser, and Wim M. De Borggraeve

Contents

1	Introduction	136
2	Formation of Five-Membered Heterocycles	136
2.1	Five-Membered Heterocycles Containing One Heteroatom	136
2.2	Five-Membered Heterocycles Containing Two Heteroatoms	137
2.3	Five-Membered Heterocycles Containing Three Heteroatoms	142
3	Formation of Six-Membered Heterocycles	147
3.1	Six-Membered Heterocycles Containing One Heteroatom	147
3.2	Six-Membered Heterocycles Containing Two Heteroatoms	151
4	Formation of Seven- and Higher-Membered Heterocycles	154
5	Conclusion and Future Perspectives	155
	References	157

Abstract Multicomponent reactions (MCRs) are of great significance in organic synthesis. They often decrease the number of synthesis steps since three or more reactants are incorporated in the product in a single step. This increases the number of combinatorial options and allows more efficient processes in less time. The pharmaceutical industry is therefore very fond of MCRs for the construction of libraries. As a consequence, the field is being investigated intensely for the enhancement of chemical processes and the discovery of new types of MCRs.

The combination of the benefits of flow technology and MCRs for heterocycle synthesis is an interesting and specialized field. This chapter serves as an overview of the literature covering this topic starting from 2010, up to when the literature on this matter is reviewed in a book chapter in this book series by Cukalovic et al. (Top Heterocycl Chem 23:161–198, 2010).


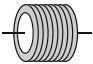
Keywords Continuous flow · Heterocycles · Multicomponent reactions · Synthesis

S. Van Mileghem, C. Veryser, and W. M. De Borggraeve (✉)
Molecular Design and Synthesis, Department of Chemistry, KU Leuven, Leuven, Belgium
e-mail: wim.deborggraeve@kuleuven.be

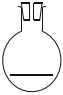




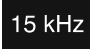

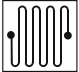





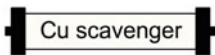

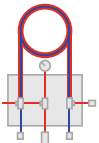

Abbreviations

2-MeTHF	2-Methyltetrahydrofuran
AcOH	Acetic acid
Boc	<i>tert</i> -Butoxycarbonyl
BPR	Back-pressure regulator
DBU	1,8-Diazabicyclo[5.4.0]undec-7-ene
DCM	Dichloromethane
DIPEA	<i>N,N</i> -Diisopropylethylamine
DMA	<i>N,N</i> -Dimethylacetamide
DMAP	4-Dimethylaminopyridine
DME	1,2-Dimethoxyethane
DMF	<i>N,N</i> -Dimethylformamide
EDC	1-Ethyl-3-(3-dimethylaminopropyl)carbodiimide
eq	Equivalents
Et ₂ O	Diethyl ether
Et ₃ N	Triethylamine
EtOAc	Ethyl acetate
EtOH	Ethanol
HOBt	1-Hydroxybenzotriazole
kHz	Kilohertz
M	Molar
MCR	Multicomponent reaction
MeCN	Acetonitrile
MeOH	Methanol
MW	Microwave
PEG200	Polyethylene glycol 200
PEG300	Polyethylene glycol 300
PFA	Perfluoroalkoxy alkane
psi	Pound-force per square inch
PTFE	Polytetrafluoroethylene (Teflon [®])
<i>t</i> -BuONO	<i>tert</i> -Butyl nitrite
TMSN ₃	Trimethylsilyl azide

Legends

	Back-pressure regulator (BPR)
	Coil reactor (copper/PTFE/stainless steel)

(continued)

	Collection flask
	Continuous extraction
	Control flow unit (CFU)
	Heat exchanger
	In-line infrared flow cell
	Magnetic field generator working at 15 kHz
	Mass flow controller (MFC)
	Microreactor chip
	Mixer
	Ozone generator
	Reagent loop
	Photo reactor
	Pump
	QuadraPure TU scavenging resin
	Residence time unit (RTU)
	Telfon AF-2400 tube-in-tube reactor
	Tubular column reactor

1 Introduction

Multicomponent reactions (MCRs) are considered an important tool in organic synthesis [1]. By definition, MCRs combine at least three reactants that generate a product containing most atoms of the starting materials. Examples of classic MCRs are the Ugi, Mannich, Hantzsch, Strecker, and Biginelli reactions [2–7]. All of these have been explored and further adapted over the years. In recent decades, the notion of green and sustainable chemistry has reshaped the way chemists conceive synthesis; the focus is not only on the development of novel methods but also on finding more sustainable alternatives for existing ones [8–10]. In this respect, MCRs are gaining attention because they can be used to produce diverse compound libraries in a single step, drastically reducing the environmental footprint of the chemistry, compared to sequential reaction approaches. Moreover, the time saved by this approach in library synthesis is an added financial benefit. Therefore, pharmaceutical research has shown significant interest in MCRs for the ease of construction of libraries and is probably the main industry strongly supporting the further development of MCR research, especially for heterocycle synthesis. The MCR field is thus explored intensively and is expected to receive further attention in the future.

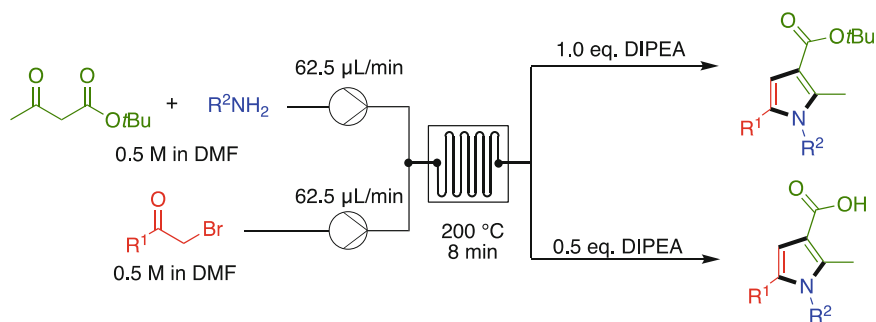
While the combination of flow technology and MCRs for heterocycle synthesis offers interesting advantages, the literature covering this specialized topic is still rather limited. Moreover, in batch, the difference between MCRs and one-pot multistep reactions is clear, but this is less so when dealing with flow chemistry. Here, only a thin line differentiates MCRs from telescoped/multistep protocols and investigators prefer using the terms telescoped and multistep reactions over MCR. Strictly speaking, in an MCR (in batch), all reactants are added at once, and three or more compounds are (partially) incorporated in the product. Due to technical constraints in continuous flow (four-way valves and higher), reactions involving three or more reagents are often performed in a telescoped manner: two streams are connected via a T-piece. The combined stream is then connected to another stream via a T-piece, introducing another reagent, etc. We prefer to also incorporate these reactions in this review and hence extend the concept of MCRs in flow to telescoped reactions where no in-line purification of intermediates is performed before the next reactant is added.

This review gives an overview of the literature since 2010 covering the combination of MCRs with continuous flow chemistry for the synthesis of heterocycles. Literature before 2010 has been covered in a review by Cukalovic et al. in this book series [1].

2 Formation of Five-Membered Heterocycles

2.1 *Five-Membered Heterocycles Containing One Heteroatom*

In 2010, Cosford and coworkers reported a one-step continuous flow procedure to produce highly substituted pyrrole-3-carboxylic acids [11]. The synthetic strategy relied on the Hantzsch pyrrole synthesis [3], starting from *tert*-butyl acetoacetates,



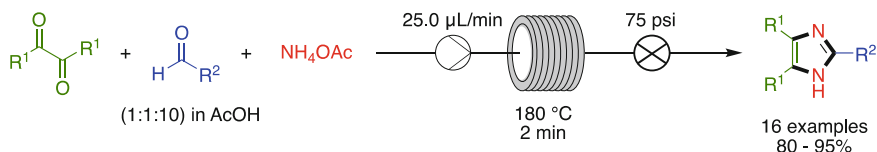
Scheme 1 Synthesis of highly substituted pyrrole-3-carboxylic acid derivatives via in situ hydrolysis of tert-butyl esters [11]

2-bromoketones, and primary amines (or ammonia). This three-component reaction results in the formation of pyrrole-3-carboxylic esters. When the HBr by-product is not neutralized, in situ deprotection of the *tert*-butyl ester yields pyrrole-3-carboxylic acids in an uninterrupted flow sequence (Scheme 1). Noteworthy, when the optimized flow conditions were translated to batch synthesis, the pyrrole-3-carboxylic acid was isolated in significantly lower yield (40% instead of 65%).

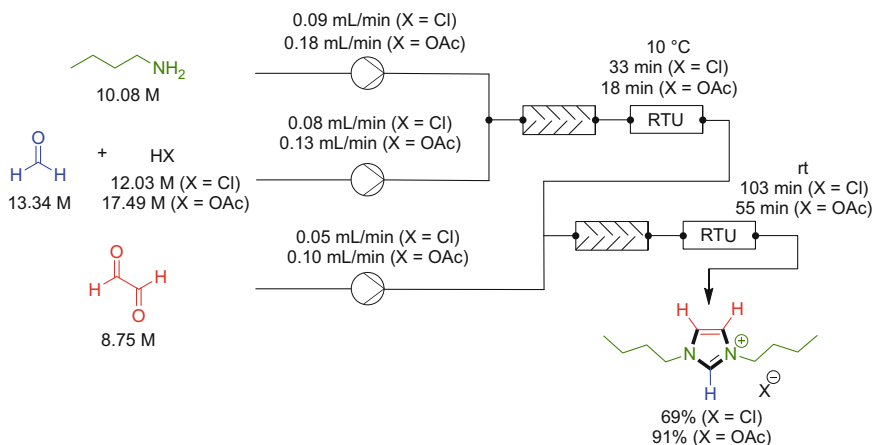
2.2 Five-Membered Heterocycles Containing Two Heteroatoms

The Debus–Radziszewski synthesis is one of the classical strategies to generate imidazoles [12, 13]. This MCR starts from a 1,2-dicarbonyl compound, an aldehyde, and ammonia (or a primary amine). In batch, this reaction requires harsh conditions (reflux in acetic acid) and prolonged reaction times, which often results in low yields of product. The Jia group envisioned that flow chemistry could serve as a viable alternative to improve this reaction, as heat transfer in a flow reactor is significantly better than in a batch reactor. They developed an efficient synthesis of imidazoles under superheating conditions by using a continuous flow microreactor system under pressure [14]. This process greatly enhanced the reaction rate of the imidazole formation and near quantitative yields were achieved (Scheme 2).

The Stark group developed an efficient flow procedure to provide 1,3-dialkylimidazolium-based ionic liquids, starting from readily available commodity chemicals such as glyoxal, monoalkylamines, formaldehyde, and an acid (Scheme 3) [15]. This modified Radziszewski reaction demonstrates high atom efficiency as water is the only by-product formed. Key to the success of this approach is the enhanced mixing and heat transfer in the flow setup. These intensified conditions reduced the reaction time by a factor of 3 compared to a traditional batch setup under similar conditions, while slightly improved yields were obtained.



Scheme 2 Synthesis of imidazoles from 1,2-diketones, aldehydes and ammonium acetate under superheating conditions in a microreactor [14]

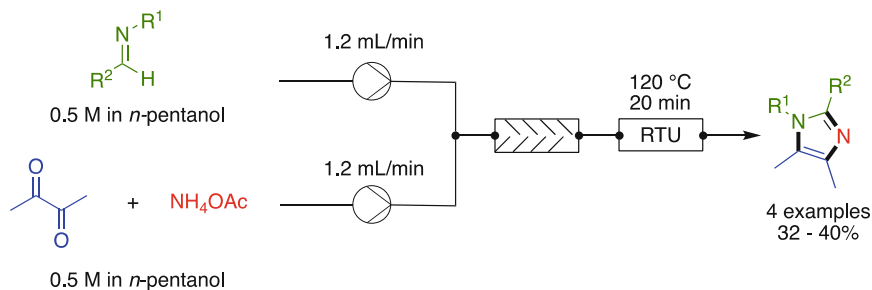


Scheme 3 Synthesis of 1,3-dialkylimidazolium-based ionic liquids under continuous flow conditions [15]

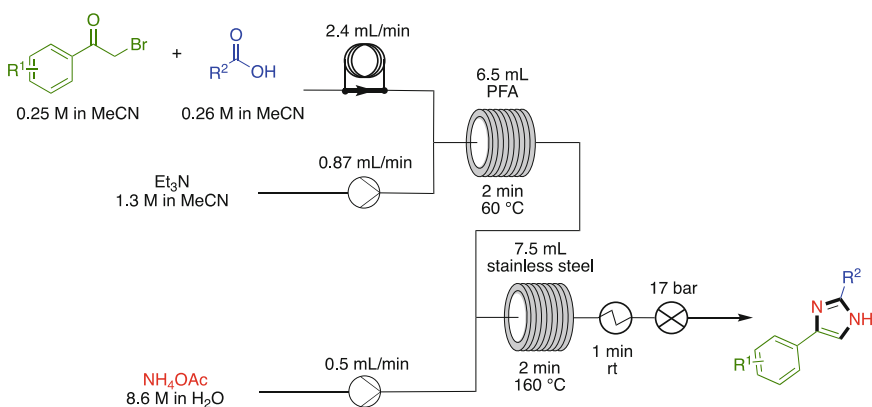
Another modification of the Radziszewski MCR was used by Maton et al. to synthesize tetrasubstituted imidazoles under continuous flow conditions [16]. First, the imine building block was generated in batch from the corresponding aldehyde and amine. This intermediate was subsequently mixed with a stream of diacetyl and ammonium acetate in a microreactor. After a residence time of 20 min at 120 $^{\circ}\text{C}$, the desired tetrasubstituted imidazoles were produced in moderate yields (Scheme 4).

Carneiro et al. applied continuous flow technology to synthesize 1*H*-4-substituted imidazoles [17]. In this two-step flow protocol, the intermediate α -acyloxy ketone is first generated from α -bromoacetophenone and a carboxylic acid, which subsequently undergoes a condensation reaction with ammonium acetate to the 1*H*-4-substituted imidazoles (Scheme 5). The reaction was performed at 160 $^{\circ}\text{C}$, which is far above the normal boiling point of the solvent used. A back-pressure regulator (BPR) ensured that all volatiles remained in solution. Under these intensified conditions, excellent yields of the desired imidazoles were achieved after a residence time of 4 min. Moreover, this flow process was successfully utilized for the continuous production of the NS5A inhibitor Daclatasvir.

The Patel group designed a two-step gas/liquid–liquid/liquid flow system for the synthesis of 4-fluoropyrazoles [18]. The first step consists of direct fluorination of a diketone, followed by cyclization of the fluorodiketone intermediate with hydrazine



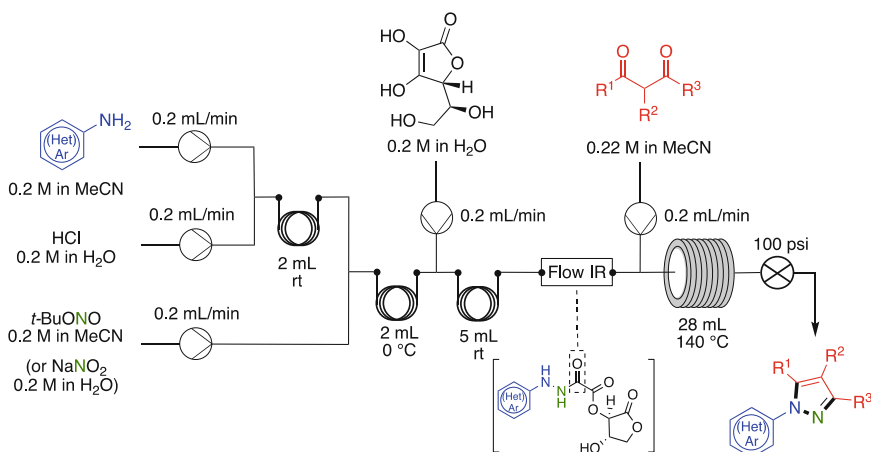
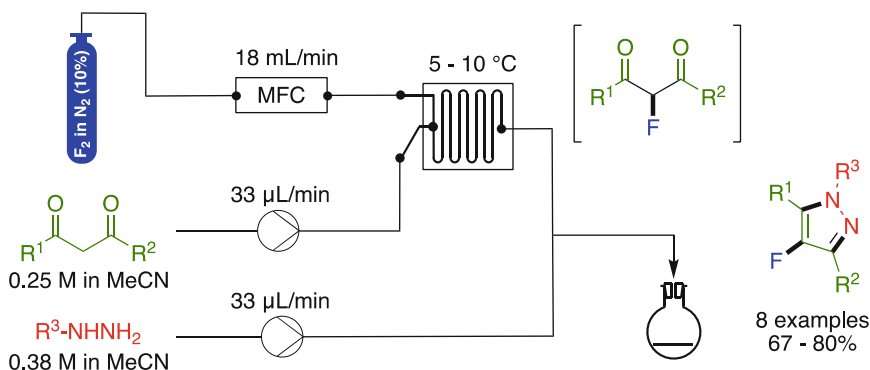
Scheme 4 Synthesis of tetrasubstituted imidazoles from imines, diacetyl, and ammonium acetate [16]



Scheme 5 Two-step flow process towards 1*H*-4-substituted imidazoles [17]

(Scheme 6). Direct fluorination in flow was achieved using a diluted stream of fluorine gas (10% v/v with nitrogen gas). In order to regulate off-gassing in the micro-reactor, a mass flow controller (MFC) was used. After reaction, the crude mixture was neutralized to remove the HF formed during the reaction. Subsequent extraction and purification by crystallization or column chromatography furnished the fluoropyrazoles in good yields. Of note, this is the first example where the carbon–fluorine bond is installed at the beginning of a continuous gas/liquid–liquid/liquid process in flow.

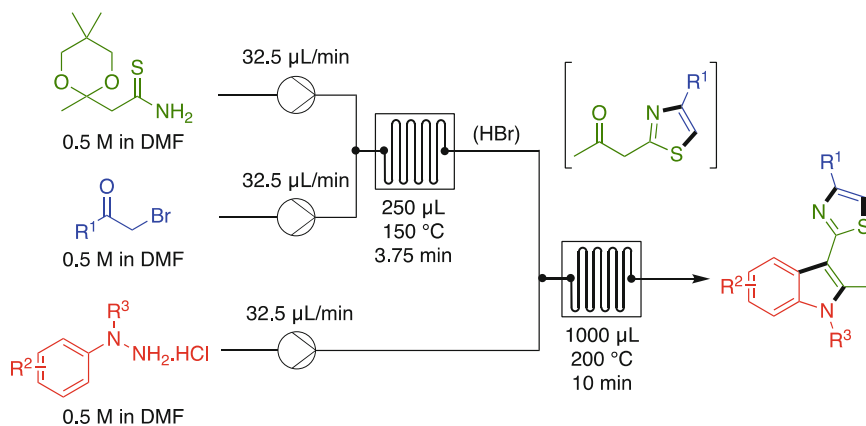
Pyrazoles can also be synthesized in flow from amines using four consecutive chemical transformations: diazotization, reduction, hydrolysis, and cyclization (Scheme 7) [19]. An in-line flow IR device monitored the formation of the intermediate oxamate (C=O stretch) and the levels of unreacted diazonium compound (N₂⁺ stretch). This information was then used to automatically adjust the flow rate of the 1,3-dione stream in order to match it with the concentration of the oxamate stream. This multistep flow setup mitigates safety concerns associated with unstable and explosive chemicals as the required diazonium compound was generated on demand in a closed system. Storage and direct contact with hazardous chemicals are therefore avoided. Poh et al.



utilized this four-step continuous process to synthesize the COX-2 selective non-steroidal anti-inflammatory drug Celecoxib, in an overall yield of 48%.

Pagano et al. developed a multistep flow strategy towards 2-(1*H*-indol-3-yl)thiazoles [20]. This heterocyclic framework was generated in a continuous sequence of three chemical transformations (Hantzsch thiazole synthesis [2], deketalization, and Fischer indole synthesis [21, 22]) without isolation or purification of the intermediates (Scheme 8). In this case, the HBr released during the Hantzsch thiazole synthesis served to remove the ketal and catalyzed the subsequent Fischer indole reaction.

Gases can readily be implemented in flow synthesis using a membrane microreactor: one such example is a tube-in-tube reactor [23]. This device consists of an impermeable outer tube, within which rests a second one, made out of semipermeable Teflon AF-2400 [24]. The authors implemented this device to synthesize the anti-inflammatory

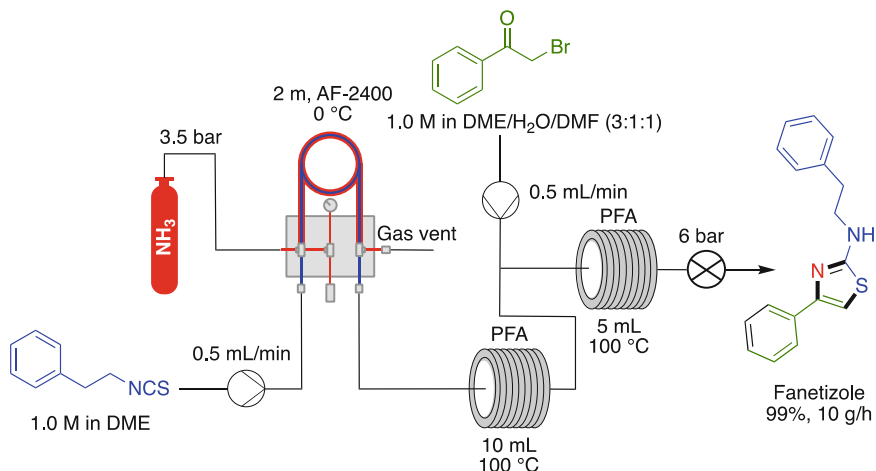


Scheme 8 A three-step synthesis of 2-(1*H*-indol-3-yl)thiazoles: Hantzsch thiazole formation, deketalization, and Fischer indole synthesis [20]

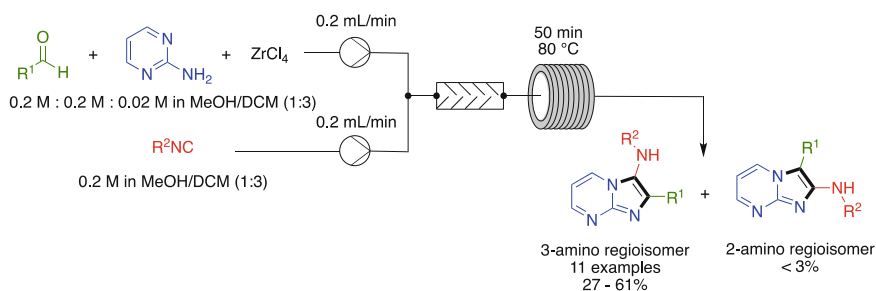
agent fanetizole in gram scale with gaseous ammonia [25]. The uptake of ammonia from the gas stream (outer tube) into the liquid stream (inner tube) was quantified by in-line flow titration with visual inspection. This allowed regulation of the ammonia concentration by varying the flow parameters. This two-step synthesis starts from the reaction of the appropriate isothiocyanate and ammonia to generate the corresponding alkyl thiourea, which subsequently reacts with 2-bromoacetophenone to deliver the thiazole in nearly quantitative yield (99%) (Scheme 9). Since the volume of gas in a tube-in-tube reactor is limited, it facilitates the safe and reliable use of a hazardous gas and circumvents the problems associated with a pressurized batch reactor.

One of the classical strategies to synthesize fused imidazoles is the Groebke–Blackburn–Bienaymé reaction [26–28]. This three-component reaction uses 2-aminoazines, aldehydes, and isocyanides as building blocks and provides access to multiple imidazole based heterocycles, depending on the nature of the 2-aminoazine. For example, 2-aminopyrimidines are used to generate aminoimidazo[1,2-*a*]pyrimidines. Under conventional batch conditions, this reaction will produce a mixture of regioisomers (2-amino and 3-aminoimidazo[1,2-*a*]pyrimidines). However, Chen et al. developed a continuous flow process to steer the reaction outcome towards the 3-amino regioisomer (Scheme 10) [29]. Key to the success was the greater control of the reaction parameters in a flow setup. After a thorough optimization study (reaction temperature, residence time, and catalyst loading), high regioselectivity towards the 3-amino product was observed. In all cases, the formation of the undesired 2-amino regioisomer was low or undetectable.

The Bucherer–Bergs hydantoin synthesis is the reaction of a ketone (or aldehyde) with ammonium carbonate and a cyanide salt [30]. Under traditional batch conditions, product formation is often hampered by loss of volatile reagents, such as ammonia and carbon dioxide that are formed in situ or by solubility issues associated with the highly polar reaction mixture. These problems were solved with an intensified continuous flow process reported by the Kappe group [31]. They assembled a



Scheme 9 Continuous and scalable process towards the anti-inflammatory agent fanetizole [25]

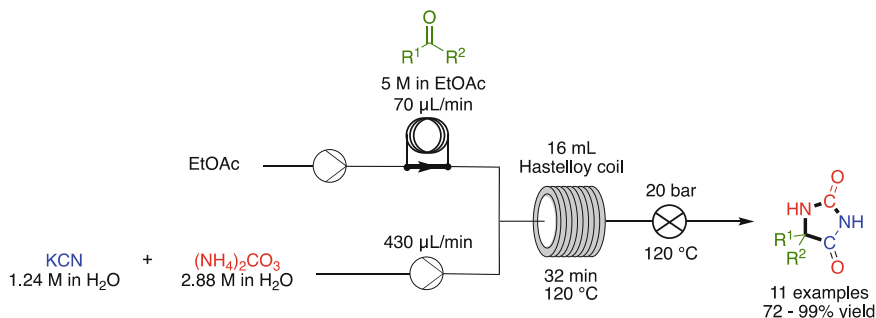


Scheme 10 Regioselective synthesis of 3-aminoimidazo[1,2-*a*]pyrimidines [29]

two-feed flow setup, one for the organic components and one for the highly polar components (Scheme 11). After optimization of the flow parameters, a well-defined segmented flow pattern was created that significantly enhanced the interfacial area compared to a batch approach and eliminated the associated solubility issues. As the flow process was conducted at 120 °C, high-pressure conditions were applied to ensure that all reagents remained in solution. This highly intensified Bucherer–Bergs reaction yielded the desired hydantoin in excellent yields.

2.3 Five-Membered Heterocycles Containing Three Heteroatoms

Triazoles are omnipresent since the discovery of the 1,3-dipolar cycloaddition of azides and alkynes [32–35]. In a traditional batch setup, the organic azides are usually first prepared and purified before they undergo cycloaddition with the appropriate alkyne.



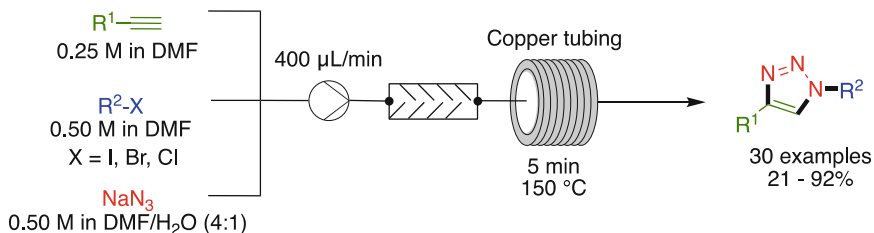
Scheme 11 Intensified continuous Bucherer–Bergs hydantoin synthesis [31]

However, as azides are prone to decompose, their manipulation raises serious safety concerns. Flow chemistry is an emerging technology that can (partially) address these issues as it allows to generate the organic azide in situ. More importantly, accumulation of the organic azide is avoided as it directly reacts in a subsequent reaction. Furthermore, the amount of in situ generated energetic intermediates (diazonium salts and azides) is limited by the spatial dimensions of the reactor. These safety improvements offered by flow chemistry were also recognized by the community and resulted in numerous publications in which azides are generated in situ and applied in the synthesis of 1,2,3-triazoles.

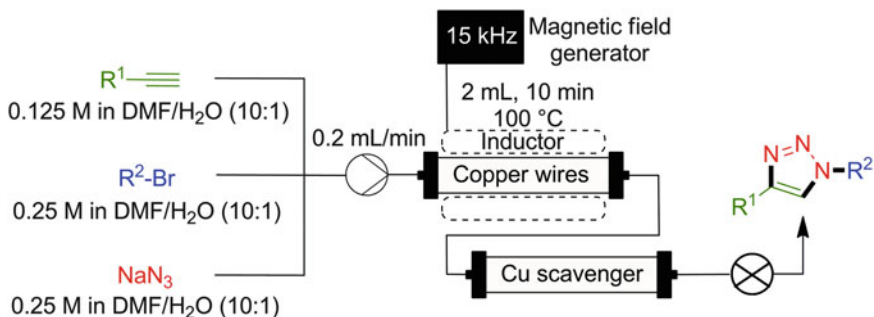
One example is reported by Bogdan and Sach [36], who used a copper flow reactor for the continuous synthesis of 1,4-disubstituted 1,2,3-triazoles. In this setup, the reaction was catalyzed by the copper reactor itself, thus eliminating the need for additional copper catalyst. In order to exclude that a thermal cycloaddition pathway was ongoing, the same reaction was performed with a traditional (non-copper-based) reactor. As expected, no conversion of starting material was observed in this case. One of the drawbacks of the copper reactor is the associated metal leaching. The authors reported up to 300 ppm of copper in the reactor effluent stream when DMF was used as solvent. However, this could be reduced to an acceptable limit by the addition of a QuadraPure TU scavenging resin. Using this flow setup, a library of 1,2,3-triazoles was synthesized from six different alkyl halides, six different acetyl- enes, and sodium azide in moderate to good yields (Scheme 12).

Kirschning and coworkers reported an inductively heated flow reactor for the synthesis of 1,4-disubstituted 1,2,3-triazoles [37]. This reactor was filled with copper wires that catalyzed the cycloaddition while inductively heating the reaction mixture. Copper leaching was again minimized by implementing a QuadraPure TU scavenger at the end of the flow setup. A few selected examples demonstrated the feasibility of an inductively heated reactor as the triazoles were achieved in high yields (Scheme 13).

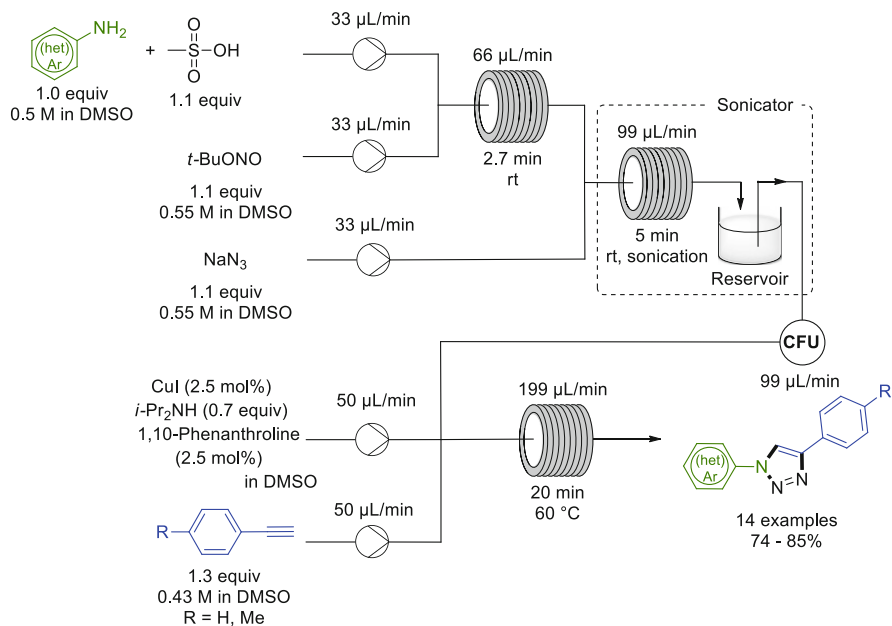
The Organ group designed a telescoped three-reactor flow process for the synthesis of various 1,4-diaryltriazoles from anilines [38]. The process relied on three consecutive chemical transformations: diazotization, azidodediazotization, and [3 + 2] copper-catalyzed azide–alkyne cycloaddition (Scheme 14). An automatic continuous flow unit



Scheme 12 Continuous synthesis of 1,4-disubstituted 1,2,3-triazoles in a copper reactor [36]



Scheme 13 1,2,3-Triazole formation in an inductively heated copper flow reactor [37]



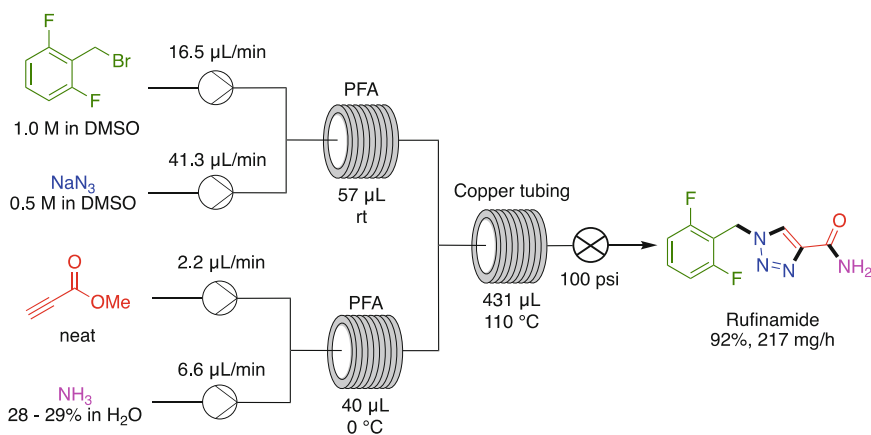
Scheme 14 Synthesis of 1,4-diaryltriazoles from anilines in a telescoped three-step flow process [38]

operated by an in-house created software was incorporated to regulate the whole system. In order to accelerate the diazotization–azidodediazotization sequence, the second reactor was submerged in a sonicator bath, resulting in a degassed, segmented effluent. The authors also demonstrated that malononitrile and 1,3-cyclohexanedione could be used as dipolarophiles to construct, respectively, 5-amino-4-cyano-[1,2,3]-triazoles and fused 1-aryl triazoles in good yields (not shown).

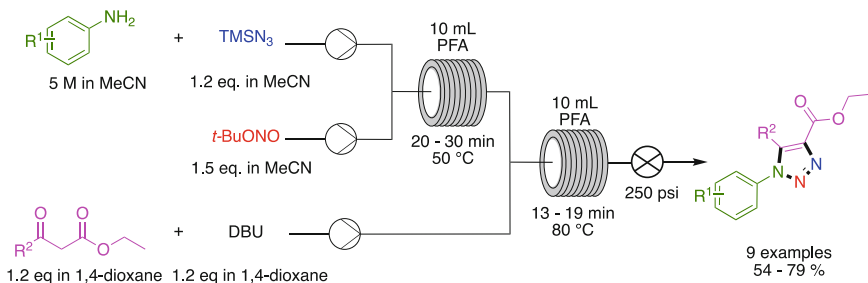
In the total synthesis of the antiepileptic agent Rufinamide by Jamison et al. [39], the 1,2,3-triazole core of this molecule was formed in a copper reactor as it is known to catalyze the azide–alkyne cycloaddition reaction. The appropriate intermediates were prepared in-line from readily available reagents in two separate reactors. The azide building block was obtained after nucleophilic substitution of 2,6-difluorobenzyl bromide with sodium azide in DMSO. Propiolamide was synthesized from methyl propiolate and aqueous ammonia at 0 °C to avoid undesired polymerization reactions. This convergent strategy afforded Rufinamide in an overall yield of 92% with a residence time of 11 min (Scheme 15).

1,3- β -Ketoesters can also be used as a dipolarophile to construct 1,4-disubstituted 1,2,3-triazoles under continuous flow conditions [40]. The reported two-step procedure starts from aniline derivatives that are first converted into their corresponding aryl azides in the presence of *tert*-butyl nitrite and trimethylsilyl azide. Next, base-mediated cyclization of the intermediate with the appropriate 1,3- β -ketoester furnished the 1,4-disubstituted regioisomer selectively in moderate to good yields (Scheme 16).

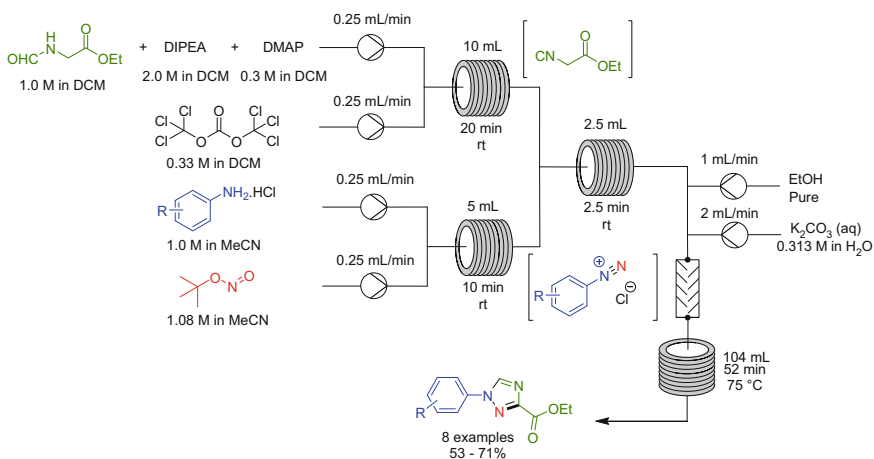
The Baxendale group developed a flow synthesis for the in situ preparation of ethyl isocyanoacetate [41]. This was achieved through dehydration of the commercially available ethyl *N*-formylglycine ethyl ester. Triphosgene was selected as the dehydrating agent as it is an easy-to-handle crystalline solid that only generates HCl and CO₂ as by-products while eliminating up to three equivalents of water. The in-line produced ethyl isocyanoacetate is a versatile building block for the synthesis of heterocycles [42]. In this report, it was mixed with aryl diazonium salts for the synthesis of



Scheme 15 Total synthesis of the antiepileptic agent Rufinamide in a continuous flow system [39]



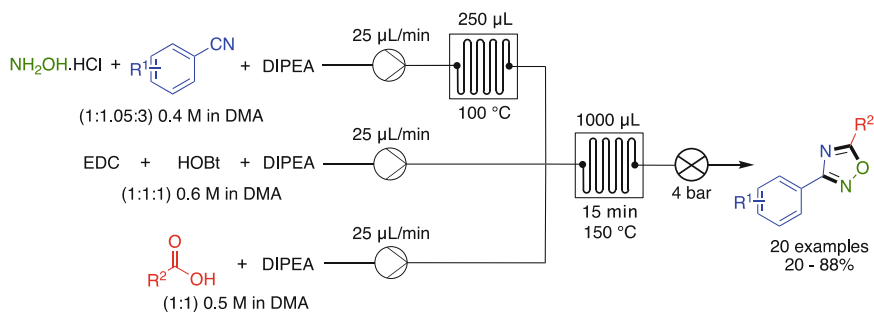
Scheme 16 Synthesis of aryl 1,2,3-triazoles from anilines and 1,3- β -ketoesters [40]



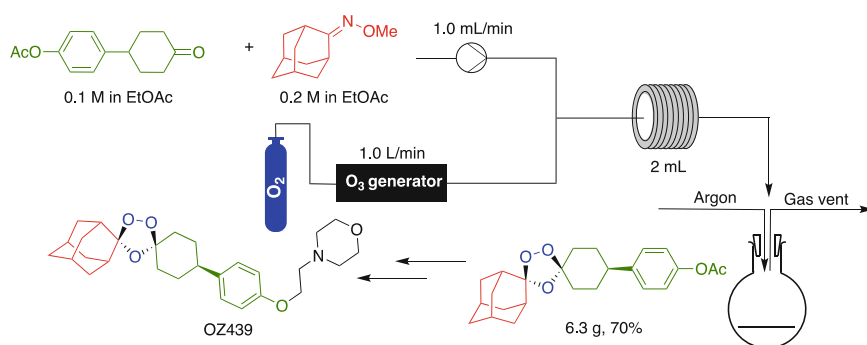
Scheme 17 In situ preparation of ethyl isocyanoacetate as key intermediate in the synthesis of 1,2,4-triazoles [41]

1,2,4-triazoles. The diazonium coupling partners were also prepared in situ from aniline derivatives and *tert*-butyl nitrite. This convergent multistep flow sequence provided the 1,2,4-triazoles in moderate to good yields (Scheme 17).

A continuous flow sequence towards highly functionalized 1,2,4-oxadiazoles starting from carboxylic acids was reported by Cosford et al. [43]. Amidoximes are first formed by premixing a benzonitrile with hydroxylamine at 100 °C. The carboxylic acids are activated in situ with coupling reagents and combined with the preformed amidoximes, furnishing the 1,2,4-oxadiazoles after intramolecular cyclodehydration in good to excellent yields (Scheme 18). The continuous flow procedure for the synthesis of amidoximes was previously developed by the same group [44]. The flow synthesis of the oxadiazoles was suitable for the gram-scale synthesis of a metabotropic glutamate subtype 5 receptor negative allosteric modulator (mGlu₅ NAM). A liquid–liquid micro-extraction module was added at the end of the flow setup to facilitate the removal of the high boiling reaction solvent. This flow setup allowed production of 3.5 g of mGlu₅ NAM in an overall yield of 70%.



Scheme 18 Synthesis of highly functionalized 1,2,4-oxadiazoles in a continuous flow process [43]



Scheme 19 Flow-assisted synthesis of the trioxolane core in the antimalarial drug candidate OZ439 [45]

The Ley group described a flow-assisted synthesis of the antimalarial drug candidate OZ439 [45], which belongs to a new class of antimalarial agents characterized by a trioxolane core [46]. The classical method to synthesize this structural motif is via the Griesbaum co-ozonolysis [47]. Ley and coworkers implemented this MCR for the construction of the heterocyclic core by mixing *O*-methyl 2-adamantanone oxime and the appropriate ketone with a stream of ozone. After optimization of the liquid and gas flow rates, the key intermediate in the synthesis of OZ439 was realized in 70% yield with a throughput of 1.9 g/h. The synthesis was finalized in batch after removal of the acetyl group, followed by nucleophilic substitution on 4-(chloroacetyl)-morpholine and selective reduction of the amide group (Scheme 19).

3 Formation of Six-Membered Heterocycles

3.1 Six-Membered Heterocycles Containing One Heteroatom

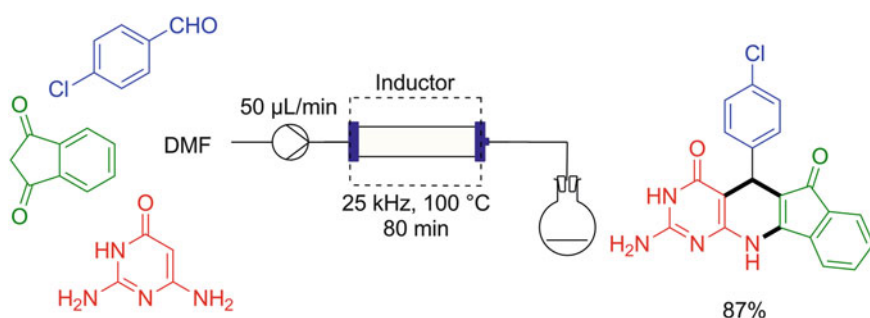
Kirschning and coworkers used inductive heating with magnetic nanoparticles to synthesize a tetracycle containing a dihydropyridine. A solution of *p*-chlorobenzaldehyde,

2,6-diaminopyrimidin-4(3*H*)-one, and indane-1,3-dione in DMF was passed through a reactor packed with MAGSILICA at 100°C, with a residence time of about 80 min (Scheme 20) [48]. The product was precipitated after addition of water and isolated in 87% yield, which was an improvement over the reaction in batch (70% yield after 3 h).

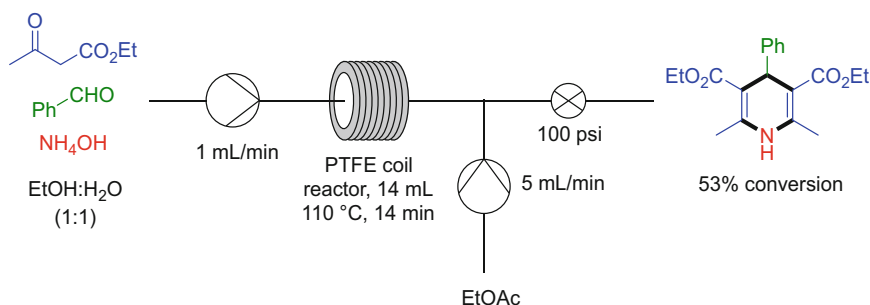
A Hantzsch dihydropyridine synthesis in flow was described by Leadbeater and coworkers in 2011 (Scheme 21) [49]. Benzaldehyde, ethyl acetoacetate, and aqueous ammonia were dissolved in a 1:1 ethanol/water mixture and pumped through a PTFE coil reactor. Then, a stream of ethyl acetate was introduced in order to avoid clogging in the BPR. A conversion of 53% to the product was obtained.

An alternative Hantzsch dihydropyridine synthesis in flow was described by Bagley et al. [50]. A mixture of an aldehyde, ethyl acetoacetate, and aqueous ammonia was passed through a stainless steel coil reactor at 140°C with a residence time of 10 min (Scheme 22). After collection, extraction, and purification, the products were isolated in moderate yields.

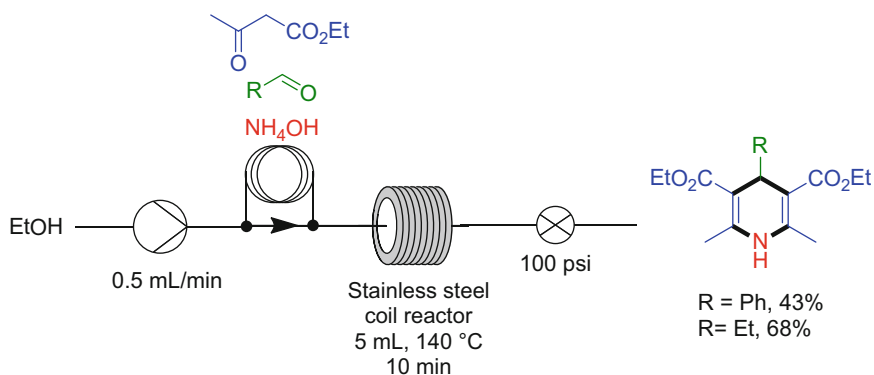
In a further attempt to improve this flow synthesis, a microwave flow reactor setup was used (Scheme 23). A mixture of phenylpropargyl aldehyde, ethyl acetoacetate, and aqueous ammonia in ethanol–acetic acid (5:1) was passed through a glass tube flow cell which was filled with sand at 120°C. The product precipitated after collecting



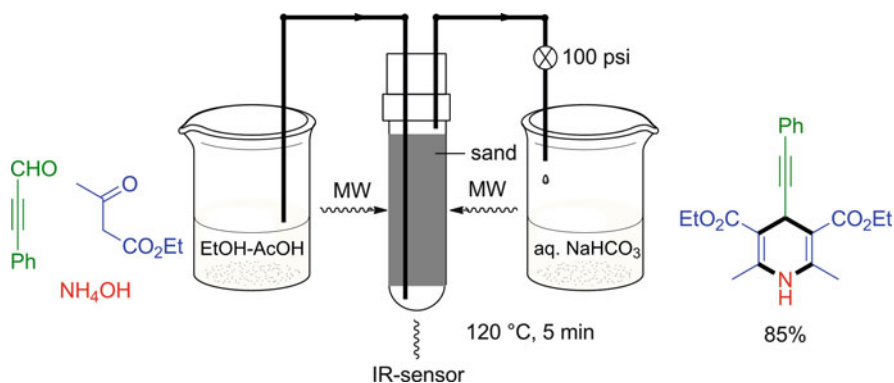
Scheme 20 Flow-assisted synthesis of a dihydropyridine by inductive heating [37]



Scheme 21 Hantzsch dihydropyridine flow synthesis reported by the Leadbeater group. The stream of ethyl acetate is added to prevent clogging [49]



Scheme 22 Hantzsch dihydropyridine flow synthesis by Bagley et al. [50]

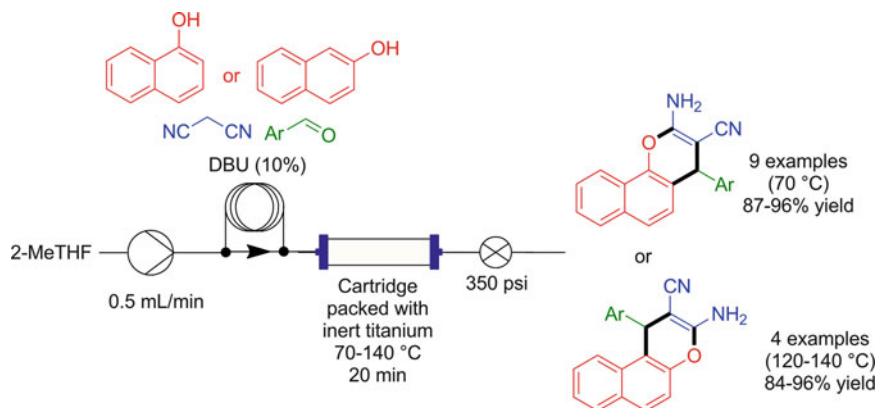


Scheme 23 Another improvement of continuous Hantzsch dihydropyridine synthesis using a microwave flow reactor. The product was purified by precipitation in aqueous sodium bicarbonate [50]

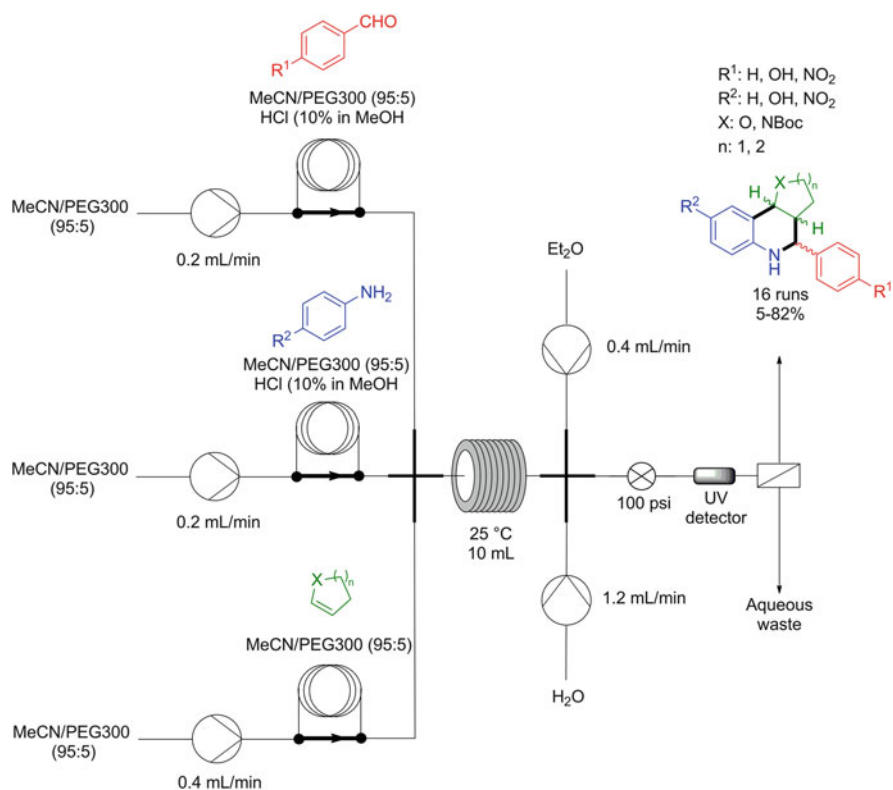
the eluting stream in aqueous sodium bicarbonate. Following filtration, the yields in either setup were slightly lower than performing this cyclization in batch under microwave irradiation.

Gonzalez et al. reported a multicomponent flow approach for the synthesis of chromenes, which are motifs found in natural products and can be used as pigments in cosmetics and agrochemicals (Scheme 24) [51]. Equimolar amounts of an aldehyde, malononitrile, and 1- or 2-naphthol were passed through a cartridge packed with inert titanium in the presence of DBU as catalyst. After a 20 min residence time at elevated temperature, the products were isolated in high yields by recrystallization or flash column chromatography.

Gioiello et al. developed a library of tricyclic tetrahydroquinolines by using the Povarov reaction (Scheme 25) [52]. The protocol was applied to different benzaldehydes, anilines, and dienophiles. After reaction at room temperature, continuous



Scheme 24 Flow synthesis of chromene derivatives using DBU as catalyst [51]



Scheme 25 Flow-assisted synthesis of tricyclic tetrahydropyridines as potential medicinal scaffolds [52]

extraction was performed after adding diethyl ether and water. Sixteen sets of diastereomers were generated in moderate to good yields, of which 12 were purified by flash column chromatography.

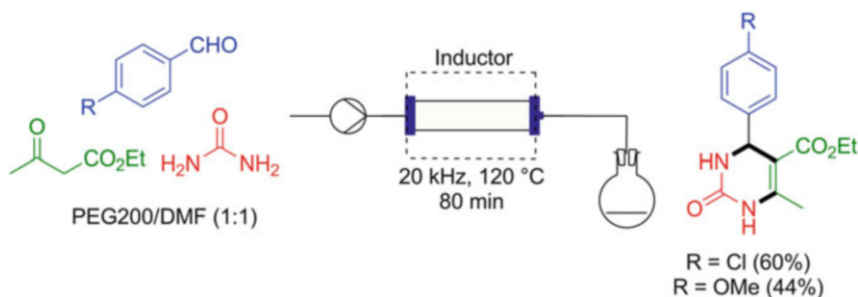
3.2 Six-Membered Heterocycles Containing Two Heteroatoms

The Kirschning group reported the synthesis of a pyrimidinone ring via a Biginelli reaction under flow conditions [48]. A cartridge filled with steel beads was used to inductively heat the reactor (Scheme 26). A solution of equimolar amounts of an aldehyde, urea, and ethyl acetoacetate together with a catalytic amount of PTSA was pumped through the inductively heated cartridge. After extraction and chromatography, the products were obtained in moderate yields, similar to that obtained when the same transformations were conducted in batch.

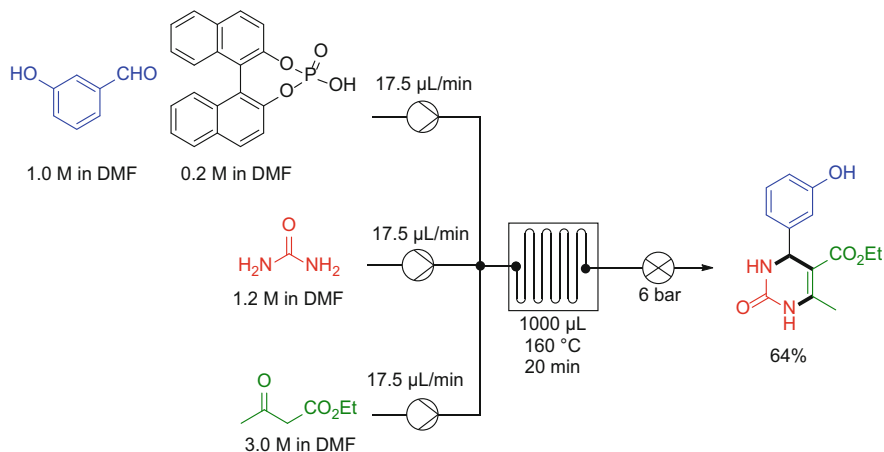
Another example of a pyrimidone MCR synthesis in flow was described by Cosford et al. [53]. Based on earlier work in batch [54], they developed an acid catalyzed Biginelli reaction under microflow conditions (Scheme 27). After reaction, the product was purified via column chromatography and isolated in 64% yield.

The authors implemented this methodology to develop a reaction cascade that gives access to 5-(thiazol-2-yl)-3,4-dihydropyrimidin-2(1H)-one derivatives (Scheme 28) [55]. The authors made elegant use of the water and HBr by-products from the thiazole formation in the subsequent acid-catalyzed acetal hydrolysis. In the next step, the MCR takes place, again catalyzed by HBr. The products were isolated after column chromatography in about 40% yield over three steps. Recently, this method was employed for fast hit-to-lead optimization to yield novel HIV replication inhibitors, with activity comparable to the clinically used drug Nevirapine [56].

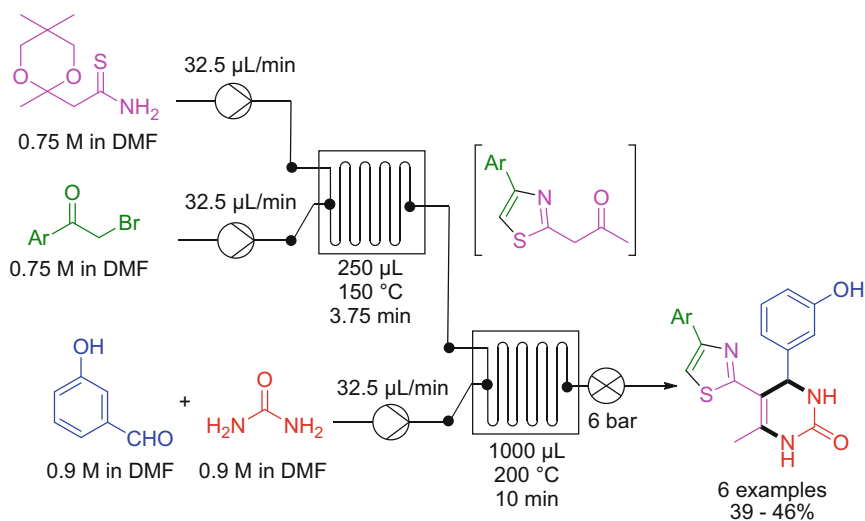
A final example of a Biginelli reaction in flow was reported by Neto et al. [57]. Equimolar amounts of an aldehyde, a 1,3-dicarbonyl derivative, and urea or thiourea were pumped through a packed bed reactor using DMF as solvent and a coordination polymer as catalyst for the synthesis of pyrimidinone and -thione derivatives



Scheme 26 Biginelli reaction under flow conditions for the synthesis of pyrimidinone derivatives [48]



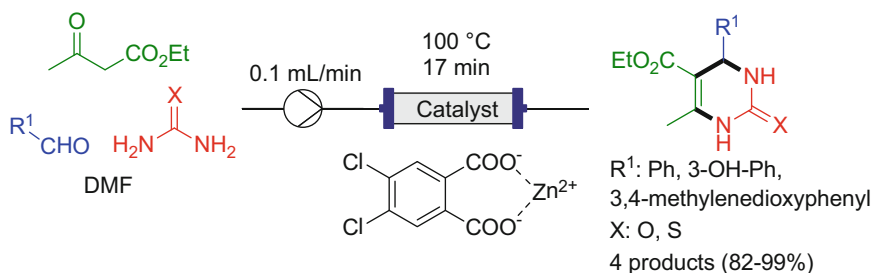
Scheme 27 Acid-catalyzed Biginelli reaction for the synthesis of pyrimidinones in microflow [53]



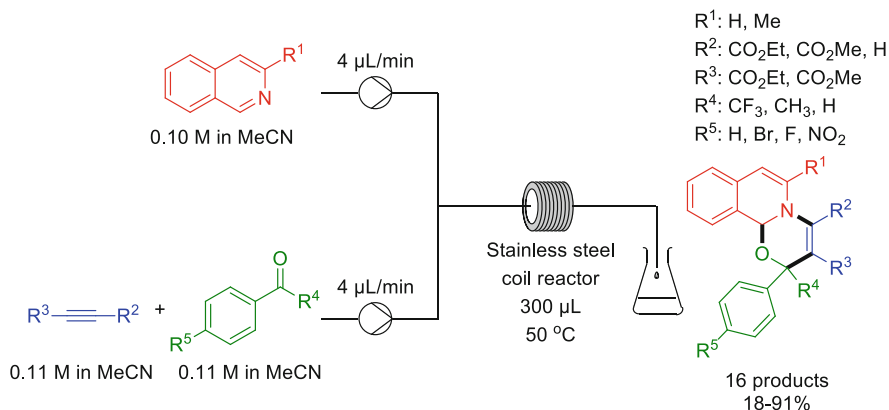
Scheme 28 Flow cascade of thiazole synthesis followed by Biginelli reaction to yield 5-(thiazol-2-yl)-3,4-dihydropyrimidin-2(1H)-one derivatives [53]

as antitumor candidates (Scheme 29). After reaction, the products are purified by column chromatography and obtained in excellent yields similar to the yields obtained under batch conditions.

In 2012, Zhang and coworkers developed a 1,4-dipolar cycloaddition using a stainless steel coil reactor leading to a series of 2-(trifluoromethyl)-2H-[1,3]oxazino[2,3-*a*]isoquinolines (Scheme 30) [58]. While significant amounts of side products were formed under batch conditions, this was not the case in the flow setup, which the



Scheme 29 Flow-assisted Biginelli reaction using a coordination polymer for the synthesis of pyridinone and -thione derivatives [57]



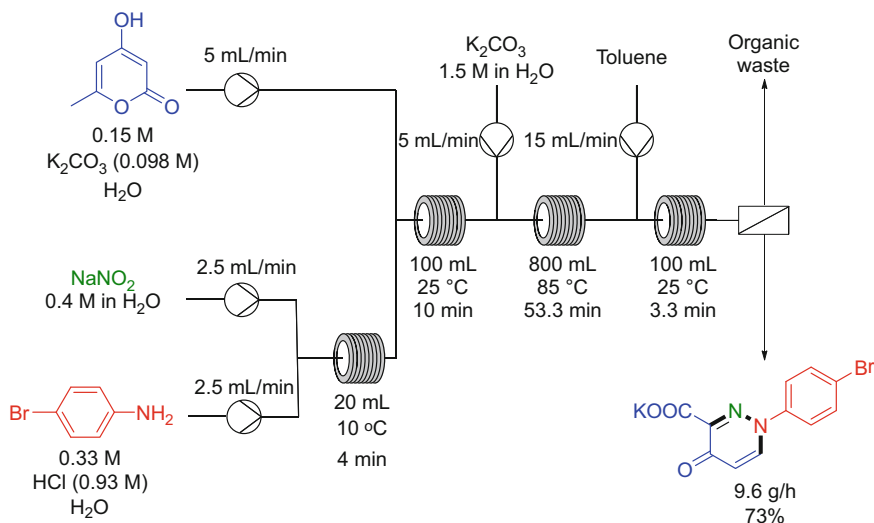
Scheme 30 Synthesis of 1,3-dihydro-oxazines by cycloadditions in flow [58]

authors attributed to the excellent mixing in the microflow system. The products were isolated in varying yields after column chromatography.

The Larhed group reported a continuous synthetic route towards spiro-oxindole-dihydroquinazolinones, which are drug-like insulin-regulated aminopeptidase (IRAP) inhibitors (Scheme 31) [59]. Silicon carbide (SiC) tubular reactors were used in combination with microwave heating. After reaction, recrystallization or column chromatography was performed to isolate the products in moderate to excellent yields.

Jamison et al. developed a mild protocol for the synthesis of pyrrolo[1,2-*a*]quinoxaline (Scheme 32) [60]. Starting from 2-(1*H*-pyrrol-1-yl)aniline, in situ formation of the corresponding isocyanide was performed, which avoids exposure to this toxic and foul-smelling intermediate. This was followed by an iridium-catalyzed photoredox cyclization. Offline extraction and column chromatography furnishes the product in 47% yield.

In 2016, Baxendale and coworkers reported a large-scale synthesis of a pyridazinone, a common intermediate in the synthesis of modulators of bromodomain-containing protein (Scheme 33) [61]. The intermediate hydrazone is poorly soluble in both organic and aqueous solvents, and copious amounts of CO_2 are liberated when



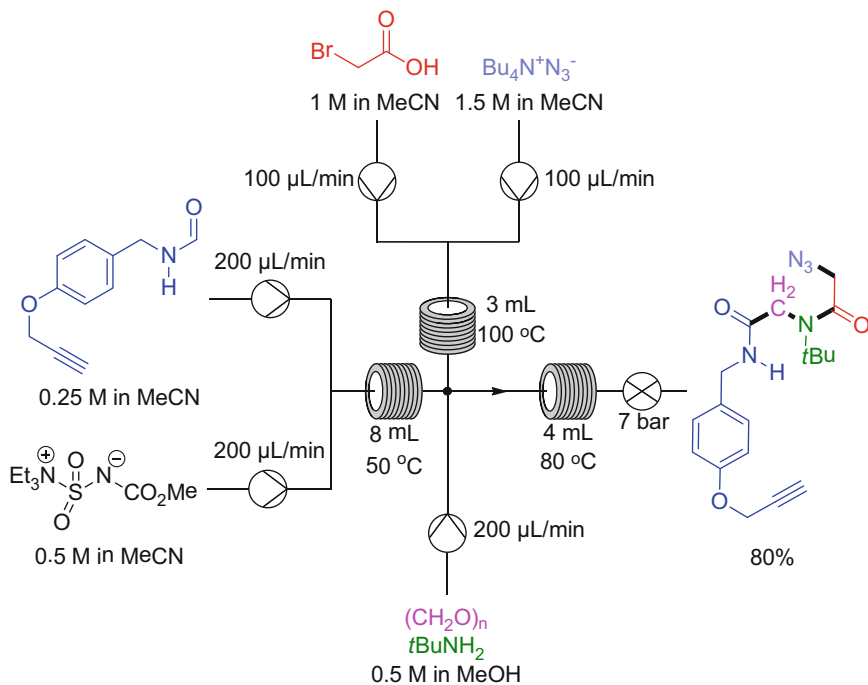
Scheme 33 Large-scale pyridazinone flow synthesis [61]

and dangerous reactants, such as isonitriles and azides, by generating them in situ and consuming them in the subsequent Ugi reaction to afford the product in 80% yield (after chromatography). This linear peptoid was pumped through a copper coil reactor at 140 °C to yield the cyclized compound in 80% yield following preparative HPLC. No homocoupled product was formed using this procedure. (While, strictly speaking, this example does not fall under our applied definition, it could arguably also be included in the chapter of formation of five-membered heterocycles.)

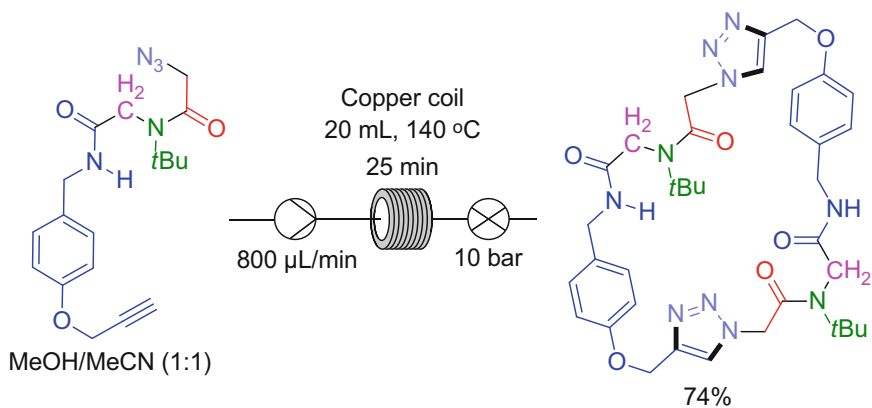
5 Conclusion and Future Perspectives

The recent achievements in the field of MCRs in continuous flow for the synthesis of heterocycles were reviewed. While in the time period covered by this review, no examples are found of syntheses of four-membered heterocycles, a fair amount of five- and six-membered heterocycle preparations are reported as well as one example of a macrocycle synthesis. Flow chemistry examples with batch counterparts in most cases performed better in terms of safety, conversion, selectivity, and space–time yield. Moreover, in telescoped reactions, side products can elegantly be used as reactant for the following step. Also, some of these examples benefit from the in situ formation of sensitive, dangerous, and/or toxic products drastically reducing safety concerns related to storage of these chemicals.

Due to the attractiveness of MCRs as well as the safety and processing advantages of flow chemistry, we expect a more generalized adoption of the combination of MCRs and flow techniques for the synthesis of heterocycles and other fine chemicals both in academia and industry.



Scheme 34 In situ synthesis of isonitriles and organic azides followed by Ugi reaction [62]



Scheme 35 Copper catalyzed cyclization [62]

References

1. Cukalovic A, Monbaliu J-CMR, Stevens CV (2010) Microreactor technology as an efficient tool for multicomponent reactions. *Top Heterocycl Chem* 23:161–198
2. Hantzsch A, Weber JH (1887) Ueber Verbindungen des Thiazols (Pyridins der Thiophenreihe). *Ber Dtsch Chem Ges* 20(2):3118–3132
3. Hantzsch A (1890) Ueber das sogenannte Cyanaceton. *Ber Dtsch Chem Ges* 23(1):1472–1474
4. Ugi I (1962) The α -addition of immonium ions and anions to isonitriles accompanied by secondary reactions. *Angew Chem Int Ed* 1(1):8–21
5. Mannich C, Krösche W (1912) Ueber ein Kondensationsprodukt aus Formaldehyd, Ammoniak und Antipyrin. *Arch Pharm* 250(1):647–667
6. Strecker A (1850) Ueber die künstliche Bildung der Milchsäure und einen neuen, dem Glyco-coll homologen Körper. *Justus Liebigs Ann Chem* 75(1):27–45
7. Biginelli P (1893) Aldehyde-urea derivatives of aceto-and oxaloacetic acids. *Gazz Chim Ital* 23:360–413
8. Cioc RC, Ruijter E, Orru RVA (2014) Multicomponent reactions: advanced tools for sustainable organic synthesis. *Green Chem* 16(6):2958–2975
9. Bienayme H, Hulme C, Oddon G, Schmitt P (2000) Maximizing synthetic efficiency: multi-component transformations lead the way. *Chem Eur J* 6(18):3321–3329
10. Syamala M (2009) Recent progress in three-component reactions. An update. *Org Prep Proced Int* 41(1):1–68
11. Herath A, Cosford NDP (2010) One-step continuous flow synthesis of highly substituted pyrrole-3-carboxylic acid derivatives via in situ hydrolysis of tert-butyl esters. *Org Lett* 12(22):5182–5185
12. Debus H (1858) Ueber die Einwirkung des Ammoniaks auf Glyoxal. *Justus Liebigs Ann Chem* 107(2):199–208
13. Radziszewski B (1882) Ueber Glyoxalin und seine Homologe. *Ber Dtsch Chem Ges* 15(2):2706–2708
14. Kong LJ, Lv XM, Lin Q, Liu XF, Zhou YM, Jia Y (2010) Efficient synthesis of imidazoles from aldehydes and 1,2-diketones under superheating conditions by using a continuous flow micro-reactor system under pressure. *Org Process Res Dev* 14(4):902–904
15. Zimmermann J, Ondruschka B, Stark A (2010) Efficient synthesis of 1,3-dialkylimidazolium-based ionic liquids: the modified continuous Radziszewski reaction in a microreactor setup. *Org Process Res Dev* 14(5):1102–1109
16. Maton C, De Vos N, Roman BI, Vanecht E, Brooks NR, Binnemans K, Schaltin S, Fransaer J, Stevens CV (2012) Continuous synthesis of peralkylated imidazoles and their transformation into ionic liquids with improved (electro)chemical stabilities. *ChemPhysChem* 13(13):3146–3157
17. Carneiro PF, Gutmann B, de Souza ROMA, Kappe CO (2015) Process intensified flow synthesis of 1H-4-substituted imidazoles: toward the continuous production of daclatasvir. *ACS Sustain Chem Eng* 3(12):3445–3453
18. Breen JR, Sandford G, Yufit DS, Howard JAK, Fray J, Patel B (2011) Continuous gas/liquid-liquid/liquid flow synthesis of 4-fluoropyrazole derivatives by selective direct fluorination. *Beilstein J Org Chem* 7:1048–1054
19. Poh JS, Browne DL, Ley SV (2016) A multistep continuous flow synthesis machine for the preparation of pyrazoles via a metal-free amine-redox process. *React Chem Eng* 1(1):101–105
20. Pagano N, Heil ML, Cosford NDP (2012) Automated multistep continuous flow synthesis of 2-(1H-indol-3-yl)thiazole derivatives. *Synthesis* 44(16):2537–2546
21. Fischer E, Jourdan F (1883) Ueber die Hydrazine der Brenztraubensäure. *Ber Dtsch Chem Ges* 16(2):2241–2245
22. Fischer E, Hess O (1884) Synthese von Indolderivaten. *Ber Dtsch Chem Ges* 17(1):559–568
23. Noël T, Hessel V (2013) Membrane microreactors: gas–liquid reactions made easy. *Chemsuschem* 6(3):405–407
24. Polyzos A, O'Brien M, Petersen TP, Baxendale IR, Ley SV (2011) The continuous-flow synthesis of carboxylic acids using CO₂ in a tube-in-tube gas permeable membrane reactor. *Angew Chem Int Ed* 50(5):1190–1193

25. Pastre JC, Browne DL, O'Brien M, Ley SV (2013) Scaling up of continuous flow processes with gases using a tube-in-tube reactor: inline titrations and fanetizole synthesis with ammonia. *Org Process Res Dev* 17(9):1183–1191
26. Groebke K, Weber L, Mehlin F (1998) Synthesis of imidazo[1,2-a] annulated pyridines, pyrazines and pyrimidines by a novel three-component condensation. *Synlett* 1998(6):661–663
27. Blackburn C, Guan B, Fleming P, Shiosaki K, Tsai S (1998) Parallel synthesis of 3-aminoimidazo [1,2-a]pyridines and pyrazines by a new three-component condensation. *Tetrahedron Lett* 39(22):3635–3638
28. Bienaymé H, Bouzid K (1998) A new heterocyclic multicomponent reaction for the combinatorial synthesis of fused 3-aminoimidazoles. *Angew Chem Int Ed* 37(16):2234–2237
29. Butler AJE, Thompson MJ, Maydom PJ, Newby JA, Guo K, Adams H, Chen BN (2014) Regioselective synthesis of 3-aminoimidazo 1,2-a-pyrimidines under continuous flow conditions. *J Org Chem* 79(21):10196–10202
30. Ware E (1950) The chemistry of the hydantoins. *Chem Rev* 46(3):403–470
31. Monteiro JL, Pieber B, Corea AG, Kappe CO (2016) Continuous synthesis of hydantoins: intensifying the Bucherer-Bergs reaction. *Synlett* 27(1):83–87
32. Huisgen R (1963) 1,3-dipolar cycloadditions. Past and future. *Angew Chem Int Ed* 2(10):565–598
33. Rostovtsev VV, Green LG, Fokin VV, Sharpless KB (2002) A stepwise Huisgen cycloaddition process: copper(I)-catalyzed regioselective “ligation” of azides and terminal alkynes. *Angew Chem Int Ed* 41(14):2596–2599
34. Tornøe CW, Christensen C, Meldal M (2002) Peptidotriazoles on solid phase: 1,2,3-triazoles by regiospecific copper(I)-catalyzed 1,3-dipolar cycloadditions of terminal alkynes to azides. *J Org Chem* 67(9):3057–3064
35. Kolb HC, Finn MG, Sharpless KB (2001) Click chemistry: diverse chemical function from a few good reactions. *Angew Chem Int Ed* 40(11):2004–2021
36. Bogdan AR, Sach NW (2009) The use of copper flow reactor technology for the continuous synthesis of 1,4-disubstituted 1,2,3-triazoles. *Adv Synth Catal* 351(6):849–854
37. Ceylan S, Klande T, Vogt C, Friese C, Kirschning A (2010) Chemical synthesis with inductively heated copper flow reactors. *Synlett* (13):2009–2013
38. Teci M, Tilley M, McGuire MA, Organ MG (2016) Handling hazards using continuous flow chemistry: synthesis of N1-aryl-[1,2,3]-triazoles from anilines via telescoped three-step diazotization, azidodediazotization, and [3 + 2] dipolar cycloaddition processes. *Org Process Res Dev* 20(11):1967–1973
39. Zhang P, Russell MG, Jamison TF (2014) Continuous flow total synthesis of rufinamide. *Org Process Res Dev* 18(11):1567–1570
40. Stazi F, Cancogni D, Turco L, Westerduin P, Bacchi S (2010) Highly efficient and safe procedure for the synthesis of aryl 1,2,3-triazoles from aromatic amine in a continuous flow reactor. *Tetrahedron Lett* 51(41):5385–5387
41. Baumann M, Garcia AMR, Baxendale IR (2015) Flow synthesis of ethyl isocyanoacetate enabling the telescoped synthesis of 1,2,4-triazoles and pyrrolo-[1,2-c] pyrimidines. *Org Biomol Chem* 13(14):4231–4239
42. Matsumoto K, Suzuki M (2001) Ethyl isocyanoacetate. *Encyclopedia of reagents for organic synthesis*. Wiley, Hoboken
43. Herath A, Cosford NDP (2017) Continuous-flow synthesis of highly functionalized imidazo-oxadiazoles facilitated by microfluidic extraction. *Beilstein J Org Chem* 13:239–246
44. Grant D, Dahl R, Cosford ND (2008) Rapid multistep synthesis of 1,2,4-oxadiazoles in a single continuous microreactor sequence. *J Org Chem* 73(18):7219–7223
45. Lau SH, Galvan A, Merchant RR, Battilocchio C, Souto JA, Berry MB, Ley SV (2015) Machines vs malaria: a flow-based preparation of the drug candidate OZ439. *Org Lett* 17(13):3218–3221
46. Barnett DS, Guy RK (2014) Antimalarials in development in 2014. *Chem Rev* 114(22):11221–11241
47. Griesbaum K, Liu XJ, Kassiaris A, Scherer M (1997) Ozonolyses of O-alkylated ketoximes in the presence of carbonyl groups: a facile access to ozonides. *Liebigs Ann Recl* (7):1381–1390

48. Ceylan S, Coutable L, Wegner J, Kirschnig A (2011) Inductive heating with magnetic materials inside flow reactors. *Chem Eur J* 17(6):1884–1893
49. Devine WG, Leadbeater NE (2011) Probing the energy efficiency of microwave heating and continuous-flow conventional heating as tools for organic chemistry. *Arkivoc*:127–143
50. Bagley MC, Fusillo V, Jenkins RL, Lubinu MC, Mason C (2013) One-step synthesis of pyridines and dihydropyridines in a continuous flow microwave reactor. *Beilstein J Org Chem* 9:1957–1968
51. Vaddula BR, Yalla S, Gonzalez MA (2015) An efficient and more sustainable one-step continuous-flow multicomponent synthesis approach to chromene derivatives. *J Flow Chem* 5(3):172–177
52. Cerra B, Mostarda S, Custodi C, Macchiarulo A, Gioiello A (2016) Integrating multicomponent flow synthesis and computational approaches for the generation of a tetrahydroquinoline compound based library. *MedChemComm* 7(3):439–446
53. Pagano N, Herath A, Cosford NDP (2011) An automated process for a sequential heterocycle/multicomponent reaction: multistep continuous flow synthesis of 5-(thiazol-2-yl)-3,4-dihydropyrimidin-2(1H)-ones. *J Flow Chem* 1(1):28–31
54. Chen XH, Xu XY, Liu H, Cun LF, Gong LZ (2006) Highly enantioselective organocatalytic Biginelli reaction. *J Am Chem Soc* 128(46):14802–14803
55. Kim J, Cechetto J, No Z, Christophe T, Kim T, Nam JY, So W, Jo M, Ok T, Park C (2011) Anti viral compounds. WO 2010 046780
56. Pagano N, Teriete P, Mattmann ME, Yang L, Snyder BA, Cai Z, Heil ML, Cosford NDP (2017) An integrated chemical biology approach reveals the mechanism of action of HIV replication inhibitors. *Bioorg Med Chem* 25(23):6248–6265
57. Silva GCO, Correa JR, Rodrigues MO, Alvim HGO, Guido BC, Gatto CC, Wanderley KA, Fioramonte M, Gozzo FC, de Souza ROMA, Neto BAD (2015) The Biginelli reaction under batch and continuous flow conditions: catalysis, mechanism and antitumoral activity. *RSC Adv* 5(60):48506–48515
58. Lei M, Tian W, Hu R, Li W, Zhang H (2012) An efficient synthesis of 2-(trifluoromethyl)-2H-1,3-oxazino 2,3-a isoquinolines via a three-component cascade approach using a continuous-flow microreactor. *Synthesis* 44(16):2519–2526
59. Engen K, Savmarker J, Rosenstrom U, Wannberg J, Lundback T, Jenmalm-Jensen A, Larhed M (2014) Microwave heated flow synthesis of spiro-oxindole dihydroquinazolinone based IRAP inhibitors. *Org Process Res Dev* 18(11):1582–1588
60. He Z, Bae M, Wu J, Jamison TF (2014) Synthesis of highly functionalized polycyclic quinoxaline derivatives using visible-light photoredox catalysis. *Angew Chem Int Ed* 53(52):14451–14455
61. Filipponi P, Gioiello A, Baxendale IR (2016) Controlled flow precipitation as a valuable tool for synthesis. *Org Process Res Dev* 20(2):371–375
62. Salvador CEM, Pieber B, Neu PM, Torvisco A, Andrade CKZ, Kappe CO (2015) A sequential Ugi multicomponent/Cu-catalyzed azide-alkyne cycloaddition approach for the continuous flow generation of cyclic peptoids. *J Org Chem* 80(9):4590–4602

Flow-Assisted Synthesis of Heterocycles at High Temperatures



Ryan J. Sullivan and Stephen G. Newman

Contents

1	Introduction	162
2	Synthesis of Heterocycles by Pericyclic and Related Reactions	164
2.1	Five-Member Ring Systems	164
2.2	Six-Member Ring Systems	167
3	Synthesis of Heterocycles by Challenging Condensation Reactions	169
3.1	Five-Member Ring Systems	170
3.2	Six-Member Ring Systems	173
3.3	Seven-Member Ring Systems	175
4	Heterocycle Modification Enabled by High Temperatures	176
4.1	Substitution	177
4.2	Deprotections	179
5	Conclusions	180
	References	183

Abstract Performing selective and high-yielding transformations on complex organic molecules at temperatures in the range of 200–450°C may at first seem counterintuitive or even impossible. However, using continuous flow systems, conditions of this sort are indeed accessible and viable for useful chemistry. This review highlights recent endeavors in heterocycle synthesis and modification enabled by high-temperature (>200°C) flow chemistry, with emphasis placed on showcasing the variety and synthetic utility of different high-temperature enabled transformations. The reviewed content naturally falls into three categories: pericyclic transformations, condensation reactions, and modification/functionalization of heterocycles. Different shortcomings and considerations necessary when planning high-temperature flow reactions have also been highlighted where applicable.

R. J. Sullivan and S. G. Newman (✉)

Centre for Catalysis Research and Innovation, Department of Chemistry and Biomolecular Sciences, University of Ottawa, Ottawa, ON, Canada

e-mail: stephen.newman@uottawa.ca

Keywords Condensation · Flow chemistry · Heterocycles · High-temperature high-pressure · Novel process windows · Pericyclic

1 Introduction

Most lab-scale chemical reactions are performed in round bottom flasks, which have remained – essentially unchanged – the principle piece of equipment used by laboratory chemists for over 200 years. As a consequence, the vast majority of these reactions are run at atmospheric pressure and are limited to either temperatures up to the boiling point of the solvent (i.e., operating under reflux) or the safe operating limit of the bath used to heat the flask (e.g., mineral oil $\approx 120^\circ\text{C}$, silicone oil $\approx 180\text{--}230^\circ\text{C}$ ¹) [1].

Advantages exist for performing reactions at higher temperatures, although two additional requirements become necessary: (1) a convenient and safe heating source and (2) a strategy to prevent solvent boiling by providing system pressure. If these two requirements are met, kinetic benefits can be realized since reaction rate constants increase exponentially with temperature (as described by the Arrhenius equation: $k = Ae^{-E_a/RT}$) [2]. This extends far beyond the convenience of completing reactions in minutes instead of hours: many transformations that do not occur to any observable extent at modest temperatures and pressures can be performed efficiently at highly elevated ones.

In the 1990s, microwave chemistry received much attention as a practical technique to perform reactions at temperatures above atmospheric solvent boiling points through rapid heating in sealed vessels [3–8]. While very convenient for small-scale discovery work, many limitations exist, including relatively poor energy efficiency, modest upper temperature limits, poor scalability, challenges with analysis and screening, glass explosion hazards, and the necessity for either a solvent that efficiently absorbs microwaves (i.e., a polar solvent, H_2O , DMF, etc.) or an alternative mechanism for absorbing and dissipating the energy (e.g., addition of graphite or SiC as microwave susceptors) [9–11]. For example, with a maximum operating pressure of around 20–30 bar, an upper limit is found for toluene $\approx 230^\circ\text{C}$, DMF $\approx 290^\circ\text{C}$, and $\text{H}_2\text{O} \approx 200^\circ\text{C}$.

Flow reactors present a unique opportunity for high-temperature chemistry since they are often capable of safely handling exceptionally high temperatures and pressures without the limitations inherent with batch microwave reactors [12–21]. For instance, an HPLC pump and stainless steel tube can reasonably handle pressures of 200 bar at 350°C , conditions under which nearly all common organic solvents exist as supercritical fluids [12]. Since the physical properties of substances in the supercritical state can differ significantly from the liquid state (e.g., density, viscosity, thermal conductivity, etc.) [22–24], the possibility of performing

¹Depending on the functionalization: 180°C for methyl silicone oils and 230°C for phenyl methyl silicone oils.

chemistry in supercritical fluids is in itself intriguing, and some examples of this will be discussed.

This also highlights the fact that performing *liquid* phase chemistry under high-temperature, high-pressure flow conditions is, in many cases, not limited by the shortcomings of the equipment but in fact by the inherent physical properties (i.e., the critical point) of the desired solvent [12]. Liquids and gasses can also display complex behavior at subcritical temperatures and pressures, including changes in compressibility, diffusivity, and solubility. Significant expansion of the reaction solvent can also occur, resulting in a reduction in residence time as temperature increases [25]. While this is generally of minor consequence when initially optimizing a reaction, further experiments may be required for reliable scale-up.

Furthermore, the relevance of flow chemistry on industrial scale – where cost considerations also factor into process design – necessitates mentioning that the increase in energy usage for a high-temperature, high-pressure flow process is frequently offset by the many benefits of process intensification (e.g., increased throughput, decreased reactor volume, etc.) [12].

This is best illustrated by an example. The condensation reaction between *o*-phenylenediamine and acetic acid to produce 2-methylbenzimidazole has an experimentally determined pre-exponential factor $A = 3.1 \times 10^8$ and activation energy $E_a = 73.43 \text{ kJ mol}^{-1}$ [10]. This translates to a reaction time of 9 weeks at 25°C while only ca. 1 s is needed at 270°C (with 1 M starting concentrations) [10, 12]. For comparison, this means that if one wanted to produce 1 metric ton of this material, they could in theory run an ~8,000 L batch reaction at room temperature for 9 weeks or process the same volume of material through a ~1.5 mL flow reactor (at 270°C with 1 s residence time) in the same time frame. Alternatively, using a 250 mL flow reactor could allow this volume of material to be processed in only ~9 h.

Furthermore, utilizing a flow system under elevated pressure allows use of low- or moderate-boiling solvents at temperatures well above their atmospheric boiling points. This is highly desirable compared to the alternative strategy most commonly used in batch experiments – namely, selection of high-boiling solvents (e.g., *o*-dichlorobenzene, b.p. 178°C; DMSO, b.p. 189°C; nitrobenzene, b.p. 211°C; diphenyl ether, b.p. 259°C) – that greatly complicates product isolation and purification [26].

A common trepidation for newcomers to the field of high-temperature chemistry is a belief that at highly elevated temperatures, compound decomposition pathways will predominate, and therefore synthetic utility will be lost. As numerous reports have now shown – and this chapter will highlight – this is not the case as long as exposure time at temperature is controlled [12]. Flow systems are ideally suited to provide this control via tightly regulated residence times in heated zones in addition to numerous other advantages including flash heating and cooling.

For selection of transformations to include in this chapter, high temperature was arbitrarily defined as $T \geq 200^\circ\text{C}$, which is well above the boiling point of most

common and practical organic solvents. The great synthetic utility of flow processes conducted under these conditions will be illustrated through a selection of diverse heterocycle syntheses, chosen to highlight how complex organic molecules can be made at high temperature. This is not intended to be a comprehensive review, but rather representative examples have been selected to showcase the various benefits and/or considerations necessary when conducting high-temperature, high-pressure flow chemistry. Specific setups will be discussed in the subsequent examples.

2 Synthesis of Heterocycles by Pericyclic and Related Reactions

Pericyclic reactions often have relatively high activation energies. It is not atypical to require temperatures above 150°C, even when tuning the electronics of the reactants to enhance reactivity [27–29]. With substrates that are not favorably electronically biased, the temperatures required for synthetically useful reaction rates can be prohibitively high – even inaccessible – using traditional equipment. Flow chemistry on the other hand can provide access to the high temperatures necessary for these reactions to become synthetically useful.

In this section, procedures to synthesize heterocycles by challenging pericyclic reactions will be presented. Examples to illustrate how different challenges have been overcome through development of high-temperature flow processes, including accelerating prohibitively slow reactions, using unactivated substrates or hazardous reagents and efficiently forming highly reactive intermediates (e.g., ketenes in Gould-Jacobs reactions) are presented.

2.1 *Five-Member Ring Systems*

Two examples of high-temperature flow pericyclic transformations to generate five-member heterocycles have been presented in the literature [30–32]. Hessel and coworkers demonstrated the use of a high-temperature flow process to allow convenient access to substituted triazole cores without the need for a transition metal catalyst [30]. Selecting an intermediate in the synthesis of rufinamide (Fig. 1, top), a drug used for treatment of Lennox-Gastaut syndrome, the authors showed that high temperatures enabled use of a dipolarophile that, while less reactive than alternative options, gave excellent regioselectivity due to the presence of a methoxy leaving group.

Using a continuous flow reactor fabricated from 1/16" outer diameter (OD) stainless steel tubing heated in oil baths (Fig. 1, bottom), the authors found

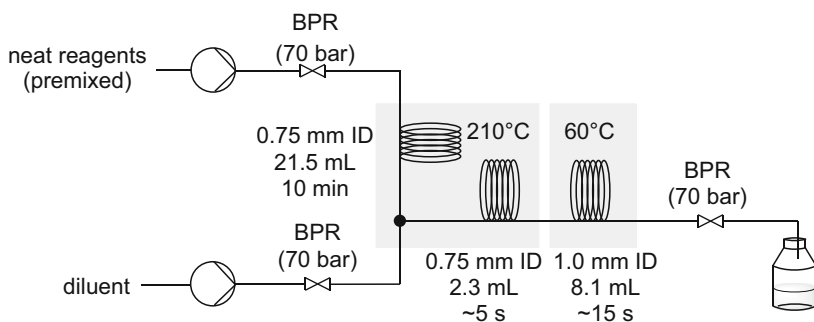
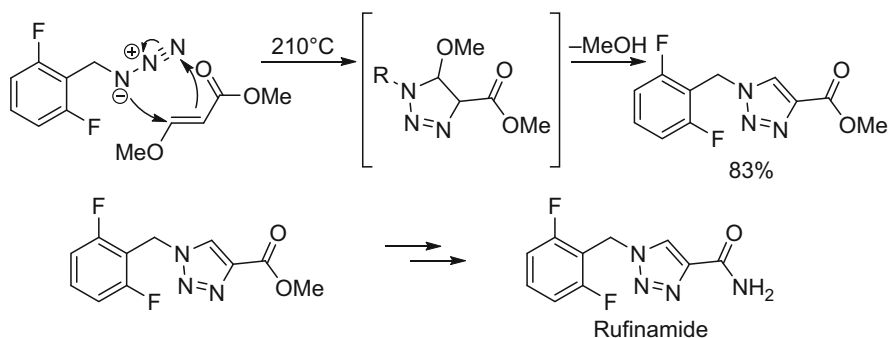


Fig. 1 1,3-Dipolar cycloaddition for introduction of the triazole ring on route to rufinamide and schematic of reactor used

that the optimal reaction temperature was 210°C with a 10 min residence time, balancing rate acceleration of the desired 1,3-dipolar cycloaddition with undesired azide decomposition to 2,6-difluorobenzylamine and 2,6-difluorotoluene.

The authors also incorporated semicontinuous purification of the product by the addition of a diluent stream of either MeCN (10:1 *v/v* to product stream) or MeOH (15:1 *v/v*) that was mixed with the neat product stream at the reaction temperature (210°C) then cooled in the receiving flask to affect crystallization giving 83% yield of the desired product.

Kappe and coworkers demonstrated a conceptually similar high-temperature enabled 1,3-cycloaddition between organic nitriles and in situ generated hydrazoic acid for the synthesis of various substituted tetrazoles (Fig. 2, top) [31, 32]. In this case, 220°C and 10 min residence time was suitable to promote the cycloaddition reaction with yields typically $\geq 90\%$.

The authors used a reactor setup with two reagent feeds as shown in Fig. 2, bottom. One pump delivered the organic nitrile and acetic acid in NMP, while a second pump dosed NaN_3 as an aqueous solution. These were combined in a glass chip microreactor, generating HN_3 that remained in solution at the elevated pressure.

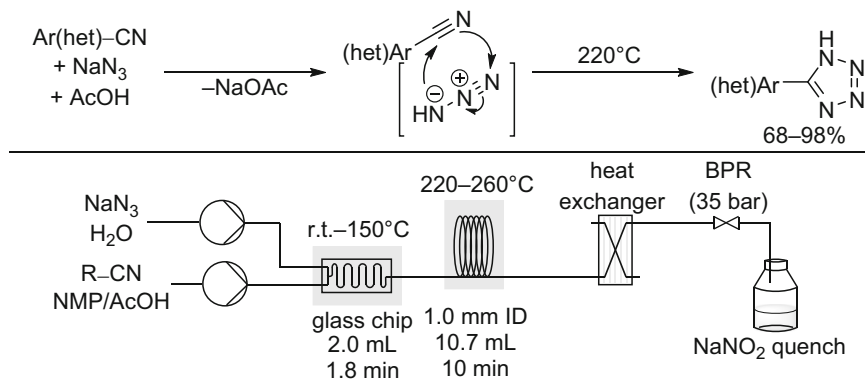


Fig. 2 Tetrazole synthesis by 1,3-dipolar addition of organic nitriles with in situ generated HN_3 and schematic of reactor setup

In most cases, the microreactor was kept at room temperature (r.t.), but for organic nitriles that exhibited poor solubility after addition of the aqueous solution, the microreactor was heated at 150°C .

Subsequent heating to 220°C for 10 min in a passivated silica-coated stainless steel coil (Sulfinert²) afforded the cycloaddition product. Product isolation was achieved by either simple liquid-liquid extraction or precipitation of the product by addition of HCl .

Importantly, the authors noted that the heating mechanism used had a significant impact on product yield. Using a flow reactor that heated the reaction coil by direct electric resistance heating (ThalesNano X-Cube Flash) resulted in no yield of desired tetrazole, while a flow reactor that heated the coil by conductive heating (Uniqsis FlowSyn) gave excellent yields. The authors determined the problem was greatly accelerated decomposition of the formed tetrazole ring under the electric resistance heated conditions and attributed this to the presence of uneven temperature distributions and local hot spots with this heating source [33].

An additional triazole synthesis using a homogenous copper catalyst at a slightly lower temperature of 180°C has also been reported by the group of Hessel [34], and a very similar tetrazole synthesis using catalytic rather than stoichiometric amount of acid at 190°C was reported by the group of Jamison [35]. While these reports don't meet our arbitrary cutoff of 200°C for discussion in this chapter, they are conceptually very similar.

²Sulfinert is a Siltek-treated stainless steel coil (i.e., chemical vapor deposition multilayer silica coating) that has the advantages of Teflon coatings or glass/fused silica coils without the temperature limitations and gas permeability concerns of Teflon and with much greater flexibility and temperature stability than glass or fused silica coils. For more information, see www.Restek.com.

2.2 Six-Member Ring Systems

Several examples have been reported of pericyclic transformations enabled by high-temperature flow chemistry for the generation of six-member heterocycles, including 6π electrocyclizations to make various pyrimidinones and quinolones [36–38], oxazinones [39] and chromenes [40], and $4\pi + 2\pi$ cycloadditions to make pyridines [41, 42] and tetrahydroisoquinolines [43]. From these, two representative examples will be highlighted to illustrate controlled formation of difficult to generate, high-energy intermediates, wide functional group tolerance at high temperatures, use of low-boiling solvents via back pressure regulation to simplify product isolation and purification, and reactivity enabled for unactivated substrates.

Wang and coworkers detailed the use of high-temperature flow chemistry to access various pyrimidinones and hydroxyquinolines via the Gould-Jacobs reaction – a reaction typically necessitating high temperatures but short reaction times to avoid over reaction and decomposition (Fig. 3, top) [38].

Using a 2.0 mL stainless steel coil in a heated oven (ThalesNano Phoenix flow reactor) and a liquid handling robot as shown in Fig. 3, bottom, the authors prepared a library of substituted pyrimidinones and quinolones. Optimal reaction conditions of 390°C with 30 s residence time gave high yields of the desired products, which could be isolated in good purity on ~60 mg scale simply by evaporation of the THF solvent followed by trituration with EtOAc. Production of gram-scale quantities was also demonstrated by delivering reagents continuously rather than as sample plugs. In contrast to typical Gould-Jacobs batch reactions (necessitating diphenyl ether as solvent), the isolation and purification was greatly improved.

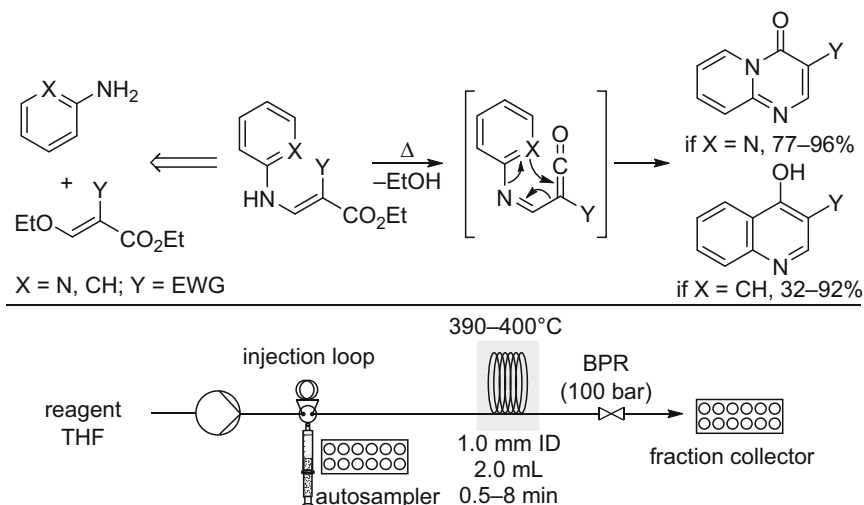


Fig. 3 Gould-Jacobs reaction sequence for the synthesis of pyrimidinones or quinolones and schematic of reactor used

The authors also demonstrated that modification of the reaction conditions by lengthening the residence time to 8 min and raising the temperature to 400°C allowed production of decarboxylated products in the case when the electron withdrawing group was an ethyl ester (Y = CO₂Et in Fig. 3, top). A selected summary of their demonstrated scope is reproduced in Table 1.

Martin and coworkers developed a high-temperature flow Kondrat'eva reaction to make substituted pyridines from deactivated oxazoles [42]. Traditionally, the Kondrat'eva reaction – an inverse electron demand Diels-Alder reaction between an electron-rich oxazole and electron-poor dienophile (Fig. 4, top) – requires an electron-donating alkoxy or amino group at the 5-position of the oxazole and

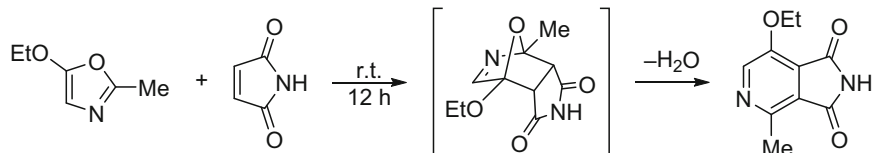
Table 1 Selected entries from the scope of Gould-Jacobs reaction reported by Wang and coworkers [38]

Product	Yield (%)	Product	Yield (%)	Product	Yield (%)
	94 ^a		32 ^a		59 ^b
	88 ^a		82 ^a		84 ^b
	96 ^a				73 ^b
	94 ^a		92 ^a		63 ^b
	77 ^a		95 ^a		67 ^b

^a390°C, 30 s residence time

^b400°C, 8 min residence time, Y = CO₂Et

Example of typical Kondrat'eva reaction:



Britton and coworkers:

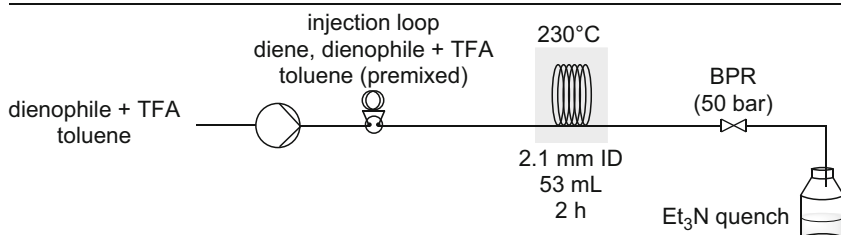
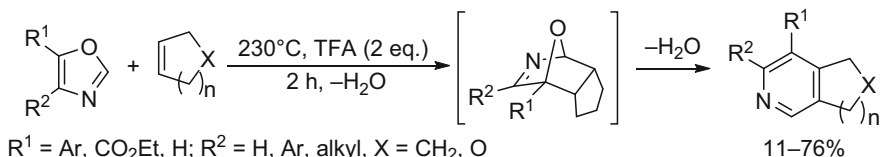


Fig. 4 Example of typical room temperature Kondrat'eva reaction [44], high-temperature flow Kondrat'eva reaction, and schematic of reactor used

dienophiles with electron withdrawing substituents for intermolecular reactions. Using temperatures of 230°C and 2 h residence time, however, a collection of 5-aryl- and 5-CO₂Et-substituted oxazoles was successfully used as dienes in the Kondrat'eva reaction with electron neutral dienophiles, greatly broadening the accessible scope of this reaction.

The authors used a 304 stainless steel coil inside a GC oven for the reactions as shown in Fig. 4, bottom. Reagents were introduced as 2.5 mL premixed sample plugs (diene + dienophile + TFA in toluene), buffered by an additional 1.0 mL of premixed dienophile + TFA of the same concentration on both the leading and tailing edges (before and after) of the sample plug.

3 Synthesis of Heterocycles by Challenging Condensation Reactions

Condensation reactions represent the most common method of forming carbon–heteroatom bonds [45, 46]. While many condensations are facile, others can be very challenging and are not feasible at moderate temperatures. This has been solved in the past by different approaches such as pre-activation of starting materials (e.g., converting organic acids to acid chlorides or addition of activating substituents), use

of acid or base catalysis, etc. While these strategies are usually effective to access the desired heterocycle cores, they often necessitate additional reaction steps and decrease overall atom economy.

The relative ease by which high temperatures are accessed in continuous flow systems makes it a very powerful strategy to enable these less favored but still highly valuable condensation reactions. In this section, the application of high-temperature flow chemistry to challenging condensation reactions, forming heterocycles of ring sizes from 5–7 atoms, will be discussed.

3.1 Five-Member Ring Systems

Condensation reactions enabled by high-temperature flow chemistry have been reported for the construction of pyrroles [47], pyrazoles [48, 49], benzazoles [10, 50], oxadiazoles [51], thiophenes [49], imidazolidinones [52, 53], oxazolidinones [53], and pyrrolidines [53]. Three representative examples will be highlighted to illustrate acceleration of prohibitively slow condensation reactions, use of supercritical water to negate the need for added acid catalysts, unanticipated catalysis by reactor material, and potential considerations necessary when telescoping multiple reaction steps into a process with a high-temperature stage.

Kawanami and coworkers demonstrated the production of various benzazole ring systems enabled by reaction temperatures of 340–445°C [50]. Residence times of <10 s provided near quantitative yields of benzimidazoles, benzoxazoles, and benzothiazoles starting from ortho-substituted anilines and benzoyl anhydrides (Fig. 5, top).

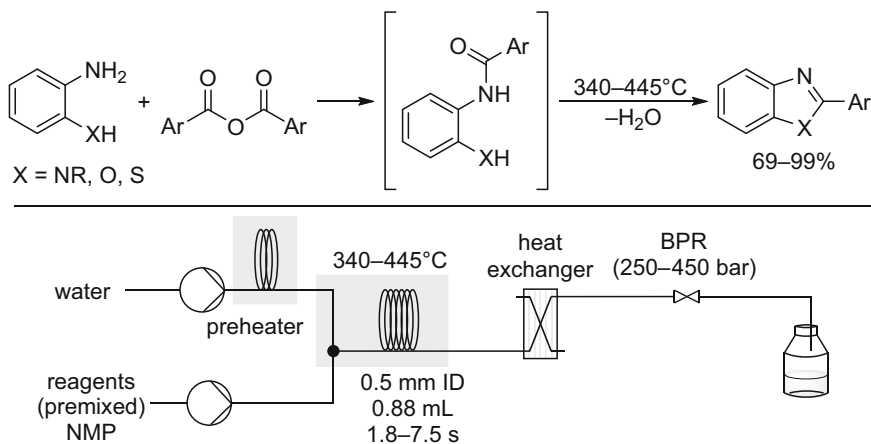


Fig. 5 Synthesis of benzazole heterocycles by a tandem acylation, dehydration reaction sequence, and schematic of reactor used

The authors used a 0.5 mm ID 316 stainless steel coil microreactor as summarized in Fig. 5, bottom, and supercritical water as the reaction medium, negating the need for an added acid catalyst.³ The premixed reagents were delivered as a solution in NMP and mixed with scH₂O at temperature to affect the tandem acylation-dehydration reaction. The scope reported is reproduced in Table 2.

Kappe and coworkers used high-temperature flow chemistry to demonstrate improvement of a substituted pyrazole synthesis needed for preparation of discovery libraries for Ca²⁺ channel inhibitors (potential treatments of various systemic diseases) [48]. The targeted pyrazole system can be prepared by traditional batch methods in two steps by first condensation of 4-nitrophenylhydrazine with hexafluoroacetylacetone and then reduction of the nitro-substituted intermediate to the desired aniline, requiring multiple days and giving overall yields <30% (Scheme 1, top).

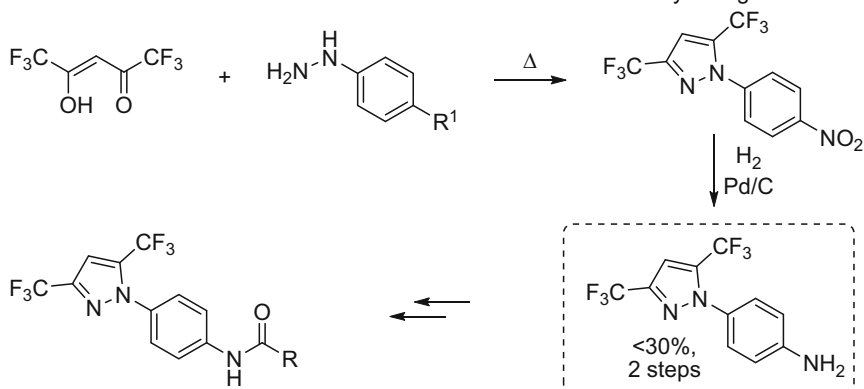
By converting to a high-temperature flow process with acetic acid as the solvent, the authors found that reaction temperatures of 265°C in a stainless steel coil (1 mm ID, heated by direct electric resistance) were effective not only for the condensation reaction but also serendipitously resulted in reduction of the nitro group to the desired free aniline (Bechamp reaction, catalyzed by the stainless steel reaction coil). This combined the original two reaction steps into one, reducing reaction

Table 2 Scope of benzazole heterocycle synthesis reported by Kawanami and coworkers [50]

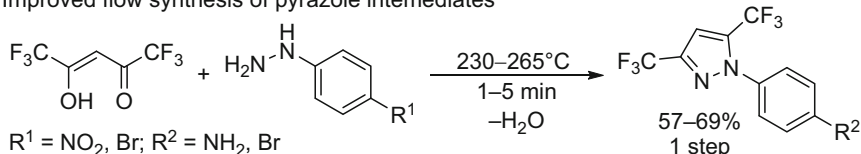
Product/functional groups	Conditions (°C/MPa/s)	Yield (%)	
	R ¹ = OMe	445/45/3.87	90
	R ¹ = CF ₃	445/45/3.87	>99
	R ² = H	445/35/2.26	98
	R ² = Br	400/25/1.77	>99
	R ² = F	400/40/5.55	>99
	R ² = COPh	445/45/3.87	>99
	R ² = NO ₂	340/45/7.45	>99
	X = NMe, R ³ = H	400/25/1.77	81
	X = O, R ³ = H	445/45/3.87	69
	X = O, R ³ = CF ₃	445/45/3.87	84
	X = O, R ³ = OMe	400/30/3.79	>99
	X = S, R ³ = H	400/40/5.55	92

³The ionic constant (K_w) of scH₂O is highly pressure dependent and can be greater than that of subcritical water at high pressures, i.e., both [H₃O⁺] and [OH⁻] can be higher in scH₂O at high pressures.

Traditional route toward Ca^{2+} channel inhibitors was slow and low yielding



Improved flow synthesis of pyrazole intermediates



Scheme 1 Traditional batch synthesis of pyrazole intermediate on route to Ca^{2+} channel inhibitors and improved flow synthesis incorporating potential for either amide bond formation or Buchwald-Hartwig amination reactions to generate screening libraries

times to 1 min and increasing the yield to 57% of the desired pyrazole substituted aniline (Scheme 1, bottom).

Additionally, based on the possibility of using a Buchwald-Hartwig amination instead of amide bond formation for library population, a high-temperature flow route to the bromo-substituted analogue was also developed. In this case, temperatures of 230°C with 5 min residence time were sufficient for the condensation reaction (Scheme 1, bottom).

Cosford and coworkers reported the synthesis of various oxadiazole systems by a telescoped flow reaction sequence concluding with a high-temperature condensation [51]. They developed an automated three-step reaction between first aryl nitriles and hydroxylamine to give an amidoxime intermediate, then acylation with an acyl chloride, and finally heating to 200°C to affect cyclization (Fig. 6, top).

The authors used etched glass microreactor chips heated in the Africa flow system (Syrris) and 0.05 mm ID PTFE capillaries in the arrangement shown in Fig. 6, bottom. The intermolecular acylation reaction between the amidoxime and the acid chloride was low yielding at elevated temperatures due to decomposition of the acid chloride, thus necessitating a cooling stage after the first reaction and a 2 min residence time at room temperature for the acylation before heating to 200°C for 10 min to affect the condensation and form the oxadiazole ring. A variety of functional groups and heterocycles were tolerated with little effect on yield (typically 45–60% over the three steps).

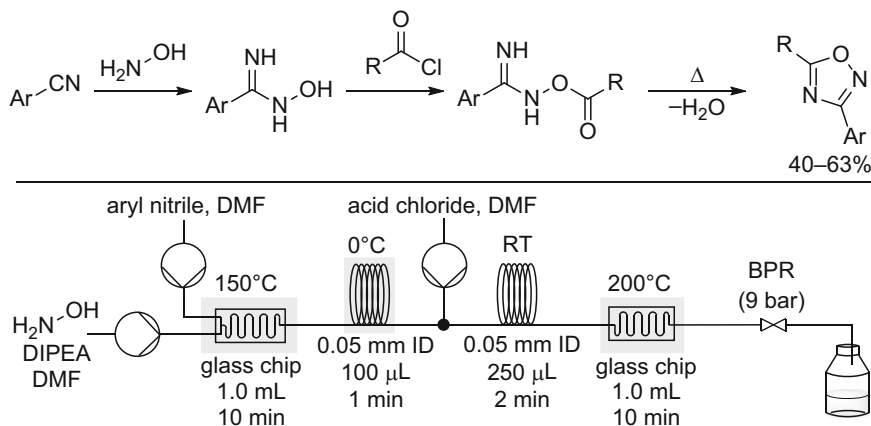


Fig. 6 Oxadiazole synthesis and schematic of reactor used

3.2 Six-Member Ring Systems

High-temperature flow conditions have been used to enable the synthesis of piperidines [53], morpholines [53], piperazines [53], dihydropyrimidinones [54], and quinolines [55] by condensation reactions. Two representative examples will be highlighted that illustrate process intensification of multicomponent reactions, elegant use of by-products from one reaction step to catalyze subsequent reactions in a telescoped process, and use of heterogeneous catalysts in packed bed reactors.

Cosford and coworkers demonstrated a high-temperature enabled three-component reaction yielding substituted dihydropyrimidinones via a Biginelli reaction (Fig. 7, top) [54]. The authors desired a process intensified synthesis that would enable rapid generation of libraries for biological activity screening. Therefore, they developed a telescoped approach, starting with first facile and rapid formation of substituted thiazoles via a Hantzsch thiazole synthesis. The released HBr generated in this step also affected an acid-catalyzed ketone deprotection to generate the ketone intermediate needed for the Biginelli reaction.

Addition of the urea and aldehyde reagents to the ketone stream exiting the 1st reactor and heating to 200°C for 10 min in the 2nd reactor affected the desired Biginelli reaction (Fig. 7, bottom), also catalyzed by the HBr by-product released during the previous thiazole formation. The authors used etched glass microreactor chips (Syrris Africa flow system) for the synthesis and estimated that ~100 derivatives could be prepared and purified (using preparative HPLC) by a fully automated system in 1 week.

Poliakoff and coworkers demonstrated a high-temperature Skraup reaction catalyzed by a heterogeneous $\text{Nb}_3(\text{PO}_4)_5$ acid catalyst in a packed bed reactor (PBR) to make quinolines from solketal and aniline at 250°C (Fig. 8, top) [55]. The authors used the reactor setup shown in Fig. 8, bottom, with two liquid feeds mixed by downward flow through an inert bed of packed sand and then reacted over a bed of

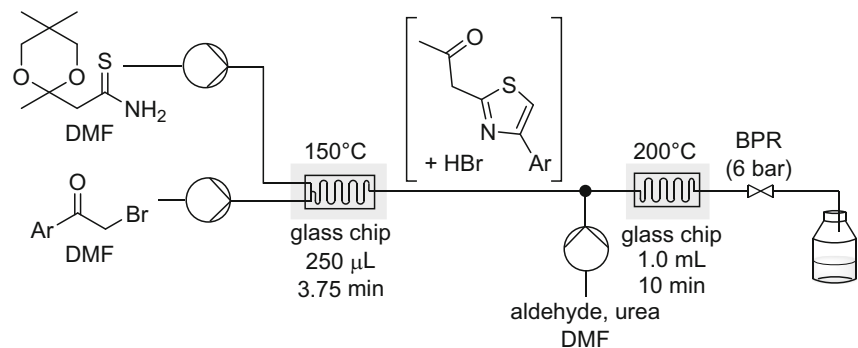
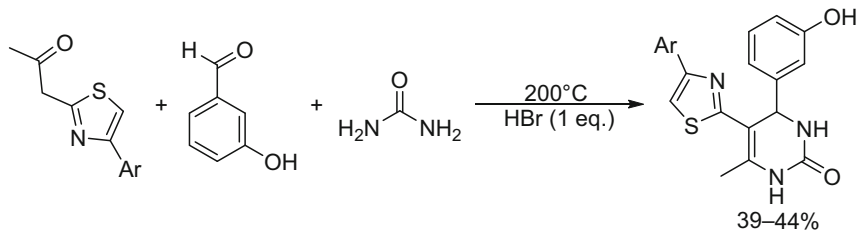


Fig. 7 Three-component Biginelli reaction accelerated by high-temperature flow and schematic of reactor used

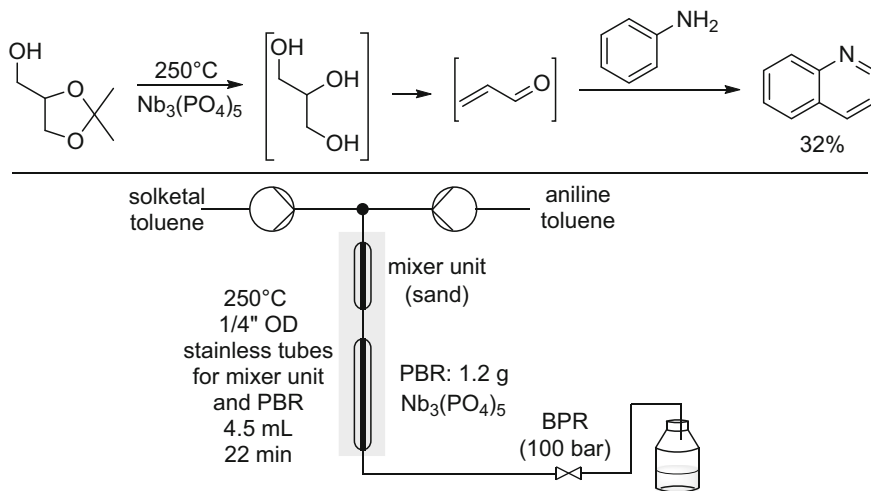


Fig. 8 High-temperature flow Skraup reaction over $\text{Nb}_3(\text{PO}_4)_5$ catalyst and schematic of reactor used

niobium phosphate catalyst. 0.25" OD stainless steel tubes fitted with end frits and heated in an aluminum block were used to make the packed bed reactors.

3.3 Seven-Member Ring Systems

Fewer examples of seven-member ring systems formed by high-temperature flow condensation reactions have been demonstrated, with examples of azepane [53] and ϵ -caprolactam [56] syntheses presented in the literature.

Poliakoff and coworkers demonstrated the formation of 1-methylazepane from 6-amino-1-heptanol and methanol over a γ -Al₂O₃ catalyst in supercritical CO₂ [53]. Reaction temperatures of 380°C were necessary to affect efficient cyclization reactions with lower temperatures (340°C) favoring *N*- and *O*-methylation (Fig. 9, top). The authors used a packed bed reactor combined with online GC analysis via a high-pressure sampling valve to allow automated reaction optimization as shown in Fig. 9, bottom.

Poliakoff and coworkers also demonstrated the synthesis of ϵ -caprolactam by a tandem hydrolysis, condensation reaction sequence from 6-aminocapronitrile (Fig. 10, top) [56]. In this case, the authors used the reactor setup shown in Fig. 10, bottom, consisting of 1/16" OD stainless steel tubing coiled around aluminum heating blocks.

Of note is the large dependence on pressure observed for both conversion and selectivity, resulting from two factors: (1) the relatively greater compressibility of

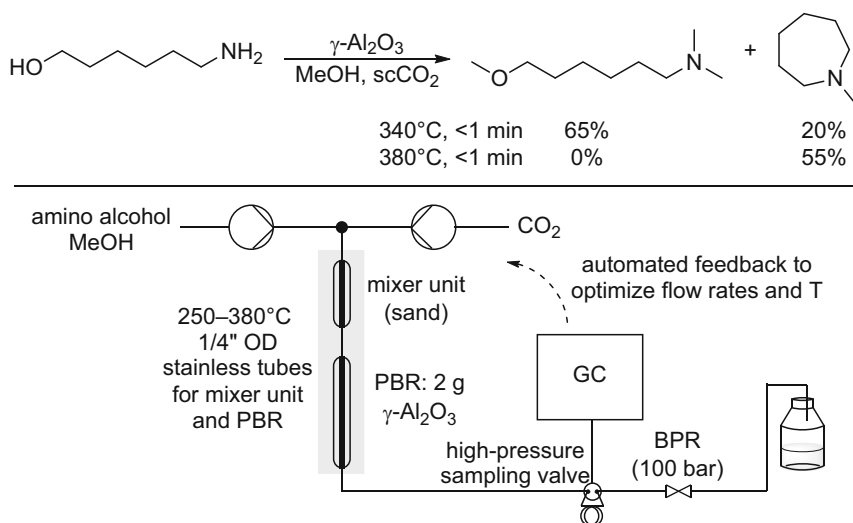


Fig. 9 Product selectivity in the high-temperature condensation reaction to form 1-methylazepane and schematic of reactor used

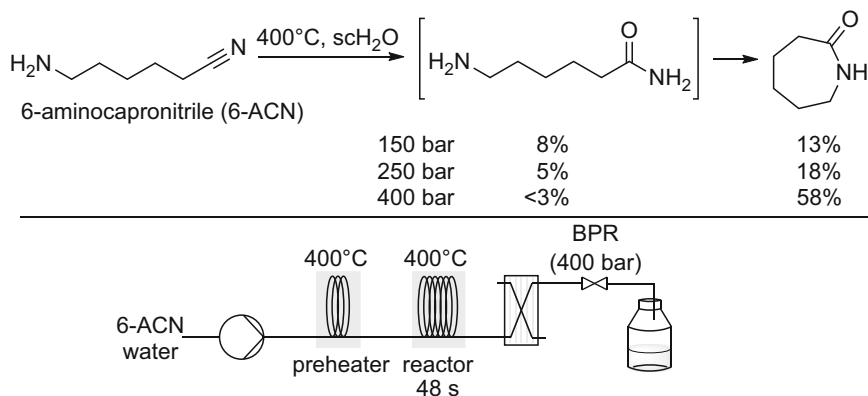


Fig. 10 High-temperature, pressure-dependent flow ϵ -caprolactam synthesis and simplified schematic of reactor used

supercritical fluids compared to liquids resulting in changing residence time as a function of pressure (6 s at 150 bar⁴ vs. 48 s at 400 bar) and (2) the effect of pressure on the ionic constant (K_w) of scH_2O which increases from $10^{-16.6}$ at 250 bar, 400°C⁵ to $10^{-12.5}$ at 400 bar, 400°C, greatly affecting the concentration of H_3O^+ present to catalyze the condensation reaction.

4 Heterocycle Modification Enabled by High Temperatures

The previous sections focused on the construction of heterocycles using chemical reactions that benefitted from or necessitated high temperatures, namely, pericyclic and condensation reactions. Beyond the construction of heterocycle rings, however, modification of functionalized heterocycles is also of great importance. In this arena as well, reactions that are mechanistically simple yet kinetically challenging can be enabled with high-temperature flow chemistry, negating the need for expensive additives, transition metal catalysts, or other harsh conditions typically required to accelerate reactions that are prohibitively slow at accessible batch temperatures. In this section, we focus on two such reaction classes that particularly benefit from being performed under high-temperature flow conditions: challenging substitutions and pH-neutral deprotections.

⁴The critical point of water is 374°C, 218 bar. At 400°C, 150 bar, the water is present as superheated steam but not yet as a supercritical fluid.

⁵When keeping the temperature constant at 400°C, K_w is at a minimum when $P = 250$ bar.

4.1 Substitution

Nucleophilic aromatic substitution (S_NAr) reactions are powerful for the straightforward and rapid synthesis of functionalized heterocycles. However, the need to form reactive, dearomatized intermediates along the reaction pathway often leads to high activation energies, necessitating temperatures beyond the atmospheric boiling point of common organic solvents in the absence of highly activating substituents (e.g., additional NO_2 groups) [57, 58]. While Buchwald-Hartwig cross-couplings and related reactions provide a viable alternative to challenging S_NAr reactions, the requirement of expensive metals and ligands, stoichiometric additives, and extensive optimization is unappealing. Furthermore, the use of transition metal catalysts can introduce additional purification challenges to achieve the (sub)ppm level metal residues mandated in the APIs.

To enable S_NAr chemistry in the absence of additional activating groups, additives, or catalysts, high-temperature flow chemistry has been used to perform S_NAr reactions of 2-chlorosubstituted pyridines, quinolines and pyrazines [12, 59–61], and 2-chloro-substituted quinazolines, quinoxalines, and benzimidazoles [62]. Hamper and coworkers reported an S_NAr reaction between 2-chloropyridine/quinoline/pyrazine and secondary amine nucleophiles – reactions that usually require multiple days in batch under pressurized conditions (autoclaves or sealed tubes) – enabled by temperatures of $260^\circ C$ and 10 min residence time in flow (Fig. 11, top) [60]. The authors used a 2.0 mL stainless steel coil enclosed in an aluminum heating block and an injection loop as shown in Fig. 11, bottom.

The authors noted the importance of considering solvent stability at elevated temperature during reaction development. Initial reaction optimization was performed using piperidine as the nucleophile and DMF as the solvent.

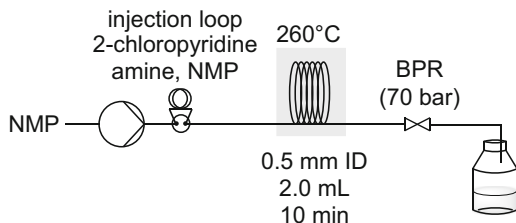
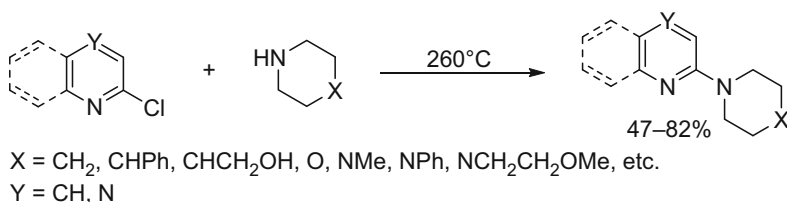
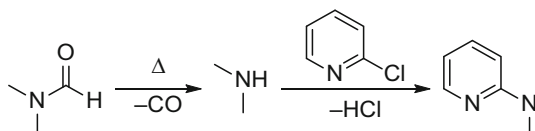


Fig. 11 High-temperature S_NAr reaction between 2-chloropyridine/quinoline/pyrazine and 2° amine nucleophiles and schematic of reactor used

2-(Dimethylamino)pyridine was observed as a major side product (up to 37%), produced by thermal decarbonylation of DMF to give dimethylamine and then S_NAr with the substrate as shown in Scheme 2. Substituting DMA for DMF was similarly problematic, with the same impurity forming, but changing to NMP removed by-product formation. Similar observations of problematic DMF decomposition at high temperature and intentional exploitation of this decomposition pathway to generate dimethylamine in situ have been reported elsewhere as well [51, 61].

Bogdan and coworkers reported a similar high-temperature flow S_NAr reaction between 2-chloroquinazoline/quinoxaline/benzimidazole and $1^\circ/2^\circ$ amines (Fig. 12, top) [62]. In this case, reaction temperatures of 225°C with 16 min residence time gave good to high yields for a wide variety of nitrogen nucleophiles. The reactor setup used was an 8 mL stainless steel coil heated in the Phoenix flow reactor in combination with an injection loop as shown in Fig. 12, bottom. Although EtOH was



Scheme 2 Decomposition of DMF at high temperature and by-product formation by S_NAr reaction with 2-chloropyridine

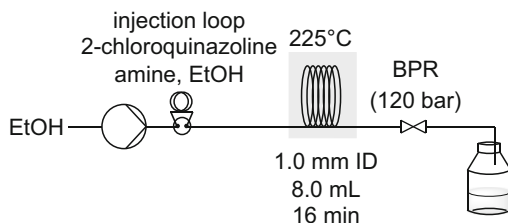
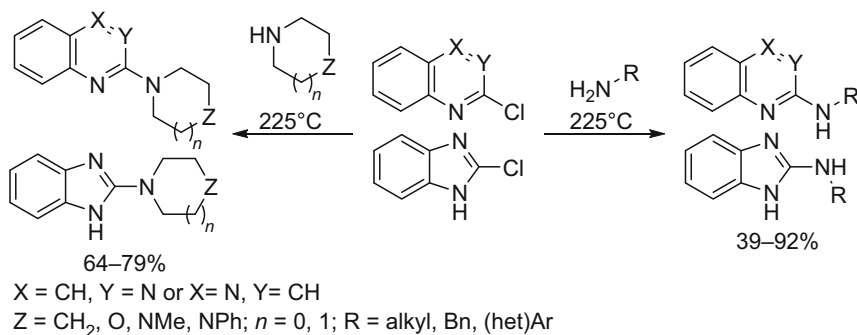


Fig. 12 High-temperature S_NAr reaction of 2-chloroquinazoline/quinoxaline/benzimidazole with $1^\circ/2^\circ$ N nucleophiles and schematic of reactor used

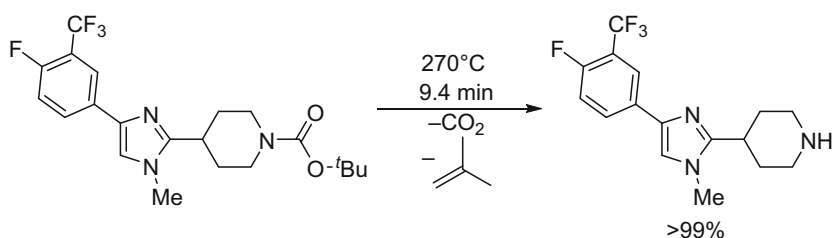
used as the solvent, no formation of 2-ethoxyquinazoline/quinoxaline/benzimidazole was observed.

4.2 Deprotections

The use of high-temperature flow conditions has been very elegantly applied to the deprotection of *N*-Boc-protected amines. Although deprotection of Boc groups is usually facilely achieved by simple treatment under mildly acidic conditions, application of high temperatures in flow has been demonstrated to be an effective alternative and orthogonal deprotection strategy that generates only easily separated, gaseous by-products and does not destroy other acid-sensitive functional groups or stereocenters.

Johnson and coworkers developed a high-temperature flow thermal Boc deprotection on kg scale for the transformation shown in Scheme 3 [26]. The authors performed the reaction under supercritical conditions at 270°C, 70 bar with 95:5 THF:MeOH as the solvent, allowing single-phase operation in the reactor despite the evolution of CO₂ and isobutylene. A 221 mL coiled stainless steel tubular reactor was used with 3.18 mm OD, 1.96 mm ID, and 73.6 m length, giving 9.4 min residence time and providing the desired product in quantitative yield and 97% purity simply by evaporation of the solvent.

Bogdan and coworkers demonstrated a wide substrate scope for thermal Boc deprotections at 300°C with 2 min residence time in MeCN [63]. A 2.0 mL, 1 mm ID stainless steel coil in the Phoenix flow reactor was used in the setup shown in Fig. 13.



Scheme 3 Thermal Boc deprotection reported by Johnson and coworkers

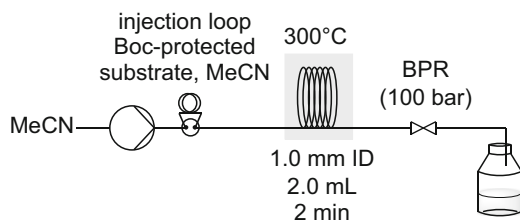


Fig. 13 Schematic of reactor setup used for thermal Boc deprotection reported by Bogdan and coworkers

Many functional groups were stable under these conditions, giving the desired amine products in high yield and good purity by simple evaporation of the solvent. Further, various other acid-sensitive protecting groups were unaffected demonstrating the ability to orthogonally deprotect with these conditions. A summary of the reported scope is reproduced in Table 3.

5 Conclusions

This chapter showcased an array of synthetically useful transformations enabled by high-temperature flow chemistry, in the context of heterocycle synthesis and functionalization. Examples ranging from mg to kg scale have been discussed, highlighting selective and high-yielding transformations that either do not occur at all or are too prohibitively slow to be synthetically useful under typical batch conditions (i.e., reflux in open flasks). Surprisingly wide substrate scopes have been demonstrated in many cases, showing that many functional groups are stable under high-temperature conditions as long as residence time is controlled.

Improvements in product isolation and purification – concerns often overlooked in academia but of great importance in industrial processes – have also been highlighted where applicable, usually stemming from the ability to use low-boiling solvents for high-temperature processes but also arising from the ability to perform reactions without catalyst or other additives in some cases.

We hope that the reader has also gained an appreciation of the relatively simple equipment (e.g., HPLC pumps, stainless steel tubing, a heat source and back pressure regulator) needed to conduct high-temperature flow experiments, in stark contrast to the expensive and specialized equipment (i.e., high pressure autoclaves) that would be needed for similar batch experimentation.

Furthermore, the pressures and temperatures accessible in a flow system far exceed those that could be safely investigated even in batch autoclaves, and many examples highlighting new reactivity only possible in these novel process windows have been highlighted. Additionally, examples highlighting the need for controlled, short reaction time have also demonstrated the synthetic opportunities available with high-temperature flow chemistry that would be impossible to achieve in batch systems at any sort of useful preparative scale.

Also highlighted were various examples selected to give an idea of the considerations and possible complications involved when performing chemistry at $T > 200^{\circ}\text{C}$. These included deleterious effects of different heating mechanisms, unanticipated reactivity catalyzed by reactor material (e.g., stainless steel), situations necessitating cooling of reaction effluent before subsequent reagent addition in telescoped processes, the impact of system pressure under supercritical conditions, and the possibility of solvent decomposition leading to impurity formation.

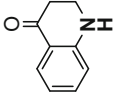
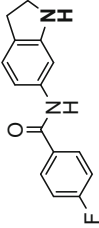
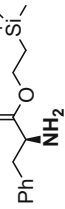
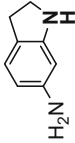
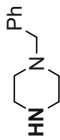
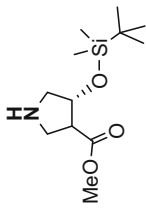
Many traditional (named) heterocycle syntheses include condensation as part of reaction cascades to form heterocycle cores. As shown in this chapter, ring-closing condensation reactions are particularly well suited for high-temperature conditions,

Table 3 Scope of thermal Boc deprotection reported by Bogdan and coworkers [63]^a

Product	Yield (%) ^b	Product	Yield (%) ^b	Product	Yield (%) ^b
$\begin{array}{c} \text{O} \\ \parallel \\ \text{R}^1\text{-N-C-O}^t\text{Bu} \\ \\ \text{R}^2 \end{array}$ $\xrightarrow[300^\circ\text{C, 2 min}]{-\text{CO}_2, \text{-isobutylene}}$ $\begin{array}{c} \text{R}^1\text{-NH} \\ \\ \text{R}^2 \end{array}$					
	>95		>95		85
	92		94		>95
	>95		>95		>95
	>95		>95		89
	>95		>95		

(continued)

Table 3 (continued)

Product	Yield (%) ^b	Product	Yield (%) ^b	Product	Yield (%) ^b
	>95		85		93
	78		>95		54 ^c

^aThe nitrogen atom in bold was deprotected

^bIsolated yield after evaporation of solvent

^cIsolated yield by column chromatography

especially in cases when substituent effects or ring size cause the reaction rates to be prohibitively slow at commonly accessible batch temperatures.

Concerted pericyclic reactions in the absence of activating groups also generally exhibit high activation barriers and therefore prohibitively slow reaction rates, but high-temperature flow chemistry can enable this type of chemistry to access different substitution profiles. Reactivity dominated by an entropy driving force (i.e., release of gaseous by-products) but with a high activation barrier can also be elegantly accessed through high-temperature flow and dealing with the evolved gasses nicely handled by working under supercritical conditions.

Future research in these areas will undoubtedly continue to expand upon these themes, while additional new and exciting transformations enabled by high temperatures are sure to follow as well. It will undoubtedly be interesting to see the creative solutions enabled by high-temperature flow chemistry for challenging heterocycle syntheses in the years to come.

References

1. Rudnick LR, Bartz WJ (2013) Comparison of synthetic, mineral oil, and bio-based lubricant fluids. In: Rudnick LR (ed) *Synthetics, mineral oils, and bio-based lubricants*, 2nd edn. CRC Press, Boca Raton, pp 347–366
2. Atkins P, De Paula J (2010) *Atkin's physical chemistry*, 9th edn. Oxford University Press, Oxford
3. Kappe CO, Dallinger D, Murphree SS (2009) *Practical microwave synthesis for organic chemists – strategies, instruments, and protocols*. Wiley-VCH, Weinheim
4. Leadbeater NE (ed) (2010) *Microwave heating as a tool for sustainable chemistry*. CRC Press, Boca Raton
5. Larhed M, Olofsson K (eds) (2006) *Microwave methods in organic synthesis*. Springer, Heidelberg
6. Galema SA (1997) Microwave chemistry. *Chem Soc Rev* 26:233–238
7. Lidström P, Tierney J, Wathey B, Westman J (2001) Microwave assisted organic synthesis – a review. *Tetrahedron* 57:9225–9283
8. Kappe CO (2004) Controlled microwave heating in modern organic synthesis. *Angew Chem Int Ed* 43:6250–6284
9. de la Hoz A, Diaz-Ortiz A, Prieto P (2016) Microwave-assisted green organic synthesis. In: Stefanidis G, Stankiewicz A (eds) *Alternative energy sources for green chemistry*. Royal Society of Chemistry, Cambridge, pp 1–33
10. Damm M, Glasnov TN, Kappe CO (2010) Translating high-temperature microwave chemistry to scalable continuous flow processes. *Org Process Res Dev* 14:215–224
11. Glasnov TN, Kappe CO (2011) The microwave-to-flow paradigm: translating high-temperature batch microwave chemistry to scalable continuous-flow processes. *Chem Eur J* 17:11956–11968
12. Razzaq T, Kappe CO (2010) Continuous flow organic synthesis under high-temperature/pressure conditions. *Chem Asian J* 5:1274–1289
13. Gutmann B, Cantillo D, Kappe CO (2015) Continuous-flow technology – a tool for the safe manufacturing of active pharmaceutical ingredients. *Angew Chem Int Ed* 54:6688–6728
14. Plutschack MB, Pieber B, Gilmore K, Seeberger PH (2017) The hitchhiker's guide to flow chemistry. *Chem Rev* 117:11796–11893

15. Porta R, Benaglia M, Puglisi A (2016) Flow chemistry: recent developments in the synthesis of pharmaceutical products. *Org Process Res Dev* 20:2–25
16. Malet-Sanz L, Susanne F (2012) Continuous flow synthesis. A pharma perspective. *J Med Chem* 55:4062–4098
17. Movsisyan M, Delbeke EIP, Berton JKET, Battilocchio C, Ley SV, Stevens CV (2016) Taming hazardous chemistry by continuous flow technology. *Chem Soc Rev* 45:4892–4928
18. Britton J, Raston CL (2017) Multi-step continuous-flow synthesis. *Chem Soc Rev* 46:1250–1271
19. Newman SG, Jensen KF (2013) The role of flow in green chemistry and engineering. *Green Chem* 15:1456–1472
20. Vaccaro L (ed) (2017) Sustainable flow chemistry: methods and applications. Wiley-VCH, Weinheim
21. Lummiss JAM, Morse PD, Beingssner RL, Jamison TF (2017) Towards more efficient, greener syntheses through flow chemistry. *Chem Rec* 17:667–680
22. Eckert CA, Knutson BL, Debenedetti PG (1996) Supercritical fluids as solvents for chemical and materials processing. *Nature* 383:313–318
23. Jessop PG, Leitner W (eds) (1999) Chemical synthesis using supercritical fluids. Wiley-VCH, Weinheim
24. van Eldik R, Klärner F-G (eds) (2002) High pressure chemistry: synthetic, mechanistic, and supercritical applications. Wiley-VCH, Weinheim
25. Adeyemi A, Bergman J, Brånalt J, Sävmarker J, Larhed M (2017) Continuous flow synthesis under high-temperature/high-pressure conditions using a resistively heated flow reactor. *Org Process Res Dev* 21:947–955
26. May SA, Johnson MD, Braden TM, Calvin JR, Haerberle BD, Jines AR, Miller RD, Plocharczyk EF, Rener GA, Richey RN, Schmid CR, Vaid RK, Yu H (2012) Rapid development and scale-up of a 1H-4-substituted imidazole intermediate enabled by chemistry in continuous plug flow reactors. *Org Process Res Dev* 16:982–1002
27. Houk KN, Gonzalez J, Li Y (1995) Pericyclic reaction transition states: passions and punctilios, 1935–1995. *Acc Chem Res* 28:81–90
28. Fleming I (2015) Pericyclic reactions, 2nd edn. Oxford University Press, Oxford
29. Spangler CW (1976) Thermal [1,j] sigmatropic rearrangements. *Chem Rev* 76:187–217
30. Borukhova S, Noël T, Metten B, de Vos E, Hessel V (2013) Solvent- and catalyst-free Huisgen cycloaddition to rufinamide in flow with a greener, less expensive dipolarophile. *ChemSusChem* 6:2220–2225
31. Gutmann B, Roduit J-P, Roberge D, Kappe CO (2010) Synthesis of 5-substituted 1H-tetrazoles from nitriles and hydrazoic acid by using a safe and scalable high-temperature microreactor approach. *Angew Chem Int Ed* 49:7101–7105
32. Gutmann B, Obermayer D, Roduit J-P, Roberge DM, Kappe CO (2012) Safe generation and synthetic utilization of hydrazoic acid in a continuous flow reactor. *J Flow Chem* 2:8–19
33. Gutmann B, Glasnov TN, Razzaq T, Goessler W, Roberge DM, Kappe CO (2011) Unusual behavior in the reactivity of 5-substituted-1H-tetrazoles in a resistively heated microreactor. *Beilstein J Org Chem* 7:503–517
34. Varas AC, Noël T, Wang Q, Hessel V (2012) Copper(I)-catalyzed azide–alkyne cycloadditions in microflow: catalyst activity, high-T operation, and an integrated continuous copper scavenging unit. *ChemSusChem* 5:1703–1707
35. Palde PB, Jamison TF (2011) Safe and efficient tetrazole synthesis in a continuous-flow microreactor. *Angew Chem Int Ed* 50:3525–3528
36. Lengyel L, Nagy TZ, Sipos G, Jones R, Dormán G, Üрге L, Darvas F (2012) Highly efficient thermal cyclization reactions of alkylidene esters in continuous flow to give aromatic/heteroaromatic derivatives. *Tetrahedron Lett* 53:738–743
37. Lengyel LC, Sipos G, Sipócz T, Vágó T, Dormán G, Gerencsér J, Makara G, Darvas F (2015) Synthesis of condensed heterocycles by the Gould–Jacobs reaction in a novel three-mode pyrolysis reactor. *Org Process Res Dev* 19:399–409

38. Tsoung J, Bogdan AR, Kantor S, Wang Y, Charaschanya M, Djuric SW (2017) Synthesis of fused pyrimidinone and quinolone derivatives in an automated high-temperature and high-pressure flow reactor. *J Org Chem* 82:1073–1084
39. Cantillo D, Sheibani H, Kappe CO (2012) Flash flow pyrolysis: mimicking flash vacuum pyrolysis in a high-temperature/high-pressure liquid-phase microreactor environment. *J Org Chem* 77:2463–2473
40. Bogaert-Alvarez RJ, Demena P, Kodersha G, Polomski RE, Soundararajan N, Wang SSY (2001) Continuous processing to control a potentially hazardous process: conversion of aryl 1,1-dimethylpropargyl ethers to 2,2-dimethylchromenes (2,2-dimethyl-2H-1-benzopyrans). *Org Process Res Dev* 5:636–645
41. Martin RE, Morawitz F, Kuratli C, Alker AM, Alanine AI (2012) Synthesis of annulated pyridines by intramolecular inverse-electron-demand hetero-Diels–Alder reaction under superheated continuous flow conditions. *Eur J Org Chem* 2012:47–52
42. Lehmann J, Alzieu T, Martin RE, Britton R (2013) The Kondrat'eva reaction in flow: direct access to annulated pyridines. *Org Lett* 15:3550–3553
43. Tsoung J, Wang Y, Djuric SW (2017) Expedient Diels–Alder cycloadditions with ortho-quinodimethanes in a high temperature/pressure flow reactor. *React Chem Eng* 2:458–461
44. Jouanno L-A, Chevalier A, Sekkat N, Perzo N, Castel H, Romieu A, Lange N, Sabot C, Renard P-Y (2014) Kondrat'eva ligation: Diels–Alder-based irreversible reaction for bioconjugation. *J Org Chem* 79:10353–10366
45. Alvarez-Builla J, Vaquero JJ, Barluenga J (eds) (2011) *Modern heterocyclic chemistry*. Wiley-VCH, Weinheim
46. Joule JA, Mills K (2010) *Heterocyclic chemistry*, 5th edn. Wiley-Blackwell, New York
47. Herath A, Cosford NDP (2010) One-step continuous flow synthesis of highly substituted pyrrole-3-carboxylic acid derivatives via *in situ* hydrolysis of tert-butyl esters. *Org Lett* 12:5182–5185
48. Obermayer D, Glasnov TN, Kappe CO (2011) Microwave-assisted and continuous flow multistep synthesis of 4-(pyrazol-1-yl)carboxanilides. *J Org Chem* 76:6657–6669
49. Darvas F, Dorman G, Lengyel L, Kovacs I, Jones R, Urge L (2009) High pressure, high temperature reactions in continuous flow; merging discovery and process chemistry. *Chim Oggi Chem Today* 27:40–43
50. Nagao I, Ishizaka T, Kawanami H (2016) Rapid production of benzazole derivatives by a high-pressure and high-temperature water microflow chemical process. *Green Chem* 18:3494–3498
51. Grant D, Dahl R, Cosford NDP (2008) Rapid multistep synthesis of 1,2,4-oxadiazoles in a single continuous microreactor sequence. *J Org Chem* 73:7219–7223
52. Seki T, Kokubo Y, Ichikawa S, Suzuki T, Kayaki Y, Ikariya T (2009) Mesoporous silica-catalysed continuous chemical fixation of CO₂ with N,N'-dimethylethylenediamine in supercritical CO₂: the efficient synthesis of 1,3-dimethyl-2-imidazolidinone. *Chem Commun*:349–351
53. Streng ES, Lee DS, George MW, Poliakkoff M (2017) Continuous N-alkylation reactions of amino alcohols using γ -Al₂O₃ and supercritical CO₂: unexpected formation of cyclic ureas and urethanes by reaction with CO₂. *Beilstein J Org Chem* 13:329–337
54. Pagano N, Herath A, Cosford NDP (2011) An automated process for a sequential heterocycle/multicomponent reaction: multistep continuous flow synthesis of 5-(thiazol-2-yl)-3,4-dihydropyrimidin-2(1H)-ones. *J Flow Chem* 1:28–31
55. Jin J, Guidi S, Abada Z, Amara Z, Selva M, George MW, Poliakkoff M (2017) Continuous niobium phosphate catalysed Skraup reaction for quinoline synthesis from solketal. *Green Chem* 19:2439–2447
56. Yan C, Fraga-Dubreuil J, Garcia-Verdugo E, Hamley PA, Poliakkoff M, Pearson I, Coote AS (2008) The continuous synthesis of ϵ -caprolactam from 6-aminocapronitrile in high-temperature water. *Green Chem* 10:98–103
57. Bunnett JF, Zahler RE (1951) Aromatic nucleophilic substitution reactions. *Chem Rev* 49:273–412

58. Terrier F (2013) *Modern nucleophilic aromatic substitution*. Wiley-VCH, Weinheim
59. Razzaq T, Glasnov TN, Kappe CO (2009) Continuous-flow microreactor chemistry under high-temperature/pressure conditions. *Eur J Org Chem* 2009:1321–1325
60. Hamper BC, Tesfu E (2007) Direct uncatalyzed amination of 2-chloropyridine using a flow reactor. *Synlett* 2007:2257–2261
61. Petersen TP, Larsen AF, Ritzén A, Ulven T (2013) Continuous flow nucleophilic aromatic substitution with dimethylamine generated *in situ* by decomposition of DMF. *J Org Chem* 78:4190–4195
62. Charaschanya M, Bogdan AR, Wang Y, Djuric SW (2016) Nucleophilic aromatic substitution of heterocycles using a high-temperature and high-pressure flow reactor. *Tetrahedron Lett* 57:1035–1039
63. Bogdan AR, Charaschanya M, Dombrowski AW, Wang Y, Djuric SW (2016) High-temperature Boc deprotection in flow and its application in multistep reaction sequences. *Org Lett* 18:1732–1735

Flow Chemistry Approaches Applied to the Synthesis of Saturated Heterocycles



Marcus Baumann and Ian R. Baxendale

Contents

1	Background	188
1.1	Synthesis of Saturated Heterocycles via Cycloaddition Reactions	188
1.2	Synthesis of Saturated Heterocycles Through Cyclodehydration and Related Reactions	200
1.3	Catalysis Applied to the Assembly of Saturated Heterocycles	206
1.4	Miscellaneous Approaches for the Synthesis of Saturated Heterocycles	216
1.5	Target-Driven Synthesis of Saturated Heterocycles	224
2	Summary and Conclusions	230
	References	231

Abstract Continuous-flow processing approaches are having a significant impact on the way we devise and perform chemical synthesis. Flow chemistry has repeatedly demonstrated numerous improvements with respect to synthesis efficiency, process safety and ease of reaction scale-up. In recent years flow chemistry has been applied with remarkable success to the generation of valuable target structures across a range of industries from basic bulk chemical manufacture and materials development to flavours, food and cosmetic applications. However, due to its earlier implementation, it has found so far many more advocates in areas of medicinal and agrochemical research and manufacture. In this review article, we summarise the key developments that continuous-flow synthesis has had in the area of saturated heterocycles, specifically focusing on approaches that generate these important entities from acyclic precursors.

Keywords Continuous processing · Flow chemistry · Heterocycles · Synthesis

M. Baumann and I. R. Baxendale (✉)
Department of Chemistry, University of Durham, Durham, UK
e-mail: i.r.baxendale@durham.ac.uk

1 Background

Over the last 20 years, flow synthesis has experienced a steady growth in popularity within the chemical community as it enables chemists to streamline their efforts by conducting chemistry in a more efficient, safe and often more environmentally benign fashion [1–9]. As such numerous applications have been reported detailing improvements with regard to extending traditional processing windows (temperature and pressure) [10–14], executing multistep sequences with in-line analysis and purification [15–18], as well as safely performing otherwise ‘forbidden’ reactions [19]. Unsurprisingly, this has attracted considerable interest from chemists in the pharmaceutical and agrochemical industries where increasing pressure to rapidly deliver new biological actives has been linked with the hope of utilising continuous-flow technologies to access unexplored chemical space [20–22]. Consequently, chemists from both industry and academia have been focused on utilising flow chemistry to efficiently prepare new classes or improve access to difficult to generate heterocyclic moieties. In general most of these target heterocycles have been based on five- or six-membered aromatic ring systems [23–25], rather than saturated heterocycles, which disregards the immense potential with respect to three-dimensionality as well as structural diversity that such saturated heterocycles would bring to drug development programmes [26, 27]. As there is a progressive change in mind-set regarding these untapped opportunities in both industry and academia (moving away from flatland structures) [28, 29], this review focuses on surveying recent developments in the area of non-aromatic heterocycles as prepared in flow, organised into five subsections each highlighting strategic approaches applied to the flow assembly of various saturated heterocyclic structures:

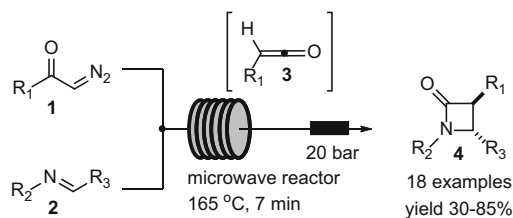
1. Synthesis of saturated heterocycles via cycloaddition chemistry
2. Synthesis of saturated heterocycles via cyclodehydration and related reactions
3. Catalysis applied to the assembly of saturated heterocycles
4. Miscellaneous approaches for the synthesis of saturated heterocycles
5. Target-driven synthesis of saturated heterocycles

1.1 Synthesis of Saturated Heterocycles via Cycloaddition Reactions

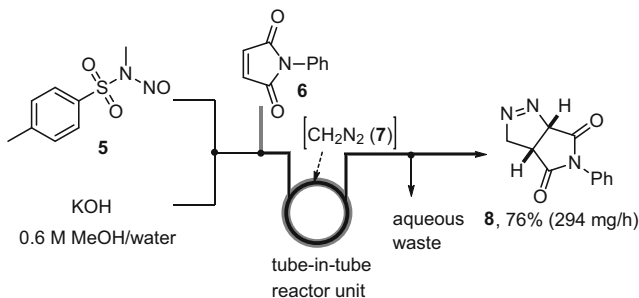
Cycloaddition reactions are amongst the most powerful and atom-economic processes available to chemists allowing multiple bonds to be formed in a single transformation. Typically as these reactions follow concerted and well-defined transition states, they are accompanied by a high degree of regioselectivity and have high potential interactions with catalysts leading to stereocontrolled ring-forming processes. Furthermore, numerous variations have been reported permitting access to both functional carbocyclic and heterocyclic structures of variable ring size.

In a recent application, heterocyclic ring construction has been exemplified by devising a microwave flow approach to various β -lactams via a Wolff-Staudinger cascade reaction (Scheme 1) [30]. In this study, different 2-diazo ketones **1** were combined with preformed imine substrates **2** via a T-piece mixer and directed into a flow microwave cavity where under irradiation (165 °C, 7 min) the rearrangement of the 2-diazo ketone into a ketene **3** was achieved, which then underwent the expected [2 + 2] cycloaddition yielding a selection of β -lactam products **4** typically in good yield and diastereoselectivity. Improvements regarding the safe generation of the ketene intermediate and its efficient transformation into various β -lactams are reported as the main benefits of this flow approach which was followed up with DFT studies addressing the observed preference for the trans-diastereomer as main product.

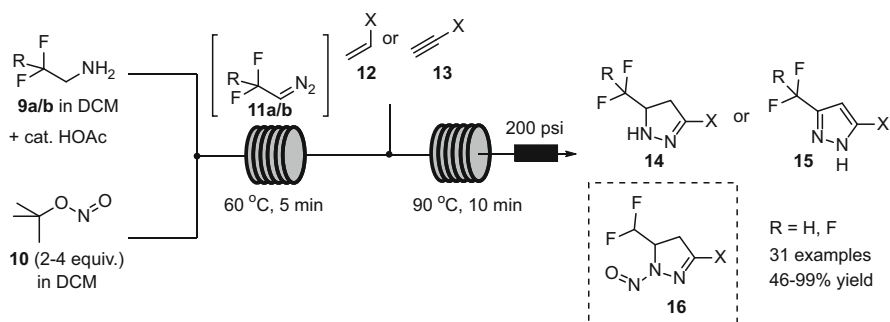
The desire to safely generate and utilise the highly reactive diazomethane reagent **7** was identified as the driving force in a related study for the development of a continuous-flow approach [31]. In this sequence a tube-in-tube [32, 33] flow reactor set-up was employed to allow diazomethane, prepared in situ by the base-mediated decomposition of commercially available Diazald **5**, to permeate across a Teflon AF-2400 membrane into a stream of the reacting substrate. Upon optimisation, this approach was successfully demonstrated on several important transformations including a dipolar cycloaddition reaction with *N*-phenyl maleimide **6** yielding the saturated 1-pyrazoline species **8** in good yield and throughput (Scheme 2).



Scheme 1 Continuous-flow microwave synthesis of β -lactams **4**



Scheme 2 Generation of diazomethane **7** in flow and its application to dipolar cycloaddition reactions

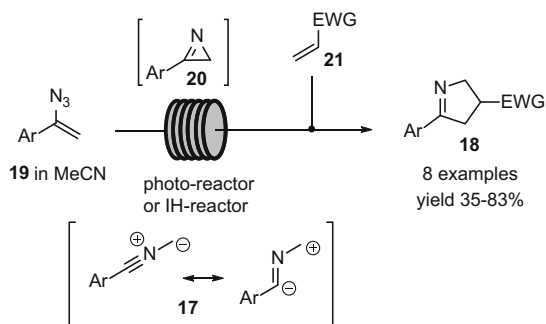


Scheme 3 Synthesis of heterocycles **14–16** derived from di- or trifluoromethyl diazomethane

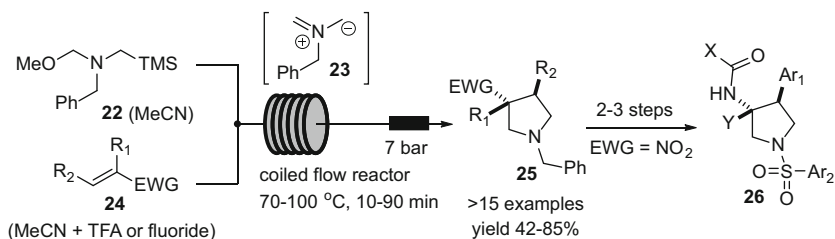
More recently, a related study was disclosed detailing the generation of di- and trifluoromethyl diazomethane **11a/b** prepared in situ by reacting *t*-butyl nitrite **10** with the corresponding amine precursors **9a/b** as a flow operation [34] (Scheme 3). The subsequent dipolar cycloaddition of **9a/b** with a selection of alkenes **12** and alkynes **13** resulted in the formation of a series of di- and trifluoromethylated pyrazolines **14** and pyrazoles **15** which are important motifs in medicinal chemistry. Using a telescoped flow process for the generation and subsequent consumption of the di-/trifluoromethyl diazomethane not only allowed for a safe and scalable process to deliver the desired heterocyclic targets but moreover provided excellent control over the reaction conditions with respect to mass and heat transfer. It was additionally found that doubling the stoichiometry of *t*-butyl nitrite **10** enabled the synthesis of new *N*-nitroso pyrazolines **16** in good to excellent yields.

Another recent application highlighting the salient benefits of continuous-flow chemistry towards the safe generation and use of highly reactive species demonstrates a series of [3 + 2]-cycloaddition reactions between nitrile ylides **17** and alkenes yielding different dihydropyrroles **18** [35]. In this study, the nitrile ylide species were generated by photolysis of vinyl azides **19** via intermediacy of isolable *2H*-azirines **20** prior to reaction with electron-deficient alkenes **21** as dipolarophiles (Scheme 4). Additionally, this report outlines the complimentary use of either photolysis or inductive heating (IH-reactor) as a means of generating *2H*-azirines in flow.

The diastereoselective synthesis of substituted pyrrolidines based on azomethine ylide chemistry is a very popular entry into chiral heterocycles that are starting to feature as common fragments in many drug structures. Consequently, several approaches detailing this [3 + 2]-cycloaddition reaction have been developed using continuous-flow technology [36, 37]. The commercially available silylated amination ether **22** in the presence of either TFA (trifluoroacetic acid) or a fluoride source was used to generate an unstabilised azomethine ylide **23** in situ then goes on to react with different dipolarophiles **24** including acrylate esters, acrylonitriles and nitro olefins (Scheme 5). Using a commercially available Vapourtec flow system, it was possible to generate small sets of pyrrolidine products **25** in both high yield and purity. The main benefits of this flow approach were identified as the short reaction



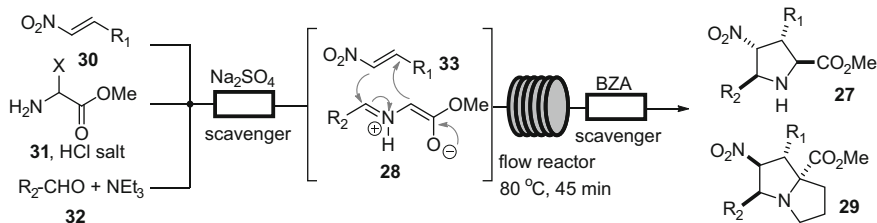
Scheme 4 Synthesis of dihydropyrroles **18** via dipolar cycloaddition of in situ generated nitrile ylides



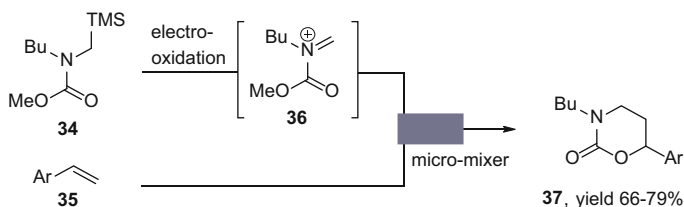
Scheme 5 Synthesis of pyrrolidines **25** via dipolar cycloaddition of unstabilised azomethine ylides **26**

time (10–90 min) and in mitigating the risks associated with the highly exothermic nature of the transformation. Additionally, the use of in-line cartridges of scavengers such as benzylamine resin (BZA) in combination with small plugs of silica was reported as a simple yet efficient means of performing direct purification of the crude reaction stream. Furthermore, this facile entry into diastereopure nitropyrrolidines was exploited in their transformation into a series of elaborated drug-like architectures **26** based on nitro reduction and acylation/sulfonylation reactions, which were performed by a suite of batch and flow processes [38].

A related study details the flow synthesis of tetrasubstituted pyrrolidines **27** via reaction of different dipolarophiles with stabilised azomethine ylides **28** that were prepared in situ from aldehydes and amino esters (Scheme 6) [39]. This multicomponent approach towards these interesting structures was realised using a three-pump assembly to direct each substrate via a mixing element into a glass column containing anhydrous sodium sulfate to aid in the formation of the glycine imine intermediate. The imine then underwent dipolar cycloaddition with the desired dipolarophile. Extending the choice of amino esters to also include proline derivatives enabled the efficient generation of structurally more complex bicyclic pyrrolizidine structures **29**.



Scheme 6 Multicomponent synthesis of pyrrolidines **27** and pyrrolizidines **29** in flow (predominant diastereomer shown)

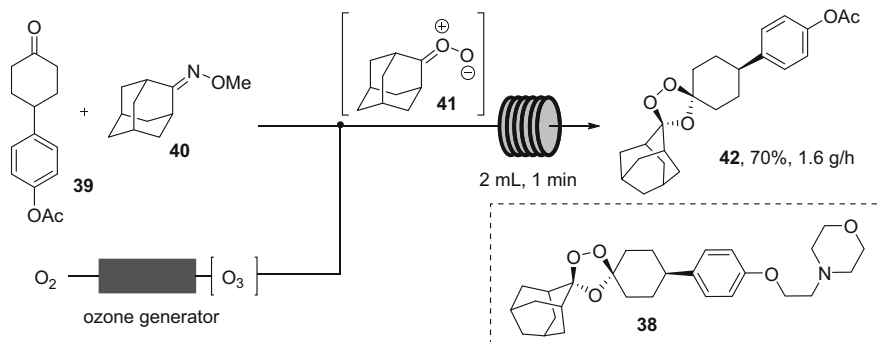


Scheme 7 Diels-Alder cycloaddition reactions of electrochemically generated *N*-acyliminium species

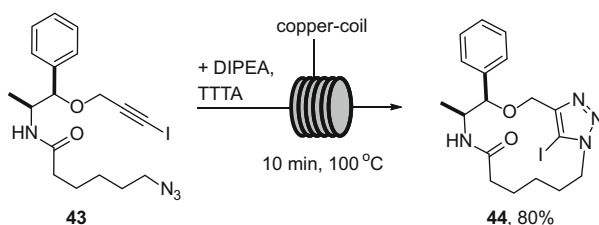
A related study detailing the benefits of flow chemistry in generating and utilising highly reactive *N*-acyliminium species was enabled by exploiting an efficient electrochemical approach [40, 41]. In this instance, the desired *N*-acyliminium species **36** was prepared from a silylated precursor **34** under low temperature electrolysis conditions prior to micro-mixing with different alkene and alkyne dienophiles rendering upon cycloaddition various 1,3-oxazine products (**37**, Scheme 7) in yields surpassing those obtained in comparable batch reactions that were reported to suffer from competition of several side reactions.

An interesting flow approach towards the antimalarial drug candidate OZ439 **38** was recently reported [42]. As the target structure contains a 1,2,4-trioxolane ring system, a concise approach was chosen that generated this pharmacophore by a Griesbaum co-ozonolysis, which is a [3 + 2] cycloaddition reaction between a ketone and a carbonyl oxide generated in situ from an alkylated oxime [43]. To achieve this transformation in flow, a mixture of ketone **39** and oxime derivative **40** was prepared in ethyl acetate and combined in a T-piece with a stream of ozone allowing the desired transformation to take place in a small volume flow coil (2 mL) prior to product isolation (Scheme 8). Crucially, the desired product was produced in high yield (70%, d.r. 9:1 *cis-trans*) at a rate of 1.9 g/h allowing the safe generation of multigramme quantities of **42**, the precursor to OZ439, in a single working day.

A final case highlighting the value of dipolar cycloadditions performed to generate interesting heterocyclic scaffolds is shown in Scheme 9 where a transannular click reaction between an azide and an alkyne furnishes not only the common 1,2,3-triazole but moreover a 12- to 31-membered macrocycle **44** [44]. This transformation is accelerated through the use of a copper reactor coil that is proposed to



Scheme 8 Griesbaum co-ozonolysis flow approach towards drug OZ439 **38**

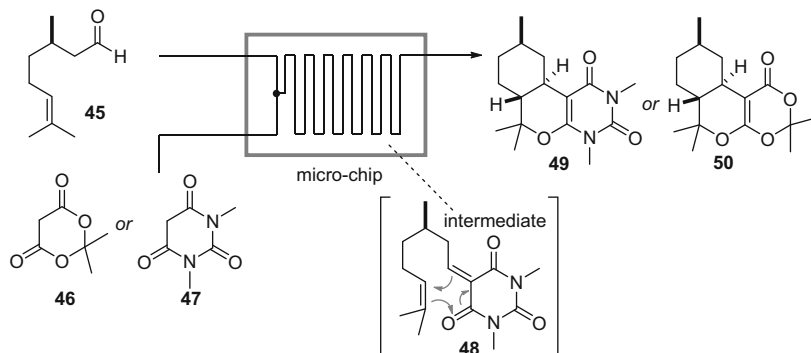


Scheme 9 Click-based approach to triazole containing macrocycles

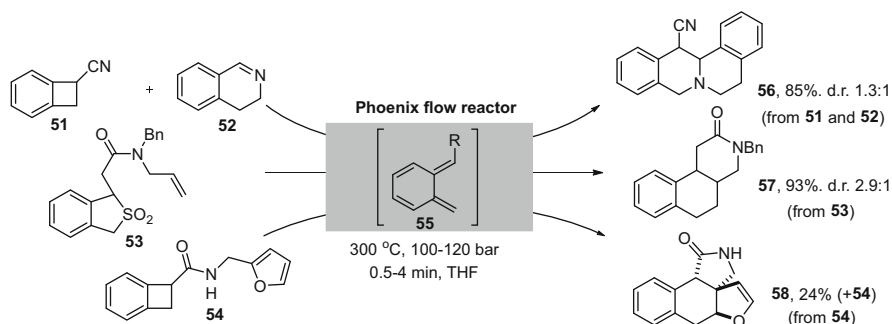
release catalytic amounts of copper ions into the passing substrate solution aiding in the cycloaddition event. Using short residence times of 10 min and a temperature of 100 °C enabled the efficient generating of a small collection of macrocyclic products. Importantly, it was found that DIPEA (2 equiv.) and TTTA [*tris*((1-*tert*-butyl-1*H*-1,2,3-triazol-4-yl)methyl)amine, 0.1 equiv.] as additives were crucial for isolating the desired products in good yields.

The preparation of drug-like heterocyclic scaffolds via Diels-Alder processes has for many years attracted the attention of flow chemists as a readily scalable technique towards their efficient assembly. In an early example, this was exemplified via a microreactor chip-based approach in which citronellal **45** was first subjected to a Knoevenagel condensation reaction with either Meldrum's acid **46** or 1,3-dimethylbarbituric acid **47** resulting in an adduct (i.e. **48**). This intermediate was nicely set up for intramolecular hetero Diels-Alder reactions to yield the desired cycloadducts (Scheme 10) [45].

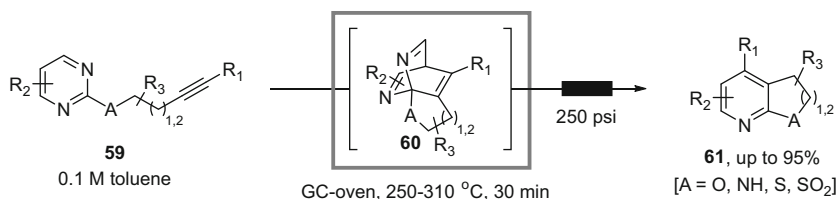
More recently, drug-like heterocyclic systems have also been prepared under flash chemistry conditions exploiting new high temperature and pressure reactions that were previously hard to access without dedicated high-pressure autoclave equipment [46, 47]. The benefit of the flow approach was demonstrated by the efficient generation of various *ortho*-quinodimethanes **55** that underwent smooth Diels-Alder reactions with various dienophiles furnishing several different drug-like scaffolds (e.g. **56–58**) typically in good isolated yields (Scheme 11) [48]. Being able to safely



Scheme 10 A microchip approach to tricyclic products **49–50**



Scheme 11 Selected examples of Diels-Alder cycloadditions of *ortho*-quinodimethanes in flow



Scheme 12 Hetero-Diels-Alder cycloaddition reactions of alkynyl pyrimidines in flow

perform these transformations in a Phoenix Flow Reactor system at high temperature (300 °C) and pressures (100–120 bar) not only allowed for significantly shortened reaction times (0.5–4 min) but additionally also permitted the use of a low boiling organic solvent (THF) due to inbuilt back pressure regulators. This simplified product isolation at the end of the reaction by simple evaporation.

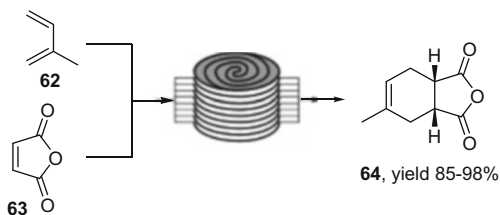
A further example of high-temperature Diels-Alder reactions yielding drug-like scaffolds was demonstrated in flow by converting a series of 2-alkynyl pyrimidines **59** into the corresponding bicyclic pyridines **61** (Scheme 12) [49]. This approach is

based on a less common inverse electron demand hetero-Diels-Alder reaction that was performed as a continuous process by passing the substrate solution through a GC oven maintained at high temperature (250–310°C). Pleasingly, it was observed that residence times of 30 min were sufficient to generate the desired products in good to excellent isolated yields. The HCN that was released in the process was trapped as a cyanohydrin species by blending the toluene solvent with pentan-3-one (1% v/v). The reaction was subsequently applied to several different substrates allowing variation of the substitution pattern as well as in the ring size of final products.

Several research groups have investigated the process intensification of the Diels-Alder cycloaddition. A common example in the context of this review is the reaction scale-up of isoprene **62** with maleic anhydride **63** under continuous-flow conditions furnishing the valuable intermediate structure 3 α ,5,7 α -trimethyl-3 α ,4,7,7 α -tetrahydroisobenzofuran-1,3-dione **64** (Scheme 13). Although using a stainless steel reactor [50, 51] often allows higher temperature and pressures to be accessed, this particular cycloaddition is more facile allowing other reactor construction materials to be employed. Mackley and co-workers engineered a polymeric microchannel disk reactor (micro flow disk – MFD) which comprised eight parallel channels (~200 μm i.d.) prepared in a tape which could be easily coiled to create a spool [52]. Direct immersion of the reactor in an oil or water bath allowed efficient temperature regulation, and at 60°C, isolated yields of 85–98% in 28–113 min residence times could be achieved. Under optimised processing conditions, a throughput of 1.05 kg/day was obtained. In an example, the ability to rapidly increase throughput using the concept of numbering up, the same process was run using eight parallel MFDs (I_{cap} 40 m) [53]. The isolated yield was maintained between 85 and 98% at flow rates of 2–6 mL/min. When the reactor was working at full capacity (6 mL/min), an output of 2.73 g/min equating to an impressive 3.93 kg/day was obtained requiring only solvent removal to isolate the final crystalline product **64**. More recently this same process has been reinvestigated using a statistical modelling approach leading to revised conditions and an improved kinetic profile which allowed the reaction to be scaled directly by a factor of 500 from a microreactor to a Corning flow reactor [54].

In an example of employing the Diels-Alder reaction in a target-orientated synthesis, a short two-stage continuous-flow synthesis of a spirocyclic fragrance component has been realised in a multistep sequence [55]. A Baylis-Hillman reaction preformed in a set of CSTRs enables sufficient residence time for the slow transformation (Scheme 14). Telescoping the product into a more rapid acetic

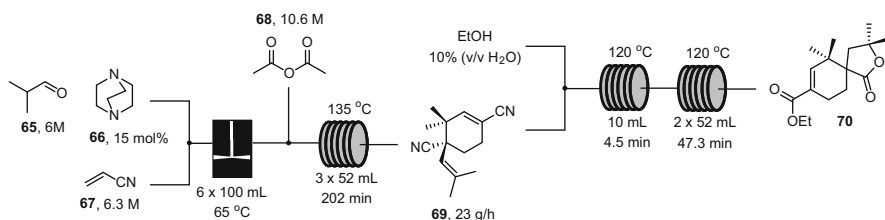
Scheme 13 Diels-Alder cycloaddition using an MFD device



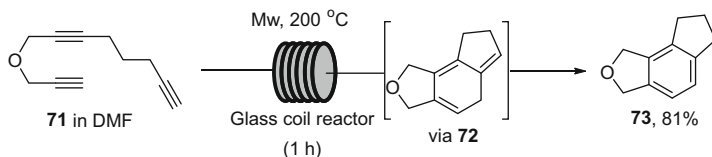
anhydride promoted acylation-elimination and Diels-Alder cycloaddition sequence gave the intermediate cyclohexene **69** with a productivity of 23 g/h (isolated). Acid alcoholysis at elevated temperature facilitated spirocyclisation and interconversion of the vinyl nitrile to its ester analogue. The reactor was run uninterrupted for over 6 days generating multi-kilogramme quantities of the desired product.

Accessing high-temperature heating zones to drive reactions is often pursued in the laboratory using microwave reactors. It has been demonstrated that flow chemistry and microwave irradiation can be unified to deliver processing advantages [56–59], for example, a metal-free intramolecular alkyne cyclotrimerisation of an oxygen-bridged triyne **71** to generate cyclic ether with an aromatic core **73** (Scheme 15) [60]. The reaction was easily processed by pumping the solution of the starting material through a glass coil located within the microwave reaction cavity; pressure was maintained using a back pressure regulator positioned at the output. The flow process gave an identical yield to the batch equivalent reaction but was readily scaled based upon extended run times under continuous operation.

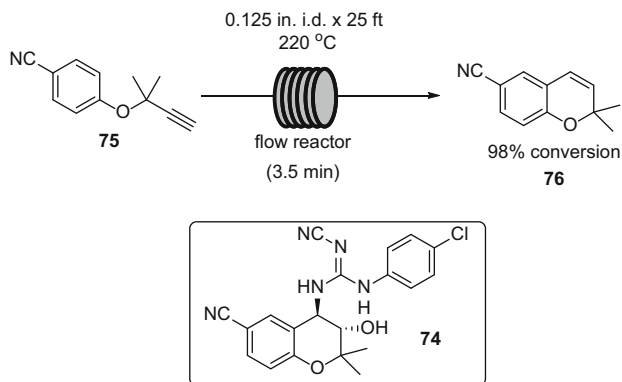
The requirement to perform safely and consistently a high-temperature Claisen rearrangement (220°C) during a scale-up campaign towards the preparation of a drug candidate **74** inspired chemists at Bristol-Myers Squibb to develop a continuous-flow approach (Scheme 16) [61]. Using a coiled steel tube reactor, residence times of between 3.5 and 17.7 min were evaluated for the transformation of propargyl ether **75** to 6-cyano-2,2-dimethylchromene **76** achieving >96% conversion under the range of conditions tested. During the campaign over 50 kg of material was processed with a production capability of >7 kg/h. In addition, the scope of the reaction was evaluated based upon an expanded range of propargyl ethers which also underwent smooth reaction giving high yields (74–96%) although certain species required higher reaction temperatures >240°C.



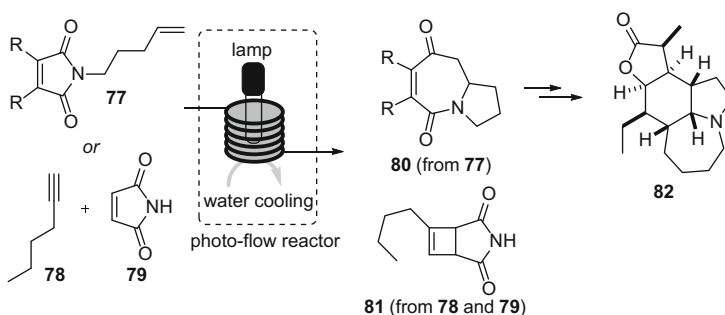
Scheme 14 Synthesis of 2-oxaspiro[4.5]decan-1-one **70**



Scheme 15 Microwave thermal cyclisation



Scheme 16 Thermal Claisen rearrangement in flow



Scheme 17 Photocycloaddition reactions in continuous-flow mode

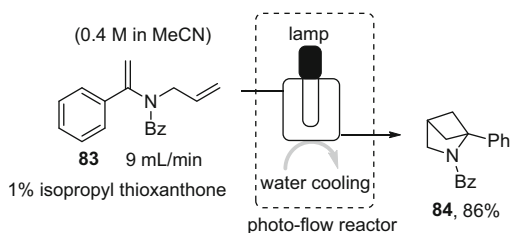
Photocycloadditions represent a further subsection of this important cyclisation mode that has in recent years seen growing interest regarding continuous processing options. This is owed to the improved efficiency and scalability such photochemical reactions can realise when performed in flow mode. A popular entry into this chemistry was reported for [2 + 2]- as well as [5 + 2]-photocycloadditions between maleimides and alkenes or alkynes as reaction partners (Scheme 17) [62]. For this purpose, a simple photochemical reactor was built by winding fluoruous polymer tubing around a cooled immersion well, inside which a light source was placed. Upon passing solutions of substrates through this reactor set-up then allowed for the efficient generation of the heterocyclic target compounds with throughputs of >100 g/day. The value of generating these architectures was more recently demonstrated in the flow-assisted total synthesis of neostenine (Scheme 17) **82** [63].

A higher specification bespoke engineered photoflow reactor given the name the firefly was developed for scale-up operation [64]. The new system was based upon an array of sequentially linked quartz tubes arranged axially around the central light source (400 W Hg lamp) with a water cooling surround jacket. This enabled the same maleimide **79** with alkyne **78** [2 + 2]-cyclisation to be run with a productivity

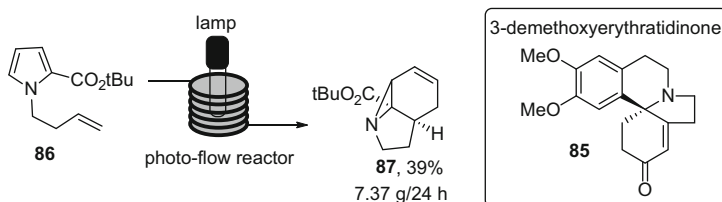
of 3.41 g/h. However, running at a higher power setting of 3 kW allowed further scaling on a range of different reactions, for example, the bridged pyrrolidine **84** could be produced at 49 g/h which was an 11-fold increase on what had previously been reported in batch (Scheme 18).

Photochemistry has also been used to help prepare sufficient starting material for a natural product total synthesis of the alkaloid 3-demethoxyerythratidinone **85**. The key transformation of pyrrole **86** gave the desired aziridine **87** in a 39% yield (Scheme 19) [65]. This transformation which must be run under high dilution and has a low quantum yield was difficult to scale in batch. Using a three-lamp (254 nm) FEP-flow (fluorinated ethylene propylene) reactor gave access to 1.91 g of aziridine in a single 373 min run which would equate to a productivity of 7.37 g/24 h. This generated adequate material to complete the total synthesis.

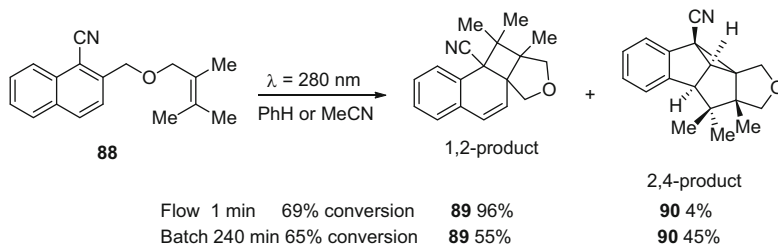
A series of intramolecular photocycloadditions of alkenyl naphthalene derivatives leading to polycyclic structures through [2 + 2] and [2 + 3] processes were compared under batch and flow conditions (Scheme 20) [66]. For the flow processing, a Pyrex glass micro-channelled (100 μm width \times 60 μm depth and 120 mm length, flow rate 0.03 mL/h) reactor was used, irradiation being supplied by a high-power xenon lamp (500 W, $\lambda = 280$ nm) as the light source. A significant reduction in the required irradiation time from 240 min in batch to 1 min in flow was noted, but importantly this was also accompanied with a diminished amount of photocycloreversion product being observed. The authors demonstrated a scale-up using a wider bore reactor (2.5 mm width \times 50 μm depth and 60 mm length with a flow rate of 0.45 mL/h) to affect a 25-fold increase in the quantity of product that could be generated in essentially equivalent selectivity and yield.



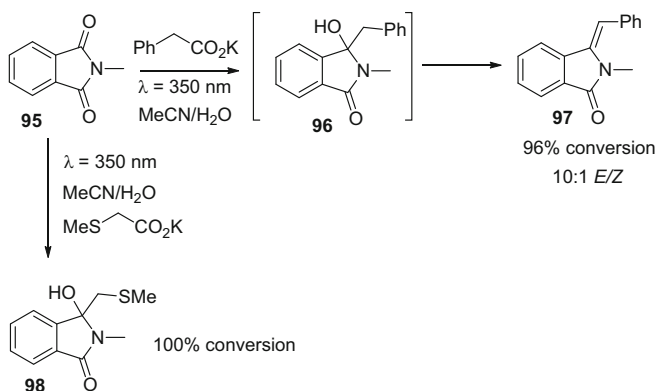
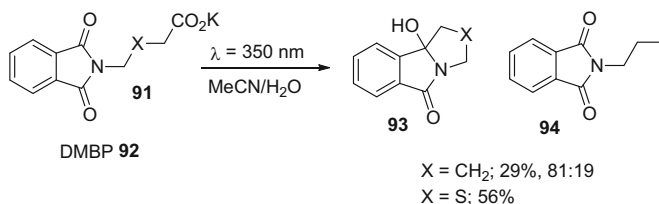
Scheme 18 Scale-up flow photocycloaddition reactions



Scheme 19 Photocycloaddition cyclisation to generate starting materials for the synthesis of 3-demethoxyerythratidinone **85**



Scheme 20 Intramolecular photocycloaddition of 2-(2-alkenyloxymethyl)-naphthalene-1-carbonitriles



Scheme 21 Photochemical promoted addition and intramolecular cyclisation

Finally, photodecarboxylation reactions have emerged as efficient (quantum yields of up to 60%) and powerful methods of inducing metal-free alkylations. In a photochemical process promoted by the sensitiser 4,4'-dimethoxybenzophenone (DMBP) **92**, the decarboxylation and radical trapping into phthalimides was explored [67]. A simple set-up employing a commercial Foturan microreactor (volume = 1.6 mL) and an array of five 8 W UVA lamps was assembled. In reaction times of approximately 1 h, high conversions and in most cases good recovery of the products were achieved after chromatographic purification (Scheme 21). A similar approach with more selective excitation has also been reported by DeLaney et al. delivering pyrrolizidine structures [68].

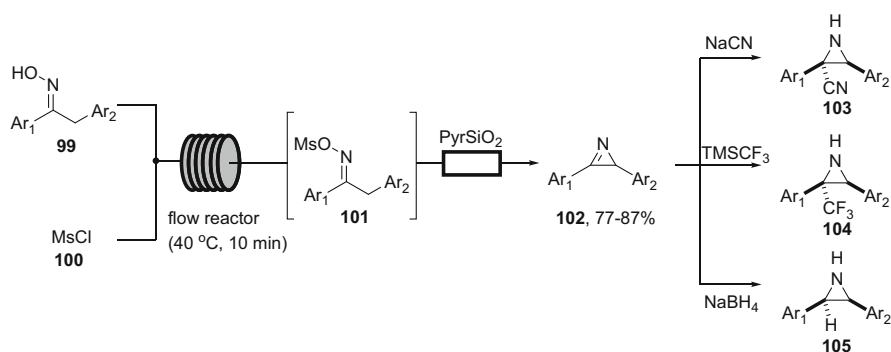
1.2 Synthesis of Saturated Heterocycles Through Cyclodehydration and Related Reactions

Cyclodehydration reactions represent another versatile entry to heterocyclic scaffolds often from more readily prepared acyclic precursors. A range of dehydration agents can be utilised to activate a leaving group (often hydroxy) and achieve the cyclisation step via an intramolecular nucleophilic substitution reaction. Several flow approaches have harnessed such cyclodehydration strategies in the synthesis of valuable heterocyclic architectures.

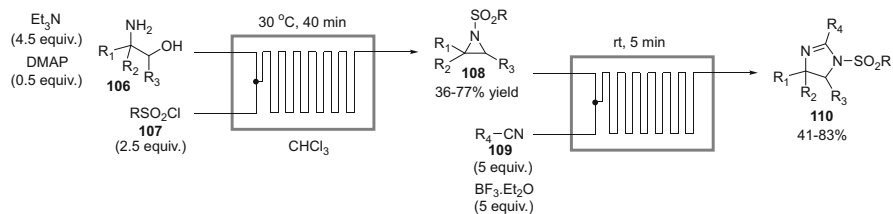
In a recent study, a small series of *2H*-azirines **102** was prepared in flow via activation of an oxime using mesyl chloride followed by a base-promoted cyclisation reaction [69]. A simple set-up was constructed involving combining a stream of the oxime substrate **99** with a solution of mesyl chloride **100** prior to entering a tubular flow reactor (Scheme 22). Upon exiting the flow coil, the mesylated oxime intermediate **101** passed through a cartridge containing silica-supported pyridine (ambient temperature, ~4 min residence time) resulting in the clean formation of the desired *2H*-azirines **102**. It was demonstrated that these species could be either isolated or directly converted into various aziridines via telescoped flow procedures. Example derivative transformations included cyanation, nucleophilic trifluoromethylation and hydrogenation reactions that yielded the desired aziridine products **103–105** in high yield and excellent diastereoselectivity (>19:1).

A telescoped flow processes for the synthesis and ring expansion of *N*-sulfonyl aziridines to imidazolines has also been reported [70]. Starting from readily available β -amino alcohols, the aziridines **108** were formed by activation with various sulfonyl chlorides **107** in the presence of excess triethylamine and a DMAP catalyst. The highly strained aziridines **108** could be induced to ring open with direct trapping by a nitrile followed by re-cyclisation to deliver the corresponding imidazoline **110** (Scheme 23).

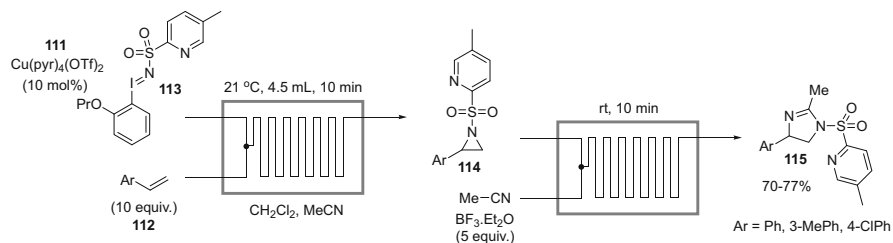
In a follow-up publication, the same group expanded the range of starting materials by applying hypervalent iodine reagents for the direct aziridination of



Scheme 22 Flow synthesis of *2H*-azirines and aziridines



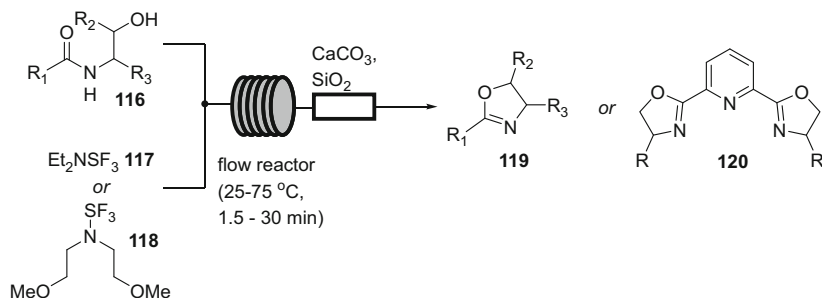
Scheme 23 Aziridine formation and ring expansion



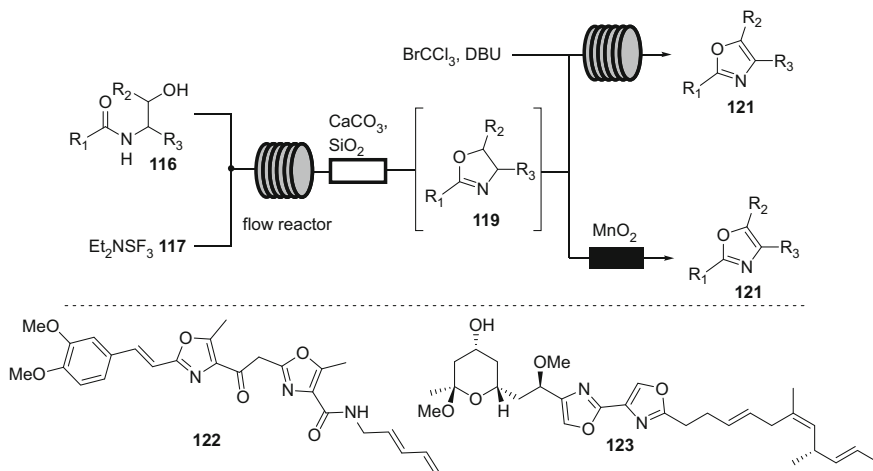
Scheme 24 Aziridine formation and ring expansion starting from alkene precursors

alkenes [71]. Several styrenes and cyclic alkenes **112** were readily converted into their aziridine products **114** in good yield promoted by a homogeneous copper(II) catalyst **111** in a flow process. Once formed various nucleophiles (alcohols and chloride) were exploited in ring opening reactions giving good yields of the β -amino adducts also performed in flow. In addition to further expand on the chemotypes prepared, acetonitrile was employed to generate a small example collect of imidazolines **115** in a telescoped sequence (Scheme 24).

Another common class of saturated heterocycles that has been prepared using continuous-flow mode operations are the oxazoline system **119** which can be generated effectively via cyclodehydration of β -hydroxy amides **116** using reagents like DAST (diethylaminosulfur trifluoride, **117**) or Deoxo-Fluor[®] **118**. Due to their reactive nature and propensity to dismutate and also form hydrogen fluoride as a highly toxic by-product, these reagents must be handled with care in batch; however, their use in flow mode was found to be much more straightforward due to their containment within the flow system. As such both DAST and Deoxo-Fluor[®] have also found widespread applications in other flow-based applications such as deoxyfluorination reactions of various alcohols and carbonyl substrates [72]. For the synthesis of oxazolines, a typical flow set-up can be used which allows mixing of streams of the substrate and the dehydrating agent (DAST or Deoxo-Fluor[®]) at a T-piece prior to undergoing the desired reaction in a tubular flow reactor (Scheme 25) [73]. To safely quench any residual reagent and at the same time eliminate hydrogen fluoride, several in-line purification procedures have been reported. These include using calcium carbonate as a basic scavenger within a glass column as well as aqueous extractions in which a solution of sodium bicarbonate is blended with the crude reaction mixture prior to separation and product collection. Both options have been



Scheme 25 Flow synthesis of oxazolines by cyclodehydration of β -hydroxy amides



Scheme 26 Generation of oxazoles from intermediate oxazolines in flow mode

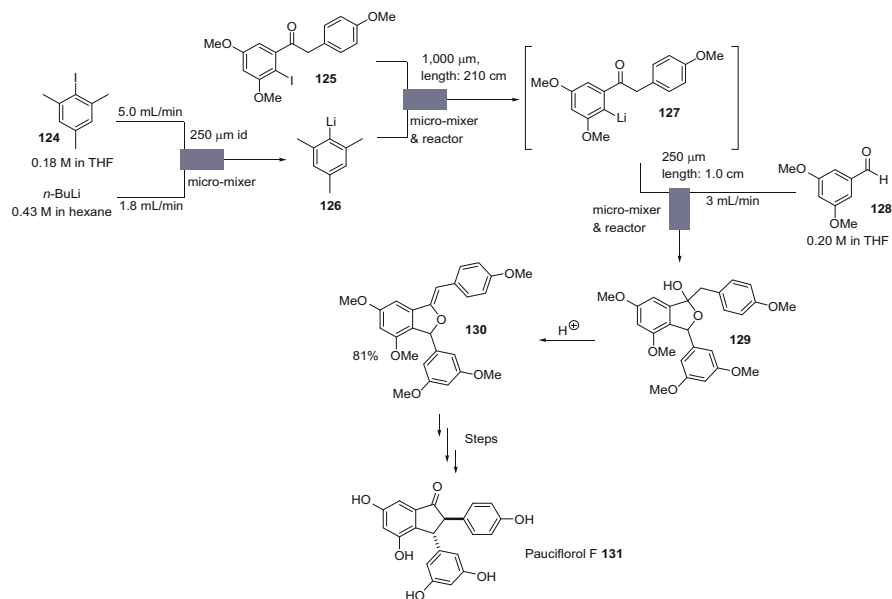
successfully demonstrated to aid the synthesis of the oxazoline species **119** as well as providing access to important *bis*-oxazoline ligands such as the PyBox structure **120** [74].

Moreover, the effectiveness of generating diversely substituted oxazolines also enabled the application of this methodology for the synthesis of several oxazole-containing natural products such as *O*-methyl siphonazole A [75] **122** and (–)-hennoxazole A [76] **123** utilising a suite of integrated batch and flow-based approaches. Whilst the formation of the oxazoline ring system is accomplished as outlined above, its oxidation to the corresponding di- and tri-substituted oxazoles **121** is reported in a telescoped fashion by employing either homogeneous (bromochloroform and DBU) or heterogeneous conditions (MnO_2 powder placed in glass cartridges [77], Scheme 26).

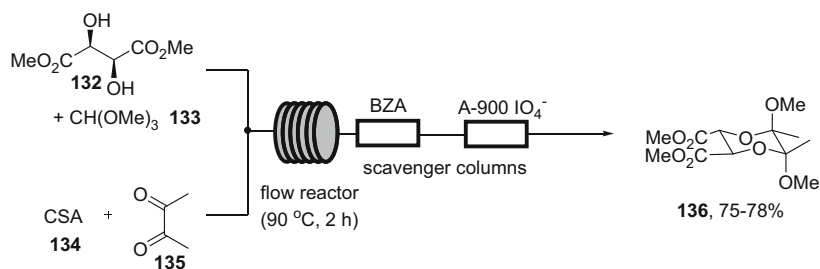
In many chemical transformations, it is necessary to install protecting groups on sensitive functional units in order to provide sufficient chemical reactivity distinction to avoid competing reactions at multiple site. A facet of microreactor technology is

the ability to rapidly generate and also intercept transiently stable intermediates with reagents before other promiscuous reactions leading to by-products or decomposition can happen. Yoshida and co-workers have reported [78] a protecting group-free approach to the use of organolithium species in flow. Under conventional batch conditions, the mixing of an organolithium reagent with a reactive carbonyl functionality, such as ketones, would result in an addition reaction. However, by ensuring exacting control over reaction time in a micromixer (<0.003 s), it was shown that an aryllithium intermediate **127** could be generated from substrates possessing a ketone functionality without the need for protection. As an exemplification of the synthetic utility of the methodology, it was used to prepare compound **130** on route to the natural product pauciflorol F **131** which was synthesised in 81% yield with a throughput of 12.72 g/h (Scheme 27).

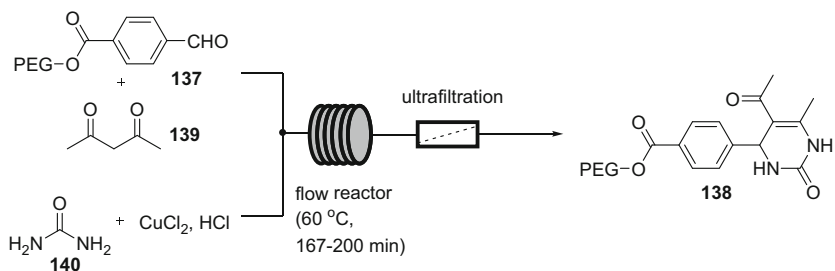
Apart from classical cyclodehydration reactions that as outlined above are typically intramolecular processes, related intermolecular cyclocondensation processes have been reported in flow mode. One early example details this approach in the continuous-flow synthesis of butane-2,3-diacetal building blocks (**136**, BDA) which have found widespread applications in the synthesis of complex natural products (Scheme 28) [79, 80]. Although several batch procedures had already been reported, these involved several labour- and time-intensive isolation and purification steps that resulted in reduced isolated yields. Thus, it became desirable to establish an efficient continuous-flow approach rendering BDA building blocks in a more robust and streamlined manner. To this end a commercial Uniqsis FlowSyn platform was utilised to combine methanolic streams containing trimethyl orthoformate **133** and



Scheme 27 Intermediate **130** on route to pauciflorol F **131**



Scheme 28 Flow synthesis of BDA building blocks



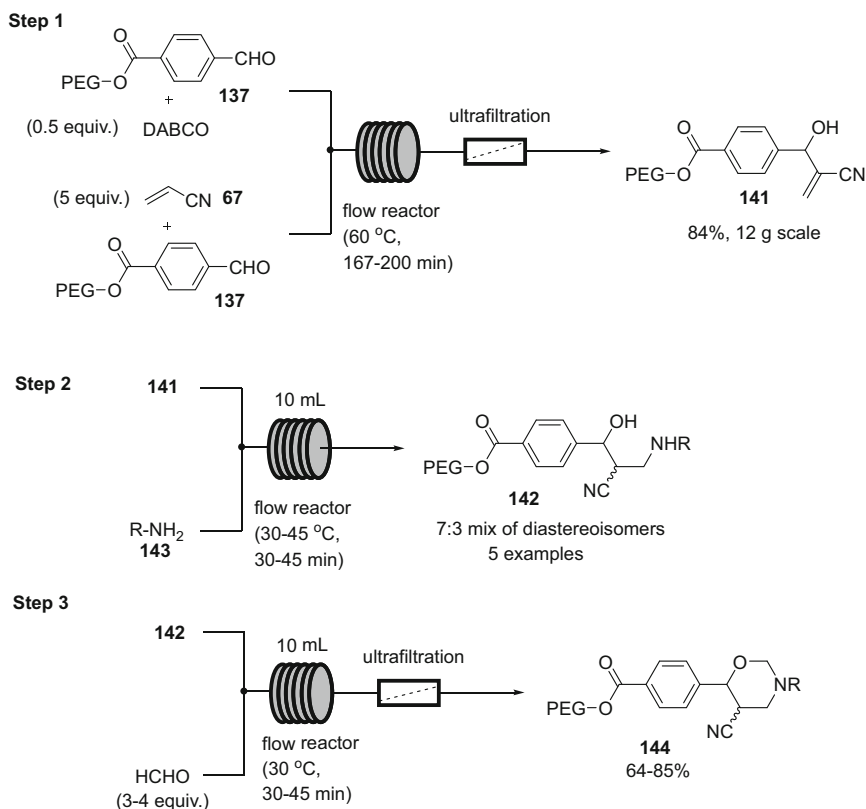
Scheme 29 Example Biginelli reaction towards PEG-functionalised heterocycles

dimethyl-*L*-tartrate **132** (stream A) with *DL*-camphorsulfonic acid (CSA) **134** and butanedione **135** (stream B) in a T-piece mixer before entering a heated flow coil reactor (14 mL, PTFE, 90 °C, 2 h residence time). Upon exiting the reactor, the crude reaction stream was directed through sequential columns containing benzylamine scavenger (BZA, removes CSA and unreacted butanedione) as well as immobilised periodate (effects glycol cleavage of remaining dimethyl-*L*-tartrate into volatile by-products). The product stream was collected, and after evaporation, the desired BDA building block **136** was obtained in 78% yield (2 mmol scale) and in excellent purity. Importantly, the efficient scale-up of this process was demonstrated in flow, which during a 10 h campaign allowed 200 mmol of substrate to be processed leading to the isolation of 40 g of elementally pure **136** in 75% yield.

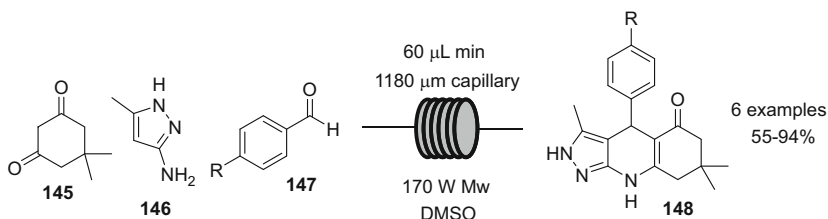
Another example of generating saturated heterocycles in flow mode via a cyclocondensation reaction is outlined in Scheme 29 where a PEG-linked aldehyde substrate **137** was used as a substrate in Biginelli as well as Baylis-Hillman reactions employing water as the solvent [81]. To realise the synthesis of 3,4-dihydropyrimidin-2(1*H*)-ones **138**, a copper-catalysed Biginelli reaction was demonstrated in which an aqueous stream containing the PEG-linked aldehyde **137** and acetylacetone **139** was united with a second stream of urea **140** and aqueous CuCl₂ before entering a heated flow coil (60 °C, 167–200 min residence time). The exiting flow stream containing the crude product was collected and purified by ultrafiltration.

In an analogous fashion, a series of tetrahydro-1,3-isoxazines **144** was prepared in a three-step sequence consisting of a Baylis-Hillman reaction between **137** and acrylonitrile **67**, followed by an in situ aza-Michael addition \rightarrow **142** and subsequent cyclocondensation \rightarrow **144** with aqueous formaldehyde (Scheme 30) [81].

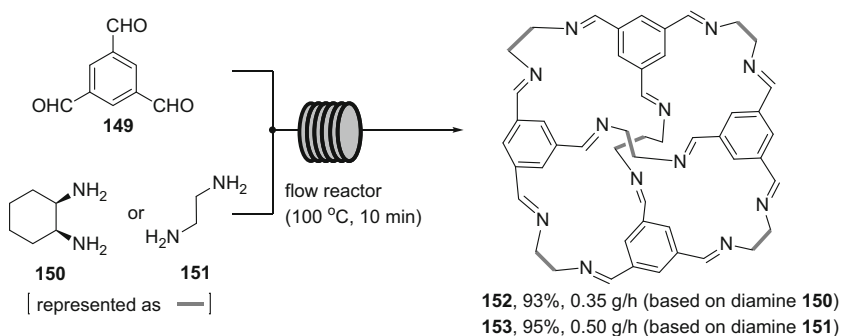
The popularity of multicomponent reactions for the rapid assembly of diverse heterocyclic scaffolds has also featured in a microwave-assisted flow approach towards a small selection of tricyclic products **148** resulting from the condensation of equimolar amounts of a benzaldehyde **147** with dimedone **145** and 2-aminopyrazoles **146** (Scheme 31) [82]. Of particular note was that much higher yields of the tetrahydropyrazolo[3,4-b]quinolin-5(6*H*)-one cores **148** were achieved in very short residence times compared to the need for prolonged refluxing in absolute ethanol which had previously been the optimised conditions. This gave two major benefits regarding the combinatorial efficiency of the system for library preparation first from the higher throughputs and thus quicker access to new structures but also from an associated reduction in the required purification times due to the higher starting purity of the crude materials.



Scheme 30 Three-step Baylis-Hillman promoted assembly of PEG-linked heterocycles in flow



Scheme 31 Three-component condensation reactions performed under microwave irradiation in a capillary reactor



Scheme 32 Dynamic flow synthesis of organic cage structures

A final example detailing cyclocondensation reactions applied to the flow preparation of partially saturated heterocycles was recently reported through a dynamic flow synthesis of porous organic cages [83]. In this approach, mixtures of triformylbenzene **149** and (1*R*,2*R*)-cyclohexanediamine **150** or ethylenediamine **151** were obtained by blending individual streams of these components that subsequently entered a heated flow coil reactor (100°C, 10 min) where multiple, reversible imine-forming reactions took place generating the thermodynamic cage structure **152** or **153** as the predominant product (Scheme 32). Using two different diamine inputs **150** and **151**, it was possible to generate the desired cage structure in short times and excellent yields allowing throughputs of 0.35–0.5 g/h. This outcome is far superior to the previously reported batch procedures, where the requirement of high dilution together with the inability to superheat solvent mixtures dictates reaction times of 3–5 days.

1.3 Catalysis Applied to the Assembly of Saturated Heterocycles

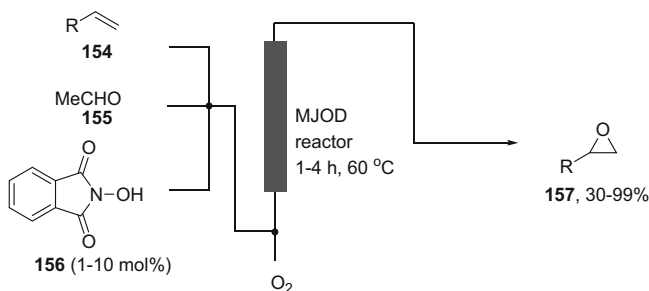
As the above sections have outlined, several benefits have been realised when generating saturated heterocyclic architectures under flow conditions, including the

safe in situ formation of highly reactive intermediates, the application of in-line analysis and purification methods and the ability to directly translate such steps into telescoped multistep sequences or scaled processes. A further field which is experiencing a rapid growth in popularity is the performing of catalysis in flow. As such several studies have been reported in which homogeneous as well as heterogeneous catalysis has been applied to the efficient formation of various saturated heterocyclic structures.

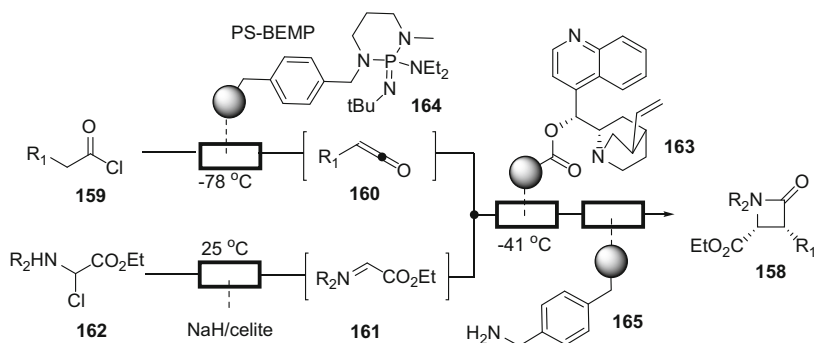
An early example details the organocatalyzed Minisci epoxidation of different alkenes using a multi-jet oscillating disk reactor (MJOD) [84]. In this reactor system, streams of the alkene substrate **154**, acetaldehyde **155** and *N*-hydroxyphthalimide catalyst **156** were mixed at the bottom of the reactor and combined with oxygen gas (Scheme 33). Upon passing through the heated reactor body oscillation is applied to establish rapid mass and heat exchange which results in improved reaction kinetics compared to analogous batch Minisci epoxidation reactions. Using the optimised system, a number of terminal and cyclic alkenes were successfully converted into their epoxide counterparts **157** in modest to excellent yields.

The application of catalytic approaches for the continuous synthesis of lactones is a well-established means for their effective generation. Consequently, a nanoflow approach for the regioselective Baeyer-Villiger oxidation of cyclic ketones mediated by hydrogen peroxide has been reported using a low loading of a fluoros lanthanide catalyst [85]. In addition, a recent study describes the effective synthesis of related lactones by a cycloisomerisation cascade [86]. Importantly, this approach utilises a silica-supported phenylmercuric triflate catalyst to affect this transformation, with only negligible amounts of mercuric salts being detected as a result of leaching from the support.

Apart from using homogeneously catalysed transformations to furnish heterocyclic scaffolds in flow mode, the complementary approach using immobilised organocatalysts has gained considerable attention. Many benefits regarding the simplicity of catalyst recovery and its recyclability can be derived from using fixed bed flow systems in addition to fundamentally changing the effective concentration of catalyst experienced by a solution progressing through the reactor. An early example is depicted in Scheme 34 outlining an immobilised quinine catalyst being used to affect the asymmetric synthesis of a series of β -lactams **158** [87]. This



Scheme 33 Minisci epoxidation in flow



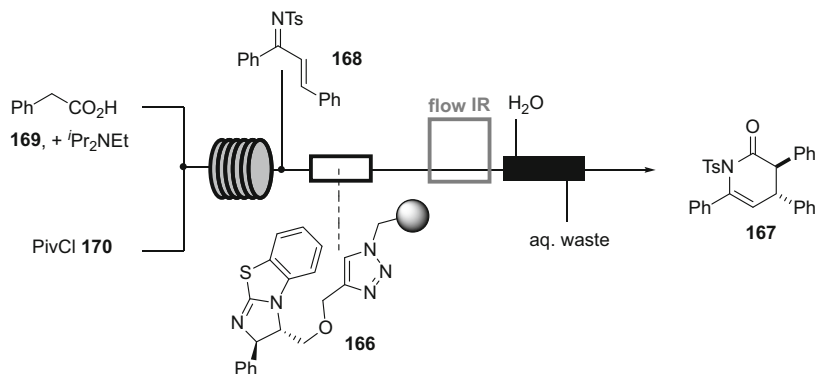
Scheme 34 Asymmetric flow synthesis of β -lactams **158**

assembly was accomplished by passing a stream of an acid chloride **159** through a column containing immobilised BEMP **164** as base, thus generating in situ a ketene species **160**. This stream was next blended with a second stream containing an imine **161**, also generated in situ by dehydrochlorination of a chloroglycine derivative **162**. The mixture was immediately passed into a packed bed column reactor containing the immobilised quinine catalyst **163**. After scavenging residual starting materials and by-products aided by an immobilised benzylamine species **165**, the desired β -lactam products were isolated in good yield and stereoselectivity.

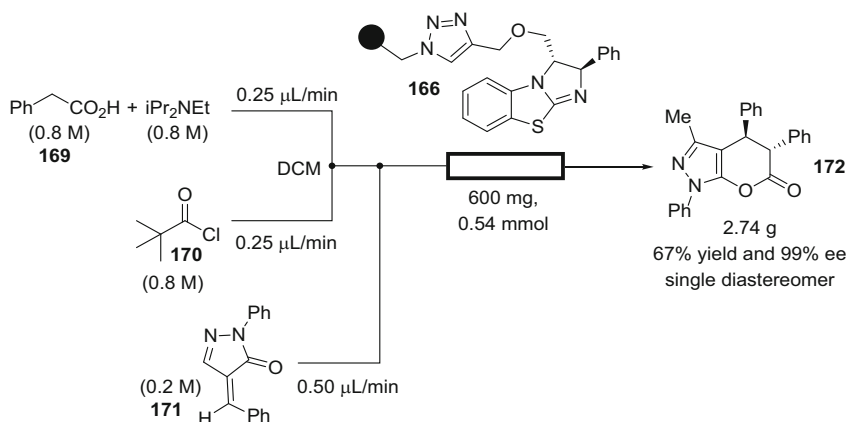
In a more recent demonstration, a benzo-tetramisole catalyst **166** was immobilised via a copper-catalysed click reaction onto a polystyrene resin allowing it to be used as an immobilised catalyst for enantioselective domino Michael addition – cyclisation reactions performed both in batch and flow mode [88]. With a catalyst loading of the resin of 0.9 mmol/g, the desired transformation was studied in a continuous fashion and pleasingly was found to deliver the desired product **167** not only in high yield and stereoselectivity but moreover in a short residence time of 7.5 min (Scheme 35). To increase the effectiveness of this continuous-flow approach, in-line IR and in-line extraction techniques were successfully coupled with the synthesis effort.

The same polystyrene-supported isothiourea catalyst **166** has also been utilised in asymmetric [4 + 2] annulation reactions generating six-membered heterocycles and spiroheterocycles consisting of oxindole units in high yields and e.e. (32 examples) [89]. In a demonstration of the catalyst robustness, a flow sequence was run involving packing the catalyst material into a cartridge and flowing the substrates through (Scheme 36). The supported catalyst showed no deterioration in the resultant yield or e.e. of the product exiting the reactor even after 18 h of continuous operation (TON ~77).

In a related study, a squaramide catalyst **173** was immobilised onto a polystyrene resin providing a cost-effective and recyclable catalyst system that was successfully applied to the two-step synthesis of a selection of pyranonaphthoquinones **174** [90]. This sequence commences with the enantioselective Michael addition reaction between 2-hydroxy-1,4-naphthoquinone **175** and different nitro olefins **176**



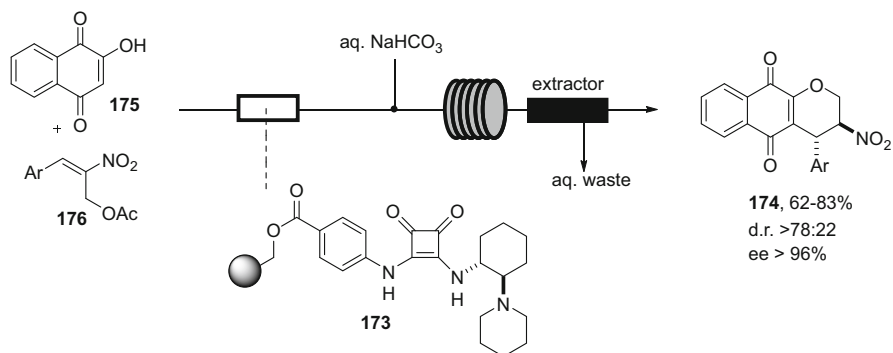
Scheme 35 Asymmetric flow synthesis of dihydropyridinones **167** using organocatalyst **166**



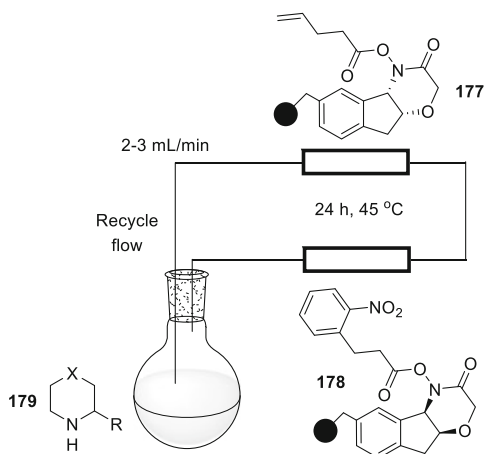
Scheme 36 Organocatalytic enantioselective annulation reaction using an immobilised catalyst

promoted by the immobilised squaramide catalyst (400 mg resin), followed by an oxa-Michael cyclisation reaction. Combined with an in-line extraction procedure, this efficient process allowed the rapid construction of the desired products in high yields and stereoselectivities in a total residence time of approximately 30 min (Scheme 37).

Kinetic resolution is a principal method of enantiomer separation allowing access to a single chiral compound from a racemic mixture by enantioselective derivatisation. An approach using immobilised chiral acyl hydroxamic acid catalysts **177** and **178** has been used for the kinetic resolution of several saturated *N*-heterocycles generating enantio-enriched amide products (Scheme 38) [91]. The methodology employs two sequentially linked packed bed cartridge reactors filled with polymeric chiral acyl derivatising agents which are chosen to react preferentially with the different enantiomers of the racemic mixture. This approach generates a



Scheme 37 Immobilised squaramide catalyst **173** for the flow synthesis of pyranonaphthoquinones **174**



Substrates				
180	181	182	183	184
90%ee (50% yield) 85%ee (48% yield)	89:11 (45% yield) 95:5 (35% yield)	92%ee (28% yield) 88%ee (35% yield)	94%ee (40% yield) 92%ee (48% yield)	88%ee (18% yield) 92%ee (17% yield)

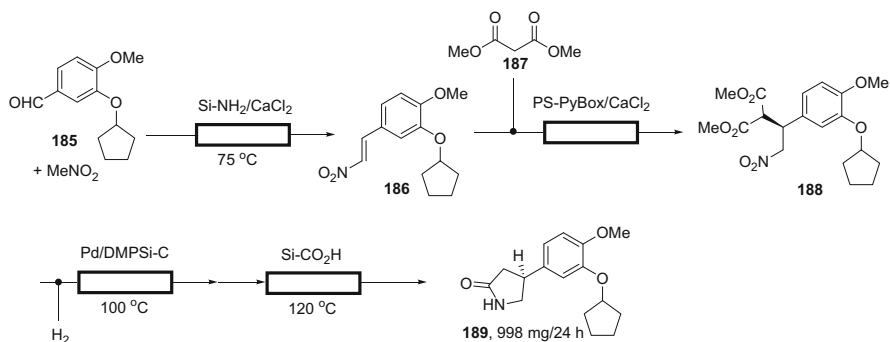
Scheme 38 Kinetic resolution of *N*-heterocyclic structure

mixture of differentiated amide products **180–184** which can be separated and the amide bond cleaved.

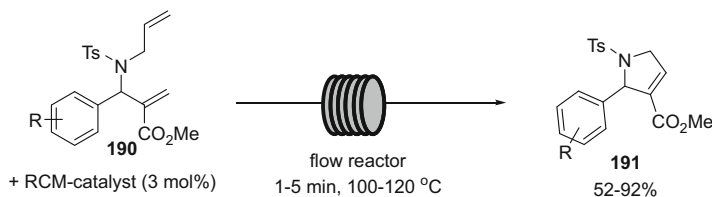
The added value that can be gained when combining multistep flow synthesis with effective catalytic transformations has recently been demonstrated by a continuous-flow synthesis of the anti-inflammatory drug (*S*)-rolipram **189** [92].

To prepare this target compound, a sequence was devised starting with a Henry reaction between aldehyde **185** and nitromethane catalysed by calcium chloride on a silica-supported amine construct. The resulting nitro olefin solution was then mixed with dimethyl malonate **187**, passed through a small column containing molecular sieves to remove traces of water before being directed into two successive cartridges containing CaCl_2 -(*S*)-PyBox as a chiral catalyst to promote an asymmetric Michael addition. The resulting product was collected and combined with hydrogen gas to pass through a column containing a polysilane-supported Pd-catalyst to affect the reduction of the nitro group. The resultant amine directly cyclises onto the adjacent ester group to furnish (*S*)-rolipram **189** after hydrolysis and decarboxylation of the superfluous ester moiety (Scheme 39). After preparative thin-layer chromatography and crystallisation, (*S*)-rolipram **189** was isolated optically pure in 50% yield with a reported throughput of 998 mg per 24 h.

In addition to several organocatalytic transformations, related metal-catalysed processes have been reported in continuous-flow mode. For instance, a recent study details the development of an efficient flow approach utilising ruthenium-catalysed ring-closing metathesis (RCM) to furnish a selection of valuable 2,5-dihydro-1*H*-pyrrole-3-carboxylates **191** [93]. To affect this important transformation, a stream of a suitably functionalised substrate **190** and the homogeneous metathesis catalyst (3 mol%) were directed into a flow reactor maintained at elevated temperature (Scheme 40).



Scheme 39 Continuous-flow synthesis of (*S*)-rolipram **189** employing multiple catalytic transformations



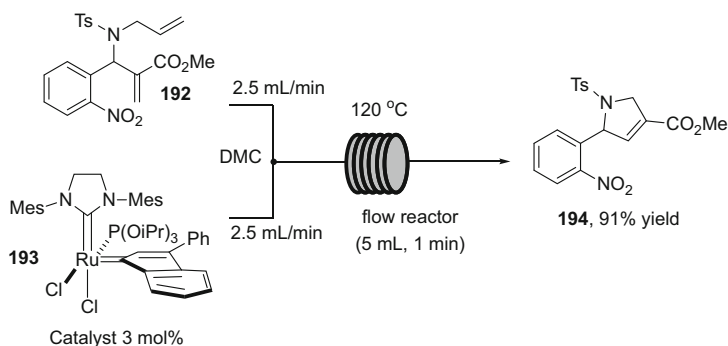
Scheme 40 Ring closing metathesis towards 2,5-dihydro-1*H*-pyrrole-3-carboxylates **191** in flow mode

Having demonstrated the reaction at small scale on a range of substrates (seven examples; 52–92% yield), a scale-up process was then conducted. The reaction was performed in the green solvent dimethyl carbonate (DMC), using a residence time of only 1 min at 120 °C enabling the processing of 10 g of diene starting material in 37 min; this yielded the desired product in 91% after filtration through silica (Scheme 41).

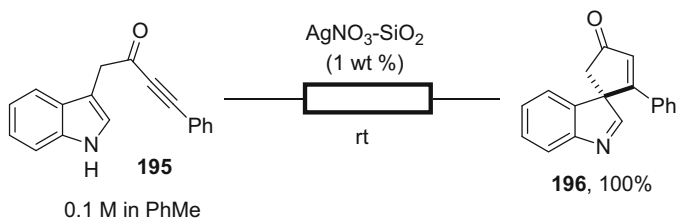
Other reports detailing the efficient synthesis of heterocyclic entities through ring closing metathesis reactions via microwave-assisted capillary synthesis [94] as well as silica-supported catalyst constructs [95] have also been disclosed.

In an interesting re-evaluation of an old reagent system, the application of a $\text{AgNO}_3\text{-SiO}_2$ heterogeneous catalyst for the dearomatising spirocyclisation reactions of a range of alkyne functionalised aromatics has been demonstrated [96]. Although the work was primarily performed in batch including a comprehensive mechanistic investigation, the authors explored a synthesis which yielded 23.6 g of a spirocycle **196** from 19.3 mg of the catalyst using a simple packed bed continuous-flow set-up (Scheme 42). The reaction was continuously processed for a period of 51 h being accessed by aliquot sampling and NMR analysis demonstrating the product was consistently being quantitatively formed.

As outlined in the introduction, pharmaceutical structures are rapidly moving away from the classical flat aromatic motifs of the past 30 years with the introduction



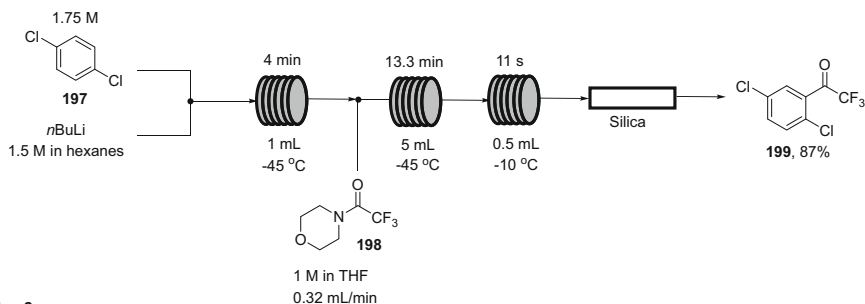
Scheme 41 Ring closing metathesis for the synthesis of 2,5-dihydro-1*H*-pyrroles in flow



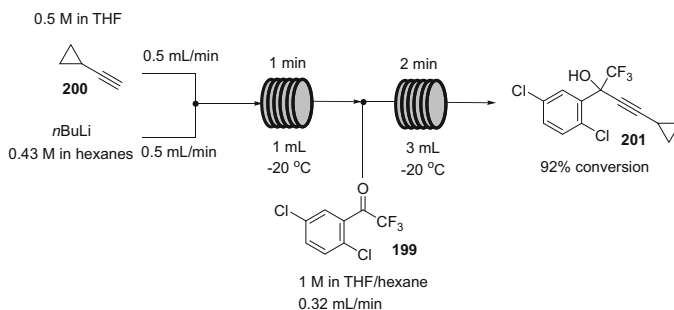
Scheme 42 Example dearomatising spirocyclisation reaction using a packed bed reactor

of more saturated heterocycles which possess prominent chiral display elements; a notable example which has recently been translated to a flow synthesis is efavirenz (**202**; Scheme 43) [97]. This semi-continuous three-step process provided *rac*-efavirenz **202** in a reasonable overall yield of 45% utilising a key copper-catalysed installation/cyclisation of the carbamate ring. In the first stage of the sequence, trifluoroacetylation \rightarrow **199** was achieved using a modified trifluoroacetylmorpholine reagent **198** to acylate a rapidly formed 2,5-dichlorophenyllithium species. Through the application of a short in-line silica cartridge, acidic workup and removal of the morpholine by-product and additional inorganic salts could be affected. A further organometallic addition of lithium cyclopropylacetylide prepared in situ furnished the propargylic alcohol **201** which in the final step was cyclised to the product **202**. A combination of a soluble amine chelated copper catalyst with a mixed bed of copper metal, Celite (as a dispersant) and sodium cyanate packed into a cartridge proved suitable for this transformation.

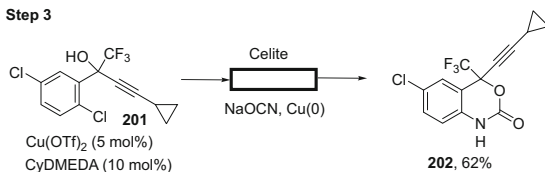
Step 1



Step 2



Step 3

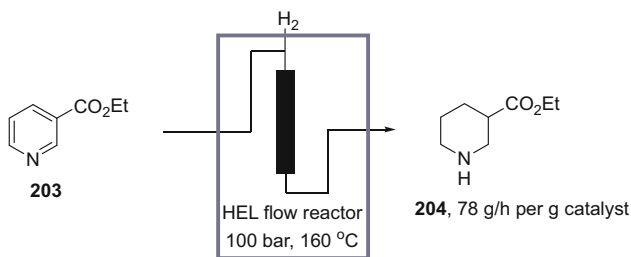


Scheme 43 Flow synthesis of *rac*-efavirenz **202**

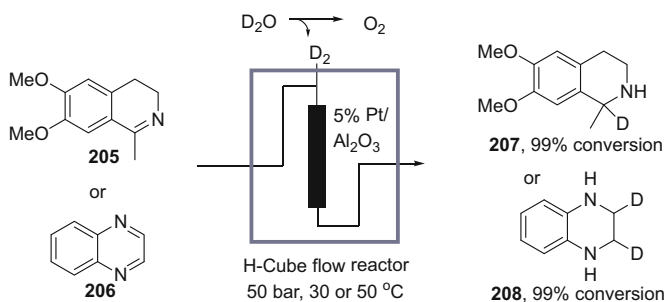
In addition to flow transformations based on homogeneous metal catalysts, a growing number of examples report the use of heterogeneous metal catalysts for the construction of saturated heterocycles. A recent publication describes a scalable approach in which ethyl nicotinate **203** was converted in a trickle bed reactor into its saturated piperidine counterpart **204** under hydrogenation conditions (Scheme 44) [98]. Using the HEL flow system, streams of the dissolved substrate and hydrogen gas were mixed and passed through a heated stainless steel column containing the heterogeneous catalyst (Pd or Rh on carbon or alumina). Upon optimisation of this process, the full hydrogenation of **203** was achieved with a throughput of 408 g/h of product per gramme of catalyst. This showcases the successful scale-up of the transformation.

An analogous small-scale approach towards various saturated heterocycles (e.g. **207**, **208**) was recently reported using the popular H-Cube system [99]. In this set-up hydrogen is produced in situ by electrolysis of water allowing the desired hydrogenation to occur in cartridges containing the heterogeneous catalyst (Scheme 45). In addition, this approach was applied to the successful deuteration of several heterocycles such as dihydroquinolines and dihydroisoquinolines as well as quinoline and quinoxaline.

A combined flow stream of phenethylamine **209** and levulinic acid (**210**, itself prepared under flow conditions from D-fructose) [100] has been processed under hydrogenation conditions employing the H-Cube Pro and a carbon-supported



Scheme 44 Scaled flow synthesis of piperidine **204** continuous-flow mode

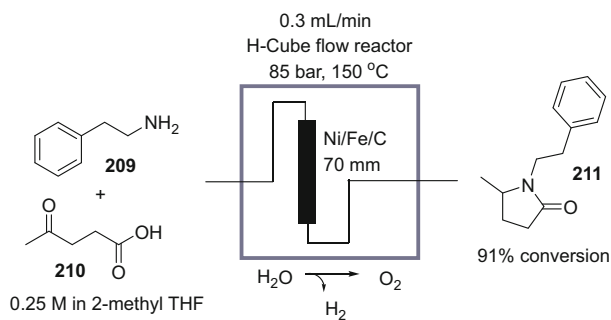


Scheme 45 Hydrogenation and deuteration in continuous-flow mode

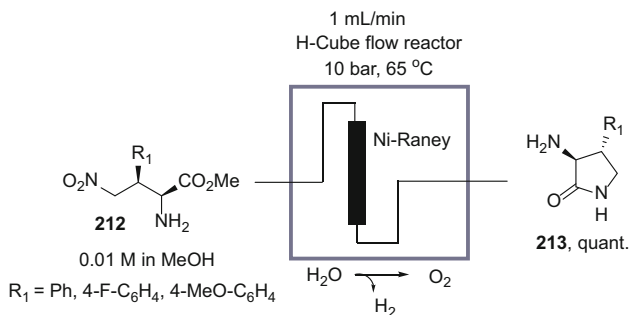
bimetallic Fe/Ni alloy (Scheme 46). This provided the corresponding pyrrolidinones **211** in high conversion via a stepwise reductive amination and cyclisation sequence [101]. This particular process represents a good example of an intensified process which was capable of delivering large amounts of material with only simple solvent removal giving high-quality isolated product.

Similarly a series of H-Cube-mediated reductions of γ -nitro- α -amino esters **212** have been utilised to prepare following cyclisation small subsets of libraries of lactams (**213**, Scheme 47) [102]. Interestingly the *syn* configured materials selectively gave the *trans* pyrrolidinones in high yields and diastereoselectivities, whereas the corresponding *anti* nitro materials furnished the *cis* cyclic derivatives.

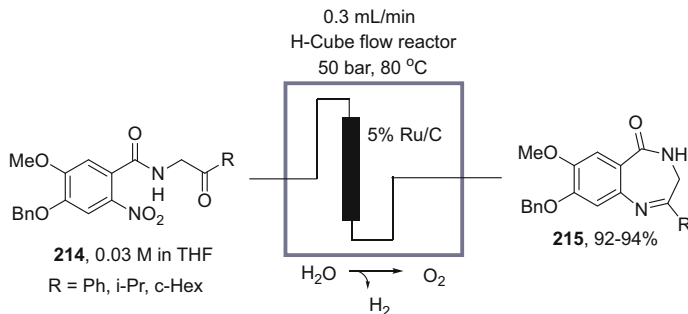
A readily scalable continuous-flow protocol for the synthesis of the privileged structure 3,4-dihydro-5H-benzo[e][1,4]diazepin-5-one **215** from easily prepared 2-nitro-benzamides **214** using a key reductive-cyclisation procedure has been developed (Scheme 48) [103]. Selectivity through exacting control over the reaction conditions in the catalytic hydrogenation step was required to avoid several overreduction products from debenzoylation, ketone (anilino alcohol formation) and imine reduction. The additional flexibility is presented by simple modification of the flow rate which was used to regulate catalyst contact times allowing better control of the process equating to an improved yield and purity of the products.



Scheme 46 Flow reductive amination



Scheme 47 Flow reductive amination of aliphatic nitro amino esters



Scheme 48 Flow reductive cyclisation to form 3,4-dihydro-5*H*-benzo[*e*][1,4]diazepin-5-ones **215**

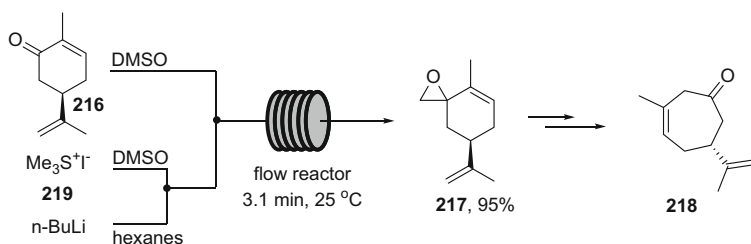
1.4 Miscellaneous Approaches for the Synthesis of Saturated Heterocycles

As demonstrated previously epoxides have evolved as popular heterocyclic scaffolds in continuous-flow mode. As such most reported approaches generate these three-membered rings by adding oxygen across an alkene. These include the aforementioned Minisci epoxidation reaction as well as the oxidative functionalisation of alkene by means of lipases and peracids [104], hydrogen peroxide and poly-L-leucine [105] or HOF·MeCN [106]. Given the industrial importance of simple epoxides such as ethylene and propylene oxide, continuous methods for their scaled synthesis have been reported [107, 108].

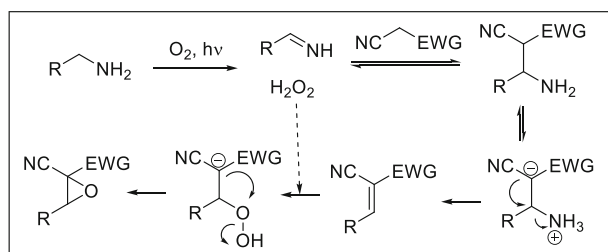
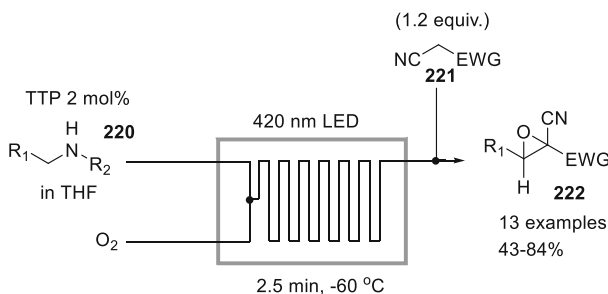
A complementary approach of adding a carbon atom across a carbonyl was recently utilised to elaborate (*R*)-(-)-carvone **216** into the corresponding epoxide derivative **217** that was later transformed into cycloheptenone **218** [109]. To accomplish this transformation, a Corey-Chaykovsky epoxidation reaction was developed in flow mode (Scheme 49). To this end, the Corey-Chaykovsky reagent **219** was dissolved in DMSO and combined with a stream of *n*-butyl dissolved in hexanes. The resulting anion was then added via a T-piece to a stream of substrate **216** prior to being directed into a residence time flow coil which was maintained at ambient temperature. After a short residence time of 3.1 min, the material was collected. In a run covering a period of 2 h, the epoxide **217** was obtained as a diastereomeric mixture in high purity and isolated yield (95%, 9.35 g).

Singlet oxygen has been used in an ingenious cascade leading to highly functionalised α -cyanoepoxides **222** products starting from 1° or 2° unactivated amines (**220**, Scheme 50) [110]. The singlet oxygen, produced in a continuous-flow photoreactor, serves as an oxidant with the hydrogen peroxide by-product acting as an epoxidation agent for an electron-deficient olefin intermediate, formed through a deaminative Mannich coupling with malononitrile or methyl cyanoacetate **221**.

Cyclic sulfonamides are an important class of bioactive compounds that can be conveniently accessed from acyclic precursors. Using a microwave approach, a



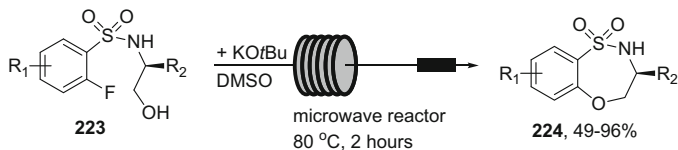
Scheme 49 Corey-Chaykovsky epoxidation of (*R*)-(-)-carvone **216** in flow mode



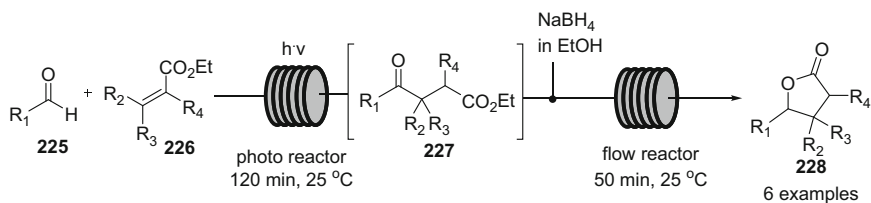
Scheme 50 Ring expansion of diazo intermediates

series of these entities were recently prepared through an intramolecular S_NAr reaction. To provide a readily scalable route, a microwave-assisted flow method was developed as depicted in Scheme 51 [111]. To this end, a stock solution of the substrates **223** and $KOtBu$ as base was prepared in DMSO and pumped through a modified microwave reactor in which the desired products **224** were formed within a residence time of 2 h at a temperature of 80°C.

To create γ -lactones that are commonly found in bioactive natural products, a continuous multistep flow sequence was developed (Scheme 52) [112]. This study combined a photochemical transformation between aldehydes **225** and α,β -unsaturated esters **226** with a $NaBH_4$ -mediated reduction of the resulting adduct **227** allowing the formation of the desired γ -lactone products **228** upon intramolecular cyclisation. To run this process in flow mode, the photocatalyst (tetrabutylammonium decatungstate, TBADT, 1%) is dissolved in a stock solution of **225** and **226** in MeCN and pumped through a coiled reactor (2 h residence time)



Scheme 51 Flow microwave approach to cyclic sulfonamides

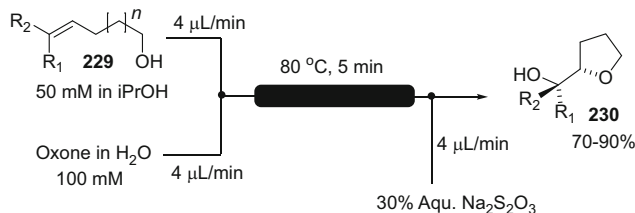


Scheme 52 Flow synthesis of γ -lactones **228** mediated by a photochemical coupling reaction

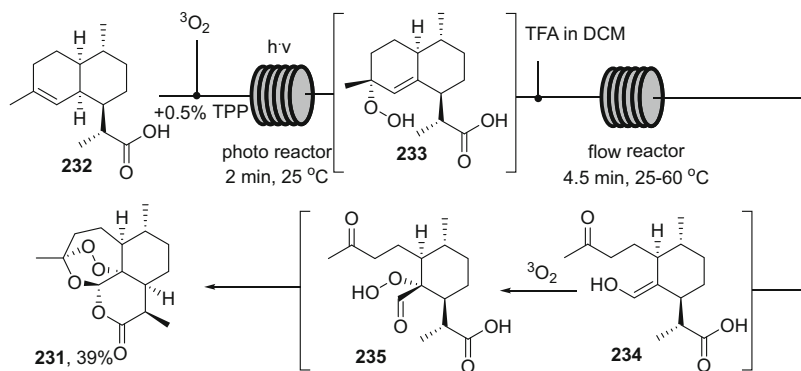
surrounding the light source (medium pressure Hg lamp, 125 W). Upon exiting this first reactor, a stream containing NaBH_4 dissolved in ethanol is mixed via T-piece prior to passing this mixture into a second coil reactor (50 min residence time) in which the reduction and cyclisation to the γ -lactone occur. After workup and purification, the desired products were isolated in good yields (51–68%) as mixtures of diastereomers.

More recently, an alternative flow approach to lactone-derived products was reported based on alkenoic acid substrates that were activated by a perselenic acid catalyst [113]. Through the efficient in-line scavenging of acidic materials (substrate and catalyst) with an immobilised tertiary amine base, this method represents a neat and eco-friendly entry to various lactones. In a related study, a series of alkenols were oxidatively cyclised using Oxone as a cheap and readily available oxidant (Scheme 53) [114]. A small selection of hydroxy-tetrahydrofuran **230** products was obtained after in-line quenching of residual oxidant with a solution of sodium thiosulfate to furnish the desired products in good to excellent yield.

A further example applying photochemical processing to the continuous-flow synthesis of an important target was recently demonstrated for the antimalaria drug artemisinin **231** (Scheme 54) [115, 116]. This multistage sequence involves first a photo-oxidation of dihydroartemisinic acid **232** in the presence of a photosensitiser such as tetraphenylporphyrin or 9,10-dicyanoanthracene. The successful flow set-up is based on combining oxygen gas with a solution of substrate **232** and the photosensitiser to result in a reaction mixture that is then pumped through the photoreactor where singlet oxygen is generated and reacts with the substrate to furnish the hydroperoxide intermediate **235**. The exiting stream is subsequently blended with TFA to affect the Hock cleavage and skeletal rearrangement to furnish artemisinin **231** in an isolated yield of 39% and an extrapolated throughput of up to 200 g/day.



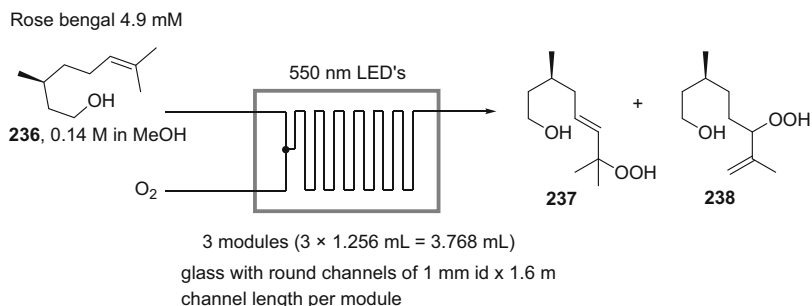
Scheme 53 Synthesis of tetrahydrofurans in flow



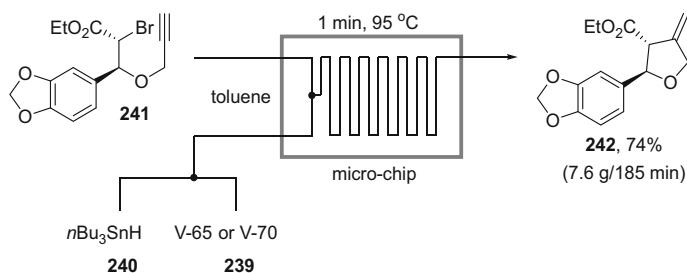
Scheme 54 Photochemical synthesis of artemisinin **231** in flow

More recently, a related gas-liquid membrane reactor system has been utilised for the generation of singlet oxygen that was then harnessed in a series of photo-oxidation reactions [117]. As an example a microstructured stacked glass reactor assembly for use under photochemical irradiation has been applied to the preparation of several products including ascaridole which was obtained in 90% conversion from α -terpinene (>85% purity as determined by GC) in a [4 + 2] cycloaddition with activated oxygen [118]. The same reactor set-up was also used in the initial oxidation step of citronellol ultimately leading to rose oxide; the photocatalysed reaction of citronellol **236** with singlet oxygen efficiently furnishes the corresponding hydroperoxides **237** and **238** (ratio undisclosed) via a Schenck ene reaction. Although not specifically performed in this investigation, the resulting peroxy species can be readily reduced to the corresponding alcohols and through subsequent cyclisation yield the desired rose oxide final product (Scheme 55) [119].

A further class of reactions that have so far been scarcely exploited in flow but are highly amenable are radical reactions. Recently, however a neat and scalable route to tetrahydrofuran systems that are precursors to furofuran lignans has been devised using a microreactor system [120]. To this end a premixed stream of tributyltin hydride and a radical initiator (**239**; V-70 or V-65) was blended with a stream of the desired substrate **241**. The combined reaction mixture was then passed through a heated microreactor (95°C) in which the cyclisation took place within a short



Scheme 55 Stacked photochemical reactor

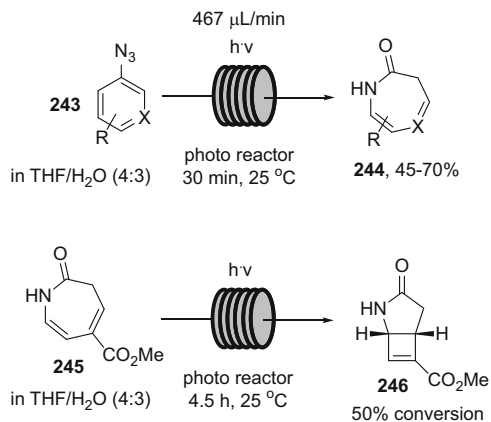


Scheme 56 Microreactor flow synthesis of furofuran precursor **242**

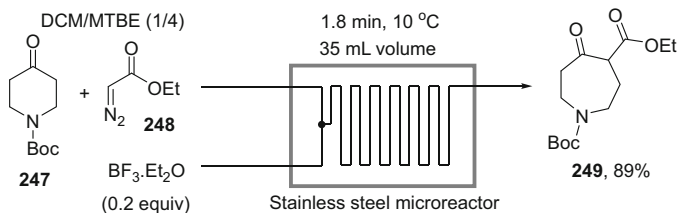
residence time of 1 min (Scheme 56). Due to these favourable parameters, multigramme quantities of the target compound **242** were accessible in a short period of time.

A flow photolysis sequence starting from aryl azides **243** which under irradiation generate reactive nitrenes that readily undergo rearrangement to didehydroazepines and can be trapped by water (or potentially other nucleophiles) to form a series of 3*H*-azepinones **244** has been reported (Scheme 57) [121]. To carry out the reaction, a simple FEP tubing photoreactor (14 mL) was constructed around a 450 W medium pressure Hg lamp. The reaction temperature was regulated by a recirculating cryostat cooling jacket and the light source fitted with a Pyrex filter to remove the IR band. Additionally a back pressure regulator (6.9 bar) was positioned at the exit of the reactor to maintain the solubility of the evolved nitrogen. Due to the inherently short irradiation times compared to batch, it was possible to minimise secondary photochemical reactions. This was exemplified by demonstrating that by increasing the residence time, the fused lactam **246** was obtained from the 3*H*-azepinones **245** via a further photochemical disrotatory electrocycloisatation (Scheme 57).

The generation and in situ utilisation of reactive intermediates in a controlled and small volume reactor is one of the major benefits of integrated flow processing. This has been used to great effect to allow many previously ‘forbidden chemistries’ to be undertaken in a safe and consistent fashion. Safety concerns regarding the scaling of reactions diazo ring expansion of *N*-Boc-4-piperidone **247** were a primary driver for



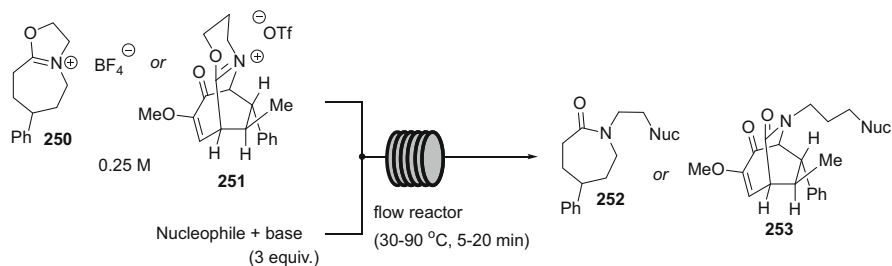
Scheme 57 Photochemical ring transformations in flow



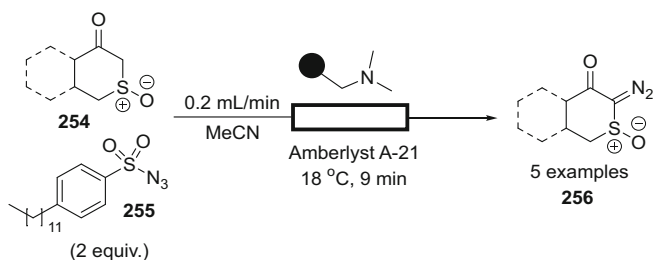
Scheme 58 Ring expansion of diazo intermediates

investigating flow by Zhang et al. [122] The highly exothermic addition of BF₃·OEt₂ to a mixture of ethyl diazoacetate **248** and the ketone **247** was of particular concern as in batch the reaction had a prolonged initiation period followed by very rapid reaction as the concentration of catalyst reached the 60 mol%, the reaction was also accompanied with the release of large volumes of gas. Such issues were mitigated working in CYTOS flow system allowing high throughputs of 91 g/h to be processed in a small footprint microreactor with a residence time of only 1.8 min (Scheme 58).

A microreactor system has been employed to investigate the reactivity patterns associated with iminium ethers as ambident electrophilic constructs for the synthesis of sets of highly functionalised heterocycles [123]. The ready availability of a wide range of structurally diverse iminium ethers and a wider selection of potential partner nucleophiles create an attractive substrate base for generating highly diverse libraries. In an attempt to expand the variety of chemotypes that can be accessed based upon controlling reaction conditions, an automated microreactor was used to perform a structured multidimensional reaction screen. Specifically using intermediate Iminium Ether salts **250**, **251** previously prepared via azido-Schmidt ring expansion, reactions of hydroxyalkyl azides were evaluated in their transformations to the bicyclo[3.2.1]octanoid and cyclohexanone derivatives **252**, **253** (Scheme 59).



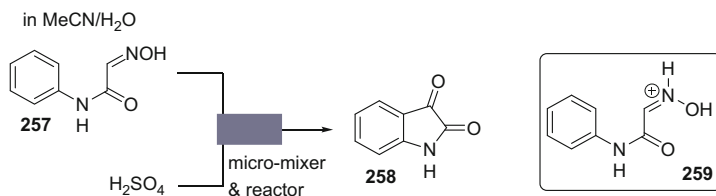
Scheme 59 Nucleophilic ring opening of diazo ether



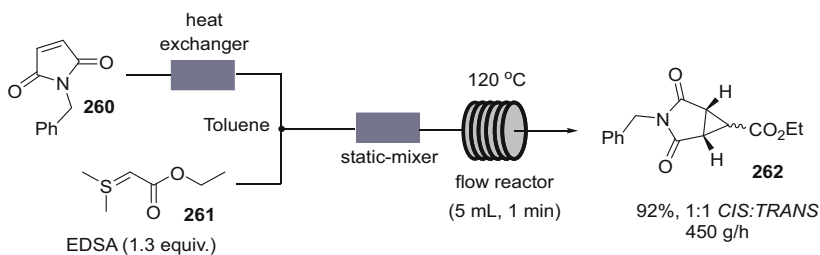
Scheme 60 Diazo transfer in flow

A further example of taming reactive intermediates through their application in flow is the use of the potentially explosive diazo transfer reagent dodecylbenzenesulfonyl azide **255** in the synthesis of lactone-derived α -diazosulfoxides **256** using the Regitz diazo transfer methodology (Scheme 60) [124]. The use of continuous flow leads to isolation of the desired compounds in an enhanced two- to threefold increased yield relative to standard batch conditions, with short reaction times and improved safety profile whilst also offering easy scale-up. Indeed, for some of the compounds processed, it was not possible to isolate the products via batch preparative condition due to the very low conversions and high rate of decomposition (hetero-Wolff rearrangement) experienced. The yield and purity improvements were indicated as being due to the short base contact times of both the reacting substrates and resultant products that were experienced in the flow reactor an aspect that was difficult to regulate in batch.

The ability to interrogate reactions by the direct introduction of analytical devices into the flow stream offers several benefits for rapid knowledge-driven optimisation and investigation of short-lived intermediates, thus generating a better mechanistic understanding. In demonstration of this approach, Santos and co-workers [125] coupled a mass spectrometer to the output of a capillary microreactor and thus were able to identify and characterise transient intermediates in the synthesis of isatins as encountered in the Sandmeyer reaction (Scheme 61). By reacting isonitrosoacetanilide **257** with sulphuric acid in a micro-T-mixer connected directly to the ESI-MS instruments source, the flow rate could be varied from 5 to 10 $\mu\text{L}/\text{min}$ giving access to very short residence times of 0.7–1.4 s providing a real-time



Scheme 61 Mass spectroscopy coupled flow investigation of reactive intermediates

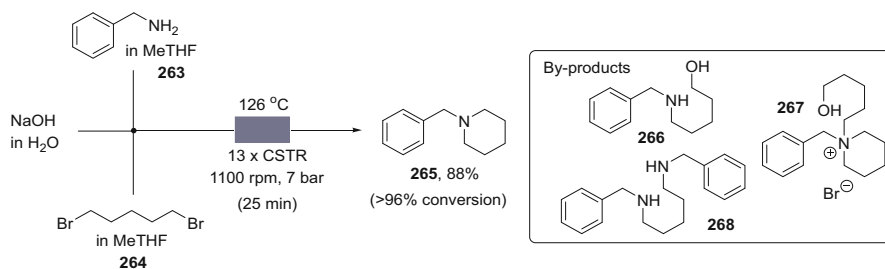


Scheme 62 Flow cyclopropanation of benzyl-protected maleimide

snapshot of the ion composition of the reaction. ESI mass (and tandem mass) spectrometric experiments enabled the authors to identify that the reaction proceeded through a previously unidentified cationic species **259**. Although not used in a preparative generation of the isatin structures **258**, this proof of concept study exemplifies how greater understanding and fast data analysis could assist elucidation of mechanisms and improve reaction optimisation.

A multi-kilogramme continuous-flow cyclopropanation of *N*-benzylmaleimide **260** using the ylide of ethyl(dimethylsulfuranylidene) acetate (**261**, EDSA) has been devised by chemists at Boehringer Ingelheim Pharmaceuticals [126]. During initial investigations of the original procedure [127], it was discovered that the yield was highly dependent on the rapid combination of the reagents which needed to be added at an elevated temperature. In batch at kilogramme scale, such addition would have been problematic due to difficulties maintaining precise temperature control and issues of imperfect mixing. It was therefore considered that the development of a robust large-scale batch procedure would present significant technical challenges, and so a flow option was considered. The final flow process was run continuously for 7 h with a throughput of 450 g product/h (at a concentration of 50 g/L) which gave a total of 3.3 kg in 92% yield (Scheme 62). Of particular note was the use of preheating of the input solutions prior to mixing leading to very short reaction times of 2 min.

Biphasic reactions in flow are becoming much more prevalent in the scientific literature especially as a means of recycling catalysts or applying differential control over reacting species. Novartis scientists have recently explored a bespoke flow approach for conducting scaled biphasic liquid/liquid reactions under superheated conditions with the aim of expanding their available processing regimes (temperature/pressure) [128]. As a model reaction, the double alkylation of benzylamine **263**

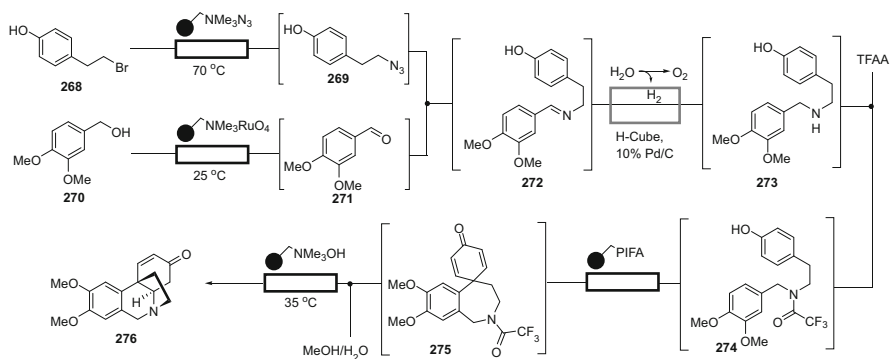


Scheme 63 Biphasic reaction process

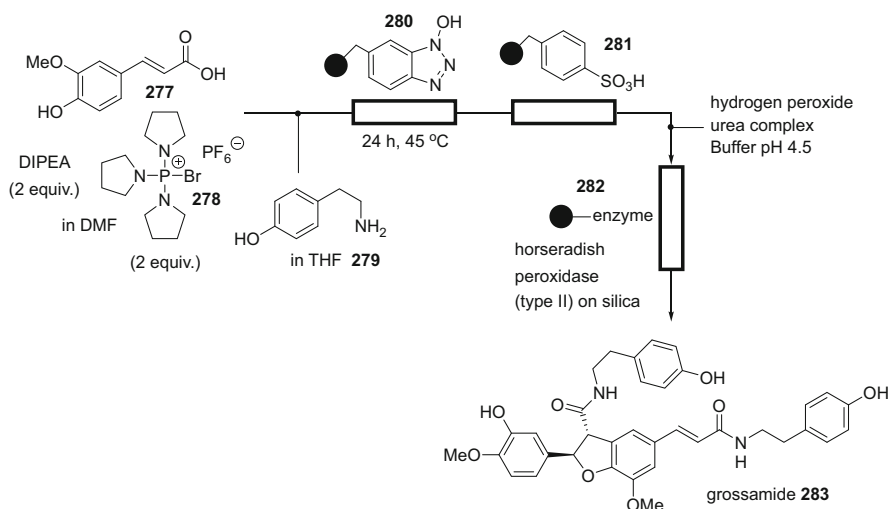
with 1,5-dibromopentane **264** was chosen as a problematic transformation (by-product formation **266–268**, Scheme 63) which following careful kinetic profiling and characterisation of the biphasic fluid dynamics enabled optimisation of the reaction (from initial 17 to 88%). The flow system comprised a set of vertically stacked continuous stirred-tank elements (13 stages) integrated to provide an unified flow tube assembly (double jacketed for thermal regulation). A principal advantage of this set-up was that the CSTR nature of the unit decouples mixing and flow rate which is normally not easily achieved in a standard plug flow reactor. However, independent control of the two immiscible flow streams entering the reactor still allows modification of stoichiometry and residence time, both of which were important variables determining the ultimate success of the reaction. Biphasic processing scenarios especially those involving liquid/liquid biphasic systems will certainly become an increasingly important aspect of future flow processes.

1.5 Target-Driven Synthesis of Saturated Heterocycles

Since its inception almost 20 years ago, flow chemistry has also been applied to the synthesis of complex target molecules such as natural products. One of the first and leading examples is the alkaloid natural product oxomaritidine **276** (Scheme 64) [129]. A fully telescoped continuous process comprising of seven distinct chemical transformations was developed to produce this compact target molecule including several immobilised reagents and scavengers. The sequence starts with converting bromide **268** via an immobilised azide species into intermediate **269**, which was combined with aldehyde **271**, prepared by in situ oxidation of alcohol **270**, in an aza-Wittig reaction to yield imine **272** (Scheme 33). Flow hydrogenation of **272** generated the amine **273** which was further protected via trifluoroacetylation to give intermediate **274**. Using an immobilised version of the PIFA reagent, substrate **274** underwent an oxidative dearomatisation to benzoazepin **275** which upon deprotection furnishes the tetracyclic scaffold of oxomaritidine. Importantly, this flow sequence not only allowed the target compound to be produced without need for intermediate purification stages but additionally shortened the synthesis from



Scheme 64 Continuous-flow synthesis of oxomaritidine **276**



Scheme 65 Synthesis of the natural product grossamide **283**

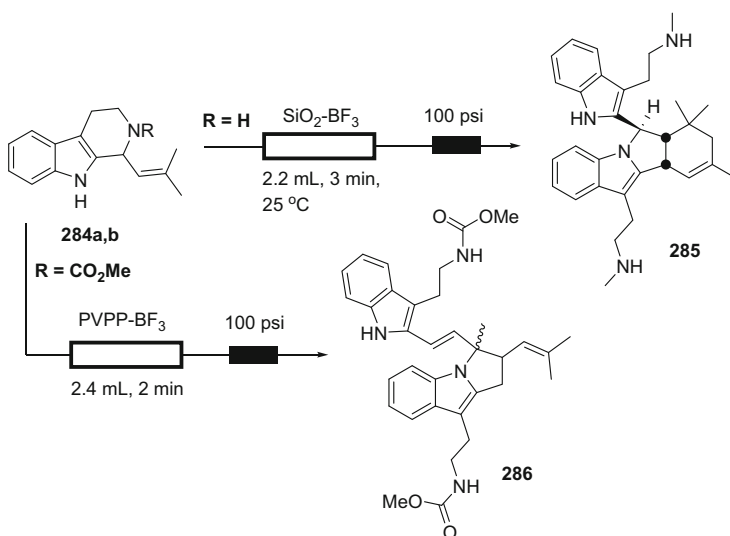
several days to about 4 h. The isolated yield for **276** was found to be ~40% indicating that apart from the less selective phenolic coupling step all other steps occurred in very high yield.

An enantioselective total synthesis of the neolignan natural product grossamide **283** using an enzyme-mediated dimerisation of a simple *N*-feruloyltyramine building block in a fully automated reactor was an early example of the potential power of flow for target synthesis [130]. The integrated process was performed using a sequence of column reactors containing immobilised reagents to effect the amide coupling of tyramine **279** and ferulic acid **277** followed by oxidative dimerisation and intramolecular cyclisation (Scheme 65). To facilitate the optimisation and allow rapid exchange of the column reactors upon depletion, a UV-Vis and MS detector

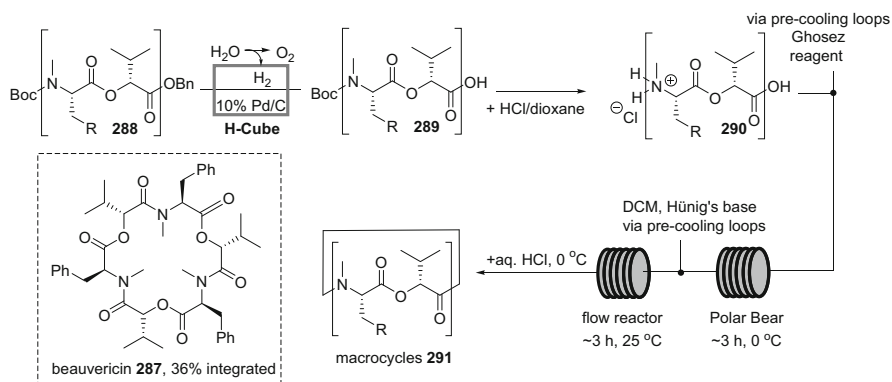
were employed in-line which signalled a series of values to select new reactors from a bank of replacements. In this way uninterrupted processing of the starting materials could be achieved and minor fluctuations in the reactor composition corrected by regulations of the various pumps (flow rates).

Another recent application detailing the use of flow techniques in the rapid assembly of complex natural products containing saturated heterocycles is given in the biomimetic synthesis of isoborreverine **285** and related **286**, precursor to the alkaloid flinderole from common borreverines **284a-b**. These syntheses were accomplished in flow mode by passing solutions of substrates **284a-b** through cartridges containing immobilised Lewis acids, especially those based on supported versions of BF_3 [131]. As such it was possible to convert the carbamate protected borreverine **284a** into **286** using PVPP- BF_3 as the immobilised Lewis acid, whilst isoborreverine **285** was readily prepared by dimerising borreverine **284b** using a more reactive silica-supported BF_3 species (Scheme 66).

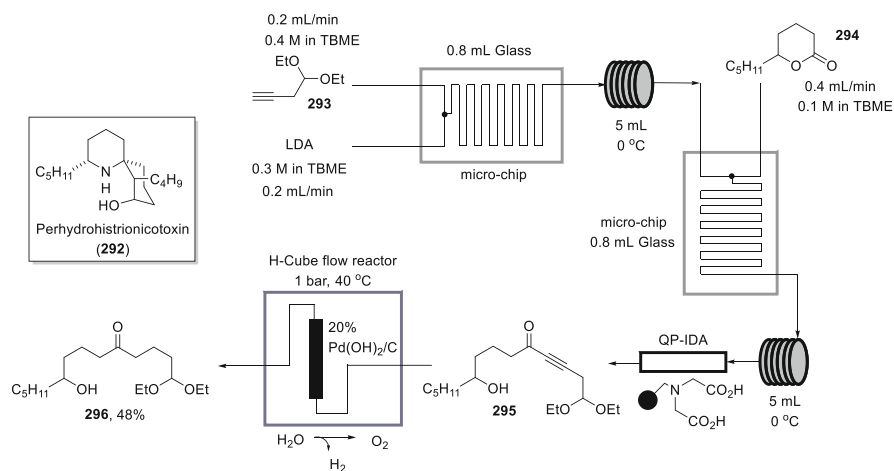
Flow chemistry techniques have been additionally applied successfully to the synthesis of several cyclo-oligomeric depsipeptides such as the natural products beauvericin **287** and related structures [132]. The assembly of these heterocyclic structures in flow mode was accomplished by initially employing the H-Cube system for debenzoylation of the C-terminus of the desired building blocks **288**, whereas the *N*-Boc groups of the products **289** were removed in a batch mode fashion using HCl in dioxane in a subsequent step (Scheme 67). A Polar Bear Plus system (operated at 0°C) was used in the activation of the resulting amino acid building blocks **290** with Ghosez reagent (2 equiv.) allowing after in-line treatment with Hünig's base the key macrocyclisation reaction to take place in a subsequent flow coil (at rt). The success of this flow approach compared to batch methods manifests itself in higher isolated



Scheme 66 Biomimetic synthesis of borreverine-derived alkaloids **285** and **286** in flow mode



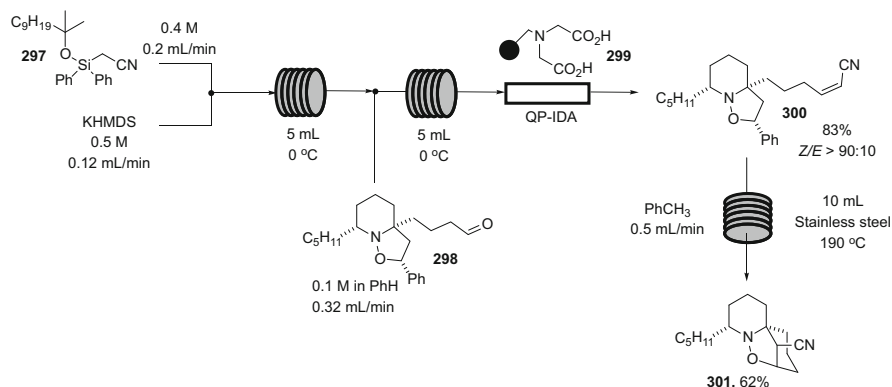
Scheme 67 Flow synthesis for peptide coupling and macrocyclisation reactions



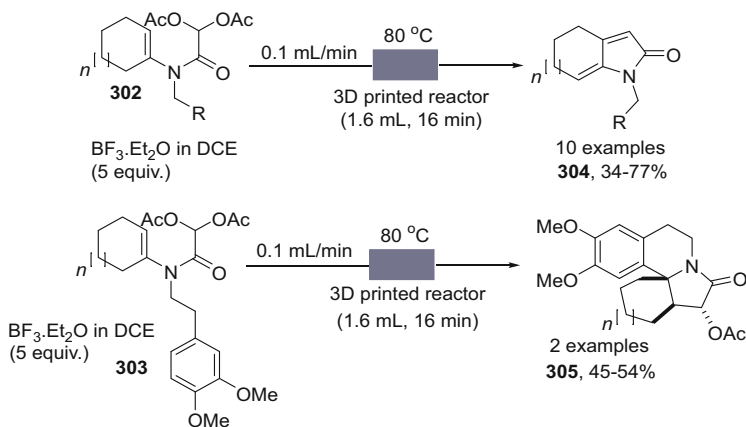
Scheme 68 Flow-assisted synthesis of key intermediates in the preparation of perhydrohistrionicotoxin **292**

yields as well as improved atom economy with respect to the ratio of coupling partners (1:1) indicating that such flow syntheses can be expected to find further applications for other solution phase peptide coupling reactions.

Flow approaches have also been employed in order to facilitate the total synthesis of the spiro-piperidine alkaloid perhydrohistrionicotoxin **292** through a combination of conventional batch techniques and microreactor technology [133]. Extended operation of the flow reactors permitted the synthesis of larger quantities of intermediate allowing easier screening of key transformations in batch (Scheme 68). In addition a final cascade to the core structure involving a Peterson olefination and high-temperature 1,3-dipolar cycloreversion-cycloaddition via an intermediate isoxazolidine **298** was also shown to be more amenable to flow processing conditions (Scheme 69).

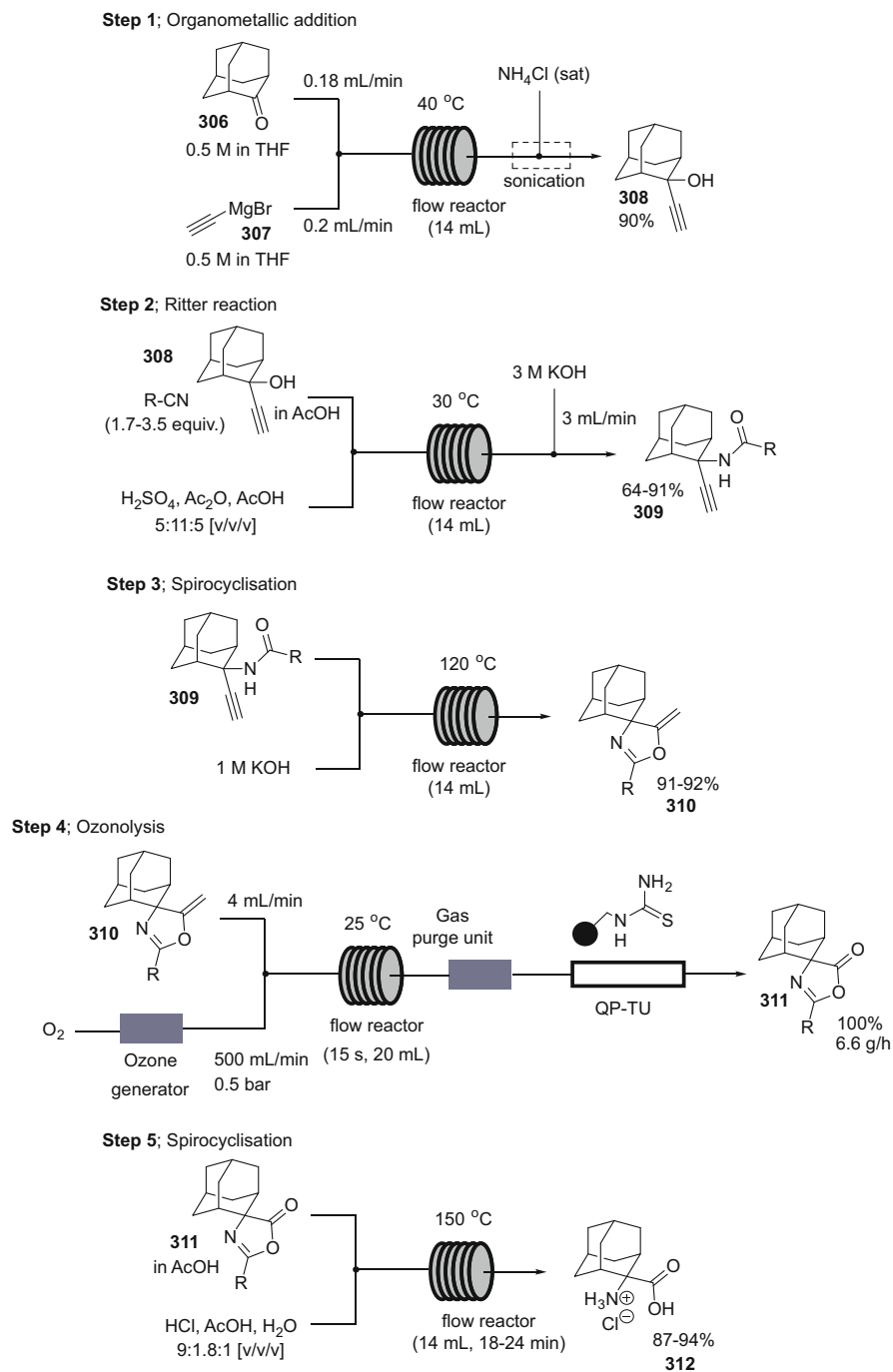


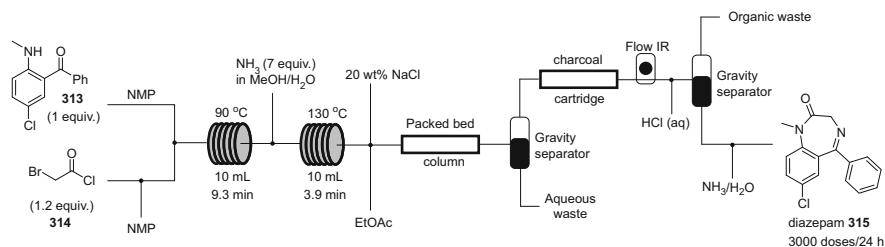
Scheme 69 Flow Peterson olefination and thermal 1,3-dipolar cycloreversion-cycloaddition used in the synthesis of perhydrohistrionicotoxin **292**



Scheme 70 The use of 3D printed column reactor for flow chemistry applications

The use of 3D printing in flow chemistry for fast prototyping of reactors with low development cost is becoming a popular tool especially as the refinement in printing technologies allows greater accuracy often in the 10–50 μm range. Recently a micro-printed polypropylene (PP) column reactor comprising an internal spiral configuration (2 mm id, Volume 1.6 mL) has been used to synthesise a range of heterocyclic compounds including the core structure of the natural product (\pm)- γ -lycorane (Scheme 70) [134]. The reactor was demonstrated to possess reasonable temperature and solvent compatibility in a range of chemistries, but prolonged usage (>5 uses) led to degradation and leakage of material at the connectors. It is apparent that this format of reactor design is rapidly evolving and aspects such as connections/joints will in the future be generated with increased robustness, thereby dramatically increasing the value of such technologies to the labs of the future.





Scheme 72 Preparation of multi-APIs using a single-flow processing device

For the synthesis of a family of neurotensin receptor probes, the amino acid fragment 2-aminoadamantane-2-carboxylic acid **313** was required at scale. As a previous microwave flow route via a Bucherer-Bergs reaction had provided inferior quality material, an alternative strategy was sought [135]. A five-step flow sequence was devised involving first addition of an acetylenic Grignard reagent to 2-adamantanone (**306**, Step 1; Scheme 71) followed by conversion of the propargylic alcohol **308** to the acyl-propargylamide derivative **309** via a Ritter reaction (Step 2; Scheme 71). A subsequent 5-enol-exo-dig cyclisation produces an oxazole derivative (**310**, Step 3; Scheme 71) which under flow ozonolysis conditions provided the azlactone (**311**, Step 4; Scheme 71). Finally, acid-catalysed hydrolysis (Step 5; Scheme 71) yielded the desired amino acid product **312** in 76% overall yield (R = Me; 70% for R = Ph).

To demonstrate a different future drug delivery scenario, a compact mini-plant synthesiser employing flow reactor technology for the continuous manufacturing of pharmaceuticals has been constructed [136]. A series of four drug substances (diphenhydramine hydrochloride, lidocaine hydrochloride, diazepam (**315**; Scheme 72) and (\pm)-fluoxetine hydrochloride) were sequentially prepared from advanced intermediates using the same unit and further progressed through formulation and tableting to prepare a representative >850 doses/24 h as an example of on-demand production. The system was designed to run under full software control and be quickly reconfigured to enable rapid delivery of directly administrable treatments responding to changes in patient demand. As a proof of concept, this certainly establishes how *at location* drug preparation services may evolve in the future aligning with the concepts of personalised medicines in terms of permitting tailored delivery of on-demand formulations.

2 Summary and Conclusions

As demonstrated in this review, flow chemistry has been applied to the synthesis of numerous saturated heterocycles with remarkable success. Although many examples concern the synthesis of five- and six-membered ring systems, flow synthesis has also found its place in the synthesis of small, medium and even macrocyclic ring systems. Despite such a variety of heterocyclic scaffolds being created, it is apparent

that classical methods, such as cycloaddition and cyclocondensation reactions, dominate in their assembly. Noticeably, many such approaches rely on using known transformations and reagents; however, at the same time, several innovative approaches demonstrate new targets and methods for their efficient assembly in flow mode. For instance, a general trend towards incorporating more catalytic processes for the synthesis of single enantiomer scaffolds is becoming more prevalent, especially in the development and exploitation of immobilised organocatalysts. In addition, the continuous synthesis of many new chemical architectures is increasingly making use of more in-line analysis and in-line purification techniques, which are vital for providing high-purity samples for biological testing in a more automated fashion. It is therefore increasingly likely that future endeavours in this field will aim to link the synthesis of target structures with the evaluation of key biological properties, which is well aligned with the concept of continuous processing, and will thus accelerate the discovery process for new bioactive entities in the years to come.

Acknowledgements We gratefully acknowledge support from the Royal Society (MB and IRB).

References

1. Fanelli F, Parisi G, Degennaro L, Luisi R (2017) *Beilstein J Org Chem* 13:520–542. <https://doi.org/10.3762/bjoc.13.51>
2. Ley SV, Fitzpatrick DE, Myers RM, Battilocchio C, Ingham RJ (2015) *Angew Chem Int Ed* 54:10122–10137. <https://doi.org/10.1002/anie.201501618>
3. Fitzpatrick DE, Battilocchio C, Ley SV (2016) *ACS Cent Sci* 2:131–138. <https://doi.org/10.1021/acscentsci.6b00015>
4. Newman SG, Jensen KV (2013) *Green Chem* 15:1456–1472. <https://doi.org/10.1039/C3GC40374B>
5. Baxendale IR, Brocken L, Mallia CJ (2013) *Green Process Synth* 2:211–230. <https://doi.org/10.1515/gps-2013-0029>
6. Baxendale IR (2013) *J Chem Technol Biotechnol* 88:519–552. <https://doi.org/10.1002/jctb.4012>
7. Ley SV (2012) *Chem Rec* 2:378–390. <https://doi.org/10.1002/tcr.201100041>
8. Wegner J, Ceylan S, Kirschning A (2011) *Chem Commun* 47:4583–4592. <https://doi.org/10.1039/C0CC05060A>
9. Hartman RL, Jensen KV (2009) *Lab Chip* 9:2495–2507. <https://doi.org/10.1039/B906343A>
10. Hessel V (2009) *Chem Eng Technol* 32:1655–1681. <https://doi.org/10.1002/ceat.200900474>
11. Razaq T, Glasnov TN, Kappe CO (2009) *Chem Eng Technol* 32:1702–1716. <https://doi.org/10.1002/ceat.200900272>
12. Razaq T, Kappe CO (2010) *Chem Asian J* 5:1274–1289. <https://doi.org/10.1002/asia.201000010>
13. Ceylan S, Coutable L, Wegner J, Kirschning A (2011) *Chem Eur J* 17:1884–1893. <https://doi.org/10.1002/chem.201002291>
14. Hessel V, Kralisch D, Kockmann N (eds) (2015) *Novel process windows: innovative gates to intensified and sustainable chemical processes*. Weinheim, Wiley-VCH
15. Webb D, Jamison TF (2010) *Chem Sci* 1:675–680. <https://doi.org/10.1039/C0SC00381F>

16. Wegner J, Ceylan S, Kirschning A (2012) *Adv Synth Catal* 354:17–57. <https://doi.org/10.1002/adsc.201100584>
17. Britton J, Raston CL (2017) *Chem Soc Rev* 46:1250–1271. <https://doi.org/10.1039/C6CS00830E>
18. Anderson NG (2001) *Org Process Res Dev* 5:613–621. <https://doi.org/10.1021/op0100605>
19. Movsisyan M, Delbeke EIP, Berton JKET, Battilocchio C, Ley SV, Stevens CV (2016) *Chem Soc Rev* 45:4892–4928. <https://doi.org/10.1039/C5CS00902B>
20. Baumann M, Baxendale IR (2015) *Beilstein J Org Chem* 11:1194–1219. <https://doi.org/10.3762/bjoc.11.134>
21. Gutmann B, Cantillo D, Kappe CO (2015) *Angew Chem Int Ed* 54:6688–6798. <https://doi.org/10.1002/anie.201409318>
22. Porta R, Benaglia M, Puglisi A (2016) *Org Process Res Dev* 20:2–25. <https://doi.org/10.1021/acs.oprd.5b00325>
23. Baumann M, Baxendale IR, Ley SV (2011) *Mol Divers* 15:613–630. <https://doi.org/10.1007/s11030-010-9282-1>
24. Glasnov TN, Kappe CO (2011) *J Heterocycl Chem* 48:11–29. <https://doi.org/10.1002/jhet.568>
25. Movsisyan M, Moens M, Stevens C (2016) In: Scriven EFV, Ramsden CA (eds) *Advances in heterocyclic chemistry: flow synthesis of heterocycles*, vol 119. Elsevier, Amsterdam, pp 22–57
26. Lovering F, Bikker J, Humblet C (2009) *J Med Chem* 52:6752–6756. <https://doi.org/10.1021/jm901241e>
27. Lovering F (2013) *Med Chem Commun* 4:515–519. <https://doi.org/10.1039/C2MD20347B>
28. Birudukota NVS, Franke R, Hofer B (2016) *Org Biomol Chem* 14:3821–3837. <https://doi.org/10.1039/C5OB02539G>
29. Karawajczyk A, Giordanetto F, Benningshof J, Hamza D, Kalliokoski T, Pouwer K, Morgentín R, Nelson A, Müller G, Piechot A, Tzalis D (2015) *Drug Discov Today* 20:1310–1316. <https://doi.org/10.1016/j.drudis.2015.09.009>
30. Musio B, Mariani F, Sliwinski EP, Kabeshov MA, Odajima H, Ley SV (2016) *Synthesis* 48:3515–3526. <https://doi.org/10.1055/s-0035-1562579>
31. Mastronardi F, Gutmann B, Kappe CO (2013) *Org Lett* 15:5590–5593. <https://doi.org/10.1021/ol4027914>
32. Brzozowski M, O'Brien M, Ley SV, Polyzos A (2015) *Acc Chem Res* 48:346–362. <https://doi.org/10.1021/ar500359m>
33. Mallia CJ, Baxendale IR (2016) *Org Process Res Dev* 20:327–360. <https://doi.org/10.1021/acs.oprd.5b00222>
34. Britton J, Jamison TF (2017) *Angew Chem Int Ed* 56:8823–8827. <https://doi.org/10.1002/anie.201704529>
35. Cludius-Brandt S, Kupracz L, Kirschning A (2013) *Beilstein J Org Chem* 9:1745–1750. <https://doi.org/10.3762/bjoc.9.201>
36. Grafton M, Mansfield AC, Fray MJ (2010) *Tetrahedron Lett* 51:1026–1029. <https://doi.org/10.1016/j.tetlet.2009.12.071>
37. Baumann M, Baxendale IR, Ley SV (2010) *Synlett* 5:749–752. <https://doi.org/10.1055/s-0029-1219344>
38. Baumann M, Baxendale IR, Kuratli C, Ley SV, Martin RE, Schneider J (2011) *ACS Comb Sci* 13:405–413. <https://doi.org/10.1021/co2000357>
39. Baumann M, Baxendale IR, Kirschning A, Ley SV, Wegner J (2011) *Heterocycles* 82:1297–1316. [https://doi.org/10.3987/COM-10-S\(E\)77](https://doi.org/10.3987/COM-10-S(E)77)
40. Yoshida J (2005) *Chem Commun* 41:4509–4516. <https://doi.org/10.1039/B508341A>
41. Suga S, Tsutsi Y, Nagaki A, Yoshida J (2005) *Bull Chem Soc Jpn* 78:1206–1217. <https://doi.org/10.1246/bcsj.78.1206>
42. Lau S-H, Galvan A, Merchant RR, Battilocchio C, Souto JA, Berry MB, Ley SV (2015) *Org Lett* 17:3218–3221. <https://doi.org/10.1021/acs.orglett.5b01307>
43. Griesbaum K, Liu X, Kassiaris A, Scherer M (1997) *Liebigs Ann Recueil* 1381–1390

44. Bogdan AR, James K (2011) *Org Lett* 13:4060–4063. <https://doi.org/10.1021/ol201567s>
45. Fernandez-Suarez M, Wong SYF, Warrington BH (2002) *Lab Chip* 2:170–174. <https://doi.org/10.1039/B202324E>
46. Yoshida J (2010) *Chem Rec* 10:332
47. Yoshida J, Takahashi Y, Nagaki A (2013) *Chem Commun* 49:9896–9904. <https://doi.org/10.1039/C3CC44709J>
48. Tsoung J, Wang Y, Djuric SW (2017) *React Chem Eng* 2:458–461. <https://doi.org/10.1039/C7RE00058H>
49. Martin RE, Morawitz F, Kuratli C, Alker AM, Alanine AI (2012) *Eur J Org Chem* 47–52. <https://doi.org/10.1002/ejoc.201101538>
50. Snyder DA, Noti C, Seeberger PH, Schael F, Bieber T, Ehrfeld W (2005) *Helv Chim Acta* 88:1–9. <https://doi.org/10.1002/hlca.200490304>
51. Wiles C, Watts P (2011) *Micro reaction technology in organic synthesis*. CRC Press, Boca Raton
52. Hallmark B, Mackley MR, Gadala-Maria F (2005) *Adv Eng Mater* 7:545–547. <https://doi.org/10.1002/adem.200400154>
53. Hornung CH, Mackley MR, Baxendale IR, Ley SV (2007) *Org Process Res Dev* 11:399–405. <https://doi.org/10.1021/op700015f>
54. McMullen JP, Jensen KF (2011) *Org Process Res Dev* 15:398–407. <https://doi.org/10.1021/op100300p>
55. Baxendale IR (2015) *Chem Eng Technol* 38:1713–1716. <https://doi.org/10.1002/ceat.201500255>
56. Baxendale IR, Hornung C, Ley SV, Molina JMM, Wikström A (2013) *Aust J Chem* 66:131–144. <https://doi.org/10.1071/CH12365>
57. Kappe CO, Dallinger D, Murphree SS (2009) *Practical microwave synthesis for organic chemists; strategies, instruments and protocols*. Wiley-VCH Verlag GmbH, Weinheim. ISBN: 978-3-527-32097-4
58. Baxendale IR, Hayward JJ, Ley SV (2007) *Comb Chem High Throughput Screen* 10:802–836. <https://doi.org/10.2174/138620707783220374>
59. Baxendale IR, Pitts MR (2006) *Chimica Oggi Chem Today* 24:41–45
60. Saaby S, Baxendale IR, Ley SV (2005) *Org Biomol Chem* 3:3365–3368. <https://doi.org/10.1039/b509540a>
61. Bogaert-Alvarez RJ, Demena P, Kodersha G, Polomski RE, Soundararajan N, Wang SSY (2001) *Org Process Res Dev* 5:636–645. <https://doi.org/10.1021/op0100504>
62. Hook BDA, Dohle W, Hirst PR, Pickworth M, Berry MB, Booker-Milburn KI (2005) *J Org Chem* 70:7558–7564. <https://doi.org/10.1021/jo050705p>
63. Lainchbury MD, Medley MI, Taylor PM, Hirst P, Dohle W, Booker-Milburn KI (2008) *J Org Chem* 73:6497–6505. <https://doi.org/10.1021/jo801108h>
64. Elliott LD, Berry M, Harji B, Klauber D, Leonard J, Booker-Milburn KI (2016) *Org Process Res Dev* 20:1806–1811. <https://doi.org/10.1021/acs.oprd.6b00277>
65. Blackham EE, Booker-Milburn KI (2017) *Angew Chem* 56:6613–6616. <https://doi.org/10.1002/anie.201701775>
66. Mukae H, Maeda H, Nashihara S, Mizuno K (2007) *Bull Chem Soc Jpn* 80:1157–1161. <https://doi.org/10.1246/bcsj.80.1157>
67. Shvydkiv O, Nolan K, Oelgemöller M (2011) *Beilstein J Org Chem* 7:1055–1063. <https://doi.org/10.3762/bjoc.7.121>
68. DeLaney EN, Lee DS, Elliott LD, Jin J, Booker-Milburn KI, Poliakov M, George MW (2017) *Green Chem* 19:1431–1438. <https://doi.org/10.1039/C6GC02888H>
69. Baumann M, Baxendale IR (2016) *Synlett* 27:159–163. <https://doi.org/10.1055/s-0035-1560391>
70. Hsueh N, Clarkson GJ, Shipman M (2015) *Org Lett* 17:3632–3635. <https://doi.org/10.1021/acs.orglett.5b01777>

71. Hsueh N, Clarkson GJ, Shipman M (2016) *Org Lett* 18:4908–4911. <https://doi.org/10.1021/acs.orglett.6b02349>
72. Baumann M, Baxendale IR, Ley SV (2008) *Synlett* 14:2111–2114. <https://doi.org/10.1055/s-2008-1078026>
73. Baumann M, Baxendale IR, Martin LJ, Ley SV (2009) *Tetrahedron* 65:6611–6625. <https://doi.org/10.1016/j.tet.2009.05.083>
74. Battilocchio C, Baumann M, Baxendale IR, Biava M, Kitching MO, Ley SV, Martin RE, Ohnmacht SA, Tappin NDC (2012) *Synthesis* 44:635–647. <https://doi.org/10.1055/s-0031-1289676>
75. Baumann M, Baxendale IR, Brasholz M, Hayward JJ, Ley SV, Nikbin N (2011) *Synlett* 22:1375–1380. <https://doi.org/10.1055/s-0030-1260573>
76. Fernandez A, Levine ZG, Baumann M, Sulzer-Mosse S, Sparr C, Schläger S, Metzger A, Baxendale IR, Ley SV (2013) *Synlett* 24:514–518. <https://doi.org/10.1055/s-0032-1318109>
77. Glöckner S, Tran DN, Ingham RJ, Fenner S, Wilson ZE, Battilocchio C, Ley SV (2015) *Org Biomol Chem* 13:207–214. <https://doi.org/10.1039/C4OB02105C>
78. Kim H, Nagaki A, Yoshida J (2011) *Nat Commun* 2:264–272. <https://doi.org/10.1038/ncomms1264>
79. Carter CF, Baxendale IR, O'Brien M, Pavey JBJ, Ley SV (2009) *Org Biomol Chem* 7:4594–4597. <https://doi.org/10.1039/B917289K>
80. Carter CF, Baxendale IR, Pavey JBJ, Ley SV (2010) *Org Biomol Chem* 8:1588–1595. <https://doi.org/10.1039/B924309G>
81. Prosa N, Turgis R, Piccardi R, Scherrmann M-C (2012) *Eur J Org Chem* 2188–2200. <https://doi.org/10.1002/ejoc.201101726>
82. Bremner WS, Organ MG (2007) *J Comb Chem* 9:14–16. <https://doi.org/10.1021/cc060130p>
83. Briggs ME, Slater AG, Lunt N, Jiang S, Little MA, Greenaway RL, Hasell T, Battilocchio C, Ley SV, Cooper AI (2015) *Chem Commun* 51:17390–17393. <https://doi.org/10.1039/C5CC07447A>
84. Spaccini R, Liguori L, Punta C, Bjorsvik H-R (2012) *ChemSusChem* 5:261–265. <https://doi.org/10.1002/cssc.201100262>
85. Mikami K, Islam MN, Yamanaka M, Itoh Y, Shinoda M, Kudo K (2004) *Tetrahedron Lett* 45:3681–3683. <https://doi.org/10.1016/j.tetlet.2004.02.157>
86. Yamamoto H, Sasaki I, Hirai Y, Namba K, Imagawa H, Nishizawa M (2009) *Angew Chem Int Ed* 48:1244–1247. <https://doi.org/10.1002/anie.200804641>
87. Hafez AM, Taggi AE, Dudding T, Lectka T (2001) *J Am Chem Soc* 123:10853–10859. <https://doi.org/10.1021/ja016556j>
88. Izquierdo J, Pericas MA (2016) *ACS Catal* 6:348–356. <https://doi.org/10.1021/acscatal.5b02121>
89. Wang S, Izquierdo J, Rodríguez-Escrich C, Pericàs MA (2017) *ACS Catal* 7:2780–2785. <https://doi.org/10.1021/acscatal.7b00360>
90. Osorio-Planes L, Rodríguez-Escrich C, Pericas MA (2016) *Cat Sci Technol* 6:4686–4689. <https://doi.org/10.1039/C6CY00473C>
91. Kreituss I, Bode JW (2017) *Nat Chem* 9:446–452. <https://doi.org/10.1038/nchem.2681>
92. Tsubogo T, Oyamada H, Kobayashi S (2015) *Nature* 520:329–332. <https://doi.org/10.1038/nature14343>. Scheme updated based upon presented material at the international conference on organic synthesis 21, IIT Bombay, India, December 2016
93. Drop M, Bantreil X, Grychowska K, Mahoro GU, Colacino E, Pawlowski M, Martinez J, Subra G, Zajdel P, Lamaty F (2017) *Green Chem* 19:1647–1652. <https://doi.org/10.1039/C7GC00235A>
94. Comer E, Organ MG (2005) *J Am Chem Soc* 127:8160–8167. <https://doi.org/10.1021/ja0512069>
95. Lim J, Lee SS, Ying JY (2010) *Chem Commun* 46:806–808. <https://doi.org/10.1039/B917986K>

96. Clarke AK, James MJ, O'Brien P, Taylor RJK, Unsworth WP (2016) *Angew Chem Int Ed* 55:13798–13802. <https://doi.org/10.1002/anie.201608263>
97. Correia CA, Gilmore K, McQuade DT, Seeberger PH (2015) *Angew Chem* 54:4945–4948. <https://doi.org/10.1002/anie.201411728>
98. Ouchi T, Battilocchio C, Hawkins JM, Ley SV (2014) *Org Process Res Dev* 18:1560–1566. <https://doi.org/10.1021/op500208j>
99. Ötvös SB, Mandity IM, Fülöp F (2011) *Mol Divers* 15:605–611. <https://doi.org/10.1007/s11030-010-9276-z>
100. Brasholz M, Von Känel K, Hornung CH, Saubern S, Tsanaktsidis J (2011) *Green Chem* 13:1114–1117. <https://doi.org/10.1039/C1GC15107J>
101. Chieffi G, Braun M, Esposit D (2015) *ChemSusChem* 8:3590–3594. <https://doi.org/10.1002/cssc.201500804>
102. Conde E, Rivilla I, Larumbe A, Cossío FP (2015) *J Org Chem* 80:11755–11767. <https://doi.org/10.1021/acs.joc.5b01418>
103. Viviano M, Milite C, Rescigno D, Castellano S, Sbardella GA (2015) *RSC Adv* 5:1268–1273. <https://doi.org/10.1039/C4RA13392G>
104. Wiles C, Hammond MJ, Watts P (2009) *Beilstein J Org Chem* 5(27). <https://doi.org/10.3762/bjoc.5.26>
105. Kee S-P, Gavriilidis A (2009) *Org Process Res Dev* 13:941–951. <https://doi.org/10.1021/op800276a>
106. McPake CB, Murray CB, Sandford G (2009) *Tetrahedron Lett* 50:1674–1676. <https://doi.org/10.1016/j.tetlet.2008.12.073>
107. Kestenbaum H, Lange de Oliveira A, Schmidt W, Schüth F, Ehrfeld W, Gebauer K, Löwe H, Richter T, Lebiez D, Untiedt I, Züchner H (2002) *Ind Eng Chem Res* 41:710–719. <https://doi.org/10.1021/ie010306u>
108. Markowz G, Schirrmeister S, Albrecht J, Becker F, Schütte R, Caspary KJ, Klemm E (2005) *Chem Eng Technol* 28:459–464. <https://doi.org/10.1002/ceat.200407146>
109. Alves L, Desidera AL, de Oliveira KT, Newton S, Ley SV, Brocksom T (2015) *Org Biomol Chem* 13:7633–7642. <https://doi.org/10.1039/C5OB00525F>
110. Ushakov DB, Gilmore K, Seeberger PH (2014) *Chem Commun* 50:12649–12651. <https://doi.org/10.1039/C4CC04932B>
111. Ullah F, Samarakoon T, Rolfe A, Kurtz RD, Hanson PR, Organ MG (2010) *Chem Eur J* 16:10959–10962. <https://doi.org/10.1002/chem.201001651>
112. Fagnoni M, Bonassi F, Palmieri A, Protti S, Ravelli D, Ballini R (2014) *Adv Synth Catal* 356:753–758. <https://doi.org/10.1002/adsc.201300859>
113. Cerra B, Mangiavacchi F, Santi C, Lozza AM, Gioiello A (2017) *React Chem Eng* 2:467–471. <https://doi.org/10.1039/C7RE00083A>
114. Yamada YMA, Torii K, Uozumi Y (2009) *Beilstein J Org Chem* 5(18). <https://doi.org/10.3762/bjoc.5.18>
115. Kopetzki D, Levesque F, Seeberger PH (2013) *Chem Eur J* 19:5450–5456. <https://doi.org/10.1002/chem.201204558>
116. Levesque F, Seeberger PH (2012) *Angew Chem Int Ed* 51:1706–1709. <https://doi.org/10.1002/anie.201107446>
117. Kouridaki A, Huvaere K (2017) *React Chem Eng* 2:590–597. <https://doi.org/10.1039/C7RE00053G>
118. Ziegenbalg D, Kreisel G, Weiß D, Kralisch D (2014) *Photochem Photobiol Sci* 13:1005–1015. <https://doi.org/10.1039/C3PP50302J>
119. Bourne RA, Han X, Poliakov M, George MW (2009) *Angew Chem Int Ed* 48:5322–5325. <https://doi.org/10.1002/anie.200901731>
120. Fukuyama T, Kobayashi M, Rahman MT, Kamata N, Ryo I (2008) *Org Lett* 10:533–536. <https://doi.org/10.1021/ol702718z>
121. Bou-Hamdan FR, Lévesque F, O'Brien AG, Seeberger PH (2011) *Beilstein J Org Chem* 7:1124–1129. <https://doi.org/10.3762/bjoc.7.129>

122. Zhang X, Stefanick S, Villani FJ (2004) *Org Process Res Dev* 8:455–460. <https://doi.org/10.1021/op034193x>
123. Treece JL, Goodell JR, Velde DV, Porco JA, Aubé J (2010) *J Org Chem* 75:2028–2038. <https://doi.org/10.1021/jo100087h>
124. McCaw PG, Buckley NM, Eccles KS, Lawrence SE, Maguire AR, Collins SG (2017) *J Org Chem* 82:3666–3679. <https://doi.org/10.1021/acs.joc.7b00172>
125. Silva BV, Violante FA, Pinto AC, Santos LS (2011) *Rapid Commun Mass Spectrom* 25:423–428. <https://doi.org/10.1002/rcm.4869>
126. Buono FG, Eriksson MC, Yang B-S, Kapadia SR, Lee H, Brazzillo J, Lorenz JC, Nummy L, Busacca CA, Yee N, Senanayake C (2014) *Org Process Res Dev* 18:1527–1534. <https://doi.org/10.1021/op500263m>
127. Payne GB (1967) *J Org Chem* 32:3351–3355. <https://doi.org/10.1021/jo01286a017>
128. Mandrelli F, Buco A, Piccioni L, Renner F, Guelat B, Martin B, Schenkel B, Venturoni F (2017) *Green Chem* 19:1425–1430. <https://doi.org/10.1039/C6GC02840C>
129. Baxendale IR, Deeley J, Griffiths-Jones CM, Ley SV, Saaby S, Tranmer GK (2006) *Chem Commun*:2566–2568. <https://doi.org/10.1039/B600382F>
130. Baxendale IR, Griffiths-Jones CM, Ley SV, Tranmer GK (2006) *Synlett*:427–430. <https://doi.org/10.1055/s-2006-926244>
131. Kamptmann S, Ley SV (2015) *Aust J Chem* 68:693–696. <https://doi.org/10.1071/CH14530>
132. Lücke D, Dalton T, Ley SV, Wilson ZE (2016) *Chem Eur J* 22:4206–4217. <https://doi.org/10.1002/chem.201504457>
133. Brasholz M, Macdonald JM, Saubern S, Ryan JH, Holmes AB (2010) *Chem Eur J* 16:11471–11480. <https://doi.org/10.1002/chem.201001435>
134. Rao ZX, Patel B, Monaco A, Cao ZJ, Barniol-Xicotà M, Pichon E, Ladlow M, Hilton ST (2017) *Eur J Org Chem*. <https://doi.org/10.1002/ejoc.201701111>. Early view
135. Battilocchio C, Baxendale IR, Biava M, Kitching MO, Ley SV (2012) *Org Process Res Dev* 16:798–810. <https://doi.org/10.1021/op300084z>
136. Adamo A, Beingsner RL, Behnam M, Chen J, Jamison TF, Jensen KF, Monbaliu J-CM, Myerson AS, Revalor EM, Snead DR, Stelzer T, Weeranoppanant N, Wong SY, Zhang P (2016) *Science* 352:61–67. <https://doi.org/10.1126/science.aaf1337>

Functionalization of Heteroarenes Under Continuous Flow



Joachim Demaerel, Vidmantas Bieliūnas, and Wim M. De Borggraeve

Contents







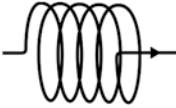

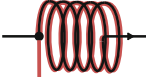



1	Introduction	239
2	C(sp ²)-C(sp) Bond Formation	240
3	C(sp ²)-C(sp ²) Bond Formation	246
	3.1 Heterogeneous Catalysis	246
	3.2 Homogeneous Catalysis	253
	3.3 Uncatalyzed Reactions	262
4	C(sp ²)-C(sp ³) Bond Formation	263
5	C-N Bond Forming Reactions	272
	5.1 Nitration	273
	5.2 Nucleophilic Substitution	278
	5.3 Rearrangements	286
	5.4 Cross-Coupling	288
6	C-O Bond Forming Reactions	296
7	C-B Bond Forming Reactions	297
8	C-X Bond Forming Reactions	302
	8.1 Fluorination	302
	8.2 Bromination	304
	8.3 Iodination	305
9	C-S Bond Forming Reactions	309
10	C-Si Bond Forming Reactions	309
11	Conclusion	311
	References	312

Abstract Aromatic heterocycles are omnipresent motifs in pharmaceutical and agrochemical structures. Functionalization of these ring systems is an important part of many synthetic procedures. In this chapter, an overview is given of how microflow technology has been employed as a powerful tool for the diversification of heteroarenes. An emphasis is put on fine chemical synthesis, although reactor design and problem solving will be discussed when relevant, as it comprises an important part of the research field. Pragmatic translations to microflow are reviewed for










J. Demaerel, V. Bieliūnas, and W. M. De Borggraeve (✉)
Molecular Design and Synthesis, Department of Chemistry, KU Leuven, Leuven, Belgium
e-mail: wim.deborggraeve@kuleuven.be

existing functionalization protocols, and a few elusive reactions are highlighted that cannot be performed satisfyingly in batch mode.

Keywords Continuous flow · Cross-coupling · Functionalization · Heterocycles

	Starting material
	Isolated intermediate
	Non-isolated intermediate
	Product
	Packed scavenger column
	Packed reactor column
	Coil reactor
	Microfluidic reactor
	Tube-in-tube reactor
	Off-line reaction or quench
	Gas bottle
	Pump

(continued)

	Injection loop
	Omitted sequence
	Mass flow controller
	Connector piece
	Connector piece or passive micromixing piece
	Micromixing piece
	Back pressure regulator
	Microwave irradiation
	Ultrasound irradiation

1 Introduction

Flow chemistry has been amply used to install new functionality onto aromatic ring systems. Whether in a multistep synthesis of high value target molecules or as broad methods for safer and more effective synthesis, chemists have demonstrated some impressive benefits of microflow technology. The reasons for these successes are well known, as flow typically warrants safer manufacturing, more facile heating and pressurization, fast mixing, high reproducibility, and potential for scale-up.

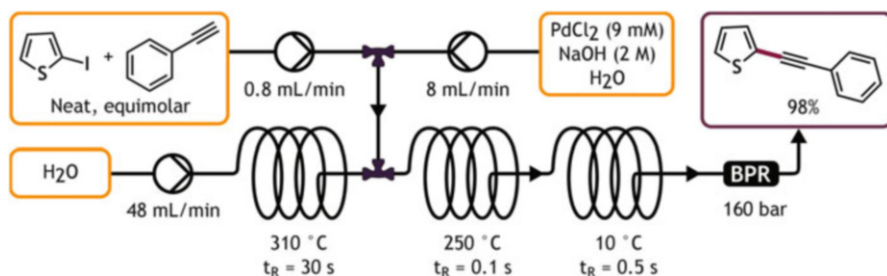
In this chapter, an overview is given of protocols to install a new bond onto heteroarenes. Either functional group interconversions or direct C-H modifications are discussed, where a new bond is formed on the ring itself. A subdivision is made based upon the type of bond which is formed, starting with C-C bond formation, then going to C-heteroatom bond formation.

To date, no review has explicitly covered continuous flow reactions for the diversification of heteroarenes. Some more specific topics have been reviewed, like hazardous and explosive reactions [1, 2], organolithium chemistry [3–5], cross-coupling chemistry [6–8], or flow syntheses of pharmaceutical intermediates [9–13]. Some relevant examples will be reproduced in this chapter, and an update of more recent methods is presented.

2 C(sp²)-C(sp) Bond Formation

Alkyne fragments are frequently encountered in both natural products and synthetic materials, where they give rise to unique structural and electronic properties as well as distinct reactivity. Therefore, aryl alkynes display diverse synthetic utility and are valued both as intermediates and as final compounds. These materials are most often produced via Castro-Stephens (Cu catalysis, 1963), Heck-Cassar (Pd catalysis, 1975), or Sonogashira (combined Pd and Cu catalysis, 1975) cross-coupling reactions, which, as the products themselves, have attracted considerable attention over the years [14–18]. Several attempts at aryl alkylation in continuous flow have also been discussed by Noel and Hessel, but the chosen examples were mostly confined to carbocyclic aromatic compounds [6]. Hence, relevant reports discussed therein will be included in this section with the emphasis on heterocyclic substrates.

An early example of flow heterocycle alkylation comes from Kawanami et al., who showcased the advantages of superior heat transfer and pressure tolerance by conducting the Heck-Cassar reaction in high pressure and high temperature (HPHT) water [19]. To accomplish that, a neat equimolar mixture of aryl iodides and phenylacetylenes was finely dispersed in ambient temperature aqueous PdCl₂ (2 mol%) and NaOH (4.5 eq.) by a 0.5 mm I.D. micromixer (Scheme 1). The formed emulsion was then merged with degassed and pressurized high temperature water in a second matching micromixer at the microreactor inlet. The superheated water brought both organic reagents into homogeneous solution and instantaneously heated it to 250 °C. This temperature was further maintained by the microreactor for 0.1 s. Active cooling of the output stream ensured the precise sub-second residence time, therefore allowing nearly quantitative yields of substituted phenylacetylenes to be obtained at a formidable 0.22 mol/h rate. The water-insoluble reaction products, including Pd⁰, readily separated from the eluted mixture and could be conveniently isolated by phase separation and/or filtration. Unfortunately, only a few substrates were investigated, with 2-iodothiophene being the single heterocyclic example. Even though high performance pumps are necessary to replicate the

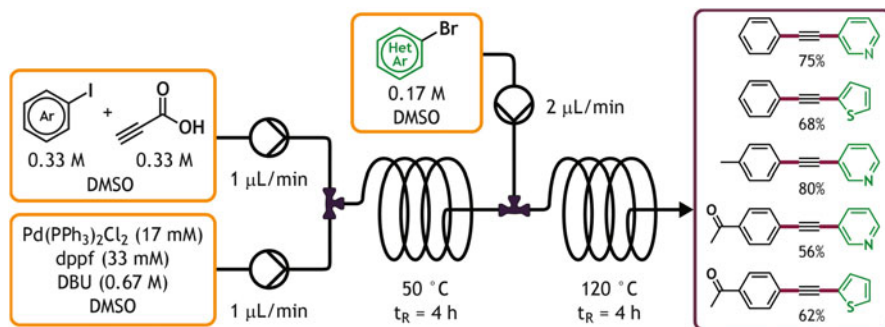


Scheme 1 Ultrafast aqueous Heck-Cassar coupling of iodothiophene in HPHT water (Kawanami et al. [19])

process, it is attractive from both high production rate and low environmental impact standpoints.

For small-scale combinatorial synthesis of unsymmetrical diaryl alkynes, a method of continuous Heck-Cassar coupling followed by decarboxylative coupling is available (Scheme 2) [20]. Early batch experiments revealed that, in the presence of $\text{Pd}(\text{PPh}_3)_2\text{Cl}_2$ (5 mol%), dppf (10 mol%) and DBU (2 eq.), propiolic acid (1 eq.) sequentially reacts with aryl iodides and bromides, simultaneously present in the mixture. To enhance the selectivity even further, both steps were spatially separated in flow. While a single stock solution is unfeasible due to DBU propiolate precipitation at ambient temperature, the first set of reagents can be reliably supplied in two separate streams through a micromixer, installed at the reactor inlet. The produced arylpropionic acid is then further coupled by introducing an aryl bromide and flowing the resulting mixture through a second 0.6 mm I.D. PTFE coil reactor. With this two-step procedure, multiple asymmetric alkynes were generated in moderate to good yields and only an electron-poor iodoarene gave significant amounts of symmetrical alkyne byproducts. Extremely low throughput and total 8-h residence times are notable disadvantages, but the method provides convenient access to a multitude of disubstituted alkynes at far greater selectivity than an equivalent batch process.

A two-stage continuous approach can also be used for fluorinated heteroaromatic alkyne production from terminal alkynes containing a tosylated sidechain (Scheme 3) [21]. In the report, a nucleophilic substitution of tosylate group was accomplished using tetrabutylammonium fluoride in a Chemtrix[®] 10 μL microfluidic chip. The internal architecture of the chip provides sufficient mixing, resulting in quantitative fluorination in less than 3 min. Simultaneous introduction of aryl halide (1 eq.), Pd(OAc)₂ (5 mol%) and tetrabutylammonium acetate (1.5 eq.) into the output stream then allowed to couple the intermediate terminal alkyne in a subsequently installed 0.40 mm I.D. PEEK tube reactor. No microchannel clogging was observed due to

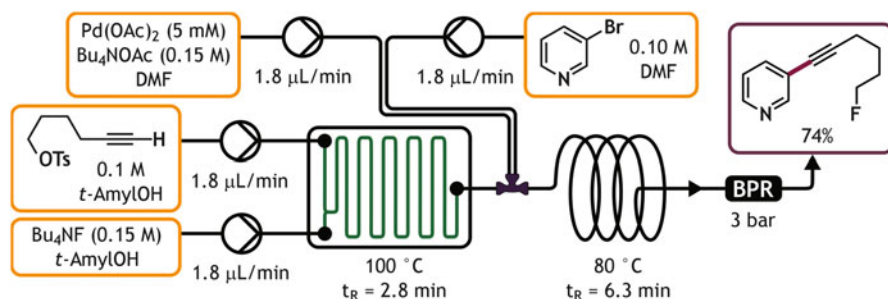


Scheme 2 Continuous sequential Heck-Cassar coupling followed by decarboxylative coupling. DBU = 1,8-Diazabicyclo(5.4.0)undec-7-ene; dppf = 1,1'-Bis(diphenylphosphino)ferrocene (Lee et al. [20])

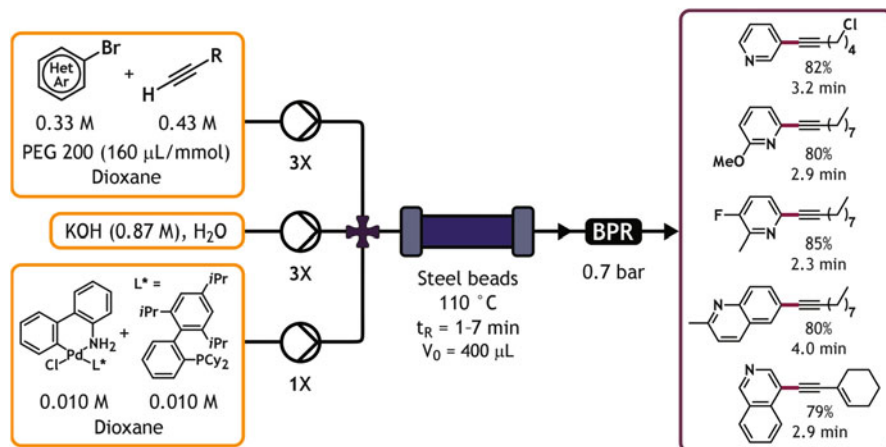
high solubility of the produced tetrabutylammonium salts in polar organic solvents. The resulting method is useful for easily automated quick access to ^{18}F labeled alkynes for positron imaging. Unfortunately, the reported substrate scope was narrow and the yield in the case of a single heterocyclic example was inferior to most carbocyclic counterparts.

The first general and efficient continuous flow protocol for terminal alkyne coupling with aryl bromides mitigated the substrate scope limitations imposed by scarcity and high price of iodinated counterparts [22]. To achieve sufficiently high reactivity under reasonable catalyst loading, a second generation Buchwald X-Phos palladacycle precatalyst, capable of rapidly providing the catalytically active species, was used. Though 0.25 mol% of both precatalyst and ligand gave satisfactory results in batch, flow conditions required 1 mol% of each for optimal performance. Initial investigations also revealed KOH to be the most effective base, therefore, dioxane-water (4:3) mixture was used to fully solubilize salts. A 60–125 μm stainless steel bead packed cartridge then provided the necessary mixing of phases, which was insufficient with segmented flow in steel tubing alone [23]. Notably, any other inert filling material, that does not cause excessive backpressure, could have also been used. Under optimized conditions, 1.3 eq. of alkynes were necessary to fully consume the aryl bromides and give good to excellent yields (Scheme 4). This protocol performed well with both electron-rich and electron-deficient aryl bromides, including ortho-substituted and heteroaromatic examples. Furthermore, the combined reported scope of both batch and flow conditions suggests an exceptionally wide substrate compatibility.

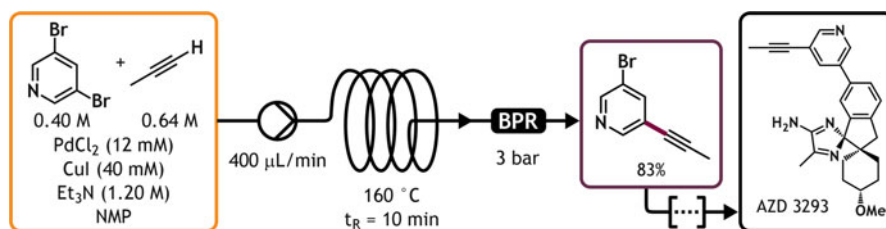
In the previous examples, only liquid and solid terminal alkynes were investigated, while gaseous counterparts remained unexplored. Indeed, the difficulty of handling gasses in a laboratory setting has even led to an almost exclusive use of liquid or solid organometallic, silylated or carboxylated derivatives for C_2 – C_4 alkyne fragment introduction [24]. While these reagents are easier to handle, they are also more expensive and offer significantly inferior atom efficiency compared to the corresponding gasses. Fortunately, flow setups, such as described above, do



Scheme 3 Continuous sequential nucleophilic fluorination of tosylated alkyne followed by Heck-Cassar coupling (Placzek et al. [21])



Scheme 4 Aryl bromide optimized Heck-Cassar coupling. Constant reagent ratios were used for each experiment (Shu et al. [22])



Scheme 5 Monopropynylation of 3,5-dibromopyridine via Sonogashira reaction with propyne in *N*-methylpyrrolidone (Znidar et al. [25])

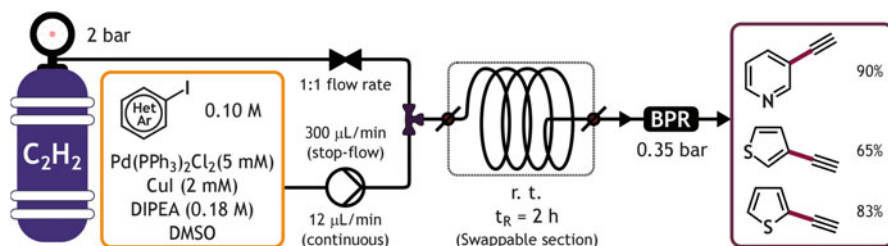
facilitate convenient use of gases with only minor modifications, therefore, enabling direct coupling of aromatic compounds to gaseous alkynes.

The effective use of propyne for flow Sonogashira coupling was demonstrated during the synthesis of an intermediate towards Alzheimer's drug AZD3293 (Scheme 5) [25]. The report particularly emphasizes the use of microwave heating for optimization experiments performed in batch to mimic the rapid heating profile of flow methods. It also highlights the headspace effect, which is encountered when volatile reagents evaporate from the mixture and collect in the vacant space of a batch reactor leading to lower availability. Fortunately, flow reactors with a back-pressure regulator can prevent void formation by maintaining a higher in-line pressure than the vapor pressure of the most volatile component at any point. Such systems enable the efficient use of volatile reagents and ensure their predictable ratios throughout the reaction.

To establish a flow protocol, the patented batch conditions of 3,5-dibromopyridine monopropynylation with TMS-propyne were initially adapted for 1-hexyne. Also, CuI loading was reduced from 30 to 10 mol% and toluene was replaced by NMP to afford homogeneous reaction mixtures. The optimized batch conditions were then applied in flow, using propyne stock solution in NMP instead of 1-hexyne, and the product was obtained in 83% yield. In comparison, the aforementioned patented industrial batch process gives only 80% yield after 18 h at 110°C and is more expensive to conduct. Furthermore, additional stages could be appended to the discussed system to provide the AZD3293 via subsequent Suzuki-Miyaura coupling in a telescoped manner.

Acetylene gas was successfully utilized for continuous Sonogashira coupling in a stop-flow micro-tubing reactor (SFMT) system by Jie Wu group (Scheme 6) [26]. The described setup is particularly suitable for reaction screening, because the reactor coil can be removed from the line after pausing the flow and closing the shut-off valves at each end of the channel. These valves hermetically seal the reactor and maintain the pressure determined by the shared backpressure regulator. As a result, a single system can quickly fill several reactor coils in sequence so that multiple slow reactions could be conducted in parallel. Formed products are then retrieved by simply reconnecting the coil to the flow system and flushing it with solvent. Although the reactions are conducted like high pressure batch experiments, the conditions mimic those encountered in continuous flow reactors barring decreased mass transfer in segmented regime [27, 28]. Furthermore, when applied to lengthy parallel experiments, this method is easy to set up, requires neither multiple high pressure reactors nor multiple flow reactors, but combines the best aspects of both.

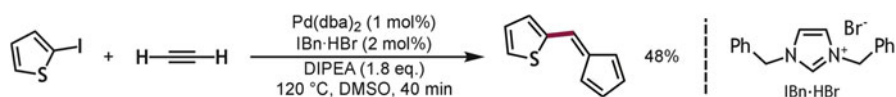
Employing the SFMT apparatus, ethyne was selectively monoarylated in swappable 0.76 mm I.D. HPFA coils after forming 1:1 gas-liquid slugs with a solution containing the substrate, 5 mol% of Pd(PPh₃)₂Cl₂, 2 mol% of CuI, and 1.8 eq. of DIPEA at 0.35 bar initial overpressure. The obtained process was readily translated into true continuous flow just by selecting an appropriate flow rate and reactor coil length to match the residence time. In both cases ethyne diarylation was negligible, contrary to the absence of known selective batch processes. Furthermore,



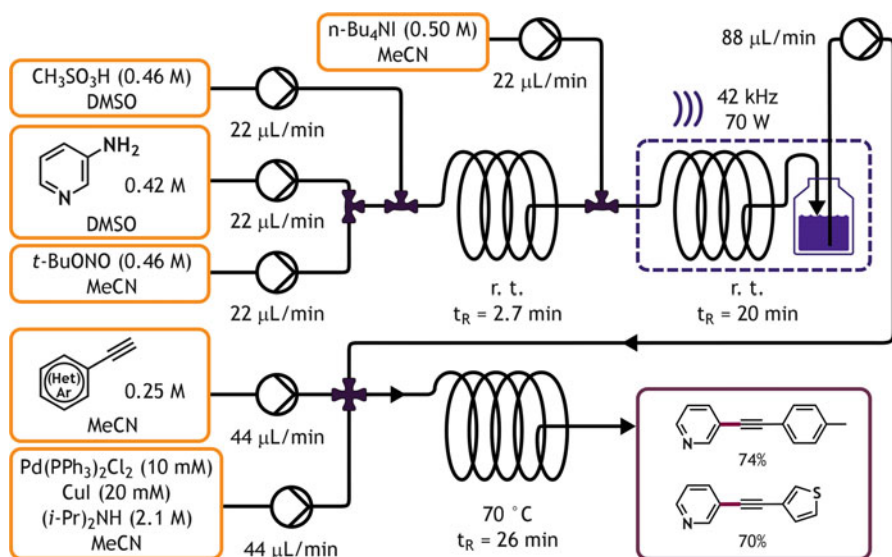
Scheme 6 Sonogashira coupling of ethyne in SFMT system with swappable coils. DIPEA = *N,N*-diisopropylethylamine (Xue et al. [26])

in the absence of copper, fulvene derivatives were formed instead of the expected Heck-Cassar products. Under reoptimized conditions, the same system produced the 2-thiophenyl derivative in 48% yield (Scheme 7).

Instead of using the aryl halide or equivalent coupling partners directly, Teci et al. established a three-step continuous telescoped diazotization/iododediazotization/cross-coupling protocol, that uses anilines as starting material en route to Sonogashira coupling products (Scheme 8) [29]. Two major challenges were encountered during development, both of them at the iododediazotization step. The precipitation of solids threatened to clog the reactor, while nitrogen evolution resulted in a randomly segmented flow mode. Therefore, the reactor was ultrasonicated to prevent clogging and to accelerate the reaction, while the effluent was dynamically ultrasonicated in an open vessel to reconstitute a continuous liquid stream, which was crucial for further reagent dosing and mixing. This also enabled convenient continuous sampling of the effluent for conversion monitoring.



Scheme 7 Flow fulvene synthesis in the aforementioned SFMT system using stainless steel coils. DIPEA = *N,N*-diisopropylethylamine (Xue et al. [26])



Scheme 8 Sequential continuous diazotization/iododediazotization/Sonogashira coupling, adaptable for Suzuki-Miyaura coupling by replacing alkynes with boronic acids (Teci et al. [29])

When 3-aminopyridine was used as substrate, the Sonogashira reaction proceeded with good yields at about 0.45 mmol/h production rate using 5 and 10 mol% of Pd and Cu catalysts, respectively. Similar performance was attained with the non-heterocyclic counterparts. Notably, the heterocyclic substrates in particular produced minor precipitate in reactor 3, possibly complicating scale-up. The same setup was also compatible with a Suzuki-Miyaura coupling when alkyne was simply replaced with a boronic acid. In that case, the performance of 3-aminopyridine remained essentially unchanged, suggesting that the first two stages could be integrated with the systems described in the next section.

3 C(sp²)-C(sp²) Bond Formation

Binding of aromatic rings to other sp² carbon atoms in either flow or batch mode is arguably most often accomplished using cross-coupling reactions, catalyzed by homogeneous or heterogeneous transition metal catalysts. These reactions have received extensive attention since their inception and are presently well established both in research and in industry setting [7, 30, 31]. Out of commonly used procedures, the Suzuki-Miyaura coupling (SMC) stands out as the most widely implemented method for both arylation and vinylation of aromatic rings, including the more challenging heterocyclic counterparts [32, 33]. This trend also extends well into flow chemistry where its robustness is utilized to the extent of creating continuous multistep syntheses without isolation of intermediates [34]. Once again, the examples mentioned in the earlier reviews are also included in this section with the emphasis on heterocyclic substrates.

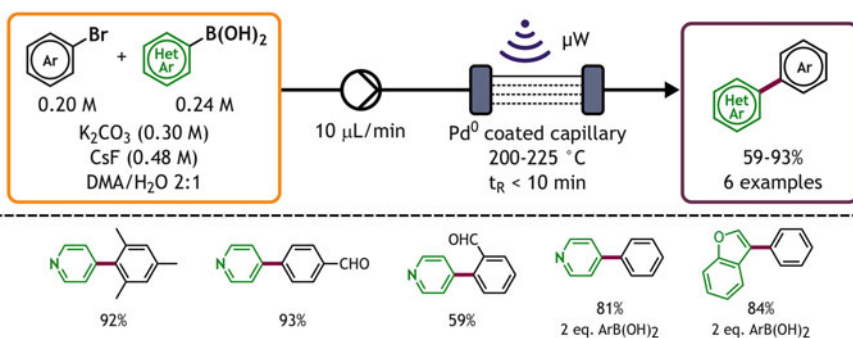
3.1 Heterogeneous Catalysis

Heterogeneous catalysts in continuous flow confine the active material to the reaction site, resulting in superb reactivity due to high local concentrations under low overall loading. Furthermore, catalysts containing metallic particles exhibit marked microwave absorption, which facilitates highly focused direct heating and enables greater suppression of catalyst-independent side-reactions in comparison to homogeneous approach [35, 36]. Also, though metal leaching from the support material is essentially unavoidable during the oxidative insertion–reductive elimination cycling, product purification is more straightforward, as observed levels are orders of magnitude lower than encountered in homogeneous catalysis. However, the gradual loss of active metal limits the lifetime of the catalyst bed, impairs reproducibility, and causes time-dependent performance [8].

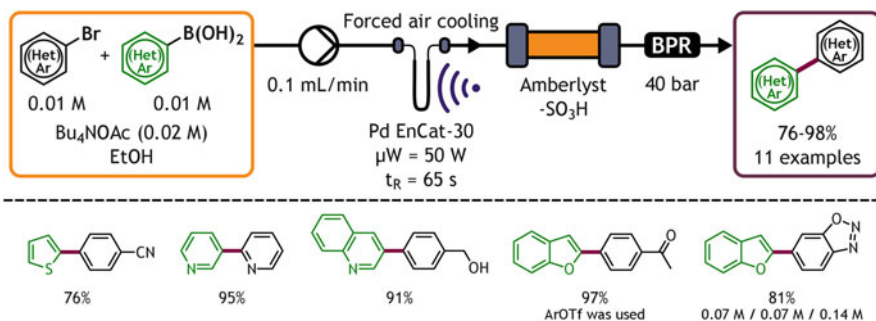
Interestingly, the early reported examples of heterogeneously catalyzed heterocyclic substrate coupling in flow utilized microwave heating, but the trend did not continue further. In one report, a capillary reactor with porous Pd black coated inner

walls successfully catalyzed the SMC of multiple substrates, including heteroarylboronic acids (Scheme 9) [35]. The reactor was manufactured in house from regular 1.15 mm I.D. glass capillaries by thermal decomposition of 0.1 M Pd(OAc)₂ in DMF. Subsequent calcination at 400°C removed organic materials and increased the surface area of the coating, resulting in porous Pd film of 6 μm thickness. The coated capillary was then inserted into a single mode microwave reactor cavity. Passing a solution of substrate, heteroarylboronic acid (1.2 eq.), K₂CO₃ (1.5 eq.) and CsF (2.4 eq.) through such microwave heated capillaries resulted in good conversion at a 0.12 mmol/h rate. Furthermore, the rate is easily multiplied by installing a mixing head to bundle several capillaries together. 19.2 ppm of Pd was detected in the eluted reaction stream, which is relatively low for an unsupported metal catalyst. Notably, equivalent conventional heating provided inferior results, indicating a discrepancy between the observed bulk temperature and the film temperature under microwave heating.

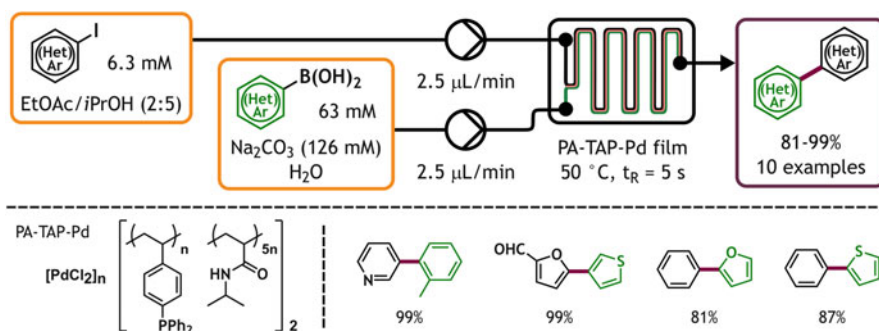
Batch SMC experiments using polyurea supported Pd(OAc)₂ catalyst Pd EnCat[®] 30 under microwave irradiation also showed an up to tenfold rate increase in comparison to conductive heating [36]. Explanation of this tremendous difference by direct heating of the metallic species gained further ground after introduction of external cooling. With it, the reaction rate was maintained even at 45°C lower bulk temperature, and previously problematic substrates began providing clean conversions. The investigation culminated with the creation of a Pd EnCat[®] 30 (180 mg) packed capillary insert, designed to fit in a microwave cavity (Scheme 10). A backpressure regulator and an Amberlyst[®] resin cartridge were installed downstream to stabilize the flow profile and to purify the product, respectively. To avoid the overheating and collapse of the polymer matrix, the reactor was operated under a pulsed protocol of alternating 30 s heating-while-cooling and 18 s cooling cycles. Under these conditions, an equimolar solution of coupling partners with 2 eq. of base gave clean and efficient conversions of most heterocyclic substrates into the corresponding biaryls. Furthermore, a library of ten products was successfully prepared in sequence using the same catalyst bed without any deterioration of



Scheme 9 Suzuki-Miyaura coupling in a Pd⁰ coated glass capillary reactor under microwave heating (Shore et al. [35])



Scheme 10 Suzuki-Miyaura coupling in a Pd EnCat[®] 30 packed glass capillary reactor under simultaneous heating and cooling (Baxendale et al. [36])



Scheme 11 Rapid Suzuki-Miyaura coupling catalyzed by Pd immobilized on a thin polymer film (Yamada et al. [37])

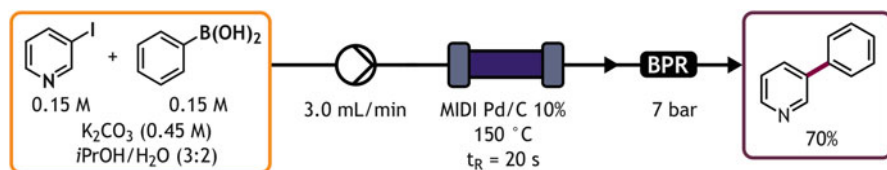
activity. The capacity for scale-up was tested by doubling the reagent concentrations and flow rate. This resulted in constant performance of 1.2 mmol/h over 36 h, which translates into 0.2% Pd loading and highlights the exceptional efficiency. Though low leaching is expected, the authors recommend installing a Quadrapure[®] scavenger resin cartridge if a completely metal-free product is desired.

A peculiar capillary reactor was created by deposition of catalytic polymer film at the laminar interface between two immiscible liquid streams (Scheme 11) [37]. The film was obtained by simultaneously passing a diphenylphosphine grafted polymer in EtOAc and [PdCl₄(NH₄)₂] in water through a 100 μm × 40 μm × 140 mm channel under laminar flow. Crosslinking of phosphine sidechains by palladium resulted in reliable and uniform precipitation of 1 μm film throughout the whole length of the channel, including the bends. Interestingly, the coupling partners were also passed in two streams, separated by the membrane. One stream contained aryl iodide in *i*PrOH and the other contained aqueous boronic acid (10 eq.) and the base (20 eq.). Though a large excess of boronic acid had to be used with heterocycles, most products were obtained in quantitative yields. Furthermore, a 60-min continuous experiment with a carbocyclic substrate pair showed no deterioration of activity, and no leached

palladium or phosphorous could be detected in the collected samples ($\text{Pd} < 0.044$ ppm, ICP-AES). Though only a modest rate of $1 \mu\text{mol/h}$ was obtained with a single reactor, the approach is certainly unique and offers quick access to pure, transition metal-free coupling products, albeit in small quantities.

Commercially available CatCart™ heterogeneous palladium catalysts based on phosphine-grafted polymer matrix were investigated for 5-formyl-2-furanylboronic acid coupling with aryl bromides on a ThalesNano X-Cube™ flow system [38]. This particular substrate attracted attention due to numerous encounters of furan biaryl motif in biologically active compounds of various different classes. Out of the tested polypropylene fiber catalyst cartridges, the $\text{PPh}_3\text{PdCl}_2\text{P}(t\text{-Bu})_3$ grafted FC1032™ showed the most promising results when used with aryl bromides and 3 eq. of TBAF in MeOH. Challenging substrates, such as chloroarenes and electron-rich bromoarenes, prompted a shift to a more active CatCart™ $\text{PdCl}_2(\text{PPh}_3)_2\text{-DVB}$ catalyst and tetrabutylammonium acetate as base. However, the $\text{PdCl}_2(\text{PPh}_3)_2\text{-DVB}$ was also less selective, producing up to 30% of homocoupling products from the most reactive substrates. Analysis of eluted crude mixtures from either cartridge showed palladium levels to be below 1 ppm—low enough for pharmaceutical applications—even under the harsher conditions used with the $\text{PdCl}_2(\text{PPh}_3)_2\text{-DVB}$ polymer.

Heterogeneous catalysts based on inorganic matrices are known for greater chemical and thermal stability, straightforward functionalization, and more attractive price. Pd/C immediately stands out as the first choice since it is one of the most known and least expensive palladium catalysts. An attempt to use it for green SMC in aqueous isopropanol on a ThalesNano H-Cube™ MIDI® system has been reported by Mateos et al. [39] 5% Pd/Al₂O₃ and Pd black catalysts were also tested, but quickly rejected due to inferior activity. Initial intentions of using purely aqueous media were also abandoned because formed slurries clogged the cartridge. Fortunately, complete reagent dissolution was achieved by adding either methanol or isopropanol. The resulting biphasic liquid was then energetically stirred during uptake into the flow system. When passed through the Pd/C (10%) cartridge, such mixture, containing equimolar amounts of 3-iodopyridine and phenylboronic acid with 3 eq. of K₂CO₃, afforded the coupling product at a formidable 19 mmol/h rate (Scheme 12). 26–44 ppm of palladium were detected with carbocyclic substrates and at least the same levels should be expected for heterocyclic congeners as well. Despite high leaching, more than 400 mmol 2-phenylbenzonitrile were produced

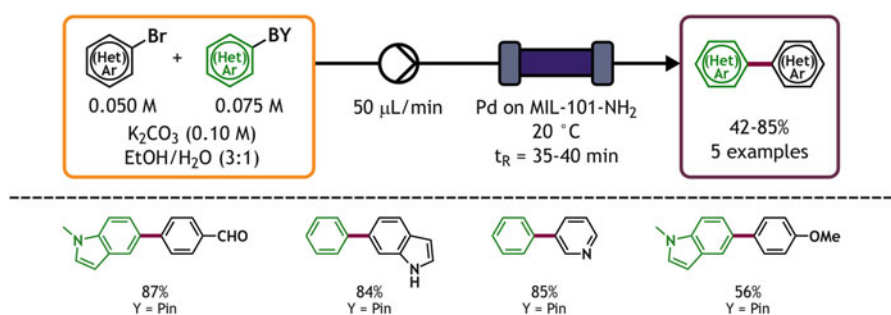


Scheme 12 High throughput Suzuki-Miyaura coupling catalyzed by 10% Pd/C on a ThalesNano H-Cube™ MIDI® (Mateos et al. [39])

with a single cartridge during a scale-out attempt, owing to high metal content of the catalyst.

Pascanu et al. pioneered the use of functionalized mesoporous metal-organic framework (MOF) supported palladium nanoparticles for SMC in continuous flow mode [40]. The entire investigation was focused primarily on challenging substrates, so this versatile, tunable, and extremely porous support material was specifically chosen to circumvent the scope limitations imposed by other common heterogeneous catalysts. MIL-101-NH₂, containing 7.29 wt.% Pd, was chosen in particular, because of its good stability and near-optimal palladium level. A wide array of heterocyclic halides and heterocyclic boron derivatives coupled exceptionally well during batch testing, prompting further study of the catalyst's behavior in flow. Good to moderate yields of heterobiaryls were obtained under ambient conditions by passing solutions of substrates and K₂CO₃ through an Ominifit[®] glass column (10 × 70 mm), packed with 350 mg of the catalyst (Scheme 13). Furthermore, the whole reported library was generated in a single continuous flow experiment simply by swapping the feed mixtures and collection flasks, therefore proving the endurance and suitability of the catalyst for focused drug candidate set generation under real-life conditions. In this case, the column did not exhibit signs of degradation before 3 mmol of aryl halides were processed. In a separate experiment it was also observed that heavy metal leaching remains insignificant until the collapse of the MOF crystal structure, which is easily identified by sharp decline of catalytic activity. Overall, as evidenced by both flow and batch experiments discussed in the work, this particular catalytic system is remarkably suitable for the synthesis of challenging heterobiaryls and offers a far wider substrate scope than is illustrated by the examples given herein.

Functionalized silica bound palladium catalysts appear to be the most popular choice for heterocyclic substrates. In an early report, containing heterocyclic examples, a silica bound phosphine/palladium complex, containing 6 wt.% of metal, was examined as catalyst for Hiyama reaction [41]. In its presence, trimethoxysilyl benzene reacted with several carbocyclic aromatic bromides completely and selectively. 2-Bromopyridine and 2-bromothiophene were poor substrates, however, and gave lesser than 50% yields.

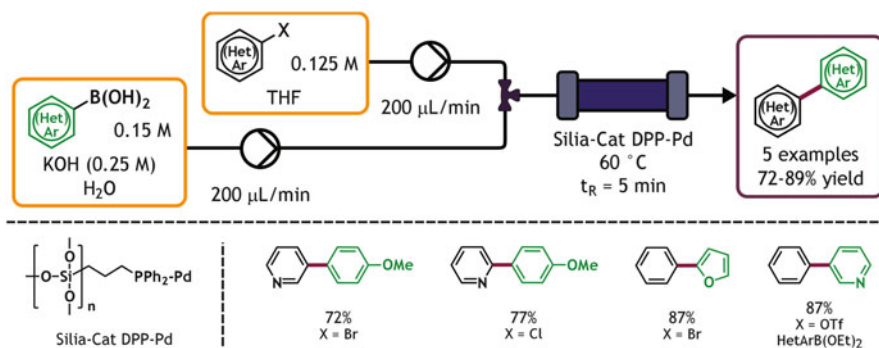


Scheme 13 Suzuki-Miyaura coupling using mesoporous metal-organic framework-supported palladium (Pascanu et al. [40])

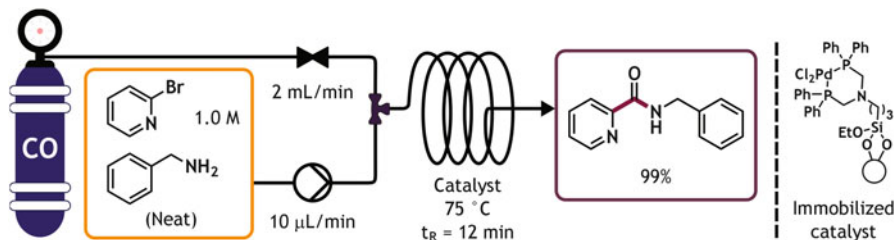
Catalysis of heterocycle SMC by a commercially available phosphine tethered silica catalyst SiliaCat[®] DPP-Pd containing ≥ 0.20 mmol of active metal per gram was found to be much more successful [42]. The investigation was conducted using 1 g of catalyst on a Vapourtec R2 + R4 setup with a 6.6 mm I.D. Omnifit[®] column (Scheme 14). A biphasic solvent system was chosen for its compatibility with inorganic bases as KOH (2.0 eq.) exhibited the best performance during initial screening. When a slight excess of boron derivatives (1.2 eq.) was used, iodides, bromides, chlorides, and triflates reacted equally well to give full conversions. Furthermore, selective coupling at the bromo substituent was achieved with bromochlorobenzene.

Good isolated yields of products were obtained from haloheteroarenes as well as heteroaryl boron derivatives at a 1 mmol scale, reaching up to 1.3 mmol/h production rate with consistent performance for at least 30 consecutive runs. An 8-h scale-out experiment with 4-methoxyphenylboronic acid and 2-bromotoluene exhibited the same consistency. ICP-MS measurements during the scale-out experiment showed minute leached Pd levels of ≤ 10 ppb and ≤ 20 ppb in organic and in aqueous phase, respectively. Unfortunately, attempts at further process intensification by increasing the concentration of reagents or reducing the residence time resulted in diminished conversion. Identical overall results were observed when the commercial flow system was replaced with dual syringe pump, re-purposed HPLC column, and a resistive column heater setup, illustrating robustness of the method itself. Furthermore, essentially the same setup, as depicted in Scheme 14, has also been used to accomplish aryl-aryl and alkyl-aryl Negishi cross-coupling with moderate success [43].

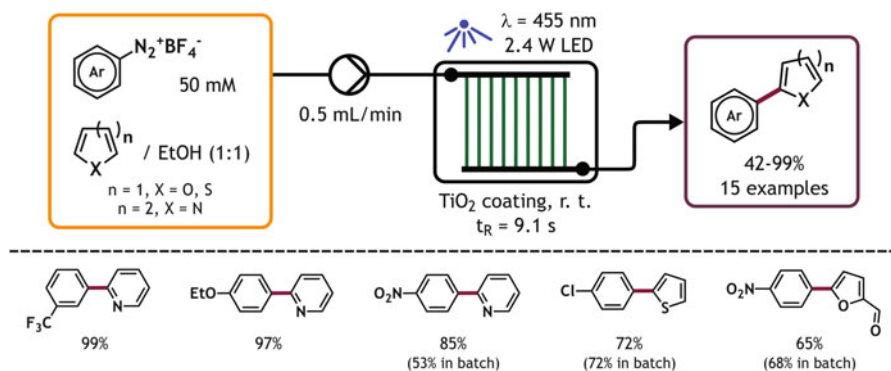
A supported diphosphine palladium catalyst, prepared in-house by treating silica with triethoxysilane tethered palladium-phosphine complex, has also been used to perform carbonylative chemistry [44]. 1 mm I.D. PTFE tube loaded with 250 mg of this catalyst, containing 1.5 wt.% of palladium, was sufficient to quantitatively aminocarbonylate 50 mmol of 2-bromopyridine in 12 min (Scheme 15). Electron-deficient carbocyclic congeners performed equally well, but drastic performance loss



Scheme 14 Silia-Cat[®] DPP-Pd catalyzed Suzuki-Miyaura coupling on a Vapourtec R2 + R4 (de Muñoz et al. [42])



Scheme 15 Heterogeneously catalyzed flow aminocarbonylation in neat amines (Miller [44])



Scheme 16 Photocatalyzed direct arylation in a TiO₂ coated microchannel reactors (Fabry et al. [46])

was observed with electron-rich substrates and plain halobenzenes. The flow aminocarbonylation provided notable improvements over a comparable batch process in terms of safety, operational simplicity, and performance. Therefore, radiolabeling with ¹¹C was also investigated, but only with carbocyclic substrates. Moderate yields and a tendency for the catalyst to permanently retain some radioactivity were observed in these experiments.

Direct C-H activation processes, such as C-H arylation, are obviously the most desired methods of heteroaryl functionalization due to superior atom efficiency in comparison to any other process. Unfortunately, the high energy of C-H bonds makes these transformations more difficult to accomplish, especially in a sufficiently selective manner [45]. Although heterocycles offer greater reactivity and innate regioselectivity even in the absence of directing functional groups, reports on heterocycle C-H activation in flow are scarce. According to the findings of Fabry et al., radical C-H arylation of pyridine, furan, and thiophene can be accomplished in a TiO₂ coated microstructured falling film reactor (FFMR) under visible light irradiation (Scheme 16) [46]. The key to this transformation, previously reported in batch, is the formation of photoactive azoethers from diazonium reagents on the catalyst's surface. Contrary to batch reactors, the TiO₂ coated microchannel reactor does not suffer from limited penetration depth and poor irradiation time control.

Therefore, the detrimental effects of overexposure are minimized and better yields can be expected. Furthermore, the rough oxide surface creates turbulence in the flowing liquid film, ensuring superb mass transfer. In the report, 2-arylation of pyridine gave extremely favorable results, universally superior to batch mode. 2-arylation of thiophene and furan, however, gave similar or inferior yields in comparison to batch. Nevertheless, the calculated specific reactor performance (mol/(L min)) was four orders of magnitude greater for the flow system, translating to 1.5 mmol/h production rate on a small scale. Also, the catalyst showed no degradation during 180-min extended run.

Attempts at direct C-H arylation using homogeneous catalysis are just as rare as the ones investigating heterogeneous catalysts. In one of the reports a direct intramolecular arylation of aryl bromobenzyl ethers and *N*-bromobenzylated heteroarenes in an ultrasonicated reactor is described [47]. However, the reaction is performed at a low rate and is of limited applicability.

3.2 Homogeneous Catalysis

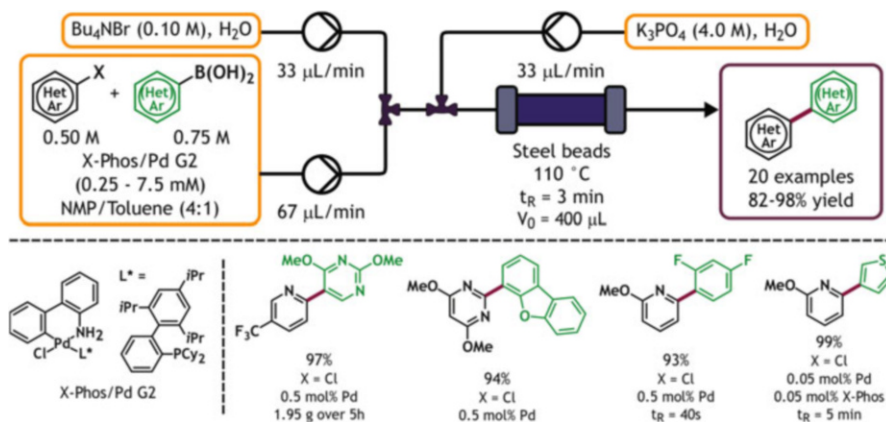
Continuous couplings catalyzed by homogeneous species closely resemble regular batch reactions and benefit from a large selection of available catalysts and ligands. Dissolution of the catalyst in the reagent stream also ensures its consistent availability and performance, particularly important when the catalyst can get poisoned by starting materials or (by)products. Furthermore, absence of packed bed cartridges in the system allows straightforward use of slurries under ultrasonic irradiation. The main drawback of homogeneous catalysis, however, is the relative difficulty of catalyst and ligand recovery, which is often highly desirable due from both scarcity and high environmental impact standpoints [48]. Furthermore, the equal distribution of homogeneous catalyst in the reactant mixture means that only the fraction that is contained in a heated loop of a flow reactor can actively participate at a time. Therefore, unnecessarily high loadings need to be applied to reach good conversions, further exacerbating the already present catalyst and ligand recovery issues.

Unsurprisingly, homogeneous SMC was used in the first reported flow protocol to effect a Csp^2 - Csp^2 bond formation at a heterocyclic ring (Scheme 17) [49]. In the report, continuous flow was investigated as a solution towards straightforward scale-up of microwave heated batch reactions. Therefore, previously reported coupling of 2-benzofuranylboronic acid with 4-bromobenzaldehyde in batch was chosen as one of the model processes. The flow reactor consisted of a helical glass tube in a protective glass sheath, fitted within a commercial single-mode microwave reactor cavity. Fortunately, the reactor retained full temperature monitoring and control functions, straightforwardly leading to results similar to the batch experiment, yet without scale limitations imposed by reactor vial size.

Generally inferior reactivity of heterocyclic substrates and the susceptibility of five-membered 2-heteroarylboronic acids towards protodeboronation under basic conditions prompted the investigation of Buchwald palladacycles as efficient



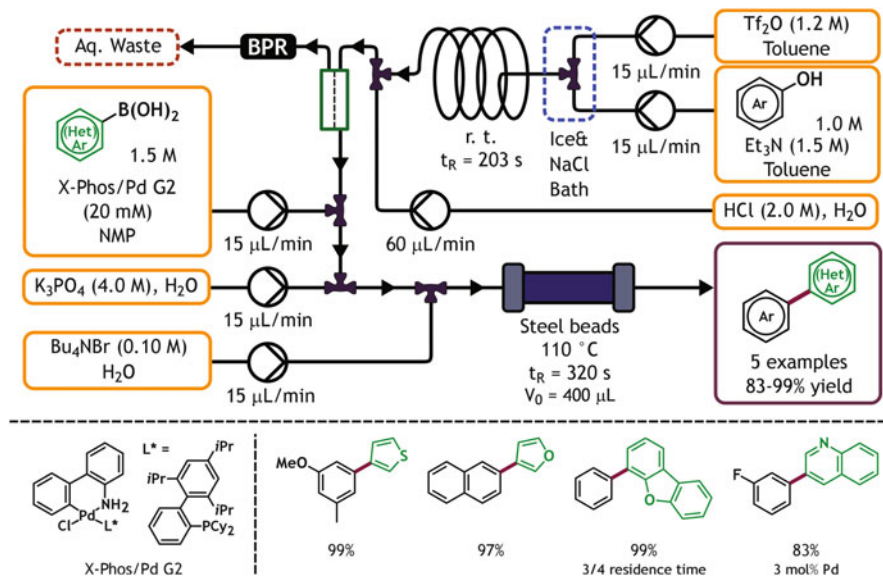
Scheme 17 Suzuki-Miyaura coupling under microwave irradiation directly transferred from batch to flow (Wilson et al. [49])



Scheme 18 Suzuki-Miyaura coupling in a steel-packed bed reactor (Noël and Musacchio [50])

catalytic palladium sources [50]. The then-novel second generation Xphos precatalyst exhibited the best performance, thus allowing the reaction to be conducted with as low as 0.5 mol% of precatalyst alone, or an unprecedented 0.05 mol%, if equal amount ligand was also added. Possibility of clogging was eliminated by conducting the reaction in biphasic NMP, toluene and water (4:1:5) system, capable of dissolving all reagents and products. A 60–125 µm stainless steel bead packed bed reactor was then used in combination with 10 mol% of phase transfer catalyst to obtain sufficient mass transfer, resulting in a sustained production rate of up to 2.0 mmol/h (Scheme 18). Furthermore, the tetrabutylammonium bromide may also act as a stabilizer for Pd in solution [51]. Both heteroaryl bromides and chlorides effectively coupled at 90 °C to furnish a wide array of biaryls in mostly excellent isolated yields. Reduction of temperature to 60 °C and increase of residence time from 2 to 5 min even permitted the effective utilization of 2-furanyl- and 2-thienylboronic acids without increasing their excess.

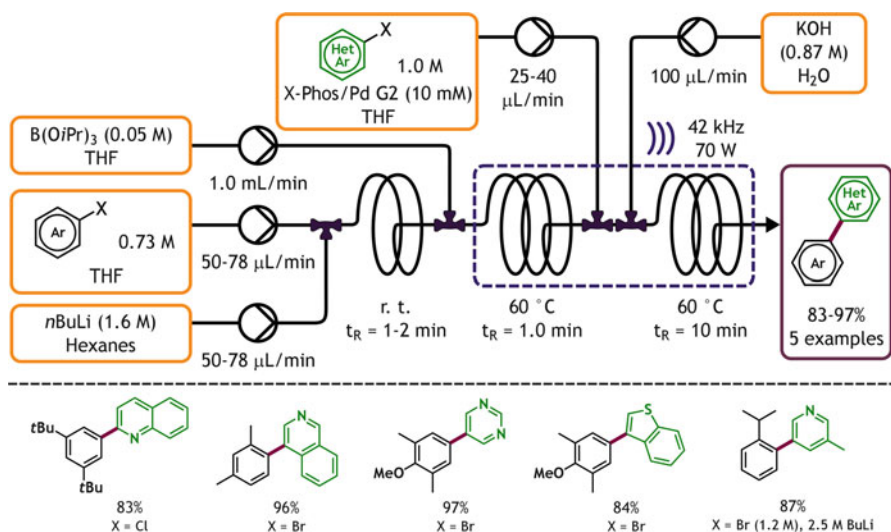
The aforementioned setup was also integrated into a more complex system, designed to carry out two-step synthesis of biaryls from readily available phenols instead of the more costly and less eco-friendly haloarenes (Scheme 19) [52]. This transformation was accomplished by first converting the phenols into corresponding



Scheme 19 Sequential triflation/Suzuki-Miyaura coupling (Noël et al. [52])

aryl triflates, which display excellent reactivity in the SMC reaction. The triflates were formed by combining a solution of triflic anhydride with a solution of a phenol and TEA in an externally cooled T-mixer, and completing the reaction in a PFA tube reactor at room temperature. Reaction was quenched with 2 M aqueous HCl in segmented flow mode and phases were separated by a selectively wettable thin porous fluoropolymer (Zefluor™) membrane. A backpressure regulator on the aqueous output was vital to stabilize the extraction process. The organic phase was then mixed with the solvents and reagents for the SMC step, conducted in the packed bed reactor, which also doubled as a second backpressure regulator. H₂O/EtOAc (1:1) was injected into the exiting stream to terminate the process and facilitate product extraction. Under optimized conditions, most heterocycles provided excellent yields, but, in comparison to the setup in Scheme 18, a more modest productivity of 1.2 mmol/h was achieved by this system. Unfortunately, only carbocyclic hydroxyarenes were tested and all heterocyclic products were formed solely from heterocyclic boronic acids. A similar idea based on in-line aryl iodide generation from corresponding anilines has also been realized by Teci et al. (see Scheme 8) [29].

The second generation Xphos palladacycle precatalyst also excelled at an opposite multistep approach with in-line generation of the boron reagent, effectively resulting in selective and efficient coupling of two aryl halides (Scheme 20) [53]. Boronate reagents were prepared by room-temperature lithium-halogen exchange and sequential quenching with dilute B(OiPr)₃ at 60 °C. Owing to outstanding efficiency of preceding reactions in flow, no in-line purification before the SMC step was necessary. However, the resulting boronate displayed poor solubility in every tested solvent, therefore, both borylation and SMC reactions had to be

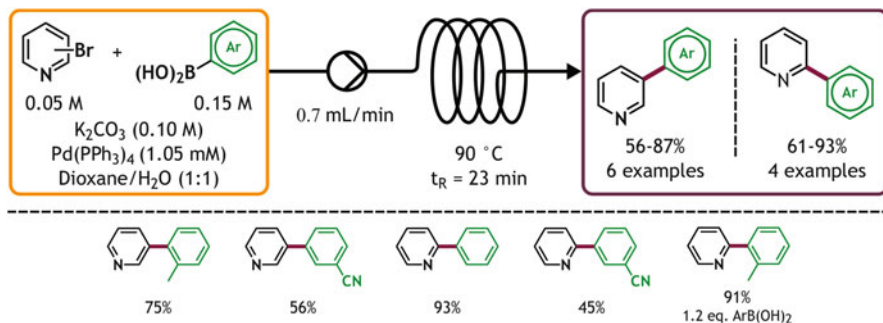


Scheme 20 Sequential lithiation/borylation/Suzuki-Miyaura coupling (Shu et al. [53])

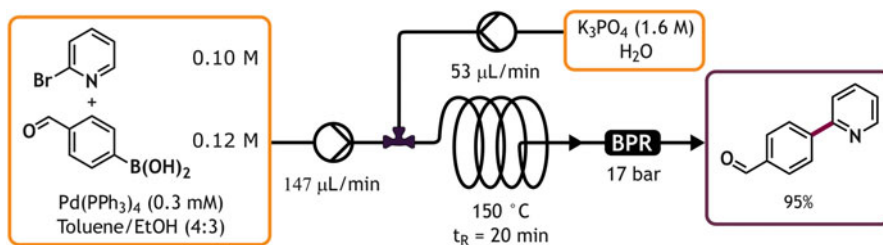
performed under ultrasonication. Induced cavitation not only did prevent clogging but also ensured sufficient mass transfer within the triphasic reaction mixture during the coupling step. Several heterocyclic haloarenes, among other substrates, were used as coupling partners to generate a library of heterocyclic biaryls in good to excellent yields at up to 2.4 mmol/h rate. Same conditions were also successfully applied for lithium-hydrogen exchange and further processing of five-membered heterocycles (see Scheme 75). Furthermore, haloarenes bearing reactive electrophilic groups have been successfully lithiated and borylated under ultrafast continuous flow by a different group, thus further expanding the reaction scope [54].

SMC reaction with heteroaryl halides in flow can also be performed using less exotic catalytic palladium sources. While attempts to use Pd(OAc)₂ for 2- and 4-Bromopyridine arylation gave unfavorable results, the reaction was successfully performed under completely homogeneous conditions in dioxane/H₂O using 3 eq. of boronic acid, 2.1 mol% of Pd(PPh₃)₄ and 2 eq. of K₂CO₃ [55]. In this case, a simple 1 mm I.D. PFA tube microreactor wrapped around a heated aluminum block was used (Scheme 21). It was noted, however, that full conversion in flow required 23 min compared to 20 min in batch under microwave heating, most likely owing to inferior heat transfer from the aluminum block to the flowing liquid. Steel tubing capable of providing better heat transfer negatively impacted the yield and was rejected after initial trials. The negative influence of different reactor material was not further investigated. While 1.2 equivalents of boronic acid were sufficient to obtain a good yield on several instances, most examples did require the full 3 equivalents, thus leaving the method open for further improvements.

An efficient Pd(PPh₃)₄ catalyzed coupling of 2-bromopyridine and 4-formylphenylboronic acid was accomplished by carrying the reaction out in a



Scheme 21 Pd(PPh₃)₄ catalyzed Suzuki-Miyaura coupling (Christakakou et al. [55])



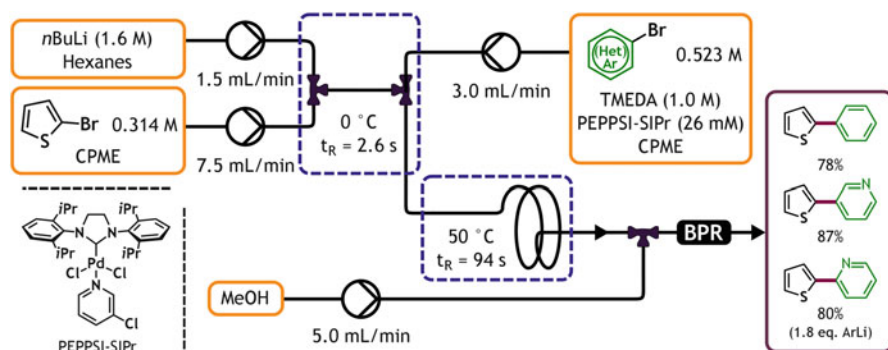
Scheme 22 Flow synthesis of Atazanavir's biaryl fragment (Dalla-Vechia et al. [56])

heterogeneous biphasic toluene/EtOH/H₂O (8:6:5) system [56]. Contrary to the report presented above, 0.3 mol% of catalyst and 1.2 equivalents of boronic acid were sufficient to achieve excellent yield in a 0.5 mm I.D. stainless steel tube reactor (Scheme 22). The narrow tubing also provided sufficient interfacial mass transfer to make a phase transfer catalyst and/or packed bed reactor completely irrelevant to the reaction outcome. Under optimized conditions, the target compound was obtained at a 1.2 mmol/h rate and satisfactory purity to be used in the subsequent step after phase separation. This homogeneous catalysis procedure, though specifically tailored for a single substrate pair, compares very favorably with each procedure described previously in this section, both in terms of efficiency with regard to each reactant and the simplicity of the system itself. Furthermore, in combination with consecutive continuous processing stages, it provided an improvement over the established batch protocol used for the synthesis of HIV protease inhibitor Atazanavir.

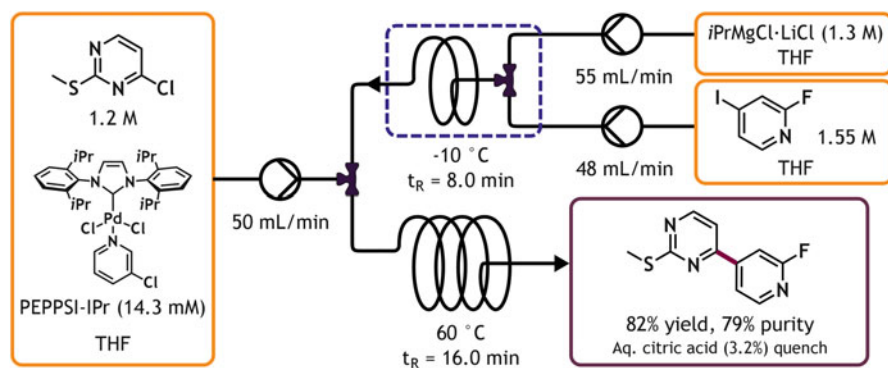
As was previously mentioned, boron reagent synthesis through lithiated intermediates is the most common route for their preparation. Therefore, Murahashi coupling – a direct, palladium catalyzed coupling of aryllithium with an aryl halide – could be said to provide a more direct and atom efficient access to products than SMC. Unfortunately, improper catalysts often prefer the competing coupling with the in situ generated butyl halide when *n*-butyllithium is used. However, pyridine stabilized *N*-heterocyclic carbene palladium precatalysts, dubbed PEPPSI (pyridine enhanced precatalyst preparation stabilization and initiation), are of comparable

effectiveness to Buchwald palladacycles at difficult couplings [57] and have been used in flow Murahashi coupling with moderate success (Scheme 23) [58]. Lithiation and subsequent coupling of unfunctionalized thiophene was also achieved in the same setup after switching to the more aggressive *s*BuLi. Notably, only aryl bromides were suitable coupling partners as chlorides were insufficiently active and iodides underwent partial halogen-lithium exchange before coupling could be completed.

A continuous approach was also used to successfully scale up a temperature dependent Kumada-Corriu reaction using an in-line generated unstable pyridylmagnesium halide (1.19 eq.) as one of the coupling partners and PEPPSI-IPr catalyst (1.19 mol%; Scheme 24) [59]. In batch, the cross-coupling gave the best results at 60 °C in spite of significant decomposition rate of the Grignard reagent at that temperature. It was therefore reasoned that the decomposition was less temperature dependent than the coupling reaction. This delicate balance of reactivity led to increasingly lowered and irreproducible yields during transition to 40 kg scale due to



Scheme 23 PEPPSI-SIPr catalyzed sequential lithiation/Murahashi coupling (Nagaki et al. [58])

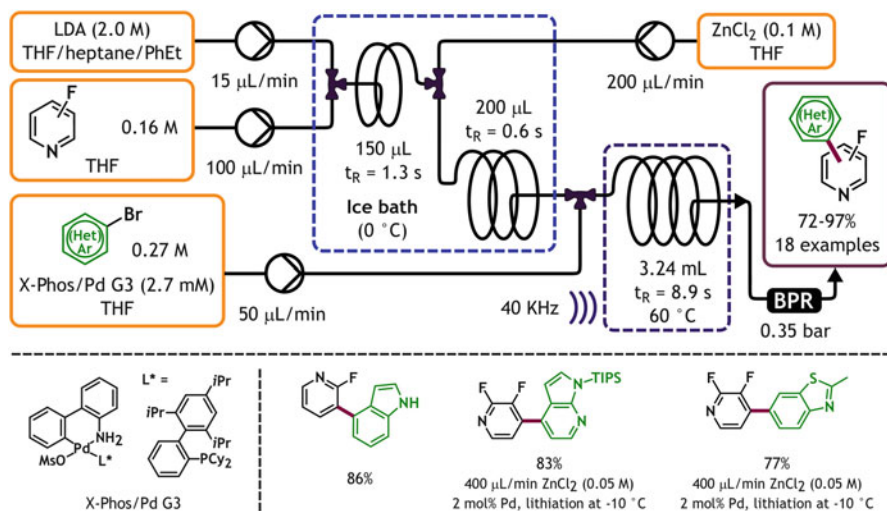


Scheme 24 Sequential magnesiation/PEPPSI-IPr catalyzed Kumada-Corriu coupling (Linghu et al. [59])

increased processing times and inferior heat/mass transfer. As expected, a two-step continuous process, where organomagnesium reagent stream was generated in a cooled tube reactor and then mixed with a stream of preheated coupling partner and catalyst to further react in a heated tube reactor, brought major improvements. Thus, it became possible to obtain consistent yields, comparable to the small scale batch experiments, even at 0.49 kg/h rate. The resulting crude product was pure enough to be used directly in the next steps towards an extracellular signal-regulated kinase inhibitor GDC-0944. In contrast, the same intermediate obtained via less demanding Suzuki-Miyaura coupling required extensive purification to ensure good reactivity.

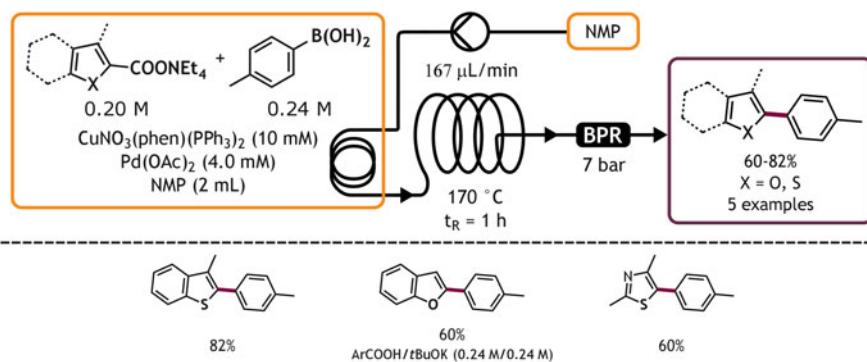
Direct lithiation of substituted aromatic rings is another atom-economical path to reactive organometallic cross-coupling reagents, that benefits from enhanced control of reaction conditions in flow [3]. Of course, the presence of a directing/activating group is necessary to accomplish this transformation with sufficient selectivity. As a directing group, fluoride is of particular interest, because it not only exerts adequate directing effect [60], but is mostly chemically inert and often imparts pharmacologically favorable properties onto biologically active compounds when substituted for hydrogen [61].

Knochel's group has reported several heterocycle flow lithiation-zincation-Negishi coupling protocols with extensive substrate scope, but the coupling step was always performed in batch by quenching the eluted organozinc reagent into the solution of the catalyst and the coupling partner [62, 63]. Roesner and Buchwald later developed an unprecedented telescoped method, which combines all three stages into a single continuous sequence (Scheme 25) [64]. It was found that LDA is sufficiently basic to fully metallate fluoropyridines, whereas fluorobenzenes require Schlosser's base for the same outcome. Stability of the heterocyclic intermediates was also greater as both metallation and transmetallation worked well at



0°C. With substituted fluorobenzenes, the zincation proceeded uneventfully, but coupling was plagued by clogging with zinc salt precipitate. The problem was considerably worse when LDA was used, with precipitation during both late steps. However, in either case it was mitigated by ultrasonic irradiation of the tube reactor and fine-tuning of concentrations and flow rates. To take full advantage of fast metalation, cross-coupling was facilitated by rapidly activating third generation Buchwald precatalyst. Bromide, chloride, and triflate coupling partners were sufficiently effective, independently of their electronic properties, and a vast fluorinated product library, including 27 regioisomerically pure heterobiaryls, was generated. More than half of the heterocycles were furnished in greater than 75% yield at greater than 1 mmol/h rate, with several pharmacologically relevant products among them.

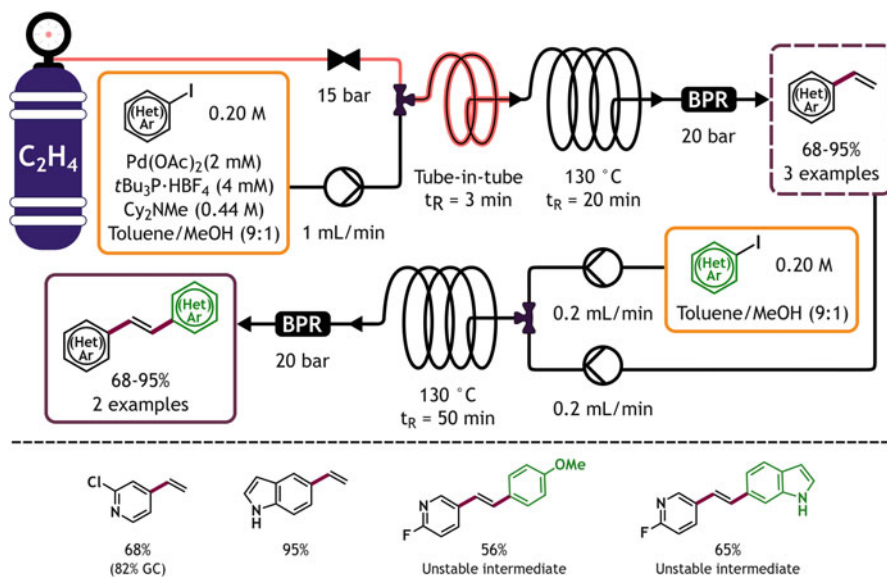
Biaryl formation via cross-coupling may also be achieved using readily available and stable aromatic carboxylates instead of laboriously prepared organometallic reagents (Scheme 26) [65]. In these cases, the reactive organometallic species is intermittently generated in situ by transition metal catalyzed decarboxylation, leaving only the relatively benign CO₂ as by-product. While outgassing of the reaction mixture might raise problems in batch, especially at larger scale, it is well handled in flow systems due to greatly reduced active zone volumes and increased temperature/pressure tolerance [66]. However, many carboxylates are poorly soluble in organic solvents, therefore extra effort is required to develop a suitable solvent-reagent system. Precipitation of salts during the reaction must also be avoided in order to keep the pressurized reactor from clogging. As evidenced by the report, good results are obtained using either preformed tetraethylammonium carboxylates or in situ generated potassium carboxylates together with aryl triflate coupling partners and plain Pd(OAc)₂ as catalytic Pd source. Under optimized conditions, several carboxylic acids based on five-membered heterocyclic scaffold can be coupled in good to moderate yields. It should be noted that, contrary to flow, extensive protodecarboxylation by *t*BuOH occurs when *t*BuOK is used to form the carboxylates in batch mode.



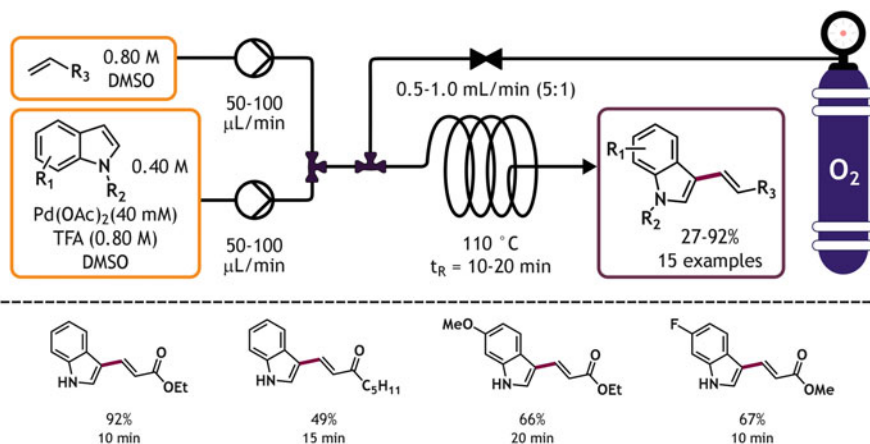
Scheme 26 Decarboxylative coupling under combined Pd (2 mol%) and Cu (5 mol%) catalysis (Lange et al. [65])

A second large group of C-C sp^2 bond forming reactions are aryl olefinations, out of which the Mizoroki-Heck coupling has been in the spotlight since its inception [67]. Unfortunately, the examples of heteroaryl olefination in flow are also scarce [6] and only a couple of reports are available at the time of writing. In one of these reports, Ley's group extensively described a Pd catalyzed aryl vinylation with ethene gas, introduced through a tube-in-tube device, assembled using commercially available Swagelok fittings, gas permeable Teflon AF-2400 inner tubing and regular PTFE outer tubing (Scheme 27) [68]. From the start, the catalytic system was tailored specifically towards working in homogeneous solutions and avoiding Pd black formation in order to evade the shortcomings of flow. A couple of 2-iodoheteroarenes did not display any reactivity during optimization and were discarded, but several other iodoheteroarenes were successfully vinylated under optimized conditions. Furthermore, the system was easily supplemented with a telescoped second coupling stage, ending in production of unsymmetrical stilbenes, including several heterocyclic examples. A different second stage, designed for rhodium catalyzed α -hydroformylation using CO/H $_2$ mixture was also described, but 2-vinylpyridine gave 2-ethylpyridine, therefore heterocycles were not further investigated. Regrettably, only iodides were reactive enough to give good conversions under indicated retention times.

Cross-dehydrogenative Heck coupling is a superior modification of the aforementioned reaction, as it bypasses the need of pre-functionalized aromatic coupling partners, greatly enhancing atom efficiency. Furthermore, it allows oxygen to be used for reoxidation of the catalyst, ending up with water as sole by-product. The



Scheme 27 Vinylation and unsymmetrical stilbene synthesis based on the use of tube-in-tube reactor (Bourne et al. [68])

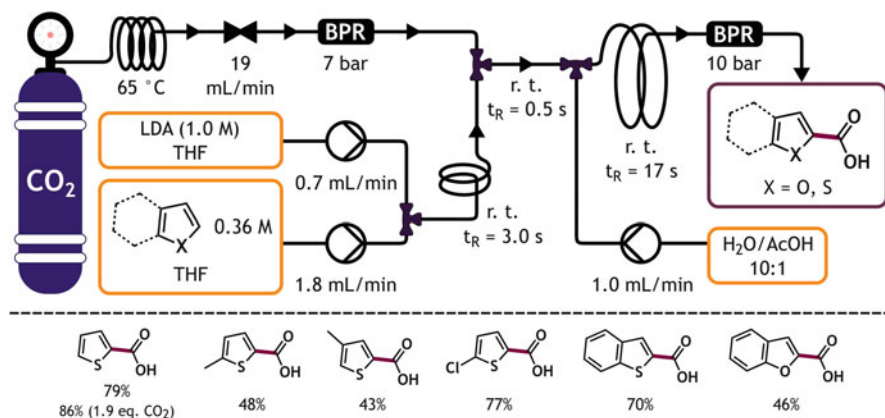


Scheme 28 Pd(OAc)₂ catalyzed dehydrogenative Heck coupling using gaseous oxygen for reoxidation of the catalyst (Gemoets et al. [69])

two-phase liquid–gas system of such reaction naturally points to segmented flow mode for optimal mass transfer and overall safety. Unsurprisingly, this idea has been developed into a 0.75 mm I.D. FEP tube reactor-based system for Pd catalyzed C-3 vinylation of NH-indoles, using DMSO as coordinating solvent to gain superb regioselectivity, and 2 eq. of TFA as catalyst activator/stabilizer (Scheme 28) [69]. Under optimized conditions, the reactor works well with acrylates and non-sterically hindered indoles, including *N*-methylindole. However, 2-methylindoles are problematic, showing sluggish reactivity, and non-activated alkenes afford significantly lower yields as well. Furthermore, a rather high catalyst loading of 10 mol% is necessary for good reactivity, partially negating the benefits of enhanced inherent atom efficiency. Nevertheless, it should be noted that this method provides access to pharmacologically relevant molecules, including a potential antitumor agent, at up to 2.2 mmol/h rate in an atom efficient manner.

3.3 Uncatalyzed Reactions

As demonstrated by Pieber et al. (Scheme 29), organometallic intermediates generated by lithiation can be directly used as nucleophiles instead of serving as feedstock to subsequent transmetalation and cross-coupling reactions [70]. According to the report, 1.1 eq. of LDA is sufficient to completely deprotonate thiophene and furan derivatives, giving soluble intermediates in the process. 1-phenylpyrazole, however, is incompatible due to poor solubility of the formed material. The amount of CO₂ is also best limited to near-stoichiometric (e.g. 1.1 eq.), as an increase to 1.9 eq. provides only marginal benefits. Interestingly, preheating of the gas may be vital for stable operation of the mass flow controller depending on the exact setup.



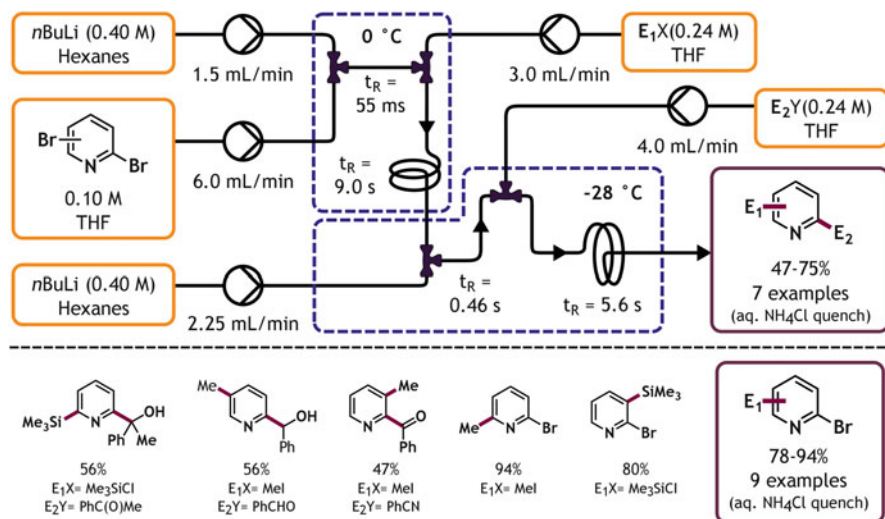
Scheme 29 Room temperature sequential direct lithiation/carboxylation (Pieber et al. [70])

Finally, quenching with pure water also causes clogging, therefore, $\text{H}_2\text{O/AcOH}$ mixture is preferred. Even then, the dissolution of formed precipitate is not instantaneous and some extra tubing has to be present prior to the backpressure regulator. Up to 40 mmol/h of starting material can be carboxylated using this method, but the reported yields do leave room for further improvements.

4 $\text{C}(\text{sp}^2)\text{-C}(\text{sp}^3)$ Bond Formation

By carrying the largest amount of substituents, sp^3 hybridized carbon atoms offer the greatest potential for structural variation. Furthermore, the available point chirality unlocks extended avenues for fine-tuning of molecular geometry at the expense of more elaborate synthetic methods. Although stereoselective synthesis is rather well established in batch, reactions that asymmetrically bind heterocycles to form new chiral centers are not well adapted to flow [71]. For non-stereoselective synthesis, organometallic compounds have been traditionally used as powerful C-Csp^3 bond-forming nucleophilic reagents. Therefore, as microreactor technology lends itself well to energetic reactions [2], it is not unexpected that a major group of transformations in this section is based on metalation and nucleophilic addition sequence.

Extreme reduction of residence time results in what are known as flash conditions that permit the practical use of intrinsically unstable molecules at otherwise prohibitively high temperatures. For example, 2,3-dibromopyridine can be lithiated and subsequently methylated in acceptable yields at room temperature if sufficiently short residence times are used [72]. Batch conditions, on the other hand, give lower yields even at $-78\text{ }^\circ\text{C}$. Eventually these findings evolved into a double sequential Br/Li exchange/electrophile capture protocol for selective disubstitution of dibromopyridines, providing products in moderate to good yields (Scheme 30).

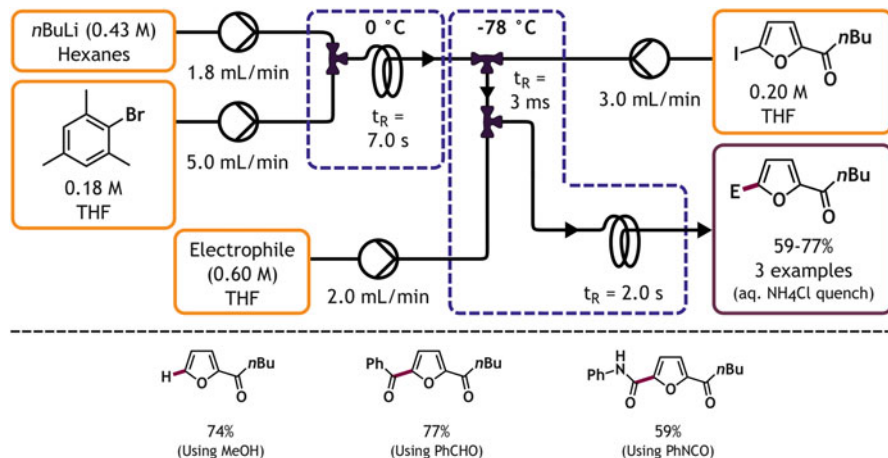


Scheme 30 Double lithiation/electrophile capture for difunctionalization of dibromopyridines in stainless steel microreactors. By omitting the third and fourth stage, monofunctionalization is achieved (Nagaki et al. [72])

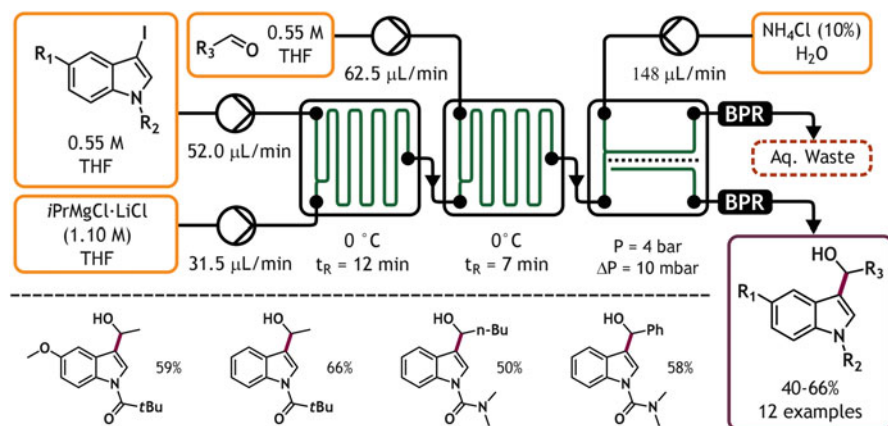
More importantly, the small scale system easily surpasses 17 mmol/h production rate without resorting to cryogenic cooling. Notably, the second pyridyllithium intermediate is more prone to side reactions, forcing to cool the second half of the system to a less convenient temperature of -28°C for optimal results. Even then it remains the major cause of reduced yield, as truncated setup provides monosubstituted products in good to excellent yields.

Application of cryogenic cooling under flash conditions offers further possibilities, such as allowing organolithium reagents to be generated from iodoaryl ketones and subsequently added to carbonyl, silicon, or tin electrophiles (Scheme 31) [73]. Such iodoarenes can be selectively lithiated with in-line generated mesityllithium, which emerged as the most effective reagent during preliminary studies. It is particularly surprising that mere two equivalents of electrophile are sufficient to quench both the formed organolithium reagent and the slight excess of mesityllithium, while still providing the products in up to excellent yields. Unfortunately, only a single heterocyclic substrate was addressed in the study. Later investigations have shown that iodoaryl nitriles and esters can also be successfully lithiated with regular alkylolithium reagents even at higher temperatures [54].

Less sensitive substrates permit the use of organometallic reagents at minute-scale residence times as illustrated by a fully automated method dedicated to the synthesis of 3-hydroxyalkylindoles (Scheme 32) [74]. To accomplish this transformation, 3-iodoindoles are first quantitatively converted into 3-indolylmagnesium chlorides under non-cryogenic conditions and then quenched with aldehydes. In this case the preference for Grignard reagents is explained by higher stability towards



Scheme 31 Use of carbonyl group-containing substrates in sequential lithiation/electrophile capture in stainless steel microreactors under cryogenic conditions (Kim et al. [73])

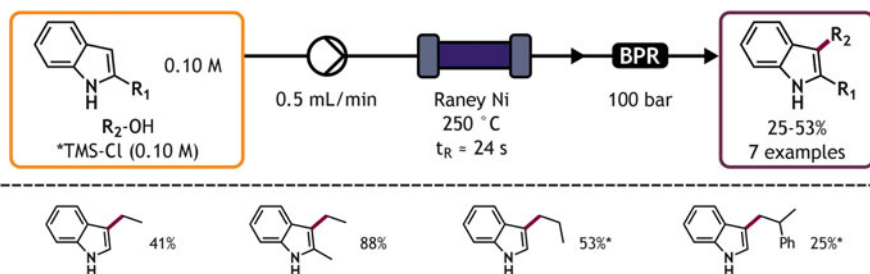


Scheme 32 Automated sequential magnesiation/hydroxyalkylation and extractive purification of 3-iodoindoles in microchip reactors using Syrris Africa flow system (Tricotet and O'Shea [74])

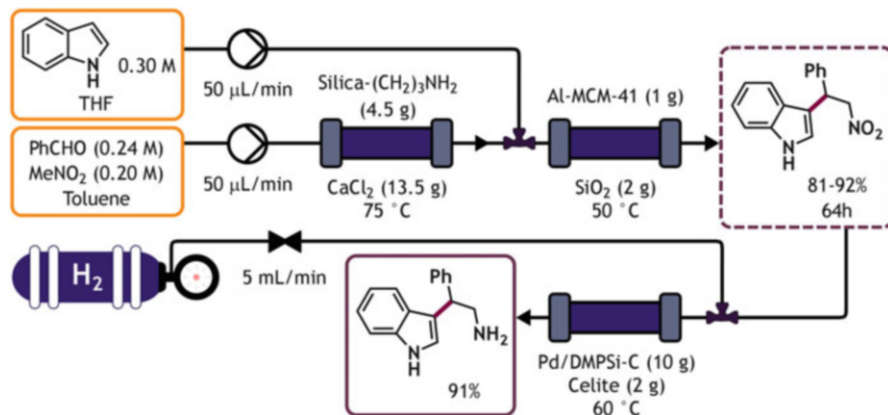
isomerization in comparison to lithiated counterparts. Further flow synthesis of methoxy or allyl derivatives from isolated 3-hydroxyalkylindoles via indolium ion formation under acidic conditions is also demonstrated in the work. In each case, continuous purification is implemented as the last step, either using liquid–liquid extraction chips or scavenger resins. However, only the methoxy derivatives are produced in nearly quantitative yields, while additional purification by column chromatography is mandatory after initial hydroxyalkylation as well as subsequent allylation. Therefore, the 3-hydroxyalkylindole synthesis cannot be directly coupled to either methylation or allylation step in a straightforward manner, preventing the development of a single continuous process.

Reactive organometallic intermediates can be avoided altogether when sufficiently active heterocycles are used. Illustrating this, several following methodologies are based upon the innate nucleophilicity of indole scaffold, which is often embedded in biologically active products. In one case, Raney Ni catalyzed indole 3-alkylation by alcohols is presented (Scheme 33) [75]. Under sufficiently high temperature and pressure, no pre-functionalization or additional substances are required for the direct alkylation, leaving water as the only by-product. However, temperature dependent *N*-alkylation and 1,3-dialkylation of unsubstituted indole is also observed. When optimized, the system displays moderate, but nearly constant performance for 24 h with ethanol as solvent/reagent. Transient *N*-TMS protection was found to enhance selectivity at the expense of atom economy, while 2-methylindole intrinsically favored 3-alkylation. Furthermore, *N*-alkylation with concomitant reduction of heterocyclic ring was the dominant reaction pathway for quinolines. Also, the method is limited to primary and secondary alcohols that are susceptible to dehydrogenation [76].

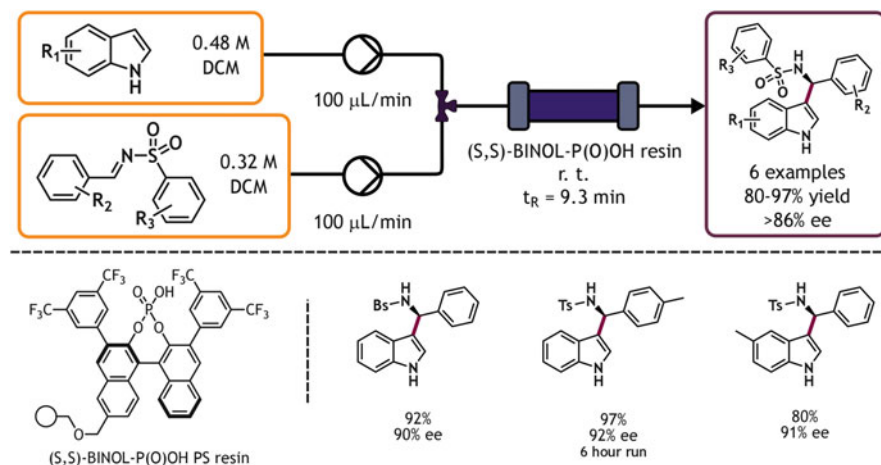
Ishitani et al. presented a highly modular system for heterogeneously catalyzed synthesis of various nitro-containing compounds from β -nitrostyrenes, which are prepared via prior in-line Henry condensation (Scheme 34) [77]. To obtain the target nitro compounds, nitrostyrenes are subjected to conjugate addition without prior purification. The exact reaction at this stage is determined by the substrate and the installed catalyst cartridge, therefore, an array of vastly different products can be generated. For example, aluminum-containing mesoporous silica MCM-41 catalyst enables α -addition of indole to β -nitrostyrene in excellent yield and selectivity. The whole system retains sufficient performance for 64 h, generating ≈ 38 mmol of product in the process. Furthermore, instead of being isolated, the nitroalkane can be further reacted with hydrogen in a downstream Pd/DMPSi-C cartridge to afford an aminoalkane product, also in excellent yield. The scope of conjugate addition reactions was investigated only with β -nitrostyrene as the acceptor, but the authors have demonstrated successful flow preparation of other nitroalkenes and do not exclude their possible application in this system.



Scheme 33 Raney Ni catalyzed indole alkylation under high temperature and pressure using combined ThalesNano H-Cube Pro™ and ThalesNano Phoenix™ reactors (Sipócz et al. [75])



Scheme 34 Sequential Henry condensation/acid-catalyzed nucleophilic addition of indole and optional sequential hydrogenation (Ishitani et al. [77])



Scheme 35 Immobilized phosphoric acid-catalyzed stereoselective imine indolylolation. Bs = benzenesulfonyl (Osorio-Planes et al. [78])

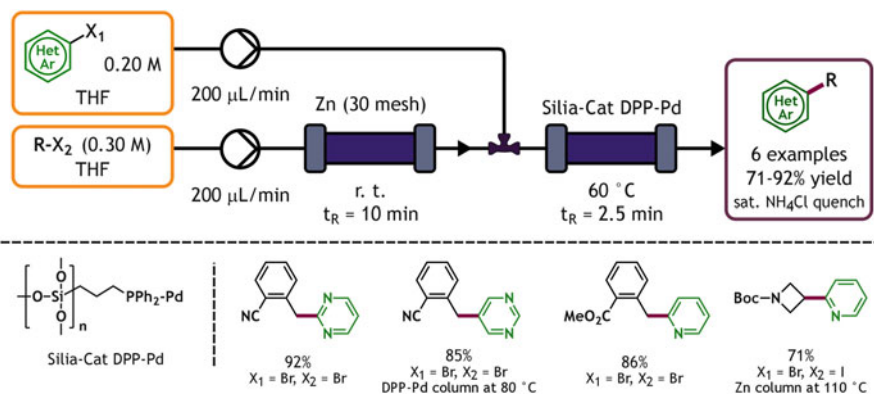
Acid-catalyzed nucleophilic addition of indole was also investigated for production of 3-indolylmethanamines (Scheme 35) [78]. In this case, polystyrene-bound BINOL-derived chiral phosphoric acid catalyst was used to promote an asymmetric attack on aromatic *N*-sulfonylketimines with marked stereoselectivity. During batch experiments, the resin proved to be highly recyclable and could be reactivated by washing with EtOAc/HCl when a decline in performance was noted. Transfer from batch to flow conditions resulted in 12-fold increase of turnover number, translating into 4.3 mmol/(h·g_{resin}) productivity. Several substrate combinations encompassing all three possible levels of diversity were investigated, generating a small library of

substituted 3-indolylmethanamines. Notably, all flow experiments, including preliminary optimization, library generation, and an extended 6-h run, were performed using the same 360 mg resin cartridge without deterioration of activity. Furthermore, the catalyst contains both Bronsted-acidic and Lewis-basic reaction sites, capable of cooperative action. Therefore, it could be suitable for other transformations as well.

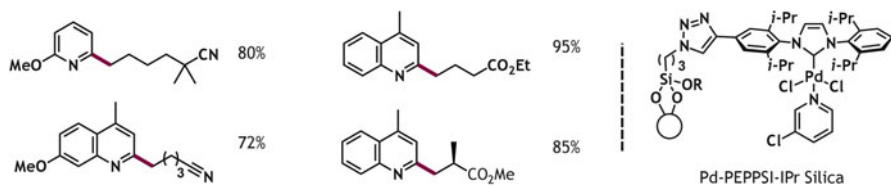
Similar reaction converts aldehydes into bis(indolyl)methanes if two equivalents of indole are available. In the presence of $\text{Sc}(\text{OTf})_2$ (5 mol%), this transformation has been shown to work nearly independently of the electronic properties of both substrates, offering target compounds in mostly good to excellent yields at room temperature [79]. The only advantage over previously reported batch conditions, however, is the reduced reaction time that results from increased reagent concentrations and a better optimized solvent.

Out of transition metal-catalyzed cross-coupling reactions the Negishi coupling has been the preferred approach to C-Csp^3 bond formation so far [80, 81]. This preference also extends to flow chemistry, where the whole organometallic cross-coupling reagent toolbox is virtually reduced to zinc-based coupling partners. In the seminal paper, SiliaCat[®] DPP-Pd was used to catalyze methylation of haloarenes, including substituted bromo- and chloropyridines, with commercially available diethylzinc, resulting in moderate to good yields with the heterocyclic substrates [43]. The same catalyst was also used for flow zincation/Negishi coupling sequence where several brominated heterocycles, among other substrates, were alkylated with in-line prepared zinc reagents in good yields (Scheme 36) [82]. Importantly, the zinc reagents were generated in-line from appropriate halides and metallic zinc after sequential preactivation with TMSCl and 1,2-dibromoethane. In both reports, the coupling step was complete within 3 min at 60°C . Furthermore, 1 g of the catalyst ($\text{Pd} \geq 0.20$ mmol/g) was sufficient to transform at least 43 mmol of starting material over 13-h interval, indicating the method's applicability on development scale.

In a more recent report, in-house prepared, Pd-PEPPSI tethered silica gel was investigated as an alternative catalyst for the Negishi reaction (Scheme 37) [83]. As



Scheme 36 Direct zincation by metallic zinc and subsequent Negishi coupling (Alonso et al. [82])

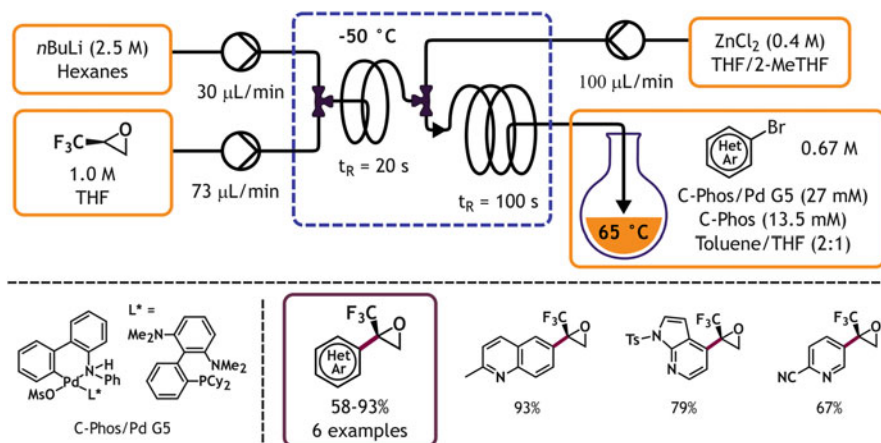


Scheme 37 Structure of the Pd-PEPPSI-IPr tethered silica and selected examples of room temperature Negishi coupling products. $t_R = 10$ min (Price et al. [83])

expected, the high intrinsic activity of the free complex was retained in the functionalized material. According to the findings, the catalyst containing 0.21 mmol/g Pd is amply active to couple heteroaromatic chlorides even at room temperature. On the other hand, the highest exhibited productivity under these conditions was about 1/3 of the SiliaCat[®] DPP-Pd and a steady decline of conversion was observed after processing about 7 mmol of substrate per gram of catalyst. The loss of activity is caused by gradual reduction of palladium content due to leaching, promoted by the excess of organozinc reagents and possibly further exacerbated by coordinating heterocyclic substrates/products. As a consequence, the method is not universal, but rather limited to coupling of unreactive aryl halides that are incompatible with the previously discussed catalyst.

Several reports covering lithium-hydrogen exchange and simultaneous transmetalation in the presence of Zn, Mg, Cu, or La halides in flow, followed by trapping with electrophile in batch are available [62, 63]. In the presented cases, the heterocyclic organometallic reagents are used either as coupling partners for arylation or as carbon nucleophiles for allylation or addition to aldehydes. Closely related method is developed for the synthesis of α -organozinc reagent from enantiopure trifluoromethyloxirane and its coupling with haloarenes in good yields and with retention of absolute configuration (Scheme 38) [84]. In this case, the steric bulk and poor nucleophilicity of the zinc reagent impedes further transmetalation onto palladium, therefore highly reactive catalysts, such as Buchwald palladacycles, are mandatory. The best performance is offered by the *N*-arylated fifth generation palladacycle, while the *N*-methylated fourth generation palladacycles are inferior even to their preceding unsubstituted counterparts. In spite of the best available catalyst, 4 mol% loading together with an additional 2 mol% of ligand is necessary to obtain good yields of heterocyclic products. These can then be further used to generate enantioenriched trifluoromethylated alcohols.

Direct trifluoromethylation of heteroarenes has also been investigated in continuous flow. Of all fluorinated pharmaceutical structures, trifluoromethyl groups are the most prevalent functionalities, because of their unique electronic behavior and metabolic stability. The installment of trifluoromethyl groups has been a topic of much attention in the last decade. Among the most common methods to accomplish a new $C(sp^2)$ -CF₃ bond is the use of a nucleophilic CF₃ source in combination with a transition metal catalyst [85]. Common nucleophiles are gaseous reagents like CF₃I, trifluoromethylsilanes or preformed organometallics like CuCF₃. Although many of

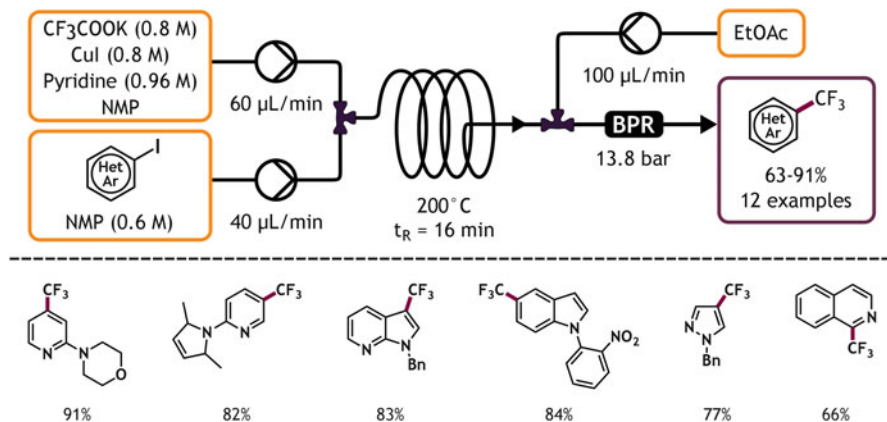


Scheme 38 Sequential flow lithiation/zincation of trifluoromethyloxirane combined with batch Negishi coupling of the organozinc reagent (Zhang and Buchwald [84])

these protocols work well, there is still room for improvement with regard to precursor availability, safety, and cost.

Chen and Buchwald addressed this challenge by using the cheap potassium trifluoroacetate salt in a flow setup to furnish trifluoromethylated arenes in minutes [86]. Although the use of trifluoroacetate for this transformation has precedence, previous methods often required large excesses of the salt and led to product mixtures [87]. Since the decarboxylation step requires high temperature, but also leads to pressure increase, continuous mode synthesis could mitigate these would-be complications at a process scale. During prior batch experiments it was found that at 200 °C two equivalents of both CF_3COOK and CuI rapidly delivered the $[\text{CuCF}_3]$ species which transformed the substrate in good yields. The last obstacle to adapt this protocol to flow was the poor solubility of the CuI salt. Fortunately, addition of pyridine as a ligand worked fruitfully. With this set of conditions a wide variety of heteroarenes were trifluoromethylated including some pharmaceutically relevant scaffolds like trifluoromethylpyrazoles, which are otherwise reluctant to engage in coupling reactions (Scheme 39).

The group of Kappe approached the same transformation from a different angle. Inspired by some recent advances in radical trifluoromethylation, like the sulfinato-Minisci reaction, or photocatalytic procedures using trifluoroacetic esters, CF_3I or $\text{CF}_3\text{SO}_2\text{Cl}$ [88], they set out to use perfluoroalkyl iodides as the source of radicals under Fenton conditions [89]. This approach was not new in itself, since alkyl iodides had been previously shown to deliver alkyl radicals when combined with a peroxide in the presence of Fe(II) [90]. However, due to the rapid nature of the reaction, careful dosing had to be performed in batch mode by slow addition of the peroxide. Continuous flow was the element of innovation towards achieving good control over this reaction. By combining a DMSO/MeCN solution of the arene, sulfuric acid, and catalytic FeSO_4 , together with a H_2O_2 30% solution stream, they

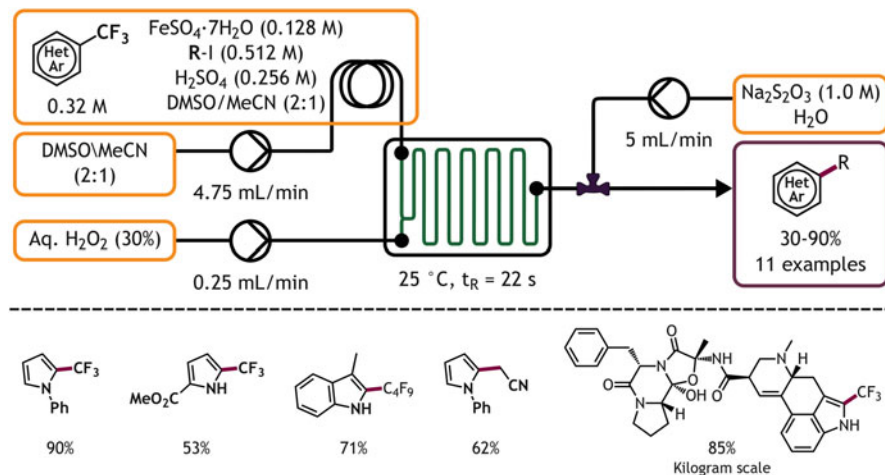


Scheme 39 Copper-catalyzed trifluoromethylation of iododienes using trifluoroacetate salt (Chen and Buchwald [86])

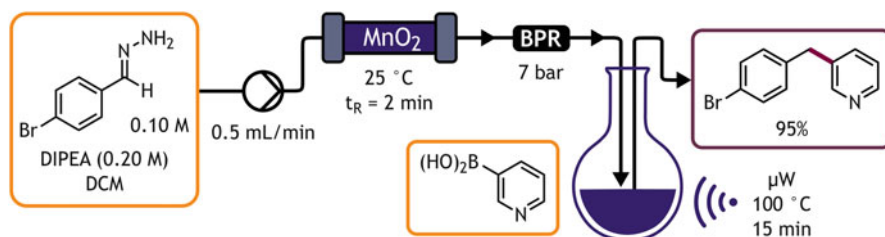
found that the desired product was formed in good yields within residence times as low as 100 ms. In-line quench with $\text{Na}_2\text{S}_2\text{O}_3$ ensured that the reaction did not continue undesirably. The rest of the scope was performed flowing through a ChemTrix microreactor for 22 s, with similar effectiveness. This way, several pyrroles and indoles were functionalized using not only trifluoromethyl iodide, but also nonafluorobutyl iodide, iodoacetonitrile, or ethyl iodoacetate as suitable radical precursors (Scheme 40).

In an innovative transformation of phenylhydrazones into α -substituted toluenes, Ley and coworkers demonstrate yet further advantages of flow chemistry [91]. Interested in the reactivity of diazo compounds, they exploited their unstable character to generate good yields for nucleophilic attack under mild conditions, which posed a significant challenge. Previous reports had used the safer tosylhydrazones, but these necessitated strongly thermal conditions to generate the diazo structure effectively, which was found to be the limiting step. To address this issue, continuous mode was opted to transform starting hydrazine to the transient diazo intermediate, which was reacted directly at the outlet. The generation was accomplished with a MnO_2 cartridge as a means of administering excess oxidant (Scheme 41). However, initial experiments yielded sluggish diazotation, as was quite accurately monitored with in-line IR spectroscopy. Activated MnO_2 displayed an improvement, but hydration still remained the major pathway, producing benzaldehyde. Only when the column was preconditioned with a hydrazone solution, was a high conversion to the diazo compound observed.

With a good generation method in hand, the diazomethane derivative was first captured with an acidic oxygen sources like carboxylic acids or phenols to furnish benzylic esters and ethers. Perhaps more interestingly, treatment of the reactive species with a boronic acid at room temperature yielded insertion of the diazomethane carbon into the C-B bond, which delivered several diarylmethanes



Scheme 40 Radical trifluoromethylation of azoles under Fenton-type conditions (Monteiro et al. [89])



Scheme 41 Phenyldiazomethane formation (after prior MnO_2 conditioning) and subsequent interception with pyridylboronic acid (Tran et al. [91])

and vinylarylmethanes after acidic protodeboronation. 3-pyridineboronic acid also reacted very well, albeit at higher temperature. One load of MnO_2 sufficed to produce 2 mmol of the desired product in 40 min reaction time. Moreover, the spent reagent could be regenerated with TBHP as the oxidant. The same authors further exploited this methodology later on by using the pinacol-trapped transient boronic acids and performing sequential interceptions with up to three diazo compounds [92].

5 C-N Bond Forming Reactions

Heteroaromatic rings bearing nitrogen substituents are extremely prevalent motifs in pharmaceutically active molecules, including some of the body's own coenzymes and nucleotides. The additional heteroatom on the ring typically enlarges the molecule's capacity to undergo non-covalent interactions with its host.

The ability to directly install a new C-N bond onto the ring system, avoiding a *de novo* synthesis of the corresponding aminated heterocycle, comprises a very important part of the medicinal chemist's toolbox.

C-N bond forming reactions described here are categorized in the following classes: nitration reactions, nucleophilic substitutions, C-N bond formation arising from rearrangements and transition metal catalyzed coupling reactions.

5.1 Nitration

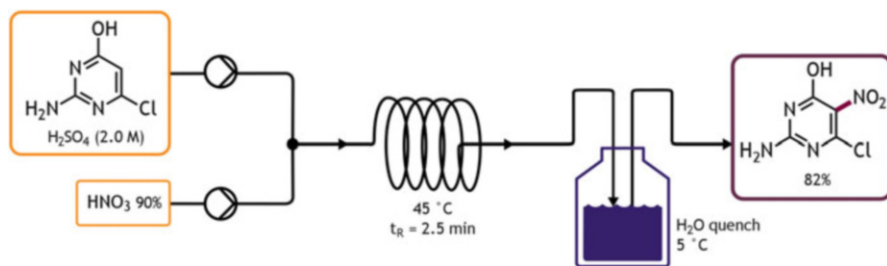
The installment of a nitro group onto an aromatic ring is an essential transformation which has been reported as early as 1834. With the discoveries in the 1850s of the nitrobenzene to aniline reduction, and of aniline *mauve* as a breakthrough synthetic dye, production of nitroarenes skyrocketed. In the twentieth century, nitrated heteroarenes such as nitrofurans and other nitroazoles or thiophenes have found their way to the dyestuff or pharmaceutical industry as valuable starting materials. Up to this date, the electrophilic aromatic nitration remains the single most important entry to anilines and other aminoheterocycles [93].

The production method has remained relatively unchanged since the 1830s. Fuming nitric acid, typically acquired by mixing nitric and sulfuric acid, still stands as the NO_2^+ source which undergoes attack from the aromatic ring. Although these conditions are hazardous enough on their own, elevated temperatures are not rarely needed for electron-poor systems such as azines. Since nitration reactions are exothermic in nature, tedious precooling of the nitration mixture is usually required, as well as rigorous temperature control of the reaction itself, making it an undesirable process to scale up.

A fully continuous process therefore warrants an almost ideal alternative from a process point of view. Narrow temperature control and superior mixing ensure a fast and chemoselective reaction, whereas the low concentration of actual nitrating acid mixture completely averts runaway events. A continuous manufacturing for simple arenes like benzene [94–97] and toluene [95, 98–101] has been widely described, as well as salicylic acid [102], phenol [103], benzaldehyde [104], and some other aromatics [105–109]. These processes have been reviewed before [110, 111], and herein we will focus our attention on the flow nitration of heteroarenes.

De Jong et al. indeed describe this predicament in the synthesis of the potent PNP inhibitor CI-972 [112]. Not only does the 2-amino-4-chloro-6-hydroxypyrimidine require heating for the nitration to work, they observe a concomitant decomposition of the material starting from 70°C, with a ferocious exotherm of 2,500 K/min at 91°C. In order not to be limited to batches of 20 L, they opted for a continuous process.

A stream of the pyrimidine in concentrated sulfuric acid was mixed with an inlet of 90% nitric acid, which was run through Teflon tubing in a 45°C water bath and eventually quenched in a cold water vessel (Scheme 42). With an optimum reaction time of 2.5 min, they were able to completely suppress the dinitration side product while at the same time having no starting material left. The precipitate was then



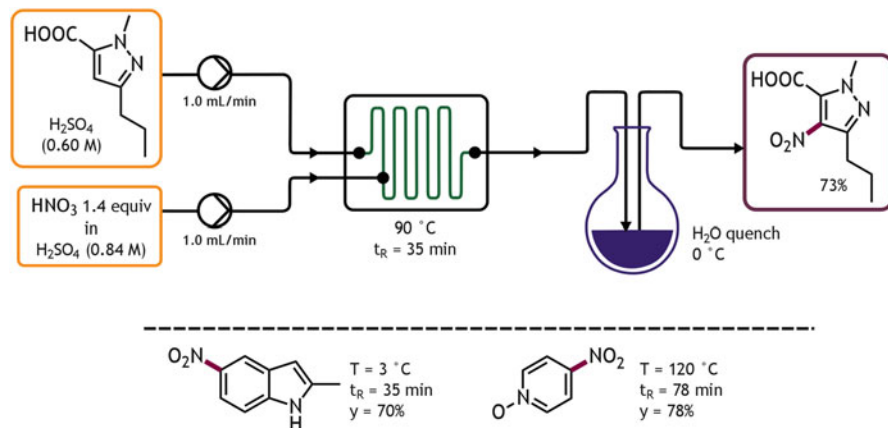
Scheme 42 Large scale continuous nitration of an aminopyrimidine (De Jong et al. [112])

turned into its diisopropylamine salt in *i*PrOH. Using these optimized conditions, they were able to produce 77 kg of the desired salt in over 96% purity with a reaction time of only 7 h.

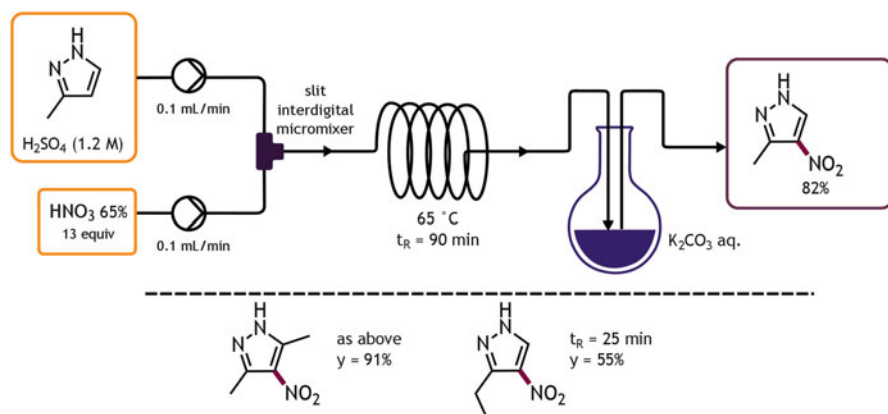
A report by Panke et al. describes their experience with a microreactor setup [113]. The custom designed CYTOS stainless steel flow chip with built-in pressure and temperature sensors allowed excellent control over the relevant parameters [114]. Because of the submillimeter dimensions, mixing and heat exchange become very efficient, thus making it an alluring arrangement for otherwise hazardous and highly exothermic reactions like nitrations. An interesting case study of this type was the pyrazole intermediate in the synthesis of Sildenafil. The electrophilic nitration of the pyrazole 3-carboxylic acid starting material is notoriously delicate: a narrow range around 90 °C is necessary for full conversion and good chemoselectivity. Spontaneous decarboxylation starts from 100 °C onward, posing yet another process hazard due to pressure build-up. These considerations make the batch production of the nitropyrazole a very tedious undertaking, and should therefore turn the operation quite amenable to continuous flow conditions.

By switching optional residence time units (RTU) on or off, the reaction time could be selected which in this case was 35 min (Scheme 43). The temperature was accurately kept at 90 °C, and under unoptimized conditions the desired product was obtained in 73% yield (prior art in batch: 75%). To further prove the usability of the reactor, the electron-rich 2-methylindole was nitrated in continuous mode. While the reported batch process requires lengthy precooling of the NaNO₃/H₂SO₄ mixture, a first attempted translation to flow at strictly 3 °C furnished 70% of the nitroindole after only 0.8 min residence time. Lastly, also pyridine N-oxide could be uncomplicatedly nitrated using the HNO₃/H₂SO₄ mixture at 120 °C, with an improved yield of 78%.

Another microreactor for efficient nitration was developed by Pelleter and Renaud [115]. A carefully chosen stainless steel coil served them well as a corrosion-resistant reactor, but the key innovation was the interslit digital micromixer which was implemented directly before. Herein, micrometer-sized channels realize a highly efficient mixing of the sulfuric acid and nitric acid streams, similar to microfluidic devices but with an overall more modular setup and higher throughput.



Scheme 43 Nitration of a Sildenafil precursor (Panke et al. [113])



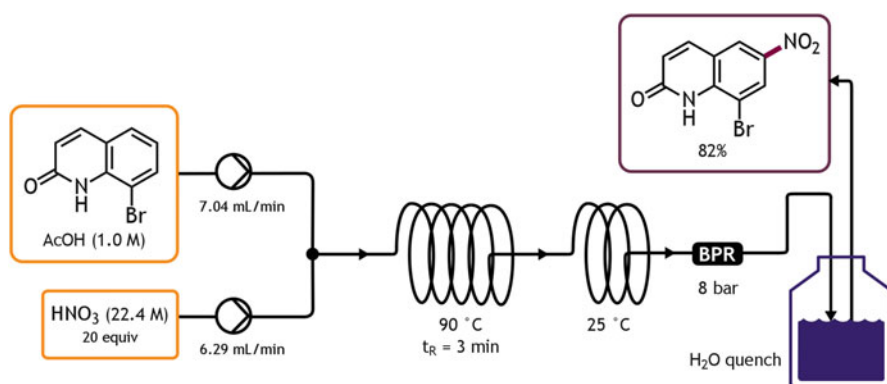
Scheme 44 Continuous nitration of different alkyldiazoles (Pelletier and Renaud [115])

Starting from an in-house need for 4-amino-3-alkylpyrazoles, different 3-alkylpyrazoles were selected as useful substrates for the aromatic nitration (Scheme 44). Having learned from previous work on pyrazole nitration and associated problems (dinitration, exothermic decomposition), it was found that this transformation could be done much more safely and mildly under continuous flow conditions. A mere 65 °C sufficed for complete conversion, while the narrow temperature range ensured an entirely chemoselective mononitration. Excellent conversion was obtained for 3-methylpyrazole when a residence time of 90 min at 0.2 mL/min was sustained, yielding 88% 3-methyl-4-nitropyrazole at a rate of 0.82 g/h.

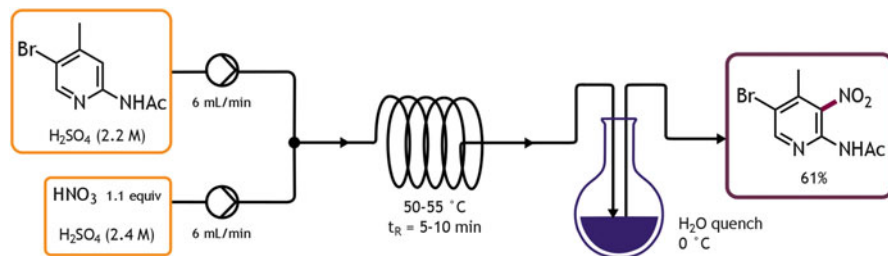
Although microfluidic chips or micromixers have demonstrable benefits for certain challenging nitrations, in other cases they can be omitted without any

diminished outcome. A team of Novartis scientists validated this two-pumps-and-some-tubing approach for the large scale synthesis of 8-bromo-6-nitro-1*H*-quinolin-2-one [106]. The Med Chem route towards this building block comprised a batch nitration in acetic acid/nitric acid mixture at 115°C. DSC measurements of the reaction mixture showed a strong exotherm from 105°C onward, partially explained by the explosiveness of acetyl nitrate. Therefore, it was reasoned that this protocol should benefit greatly from a continuous production, especially since the reaction can be manually or automatically stopped when temperature should get out of control. After some initial tests, they found that a 20-fold excess of nitric acid at 90°C could realize full conversion in only 3 min (Scheme 45). By increasing the reactor coil volume to 40 mL, followed by a 10 mL cooling coil, the flow rate could be raised to 13.3 mL/min, so that 201 g of the desired material was obtained in 86% yield and high purity, in approximately 2 h.

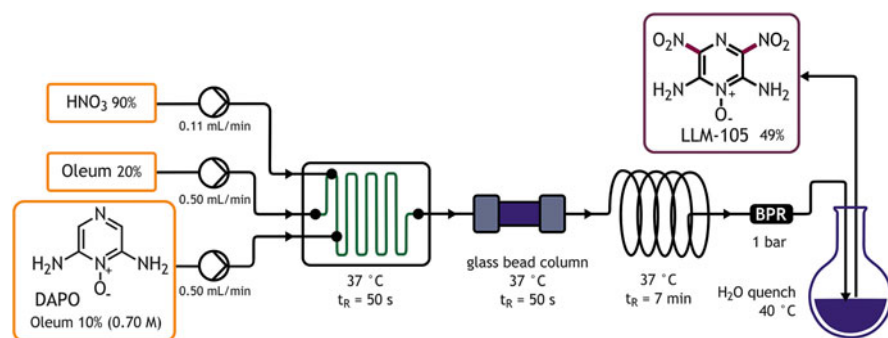
On a similarly large scale, the nitration of 2-acetamido-5-bromo-4-methylpyridine was established by an industrial team from Asymchem [116]. This multisubstituted pyridine could subsequently be engaged in the synthesis of nucleoside analogs as potential antimetabolite pharmacophores [117]. The challenge for this substrate was the decomposition which occurred from 80°C onward in nitric acid, and the side reaction where the 2-hydroxy species was formed after oxidation. The authors overcame these hurdles by using a continuous flow setup. The amount of HNO₃ proved rather delicate, although with adjustment of the feed rate, the batch yield of 55% could be increased to 61% isolated yield in good purity (Scheme 46). Translating this exact procedure to larger tubing did not give equally good results, unfortunately. Using a N₂ pressure on the feed vessels rather than pumps to insert the reactants allowed to handle the somewhat viscous streams at the inlets more reliably. Using this modified protocol, 36.5 kg of the desired nitropyridine could be produced in 2.5 days, in high purity and 50% yield.



Scheme 45 Flow nitration of the useful intermediate 8-bromoquinolin-2-one (Brocklehurst et al. [106])



Scheme 46 Flow preparation of a multisubstituted nitropyridine (Gage et al. [116])



Scheme 47 Microfluidic dinitration in the synthesis of secondary explosive LLM-105 (Zuckerman et al. [118])

Also the synthesis of nitro-containing energetic materials could clearly benefit from a drastically safer continuous manufacturing. In their efforts to investigate the properties of LLM-105 as a useful secondary explosive, the group of Zuckerman preferred a microreactor route for the multigram synthesis of this material [118]. Starting from the pyrazine DAPO, a double nitration was necessary to obtain the desired material. The batch process required the use of pure nitric acid in 10% oleum, since the presence of water was believed to aid several gas-evolving decomposition pathways. However, preferring to work with 90% nitric acid instead, it was found that with the shortened reaction times typical to flow chemistry, these side reactions could be avoided, and switching to 20% oleum ensured sufficient dehydration (Scheme 47). These two streams were then combined with an oleum solution of DAPO in a microchip reactor for highly efficient mixing, prolonged with a tubular reactor. With a residence time of only 9 min at $37\text{ }^\circ\text{C}$, they were able to produce 17.2 g of analytically pure LLM-105 (49% yield, comparable to the batch method). A key discovery to attain such high purity was the quenching temperature of $40\text{ }^\circ\text{C}$, which guaranteed the decomposition of any oxamide impurities.

5.2 Nucleophilic Substitution

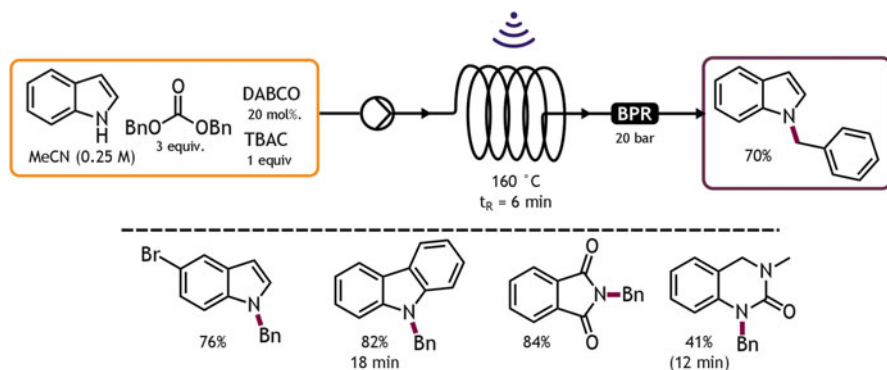
Nucleophilic substitution reactions make up another entry to new C-N bonds. The reaction between a nucleophilic amine with a carbon electrophile comprises an often efficient and reagent-economic functionalization. On a first level, the nitrogen from an azole-type heteroarene can act as a nucleophile towards, e.g., alkyl halides to form a new C-N bond. The general class of electrophile reactions with amines has been identified as one of the ten most common synthetic steps found in recent literature, even making it to 5th rank when considering production scale alone [119].

Secondly, and perhaps even more prevailing (third most commonly employed process step), is the nucleophilic aromatic substitution (S_NAr) onto a haloarene. Where this transformation with carbocycles is typically limited to electron-poor fluorobenzenes, the cards are different with, e.g., azines, whose diminished aromaticity and generally electron-poor character allows C-Cl bonds to be efficiently substituted.

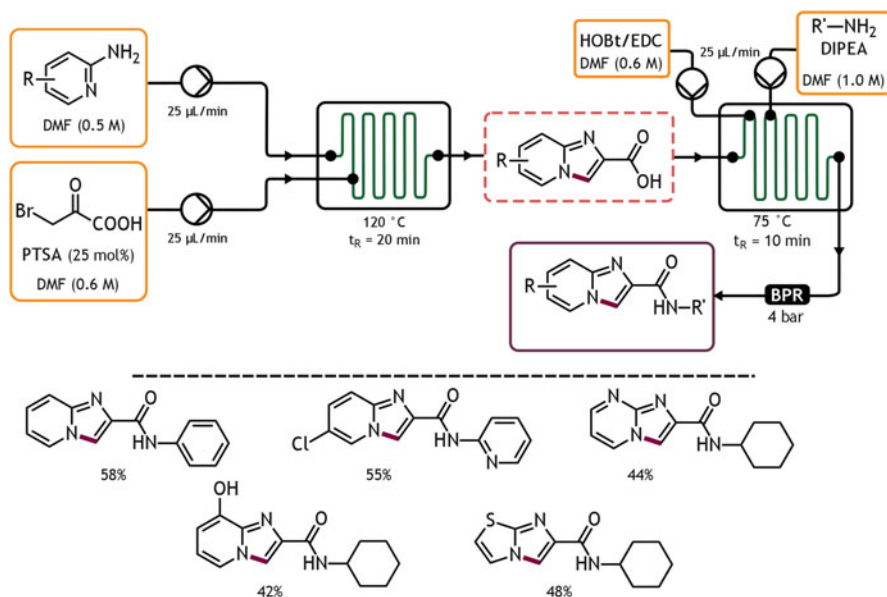
Also for these omnipresent and thermophilic C-N bond forming reactions, microreactor technology offers some benefits. Following what Kappe and coworkers coined the “microwave to flow paradigm,” flow chemistry offers a means to apply heat very locally and efficiently, so that reaction times can typically be shortened and even superheating of solvent becomes possible. Moreover, solubility is usually not an issue since organic bases can often be used, the salts of which being more soluble in the liquid phase. Some examples will be discussed wherein a new C-N bond is attained under continuous flow conditions by means of nucleophilic substitution onto a carbon center, limiting the scope of this overview to new bonds on the heteroaromatic ring itself.

Shieh et al. reported an early example of *N*-alkylations using flow techniques [120]. In a previous work, they disclosed dibenzyl carbonate (DBC) as a low-toxicity alternative to benzyl halides, although the reaction conditions gave very sluggish conversion for some indole-like nitrogen nucleophiles. It was then observed that the addition of ionic liquids like NBu_4Cl significantly enhanced reaction rate, although full potential was achieved when the reaction mixture was subjected to a continuous microwave reactor at 160°C (Scheme 48). Several heteroarenes could be benzylated in under 20 min in good yields, and a reproducible 25 g scale synthesis of 5-bromo-*N*-benzyl indole was demonstrated.

The condensation strategy toward imidazo[1,2-*a*]heterocycles as reported by Herath et al. proves the sometimes unique chemical windows that are enabled by flow chemistry [121]. The shortest route would comprise the C-N bond forming condensation of bromopyruvic acid with 2-aminopyridine. However, the necessity of long reaction times and high temperature elicited spontaneous decarboxylation, so that the batch process required using the ethyl ester with concomitant saponification thereafter. In an effort to nonetheless make the direct route happen, the authors opted for a microreactor setup. Remarkably, they found that using the right catalyst and solvent, the reaction completed in only 10 min at 125°C (Scheme 49). Several fused



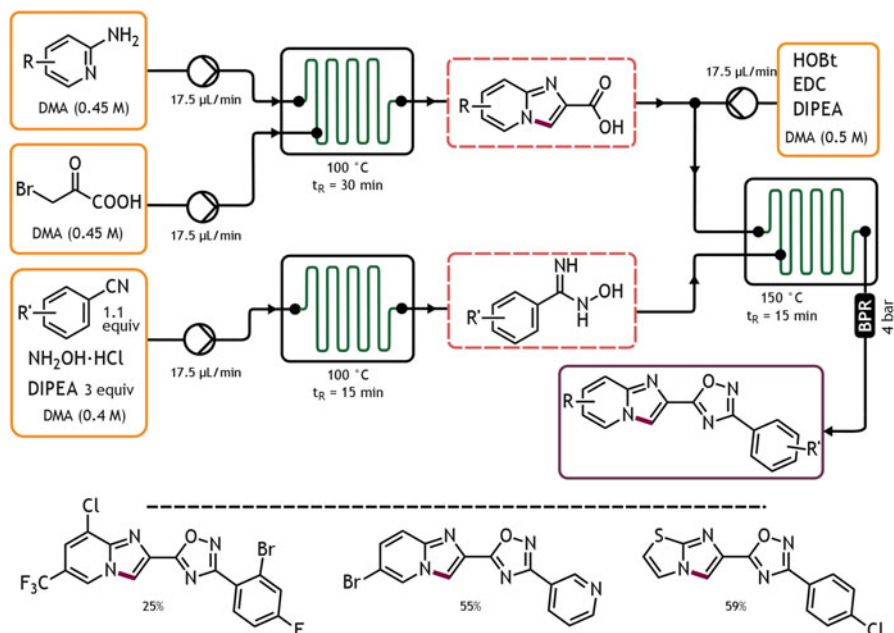
Scheme 48 Benzoylation of different heteroarenes in a microwave flow reactor (Shieh et al. [120])



Scheme 49 Microfluidic [3 + 2] cyclocondensation and subsequent amidation of various imidazo [1,2-a]arenes (Herath et al. [121])

ring systems were produced in good yields, and in-line amide formation proved to be fully compatible.

Very recently, the same authors further fine-tuned this method for the synthesis of 1,2,4-oxadiazoles [122]. By performing an in-line amidation with hydroxylamine in the presence of a benzonitrile, thermal condensation delivered them the desired teraryl structure (Scheme 50). Working on a 2.0 g scale, continuous liquid–liquid extraction as the last stage completed the elegant and chromatography-free synthesis of these highly functional drug-like scaffolds.

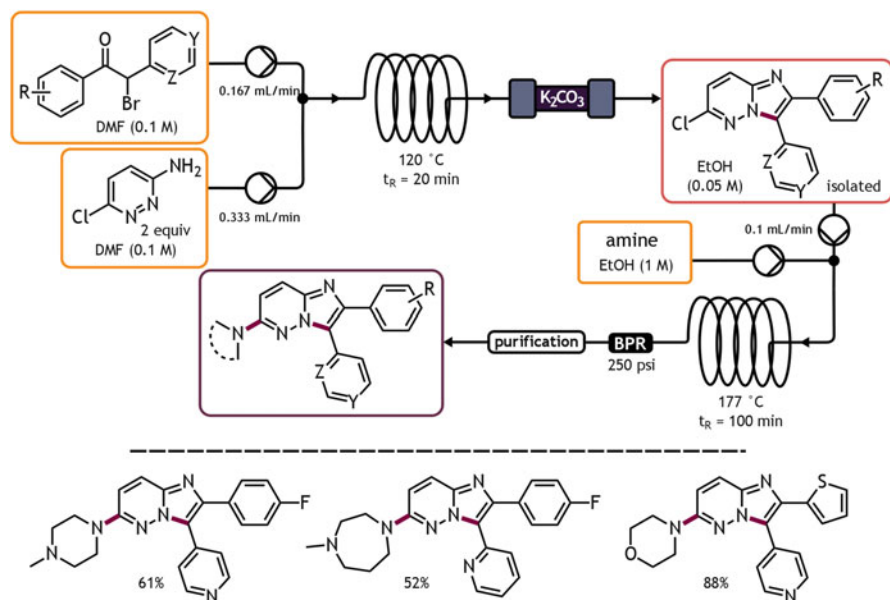


Scheme 50 Microfluidic [3 + 2] cyclocondensation and subsequent oxadiazole formation (Herath et al. [122])

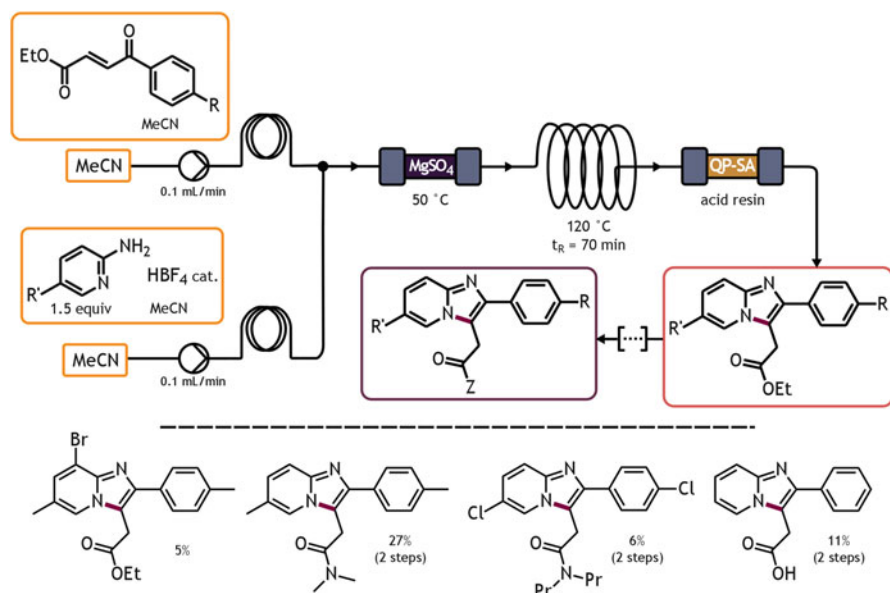
Baxendale and Ley used a similar protocol for the synthesis of casein inhibitor analogs [123]. Making use of α -bromobenzyl aryl ketones as the biselectrophile, the polysubstituted imidazo[1,2-*b*]pyridazines could be obtained in good yields from 3-aminopyridazine, a previously unreliable route (Scheme 51). The optimization of this step was a highly automated process realized by the Vapourtec R2+/R4 and the appropriate software package, requiring the operator's physical presence less than 5% of the whole time. Further derivatization was achieved by a nucleophilic displacement of the chlorine with a variety of saturated *N*-containing heterocycles at 177 °C over 100 min. Lastly, they demonstrate that purification could be achieved either by treatment with isocyanide scavenger resin to remove excess base, or with a catch-and release strategy using a sulfonic acid resin, followed by recrystallization.

The same team used this knowledge in a recent effort to arrange a fully telescoped assembly line for the production of GABA_A antagonists Zolpidem and Alpidem [124]. An unsaturated γ -keto ester was produced and purified in an upstream flow sequence, and thermally condensed with 2-aminopyridine in two steps (Scheme 52). A first dehydrating packed bed column at 50 °C ensured imine formation, whereas the subsequent loop at 120 °C established the second C-N bond formation, furnishing the desired heteroarene.

Some recent publications equally describe continuous preparation of imidazo[1,2-*a*]heterocycles, making use of multi-component reactions (MCR) to assemble the five-membered ring [125, 126]. These examples will be discussed more thoroughly in the corresponding chapter of this book.



Scheme 51 Continuous [3 + 2] condensation synthesis of imidazo[1,2-b]pyridazines and subsequent amination (Venturoni et al. [123])

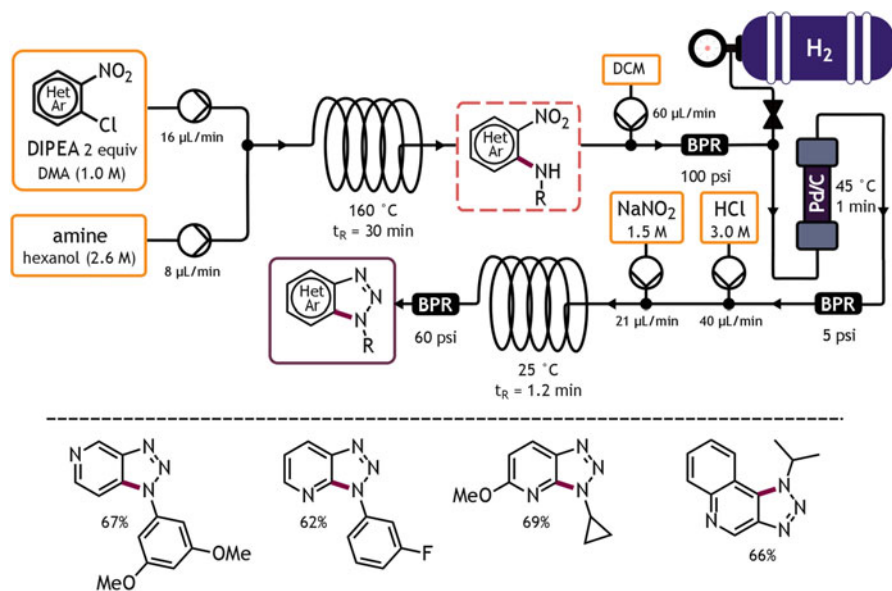


Scheme 52 Microflow [3 + 2] condensation synthesis of imidazo[1,2-a]pyridines and in-line ester derivatization (Guetzoyan et al. [124])

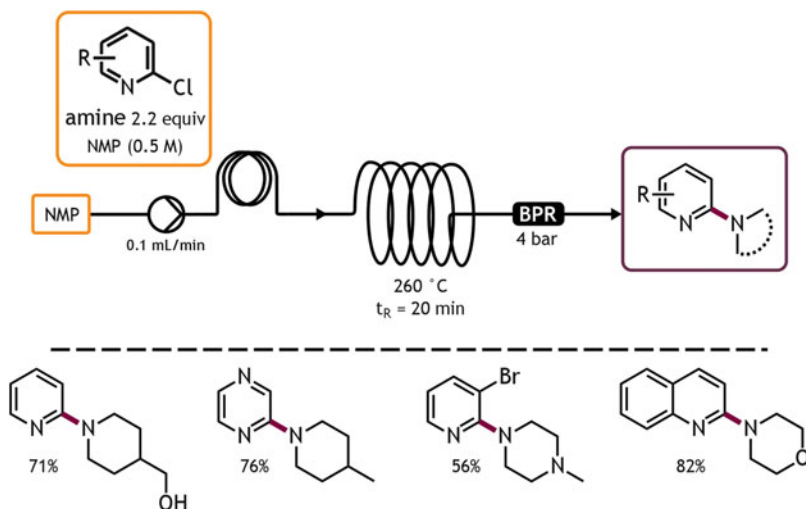
Another fused ring synthesis in flow was reported by Chen and Buchwald, with the C-N bond formation being a crucial step [127]. Previous entries to N1-functionalized benzotriazoles comprised either of *N*-alkylation of the bicyclic ring, or cycloaddition of the corresponding azide with benzyne, giving rise to either low regioselectivity or hazardous conditions, respectively. To address this need, a fully streamlined flow protocol was proposed consisting of three subsequent steps: (1) S_NAr amination, (2) nitro reduction, and (3) diazotation (Scheme 53). The first, C-N bond forming step was achieved by reacting the ortho-chloro nitropyridine in DMA with a second stream of only 1.3 equivalents of amine in *n*-hexanol at 180°C for 30 min. Several triazolopyridines or quinolines were thus produced in >60% yield in complete regioselectivity.

The “new process windows” which are uncovered by microreactor technology in terms of temperature and pressure have also captured the interest of chemists to reinvestigate the classically thermophilic S_NAr reactions. Hamper and Tesfu utilize a stainless steel coil reactor at 260°C and 70 bar to perform the amination of 2-chloropyridines and other azines (Scheme 54) [128]. Where the batch process demanded a 2-day reaction time, and where even microwave conditions could not reach over 50% conversion, the coil reactor supplied them with 2-aminopyridines in good yields. The group of Kappe has developed a similar high-temperature, high-pressure stainless steel flow reactor, and one example of the S_NAr reaction between morpholine and 2-chloropyridine gave them similar results [129].

When the former group was initially optimizing the amination reaction in DMF as the solvent, they found observable amounts of 2-dimethylaminopyridine side



Scheme 53 Continuous amination-reduction-diazotation sequence for the synthesis of benzotriazoles (Chen and Buchwald [127])

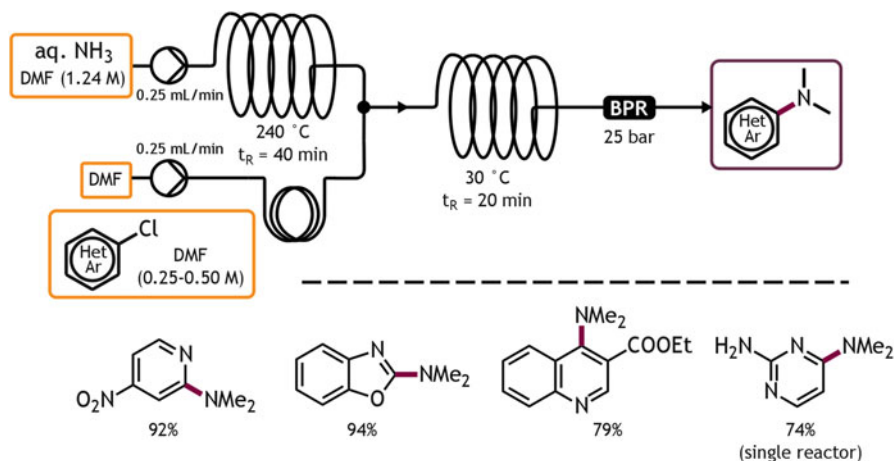


Scheme 54 Thermal S_NAr amination of chloroazines (Hamper and Tesfu [128])

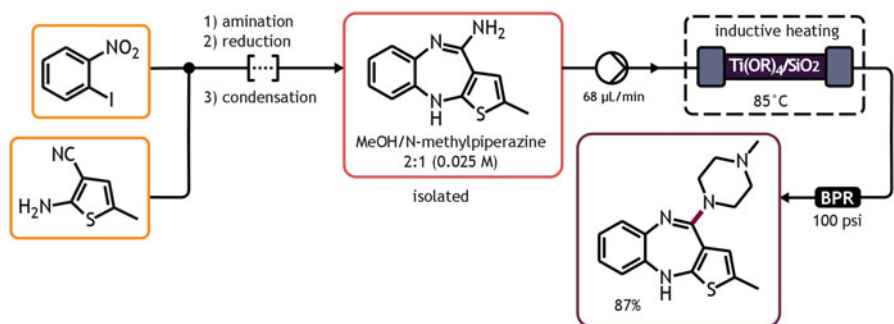
product. A decomposition of DMF into CO and dimethylamine becomes rather prevalent at this temperature, and Petersen et al. exploited this phenomenon in their study of dimethylation of heteroarenes in a high-temperature flow reactor [130]. Among a series of additives, aqueous ammonia proved excellent in promoting this decomposition. The first generation of their microreactor design consisted of a haloarene stream reacted together with an ammonia inlet in a coil heated at 250 °C for 30 min (Scheme 55). However, some starting materials decomposed at this temperature and others contained functional groups that did not tolerate the conditions. A second design therefore located the high temperature coil before the mixing T-piece, so that decomposition was realized before the substrate was brought in contact with the dimethylamine. Further S_NAr at 30–50 °C sufficed for many substrates and the method could be used to manufacture 8 g of a certain aminated pyrimidine without further modifying the setup.

An alternative heating mode for continuous mode S_NAr reactions was invented by the group of Kirschning [131]. By making use of a packed bed of ferromagnetically functionalized silica beads, high frequency inductive heating warranted an extremely rapid and efficient heating. They employed this technique in the multistep synthesis of the antipsychotic Olanzapine. Earlier on in the cascade, steel beads served as inductive heating centers for the Buchwald-Hartwig amination, and a steel capillary reactor was heated to allow the seven-membered ring to be formed. Subsequently, the nucleophilic displacement by the *N*-methyl piperazine was achieved in a MAGSILICA-filled column, while inductively heating the reactor to 85 °C (Scheme 56).

Also ultrasonication could represent a viable process intensification technique, complementary to strong heating. More often than not, ultrasound irradiation is invoked in microflow processes to sustain suspensions and avoid clogging. However, there is more to be gained from this unconventional energy source. Lee et al.



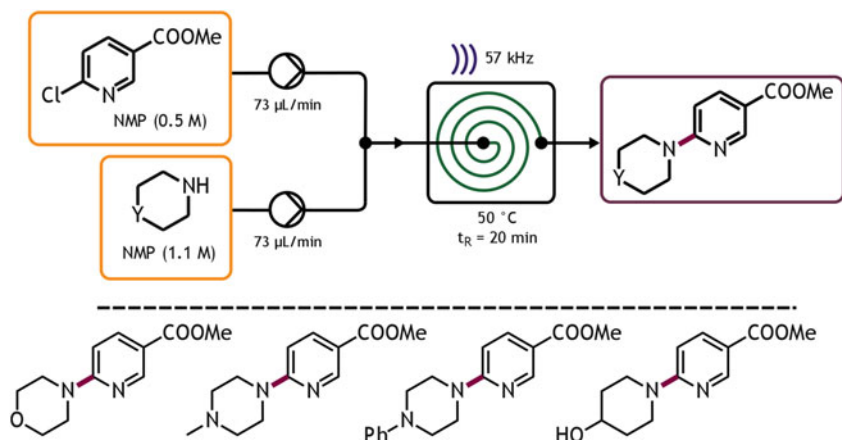
Scheme 55 Dimethylamination of chloroarenes by merit of thermal DMF decomposition (Petersen et al. [130])



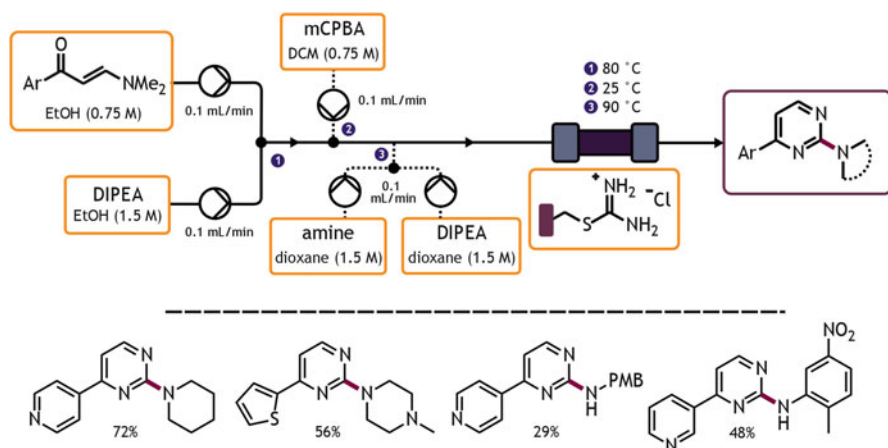
Scheme 56 Ti-catalyzed, inductively heated piperazination in the telescoped synthesis of Olanzapine (Hartwig et al. [131])

show how a microtubular reactor setup which is irradiated by piezoceramic elements can greatly enhance the amination of a substituted 2-chloropyridine with morpholine compared to the previously described method of warming up a coil to 260 °C (Scheme 57) [132]. For most of their amine scope, a twofold increase in product formation is observed compared to the thermal method, whilst reacting at a mere 50 °C. The authors motivate that not only efficient mixing but especially the cavitation-induced hotspots are responsible for this improved outcome.

An interesting approach to $\text{S}_{\text{N}}\text{Ar}$ reactions in flow was recently proposed by the group of Ley [133]. In an alternative synthesis of the blockbuster leukemia drug Imatinib, they devised a “catch-react-release” strategy to form the 2-aminopyrimidine core. An *S*-linked thiourea monolith was prepared from polymerization of the styrene-bound functional group and crosslinking with divinylbenzene. These thioureas could be further condensed with an enaminone



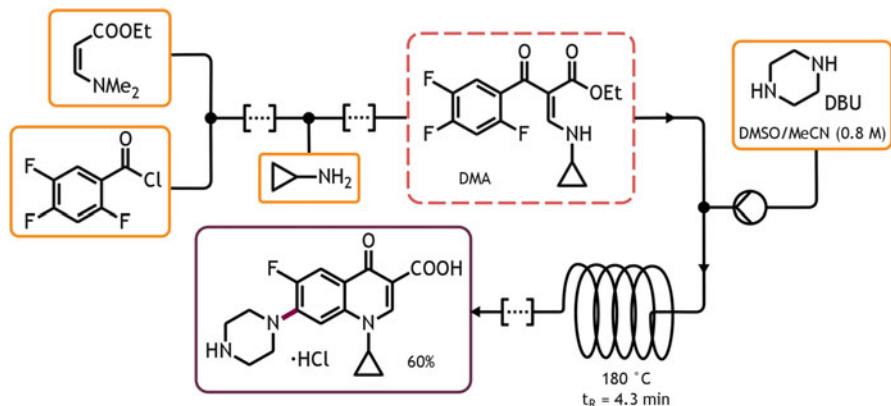
Scheme 57 Amination of a 2-chloropyridine in an ultrasonically irradiated tubular reactor (Lee et al. [132])



Scheme 58 Aminopyrimidine synthesis in a “catch-react-release” strategy from an *S*-bound thiourea column (Ingham et al. [133])

to form the 2-thiopyrimidine, whereupon the sulfur atom was oxidized to the corresponding sulfone (Scheme 58). This configuration furnished them a resin-bound leaving group as it were, and treatment with a stop-flow amine inlet at 90°C cleaved the pyrimidine off to deliver the desired Imatinib precursors.

While working on their synthesis of the antibiotic Ciprofloxacin, Lin et al. investigated a nucleophilic piperazine installment in what counts to date as the longest telescoped flow process reported [134]. Starting first from the 6,7-difluoroquinolinone precursor, the selective amination with piperazine was achieved in DMSO in a reactor coil at 150°C over 7 min. However, viewing that the preceding step consists of a S_NAr type intramolecular cyclization, they



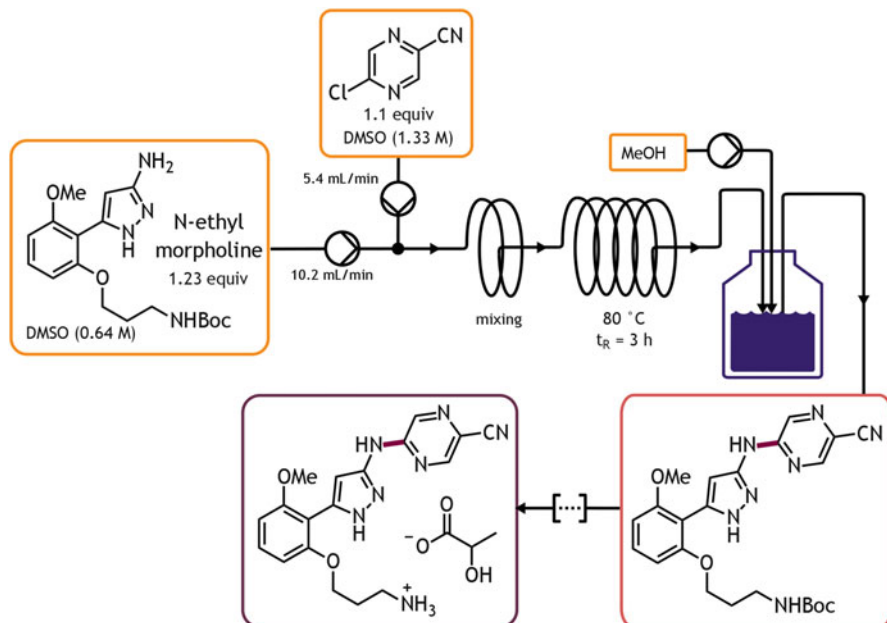
Scheme 59 One-step twofold amination in the streamlined synthesis of Ciprofloxacin (Lin et al. [134])

speculated that both steps could be realized in one reactor. Indeed, the one-pot procedure treating the trifluorobenzene with DBU and piperazine at 180°C furnished the desired quinolone in 81% yield in only 4 min (Scheme 59).

An impressive example of a fully continuous nucleophilic amination was showcased by a team from Eli Lilly [135]. In their study of the continuous, large-scale synthesis of prexasertib monolactate, an $\text{S}_{\text{N}}\text{Ar}$ -type amination was required to couple the 3-amino-5-arylpyrazole fragment with 2-chloro-5-cyanopyrazine. They found that DMSO was the solvent of choice for solubility and reactivity reasons, and both reagents were combined in a 6.35 mm (ID) \times 91 m plug flow reactor (PFR) for 3 h to afford about 2.9 kg/day of the desired compound (Scheme 60). Addition of MeOH as the antisolvent was sufficient to obtain a high purity solid, and in this way, in total 24 kg of the pure API was prepared.

5.3 Rearrangements

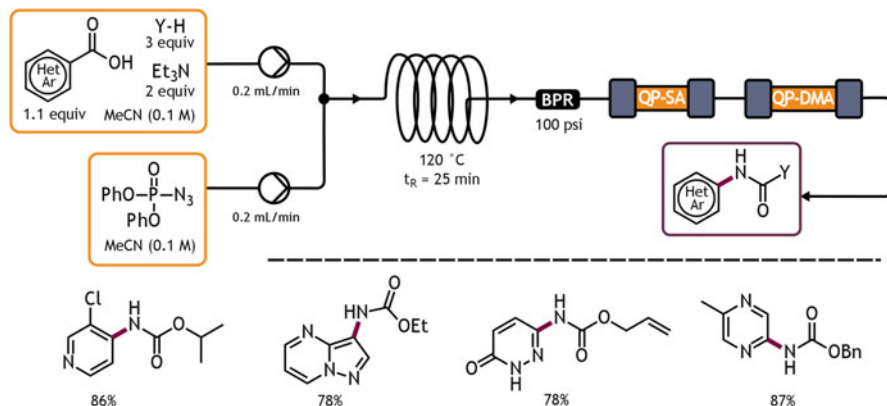
Flow chemistry lends itself very well to reactions where sensitive intermediates are formed that would pose a significant hazard in batch production. Organic azides form a classic example of materials that process chemists refuse to work with, owing to their inherent explosion risk [2]. Azide-involving reactions can nonetheless be powerful C-N bond forming routes toward aminated heterocycles. An example of these is the Schmidt reaction between azides and ketones, which affords an amide after homologation due to a denitrogenative 1,2-migration. This hazardous reaction was recently reported in flow conditions, and a variety of acetophenones were thus safely converted to acetamidobenzenes [136].



Scheme 60 Amination step in the continuous, large-scale synthesis of Prexasertib monolactate (Cole et al. [135])

Another well-known reaction which employs azides is the Curtius rearrangement. Herein, an in situ formed acyl azide thermally decomposes to the corresponding isocyanate, which can be attacked by an oxygen or nitrogen nucleophile to form carbamates or ureas, respectively. Where the application of heat to a reactive azide would never be considered an option in batch upscaling, flow chemistry offers a different way.

In 2008, Baumann et al. simultaneously published two different approaches to an in-line acyl azide formation and subsequent Curtius rearrangement. The starting point was a publication by the group of Jensen, where a sequence of microfluidic reactors and separator units was used for the divergent synthesis of several carbamates [137]. When using aqueous sodium azide as the azide source, removal of the aqueous stream was necessary to enable the following rearrangement step. Wanting to avoid this prior purification, the Cambridge team opted for an all-organic entry to acyl azides which could then be reacted as such [138]. Diphenylphosphoryl azide (DPPA) proved the reagent of choice, and combining this reagent with a stream of the carboxylic acid, Et_3N and the nucleophile into the convection flow coil at 120 °C ensured the azidation and rearrangement in one step (Scheme 61). Further downstream, a supported dimethylamine resin captured the formed diphenylphosphonic acid and the unreacted starting material as well. The subsequent Amberlyst acid resin captured the Et_3N . Thus, a wide variety of carbamate-functionalized heteroarenes were obtained in high purity.



Scheme 61 Curtius rearrangement and in-line purification for the preparation of carbamoylated heteroarenes (Baumann et al. [138])

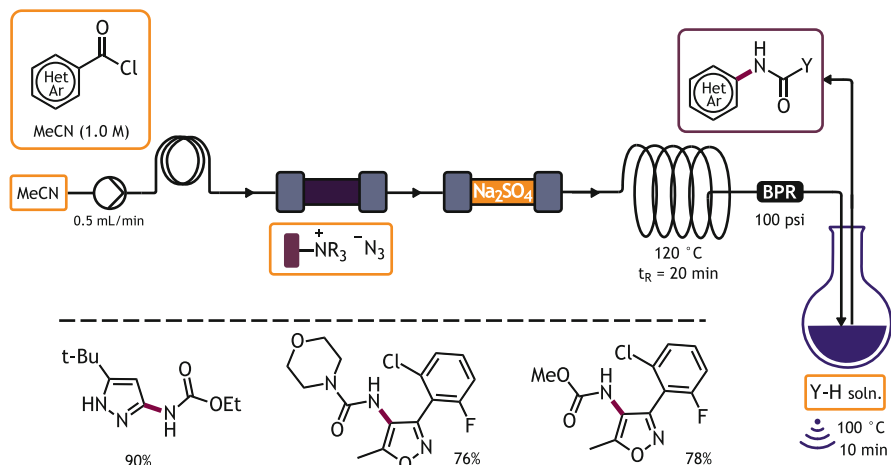
Another strategy proposed by them was composed of a packed-bed column with azide-functionalized monolith [139]. The polymerization and crosslinking of a vinyl-substituted benzyl chloride furnished them the desired macroporous material, which could then be treated with Et₃N and NaN₃ to get the tetraalkyl ammonium azide monolith. By packing this into a cartridge, 30 mmol of acyl azide per hour could be produced, starting from the acyl chloride (Scheme 62). In a further valorization, a dehydration column and reactor coil at 120 °C were sequentially connected to turn the products into their corresponding isocyanates. Collection of these in a microwave vial together with a proper nucleophile enabled a further microwave synthesis at 100 °C of several carbamates and ureas.

O'Brien et al. reported yet another “forbidden” reaction in flow [140]. The Hemetsberger-Knittel indole synthesis starts from an aryl vinyl azide, which after heating releases one N₂ molecule, so that the remaining, nitrene-like nitrogen performs a C-H bond insertion on the aromatic ring. Especially the safety benefits from microfluidic technology make this reaction very amenable for continuous processing.

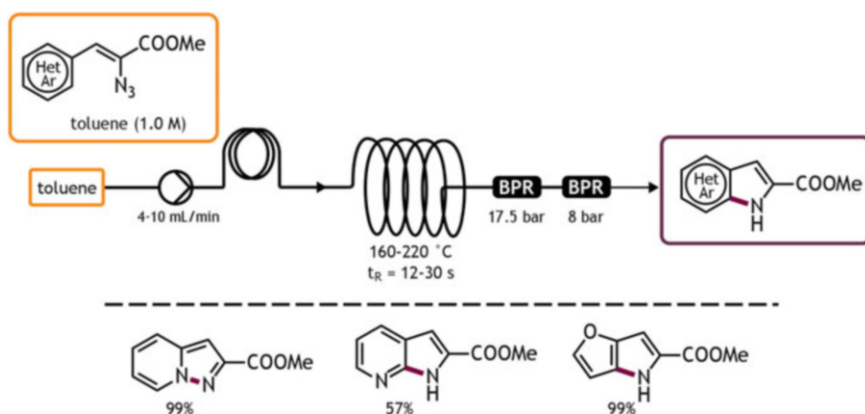
Once the 3-aryl-2-azidoacrylate starting materials were synthesized by a Knoevenagel condensation, the further rearrangement to bicyclic aromatics was optimized in flow. It was found that under optimum conditions, depending on the substrate, the products were obtained in good yields at 180–220 °C in only 6 s (Scheme 63).

5.4 Cross-Coupling

Transition metal catalyzed coupling reactions constitute a last class of transformations for the installation of C-N bonds. Whether quite old methods like the Ullmann



Scheme 62 Acyl azide synthesis from azide monolith, subsequent isocyanate formation and off-line nucleophile treatment in microwave vessel (Baumann et al. [139])



Scheme 63 Continuous Hemetsberger-Knittel indole synthesis from azidoacrylates (O'Brien et al. [140])

coupling, or more modern examples like the Buchwald-Hartwig or Chan-Lam amination, these reactions have been deeply instrumental in medicinal chemistry. In the wake of the vast amount of publications covering Suzuki-Miyaura couplings in microflow, literature has caught on with amination as well. However, it is a transformation with its own difficulties.

The palladium-catalyzed Buchwald-Hartwig amination, for example, has proven to be an especially tricky process to translate to microfluidic conditions. From the aryl bromide starting material and the typical *tert*-alkoxide base, the alkali metal bromide salt is an inevitable side product, which oftentimes causes clogging in the

channels or in the BPR in particular. Also the possible degradation to palladium black may cause the same problem. Roughly every publication concerning the Buchwald-Hartwig amination in flow evolves around precluding this obstruction.

Some prior art comes from Tundel et al., who have successfully devised a microwave protocol for the Buchwald-Hartwig amination of a variety of (hetero) arenes [141]. Aiming to render the reaction mixture entirely homogeneous for improved microwave absorption, they worked with aryl nonaflates and DBU as an organic, soluble base. However, this procedure has not been adapted to continuous flow conditions. Hartwig et al. have found that the well soluble NBu_4OAc base may indeed prevent the issue of reactor choking [131].

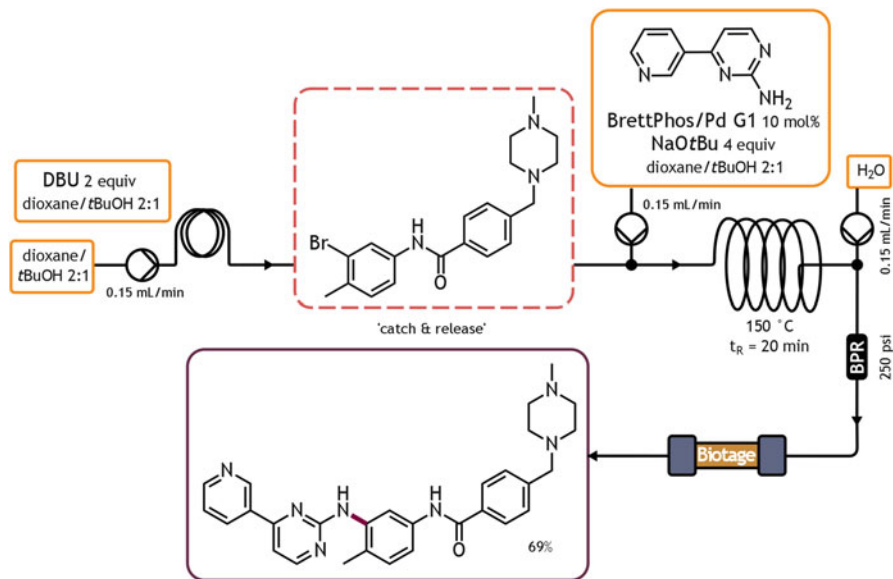
Despite promising results, a thorough investigation by Sunesson et al. pointed out that the organic base DBU could only in limited cases realize the amination, and in no case proved superior to the alkoxide bases in terms of reactivity [142]. Another approach therefore constituted a careful choice of solvent, in order to keep the base and halide salt soluble. Pomella and coworkers found that coupling between bromoxylene and piperazine worked much better in DME than in toluene since KBr precipitation from the former occurred too slow to allow clogging [143].

In the fully continuous synthesis of Imatinib, Hopkin et al. similarly found a mixture of 1,4-dioxane and *t*BuOH to be ideal for good reactivity and solubility. The piperazine-decorated benzamide was previously synthesized and captured with a sulfonic acid resin. Elution with DBU in the appropriate solvent mixture and subsequent merging with a stream of the 2-aminopyrimidine, the NaOrBu base and Pd precatalyst, allowed the amination in a reactor coil at 150°C over the course of 30 min (Scheme 64). NaBr precipitation was not avoided in this way, but a water inlet just before the BPR and a further purification step ensured full solubility. The final product was obtained in 69% yield for the amination step in good purity after in-line Biotage SPI purification.

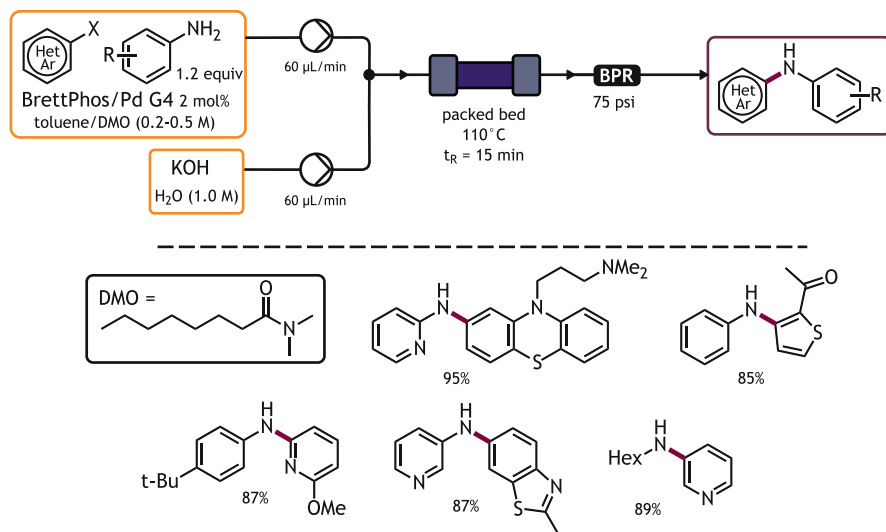
Aside from organic solvent mixtures, a biphasic approach has also been successfully employed. Naber et al. found that an aqueous KOH/toluene system could serve as a solution for the solubility problem. Furthermore the help of a PTC and a packed-bed reactor ensured high conversion [23].

The same packed-bed reactor was later used by the group to significantly expand the scope of this reaction [145]. While still using the KOH/toluene mixture, the PTC was replaced by dimethyloctamide (DMO) as an amphiphilic cosolvent. Amphiphilic solvents, containing a lipophilic and hydrophilic side, have proven their use in batch chemistry as they bring components from immiscible phases together, thus facilitating mass transfer. Also solubility is enhanced and crystallization is diminished. Good results were obtained when this protocol was translated to continuous flow, and reacting over a packed at about 120°C delivered a wide scope of aminated (hetero)arenes in good yields (Scheme 65). Especially interesting about this approach was that preceding steps could be performed without demand for a solvent switch for the C-N cross-coupling. This was demonstrated for a phenol triflation/amination sequence, and notably for the three-step synthesis of Imatinib which could be performed in a mere 2-MeTHF/ H_2O mixture in 56% overall yield.

A different approach to this problem consists not of avoiding precipitation, but of making this heterogeneous system workable. Several groups came up with the same



Scheme 64 Pd-catalyzed diarylamine synthesis in the telescoped preparation of Imatinib (Hopkin et al. [144])



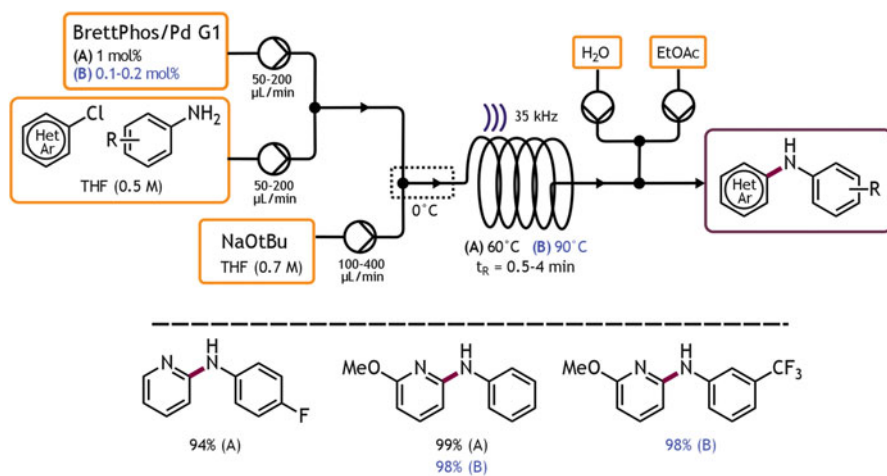
Scheme 65 Amphiphilic solvent assisted Buchwald-Hartwig amination in continuous flow (Yang et al. [145])

strategy: the use of ultrasound irradiation to break up any particles formed [146–148]. By forcing these particles to retain a small diameter, blocking mechanisms do not occur and the reactor can be maintained free of clogging.

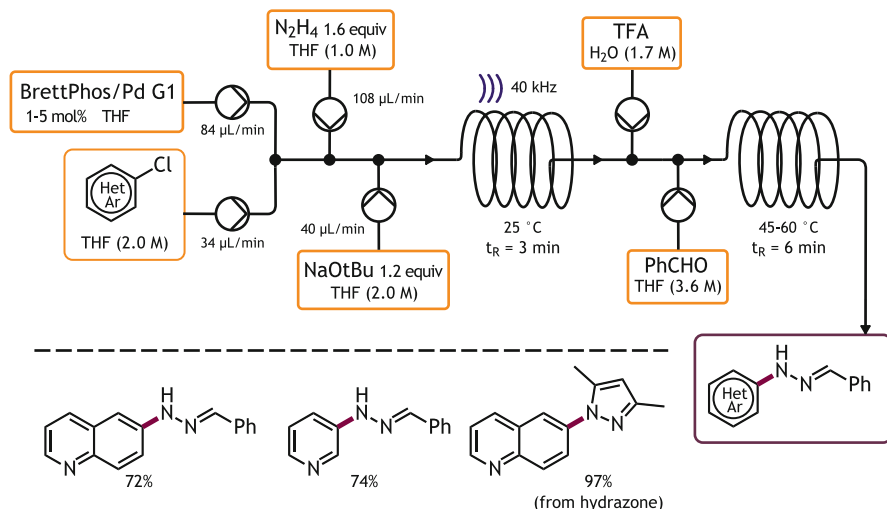
Hartman et al. describe these findings when trying to improve the Pd-catalyzed C-N coupling in flow [146]. They noticed significant clogging in a microfluidic device, due to NaCl crystal bridging or constriction. Using a PFA coil instead, and suspending it in an ultrasonication bath at 80°C, the amination reaction proceeded smoothly in a rate of 2.6 g/h without clogging.

Borrowing from this knowledge, the same group later reported a more extended protocol for the synthesis of diarylamines from aryl chlorides, bromides, or triflates [50]. With residence times ranging from 20 s to 5 min, good yields were obtained for several (hetero)aryl amines at only 60°C (Scheme 66). To demonstrate that solids formed no problem, a model reaction was subjected to the microflow reactor over 1 h to produce 2.25 g of the desired product. A further innovation comprised a fully assembled microfluidic chip reactor with a built-in piezoceramic element [150].

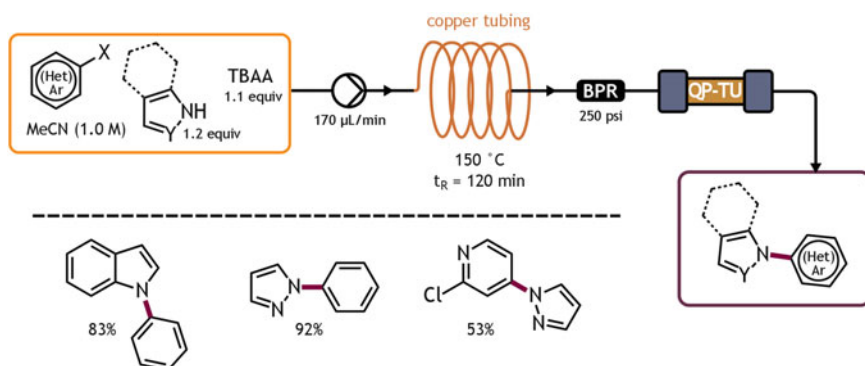
DeAngelis et al. reported the hydrazination of aryl chlorides using a similar setup [151]. The direct Buchwald-Hartwig coupling of hydrazine had previously been disclosed in a single study with several drawbacks; a more general entry was therefore still needed. Combining a THF solution of hydrazine with streams of ArCl, NaOtBu, and the Pd catalyst into a sonicated reactor coil at room temperature provided an efficient and chemoselective reaction (Scheme 67). A TFA inlet ensured dissolution of all the products and aided the subsequent trapping with benzaldehyde. They opted for in-line hydrazone formation as a safer alternative for the storage of aryl hydrazines. The trapping step could also be replaced by an immediate pyrazole formation with 1,3-dicarbonyl compounds, or by a Fischer indole synthesis with enolizable ketones.



Scheme 66 Pd-catalyzed amination protocol using a sonicated reactor coil to avoid clogging (Noel et al. [149])



Scheme 67 Continuous Pd-catalyzed hydrazination and subsequent benzaldehyde capture (DeAngelis et al. [151])



Scheme 68 Continuous Ullmann amination using a copper tubing flow reactor (Zhang et al. [153])

Beyond Pd-catalyzed coupling reactions, also copper catalysis represents a viable way to synthesize aminated heterocycles. A classical protocol for copper-catalyzed arylamine formation is the Ullmann reaction. Although this reaction traditionally requires stoichiometric amounts of copper, a good deal of more modern, catalytic variants have been described [152].

An adaptation to flow was reported by Zhang et al. [153]. They investigated a series of copper-catalyzed reactions in a copper tube flow reactor (CTFR), among others the Ullmann amination of aryl bromides and iodides. A single pump injected a MeCN solution of (hetero)aryl halide and an amine into the CTFR for 120 min followed by a subsequent thiourea copper scavenger (Scheme 68). Several arylamines were obtained in good yields.

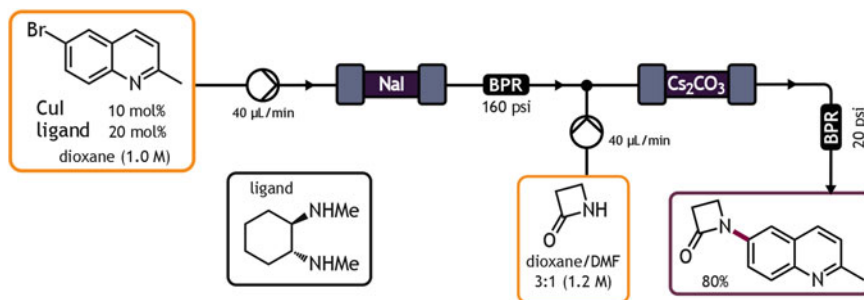
Chen et al. realized the amination of several aryl bromides by first performing the copper-catalyzed aromatic Finkelstein reaction [154] (the iodination is described in the paragraph of C-X bond formation). After exiting the NaI packed bed reactor, the CuI-containing product stream is combined with an inlet of amide into a Cs_2CO_3 packed bed reactor at 120°C (Scheme 69). These conditions sufficed to convert the aryl halides fully to their amidated analogs.

Also the Chan-Lam amination was translated to flow. This cross-nucleophile coupling is, apart from being mild and effective, also an often unpredictable reaction, which is still being refined [155]. The groups of Stevens and Van der Eycken reported the first continuous flow example of the Cu-catalyzed coupling between an arylboronic acid and a nucleophilic amine [156]. They employed a CYTOS microreactor assembly, and combined a solution of both coupling partners with a flow of $\text{Cu}(\text{OAc})_2$ and the bases at 120°C in DCM. With this method, they achieved the *N*-phenylation of a pyrazinone scaffold.

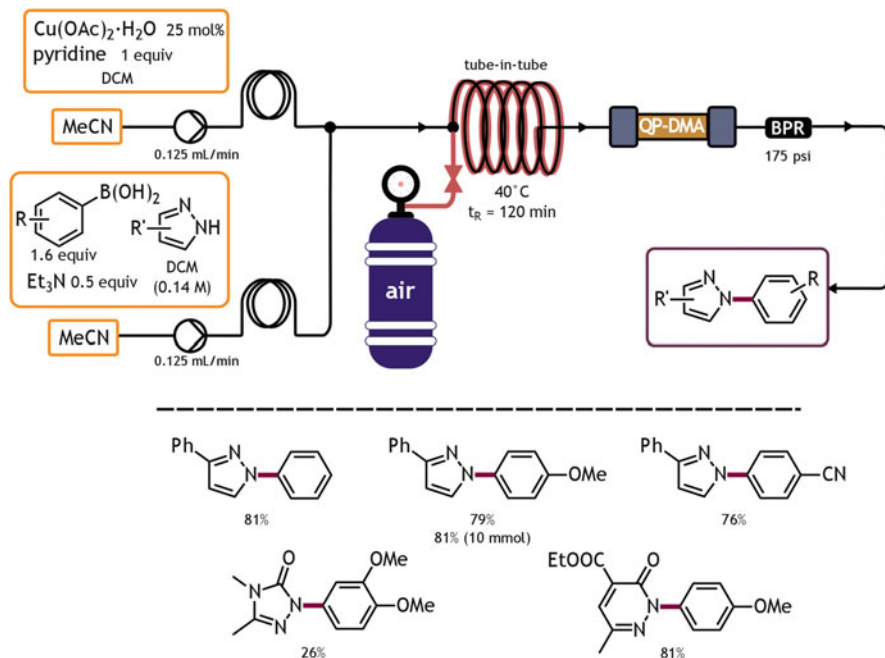
However, equimolar amounts of copper were still necessary to realize this coupling. In an attempt to transition to a catalytic system, Bao and Tranmer ran their reaction mixture through a copper coil (later through a copper powder filled column) together with TEMPO as an external oxidant, to supply a number of substituted diphenylamines [157].

The Baxendale group further developed the continuous Chan-Lam amination towards an even more waste-economical process [158]. Making use of a tube-in-tube reactor, they were able to harness oxygen gas as the stoichiometric oxidant. Merging a stream of the substrates with the catalyst/base combination, they found that high conversions were obtained when flowing the mixture through a coil for 2 h at 40°C , under an optimum O_2 pressure of 10 bar (Scheme 70). By connecting a QuadraPure supported dimethylamine column (QP-DMA), the outlet was mostly stripped of remaining boronic acid. In this way, many arylated azoles were prepared in good yields, and a 10 mmol scaled experiment showed an undiminished outcome.

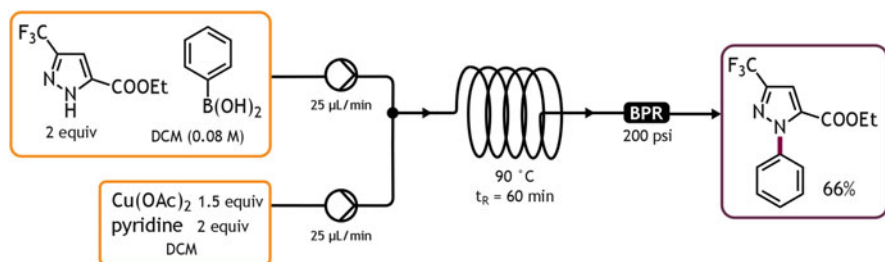
In a streamlined synthesis of highly substituted pyrazoles, Britton and Jamison recently accomplished the *N*-arylation of a trifluoromethylated pyrazole with phenylboronic acid [159]. Viewing that existing methods were not sufficient for



Scheme 69 Telescoped aromatic Finkelstein iodination and subsequent Goldberg amidation (Chen et al. [154])



Scheme 70 Tube-in-tube approach for the aerobic Chan-Lam amination of azoles with phenylboronic acids (Mallia et al. [158])



Scheme 71 Chan-Lam coupling of a substituted pyrazole and benzenboronic acid (Britton and Jamison [159])

their more demanding substrate, an optimization was necessary. It was found that best results were obtained when performing the reaction in DCM at 90 °C, which posed no problem in a microreactor (Scheme 71). A yield of 66% was obtained for this step, and they proposed this as a viable route to COX-2 inhibitors, which often carry the same *N*-aryl pyrazole motif.

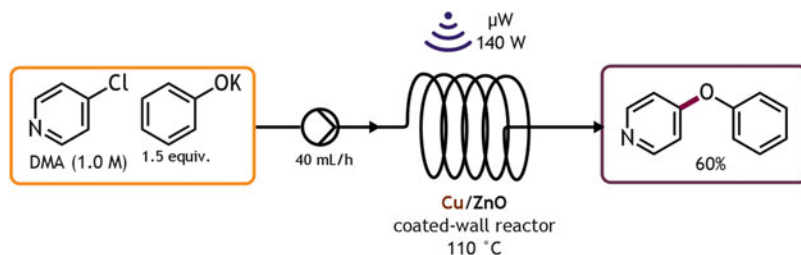
6 C-O Bond Forming Reactions

C-O bond forming reactions on heteroarenes are less prevalent than amination reactions, although oxo- or hydroxyheterocycles are no less abundant in nature. In synthesis, oxygen substituents bound to the ring often stem from carbonyl motifs already present from the de novo synthesis of the heterocycle. As a consequence, the need for etherification reactions onto the ring is abated, since alkylation or arylation of an already present oxygen functionality is usually the more viable route.

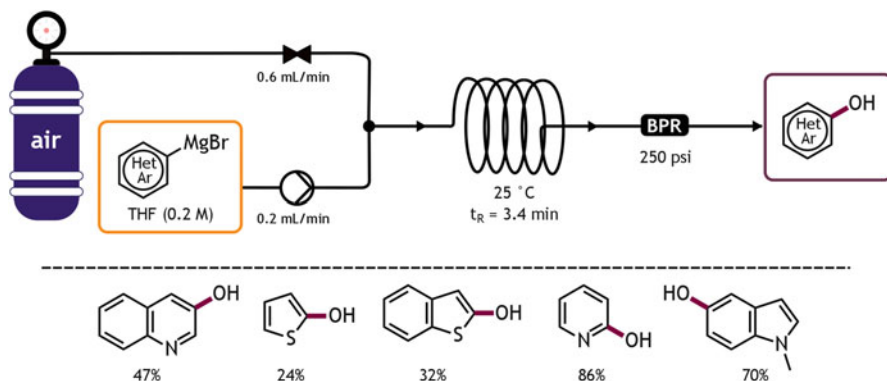
Also in the research field of microflow chemistry, reports of C-O bond forming reactions on heteroarenes have remained scarce. Nonetheless, some useful protocols have emerged, where microfluidic technology offers a unique advantage over batch chemistry. An interesting example was the metal-free, fluoride-catalyzed S_NAr -type etherification between silylated phenols and aryl fluorides [160]. The authors found that the reaction occurred most efficiently in supercritical CO_2 , and a translation to continuous flow proved an effective route to realize the high pressures.

When studying the Ullmann diaryl ether synthesis, Benaskar et al. found that microflow reactors posed a significant improvement. They had found previously that supported copper nanoparticles could serve as excellent catalysts for the etherification of 4-hydroxypyridine with potassium phenolate [161]. To further increase the reusability potential of their catalyst, they adapted the procedure to a continuous process [162]. After implementing either a fixed bed reactor using a TiO_2 support, or a ZnO supported catalyst in a wall-coated millireactor, they further investigated the mode of heating to perform this reaction (Scheme 72). They found that single mode microwave heating proved to be more efficient than multimode irradiation or oil bath heating. The intensity had a maximum of 140 W, above which catalyst decomposition became too significant. Leaching could be avoided by thermal treating of the catalyst after each cycle. In this way, the 4-phenoxy pyridine product could be obtained in 60% yield in high productivity.

In another example, He and Jamison reported the hydroxylation of arenes by aerobic treatment of an organomagnesium reagent [163]. Where the oxygenation of alkyl Grignard reagents has been successfully investigated as early as the beginning of the former century, the transformation of arylmagnesium species into its corresponding phenol proved much more prone to side reactions. The authors



Scheme 72 Copper coated wall reactor for the Ullmann etherification (Benaskar et al. [162])



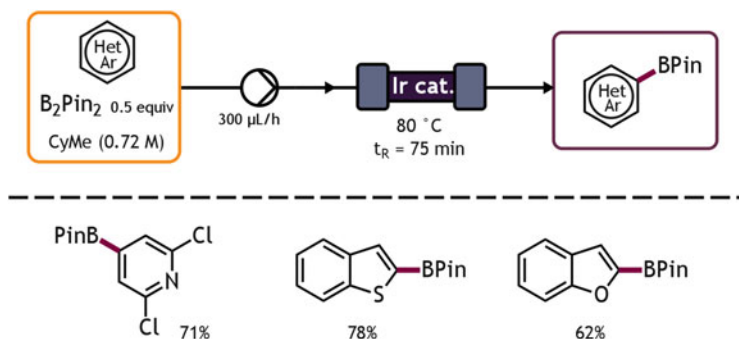
Scheme 73 Aerobic oxidation of aryl Grignard reagents to form phenols (He and Jamison [163])

postulated that a segmented flow approach should overcome this challenge by enhanced mass transfer with the gas phase. Preliminary tests with an O₂ tank at ambient conditions furnished the desired phenol in 53% yield. After some optimization, the second generation setup made use of a 3:1 air/liquid ratio in THF at 17 bar. The arylmagnesium bromide reacted with oxygen in a PFA coil over 3.4 min, supplying a variety of hydroxyheteroarenes in good yields (Scheme 73). They go on to produce *o*-substituted phenols by magnesiating 1,2-dibromobenzenes and treating the formed benzyne intermediate with a sulfur or nitrogen nucleophile, then applying their aerobic oxidation to the *ortho*-decorated arylmagnesium species.

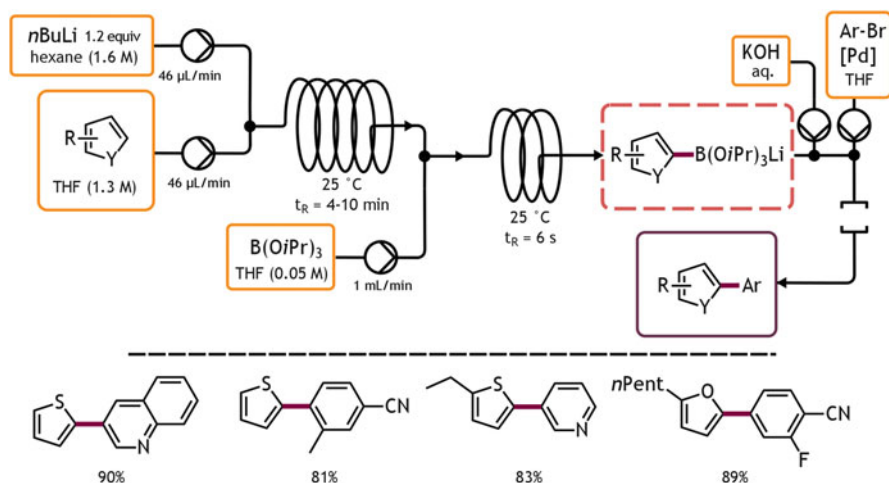
7 C-B Bond Forming Reactions

The importance of borylation on (hetero)aromatic substrates hardly needs any introduction. Research toward improved borylation methods has been incessant since the early days of palladium-catalyzed cross-coupling. Most frequently, the boron moiety is installed on a previously functionalized place of the aromatic ring, typically a (pseudo)halide. However, a direct C-H borylation comprises an appealing alternative, on account of its step and atom economy.

Tagata et al. had achieved some promising results with this concept, using an iridium catalyst [164]. They found that using the optimal ligand, 2,2'-bipyridine-4,4'-dicarboxylic acid (BPDCA), the actual catalyst became insoluble and could be reused several times. Inspired by this observation, they set out to investigate the translation to microflow conditions [165]. The unsupported catalyst was synthesized and packed into a stainless steel column inside the glovebox, but could thereafter be used outside of it. A solution of the arene and B₂pin₂ in methylcyclohexane (CyMe) or cyclopentyl methyl ether (CPME) was pumped through the packed bed at 80 °C at 0.1 mmol/h to afford a few BPin-functionalized heteroarenes (Scheme 74). Leaching



Scheme 74 C-H borylation using an insoluble Ir catalyst (Tagata et al. [165])



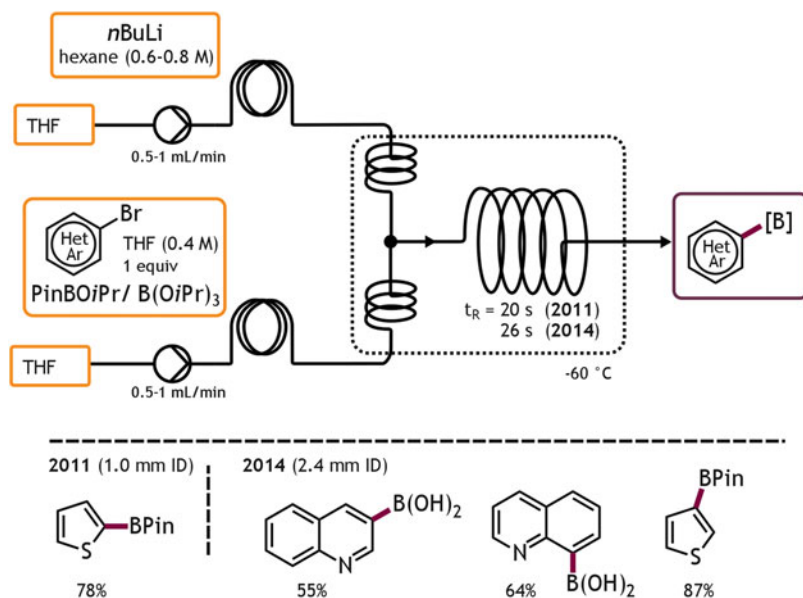
Scheme 75 Deprotonation and borate ester quench, followed by immediate Suzuki-Miyaura coupling (Shu et al. [53])

of the Ir catalyst never exceeded the 10 ppm range and the column was used well over 1 month of experimentation without diminished returns.

In 2011, two groups more or less simultaneously reported a sequential lithiation/borylation procedure for the synthesis of aryl boronic acids and esters. Shu et al. from MIT accomplished the lithiation by merging the bromobenzene and *n*BuLi solutions in a room temperature reaction loop in the range of minutes to seconds, and subsequent quenching with $\text{B}(\text{O}i\text{Pr})_3$ (Scheme 75). By maintaining the quenching solution sufficiently dilute, and with acoustic irradiation, clogging was prevented in the second reactor loop. Interestingly, for substituted thiophenes and furans, it was found that simple C-H lithiation was satisfactory. The authors then continue by using the aryl trialkoxy borate salt in a Suzuki-Miyaura cross-coupling with a second haloarene, by merging a KOH stream and a Pd precatalyst.

Browne et al. from Cambridge reported a similar strategy [166]. From previous projects involving flow chemistry under cryogenic conditions, they experienced the need for efficient cooling units which do not rely on consumable cooling liquids. Thus, they assembled a cryo unit based on refrigerator technology (aptly named “Polar Bear”), which could maintain temperatures as low as -89°C for prolonged time. With the equipment in hand, they first investigated a segmented flow approach for the halogen/lithium exchange. An inlet of aryl bromide and the boron electrophile (first $\text{B}(\text{O}i\text{Pr})_3$, later $\text{PinBO}i\text{Pr}$) was run through a precooling loop, and merged with an equally precooled stream of $n\text{BuLi}$ in hexanes (Scheme 76). Inside the reactor loop, lithiation was performed at -60°C over 20 min, and acidic workup delivered the desired arylboronic pinacol esters, including one heterocyclic example. They later explored the possibility of rendering the process fully continuous, with HPLC pumps injecting the reagents (and notably, $n\text{BuLi}$) directly from the stock solution. This was readily achieved without thickening of the reagent stream, by using larger tubing and a more polar solvent system.

The Cambridge group in a following publication expanded this methodology further [167]. A first innovation was the use of wider bore tubing in a second generation of the cryo unit. In this way, a number of arylboronic acids and esters were prepared that previously caused problematic clogging, among others from quinoline and thiophene. The next hurdle to overcome was insufficient purity for some substrates. After considering in-line and off-line purification modules, the solution to their problem consisted of a non-simultaneous lithiation/quench

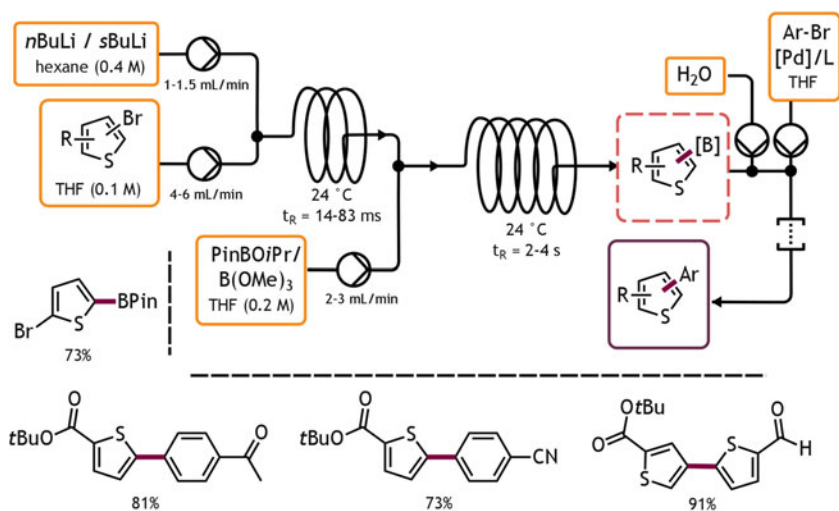


Scheme 76 Br/Li exchange and subsequent capture with boron electrophile affords boronic acids or esters (Browne et al. [166] and Newby [167])

sequence. On a larger scale, wider tubing and longer precooling and reactor loops performed the reaction equally well, and in-line liquid/liquid phase separation provided over 26 g of pure material in 30 min total reaction time.

Despite these significant advances, an important drawback with abovementioned methods is the inability to borylate sensitive group containing arenes. Electrophilic moieties like esters, nitriles, or nitro groups were not reported. The presumed incompatibility arose from the strongly nucleophilic character of the aryllithium species. However, Nagaki et al. postulated that a flash chemistry approach should counter this side reaction; owing to the very short residence times, the aryllithium species is not allowed to react with itself before it is quenched with the boron electrophile [54]. In a first reactor, the aryl halide was merged with the lithiating agent under individually optimized conditions (either a butyllithium isomer or phenyllithium) for a duration between 10 and 100 ms at a certain temperature (Scheme 77). In a subsequent mixer piece, the isopropyl pinacol borate was joined and a variety of arylboronic pinacol esters were obtained, among others the 2-thiophene variant. They then found that a space integration with the subsequent Suzuki-Miyaura coupling could be achieved. Switching to the arene dimethylboronate derivatives, hydrolysis was found to occur simply by adding base-free water, and a fourth inlet containing aryl halide and the palladium/ligand combination at 50°C enabled efficient biaryl coupling. The authors performed the same protocol more recently with a monolithic palladium-packed reactor [168].

A recent application of the lithiation/borylation procedure was demonstrated by a team from Takeda Pharmaceutical [169]. In their study of the synthesis of PI3K α inhibitor TAK-117, a problem was the large cost of the palladium catalyst and diboron species needed for the Miyaura borylation of 2-amino-6-bromobenzoxazole.

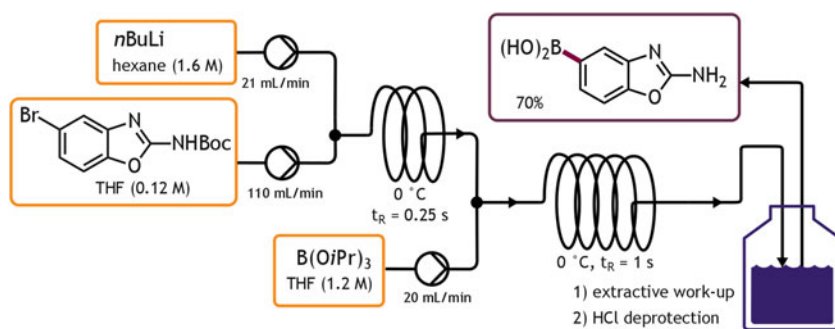


Scheme 77 Borylation and subsequent Suzuki-Miyaura coupling by Br/Li exchange and electrophile capture (Nagaki et al. [54])

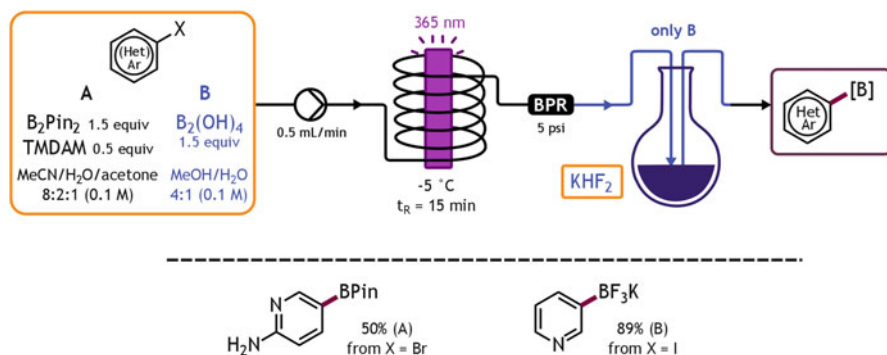
Instead, they opted for a catalyst-free organometallic approach, using the much more affordable $B(OiPr)_3$ as a boron source. As demonstrated before, flow chemistry is often highly desirable for these highly reactive intermediates, and also in their case batch lithiation was tried to no avail. Preliminary tests in flow revealed that prior Boc protection was necessary to accomplish the exchange, and although a narrow operating window was found for $0^\circ C$, a residence time of 0.21 s proved very capable of realizing the transformation. Also on a larger scale, using wider bore tubing (ID 2.17 mm) they were able to maintain a continuous borylation protocol for over 10 h, affording 1.23 kg of the desired boronic acid in excellent purity (Scheme 78). Unfortunately, due to the imperative protection and deprotection steps, the process did not end up being more cost effective, but avoiding the palladium catalyst and potentially mutagenic diboron species made it more attractive nonetheless.

An entirely metal-free alternative was recently proposed by Chen and coworkers [170]. Both in batch and in flow, they reported their discovery of the first photochemical borylation of aryl bromides and iodides. When stirring the mixture of an aryl iodide with B_2pin_2 and tetramethyl diaminomethane (TMDAM) in the bespoke MeCN/H₂O/acetone mixture, they found that under UV irradiation good conversion to the corresponding aryl pinacolyl boronate was obtained. Even better results were reported under flow conditions. The homemade flow setup consisted of a mercury lamp placed inside a jacketed quartz immersion vessel, and transparent tubing wrapped around while cooling at $-5^\circ C$ (Scheme 79). Flowing for 15–30 min furnished several borylated arenes, including the otherwise challenging electron-poor benzenes and one example of a pyridine. Interestingly, also bisboronic acid was a capable reaction partner, after which the product was captured by KHF_2 .

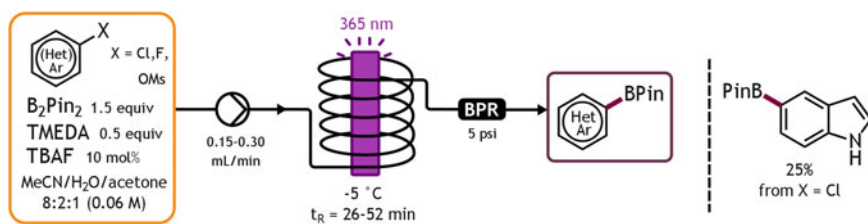
Later that year, the same group published a modification that allowed them to transform aryl chlorides, fluorides, and mesylates to their boronic counterparts [171]. This mechanistically compelling reaction made use of the same setup and comparable conditions, and was effective for electron-rich arenes after 26–52 min (Scheme 80). 5-Chloroindole was functionalized in this way, and also a high-yielding, gram scale preparation of *p*-phenolboronic acid pinacol ester was showcased.



Scheme 78 Large scale continuous preparation of 2-aminobenzoxazole-6-boronic acid (Usutani et al. [169])



Scheme 79 Flow borylation of aryl iodides and bromides under UV irradiation (Chen et al. [170])



Scheme 80 Continuous, UV-mediated borylation of electron-rich aryl chlorides, fluorides or mesylates (Chen et al. [171]). *TMEDA* *N,N,N',N'*-tetramethyl ethylene diamine, *TBAF* tetrabutylammonium fluoride

8 C-X Bond Forming Reactions

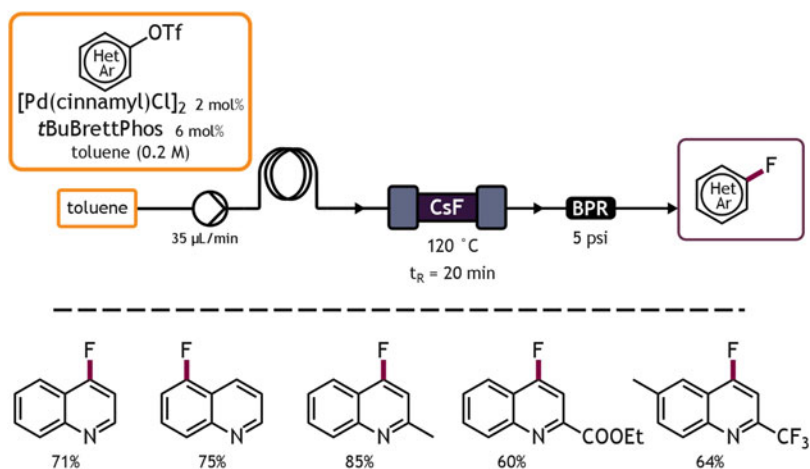
8.1 Fluorination

Of all fluorine-containing pharmaceuticals, 47% possesses an aryl fluoride bond. Several different pathways have been proposed to gain access to these important structural motifs, although these reactions have often not yet reached the same level of feasibility as other carbon-heteroatom bond formations [172]. For example, protocols for an electrophilic aromatic fluorination are often either hazardous or require expensive reagents. Also here, flow chemistry can provide a solution to this problem. The group of Yoshida used their expertise in flash chemistry to develop a sequence of halogen/lithium exchange and treatment with the relatively affordable $[\text{F}^+]$ source NFSI, to afford a variety of fluorobenzenes [173]. A similar tactic of magnesiation/fluorination was used by the group of Knochel to afford a variety of fluorinated heteroarenes, but was only reported in batch [174].

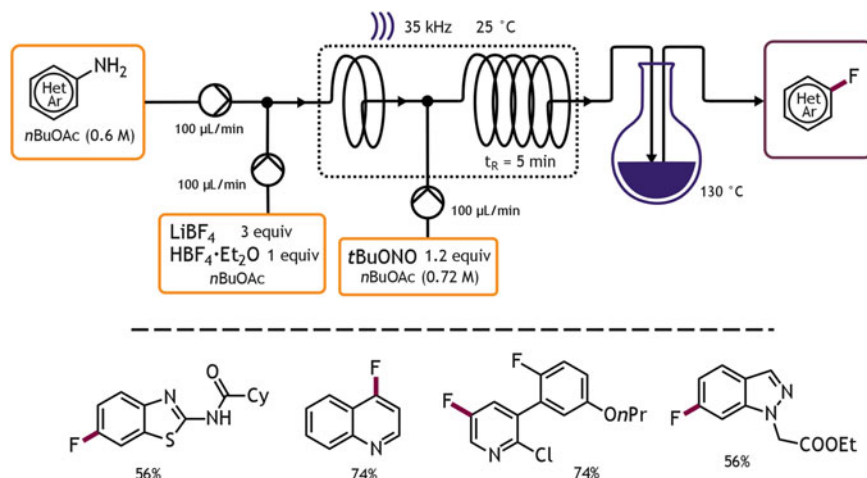
Noël et al. proposed a flow through nucleophilic aromatic fluorination [175] based on their previous work on Pd-catalyzed fluorination in batch [176]. Herein, the successful fluorination from nucleophilic fluorine sources is described for the

first time, using CsF as F⁻ source and *t*BuBrettPhos as the bulky ligand to overcome the reductive elimination hurdle. In an effort to translate this process to a continuous system, they borrowed from their previous experience with packed bed reactors to address the perennial clogging issue [23, 52], only this time replacing the packing with the poorly soluble CsF salt. Since they found that large excesses of CsF significantly increased the rate of this reaction, the packed bed approach comprised an optimum between rapid reaction and low amounts of waste. By subjecting a toluene solution of aryl triflate, catalyst and ligand to the column, over 20 min. at 120°C, they were able to supply a wide scope of (hetero)aryl fluorides in high yields (Scheme 81).

Recently, Park et al. demonstrated how an old fluorination reaction, which would otherwise be considered “forbidden chemistry,” becomes more appealing when making use of microflow techniques [177]. The Balz-Schiemann reaction consists of a thermal decomposition of an arenediazonium tetrafluoroborate salt, in a way that the corresponding aryl fluoride is obtained with the expulsion of N₂ gas. This remains one of the most important entries to fluoroarenes, because of its relatively wide scope and the accessibility aminoarenes as the feedstock for diazonium salts. However, important drawbacks from a process point of view are subjection of the labile and explosion-prone diazonium salts to harsh conditions, and the modest returns which often accompany it. A fully continuous diazonium salt formation and subsequent Balz-Schiemann reaction had been reported before [178, 179], but the need for intermediate isolation of the salt did not relieve the safety concerns inherent to these products. Where the diazotization step is typically done in water or other polar solvents, the decomposition would lead to undesired side reactions in these conditions and is therefore done in apolar aromatic solvents. The authors sought to overcome this solvent switch hurdle, and a bespoke solvent to perform



Scheme 81 Pd-catalyzed continuous fluorination of aryl triflates using a CsF packed bed reactor (Noël et al. [175])

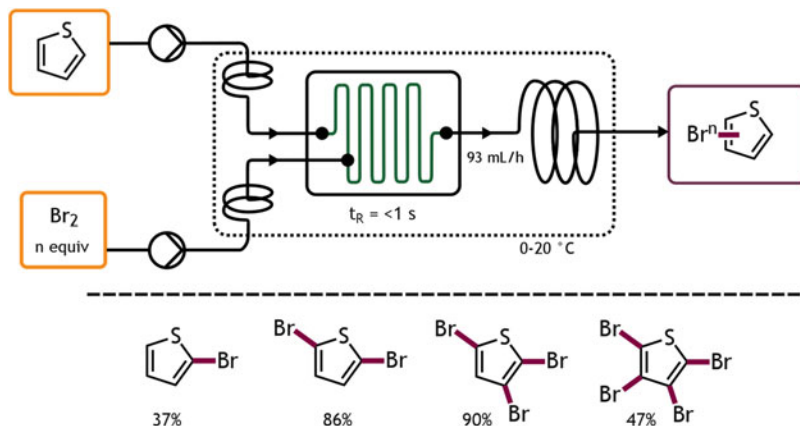


Scheme 82 Continuous flow diazotization and off-line Balz-Schiemann reaction for the synthesis of various fluoroarenes (Park et al. [177])

both steps was found in *n*-butyl acetate (*n*BuOAc). A combination of LiBF₄ and TFA were found optimal for the first step, and combining these with an inlet of the product and of *t*BuONO allowed the diazotization at room temperature while flowing for 7 min. in a sonication bath (Scheme 82). For the next step, they opted for a flow-to-stirred-tank setup. The outlet of the microreactor was connected to a vessel containing a solution of LiBF₄ in *n*BuOAc at 130°C, so that the Balz-Schiemann fluorination occurred rapidly. In this way, the concentration of hazardous diazonium salt at high temperature was kept low and clogging was avoided. A variety of fluoroarenes were synthesized with this protocol, even more challenging substrates like heteroarenes and sterically hindered benzenes.

8.2 Bromination

An early example of continuous electrophilic bromination was reported by Löb and coworkers [180]. In their extensive study of the synthesis of bromothiophenes, they found that a microreactor setup gave consistently better yields than reported batch procedures. Moreover, since this solvent and catalyst free process required less than 1 s to complete (compared to several hours in batch due to careful reagent addition), the space/time yield was drastically improved. The thiophene and Br₂ feeds were first allowed to assume the correct temperature while flowing in a thermostat bath (0–10°C), and then merged in a well-examined microfluidic mixer (Scheme 83). Quenching in a thiosulfate reservoir furnished the brominated heterocycle. By varying the ratio of bromine to thiophene, especially the 2,5-dibromo and the 2,3,5-tribromo derivative were obtained in high yields (81% and 90%, respectively).



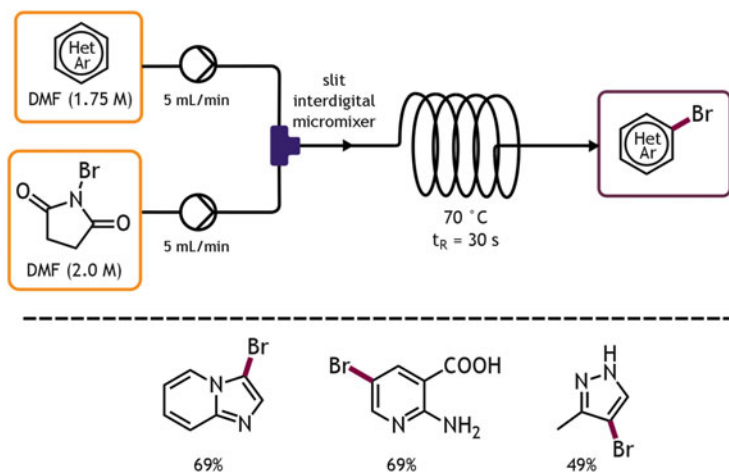
Scheme 83 Microfluidic bromination of thiophene using a caterpillar mixing element (Lob et al. [180])

Pelleter et al. likewise found that the bromination of imidazo[1,2-*a*]pyridine in a continuous system posed a significantly improved alternative to the batch reaction [115]. The safety profile in particular was affected: a previous effort to scale up the batch process proved quite susceptible to eruptive incidents, due to the reaction exotherm. They employed the same system as previously used for nitration studies, with the solvent and NBS inlets combining in the interdigital micromixer and further reacting in the residence loop. The choice for DMF as the solvent ensured full solubility. When elevating the temperature to 70°C, they noticed that a residence time of 30 s sufficed, and high throughputs of 5-bromoimidazo[1,2-*a*]pyridine were obtained in this way with excellent purity (Scheme 84). Also two other heteroarenes were successfully brominated with this protocol and even the chlorination of 3-methylpyrazole was attempted, albeit in low yield.

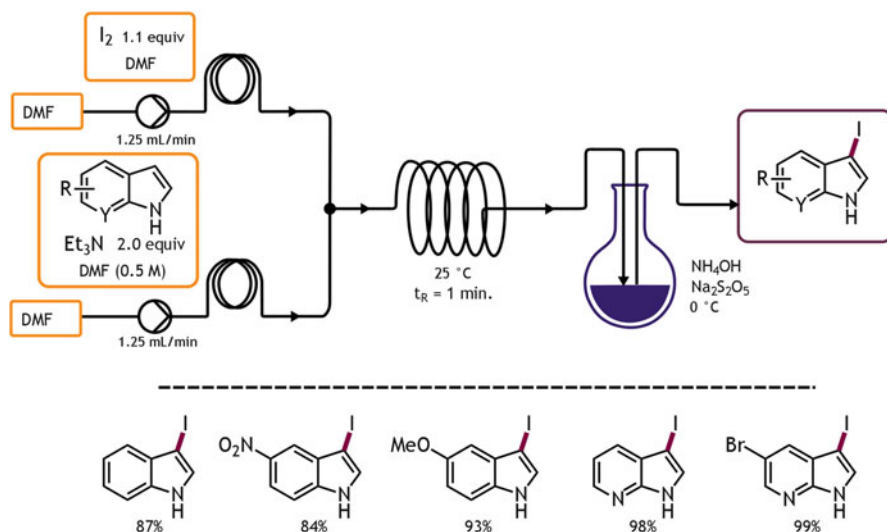
8.3 Iodination

Although the electrophilic iodination of arenes is in many ways similar to its bromination counterpart, a difference on the level of flow chemistry is the solid nature of molecular iodine. An interesting workaround was shown by Midorikawa and coworkers [181]. Molecular iodine in MeCN was treated electrochemically prior to injection, so that the reactive species CH_3CNI^+ was merged with an inlet of dimethoxybenzene for further iodination.

D'Attoma et al. recently reported a general continuous synthesis of 3-iodo(aza)indoles [182]. Starting from the heterogeneous batch protocol using KOH and I_2 in DMF, they worked toward a completely soluble variant using Et_3N as the base. Subsequently, they found that decreasing the residence time to only 1 min was sufficient to complete the reaction in yields higher than 80% (Scheme 85).



Scheme 84 Continuous electrophilic bromination with NBS using a micromixer (Pelletier and Renaud [115])



Scheme 85 Continuous 3-iodination with I_2 of several indoles and azaindoles (D'Attoma et al. [182])

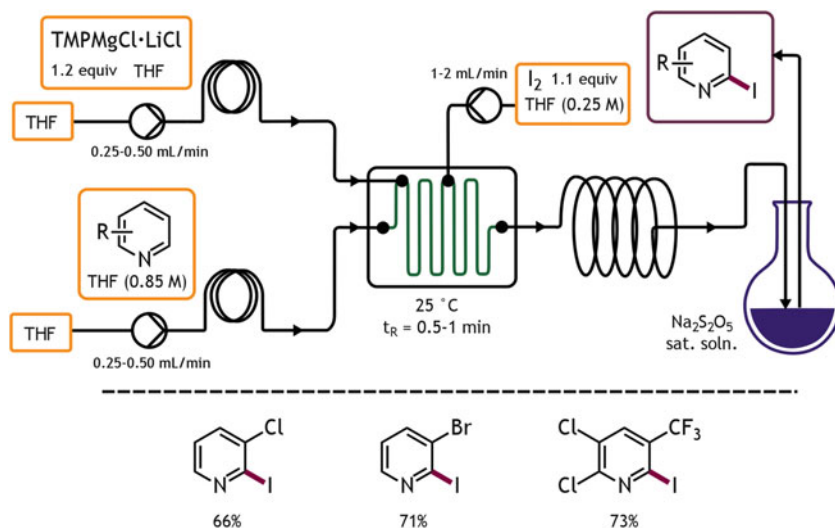
Subsequent quenching in $Na_2S_2O_5$ provided a panel of 3-iodoindoles and 3-iodoazaindoles. They then proceeded to develop a flow protocol for *N*-Boc protection and Sonogashira coupling on the 3-position.

This entry to iodoarenes directly from an unsubstituted C-H bond is an attractive pathway. Knochel adopted the same approach to functionalize an array of azines and azoles, using their previously discovered base $TMPMgCl \cdot LiCl$ [183]. In batch mode, they had been successful in the magnesiation of pyridines, albeit at cryogenic

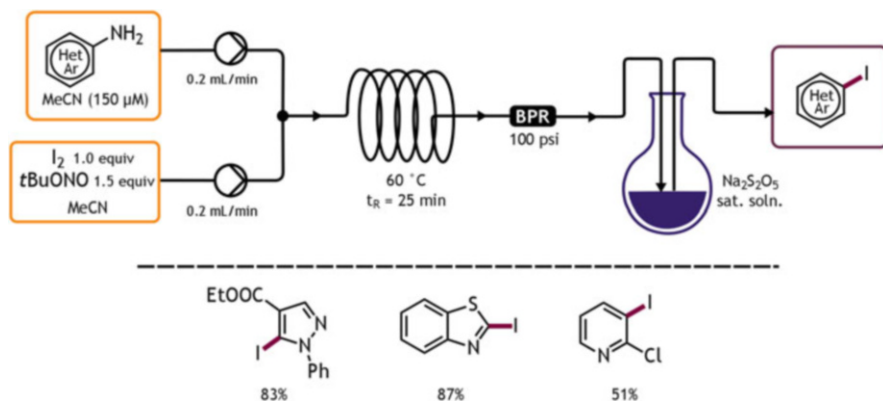
conditions (often $\leq -25^\circ\text{C}$). Now, they envisaged a microflow protocol, similar to flash lithiation chemistry, which allowed them to do the metalation at room temperature. When the combined streams of an electron-poor pyridine and a near-stoichiometric amount of $\text{TMPMgCl}\cdot\text{LiCl}$ solution were injected to a microfluidic reactor, the magnesiation was found to be complete after 30 s (Scheme 86). In the same chip, an inlet of I_2 was brought and allowed to react in the ensuing reaction loop at room temperature to realize the electrophilic quenching. Also other electrophiles were found to be successful, such as benzaldehyde, acetone, DMF, or allyl bromide. Several five- and six-membered heteroarenes were functionalized in this way in appreciable yields, and even polymerization-prone acrylates could be efficiently metalated at lower temperatures.

Similar to the Balz-Schiemann reaction, Malet-Sanz et al. set out to generate a library of aryl iodides from aminoarenes in a iododeamination reaction [184]. In contrast to the classic Sandmeyer reaction, the anhydrous counterpart between an aniline and an alkyl nitrite supposedly runs via a triazene intermediate which releases an aryl radical upon heating, capable of electrophilic quenching and thus not requiring any Cu(I) salt. This approach was used as a continuous, mild and metal-free entry to iodoarenes, which would otherwise comprise an unattractively hazardous batch protocol. Merging a stream of (hetero)arylamine in dry MeCN , with a solution of I_2 and $t\text{BuONO}$ in MeCN and subsequent heating in a 60°C coil over 25 min furnished several heteroaryl iodides in good yields (Scheme 87).

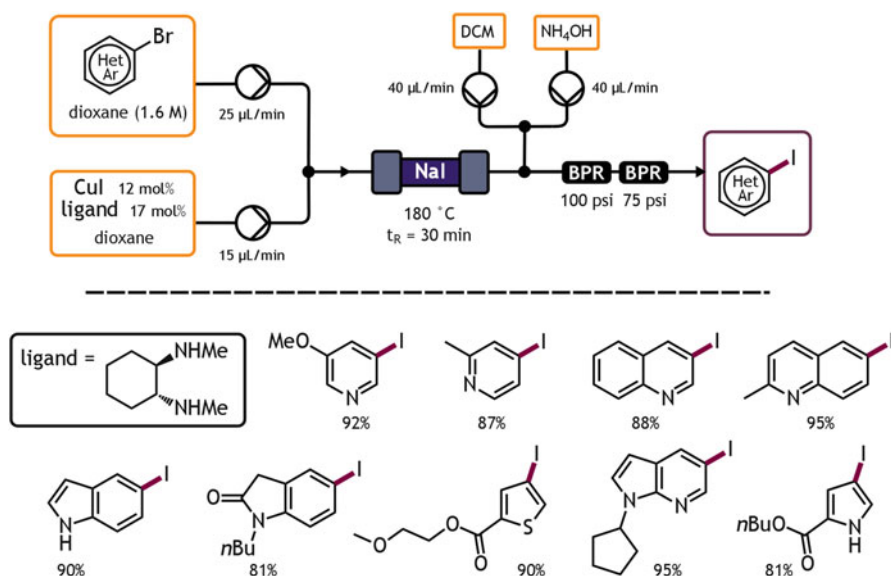
A rare example of nucleophilic iodination on heteroarenes is the aromatic Finkelstein reaction, developed by the group of Buchwald. The catalytic system for this batch transformation consisted of CuI and a diamine ligand, and was



Scheme 86 Continuous C-H magnesiation and iodination of azines (Petersen et al. [183]). *TMP* 2,2,6,6-tetramethylpiperidine



Scheme 87 Flow iododeamination of several aminoarenes (Malet-Sanz et al. [184])



Scheme 88 Aromatic Cu-catalyzed Finkelstein reaction in continuous mode using a NaI packed bed reactor (Chen et al. [154])

typically performed in dioxane at 110°C for 24 h [185]. When revisiting this reaction in order to evaluate its feasibility in microflow, they opted for a packed bed approach, on account of the low solubility of NaI in aprotic solvents [154]. Employing the same reaction conditions, only this time at 180°C, they found that the reaction reached completion in very high yield after 30 min (Scheme 88). A wide scope of pyridines and (fused) azoles was reported in typically higher than 80% yield. In the same study, they go on to investigate the streamlined S_N2 amination of these iodoarenes, as well as the Mg/I exchange followed by addition onto carbonyl electrophiles.

9 C-S Bond Forming Reactions

Good examples of the usefulness of flow chemistry can often be found in thermal rearrangements. The Newman-Kwart rearrangement (NKR) is one of those sigmatropic reactions which turns *O*-aryl thiocarbamates into *S*-aryl thiocarbamates, and thus constitutes an effective entry to thiophenols from phenols. The reaction has been shown to work for pyridines [186], and to benefit from flow conditions [187], but no heteroarenes were functionalized in the latter report.

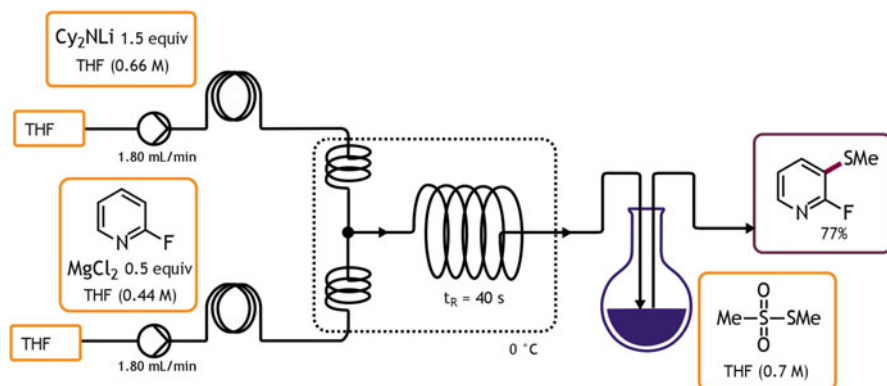
The 130-year-old Stadler-Ziegler reaction is another classic reaction for the preparation of arylthioethers. An aryldiazonium salt is herein treated with an aryl or alkyl sulfide, and after expulsion of N₂ gas, the thioether is afforded – described by the original authors as an explosive event [188]. A more modern version of this “forbidden chemistry” was reported by Wang and coworkers, who used a photocatalytic microflow procedure to generate a variety of (hetero)aryl sulfides [189] (a more elaborate discussion will be provided in [190]).

Similarly, the group of Ley proposed a flow chlorosulfonylation of aryldiazonium salts [191]. In their protocol, a solution of an aniline, a chloride salt and SO₂ in MeCN was merged with an injection of *t*BuONO, which after diazotation was treated with CuCl₂ to catalyze the denitrogenative chlorosulfonylation. This could further be reacted off-line with an amine to yield different sulfonamides, although no heteroarenes were reported.

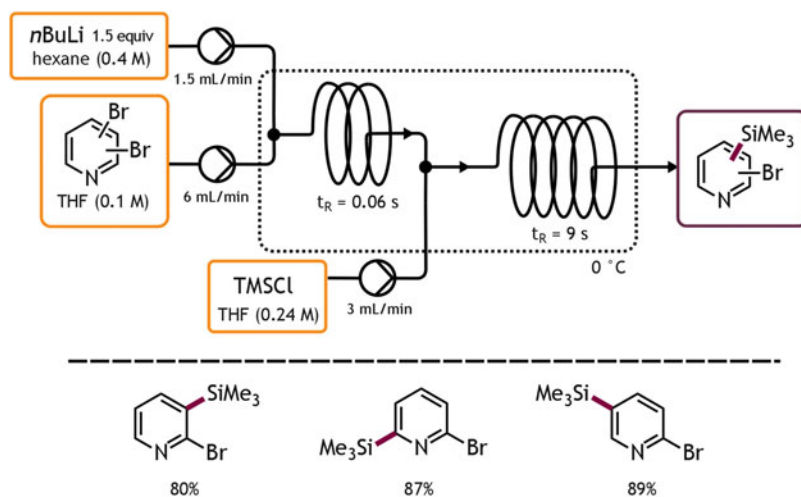
Becker et al. described a direct C-H metalation approach towards functionalized arenes [62]. In a previous report, they showed how TMPLi in the presence of metal salts emerged as a very capable base to abstract the most acidic proton off of several benzenes and heteroarenes [192]. Now, endeavoring to seek alternatives for the expensive 2,2,6,6-tetramethylpiperidine, they found that Cy₂NLi in the presence of ZnCl₂ or MgCl₂ performed at least as effectively, albeit at a 100-fold lower cost. An inlet of, e.g., 2-fluoropyridine and MgCl₂ in THF was merged with a stream of Cy₂NLi, and the formed Grignard reagent was subsequently quenched with *S*-methyl methanethiosulfonate to afford 3-methylthio-2-fluoropyridine (Scheme 89).

10 C-Si Bond Forming Reactions

A single example of direct silylation of the heteroaromatic ring in flow comes from the group of Yoshida [72]. A flash chemistry approach was used to selectively lithiate one bromide on dibrominated pyridines. Even under non-cryogenic conditions (0°C), treatment with *n*BuLi combined with a residence time of only 0.06 s with subsequent TMSCl quenching provided good yields of the silylated monobromopyridine (Scheme 90). Also a second lithiation was achieved, when a subsequent unit at –28°C was coupled. A second equivalent of *n*BuLi and a residence time of 0.5–1 s sufficiently performed Br/Li exchange, whereafter electrophile quenching afforded the disubstituted pyridine. In a later, more elaborate report, they used the same strategy to silylate monobromopyridines [193].



Scheme 89 Deprotonative magnesiation and off-line methylthiolation of 2-fluoropyridine (Becker et al. [62])



Scheme 90 Flash lithiation of dibromopyridines and subsequent trapping with the silicon electrophile (Nagaki et al. [72]) *TMSCl* trimethylsilyl chloride

More recently, Michel and Greaney used a similar lithiation approach for silyl group installment [194]. Starting from several *o*-bromophenol silyl ethers, the Br/Li exchange with *n*BuLi spontaneously effected the retro-Brook rearrangement to furnish *o*-trimethylsilylphenols. Telescoped triflation or nonaflation enabled easy access to a series of benzyne precursors, although no heteroarenes were reported.

11 Conclusion

Microflow technology has brought about some intriguing advances for heterocyclic functionalization. In some cases, flow protocols even enabled transformations which are practically unfeasible in batch mode. In many other cases, reaction times are drastically reduced, turnover is improved or safety profiles are much more workable.

From the overview in this chapter, some specific benefits of flow chemistry in the field of heteroarene functionalization can be summarized:

- **Process intensification:** reactions requiring high temperatures can be heated more efficiently in microchannels, allowing even superheating of a solvent. For this reason, flow reactions can often be conducted significantly faster than their batch counterparts.
- **Biphasic procedures:** gas/liquid reactions are typically well enhanced by microflow conditions. The ability to pressurize the reagent streams on one hand and the high contact area due to small channel dimensions on the other make for much more ideal conditions than can be obtained in batch.
- **Catalyst immobilization:** making use of packed bed reactors, flow processes may benefit from immobilized metal catalysts that can be reused multiple times. In this way, expensive metals like Pd or Ir need not be added as homogeneous catalysts, rendering the whole process more cost-effective.
- **Flash chemistry:** the ultrashort reaction times that are attainable in microflow enable some challenging lithiations, in high selectivity at non-cryogenic temperatures, which would otherwise suffer from side reactions.
- **Hazardous reagents and intermediates:** in continuous mode, the formation of dangerous intermediates like nitration mixtures or organic diazo compounds forms much less of a safety issue. This can be attributed to the fact that only minimal quantities of a certain hazardous structure exist at the same time and also because temperature control is far superior. For this reason, even deliberate, thermal decomposition of explosive compounds is allowed which would otherwise be unthinkable under batch conditions.

Although the handling of solids in microchannels will remain a perennial struggle for flow chemists, some innovations have certainly met this hardship. With the aid of ultrasound irradiation, solids can be prevented from coagulating, and packed bed reactors form a means of reacting the most insoluble of solids. Other advances will also increasingly simplify complete syntheses in flow. In-line purification modules like scavenging resins, chromatography units, membrane separation or continuous extraction are capable of delivering pure products at the end of the production line.

In recent years, some impressive continuous syntheses on process level have lifted the veil of what could be the future of API manufacturing. The inherent scalability aspect of microflow chemistry has captured interest of increasing numbers of process chemists, and steadily this mode of synthesis is becoming a fixed value in lab benches and pilot plants alike. Our prediction is that the field of heteroarene functionalization in flow will follow this trend. Not only will the

multitude of batch transformations become translatable to flow at some point, but it is also conceivable that continuous mode may surpass many batch processes in terms of versatility and reproducibility. Further research could follow up on this path by creating concepts that enable more effective reactions, easier monitoring, and practical purification.

References

1. Oger N, Le Grogne E, Felpin F-X (2015) *Org Chem Front* 2(5):590–614
2. Movsisyan M, Delbeke EI, Berton JK, Battilocchio C, Ley SV, Stevens CV (2016) *Chem Soc Rev* 45(18):4892–4928
3. Nagaki A, Yoshida J-I (2014) *Microreactor technology in lithium chemistry. Lithium compounds in organic synthesis*. Wiley-VCH Verlag GmbH, KGaA, Weinheim, pp 491–512
4. Nagaki A, Yoshida J-I (2016) Preparation and use of organolithium and organomagnesium species in flow. In: Noël T (ed) *Organometallic flow chemistry. Topics in organometallic chemistry*, vol 57. Springer, Berlin, pp 137–175
5. Degennaro L, Carlucci C, De Angelis S, Luisi R (2016) *J Flow Chem* 6(3):136–166
6. Noel T, Hessel V (2015) *Cross-coupling chemistry in continuous flow. New trends in cross-coupling: theory and applications*. The Royal Society of Chemistry, London, pp 610–644
7. Noel T, Buchwald SL (2011) *Chem Soc Rev* 40(10):5010–5029
8. Cantillo D, Kappe CO (2014) *ChemCatChem* 6(12):3286–3305
9. Baumann M, Baxendale IR, Ley SV (2011) *Mol Divers* 15(3):613–630
10. Wegner J, Ceylan S, Kirschning A (2012) *Adv Synth Catal* 354(1):17–57
11. Malet-Sanz L, Susanne F (2012) *J Med Chem* 55(9):4062–4098
12. Porta R, Benaglia M, Puglisi A (2016) *Org Process Res Dev* 20(1):2–25
13. Britton J, Raston CL (2017) *Chem Soc Rev* 46(5):1250–1271
14. Chinchilla R, Najera C (2007) *Chem Rev* 107(3):874–922
15. Doucet H, Hierso J-C (2007) *Angew Chem Int Ed* 46(6):834–871
16. Chinchilla R, Najera C (2011) *Chem Soc Rev* 40(10):5084–5121
17. Karak M, Barbosa LCA, Hargaden GC (2014) *RSC Adv* 4(96):53442–53466
18. Wang D, Gao S (2014) *Org Chem Front* 1(5):556–566
19. Kawanami H, Matsushima K, Sato M, Ikushima Y (2007) *Angew Chem Int Ed* 46(27):5129–5132
20. Lee HJ, Park K, Bae G, Choe J, Song KH, Lee S (2011) *Tetrahedron Lett* 52(39):5064–5067
21. Placzek MS, Chmielecki JM, Houghton C, Calder A, Wiles C, Jones GB (2013) *J Flow Chem* 3(2):46–50
22. Shu W, Buchwald SL (2011) *Chem Sci* 2(12):2321–2325
23. Naber JR, Buchwald SL (2010) *Angew Chem* 122(49):9659–9664
24. Negishi E-i, Kotoru M, Xu C (1997) *J Org Chem* 62(25):8957–8960
25. Znidar D, Hone CA, Inglesby P, Boyd A, Kappe CO (2017) *Org Process Res Dev* 21:878–884
26. Xue F, Deng H, Xue C, Mohamed DKB, Tang KY, Wu J (2017) *Chem Sci* 8:3623–3627
27. Kuhn S, Hartman RL, Sultana M, Nagy KD, Marre S, Jensen KF (2011) *Langmuir* 27(10):6519–6527
28. Hawbaker N, Wittgrove E, Christensen B, Sach N, Blackmond DG (2016) *Org Process Res Dev* 20(2):465–473
29. Teci M, Tilley M, McGuire MA, Organ MG (2016) *Chem Eur J* 22(48):17407–17415
30. Johansson Seechurn CCC, Kitching MO, Colacot TJ, Snieckus V (2012) *Angew Chem Int Ed* 51(21):5062–5085
31. Torborg C, Beller M (2009) *Adv Synth Catal* 351:3027
32. Miyaura N, Suzuki A (1995) *Chem Rev* 95(7):2457–2483

33. Düfert MA, Billingsley KL, Buchwald SL (2013) *J Am Chem Soc* 135(34):12877–12885
34. Len C, Bruniaux S, Delbecq F, Parmar V (2017) *Catalysts* 7(5):146
35. Shore G, Morin S, Organ MG (2006) *Angew Chem Int Ed* 45(17):2761–2766
36. Baxendale IR, Griffiths-Jones CM, Ley SV, Tranmer GK (2006) *Chem Eur J* 12(16):4407–4416
37. Yamada YMA, Watanabe T, Beppu T, Fukuyama N, Torii K, Uozumi Y (2010) *Chem Eur J* 16(37):11311–11319
38. Trinh TN, Hizartidis L, Lin AJS, Harman DG, McCluskey A, Gordon CP (2014) *Org Biomol Chem* 12(47):9562–9571
39. Mateos C, Rincón JA, Martín-Hidalgo B, Villanueva J (2014) *Tetrahedron Lett* 55(27):3701–3705
40. Pascanu V, Hansen PR, Bermejo Gómez A, Ayats C, Platero-Prats AE, Johansson MJ, Pericàs MÀ, Martín-Matute B (2015) *ChemSusChem* 8(1):123–130
41. Yang G-R, Bae G, Choe J-H, Lee S-W, Song K-H (2010) *Bull Kor Chem Soc* 31(1):250–252
42. de Muñoz JM, Alcázar J, de la Hoz A, Díaz-Ortiz A (2012) *Adv Synth Catal* 354(18):3456–3460
43. Egle B, Muñoz J, Alonso N, De Borggraeve W, de la Hoz A, Díaz-Ortiz A, Alcázar J (2015) *J Flow Chem* 4(1):22–25
44. Miller PW, Long NJ, de Mello AJ, Vilar R, Audrain H, Bender D, Passchier J, Gee A (2007) *Angew Chem Int Ed* 46(16):2875–2878
45. Hartwig JF (2015) *J Am Chem Soc* 138(1):2–24
46. Fabry DC, Ho YA, Zapf R, Tremel W, Panthöfer M, Rueping M, Rehm TH (2017) *Green Chem* 19(8):1911–1918
47. Zhang L, Geng M, Teng P, Zhao D, Lu X, Li J-X (2012) *Ultrason Sonochem* 19(2):250–256
48. Frost CG, Mutton L (2010) *Green Chem* 12(10):1687
49. Wilson NS, Sarko CR, Roth GP (2004) *Org Process Res Dev* 8(3):535–538
50. Noël T, Musacchio AJ (2011) *Org Lett* 13(19):5180–5183
51. Li J-H, Liu W-J, Xie Y-X (2005) *J Org Chem* 70(14):5409–5412
52. Noël T, Kuhn S, Musacchio AJ, Jensen KF, Buchwald SL (2011) *Angew Chem Int Ed* 50(26):5943–5946
53. Shu W, Pellegatti L, Oberli MA, Buchwald SL (2011) *Angew Chem Int Ed* 50(45):10665–10669
54. Nagaki A, Moriwaki Y, Yoshida J (2012) *Chem Commun* 48(91):11211–11213
55. Christakakou M, Schön M, Schnürch M, Mihovilovic MD (2013) *Synlett* 24(18):2411–2418
56. Dalla-Vechia L, Reichart B, Glasnov T, Miranda LSM, Kappe CO, de Souza ROMA (2013) *Org Biomol Chem* 11(39):6806–6813
57. Valente C, Çalimsiz S, Hoi KH, Mallik D, Sayah M, Organ MG (2012) *Angew Chem Int Ed* 51(14):3314–3332
58. Nagaki A, Kenmoku A, Moriwaki Y, Hayashi A, Yoshida J-i (2010) *Angew Chem Int Ed* 49(41):7543–7547
59. Linghu X, Wong N, Jost V, Fantasia S, Sowell CG, Gosselin F (2017) *Org Process Res Dev*
60. Schlosser M (2005) *Angew Chem Int Ed* 44(3):376–393
61. Gillis EP, Eastman KJ, Hill MD, Donnelly DJ, Meanwell NA (2015) *J Med Chem* 58(21):8315–8359
62. Becker MR, Ganiak MA, Knochel P (2015) *Chem Sci* 6(11):6649–6653
63. Becker MR, Knochel P (2016) *Org Lett* 18(6):1462–1465
64. Roesner S, Buchwald SL (2016) *Angew Chem Int Ed* 55(35):10463–10467
65. Lange PP, Gooßen LJ, Podmore P, Underwood T, Sciammetta N (2011) *Chem Commun* 47(12):3628
66. Bogdan AR, Charaschanya M, Dombrowski AW, Wang Y, Djuric SW (2016) *Org Lett* 18(8):1732–1735
67. Santos CIM, Barata JFB, Faustino MAF, Lodeiro C, Neves MGPMS (2013) *RSC Adv* 3(42):19219

68. Bourne SL, O'Brien M, Kasinathan S, Koos P, Tolstoy P, Hu DX, Bates RW, Martin B, Schenkel B, Ley SV (2013) *ChemCatChem* 5(1):159–172
69. Gemoets HPL, Hessel V, Noël T (2014) *Org Lett* 16(21):5800–5803
70. Pieber B, Glasnov T, Kappe CO (2014) *RSC Adv* 4(26):13430–13433
71. Puglisi A, Benaglia M, Chiroli V (2013) *Green Chem* 15(7):1790
72. Nagaki A, Yamada S, Doi M, Tomida Y, Takabayashi N, Yoshida J-I (2011) *Green Chem* 13(5):1110–1113
73. Kim H, Nagaki A, Yoshida J (2011) *Nat Commun*:2
74. Tricotet T, O'Shea DF (2010) *Chem Eur J* 16(22):6678–6686
75. Sipőcz T, Lengyel L, Sipos G, Kocsis L, Dormán G, Jones RV, Darvas F (2016) *J Flow Chem* 6(2):117–122
76. Putra AE, Takigawa K, Tanaka H, Ito Y, Oe Y, Ohta T (2013) *Eur J Org Chem* 2013(28):6344–6354
77. Ishitani H, Saito Y, Tsubogo T, Kobayashi S (2016) *Org Lett* 18(6):1346–1349
78. Osorio-Planes L, Rodríguez-Escrich C, Pericàs MA (2014) *Chem Eur J* 20(8):2367–2372
79. Mohapatra SS, Wilson ZE, Roy S, Ley SV (2017) *Tetrahedron* 73(14):1812–1819
80. Haas D, Hammann JM, Greiner R, Knochel P (2016) *ACS Catal* 6(3):1540–1552
81. Phapale VB, Cárdenas DJ (2009) *Chem Soc Rev* 38(6):1598
82. Alonso N, Miller LZ, de Muñoz JM, Alcázar J, McQuade DT (2014) *Adv Synth Catal* 356(18):3737–3741
83. Price GA, Bogdan AR, Aguirre AL, Iwai T, Djuric SW, Organ MG (2016) *Cat Sci Technol* 6(13):4733–4742
84. Zhang H, Buchwald SL (2017) *J Am Chem Soc* 139(33):11590–11594
85. Wu XF, Neumann H, Beller M (2012) *Chem Asian J* 7(8):1744–1754
86. Chen M, Buchwald SL (2013) *Angew Chem Int Ed* 52(44):11628–11631
87. Kiyohide M, Etsuko T, Midori A, Kiyosi K (1981) *Chem Lett* 10(12):1719–1720
88. Liu H, Gu Z, Jiang X (2013) *Adv Synth Catal* 355(4):617–626
89. Monteiro JL, Carneiro PF, Elsner P, Roberge DM, Wuts PGM, Kurjan KC, Gutmann B, Kappe CO (2017) *Chem Eur J* 23(1):176–186
90. Baciocchi E, Muraglia E (1993) *Tetrahedron Lett* 34(23):3799–3800
91. Tran DN, Battilocchio C, Lou S-B, Hawkins JM, Ley SV (2015) *Chem Sci* 6(2):1120–1125
92. Battilocchio C, Feist F, Hafner A, Simon M, Tran DN, Allwood DM, Blakemore DC, Ley SV (2016) *Nat Chem* 8(4):360–367
93. Booth G (2000) Nitro compounds, aromatic. *Ullmann's encyclopedia of industrial chemistry*. Wiley-VCH Verlag GmbH, KGaA, Weinheim
94. Henke L, Winterbauer H (2005) *Chem Eng Technol* 28(7):749–752
95. Burns JR, Ramshaw C (2002) *Chem Eng Commun* 189(12):1611–1628
96. Dummann G, Quittmann U, Gröschel L, Agar DW, Wörz O, Morgenschweis K (2003) *Catal Today* 79:433–439
97. Yang Jiu-Long LIJ-FLUY (2009) *Acta Phys -Chim Sin* 25(10):2045–2049
98. Ferstl W, Klahn T, Schweikert W, Billeb G, Schwarzer M, Loebbecke S (2007) *Chem Eng Technol* 30(3):370–378
99. Antes J, Boskovic D, Krause H, Loebbecke S, Lutz N, Tuercke T, Schweikert W (2003) *Chem Eng Res Des* 81(7):760–765
100. Halder R, Lawal A, Damavarapu R (2007) *Catal Today* 125(1):74–80
101. Dagade SP, Waghmode SB, Kadam VS, Dongare MK (2002) *Appl Catal A* 226(1):49–61
102. Kulkarni AA, Nivangune NT, Kalyani VS, Joshi RA, Joshi RR (2008) *Org Process Res Dev* 12(5):995–1000
103. Ducry L, Roberge DM (2005) *Angew Chem Int Ed* 44(48):7972–7975
104. Kulkarni AA, Kalyani VS, Joshi RA, Joshi RR (2009) *Org Process Res Dev* 13(5):999–1002
105. Knapkiewicz P, Skowerski K, Jaskólska DE, Barbasiewicz M, Olszewski TK (2012) *Org Process Res Dev* 16(8):1430–1435
106. Brocklehurst CE, Lehmann H, La Vecchia L (2011) *Org Process Res Dev* 15(6):1447–1453

107. Veretennikov EA, Lebedev BA, Tselinskii IV (2001) *Russ J Appl Chem* 74(11):1872–1876
108. Yu Z, Lv Y, Yu C, Su W (2013) *Org Process Res Dev* 17(3):438–442
109. Chen Y, Zhao Y, Han M, Ye C, Dang M, Chen G (2013) *Green Chem* 15(1):91–94
110. Kulkarni AA, Beilstein J (2014) *Org Chem* 10:405–424
111. Gutmann B, Cantillo D, Kappe CO (2015) *Angew Chem Int Ed* 54(23):6688–6728
112. De Jong RL, Davidson JG, Dozeman GJ, Fiore PJ, Giri P, Kelly ME, Puls TP, Seamans RE (2001) *Org Process Res Dev* 5(3):216–225
113. Panke G, Schwalbe T, Stirner W, Taghavi-Moghadam S, Wille G (2003) *Synthesis* 2003(18):2827–2830
114. Junkers M (2009) *ChemFiles* 9(4):7–9
115. Pelleter J, Renaud F (2009) *Org Process Res Dev* 13(4):698–705
116. Gage JR, Guo X, Tao J, Zheng C (2012) *Org Process Res Dev* 16(5):930–933
117. Wu R, Smidansky ED, Oh HS, Takhampunya R, Padmanabhan R, Cameron CE, Peterson BR (2010) *J Med Chem* 53(22):7958–7966
118. Zuckerman NB, Shusteff M, Pagoria PF, Gash AE (2015) *J Flow Chem* 5(3):178–182
119. Brown DG, Boström J (2016) *J Med Chem* 59(10):4443–4458
120. Shieh W-C, Lozanov M, Repič O (2003) *Tetrahedron Lett* 44(36):6943–6945
121. Herath A, Dahl R, Cosford NDP (2010) *Org Lett* 12(3):412–415
122. Herath A, Cosford NDP, Beilstein J (2017) *Org Chem* 13:239–246
123. Venturoni F, Nikbin N, Ley SV, Baxendale IR (2010) *Org Biomol Chem* 8(8):1798–1806
124. Guetzoian L, Nikbin N, Baxendale IR, Ley SV (2013) *Chem Sci* 4(2):764–769
125. Butler AJE, Thompson MJ, Maydom PJ, Newby JA, Guo K, Adams H, Chen B (2014) *J Org Chem* 79(21):10196–10202
126. Rassokhina IV, Tikhonova TA, Kobylskoy SG, Babkin IY, Shirinian VZ, Gevorgyan V, Zavarzin IV, Volkova YA (2017) *J Org Chem* 82:9682–9692
127. Chen M, Buchwald SL (2013) *Angew Chem Int Ed* 52(15):4247–4250
128. Hamper BC, Tesfu E (2007) *Synlett* 2007(14):2257–2261
129. Razaq T, Glasnov TN, Kappe CO (2009) *Eur J Org Chem* 2009(9):1321–1325
130. Petersen TP, Larsen AF, Ritzén A, Ulven T (2013) *J Org Chem* 78(8):4190–4195
131. Hartwig J, Ceylan S, Kupracz L, Coutable L, Kirschning A (2013) *Angew Chem Int Ed* 52(37):9813–9817
132. Lee CLK, Sem ZY, Hendra H, Liu XQ, Kwan WL (2013) *J Flow Chem* 3(4):114–117
133. Ingham RJ, Riva E, Nikbin N, Baxendale IR, Ley SV (2012) *Org Lett* 14(15):3920–3923
134. Lin H, Dai C, Jamison TF, Jensen KF (2017) *Angew Chem Int Ed* 56(30):8870–8873
135. Cole KP, Groh JM, Johnson MD, Burcham CL, Campbell BM, Diseroad WD, Heller MR, Howell JR, Kallman NJ, Koenig TM, May SA, Miller RD, Mitchell D, Myers DP, Myers SS, Phillips JL, Polster CS, White TD, Cashman J, Hurley D, Moylan R, Sheehan P, Spencer RD, Desmond K, Desmond P, Gowran O (2017) *Science* 356(6343):1144–1150
136. Chen Y, Liu B, Liu X, Yang Y, Ling Y, Jia Y (2014) *Org Process Res Dev* 18(11):1589–1592
137. Sahoo HR, Kralj JG, Jensen KF (2007) *Angew Chem Int Ed* 46(30):5704–5708
138. Baumann M, Baxendale IR, Ley SV, Nikbin N, Smith CD, Tierney JP (2008) *Org Biomol Chem* 6(9):1577–1586
139. Baumann M, Baxendale IR, Ley SV, Nikbin N, Smith CD (2008) *Org Biomol Chem* 6(9):1587–1593
140. O'Brien AG, Levesque F, Seeberger PH (2011) *Chem Commun* 47(9):2688–2690
141. Tundel RE, Anderson KW, Buchwald SL (2006) *J Org Chem* 71(1):430–433
142. Sunesson Y, Limé E, Nilsson Lill SO, Meadows RE, Norrby P-O (2014) *J Org Chem* 79(24):11961–11969
143. Pommella A, Tomaiuolo G, Chartoire A, Caserta S, Toscano G, Nolan SP, Guido S (2013) *Chem Eng J* 223:578–583
144. Hopkin MD, Baxendale IR, Ley SV (2010) *Chem Commun* 46(14):2450–2452
145. Yang JC, Niu D, Karsten BP, Lima F, Buchwald SL (2016) *Angew Chem Int Ed* 55(7):2531–2535

146. Hartman RL, Naber JR, Zaborenko N, Buchwald SL, Jensen KF (2010) *Org Process Res Dev* 14(6):1347–1357
147. Horie T, Sumino M, Tanaka T, Matsushita Y, Ichimura T, Yoshida J-i (2010) *Org Process Res Dev* 14(2):405–410
148. Sedelmeier J, Ley SV, Baxendale IR, Baumann M (2010) *Org Lett* 12(16):3618–3621
149. Noel T, Naber JR, Hartman RL, McMullen JP, Jensen KF, Buchwald SL (2011) *Chem Sci* 2(2):287–290
150. Kuhn S, Noel T, Gu L, Heider PL, Jensen KF (2011) *Lab Chip* 11(15):2488–2492
151. DeAngelis A, Wang D-H, Buchwald SL (2013) *Angew Chem Int Ed* 52(12):3434–3437
152. Monnier F, Taillefer M (2009) *Angew Chem Int Ed* 48(38):6954–6971
153. Zhang Y, Jamison TF, Patel S, Mainolfi N (2011) *Org Lett* 13(2):280–283
154. Chen M, Ichikawa S, Buchwald SL (2015) *Angew Chem Int Ed* 54(1):263–266
155. Vantourout JC, Miras HN, Isidro-Llobet A, Sproules S, Watson AJB (2017) *J Am Chem Soc* 139(13):4769–4779
156. Singh BK, Stevens CV, Acke DRJ, Parmar VS, Van der Eycken EV (2009) *Tetrahedron Lett* 50(1):15–18
157. Bao J, Tranmer GK (2016) *Tetrahedron Lett* 57(6):654–657
158. Mallia CJ, Burton PM, Smith AMR, Walter GC, Baxendale IR (2016) *Beilstein J Org Chem* 12:1598–1607
159. Britton J, Jamison TF (2017) *Angew Chem Int Ed* 56:8823–8827
160. Lee JK, Fuchter MJ, Williamson RM, Leeke GA, Bush EJ, McConvey IF, Saubern S, Ryan JH, Holmes AB (2008) *Chem Commun* 39:4780–4782
161. Benaskar F, Engels V, Patil N, Rebrov EV, Meuldijk J, Hessel V, Hulshof LA, Jefferson DA, Schouten JC, Wheatley AEH (2010) *Tetrahedron Lett* 51(2):248–251
162. Benaskar F, Patil NG, Engels V, Rebrov EV, Meuldijk J, Hulshof LA, Hessel V, Wheatley AEH, Schouten JC (2012) *Chem Eng J* 207:426–439
163. He Z, Jamison TF (2014) *Angew Chem* 126(13):3421–3425
164. Tagata T, Nishida M, Nishida A (2009) *Tetrahedron Lett* 50(45):6176–6179
165. Tagata T, Nishida M, Nishida A (2010) *Adv Synth Catal* 352(10):1662–1666
166. Browne DL, Baumann M, Harji BH, Baxendale IR, Ley SV (2011) *Org Lett* 13(13):3312–3315
167. Newby JA, Huck L, Blaylock DW, Witt PM, Ley SV, Browne DL (2014) *Chem Eur J* 20(1):263–271
168. Nagaki A, Hirose K, Moriwaki Y, Mitamura K, Matsukawa K, Ishizuka N, Yoshida J (2016) *Cat Sci Technol* 6(13):4690–4694
169. Usutani H, Nihei T, Papageorgiou CD, Cork DG (2017) *Org Process Res Dev* 21:669–673
170. Chen K, Zhang S, He P, Li P (2016) *Chem Sci* 7(6):3676–3680
171. Chen K, Cheung MS, Lin Z, Li P (2016) *Org Chem Front* 3(7):875–879
172. Campbell MG, Ritter T (2015) *Chem Rev* 115(2):612–633
173. Nagaki A, Uesugi Y, Kim H, Yoshida J-i (2013) *Chem Asian J* 8(4):705–708
174. Yamada S, Gavryushin A, Knochel P (2010) *Angew Chem* 122(12):2261–2264
175. Noël T, Maimone TJ, Buchwald SL (2011) *Angew Chem Int Ed* 50(38):8900–8903
176. Watson DA, Su M, Teverovskiy G, Zhang Y, García-Fortanet J, Kinzel T, Buchwald SL (2009) *Science* 325(5948):1661–1664
177. Park NH, Senter TJ, Buchwald SL (2016) *Angew Chem* 128(39):12086–12090
178. Yu ZQ, Lv YW, Yu CM, Su WK (2013) *Tetrahedron Lett* 54(10):1261–1263
179. Yu Z, Lv Y, Yu C (2012) *Org Process Res Dev* 16(10):1669–1672
180. Lob P, Hessel V, Klefenz H, Lowe H, Mazanek K (2005) *Lett Org Chem* 2(8):767–779
181. Midorikawa K, Suga S, Yoshida J-i (2006) *Chem Commun* 36:3794–3796
182. D'Attoma J, Cozien G, Brun PL, Robin Y, Bostyn S, Buron F, Routier S (2016) *ChemistrySelect* 1(3):338–342
183. Petersen TP, Becker MR, Knochel P (2014) *Angew Chem Int Ed* 53(30):7933–7937

184. Malet-Sanz L, Madrzak J, Holvey RS, Underwood T (2009) *Tetrahedron Lett* 50 (52):7263–7267
185. Klapars A, Buchwald SL (2002) *J Am Chem Soc* 124(50):14844–14845
186. Beaulieu F, Snieckus V (1992) *Synthesis* 1992(1/2):112–118
187. Lin S, Moon B, Porter KT, Rossman CA, Zennie T, Wemple J (2000) *Org Prep Pced Int* 32 (6):547–555
188. Stadler O (1884) *Ber Dtsch Chem Ges* 17(2):2075–2081
189. Wang X, Cuny GD, Noël T (2013) *Angew Chem* 125(30):8014–8018
190. Glasnov T (2018) Photochemical synthesis of heterocycles: merging flow processing and metal-catalyzed visible light photoredox transformations. *Top Heterocyclic Chem.* https://doi.org/10.1007/7081_2018_20
191. Malet-Sanz L, Madrzak J, Ley SV, Baxendale IR (2010) *Org Biomol Chem* 8(23):5324–5332
192. Becker MR, Knochel P (2015) *Angew Chem Int Ed* 54(42):12501–12505
193. Nagaki A, Yamada D, Yamada S, Doi M, Ichinari D, Tomida Y, Takabayashi N, Yoshida J-I (2013) *Aust J Chem* 66(2):199–207
194. Michel B, Greaney MF (2014) *Org Lett* 16(10):2684–2687

Flow Chemistry as a Drug Discovery Tool: A Medicinal Chemistry Perspective



Andrew R. Bogdan and Michael G. Organ

Contents

1	Introduction	320
2	From Batch to Flow	320
3	Library Synthesis Using Flow: Efforts to Decrease Cycle Times	321
3.1	Drug Discovery Cycle Times	321
3.2	Segmented Flow Approaches to Library Synthesis	322
3.3	Integrated Flow Synthesis Platforms	324
4	Flow Chemistry Support for Lead Optimization Programs	329
5	Emerging Flow Technologies and Future Opportunities	332
5.1	High-Temperature Flow Reactions	332
5.2	Hazardous Gas Chemistry	335
5.3	Flow Photochemistry Examples in Medicinal Chemistry	337
6	Conclusion and Outlook	339
	References	339

Abstract The applications of flow chemistry in a drug discovery environment are discussed within. The development of integrated synthesis–bioassay platforms is discussed in the context of enabling medicinal chemistry programs, as is the use of flow chemistry to facilitate intermediate scale-up in a lead optimization setting. Emerging chemical technologies are also discussed, highlighting the use of high temperatures, hazardous gases, and photochemistry in flow to support medicinal chemistry efforts.

Keywords Drug discovery · Emerging technologies · Flow chemistry · Integrated systems · Lead optimization · Medicinal chemistry

A. R. Bogdan (✉)
Discovery Chemistry and Technology, AbbVie, Inc., North Chicago, IL, USA
e-mail: andrew.bogdan@abbvie.com

M. G. Organ
Department of Chemistry and Biomolecular Sciences, University of Ottawa, Ottawa, ON,
Canada
e-mail: organ@uOttawa.ca

1 Introduction

The world of drug discovery is often times described as a race, in which several companies are competing for the regulatory approval of active pharmaceutical ingredients (APIs) with similar mechanisms of action [1]. For this reason, it has become imperative for pharmaceutical companies to begin to develop new, enabling technologies that can be used to expedite the drug discovery process, either by reducing cycle times or by facilitating new synthetic methodologies. Over the past few decades, one such technology, flow chemistry, has had continuous growth in the number of manuscripts being published (for example reviews, please see: Refs. [2–11]). While a significant number of these publications are applicable to improving reaction scale-up and manufacturing, this technology has not been widely adopted for drug discovery.

Many of the benefits of using flow-based processes (such as cost and energy savings) become more quantifiable when chemistry is run on process scale. For drug discovery, flow chemistry is often used to address other concerns and will have different applications depending on the stage at which it is being used. In a traditional medicinal chemistry program, the amount of material that is required over the life of the program increases as time goes on. For instance, in earlier stage projects where “go/no-go” decisions are made from mainly primary assay and ADME data, only a few milligrams of final compound is required for the appropriate assays. As projects progress from hit-to-lead to lead optimization, more final material is required as compounds begin to be profiled in a greater number of assays. For this reason, compounds may frequently be synthesized on multi-gram scale in order to provide ample amount of material for pharmacokinetic and toxicology studies. In this review, we present recent examples of where flow chemistry has had an impact on drug discovery and discuss possible avenues flow chemistry would need to take in order for it to reach its fullest potential. Due to space constraints, we will focus mainly on specific internal examples of flow chemistry in discovery and highlight external examples when relevant. We will discuss how flow chemistry has been applied to the different areas of drug discovery, beginning with examples of how flow chemistry has been used to generate chemical libraries for early stage programs (milligram scale). The application of flow chemistry to intermediate scale-up and multistep reaction sequences (gram scale) will also be highlighted. Lastly, emerging technologies to access novel chemical space (such as the use of elevated temperatures, hazardous gases, and photochemistry) will be discussed in the context of drug discovery programs.

2 From Batch to Flow

Organic synthesis is a field historically dominated by batch processes, in which reaction is carried out in round-bottom flasks or batch reactors. In the pharmaceutical industry, these reactors are mainstays, partly due to the overall complexity of the synthesis being carried out. With the need for workups, reaction quenching, phase

separations, and solvent switches that are required in a multistep reaction sequences, the use of batch chemistry is preferred. Alternative synthetic techniques such as flow chemistry, however, have been widely adopted by the fine chemical industry for decades, where comparatively simple commodity chemicals are being synthesized. Over the past few years however, significant advantages have been made in the area of flow chemistry that are enabling members of the pharmaceutical industry to embrace the field. Initially, more complicated multistep reaction sequences involved the careful use of solid-supported reagents and scavengers to facilitate the synthesis of natural products and pharmaceutical agents [12]. Now, due to the advancement of a number of new flow technologies, APIs can be synthesized on demand using multistep sequences using a compact, highly configurable setup [13].

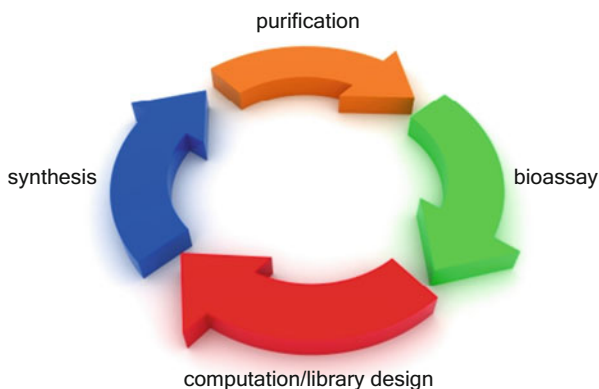
Benefits of using flow reactors have been well-documented in a number of reviews [2–11]. One key reason for these benefits is the increased surface area-to-volume ratio, which leads to improvements in heat transfer and mixing. Flow chemistry also lends itself to automation, resulting in significant gains in efficiency.

3 Library Synthesis Using Flow: Efforts to Decrease Cycle Times

3.1 Drug Discovery Cycle Times

Cycle times in drug discovery are defined by the amount of time that is required to design compounds based upon existing structural activity relationships (SAR), synthesize and purify those compounds, obtain/analyze bioassay data, and design new compounds (Fig. 1). In a traditional pharmaceutical environment, each iteration of this cycle involves the close collaboration of a multidisciplinary team of scientists. The result is an inherently slow process that has responsibilities divided among a number of different groups, each responsible for completing separate tasks before the drug discovery cycle can progress. For this reason, a number of new platforms

Fig. 1 Drug discovery cycle



have been developed with hopes of removing or streamlining steps in the drug discovery cycle, making the overall process much more efficient. One such technology frequently utilized is flow chemistry, specifically in the context of generating small-molecule libraries.

3.2 *Segmented Flow Approaches to Library Synthesis*

Many drug discovery programs have a high-throughput synthesis organization that is responsible for the synthesis of small-molecule libraries, typically designed to support early stage medicinal chemistry programs. Far from the old days of combinatorial chemistry, library synthesis now typically involves more design and property computation, using a variety of cheminformatics tools. As a result, there has been an overall decline in the total number of compounds being synthesized. With this change in mentality with regard to library design, there has come a complimentary change in library synthesis. Historically, parallel chemistry efforts have consisted of the use of polymer-supported reagents and catalysts, microwave chemistry, and multi-component reactions to facilitate library synthesis. The resulting compounds from the library synthesis are subsequently purified, frequently by a separate purifications group. As a result, the entire process of synthesizing and purifying chemical libraries can take at least 7–10 days to complete. From a medicinal chemistry perspective, speeding up library synthesis would be highly advantageous as it could speed up cycle times.

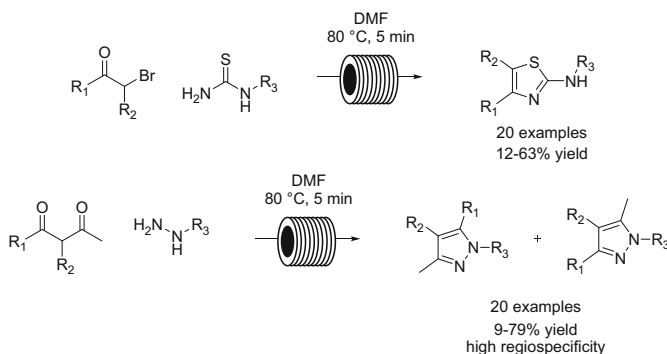
Flow chemistry has been used in drug discovery programs to generate small-molecule libraries in a highly efficient manner. A number of these studies were carried out using segmented flow techniques to prepare small-molecule libraries. Segmented flow chemistry relies on the use of an immiscible fluoruous spacer, such as perfluorodecalin or perfluoromethyldecalin, to separate reaction segments and prevents cross-contamination of sequential reactions. For segmented flow, individual reactions (i.e., library elements) can be carried out in sequence separated by fluoruous spacer, permitting multiple reactions to be carried out in the same reaction path (Fig. 2).



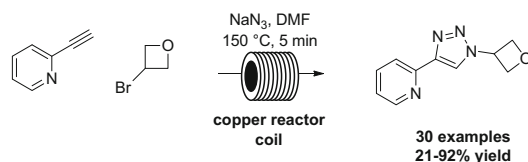
Fig. 2 Segmented flow schematic

Using this technique, a series of thiazole and pyrazole heterocycles were synthesized in sequence on small scale, with purification being performed off-line using preparative reverse-phase HPLC/MS (Scheme 1) [14]. While this was an early example of library synthesis using a segmented flow approach, the overall turnaround time of the library compared to traditional methods was not improved as the procedure relied on the manual setup and purification of each library element. For this reason, a fully automated synthesis and purification platform was investigated.

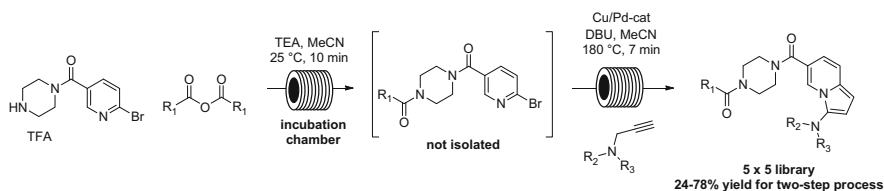
The Accendo Conjure flow reactor has been demonstrated to synthesize small-molecule libraries using this segmented flow approach. The seminal publication using the Conjure reactor uses a copper reactor coil to synthesize small-molecule 1,2,3-triazole libraries [15]. In this system, low-molecular weight azides are generated in situ by the reaction of alkyl halides with sodium azide. The resultant azides are reacted with terminal alkynes, providing the 1,2,3-triazole products in modest to excellent yield (Scheme 2). The Conjure reactor was subsequently used in the preparation of small-molecule libraries of 3-aminoindolizines [16], which could rapidly be synthesized via a multistep protocol (Scheme 3) [17]. While both of these manuscripts demonstrated that library production could be rapidly facilitated using automated flow reactors, the purification of these libraries was again carried out off-line.



Scheme 1 Flow-mediated synthesis of thiazole and pyrazole libraries using segmented flow chemistry [14]



Scheme 2 One-pot triazole library synthesis using copper reactor coil [15]



Scheme 3 Multistep library capabilities using segmented flow in Conjure flow reactor [16]

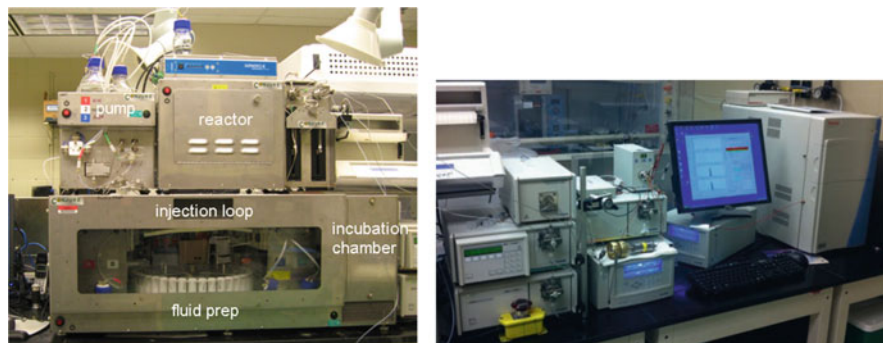


Fig. 3 The Synthesis With Integrated Flow Technology (SWIFT) platform for flow library synthesis [18]

3.3 Integrated Flow Synthesis Platforms

It is with the development and implementation of the SWIFT (Synthesis With Integrated Flow Technology) system at AbbVie that the library synthesis and purification aspects were fully integrated [18, 19]. The SWIFT platform consists of the Accendo Conjure flow reactor integrated with a mass-triggered preparative reverse-phase HPLC/MS (Fig. 3). This setup enables reactions (i.e., individual library elements) to be prepared as segments and immediately purified upon reactor exit, resulting in six pure compounds per hour (using a standard 10-min preparative HPLC method). Libraries run using the SWIFT platform use on average 15–20 mg of starting material, providing enough final compound to be screened in both primary assays and Tier 1 ADME studies.

Chemistry capable of being performed on the SWIFT system includes many of the traditional high-throughput synthetic methods, such as acylations, reductive aminations, sulfonylations, N- and O-alkylations, S_NAr, and heterocycle formations. The scope of this chemistry is dictated by the solubility of reagents, starting materials, and products as heterogeneous chemistry is well-known to pose problems when using flow chemistry. Since the introduction of the SWIFT platform at AbbVie, >7,500 compounds have been synthesized, supporting a number of early discovery programs. While success rates and average yields remain comparable to batch processes, the overall turnaround time of synthesis–purification–registration has been significantly decreased from 7–10 days

down to 2–4 days. These efficiency gains have been the key to driving early stage medicinal chemistry programs towards candidate selection.

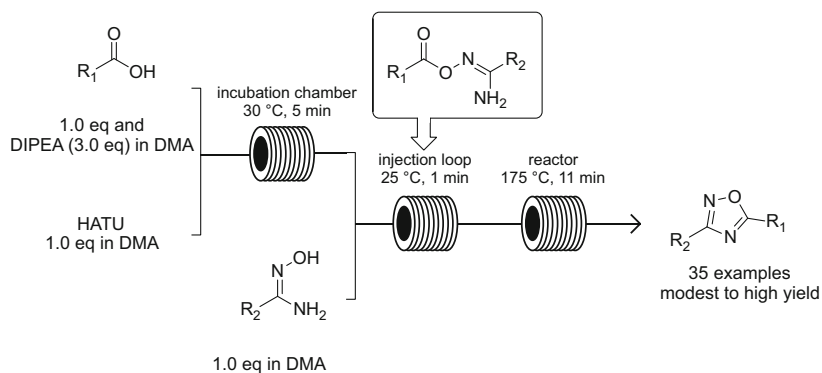
The SWIFT platform was also demonstrated to exhibit enhanced heterocycle formations when using high temperatures. As heterocycles are very common motifs in the pharmaceutical industry, developing novel synthetic methods from readily available starting materials is of high value. For this reason, the synthesis of 1,2,4-oxadiazoles and 1,2,4-triazoles was investigated using the SWIFT system [20].

As previously demonstrated by Lange and James [17], the Conjure flow reactor consists of an incubation chamber that can be utilized when carrying out multistep reaction sequences. In the synthesis of heterocycle libraries, this incubation chamber was used to synthesize activated esters, by the coupling of carboxylic acids and HATU. After mixing this material with a hydroxyamidine and base, the reaction mixture is heated to 175 °C for 11 min, to afford the 1,2,4-oxadiazole products in modest to excellent yields (Scheme 4). By using hydrazonamides and hydrazinopyridines, 1,2,4-triazoles can also be synthesized using similar variations of this methodology (Scheme 5).

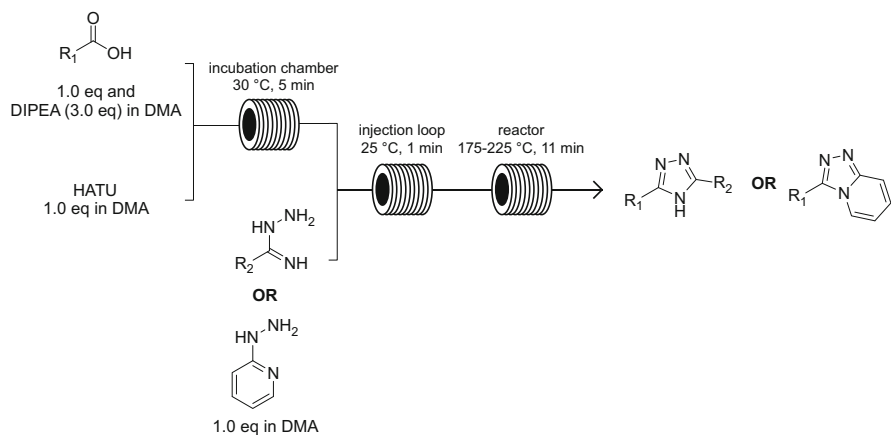
Methodologies such as these have been utilized on the SWIFT platform in support of a number of medicinal chemistry programs. While these examples highlight the benefits of using flow chemistry mainly from a synthetic efficiency perspective, assay data for these libraries is not immediately generated after the synthesis, meaning that there is still room to further improve upon drug discovery cycle times.

Additional modifications to the back end of the SWIFT platform were also made to reduce cycle times. HPLC fractions of final compounds were quantified via NMR, sampled, diluted with DMSO, and handed off to project team biologists for rapid turnaround of bioassay data. An automated platform was also developed and implemented with SWIFT to permit sample dry down, barcode labeling, quantification, and dry down in a continuous process [19].

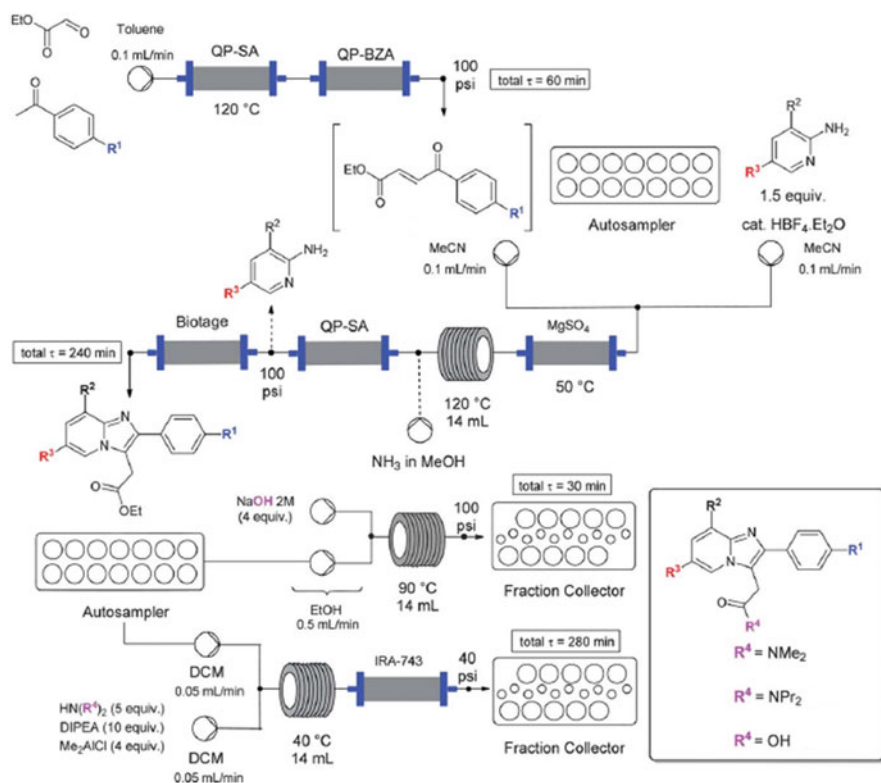
Albeit not a segmented flow approach, the Ley group has reported an elaborate multistep synthetic route to imidazo[1,2- α]pyridine libraries to be profiled in a frontal affinity chromatography (FAC) assay [21]. The synthetic route shown in Scheme 6



Scheme 4 Conjure-enabled synthesis of 1,2,4-oxadiazole libraries [20]. Reproduced from Ref. [20] with permission from the Royal Society of Chemistry



Scheme 5 Conjugate-enabled synthesis of 1,2,4-triazole libraries [20]. Reproduced from Ref. [20] with permission from the Royal Society of Chemistry



Scheme 6 Multistep flow synthesis of imidazo[1,2-a]pyridine library [21]

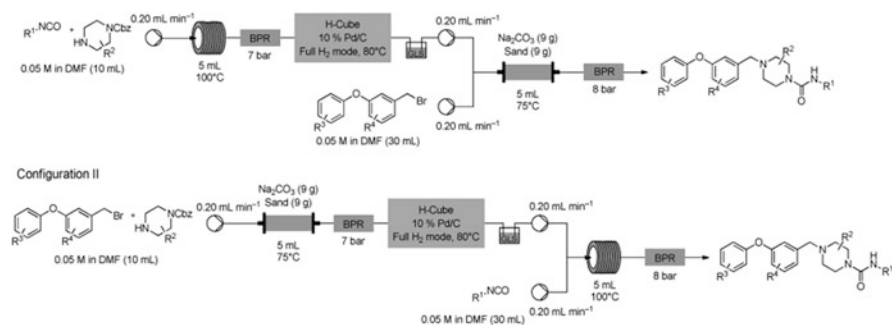
was carried out using a series of Vapourtec R2 + R4 systems, coupled with auto-samplers, fraction collectors, and purification systems. The flow synthesis of these analogs has numerous advantages over traditional batch processes, being able to superheat reaction solvents to decrease reaction times, in some cases reducing overnight processes down to a matter of hours. Pure products are subsequently sampled and diluted for use in off-line FAC assays. While the assay is not fully integrated with the flow chemistry platform, this work highlights that libraries of compounds can be rapidly prepared to be tested in an assay.

Petersen and coworkers have used multistep flow syntheses to enable the rapid generation of SAR for CCR8 ligands [22]. In this work, a multistep batch synthesis was translated into a continuous flow process (Scheme 7). Having optimized the sequence using one set of starting materials, facile library synthesis was allowed by simply varying the commercially available building blocks. Reaction was subsequently purified off-line and screened in a CCR8 assay, leading to the rapid discovery of a series of single-digit nanomolar compounds.

While many of the benefits of the aforementioned systems stem from the increased efficiency in compound production, running an assay off-line is still a limiting factor in reducing drug discovery cycle times. In drug discovery programs, assays are typically scheduled to run on a weekly basis, meaning that regardless of how fast a compound is synthesized, compounds may wait a week or more before they are tested. For this reason, further integration of a flow chemistry platform with an assay is highly advantageous.

GlaxoSmithKline reported pioneering work in the development of an integrated synthesis and bioassay platform [23]. In this chip-based approach, a small series of sulfonamides was prepared and screened for the inhibition of T-cell tyrosine phosphatase (TCPTP). After the flow reaction, passed through an LC column, and the sample is split into two streams, one for analysis via UV and MS detection, and the second for screening (Fig. 4). While this early proof-of-concept example demonstrated the value of having assays integrated with synthesis, its full potential would be realized if used in support of lead optimization programs to increase SAR generation.

Cyclofluidic has developed an integrated system that has been used to generate SAR for the discovery of Abl kinase inhibitors [24] and DPP4 inhibitors [25]. In these examples, the flow reactions are carried out using a Vapourtec R2 + R4 flow reactor



Scheme 7 Continuous flow synthesis of CCR8 ligands [22]

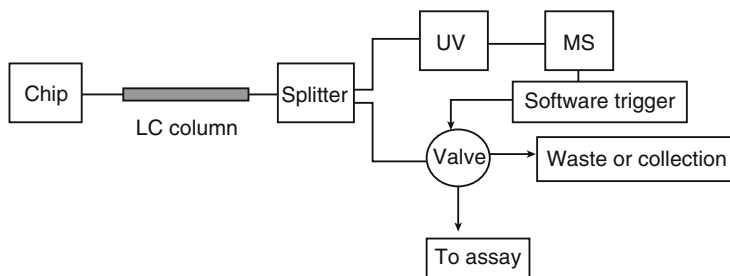


Fig. 4 GlaxoSmithKline's integrated chemistry and bioassay platform [23]

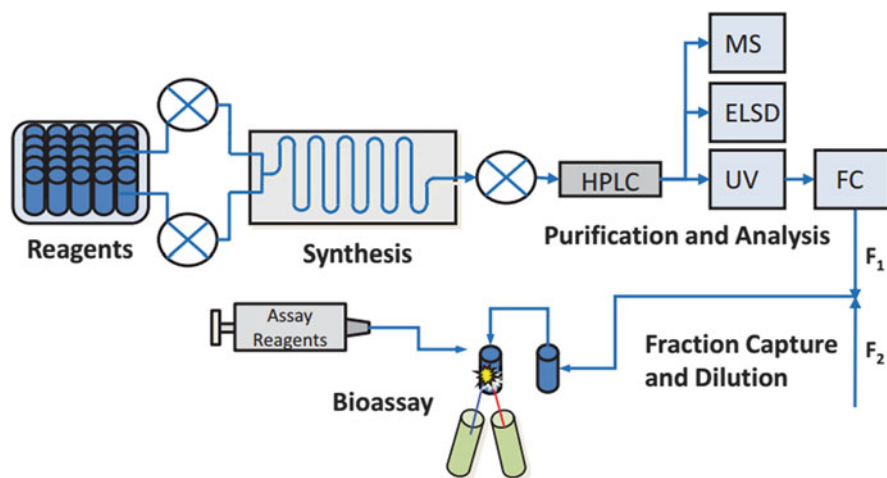
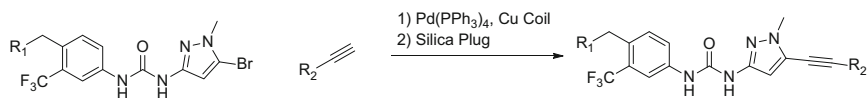


Fig. 5 Cyclofluidic's integrated synthesis-purification-bioassay platform [24]

setup, equipped with a liquid handling robot that will deliver reagents and starting materials to injection loops (Fig. 5). Upon completion of the reaction, a 10 μL aliquot of the reaction segment is purified via analytical HPLC, quantified using an evaporative light scattering detector (ELSD) and collected in a fraction collector. The sample is subsequently diluted with assay buffer. This diluted sample is transferred to a liquid handling robot that prepares assay plates that can be analyzed using fluorescence-based assays and a plate reader. For the study of Abl inhibitors, a single round of SAR generation from 29 compounds took roughly 30 h to complete. From this data, SAR heat maps could be generated, enabling subsequent libraries to be carried out in a highly efficient manner.

For Abl1 inhibitor libraries, the chemistry explored using this system includes palladium-mediated Sonogashira couplings using a copper flow reactor coil (Scheme 8), followed by filtration through a silica plug (Fig. 6).

Additionally, for the synthesis of DPP4 inhibitors, a multistep process was employed. In the first step, xanthine starting materials were coupled with a Boc-protected diamine or amino alcohol at high temperature, followed by deprotection (Scheme 9 and Fig. 7).



Scheme 8 Representative Sonogashira coupling reaction for Abl1 library synthesis [24]

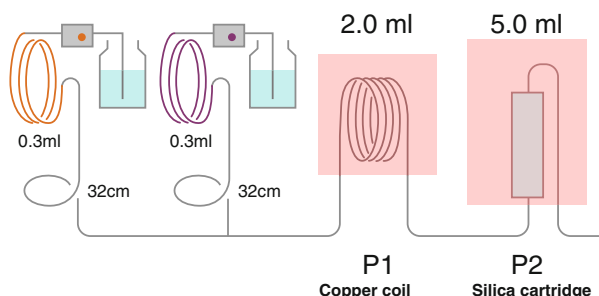
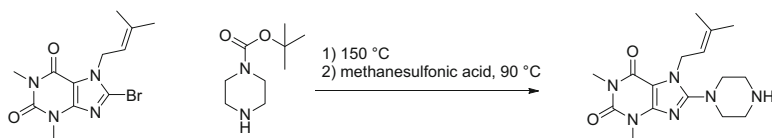


Fig. 6 Flow setup for Sonogashira flow library [24]



Scheme 9 Representative multistep process DPP4 library synthesis [25]

Researchers at Hoffman-LaRoche have developed a similar synthesis–purification–bioassay platform, this time using a chip-based assay to generate SAR for BACE1 inhibitors [26]. Similar to the Cyclofluidic system, flow reactions are carried out using a Vapourtec R2 + R4 system in conjunction with a liquid handler. In this setup, reactions are purified via preparative HPLC. Aliquots of the pure fraction are analyzed by analytical HPLC and quantitated via ELSD to determine the final concentration of product. This material is subsequently used in a chip-based assay to provide IC₅₀ values with high reproducibility. In total, the synthesis–purification–bioassay workflow was completed in roughly 60 min per compound (Fig. 8). Specifically in their study of BACE1 inhibitors, a flow-mediated peptide coupling was carried out on a 5-mg scale (Scheme 10).

4 Flow Chemistry Support for Lead Optimization Programs

An additional benefit of flow chemistry is the facile nature of reaction scale-up. In comparison, scale-up using traditional batch techniques can be less straightforward as a process that works on milligram scale in a vial may not translate to multi-gram scale in a larger reactor. Issues such as mixing and heat transfer need to be taken into consideration upon scale-up, meaning that an entire process may need to be

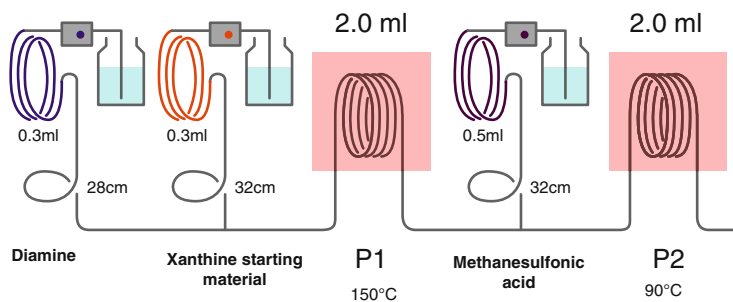


Fig. 7 Flow setup for multistep flow library [25]

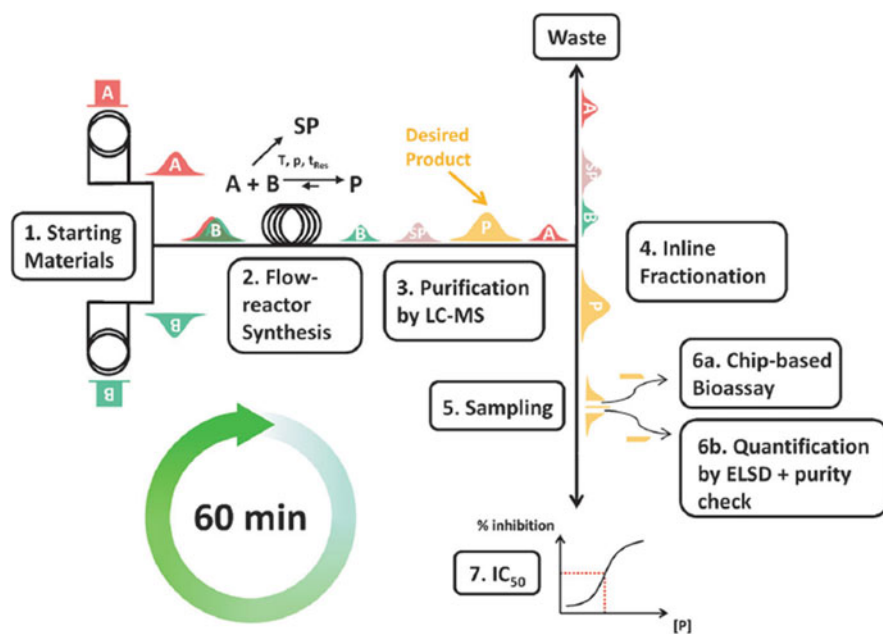
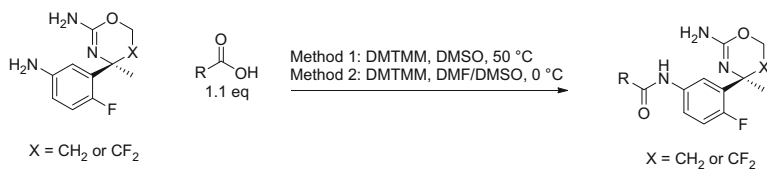


Fig. 8 Schematic for the integrated synthesis-purification-bioassay platform at Hoffman-LaRoche [26]



Scheme 10 General reaction scheme for BACE1 inhibitor synthesis [26]

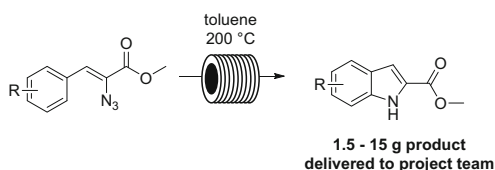
reengineered to be successful. For flow chemistry however, reaction scale-up can be much more straightforward as scale-up can either be carried out via a process known as numbering up (i.e., adding more reactors in parallel) or by simply pumping reagents into the flow reactor for a longer period of time. Scale-up in flow also permits potentially reactive or hazardous intermediates to be utilized on scale, as active chemistry volumes are minimized (i.e., flow reactor internal volumes are less than batch reactor volumes). Reasons such as these provide rationale for flow chemistry to be used in medicinal chemistry, specifically in the scale-up of intermediates or final compounds.

Heterocycles are ubiquitous in drug discovery programs and are common elements in many marketed APIs. Due to their importance, novel methodologies for the synthesis of heterocycles are constantly under investigation. The Hemetsberger–Knittel reaction, for instance, can be used to synthesize compounds relevant to medicinal chemistry; however, the use of high temperatures and organic azides often times leads to the exploration of other routes. The work of O'Brien and Seeberger demonstrated a flow-enabled synthesis of indoles using the Hemetsberger–Knittel reaction at temperatures between 160 and 220°C, using reaction times <1 min [27]. This methodology has subsequently been used by drug discovery programs to enable the synthesis of highly functionalized indoles (Scheme 11) (Bogdan, unpublished results).

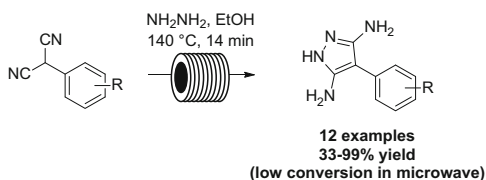
Multi-gram quantities of heterocycles have also been synthesized using flow chemistry, specifically in the synthesis of diaminopyrazoles [28]. These heterocycles were synthesized by the coupling of hydrazine with substituted malononitriles at elevated temperatures (Scheme 12). While limited to aryl malononitriles, the substrate scope shows a wide array of substitution patterns around the aromatic ring, as well as different electron-withdrawing and electron-donating groups. Superior yields were obtained when using the flow system in comparison to microwave chemistry, showing an added benefit to flow chemistry. Furthermore, it was determined that the resulting diaminopyridine analogs could be coupled with acetylacetone to provide gram quantities of phenyl pyrazolopyridinamine in high conversion (Scheme 13).

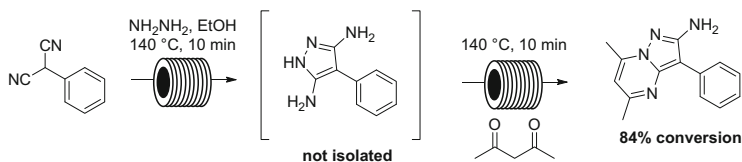
Using microwave-assisted, continuous flow organic synthesis (MACOS), a series of sultams could be prepared on gram scale (Scheme 14) [29]. In this system, the combination of flow and microwave chemistry enabled the rapid scale-up of

Scheme 11 Scale-up of indole using Hemetsberger–Knittel indole formation in flow (Bogdan, unpublished results)

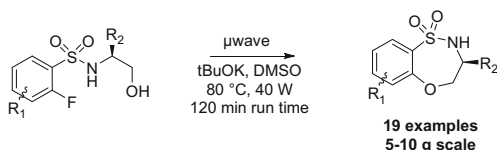


Scheme 12 The flow synthesis of diaminopyrazoles [28]





Scheme 13 The multistep synthesis of phenyl pyrazolopyridinamine [28]



Scheme 14 Scale-up of sultams using microwave-assisted, continuous flow organic synthesis (MACOS) system [29]

19 compounds and eliminated the need for optimization on large scale. In these examples, scale is a function of time and not vessel size.

5 Emerging Flow Technologies and Future Opportunities

A number of emerging flow technologies have been developed over the past number of years that have shown application in drug discovery. The technologies can benefit medicinal chemistry programs in a number of ways, by simplifying synthetic strategies, streamlining syntheses, providing superior results in comparison to batch chemistry, or permitting hazardous chemistry to be used in a safe manner.

5.1 High-Temperature Flow Reactions

As stated previously, a number of the advantages associated with flow reactors are attributed to large surface area-to-volume ratios that allow rapid heat transfer and efficient mixing. Using a combination of instruments such as gas chromatograph ovens, hot plates, HPLC pumps, and back-pressure regulators allows forcing conditions (i.e., elevated temperatures and pressures) to be readily and safely achieved. The use of elevated pressures allows solvents to be used well beyond their boiling points, permitting green solvents to be used in place of traditional high-boiling solvents, such as diphenyl ether or diglyme.

Early examples of high-temperature flow chemistry were carried out at Roche, where a series of annulated pyridine analogs were synthesized via an intramolecular

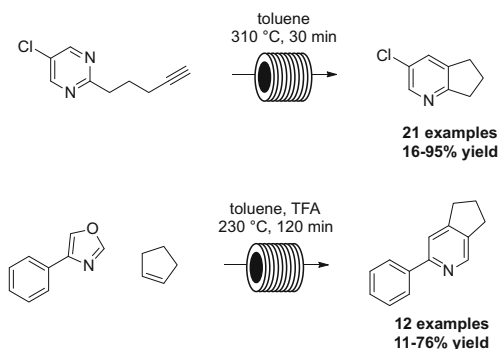
cyclization at temperatures between 250 and 310 °C in toluene (Scheme 15) [30]. Additionally, a similar protocol was developed to prepare different annulated pyridine regioisomers using an intermolecular flow-mediated Kondrat'eva reaction (Scheme 15) [31]. For these systems, a Vapourtec R2 + R4 system was interfaced with a GC oven and a back-pressure regulator, permitting high temperatures and pressures to be readily obtained.

Alternative high-temperature flow reactors such as the Phoenix from Thales Nano have also been used in a drug discovery setting, both in terms of library generation and simplifying common multistep reaction sequences. In the first example, a library of 2-aminoquinazolines was prepared using a high-temperature mediated SNAr (Scheme 16) [32]. The methodology is straightforward and uses a green solvent (ethanol) at temperatures well above its boiling point. Furthermore, the substrate scope can be expanded to include 2-chloroquinoxalines and 2-chlorobenzimidazoles.

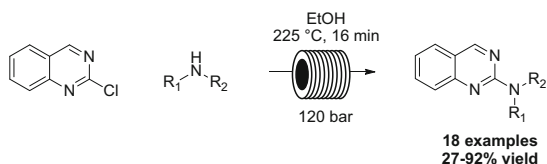
The synthesis of a diverse set of drug-like heterocycles has also been expanded beyond SNAr, to include both the Gould–Jacobs cyclization and Diels–Alder cycloaddition. The Gould–Jacobs reaction has been studied by both the Darvas group [33] and AbbVie [34] to synthesize fused pyridine and quinolone type structures. In the former example, temperatures exceeding 300 °C are used to synthesize novel aromatic and heterocyclic structures starting from alkylidene esters (Scheme 17). Tsoung expanded upon this high-temperature methodology to improve the selectivity of the reaction by adding trace amounts of water to the reaction, thus providing a more-general set of reaction conditions (Scheme 18) [34].

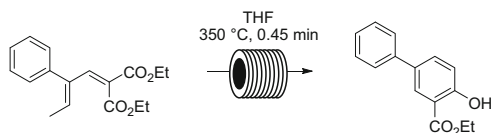
High-temperature chemistry was further expanded to Diels–Alder cyclizations, enabled by the high-temperature ring-opening of benzocyclobutanes and benzothiopen-2,2-dioxides [35]. The resulting o-diquinomethane diene was trapped with a wide variety

Scheme 15 High-temperature mediated synthesis of annulated pyridines [30, 31]

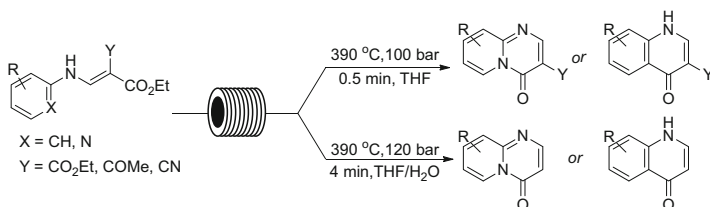


Scheme 16 The synthesis of 2-aminoquinazolines using high-temperature flow chemistry [32]

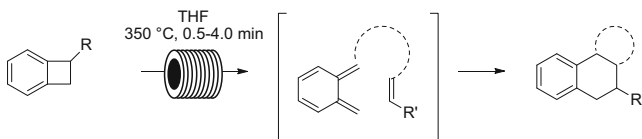




Scheme 17 High-temperature mediated Gould–Jacobs cyclization [33]



Scheme 18 The selective synthesis of functionalized pyrimidone and quinolone derivatives [34]



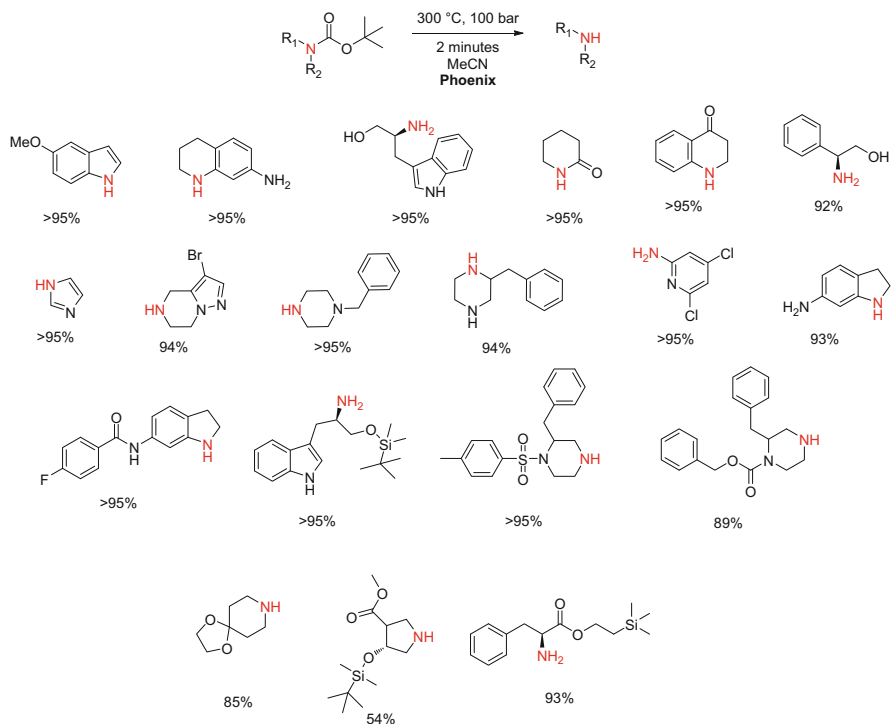
Scheme 19 Diels–Alder cyclization of benzocyclobutanes [35]

of dienophiles in both intra- and intermolecular fashion (Scheme 19). It is also worth noting that for this Diels–Alder, along with the Gould–Jacobs couplings, THF was used as the solvent at temperatures far exceeding its boiling point, thus removing the requirement to use more traditional high-boiling solvents.

The Phoenix has also been used in the high-temperature N-Boc deprotection of a series of amines [36]. Substrates were simply dissolved in acetonitrile (0.1–1.0 M final substrate concentration) and injected into the flow reactor for 2 min at 300 °C. Final deprotected materials were isolated in quantitative yield and had a very broad substrate scope (Scheme 20).

In an example relevant to medicinal chemistry, two common multistep syntheses were carried out using this high-temperature mediated Boc deprotection. These two protocols (functionalization–deprotection–functionalization) are common medicinal chemistry procedures and allow a three-step process to be completed in a matter of minutes to generate >180 mg of final material without the need for intermediate purifications or workups (Scheme 21).

The MACOS system described earlier can also be used to run reactions at high temperatures. By irradiating capillaries that have been coated with a thin film of copper or gold with microwaves, temperatures >900 °C can readily be achieved. Using a multicomponent reaction, highly functionalized propargyl amines can be synthesized in high yield, on up to a 495-mg scale (Scheme 22) [37].

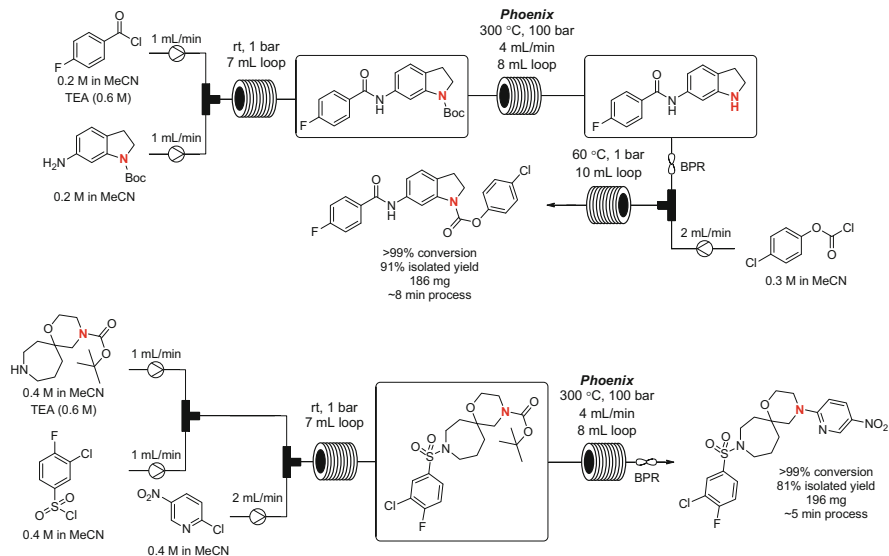


Scheme 20 Substrate scope for high-temperature Boc deprotection [36]. Reprinted with permission from Bogdan AR, Charaschanya M, Dombrowski AW, Wang Y, Djuric SW (2016) *Org Lett* 18:1732–1735. Copyright 2016 American Chemical Society

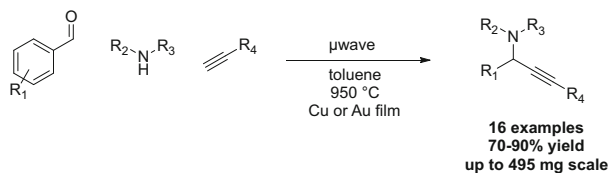
5.2 Hazardous Gas Chemistry

Medicinal chemistry programs can benefit from the use of flow chemistry when hazardous gases are required as part of the synthetic route. The benefits of performing gas-mediated reactions in flow have been recently reviewed [38]. A common technique used to introduce gases into a flow reactor is via a tube-in-tube reactor, in which an inner gas-permeable tube (commonly made of Teflon AF-2400) is pressurized with gas and an outer tube contains a stream of reagents [39]. This tube-in-tube technique also permits hazardous gases to be generated in situ and used on demand, such as with the case of diazomethane (Fig. 9) [40–43]. In the context of drug discovery efforts, this diazomethane reactor has been used to prepare novel building blocks.

Koolman and coworkers reported an automated tube-in-tube flow reactor that can be used for library generation or reaction scale-up using diazomethane generated in situ from the reaction of Diazald with KOH [40]. This system uses the tube-in-tube reactor to prepare a solution of diazomethane in THF, as opposed to passing



Scheme 21 Multistep syntheses carried out using high-temperature Boc deprotection [36]. Reprinted with permission from Bogdan AR, Charaschanya M, Dombrowski AW, Wang Y, Djuric SW (2016) *Org Lett* 18:1732–1735. Copyright 2016 American Chemical Society



Scheme 22 Thin-film catalysis using MACOS flow system [37]

the reaction stream over the gas-permeable tubing [38]. In the latter case, it has been observed that nanoparticles can form blockages in the surface of the gas-permeable tubing, limiting its long-term use. Alternatively, generating a solution of diazomethane and subsequently mixing it with a reagent stream (as shown in Fig. 10) was demonstrated to exhibit long-term use in an array of different chemistries.

Using this platform, a series of arylcyclopropyl boronates have been synthesized starting from the analogous styryl starting materials (Scheme 23). While being operated in library production mode, a series of 15 substrates could be synthesized in sequence. Furthermore, compounds of interest could be scaled-up at rates of up to 190 mg/h. Products such as these are of high value to drug discovery programs, however are not commercially available.

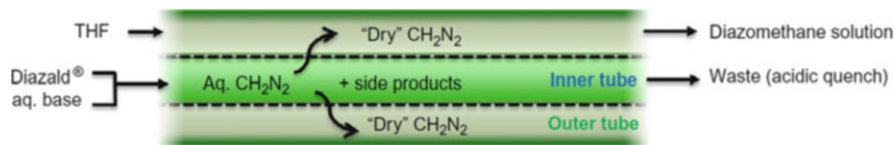


Fig. 9 Tube-in-tube flow reactor for diazomethane production [40]

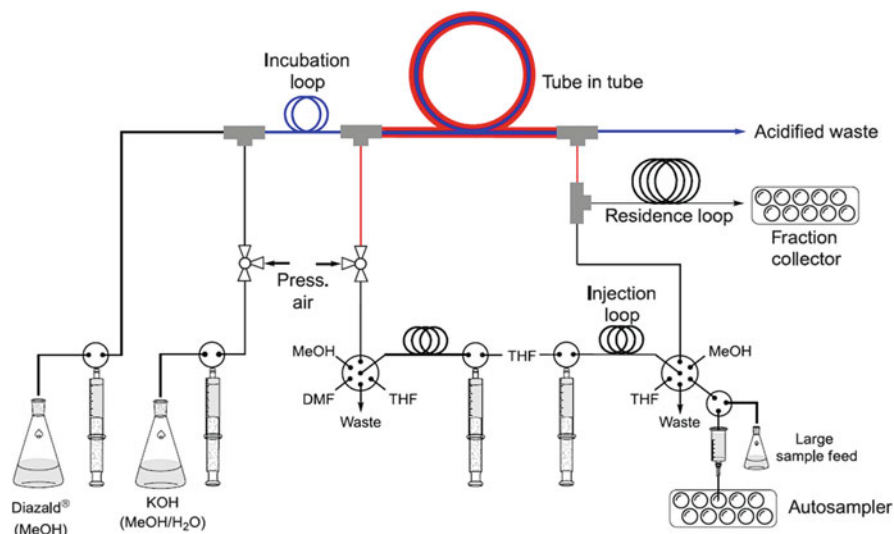
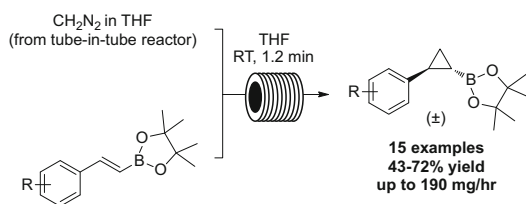


Fig. 10 Schematic of the diazomethane tube-in-tube flow reactor [40]. Reproduced from Ref. [40] with permission from the Royal Society of Chemistry



Scheme 23 Arylcyclopropyl boronate synthesis using tube-in-tube diazomethane reactor [40]

5.3 Flow Photochemistry Examples in Medicinal Chemistry

Many of the most recent advances in flow chemistry have involved the use of photochemistry [44–46]. The tubing used in traditional flow reactors results in short path lengths upon irradiation with light (both UV and visible). As a result,

reactions traditionally run in batch photochemical reactors can be carried out in flow, providing high yields and shorter reaction times [47]. Within drug discovery at AbbVie, flow photochemistry has been used to prepare a number of stereocomplex, high-sp³ character structures. The LOPHTOR (*flow-through photochemical microreactor*) uses microchannels etched into a stainless steel housing, covered with a Pyrex plate or polymeric ETFE membrane (Fig. 11) [48]. The plate can subsequently be irradiated with UV or visible light. Using this setup, it was observed that intramolecular [2 + 2] cycloadditions performed much more efficiently when run in flow (Scheme 24). Similarly, a photochemical cyclization was carried out on gram scale, providing a key intermediate for a 5-HT_{2C} program (Scheme 25) [49].

Flow photochemical transformations have also been used to synthesize building novel building blocks in support of medicinal chemistry programs. Using the LOPHTOR, a photochemistry-enabled bromination to synthesize the building block in Scheme 26 was carried out in high yields on gram quantities.

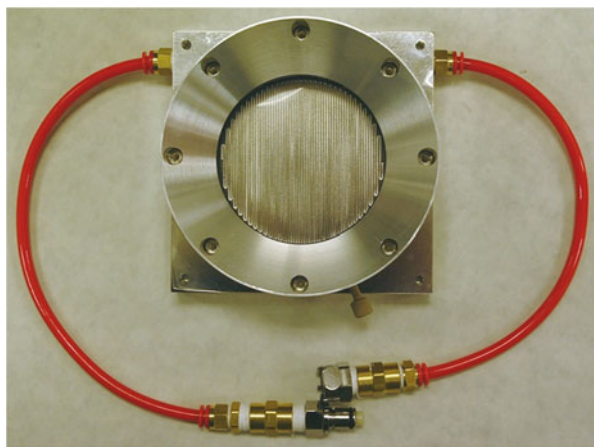
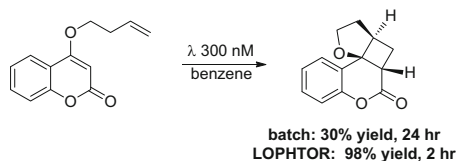
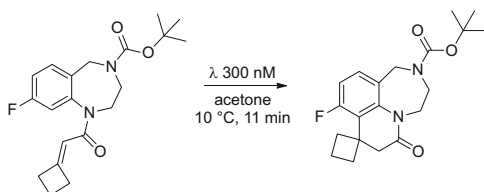


Fig. 11 The *flow-through photochemical microreactor* (LOPHTOR) photochemical reactor [48]

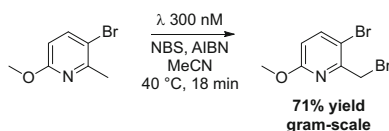


Scheme 24 Batch to flow comparison using LOPHTOR flow photochemical reactor [48]

Scheme 25 Photochemical synthesis of 5-HT_{2C} intermediate [49]



Scheme 26 Flow photochemistry-enabled bromination



6 Conclusion and Outlook

The field of medicinal chemistry is constantly evolving. For a specific program, the lead series or structural motifs can change on a weekly basis, meaning that chemistry efforts must constantly adapt to continue generating SAR in a highly efficient manner. With that said, the advantages of using flow chemistry seem far more apparent for process chemistry, where the chemistry demands are more static in comparison to discovery. In process chemistry, the benefits of flow chemistry can significantly reduce cost, energy requirements, and safety concerns. These factors are not necessarily determining factors when deciding to run flow chemistry in a drug discovery setting. Early stage discovery programs can greatly benefit from the increased efficiency and improved cycle times by way of flow-enabled library production. Perhaps one of the greatest achievements in this area is the incorporation of in-line assays, which enable the rapid generation of SAR. Further along in the drug discovery process, the facile scale-up of intermediates can prove to be of value, when other routes may not be synthetically tractable. Added complexity can also be brought into medicinal chemistry via high temperatures, hazardous gases, and photochemistry, in a manner that is unparalleled in batch.

The successful implementation of platforms such as the ones mentioned throughout this review is contingent upon the close work of a multidisciplinary team of scientists and engineers with an aligned set of strategic goals. For flow chemistry to reach its fullest potential in drug discovery, chemists, biologists, and engineers need to be prepared to challenge the status quo when approaching problems. Additional alignment of medicinal and process chemists might also streamline the transition from gram to kilogram scale-up, enabling a more rapid delivery of API.

References

1. DiMasi JA, Faden LB (2011) *Nat Rev Drug Discov* 10:23–27
2. Plutschack MB, Pieber B, Gilmore K, Seeberger PH (2017) *Chem Rev.* <https://doi.org/10.1021/acs.chemrev.7b00183>

3. Porta R, Benaglia M, Puglisi A (2016) *Org Process Res Dev* 20:2–25
4. McQuade DT, Seeberger PH (2013) *J Org Chem* 78:6384–6389
5. Pastre JC, Browne DL, Ley SV (2013) *Chem Soc Rev* 42:8849–8869
6. Wegner J, Ceylan S, Kirschning A (2011) *Chem Commun* 47:4583–4592
7. Mason BP, Price KE, Steinbacher JL, Bogdan AR, McQuade DT (2007) *Chem Rev* 107:2300–2318
8. Hessel V, Lowe H (2005) *Chem Eng Technol* 28:267–284
9. Ahmed-Omer B, Brandt JC, Wirth T (2007) *Org Biomol Chem* 5:733–740
10. Gutmann B, Cantillo D, Kappe CO (2015) *Angew Chem Int Ed* 54:6688–6728
11. Malet-Sanz L, Flavien SJ (2012) *Med Chem* 55:4062–4098
12. Baxendale IR, Deeley J, Griffiths-Jones CM, Ley SV, Saaby S, Tranmer GK (2006) *Chem Commun*:2566–2568
13. Adamo A, Beignessner RL, Behnam M, Chen J, Jamison TF, Jensen KF, Monbaliu J-CM, Myerson AS, Revalor EM, Snead DR, Stelzer T, Weeranoppanant N, Wong SY, Zhang P (2016) *Science* 352:61–67
14. Thompson CM, Poole JL, Cross JL, Akritopoulou-Zanze I, Djuric SW (2011) *Molecules* 16:9161–9177
15. Bogdan AR, Sach NW (2009) *Adv Synth Catal* 351:849–854
16. Lange PP, Bogdan AR, James K (2012) *Adv Synth Catal* 354:2373–2379
17. Lange PP, James K (2012) *ACS Comb Sci* 14:570–578
18. Hochlowski JE, Searle PA, Tu NP, Pan JY, Spanton SG, Djuric SW (2011) *J Flow Chem* 2:56–61
19. Sutherland JD, Tu NP, Nemcek TA, Searle PA, Hochlowski JE, Djuric SW, Pan JY (2014) *J Lab Autom* 19:176–182
20. Bogdan AR, Wang Y (2015) *RSC Adv* 5:79264–79269
21. Guetzoyan L, Nikbin N, Baxendale IR, Ley SV (2013) *Chem Sci* 4:764–769
22. Petersen TP, Mirsharghi S, Rummel PC, Thiele S, Rosenkilde MM, Ritzen A, Ulven T (2013) *Chem Eur J* 19:9343–9350
23. Wong Fawkes SYF, Chapela MJV, Montembault M (2005) *QSAR Combi Sci* 24:712–717
24. Desai B, Dixon K, Farrant E, Feng Q, Gibson KR, van Hoorn WP, Mills J, Morgan T, Parry DM, Ramjee MK, Selway CN, Tarver GJ, Whitlock G, Wright AG (2013) *J Med Chem* 56:3033–3047
25. Czechtizky W, Dedio J, Desai B, Dixon K, Farrant E, Feng Q, Morgan T, Parry DM, Ramjee MK, Selway CN, Schmidt T, Tarver GJ, Wright AG (2013) *ACS Med Chem Lett* 4:768–772
26. Werner M, Kuratli C, Martin RE, Hochstrasser R, Wechsler D, Enderle T, Alanine AI, Vogel H (2014) *Angew Chem Int Ed* 53:1704
27. O'Brien AG, Levesque F, Seeberger PH (2011) *Chem Commun* 47:2688–2690
28. Wilson NS, Osuma AT, Van Camp JA, Xu X (2012) *Tetrahedron Lett* 53:4498–4501
29. Ullah F, Samarakoon T, Rolfe A, Kurtz RD, Hanson PR, Organ MG (2010) *Chem Eur J* 16:10959–10962
30. Martin RE, Morawitz F, Kuratli C, Alker AM, Alanine AI (2012) *Eur J Org Chem*:47–52
31. Lehmann J, Alzieu T, Martin RE, Britton R (2013) *Org Lett* 15:3550–3553
32. Charaschanya M, Bogdan AR, Wang Y, Djuric SW (2016) *Tetrahedron Lett* 57:1035–1039
33. Lengyel L, Nagy TZ, Sipos G, Jones R, Dorman G, Urge L, Darvas F (2012) *Tetrahedron Lett* 53:738–743
34. Tsoung J, Bogdan AR, Kantor S, Wang Y, Charaschanya M, Djuric SW (2017) *J Org Chem* 82:1073–1084
35. Tsoung J, Wang Y, Djuric SW (2017) *React Chem Eng* 2:458–461
36. Bogdan AR, Charaschanya M, Dombrowski AW, Wang Y, Djuric SW (2016) *Org Lett* 18:1732–1735
37. Shore G, Yoo W-J, Li C-J, Organ MG (2010) *Chem Eur J* 16:126–133
38. Mallia CJ, Baxendale IR (2016) *OPRD* 20:327–360
39. Brzozowski M, O'Brien M, Ley SV, Polyzos A (2015) *Acc Chem Res* 48:349–362

40. Koolman HF, Kantor S, Bogdan AR, Wang Y, Pan JY, Djuric SW (2016) *Org Biomol Chem* 14:6591–6596
41. Mastronardi F, Gutmann B, Kappe CO (2013) *Org Lett* 15:5590–5593
42. Dallinger D, Pinho VD, Gutmann B, Kappe CO (2016) *J Org Chem* 81:5814–5823
43. Polyzos A, O'Brien M, Baxendale IR, Ley SV (2010) *Org Lett* 12:1596–1598
44. Ciriminna R, Delisi R, Xu Y-J, Pagliaro M (2016) *OPRD* 20:403–408
45. Su Y, Straathof NJW, Hessel V, Noel T (2014) *Chem Eur J* 20:10562–10589
46. Gilmore K, Seeberger PH (2014) *Chem Rec* 14:410–418
47. Elliott LD, Knowles JP, Koovits PJ, Maskill KG, Ralph MJ, Lejeune G, Edwards LJ, Robinson RI, Clemens IR, Cox B, Pascoe DD, Koch G, Eberle M, Berry MB, Booker-Milburn KI (2014) *Chem Eur J* 20:15226–15232
48. Vasudevan A, Villamel C, Trumbull J, Olson J, Sutherland D, Pan J, Djuric S (2010) *Tetrahedron Lett* 51:4007–4009
49. Koolman HF, Braje WM, Haupt A (2016) *Synlett* 27:2561–2566

Safe Use of Hazardous Chemicals in Flow



Md Taifur Rahman and Thomas Wirth

Contents

1	<i>Fast and Furious</i> Chemical Processes	344
2	Reactions of Explosive Nature: Nitration	356
3	In Situ Generation of Hazardous Reagents and Intermediates	360
3.1	Diazo Compounds and Diazonium Salts	360
3.2	Phosgene	362
4	Reactions Involving Toxic, Corrosive and Flammable Gaseous Reagents	363
4.1	Oxygen (Triplet and Singlet States)	363
4.2	Halogens: Fluorine and Chlorine (Both in Gaseous State and In Situ Generated) ..	369
	References	370

Abstract Flow chemistry has evolved into an excellent toolkit for handling challenging chemical transformations during the past decade. Highly exothermic and kinetically fast reactions are difficult to handle even on a small scale, whereas any scale-up poses significant risks when conventional reactors are considered. Flow chemistry enables exquisite control over mixing sequences, reaction time and quenching that ultimately paves the way for the fine-tuning of chemical reactivity in ‘space and time’. This chapter describes recent advances of flow chemistry in controlling and even discovering new reactivities of highly hazardous chemical species and unstable intermediates. This chapter compiles intriguing recent examples manifesting the power of flow chemistry to perform commonly known, cryogenic reactions at or near room temperature, safe-handling and in situ production of hazardous or toxic reagents for chemical transformations that are generally considered unsafe in conventional reactors.

M. T. Rahman
School of Chemistry and Chemical Engineering, Queen’s University Belfast, Belfast, UK

T. Wirth (✉)
School of Chemistry, Cardiff University, Cardiff, UK
e-mail: wirth@cf.ac.uk; WirthT@cardiff.ac.uk

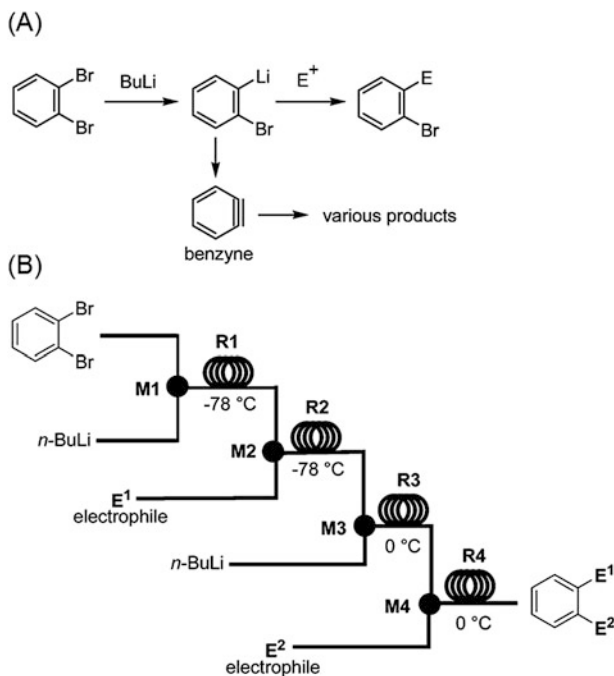
Keywords Diazo and diazonium reagents · Exothermic reactions · Fast reactions · Flash chemistry · Halogenation · Hazardous reagents · Nitration · Organometallic reagents · Oxygenation · Unstable intermediates

1 *Fast and Furious* Chemical Processes

Chemical transformations involving organometallic reagents, such as alkyl/aryl lithium or Grignard reagents, typically and invariantly require cryogenic, inert and special reaction conditions. This is not only due to inherent hazards posed by the corrosive, moisture-sensitive and often flammable reagents but also due to their highly exothermic enthalpy that may lead to hotspot generation, runaway reactions and possible explosions. Apart from safety concerns, such transformations are immensely challenging from the molecular point of view as well: intermediates generated during the course of the reactions are generally prone to isomerize, decompose or deviate towards competing reaction pathways – hence producing undesired by-products. All these factors become an intractable challenge for any scale-up operation using such reactive reagents or intermediates thus produced.

Flow chemistry can tackle safety hazards, cryogenic reaction conditions and the treacherous chemical outcome (by-product formation) associated with such reactions. Thanks to small reaction volumes and excellent heat and mass transfer capabilities, microflow platforms minimize the explosion possibility of the exotherms by removing heat from the reaction mixture instantaneously, even at higher than typical cryogenic temperatures. Moreover and most importantly, since the overreactive intermediates can be made to react in a subsequent reaction within a sub-second or millisecond time regime, any undesirable isomerization, decomposition or side reactions can be mostly and in many cases totally short-circuited and avoided. This is made possible by intelligent design and assembly of the mixing and reaction regions (namely, known as residence time units) to perform the chemistry in millisecond time scale, which is the basis of the so-called *Flash Chemistry*. Hence, now a chemist has a ‘switch’ to choose between reaction pathways in *space and time* for these ‘fast and furious’ organometallics-assisted transformations [1, 2].

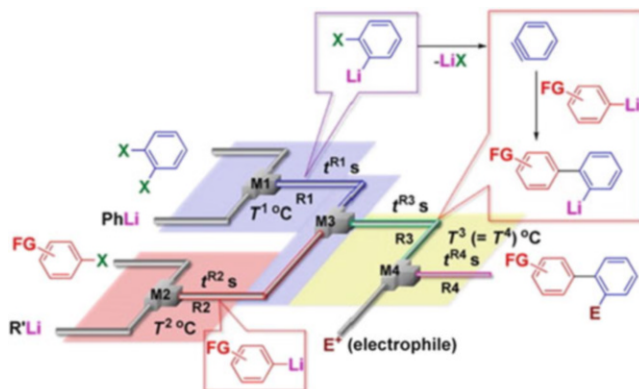
In the seminal work by the Yoshida group, an elegant and simple approach was reported for the lithiation of dibromobenzene for generating *ortho*-bromophenyllithium which could react with electrophiles (E) (Scheme 1) [3]. In typical Schlenk tube, such transformation is performed below -100°C to avoid formation of benzyne and by-products from benzyne that occur even at -78°C . Quick optimization in a simple flow chemistry set-up revealed that such reactions could be performed at -78°C where the incipient *ortho*-bromophenyllithium is made to react with electrophiles E before decomposition towards benzyne is possible. An obvious extension of the idea of sequential double substitution of the dibromoaryl species was also demonstrated in this work. Interestingly, while the first lithiation was performed at -78°C to avoid any decomposition towards benzyne formation, the second lithiation and electrophilic attachment was done at 0°C which is again ‘atypical’ of lithiation chemistry practice in synthesis laboratories.



Scheme 1 (a) Reaction pathways leading to different products during lithiation of *ortho*-dibromoarenes. (b) Flash flow chemistry schemes for controlling the reagent mixing and reaction temperature in space and time (Reproduced with permission from ACS) [3]

The work of Yoshida's group paved the way to re-examine the boundary of aggressive chemistries, especially those involving short-lived organometallics (Scheme 1). A number of other groups around the globe joined this endeavour to harness the unprecedented attributes of microfluidic flash chemistry to access or avoid certain reaction pathways that are quite formidable to realize in conventional batch (Schlenk) reactors.

While in their seminal work, Yoshida et al. showed how intricate control over residence time of bromophenyllithium may avoid the formation of benzyne from it, in a subsequent work they reported that flow chemistry can be used as a tool to rather generate benzyne and made it controllably react with another molecule of aryllithium, followed by the trapping with an electrophile E, hence furnishing a wide range of biaryl molecules (Scheme 2) [4]. As a practical application, they used this three-component flow chemistry process to synthesize boscalid, an important fungicide. Formation of benzyne from 1-bromo-2-iodobenzene was accomplished by allowing the decomposition of initially formed bromophenyllithium at a higher temperature zone (-30°C). Hence, this system represents an interesting extension of flash chemistry that exploits the excellent control over the residence time and corresponding temperature within that residence time unit and enables switching between reaction pathways at will: such as 'to benzyne, or not to benzyne'.

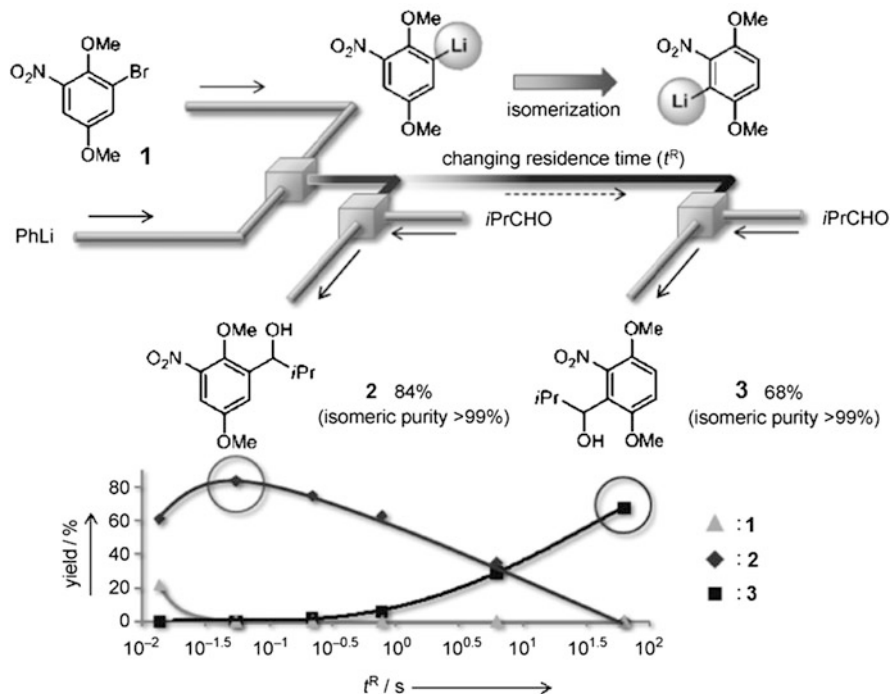


Scheme 2 An integrated flow microreactor system for the three-component coupling of benzyne, functionalized aryllithiums and electrophiles. T-shaped micromixers, M1, M2, M3 and M4; microtube reactors, R1, R2, R3 and R4 (Reproduced from [4] with permission from ACS)

Lithiation of nitro group-containing arylbromide **1** is challenging due to spontaneous isomerization of the nitroaryl lithium species into thermodynamically more stable intermediates. Nagaki et al. (Scheme 3) had demonstrated that by tuning of the time gap between the generation of nitroaryl lithium and the subsequent reaction with electrophiles, a complete control over kinetic vs. thermodynamic products, **2** and **3**, respectively, could be achieved via immediate trapping of the kinetic intermediate or allowing it to isomerize to the thermodynamic one [5].

Exquisite control over selectivity in electrophilic additions onto certain aryllithium species is demonstrated by Kim and Yoshida in their recent work (Scheme 4) [6]. Aryl halides containing carbamate or similar substituents are challenging substrates for lithiation-based electrophilic additions, because the carbamoyl group of the carbamate substituents can migrate to the anionic (organolithium) carbon atom of the aryl ring to generate an oxy anion; hence, the oxygen atom rather than the carbon atom acts as the new nucleophile and dictates the outcome of the reaction. Such rearrangements are called Fries rearrangements. A polymeric integrated chip microreactor (CMR) was designed and employed in this work, which enables the incipient *ortho*-lithiated *O*-aryl carbamates (formed via lithiation of *o*-iodophenyl diethylcarbamate **4**) to be trapped with methyl chloroformate electrophile (E) within 0.33 ms of its generation. Such rapid trapping ‘outpaces’ any skeletal rearrangement of *ortho*-lithiated *O*-aryl carbamates and produced the expected un-rearranged product **5**. Again, by deliberately slowing down the electrophilic trapping (when residence time is longer than 628 ms), the rearranged product **6** is formed exclusively.

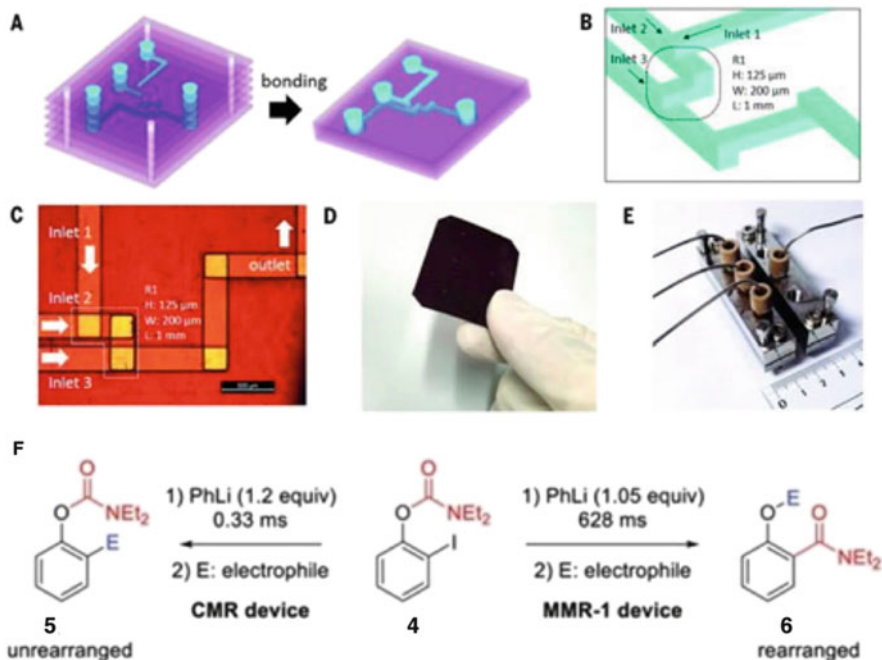
The Yoshida group reported an extension of this concept to tackle selectivity issues for homologous aryl carbamates **7**, where [1,4], [1,5] and [1,6] anionic Fries rearrangements can be controlled in a similar fashion (Scheme 5) [7]. These rearrangements are kinetically much faster than the original investigation of [1,3] Fries rearrangements.



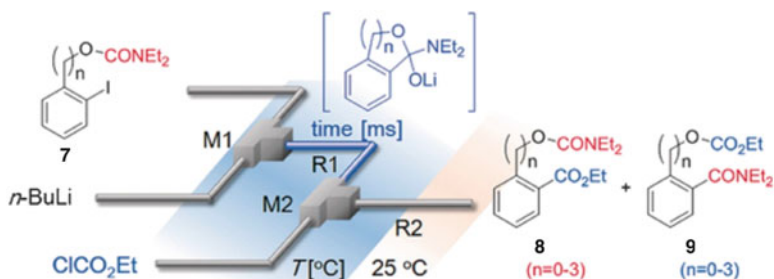
Scheme 3 Switch between kinetic and thermodynamic control by changing the residence time (Adapted from [5] with permission from Wiley-VCH)

Aryl halides containing carbonyl groups attached are challenging substrates for further functionalization via lithiation chemistry, because the carbonyl functional group on the aryl lithium can itself undergo electrophilic attack by another aryllithium species. Hence, the use of protecting groups is seen as a solution to avoid such self-degrading reactions (Scheme 6). By integrating a mixing zone in close proximity of the residence time unit, Yoshida et al. were able to reduce the residence time down to 3 ms, so that acyl-substituted aryllithiums react immediately after being formed with an electrophile, before the former can be attacked by another acyl-substituted aryllithium molecule [8]. They used this flash chemistry protocol to produce the natural product pauciflorol F where the iodine-lithium exchange reaction was performed without protecting the acyl group located *ortho* to the iodine atom.

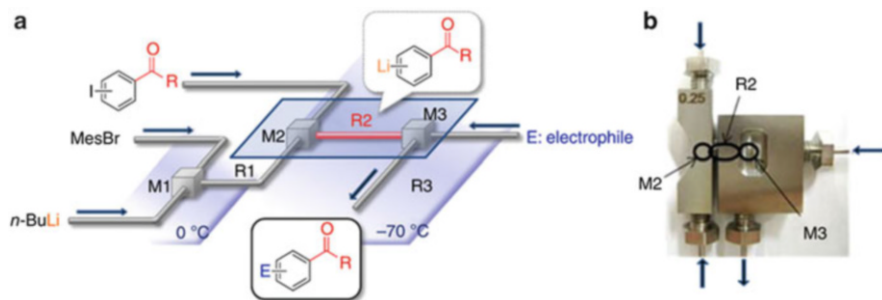
Nagaki et al. performed a tandem reaction by combining (a) in-line generation of aryllithium nucleophile Ar^1-Li (via Br-Li exchange reaction between Ar^1Br and BuLi), (b) Pd-catalysed Murahashi coupling with a second aryl halide Ar^2Br to furnish biaryls Ar^1-Ar^2 and (c) quenching of any unreacted aryllithium with MeOH. Interestingly, all steps were performed at much higher temperatures (0–20°C) than in a typical batch scenario (–78°C) (Scheme 7) [9]. Heterocyclic aromatics, such as thiophene, can be used to generate aryl-lithium species via deprotonation (instead of halogen-lithium exchange) with a lithiating agent, e.g. BuLi. A sequential flow



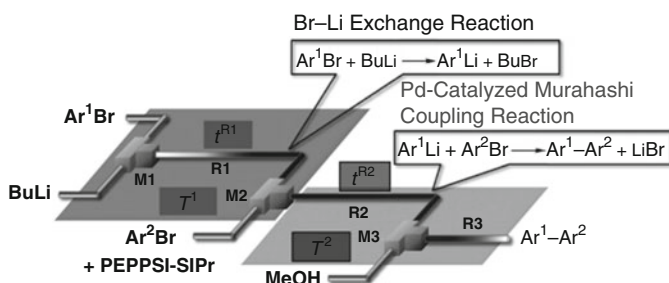
Scheme 4 (a) Conceptual scheme for fabricating 3D serpentine microchannel structure by lamination of the patterned films and one-step thermal bonding. (b) Detailed scheme for a nanolitre reaction space of rectangular 3D serpentine channels ($200\ \mu\text{m} \times 125\ \mu\text{m} \times 1\ \text{mm}$) with three inlets. (c) Optical image of the semitransparent CMR showing the nanolitre reaction space with three inlets and one outlet (top view: scale bar, $500\ \mu\text{m}$). (d) Optical image of CMR module ($4.5\ \text{cm} \times 3.5\ \text{cm}$, thickness $0.7\ \text{mm}$). (e) Optical image of CMR assembly with metal holders to connect tubes. (f) Isomerization control (kinetic vs. thermodynamic) by using different microflow reactor devices (Adapted from [6] with permission from AAAS)



Scheme 5 Controlling [1,4], [1,5] and [1,6] anionic Fries rearrangement of aryl carbamate 7 that may produce kinetic product 8 or thermodynamic product 9 depending on the residence time of the lithiated intermediate (Adapted from [7] with permission from Wiley-VCH)



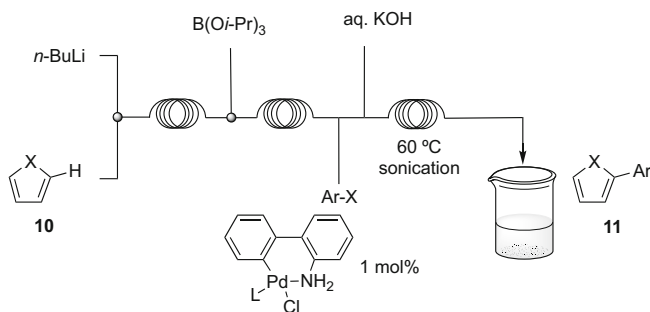
Scheme 6 (a) Flash chemistry scheme of protecting-group free approach towards lithiation and electrophilic addition to aryl compounds containing labile carbonyl groups. (b) Microreaction device with integrated mixing and residence unit components (Reproduced from [8] with permission from Nature Publishing)



Scheme 7 Integrated flow microreactor system for the lithiation and Miyaura-Suzuki cross coupling (micromixers, M1, M2 and M3; microtube reactors, R1, R2 and R3) (Reproduced from [9] with permission from Wiley-VCH)

protocol enabled deprotonation of thiophene (at 0 °C and with a residence time of 11 s), and then palladium-catalysed cross coupling with 2-bromopyridine (at 50 °C and a prolonged residence time of 94 s) produced the desired biaryl product in 80% yield.

The Buchwald group presented a flow chemistry platform that enables handling of solid precipitates formed during the course of sequential transformations such as lithiation of arenes **10**, borylation of aryl lithium and Pd-catalysed Suzuki-Miyaura reaction (Scheme 8) [10]. In this work, the aryllithium formed in the first mixing-residence unit is allowed to react with B(O*i*Pr)₃ to furnish the Suzuki-Miyaura coupling agent ArB(O*i*Pr)₃Li to be consumed in the subsequent step of the Pd-catalysed reaction under alkaline conditions. Under alkaline conditions heteroaryl borates are prone to decompose; hence, they are challenging substrates for Suzuki-Miyaura coupling reactions. This work illustrated that the in situ generation of heteroaryl borates (from heteroaryl-H and lithium exchange reaction) from both thiophene and furan derivatives **10** (X = S and O) and their immediate use to generate products **11** circumvent this long-standing synthetic challenge, which was made possible using flash chemistry. In 2012, this group extended the scope of this



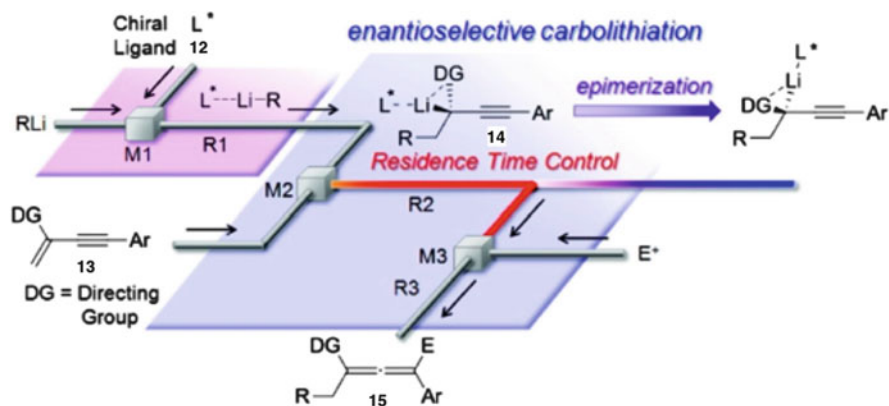
Scheme 8 Flow chemistry set-up for lithiation and Miyaura-Suzuki cross coupling

flow chemistry protocol of lithiation/borylation/catalytic reaction to accommodate asymmetric 1,4-addition of α,β -unsaturated ketones to arylboronates (formed in the same manner as their 2011 work) that furnishes chiral β -arylated ketones in high yield and excellent enantiopurity [11]. Strikingly, the lithiation step can be performed at room temperature, and the whole process (from lithiation to asymmetric 1,4-addition) takes less than 15 min of residence time.

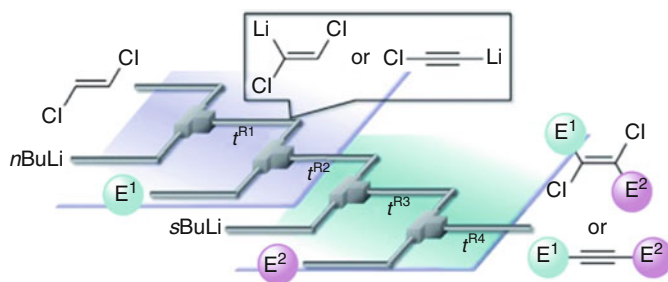
Yoshida's work on a similar reaction sequence showed that two aryl halides bearing electrophilic functional groups can be coupled in this system, and even without any added bases (such as KOH), aryl-aryl coupling can proceed [12].

An asymmetric version of the carbolithiation-mediated C–C bond formation would be an attractive method for chiral synthesis; however, rapid epimerization of the chiral carbolithium intermediate renders this process challenging. Tomida et al. applied the flash chemistry concept to tackle this problem and reported the flow version of a chiral ligand [(–)-sparteine]-assisted carbolithiation of conjugated enynes (Scheme 9) [13]. The presence of a carbamoyloxy directing group on the enyne counterpart is deemed necessary to maintain the high enantioselectivity. Conducting the flow reactions within a narrow window of residence time-temperature domain (25 s, -78°C) produced the desired chiral allene in high yield (>90% yield) and with high enantioselectivity (>90% *ee*), whereas a corresponding batch reaction with identical time and temperature conditions failed to maintain the selectivity (61% *ee*), presumably due to premature epimerization prior to the mixing and reaction with the electrophile.

The scope of flash chemistry for the lithiation of halogen-substituted alkenes to controllably synthesize either highly substituted alkenes or internal alkynes via regulating the fate of the primarily formed 2-halovinyl lithium species from *trans*-1,2-dichloroethene was examined by Nagaki et al. (Scheme 10) [14]. By suppressing β -elimination of LiCl from 2-halovinyl lithium (with millisecond residence times) and allowing immediate trapping with electrophile (E) in the downstream reaction, a variety of disubstituted dichloroalkenes could be synthesized. Through deliberate increase of the residence time for 2-halovinyl lithium species to 1–50 s, the β -elimination pathway can be switched on, and asymmetric alkenes can be produced. This work manifested the power of flash chemistry to dictate over competing



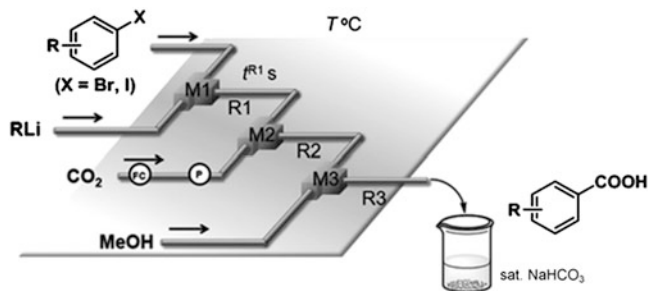
Scheme 9 Flow microreactor system for enantioselective carbolithiation followed by trapping with electrophiles (M1, M2 and M3) and three microtube reactors (R1, R2 and R3): *n*-BuLi and the chiral ligand **12** form a complex *n*-BuLi/**12** (M1 and R1). Carbolithiation of **13** with *n*-BuLi/**12** provides the chiral organolithium intermediate **14** (M2 and R2), which is then quenched with MeOH as an electrophile E (M3 and R3) to give product **15** (R = Bu, E = H) (Adapted from [13] with permission from ACS)



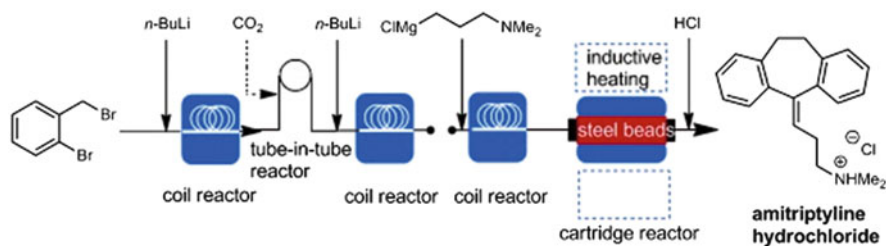
Scheme 10 An integrated flow microreactor system for the synthesis of disubstituted dichloroalkenes and asymmetric disubstituted alkynes by sequential introduction of two electrophiles (Reproduced from [14] with permission from Wiley-VCH)

reaction pathways, simply by controlling the residence time of a highly active intermediate in the reactor zone.

Facile, decomposition-free and safe generation of organometallic intermediates and their subsequent consumption with various nucleophiles prompted further research into exploiting the attributes of flash chemistry to expand into gas-liquid biphasic scenario. In this direction, the Yoshida group showed a simple but elegant example. The carboxylation of aryllithium species with CO₂ gas can produce carboxylic acids, which are important organic molecules (Scheme 11) [15]. Generally, the capture of CO₂ with organolithium compounds poses twofold of challenges. Firstly, the dissolution and diffusion of CO₂ into the organic solvent at cryogenic conditions is slow, which consequently impedes the reaction rate due to the low concentration of CO₂ in the liquid. Secondly, any electrophilic functional group



Scheme 11 A flow microreactor system for the reactions of organolithiums with CO_2 gas. T-shaped micromixers, M1, M2, M3; microtube reactors, R1, R2, R3; flow controller, FC; pressure gage, P (Reproduced from [15] with permission from Wiley-VCH)



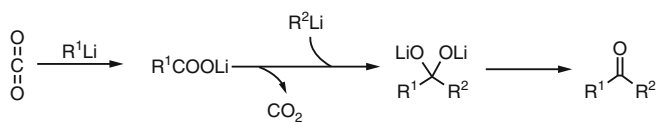
Scheme 12 Sequential flow reactions of lithiation, carbon dioxide trapping and Grignard reactions towards a medicinally active compound: the tricyclic antidepressant amitriptyline (Reproduced from [17] with permission from Wiley-VCH)

already present in the aryl skeleton may react with another molecule of organolithium species. Such a competing, self-consuming pathway inhibits the use of CO_2 as a nucleophile for such substrates. In the gas-liquid microflow regime, a precise control of aryllithium residence time coupled with fast and efficient gas-liquid mass transport enables carboxylation of diverse electrophilic functional group bearing aryl halides. Pieber et al. took terminal alkynes and heterocycles as substrates to employ fast lithiation and subsequent CO_2 capture in a flash chemistry setting that provided the corresponding carboxylated derivatives in 0.5 s reaction time [16].

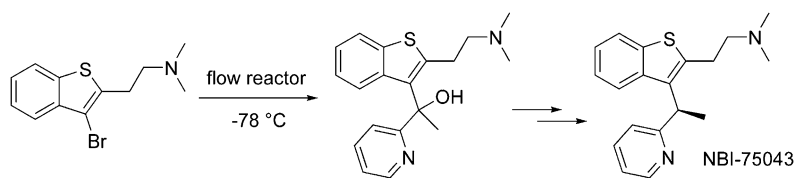
The group of Kirschning reported an interesting combination of multiple liquid-phase and liquid-gas phase organometallic reactions for the synthesis of the tricyclic antidepressant amitriptyline (Scheme 12). Lithiation-mediated Wurtz-type dimerization of *ortho*-bromobenzyl bromide, followed by a second lithiation and carboxylation (a tube-in-tube flow system incorporated for the reaction with CO_2) and in the third lithiation step a Parham cyclization furnished the key intermediate dibenzosuberone that undergoes Grignard addition with [3-(dimethylamino)propyl]magnesium chloride to provide the target product, amitriptyline, after a simple work-up. All these reactions were performed in much higher temperature (hence with increased rate) than established batch protocols [17].

With two equivalents of different organolithium species ($R^1\text{-Li}$ and $R^2\text{-Li}$) or organolithium ($R^1\text{-Li}$) and Grignard reagents ($R^2\text{MgX}$), two nucleophiles are attached to one equivalent of CO_2 , and a wide variety of ketones ($R^1\text{-CO-}R^2$) can be produced. However, low gas-liquid mass transport associated with cryogenic reaction conditions (*vide infra*), troublesome removal of excess CO_2 (to inhibit monoadduct carboxylate formation, i.e. $R^1\text{-COO}^-$ or $R^2\text{-COO}^-$ as the examples presented above) and propensity for the formation of homocoupling products (symmetric ketones: $R^1\text{-CO-}R^1$) are the major obstacles in this synthetically appealing route for *asymmetric* ketones. The Jamison group developed a telescoped three-step-one-flow process for the selective formation of asymmetric ketones via a stepwise lithiation of CO_2 followed by controlled decomposition of bimetallic intermediates to accomplish the ketones avoiding the formation of tertiary alcohols (which happens in batch conditions) (Scheme 13) [18]. In this work, both stoichiometric and excess CO_2 could be used, while for excess CO_2 a micro-degasser is placed before the second lithiation step to vent off any unused CO_2 from the reaction mixture. This constitutes a promising advance of removing reactive gases from the reaction mixture in continuous manner and hence ensures the selectivity of the subsequent reaction. The researchers extended the idea to realize a novel ketone formation protocol where both an organomagnesium (Grignard reagent) and an organolithium reagent can be used sequentially to add to CO_2 for producing asymmetric ketones.

Neurocrine Biosciences and Irix Pharmaceuticals employed flow chemistry for scaling up a process for the synthesis of histamine receptor antagonist NBI-75043 that involves a lithium-halogen exchange reaction [2-(3-bromo-benzo [b]-thiophen-2-yl)ethyl]dimethylamine and subsequent nucleophilic addition with 2-acetylpyridine (Scheme 14) [19]. *tert*-Butyllithium mixed with trimethylethylenediamine (TMEDA) was used as the lithiation reagent, which is well known for its pyrophoric nature when comes in contact with air, hence is a highly hazardous reagent for any reasonable scaled chemical transformation. Using a microreactor



Scheme 13 Flow systems for ketone synthesis from organolithiums and CO_2 (Reproduced from [18] with permission from Wiley-VCH)

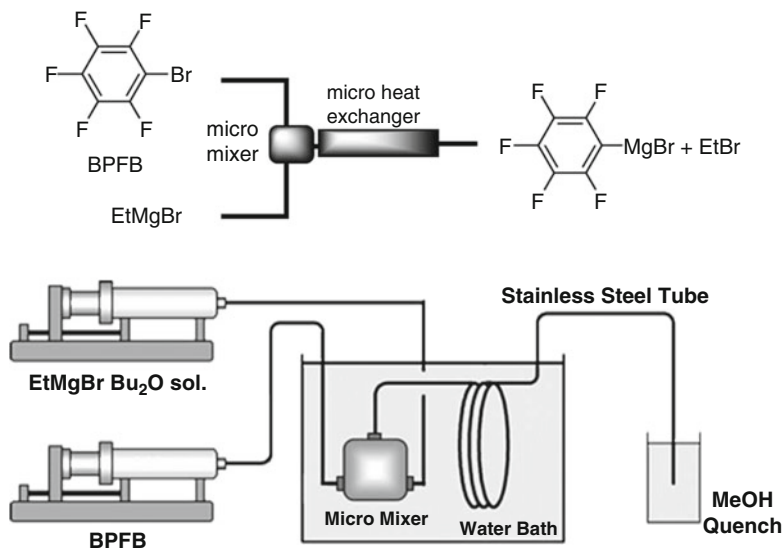


Scheme 14 Flow system for bromine-lithium exchange for a scaled-up production of NBI-75043, a sleep therapeutic (Reproduced from [19] with permission from ACS)

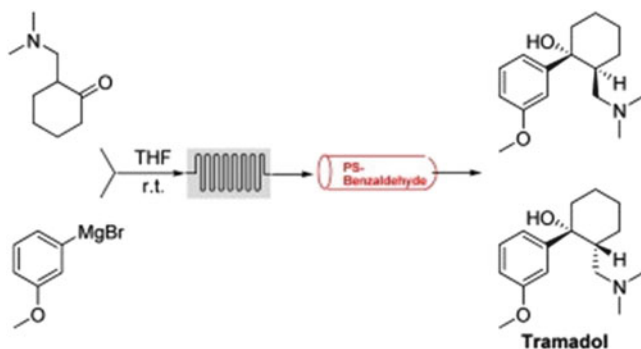
construction with T-connectors and stainless steel tubing, these groups accomplished 93% yield of the lithiation-nucleophilic addition product using 200 mL (1.7 M) *tert*-BuLi solution in a single run at cryogenic conditions (-78°C).

One of the first examples of conducting Grignard-type reactions in microreactor system came from the Yoshida group (Scheme 15) [20]. They employed commercially available micromixers such as from Toray Hi-mixer or IMM multi-lamination-based mixer and integrated those to shell and tube micro-heat exchangers. They targeted pentafluorophenylmagnesium bromide as an industrially relevant Grignard reagent, which is produced from a highly exothermic Grignard exchange reaction between ethylmagnesium bromide and bromopentafluorobenzene. After optimizing the reactions in small-scale microflow system, they opted for a pilot plant demonstration, which was successful in running the reaction under ambient condition (20°C) and with a short residence time (5 s) and for an elongated operation time (24 h). A throughput of 14.7 kg of product was obtained without any reactor fouling.

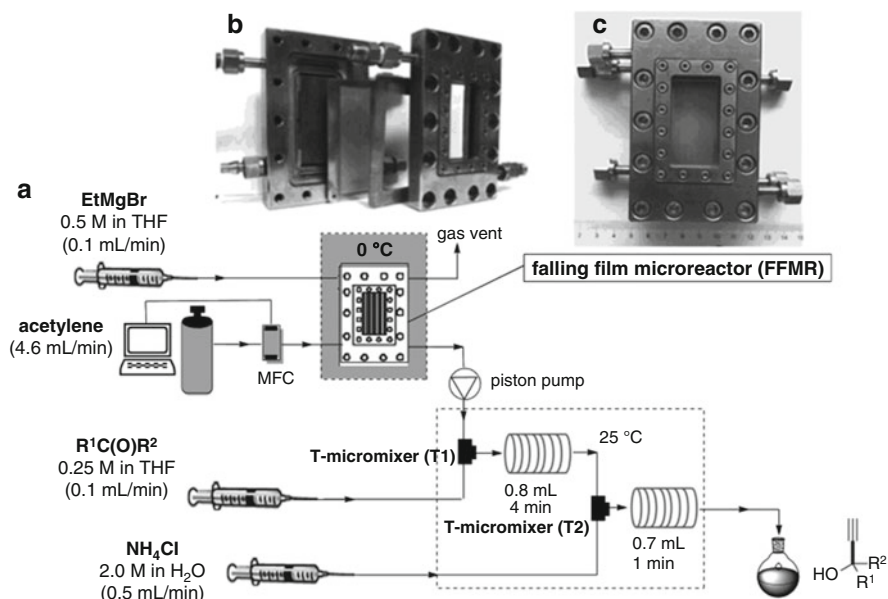
Riva et al. demonstrated a simple flow system made from polyfluoroethylene (PFE) tubing, where the addition of Grignard reagents to aldehyde and ketones (producing secondary and tertiary alcohols, respectively) could be successfully performed at room temperature, thanks to excellent heat dissipation from the reaction mixture inside the microtube residence time unit (Scheme 16) [21]. A polymer-supported benzaldehyde column was connected with the residence time unit to capture and quench any unreacted Grignard reagent, which ensured a clean and facile work-up. This microflow system was useful for the synthesis of the well-known analgesic Tramadol[®] in high yields and with improved diastereoselectivity, compared to reported batch results.



Scheme 15 Flow system for Grignard reagent production (Reproduced from [20] with permission from ACS)



Scheme 16 Flow system for producing drug molecule Tramadol[®] with an in-line quenching facility (Reproduced from [21] with permission from Elsevier)



Scheme 17 Falling film reactor for gas-liquid reaction of acetylene gas with Grignard reagent with in-line quenching. (a) Microflow set-up; (b) disassembled FFMR; (c) assembled FFMR (Reproduced from [22] with permission from ACS)

The use of acetylene gas in conjugation of alkyl Grignard reagent is an important procedure to incorporate the ethylene moiety into an alkyl backbone. This gas-liquid reaction produces propargylic alcohols (when the reaction mixture contains carbonyl compounds as electrophiles). Deng et al. capitalized on the highly efficient gas-liquid mixing and heat-transfer capabilities of falling film microreactors to perform this highly exothermic and mass-transfer regulated reaction (Scheme 17) [22]. Liquid flow rate optimization was found to be crucial for maintaining a thin film of the Grignard reagent EtMgBr solution (24×10^{-6} M), in which case fast

gas-liquid mass transfer is ensured and the propargylic alcohol is formed with excellent selectivity (over other by-products).

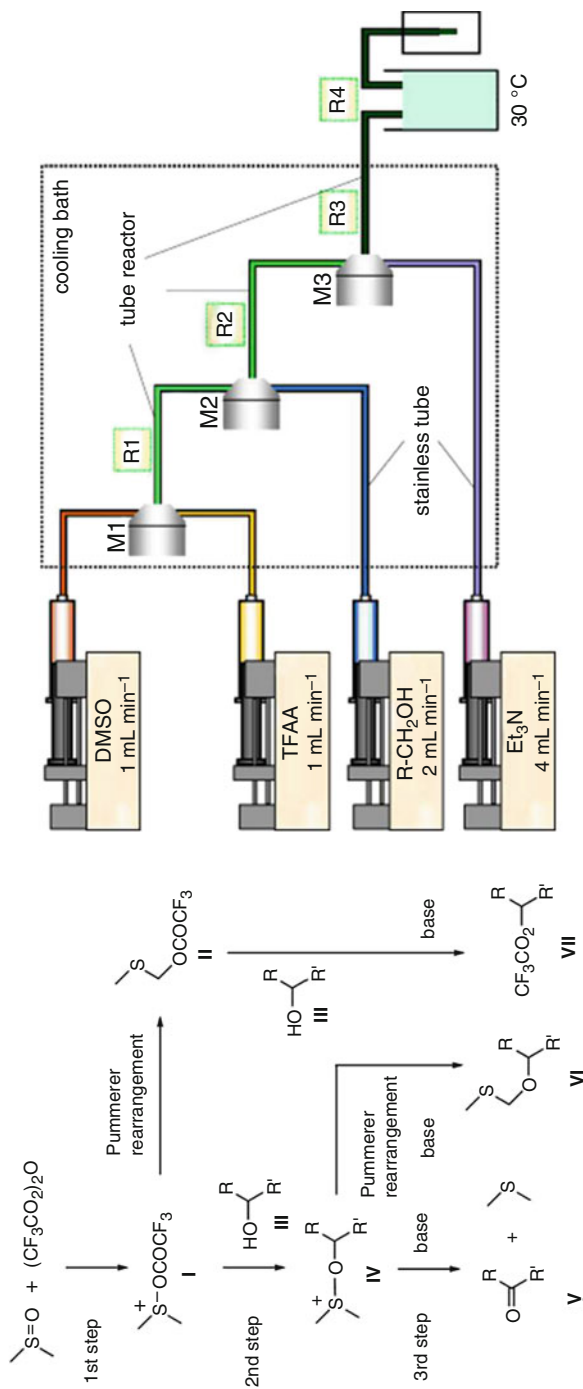
Swern oxidation is one of the most versatile methods for converting alcohols into carbonyl compounds. This is a metal-free oxidation process that requires strictly cryogenic conditions to avoid by-product formation via a Pummerer rearrangement of the intermediates (**I** and **IV**) formed during the course of the reaction (as shown in Scheme 18). Yoshida's pioneering work revealed that a flash chemistry set-up can help to circumvent such rearrangement pathways through stepwise formation of activated intermediates and allowing those intermediates to react with the next reagent/reactant within 0.01 s time scale [23]. The set-up was constructed from three micromixers (M1, M2, M3) and stainless-steel tube residence time units (R1, R2, R3, R4). As a rapid consumption of the labile intermediates occur immediately after their formation, a build-up of trifluoroacetoxy dimethylsulfonium salt (**I**) and alkoxydimethylsulfonium salt (**IV**) is avoided which manifests the safety features of the flow Swern oxidation. Aided by rapid heat dissipation from the tube, Swern oxidation could be performed even at 20°C. At 20°C a batch Swern oxidation of several primary and secondary alcohols (1-decanol, 2-octanol and cyclohexane) produced the undesired trifluoroacetates of the corresponding alcohols (**VII**) in 70–90% yield, while the flow system furnished very good to excellent yields (75–95%) of the aldehyde or ketone (**V**) with only small amount of by-products.

Such success of Swern oxidations at mild conditions prompted interest for a possible scaling up of this process. For example, Van der Linden et al. constructed a flow system to scale up the Swern oxidation of testosterone to 4-androstene-3,17-dione. A throughput of 64 g/h (volume throughput: 117 g/L/h) was achieved when the process was run at –20°C and for 1.5 h [24].

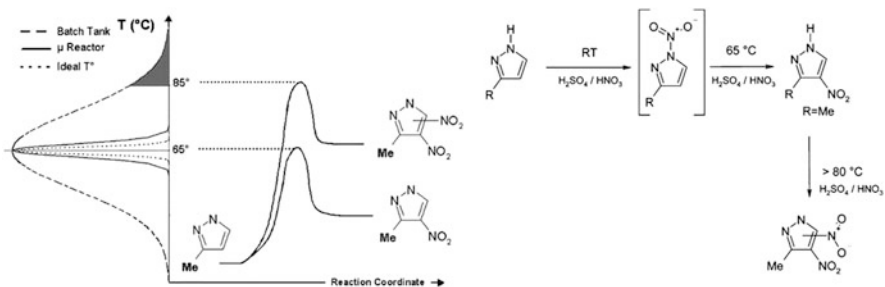
2 Reactions of Explosive Nature: Nitration

Heterocyclic nitration is an industrially important process as several drug molecules and precursor to APIs (API: active pharmaceutical intermediate) are nitrated heterocyclic molecules. Nitration of aromatics is typically highly exothermic in nature; hence, hotspot generation in the confinement of batch reactors could cause runaway reactions and pose potential for explosion. Moreover, some non-nitrated products or multiple-nitrated by-products (due to uncontrolled nitration) could be explosive themselves on their own right due to high oxygen content as well as highly demanding reaction conditions (high concentration acid mixture, high temperatures). Quenching of the unused concentrated acid mixture at the end of the reaction is another hazard, as acid/base neutralization is a highly exothermic process. This scenario becomes highly untenable for any reasonable scale-up due to safety issue. These factors prompted several academic and industrial groups to examine the scope of flow chemistry for nitration chemistries.

AstraZeneca's increased demand for nitrated pyrazole derivatives prompted them to investigate the viability of microflow reactor in scaling up hazardous nitration



Scheme 18 Reaction mechanism for Swern oxidation: possible by-product forming pathways via Pummerer rearrangement involving labile intermediates (Reproduced from [23] with permission from Wiley-VCH)

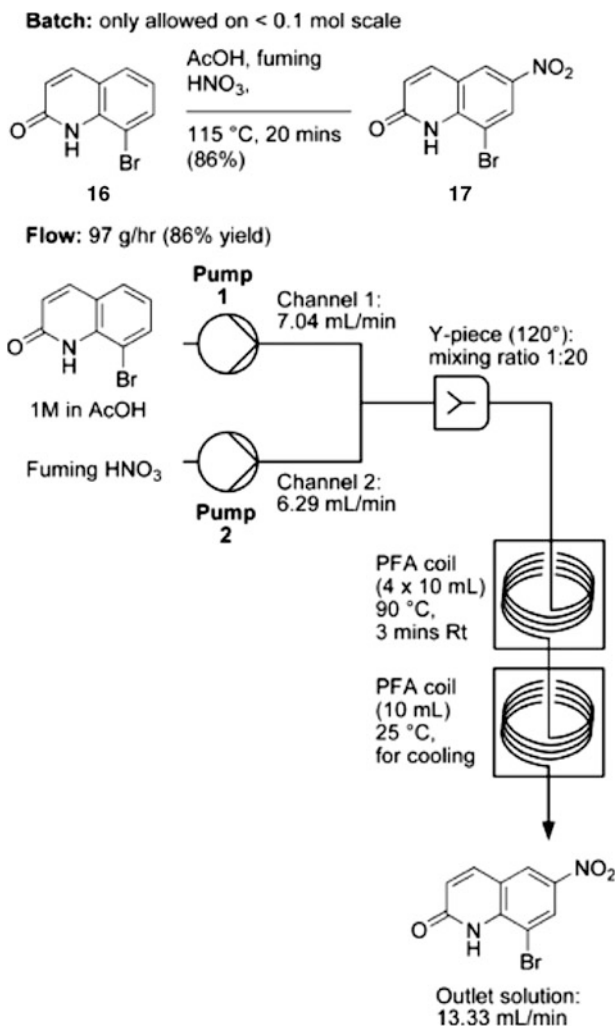


Scheme 19 Flow nitration of pyrazole: concept of controlling the selectivity via temperature control (Reproduced from [25] with permission from ACS)

chemistry, where both products and by-products are potentially explosive in nature (Scheme 19) [25]. A 2009 report from AstraZeneca showed that a combination of the IMM slit interdigital micromixer and a stainless steel tube reactor could be employed to carry on selective nitration of 3-alkyl pyrazole at a 100 g scale (at 98% conversion) under safe reaction conditions of 65°C which contrast harsh and hazardous condition (140°C) typically used for small-scale batch reactions. Apart from the scale, the most important achievement of this flow system was the ability to avoid the production of dinitro derivatives which are typically formed in the batch processes due to poor heat transfer.

Researchers from the Novartis Institute for Biomedical Research employed a commercially available microreactor system (Vapourtec) to scale up the nitration of 8-bromo-1*H*-quinolin-2-one **16** with a mixture of fuming nitric acid and acetic acid (Scheme 20) [26]. A batch reaction at 115°C, limited to <0.1 mol scale, deemed unsuitable for any conventional scale-up due to the proximity to the decomposition temperature (135°C). A Vapourtec system was used for optimization of the reaction providing a set of parameters where the best performance was achieved at 90°C with 3 min residence time, which are impressively lower than the optimized batch conditions. The group was able to produce 201 g of nitrated material **17** in just over 2 h time (throughput: 97 g/h). Similar throughput in the nitration was achieved for other aryl derivatives such as 2-amino-4-bromo-benzoic acid methyl ester (70 g/h) and 1-benzosuberone (39 g/h). In both cases significant amounts of undesired by-products were formed (17–35%) in the corresponding batch reactions.

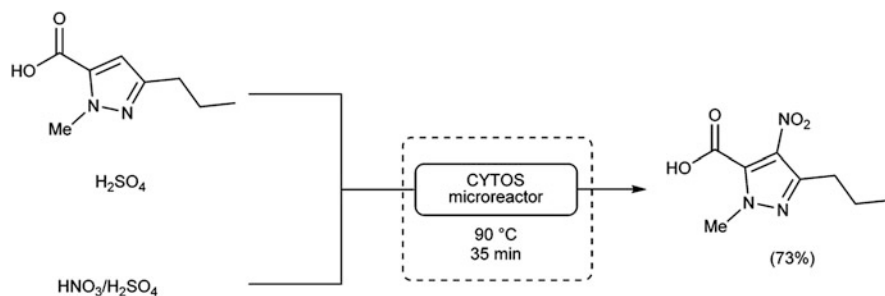
Gage et al. from Asymchem Inc. needed to meet the requirements for a large quantity of nitropyridine derivative 5-bromo-2-amino-3-nitro-4-methylpyridine, a starting material for the synthesis of an API in clinical development [27]. A conventional batch reaction sulfuric acid solution of 5-bromo-2-acetamido-4-methylpyridine with fuming nitric acid at 25–33°C provided the product (52–55% yield). A solution of the product in fuming nitric acid starts to decompose at 80°C which prohibits any scale-up for safety reasons. Hence, this group intended to implement a continuous process for safe scale-up. They used pressure-driven pumping and mixing of two liquid feeds: (1) 5-bromo-2-acetamido-4-methylpyridine in sulfuric acid and (2) a mixture of nitric acid and sulfuric acid,



Scheme 20 Scaling-up of nitration chemistry (Reproduced from [26] with permission from ACS)

while the reaction took place inside the jacketed tube reactor assembly. With 20 min residence time, a significantly higher reaction temperature 50–55 °C could be set to boost the conversion (97%) in a safe manner due to rapid heat removal from this exothermic reaction taking place inside the thermally conductive jacketed tube reactor. Although the yield of the flow reaction did not improve (compared to batch), the process could be run for 2.5 days with any hazard or fouling to furnish a total of 36.5 kg of 5-bromo-2-amino-3-nitro-4-methylpyridine with 99.7% purity.

In one of the earliest examples of microreactor-assisted nitration chemistry, the Schwalbe group demonstrated that a commercial microreactor (with an internal



Scheme 21 Scaling-up of nitration chemistry towards a key intermediate for Sildenafil drug (Reproduced from ref. [28] with permission from Springer)

reactor volume of 70 mL) enabled nitration of pyrazole-5-carboxylic acid to generate a key intermediate in the synthesis of Sildenafil (Scheme 21) [28]. Since nitration is typically performed at relatively high temperature and highly acidic condition, decarboxylation was a detrimental side reaction at temperatures above $100\text{ }^\circ\text{C}$. A microflow process operated exactly at $90\text{ }^\circ\text{C}$ and with a residence time of 30 min provided a throughput of 5.5 g/h/L with minimization of any such decomposition.

3 In Situ Generation of Hazardous Reagents and Intermediates

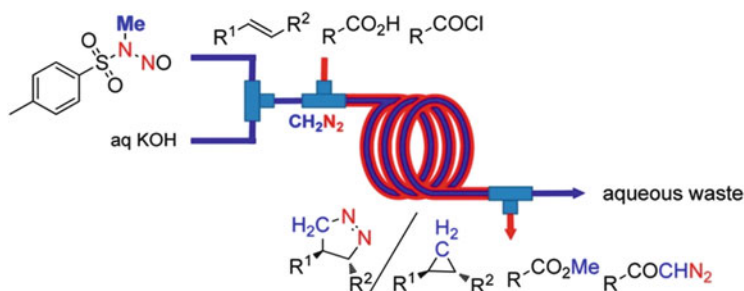
3.1 Diazo Compounds and Diazonium Salts

Diazo and diazonium compounds are versatile reagents for numerous chemical transformations. Diazoalkanes are used as alkylating reagents and α -diazocarbonyls as source of carbenes and metal carbenoids and as reactive ketenes. Diazo compounds take part as 1,3-dipoles for heterocycle-forming cycloaddition reactions. The diazonium group constitutes an excellent leaving group for numerous reactions such as Sandmeyer, Meerwein, Balz–Schiemann and palladium-catalysed cross coupling reactions. However, due to the high nitrogen content, most of the diazonium and diazo group-containing compounds are thermally unstable and are an explosion hazard. The most useful of all, diazomethane, is an excellent C_1 alkylating agent, but its application in chemical laboratories is met with severe safety concerns: toxicity, volatility and extreme shock and light and heat sensitivity. Continuous flow chemistry had proved to be a viable platform for generating and using highly reactive and hazardous diazo-based intermediates and reactants [29–31].

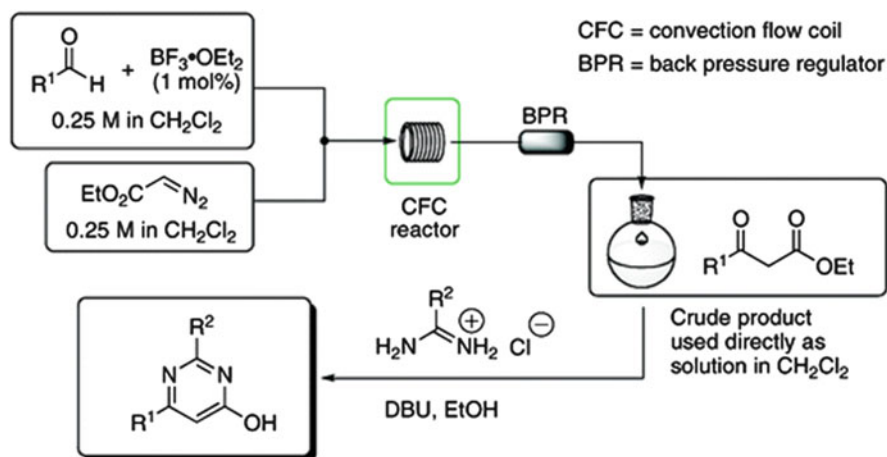
Flow chemistry enables the in situ generation of diazomethane, which is immediately consumed in-line, hence reducing the safety concern significantly [32]. Because the amount of generated diazomethane at any given time is miniscule, it is confined in a closed tubular system and then reacted with a substrate to produce desired product without any storage need. The Kappe research group generated diazomethane in a simple tube-in-a-tube reactor set-up from a well-known

reaction of alkaline decomposition of Diazald [diazald: (*N*-methyl-*N*-nitroso-*p*-toluenesulfonamide) reacted with aqueous KOH] (Scheme 22) [33]. The produced gaseous diazomethane separates through the permeable membrane of AF-2400 tube and diffuses through the THF + substrate solution flowing in the outer tube. This in situ-generated diazomethane could be used to produce heterocycles such as the methylation of 5-phenyltetrazole leading to a mixture of the 1- and 2-methyltetrazoles and the (2 + 3) cycloaddition of diazomethane to *N*-phenylmaleimide giving the respective 1-pyrazoline, in quantitative conversion. Kim et al. used a membrane-based lab-on-chip reactor to generate diazomethane in situ for organic transformations [34].

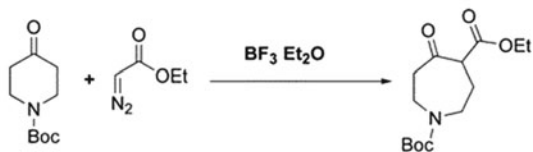
Hayes and co-workers demonstrated that ethyl diazoacetate and boron trifluoride etherate can be handled safely in a flow system where the Roskamp reaction with aldehydes provided β -ketoesters (Scheme 23) [35]. A commercial microreactor



Scheme 22 In situ generation of diazomethane and its use in a tube-in-a-tube flow arrangement (Reproduced from [33] with permission from ACS)



Scheme 23 Use of two hazardous chemicals in a single flow system: ethyl diazoacetate and boron trifluoride etherate-assisted β -ketoester synthesis (Reproduced from [35] with permission from ACS)



Scheme 24 Use of two hazardous chemicals in a single flow system: ethyl diazoacetate and boron trifluoride etherate-assisted piperidone synthesis (Reproduced from [36] with permission from ACS)

system was used in combination with a back pressure regulator (for outgassing the nitrogen gas generated from diazoacetate reagent). This system was used for rapid optimization of the reaction. β -Ketoesters exiting from the reactor were found to be sufficiently pure to be used in the second reaction (in a conventional flask reaction) with acetamidine hydrochloride that furnishes biologically important heterocycles such as pyrimidin-4-ol. This is an important advance in flow chemistry where two different hazardous reagents were used in a one-flow set-up combined with conventional batch reactor to synthesize valuable heterocyclic building blocks.

The R&D group from Johnson & Johnson Pharmaceuticals performed a similar reaction of combining diazoacetate and boron trifluoride etherate with *N*-Boc-4-piperidone in the CPC CYTOS system (a commercial microreactor) to produce *N*-tert-butoxycarbonyl-5-ethoxycarbonyl-4-perhydroazepinone as a seven-membered heterocycle. Reaction conditions of a 70 mg scale batch reaction protocol are adopted for a continuous run in the CYTOS system (with 1.8 min residence time) enabled a 91 g/h throughput, without compromising the safety (Scheme 24) [36].

3.2 Phosgene

Phosgene is an inexpensive, versatile gaseous reactant for organic transformations, yet its wide use in chemical laboratories or industries is strictly limited due to its highly toxic nature. Flow chemistry is adapted to minimize the risk of phosgene exposure via an in situ generation and immediate consumption of it. Fuse et al. demonstrated that a simple flow chemistry device comprising of T-mixers and tube can be used to generate phosgene from triphosgene and an organic base which is immediately consumed in a subsequent reaction with carboxylic acid generating acid

chlorides as reactive and versatile intermediates [37]. For chiral carboxylic acids, the generated acid chloride is prone to undergo epimerization hence jeopardizing the enantiomeric purity of the product. For the reported flow chemistry protocol, such epimerization of the acid chloride could be suppressed by telescoping to a next reaction, the amidation of the acid chloride in the second reaction zone soon after its formation. Hence, amides with >90% *ee* were obtained in most cases.

4 Reactions Involving Toxic, Corrosive and Flammable Gaseous Reagents

4.1 Oxygen (Triplet and Singlet States)

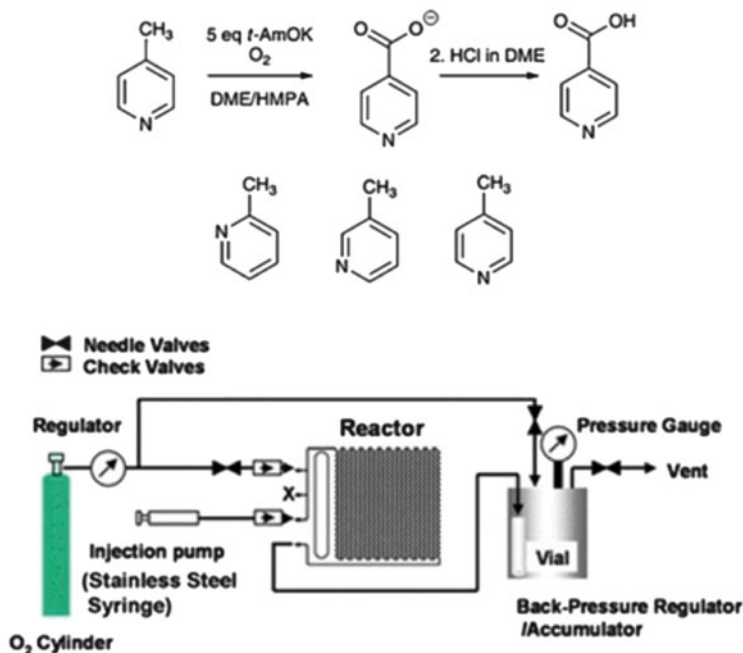
Molecular oxygen is regarded as the most benign oxidant available. Synthetically, molecular oxygen can be used either in its natural triplet or excited singlet electronic states. In both cases, formation of organic vapour-oxygen mixture poses a serious hazard due to the possibility of explosion, especially at high pressure and temperature. Moreover, the generation of highly oxygenated intermediate species such as organic peroxides raises another safety issue in oxygenation reactions.

Given the minuscule amount of molecular oxygen involved or the hazardous intermediate produced during the course of the reaction in a flow reactor system, the potential of molecular oxygen as a sustainable oxidant is gaining attention for an even larger-scale production scheme.

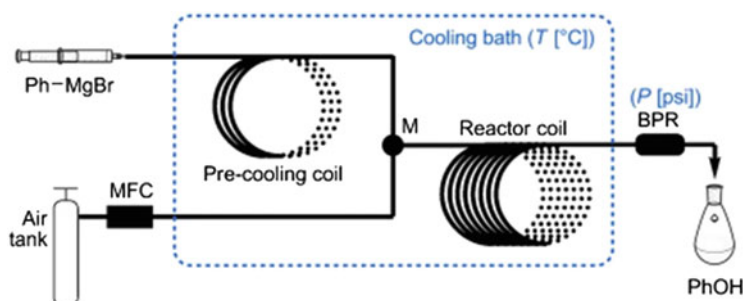
Aerobic oxidation with naturally abundant oxygen (in triplet state) typically requires metal catalysts. However, thanks to intensified heat and mass transfer within the microstructured reactor space, catalyst-free versions of such oxidation processes have been reported.

Jensen et al. demonstrated that an inherently sluggish, demanding (high temperature, high pressure and catalysts) yet low-yielding reaction such as the aerobic oxidation of picolines to provide picolinic acids can be performed in a chip reactor, which not only provides nearly quantitative conversion in much shorter reaction time but also without any catalytic assistance and at much lower pressure [38]. In this work, a silicon nitride-coated halo-etched microreactor was used (Scheme 25). With potassium *tert*-amylate (*t*-AmOK) in dimethoxyethane (DME) and hexamethylphosphoramide (HMPA) and at an oxygen pressure of 2.5 bar, 95 conversion of 3-picoline to the carboxylic acid of 3-picoline, which is known as vitamin B3, a human nutrient, was accomplished in 5 min residence time. When air (instead of pure oxygen) was used, 78% yield was obtained. Enhanced gas-liquid mass transfer was attributed to this highly efficient oxidation process.

The Jamison group at MIT worked out an unconventional protocol for the continuous production of phenol derivatives via oxygenation of Grignard reagents, a reaction which is generally known to be sluggish due to the presumed low reactivity of ArMgX species towards oxygen (Scheme 26) [39]. This report showed



Scheme 25 Oxygen-mediated oxidation of picoline to picolinic acid in a flow system (Adapted from [38] with permission from RSC)



Scheme 26 Oxygenation of aryl Grignard reagents producing phenolic derivatives (Reproduced from [39] with permission from Wiley-VCH)

that under optimized conditions (temperature and pressure), even compressed air (safer than pure oxygen) can be used in a simple gas-liquid flow set-up. ArMgX was converted to the corresponding phenols in almost quantitative conversion with excellent yields (53–87%) (-25°C , 10 bar, 3.4 min residence time), while representative batch experiments produced only 9–15% of the phenol products.

Kappe et al. reported an interesting approach of using molecular oxygen to generate reactive diimide intermediates via hydrazine oxidation under rather harsh

conditions (thanks to flow system for avoiding the risk of explosion) without necessitating the use of any catalyst: diimide is capable of reducing C=C bonds of alkenes via transfer hydrogenation [40]. In a subsequent report, they showed that using a multi-injection method, the selective reduction of artemisinic acid leads to an important precursor for the antimalarial drug artemisinin [41].

Gutmann et al. developed a flow system for the high-temperature and high-pressure Pd-catalysed aerobic oxidation of 14-hydroxymorphinone to a 1,2-oxazolidine [42] and the *N*-demethylation of 14-hydroxymorphinone-3,14-diacetate [43]. In both cases of active catalytic species, colloidal palladium is generated at a preheating step (120–140°C) that subsequently enabled quantitative conversions and sufficient purity in the reaction products.

Molecular oxygen assisted also the oxidative regeneration of Pd(II) species from Pd(0) that is formed in a Heck-type cross dehydrogenative coupling of alkenes and indoles [44].

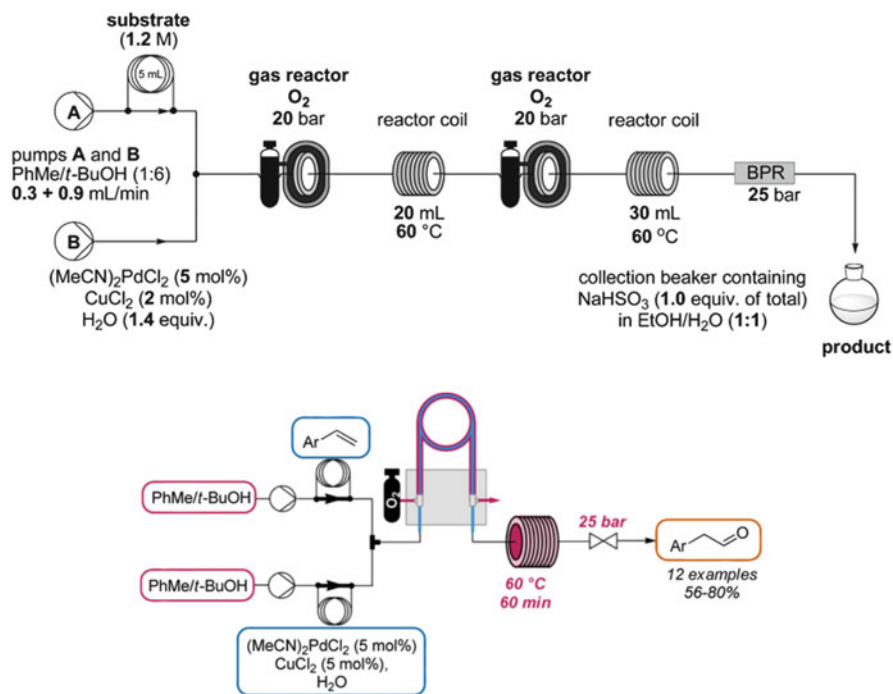
Another approach is the slow diffusion of molecular gas into the liquid. Tube-in-tube or tube-in-shell arrangements were tested for dissolving molecular oxygen into the reactants containing solution for the oxidation reactions. Gas permeable polymeric tubing is used as the gas supply conduit in to the liquid stream. In such arrangements, any reactive gas diffuses through the permeable tubing from the outer tube (or shell) [41, 42].

In the tube-in-tube arrangement, oxygen (at 25 bar pressure) diffuses from the outer tube (or stainless steel shell) through the gas-permeable polymer wall of the inner tube, and the gas dissolves into the reaction solution flowing inside the inner tube.

Boume et al. reported such tube-in-tube arrangement to carry out palladium-copper catalysed Wacker oxidation of styrene to produce *anti*-Markovnikov arylacetaldehyde derivatives (Scheme 27) [45]. In a conventional autoclave, oxygen depletion leads to lower conversion, while over-oxidation is leading to undesired by products caused by increased oxygen pressure. Such challenge is somewhat tackled in this work by minimizing the oxygen depletion via a series of connected tube-in-tube coils and maintaining an optimized oxygen pressure. This set-up was used in scaling up the process to increase the overall throughput.

A similar tube-in-tube flow set-up was employed by several groups to perform oxygen-assisted coupling reactions such as the Glaser-Hay coupling of terminal alkynes [46], Fe-catalysed nitro-Mannich reactions [47] and oxidative Heck reactions [48].

In most of the tube-in-tube flow systems, Teflon-AF 2400 is used as the most versatile polymer material as this is permeable to wide ranges of reactive gases while impermeable to most organic solvents [49]. However, due to its high price, an alternative polymer material is sought after as a gas permeable membrane. In this direction, Stahl et al. demonstrated that PTFE tubes can be used as an economic alternative of Teflon-AF 2400, thanks to the former's oxygen permeability and durability at high temperatures and pressure [50]. In this study, an extended PTFE tube was coiled inside a stainless steel shell where a sustained O₂ pressure was maintained (25 bar). Oxygen permeated through the PTFE membrane and dissolved



Scheme 27 Palladium-catalysed efficient aerobic *anti*-Markovnikov Wacker oxidation in a tube-in-tube flow reactor (Reproduced from [45] with permission from Wiley-VCH)

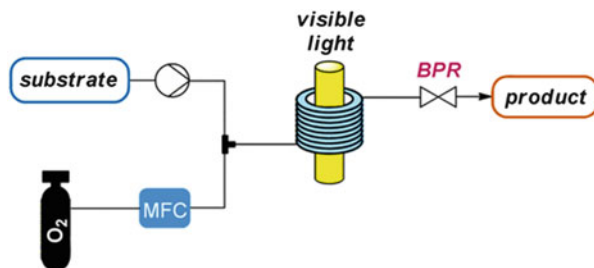
in to the substrate solution of alkyl alcohol containing the catalyst [Cu(CH₃CN)₄]OTf, a bipyridyl species (bpy or 4-MeObpy), TEMPO or ABNO and *N*-methyl imidazole (NMI) flowing inside the PTFE tube, hence enabling aerobic oxidation to alcohols to aldehydes/ketones with quantitative conversion and excellent selectivity. 10 g scale production was facilitated by numbering up of the PTFE tubes.

Flow chemistry holds special appeal to gas-liquid reactions that require photo stimuli. In addition to large surface area to volume ratio for accelerating gas-liquid mass transport, availability of transparent materials for flow reactor design (glass, PDMS and other polymers) and short optical path length facilitate efficient photo-assisted chemical processes.

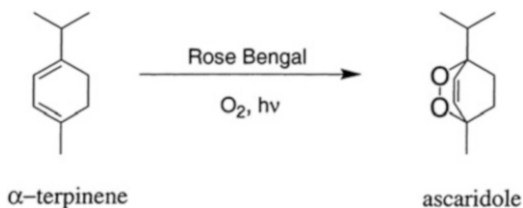
In this context, the generation of highly reactive singlet oxygen from molecular oxygen (triplet state) under photosensitization and its subsequent reaction with the substrates in the liquid phase are both easily and efficiently accomplished inside the microreactor channel. A general schematic (Scheme 28) of such flow system constitutes a simple method of supplying metered dosages of oxygen gas and a liquid stream into a transparent reactor (either glass-made chip or transparent tube coil), which is in close proximity to a light source.

Seminal work from Wootton et al. demonstrated that singlet oxygen can be generated via Rose Bengal sensitization that is used in situ to react with

Scheme 28 Concept of photochemical generation of singlet oxygen and its use in oxidation of organic substrates in flow reactor (Reproduced from [51] with permission from ACS)



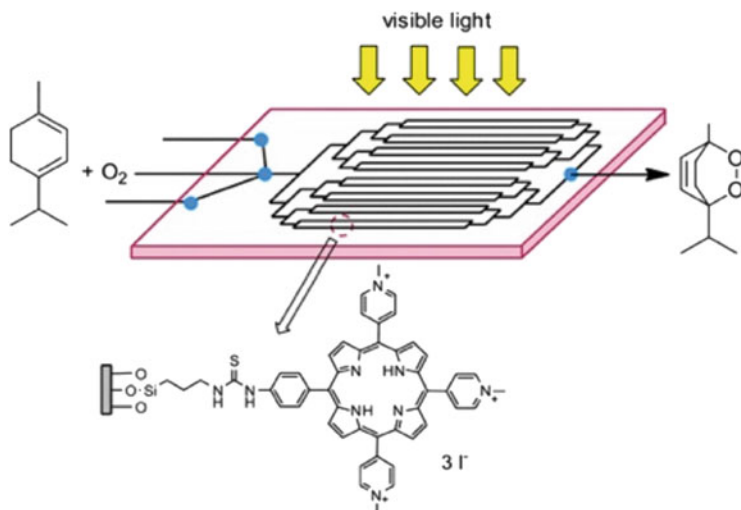
Scheme 29 Singlet oxygenation in flow reactor under photochemical irradiation (Reproduced from [52] with permission from ACS)



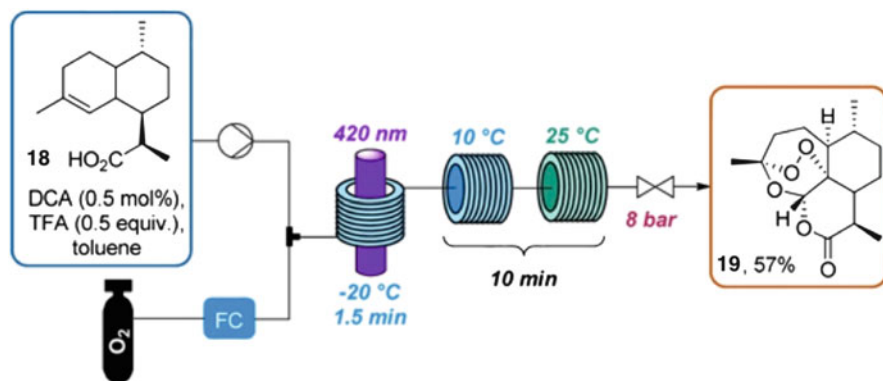
α -terpinene to produce ascaridole (peroxide) (Scheme 29) [52]. The researchers showed that within 5 s of light irradiation onto the glass chip flow reactor, over 80% conversion was achieved.

Seeberger et al. reported an innovative way of covalently attaching porphyrin photosensitizer moiety onto the microreactor channel wall. In diffusion of oxygen to the immobilized photosensitizer layer with facile penetration of UV irradiation, photosensitizer-immobilized microchannel wall hosts the photochemical generation of triplet oxygen that oxidizes α -terpinene to ascaridole (Scheme 30) [53].

Artemisinin, a sesquiterpene endoperoxide, is the number one drug for the treatment of malaria. Artemisinin can be extracted from a plant *Artemisia annua*, which is rather expensive and not supportive of the most malaria stricken developing world. A second route is the semi-synthesis from readily available artemisinic acid. Conversion of artemisinic acid **18** to artemisinin **19** involves two oxygenation steps employing both singlet and triplet oxygen. The Seeberger group made a significant advance in automated synthesis of artemisinin by employing a flow chemistry platform to produce singlet oxygen on larger scale (Scheme 31) [54]. In their 2012 work, they demonstrated that starting from dihydroartemisinic acid, the reduced form of artemisinic acid, artemisinin could be produced by singlet oxygen-mediated ene-reaction, followed by Hock cleavage, and then via hydroperoxidation by using triplet oxygen, hence leading towards target molecule artemisinin [55]. For both oxygenation steps, a coil of transparent tube wrapped around the medium-pressure Hg-lamp acted as the simple but efficient photochemical oxygenation flow reactor. They achieved 200 g/day supply of artemisinin from their flow reactor set-up which is further improved in a subsequent report [56].



Scheme 30 Photo-oxidation of α -terpinene using porphyrin immobilized on the glass channel wall (Adapted from [51] with permission from ACS)



Scheme 31 Singlet oxygen-mediated production of anti-malarial artemisinin in a flow system (Reproduced from [51] with permission from ACS)

Application of singlet oxygen in oxidation of amines in a flow photochemical set-up was also reported by the Seeberger group, who developed a continuous procedure for the formation of primary aldimines that subsequently undergo oxidative cyanation to furnish valuable α -aminonitriles [57]. A follow-up work described the use of such system for studying the regioselectivity of the photooxidation of unsymmetrical secondary amines [58].

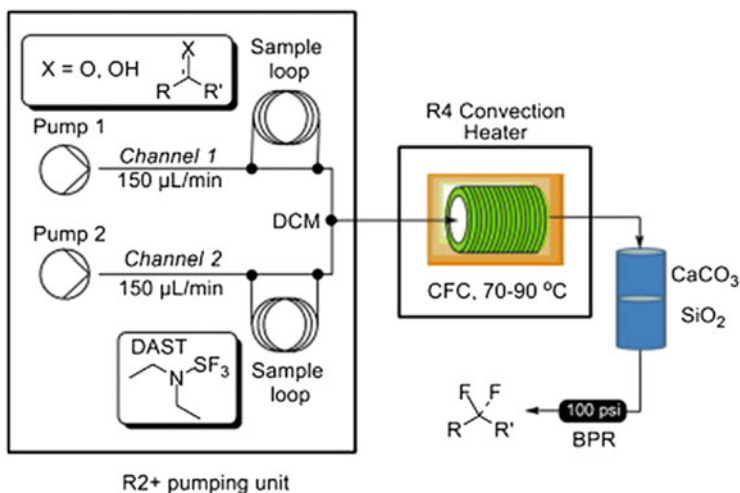
4.2 Halogens: Fluorine and Chlorine (Both in Gaseous State and In Situ Generated)

Halogenation constitutes one of the most fundamental chemical transformation in organic synthesis, as it dramatically changes the physicochemical properties of the parent molecule by introducing a halogen atom X (F, Cl, Br, I) onto the carbon-carbon chain or ring for further functionalization as well as enable further functionalization as C-X atoms are far more labile than the C-H, for diverse transformation by substituting X with numerous electrophiles and nucleophiles. Interestingly, seven of the top ten selling drugs in the USA (2014) were halogenated organic molecules [59]. The simplest way of introducing X into the molecular framework involves the use of inexpensive molecular halogen (X₂) or acids HX. However, most molecular/elemental halogen (F₂, Cl₂ and Br₂) and corresponding acids (HF, HBr, HCl, HI) are dangerously hazardous, toxic and corrosive chemicals to handle, and their reactions with most organic molecules are highly exothermic. Hence, halogenation process is typically challenging even at small scale. Understandably, flow chemistry had been used for a numerous halogenation reactions that ensure safety in the handling of the hazardous halogen reagents, conducting highly exothermic reactions and quenching of the unreacted halogen reagents [59].

Breen et al. reported the use of diluted elemental fluorine gas (a 10% fluorine in nitrogen) to convert pentane-2,4-dione into the corresponding fluorinated derivative, 3-fluoropentane-2,4-dione in a gas-liquid microflow system, which further reacted with hydrazine in a second microreactor to produce 4-fluoro-3,5-dimethyl-1*H*-pyrazole [60]. Such flow system ensures safety by minimizing the amount of fluorine gas in use at any given time as well as by immediately neutralizing the small amount of hazardous HF by-product in the collection vessel by chemical quenching.

The Ley group used few well-known fluorinating reagents such as diethylaminosulfur trifluoride (DAST), (1-chloromethyl-4-fluoro-1,4-diazoniabicyclo-[2.2.2]octane) *bis*(tetrafluoroborate) (Selectfluor[®]), and trimethylsilyl trifluoromethane (TMS-CF₃, Ruppert's reagent) for incorporating fluorine moieties into the organic molecules (Scheme 32) [61]. A commercial microreactor system was used to mix the DAST reagent stream with alcohols and carbonyl using a T-piece which is then passed through a convection flow coil (heated to 70–90°C) while generating the corresponding fluorides and difluorides, respectively. Several heterocyclic fluorides and difluoride derivatives of imidazo[1,2- α]pyridine, tetrahydro-2*H*-pyran, oxazole, quinoline etc., were synthesized using this set-up. Similarly, trifluoromethylated heterocyclic compounds were also synthesized using Ruppert's reagent in this flow reactor.

Pelleter and Renaud have reported the bromination of heterocycles using *N*-bromosuccinimide (NBS) in a simple continuous flow set-up comprising of a micromixing part and residence time loop which enabled rapid bromination (30 s) of imidazopyridine. For a scale-up process, an NBS-DMF mixture was used as an alternative to carbon tetrachloride being the typical batch solvent [25]. The process was performed with a 5 mL residence loop, at 70°C with a flow rate of 10 mL/min, accomplishing a throughput of 60 g/h leading to 3-bromo-imidazo[1,2- α]pyridine



Scheme 32 DAST (diethylaminosulfur trifluoride)-mediated fluorination of organic substrates in a flow reactor (Reproduced from [61] permission from Elsevier)

with excellent purity (99%). Similarly, the chlorination of imidazo[1,2- α]pyridine was performed by replacing NBS with *N*-chlorosuccinimide (NCS) in DMF, however with much inferior chemical conversion (40%).

References

- Mándity IM, Ötvös SB, Fülöp F (2015) Strategic application of residence-time control in continuous-flow reactors. *ChemistryOpen* 4:212–223
- Wirth T (2017) Novel organic synthesis through ultrafast chemistry. *Angew Chem Int Ed* 56:682–684
- Usutani H, Tomida Y, Nagaki A et al (2007) Generation and reactions of *o*-bromophenyllithium without benzyne formation using a microreader. *J Am Chem Soc* 129:3046–3047
- Nagaki A, Ichinari D, Yoshida JI (2014) Three-component coupling based on flash chemistry. Carbolithiation of benzyne with functionalized aryllithiums followed by reactions with electrophiles. *J Am Chem Soc* 136:12245–12248
- Nagaki A, Kim H, Yoshida J (2009) Nitro-substituted aryl lithium compounds in microreactor synthesis: switch between kinetic and thermodynamic control. *Angew Chem Int Ed* 48:8063–8065
- Kim H, Min K-I, Inoue K et al (2016) Submillisecond organic synthesis: outpacing Fries rearrangement through microfluidic rapid mixing. *Science* 352:691–694
- Kim H, Inoue K, Yoshida J (2017) Harnessing [1,4], [1,5], and [1,6] anionic Fries-type rearrangements by reaction-time control in flow. *Angew Chem Int Ed* 56:7863–7866
- Kim H, Nagaki A, Yoshida J (2011) A flow-microreactor approach to protecting-group-free synthesis using organolithium compounds. *Nat Commun* 2:264
- Nagaki A, Kenmoku A, Moriwaki Y et al (2010) Cross-coupling in a flow microreactor: space integration of lithiation and Murahashi coupling. *Angew Chem Int Ed* 49:7543–7547

10. Shu W, Pellegatti L, Oberli MA, Buchwald SL (2011) Continuous-flow synthesis of biaryls enabled by multistep solid-handling in a lithiation/borylation/Suzuki-Miyaura cross-coupling sequence. *Angew Chem Int Ed* 50:10665–10669
11. Shu W, Buchwald SL (2012) Enantioselective β -arylation of ketones enabled by lithiation/borylation/1,4-addition sequence under flow conditions. *Angew Chem Int Ed* 51:5355–5358
12. Nagaki A, Moriwaki Y, Yoshida J (2012) Flow synthesis of arylboronic esters bearing electrophilic functional groups and space integration with Suzuki–Miyaura coupling without intentionally added base. *Chem Commun* 48:11211–11213
13. Tomida Y, Nagaki A, Yoshida J (2011) Asymmetric carbolithiation of conjugated enynes: a flow microreactor enables the use of configurationally unstable intermediates before they epimerize. *J Am Chem Soc* 133:3744–3747
14. Nagaki A, Matsuo C, Kim S et al (2012) Lithiation of 1,2-dichloroethene in flow microreactors: versatile synthesis of alkenes and alkynes by precise residence-time control. *Angew Chem Int Ed* 51:3245–3248
15. Nagaki A, Takahashi Y, Yoshida J (2014) Extremely fast gas/liquid reactions in flow microreactors: carboxylation of short-lived organolithiums. *Chem Eur J* 20:7931–7934
16. Pieber B, Glasnov T, Kappe CO (2014) Flash carboxylation: fast lithiation–carboxylation sequence at room temperature in continuous flow. *RSC Adv* 4:13430–13433
17. Kupracz L, Kirschning A (2013) Multiple organolithium generation in the continuous flow synthesis of amitriptyline. *Adv Synth Catal* 355:3375–3380
18. Wu J, Yang X, He Z et al (2014) Continuous flow synthesis of ketones from carbon dioxide and organolithium or grignard reagents. *Angew Chem Int Ed* 53:8416–8420
19. Gross TD, Chou S, Bonneville D et al (2008) Chemical development of NBI-75043. Use of a flow reactor to circumvent a batch-limited metal-halogen exchange reaction. *Org Process Res Dev* 12:929–939
20. Wakami H, Yoshida JI (2005) Grignard exchange reaction using a microflow system: from bench to pilot plant. *Org Process Res Dev* 9:787–791
21. Riva E, Gagliardi S, Martinelli M et al (2010) Reaction of Grignard reagents with carbonyl compounds under continuous flow conditions. *Tetrahedron* 66:3242–3247
22. Deng Q, Shen R, Ding R, Zhang L (2014) Generation of ethynyl-Grignard reagent in a falling film microreactor: an expeditious flow synthesis of propargylic alcohols and analogues. *Adv Synth Catal* 356:2931–2936
23. Kawaguchi T, Miyata H, Ataka K et al (2005) Room-temperature Swern oxidations by using a microscale flow system. *Angew Chem Int Ed* 44:2413–2416
24. Van Der Linden JJM, Hilberink PW, Kronenburg CMP, Kemperman GJ (2008) Investigation of the moffatt-swern oxidation in a continuous flow microreactor system. *Org Process Res Dev* 12:911–920
25. Pelleter J, Renaud F (2009) Facile, fast and safe process development of nitration and bromination reactions using continuous flow reactors. *Org Process Res Dev* 13:698–705
26. Brocklehurst CE, Lehmann H, La Vecchia L (2011) Nitration chemistry in continuous flow using fuming nitric acid in a commercially available flow reactor. *Org Process Res Dev* 15:1447–1453
27. Gage JR, Guo X, Tao J, Zheng C (2012) High output continuous nitration. *Org Process Res Dev* 16:930–933
28. Schwalbe T, Autze V, Hohmann M, Stirner W (2004) Novel innovation systems for a cellular approach to continuous process chemistry from discovery to market. *Org Proc Res Dev* 8:440–454
29. Müller STR, Murat A, Maillos D et al (2015) Rapid generation and safe use of carbenes enabled by a novel flow protocol with in-line IR spectroscopy. *Chem Eur J* 21:7016–7020
30. Müller STR, Hokamp T, Ehrmann S et al (2016) Ethyl lithiodiazoacetate: extremely unstable intermediate handled efficiently in flow. *Chem Eur J* 22:11940–11942
31. Müller STR, Murat A, Hellier P, Wirth T (2016) Toward a large-scale approach to Milnacipran analogues using diazo compounds in flow chemistry. *Org Process Res Dev* 20:495–502

32. Deadman BJ, Collins SG, Maguire AR (2015) Taming hazardous chemistry in flow: the continuous processing of diazo and diazonium compounds. *Chem Eur J* 21:2298–2308
33. Mastronardi F, Gutmann B, Oliver Kappe C (2013) Continuous flow generation and reactions of anhydrous diazomethane using a teflon AF-2400 tube-in-tube reactor. *Org Lett* 15:5590–5593
34. Maurya RA, Park CP, Lee JH, Kim DP (2011) Continuous in situ generation, separation, and reaction of diazomethane in a dual-channel microreactor. *Angew Chem Int Ed* 50:5952–5955
35. Bartrum HE, Blakemore DC, Moody CJ, Hayes CJ (2010) Synthesis of β -keto esters in-flow and rapid access to substituted pyrimidines. *J Org Chem* 75:8674–8676
36. Zhang X, Stefanick S, Villani FJ (2004) Application of microreactor technology in process development. *Org Process Res Dev* 8:455–460
37. Fuse S, Tanabe N, Takahashi T (2011) Continuous in situ generation and reaction of phosgene in a microflow system. *Chem Commun* 47:12661–12663
38. Hamano M, Nagy KD, Jensen KF (2012) Continuous flow metal-free oxidation of picolines using air. *Chem Commun* 48:2086–2088
39. He Z, Jamison TF (2014) Continuous-flow synthesis of functionalized phenols by aerobic oxidation of grignard reagents. *Angew Chem Int Ed* 53:3353–3357
40. Pieber B, Martinez ST, Cantillo D, Kappe CO (2013) In situ generation of diimide from hydrazine and oxygen: continuous-flow transfer hydrogenation of olefins. *Angew Chem Int Ed* 52:10241–10244
41. Pieber B, Glasnov T, Kappe CO (2015) Continuous flow reduction of artemisinic acid utilizing multi-injection strategies - closing the gap towards a fully continuous synthesis of antimalarial drugs. *Chem Eur J* 21:4368–4376
42. Gutmann B, Weigl U, Cox DP, Kappe CO (2016) Batch- and continuous-flow aerobic oxidation of 14-hydroxy opioids to 1,3-oxazolidines – a concise synthesis of noroxymorphone. *Chem Eur J* 22:10393–10398
43. Gutmann B, Elsner P, Cox DP et al (2016) Toward the synthesis of noroxymorphone via aerobic palladium-catalyzed continuous flow *N*-demethylation strategies. *ACS Sustain Chem Eng* 4:6048–6061
44. Gemoets HPL, Hessel V, Noël T (2014) Aerobic C-H olefination of indoles via a cross-dehydrogenative coupling in continuous flow. *Org Lett* 16:5800–5803
45. Bourne SL, Ley SV (2013) A continuous flow solution to achieving efficient aerobic anti-Markovnikov Wacker oxidation. *Adv Synth Catal* 355:1905–1910
46. Petersen TP, Polyzos A, O'Brien M et al (2012) The oxygen-mediated synthesis of 1,3-butadiynes in continuous flow: using teflon AF-2400 to effect gas/liquid contact. *ChemSusChem* 5:274–277
47. Brzozowski M, Forni JA, Savage GP, Polyzos A (2015) The direct α -C(sp³)-H functionalisation of *N*-aryl tetrahydroisoquinolines via an iron-catalysed aerobic nitro-Mannich reaction and continuous flow processing. *Chem Commun* 51:334–337
48. Park JH, Park CY, Kim MJ et al (2015) Continuous-flow synthesis of meta-substituted phenol derivatives. *Org Process Res Dev* 19:812–818
49. Brzozowski M, O'Brien M, Ley SV, Polyzos A (2015) Flow chemistry: intelligent processing of gas-liquid transformations using a tube-in-tube reactor. *Acc Chem Res* 48:349–362
50. Greene JF, Preger Y, Stahl SS, Root TW (2015) PTFE-membrane flow reactor for aerobic oxidation reactions and its application to alcohol oxidation. *Org Process Res Dev* 19:858–864
51. Plutschack MB, Pieber B, Gilmore K, Seeberger PH (2017) The Hitchhiker's guide to flow chemistry. *Chem Rev* 117:11796–11893
52. Wootton RCR, Fortt R, De Mello AJ (2002) A microfabricated nanoreactor for safe, continuous generation and use of singlet oxygen. *Org Process Res Dev* 6:187–189
53. Lumley EK, Dyer CE, Pamme N, Boyle RW (2012) Comparison of photo-oxidation reactions in batch and a new photosensitizer-immobilized microfluidic device. *Org Lett* 22:5724–5727
54. Lévesque F, Seeberger PH (2011) Highly efficient continuous flow reactions using singlet oxygen as a "Green" reagent. *Org Lett* 13:5008–5011

55. Lévesque F, Seeberger PH (2012) Continuous-flow synthesis of the anti-malaria drug artemisinin. *Angew Chem Int Ed* 51:1706–1709
56. Kopetzki D, Lévesque F, Seeberger PH (2013) A continuous-flow process for the synthesis of artemisinin. *Chem Eur J* 19:5450–5456
57. Ushakov DB, Gilmore K, Kopetzki D et al (2014) Continuous-flow oxidative cyanation of primary and secondary amines using singlet oxygen. *Angew Chem Int Ed* 53:557–561
58. Ushakov DB, Plutschack MB, Gilmore K, Seeberger PH (2015) Factors influencing the regioselectivity of the oxidation of asymmetric secondary amines with singlet oxygen. *Chem Eur J* 21:6528–6534
59. Cantillo D, Kappe CO (2017) Halogenation of organic compounds using continuous flow and microreactor technology. *React Chem Eng* 2:7–19
60. Breen JR, Sandford G, Yufit DS (2011) Continuous gas/liquid-liquid/liquid flow synthesis of 4-fluoropyrazole derivatives by selective direct fluorination. *Beilstein J Org Chem* 7:1048–1054
61. Baumann M, Baxendale IR, Martin LJ, Ley SV (2009) Development of fluorination methods using continuous-flow microreactors. *Tetrahedron* 65:6611–6625

Industrial Approaches Toward API Synthesis Under Continuous-Flow Conditions



Rodrigo O. M. A. de Souza

Contents

1	Introduction	375
2	Industrial Applications	376
3	Conclusions and Perspectives	388
	References	388

Abstract The use of continuous-flow chemistry has spread to the wider chemical community and found application for the production of active pharmaceutical ingredients (APIs) as a tool for optimization, process development, and production. Herein are summarized some of the advances made by industry in the field of continuous-manufacturing during the last years.

Keywords Active pharmaceutical ingredients · Continuous-flow · Flow chemistry · Manufacturing

1 Introduction

Active pharmaceutical ingredients (APIs) are, in general, synthesized in batch manufacturing plants and then shipped to other sites to be converted into a form that can be given to patients, such as tablets, drug solutions, or suspensions. This system offers little flexibility to respond to surges in demand and is susceptible to severe disruption if one of the plants has to shut down.

The use of continuous-flow or, if you prefer, flow chemistry is not new in chemistry, although in the last 20 years it has spread to the wider chemical community and found application for the production of several high-value intermediates and

R. O. M. A. de Souza (✉)

Biocatalysis and Organic Synthesis Group, Chemistry Institute, Federal University of Rio de Janeiro, Rio de Janeiro, Brazil

e-mail: rodrigossouza@iq.ufrj.br

products [1, 2]. A synthetic organic chemist is used to working in round bottom flasks where the scale-up of the optimized process is always a challenge due to the need of additional adjustment of reaction parameters. To overcome this difficulty, continuous-flow reactors can be used as a tool for optimization and process development in organic synthesis [3–10].

Worldwide, a variety of companies are investigating continuous manufacturing of new drug substances in order to reduce their manufacturing costs and to provide a more robust way of producing the desired molecules. This demand had an incredible effect on the development of new technologies such as flow reactors, phase separators, and pumps, among others, where some companies have established a new business by designing their own reactor system [1, 2, 5, 11–14].

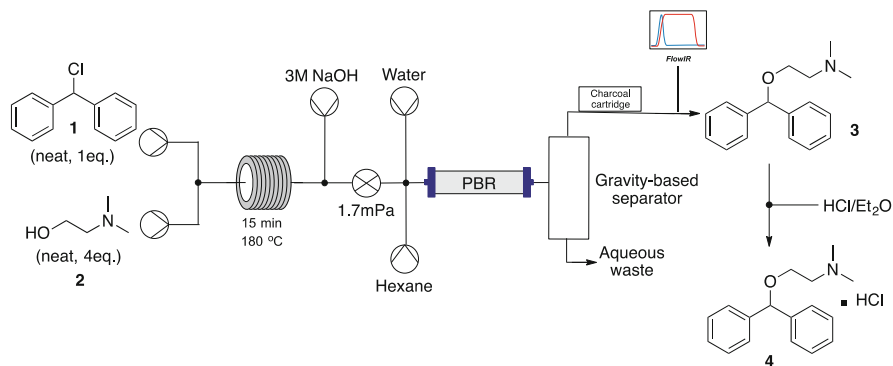
In academia, an initiative led by Prof. Frank Gupton at Virginia Commonwealth University, in collaboration with the Bill & Melinda Gates Foundation, called Medicines for All, seeks cheaper and more efficient ways to manufacture drugs, particularly those needed to treat HIV and AIDS in developing countries. The main idea behind their strategy was to start with very simple commodity chemicals, in order to make it feasible for developing economies. Nevertheless, up to now, these strategies are not completely applied in industry [15].

2 Industrial Applications

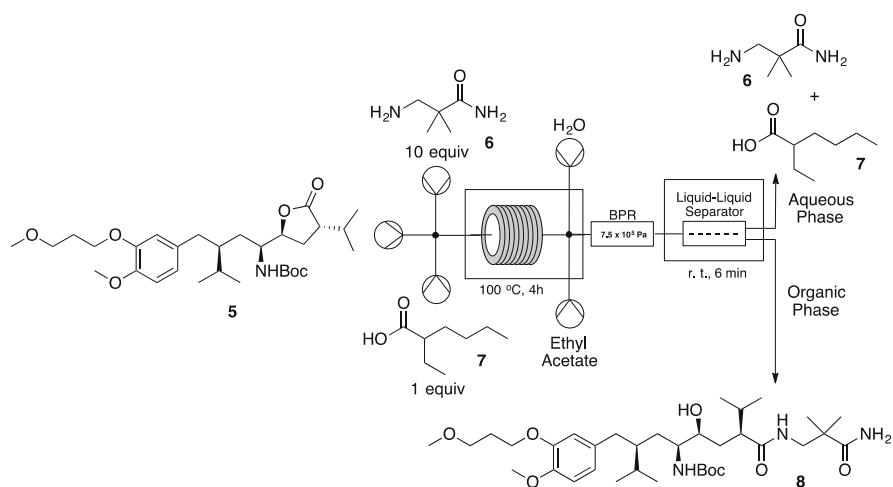
An initiative funded by the Defense Advanced Research Projects Agency (DARPA) and MIT researchers built a small transportable device suitable for small-scale synthesis of drug molecules [16]. Their new system can produce 1,000 doses of four drugs formulated as solutions or suspensions in 24 h: Benadryl, lidocaine, Valium, and Prozac. Using a refrigerator-sized continuous-flow apparatus [1.0 m (width) \times 0.7 m (length) \times 1.8 m (height), 100 kg], they are capable of complex multistep synthesis, multiple in-line purifications, post-synthesis work-up and handling, semi-batch crystallization, real-time process monitoring, and, ultimately, formulation of high-purity drug products. The scheme presented below shows the continuous-flow strategy toward the synthesis of diphenhydramine hydrochloride (**4**) (Scheme 1).

MIT researchers were also able to develop an end-to-end continuous manufacturing process for aliskiren hemifumarate, integrating synthesis, purification, and dosing [17, 18]. The synthetic strategy comprises three steps (including the hemifumarate salt formation), where in some cases the chemistry must be redesigned in order to meet the criteria needed for a continuous-flow protocol, as exemplified for the first step shown on Scheme 2.

The first step of aliskiren hemifumarate synthesis is a good example that redesigning a chemical step in order to meet continuous-flow requirements (avoiding handling of solids) can afford great rewards. Under the conditions developed for the continuous-flow process, reagents are pumped neatly through a heated coil at 100°C, leading the reaction to proceed much faster when compared to the batch process (4 h \times 72 h). Reaction work-up is also performed at 100°C, followed by membrane-based, liquid-liquid separation, leading to the desired product in 89% yield.



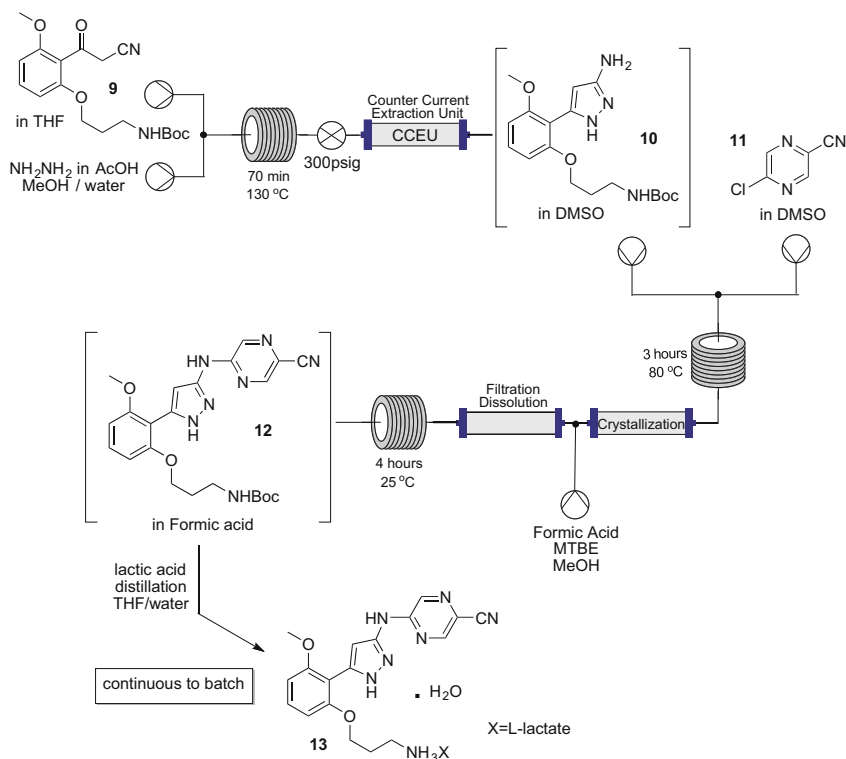
Scheme 1 Example of end-to-end continuous-flow synthesis with integrated analysis and separation for diphenhydramine hydrochloride (4) product



Scheme 2 First step of aliskiren hemifumarate continuous-flow synthesis

Recently, researchers from Lilly [19] have enabled a kilogram-scale prexasertib monolactate monohydrate synthesis (13) under continuous-flow conditions and GMP qualifications. Prexasertib (13) is being assessed in phase 1 and 2 clinical trials in combination with cytotoxic chemotherapy, targeted agents, and as a monotherapy [20]. It is the first CHK1 inhibitor to demonstrate objective clinical responses as a monotherapy [21]. During discovery and initial clinical trials, a nine-step route was used, which was deemed unsuitable for long-term manufacturing due to several hazardous reagents and moderate yields. However, researchers from Lilly have opened new windows for prexasertib synthesis by exploring continuous-flow environment (Scheme 3).

The first step has serious restrictions when conducted under batch conditions due to the use of excess hydrazine and the high temperatures needed for reaction completion. Using continuous-flow technology and a plug-flow reactor, researchers

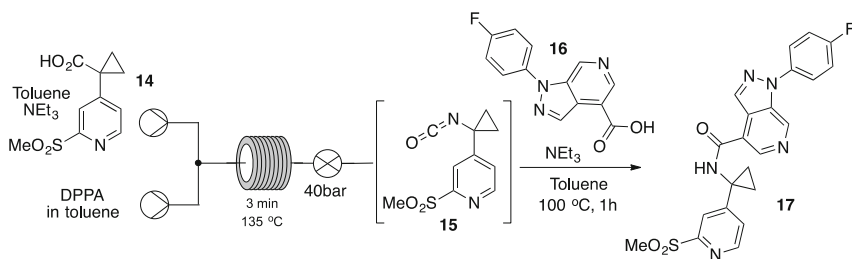


Scheme 3 Continuous-flow three-step synthesis of prexasertib monolactate monohydrate under GMP conditions

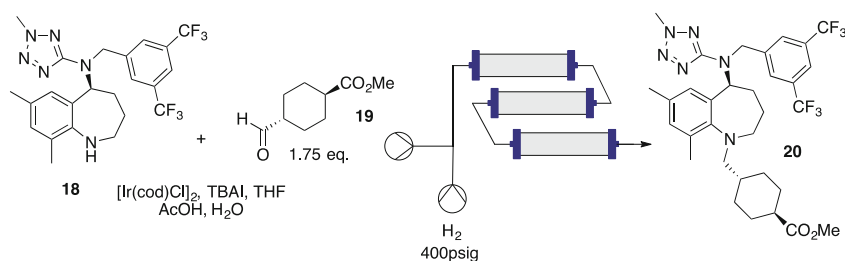
were able to reduce the amount of excess hydrazine and operate safely at 130°C. It is important to note that 0.49% of the overall production is inside the reactor at any time, reducing material at risk and increasing process safety. The first step was conducted with 89.6% yield, leading to a final product (**10**) with only 2 ppm of hydrazine and less than 1% of impurities. The next step was accomplished with 88.7% yield, and unlike the first one, this intermediate stage needed further steps of purification, since it was necessary to remove residual starting material, regioisomers, and other minor impurities. The desired product (**13**) was obtained on a continuous batch deprotection/crystallization process, leading to a final yield of 85% (1.99 kg) for the final step.

Safety was also a matter of choice for researchers from Boehringer Ingelheim Pharmaceuticals [22] when deciding to implement continuous-flow process on the synthesis of a CCR1 antagonist (**17**), with acyl azide and/or isocyanate as intermediates (Scheme 4).

The batch process started from the formation of an acyl azide, in order to obtain the carbamate product by Curtius rearrangement. Besides the fact that decoupling azide formation from isocyanate trapping was successful, researchers were keenly



Scheme 4 Semi-continuous isocyanate formation followed by Curtius rearrangement



Scheme 5 Homogeneous continuous-flow reductive amination of an intermediate of evacetrapib synthesis

aware of the key potential drawback of undesired acyl azide accumulation in the CSTR (continuous stirred-tank reactor) upon further scale-up. When implementing the continuous-flow protocol, authors could optimize intermediate isocyanate formation (**15**) to a residence time of 3 min, leading to the desired final product in a 76% overall yield and, more important, 56% more efficient than the original Curtius batch process, allowing a further scale-up to 40 kg of the final product (**17**).

Researchers from D&M Continuous Solutions, Eli Lilly, and Lilly Research Laboratories [23] have developed an efficient continuous iridium-catalyzed homogeneous high pressure reductive amination reaction to produce the penultimate intermediate (**20**) in evacetrapib synthesis. The developed continuous process operated under GMP conditions for 24 days and produced over 2 MT of the penultimate intermediate in 95% yield after batch work-up, crystallization, and isolation (Scheme 5).

After several optimization steps, researchers obtained a final reaction condition where H_2 pressure and the substrate/catalyst ratio could maximize product formation leading to minor undesired impurities, such as the *cis* regioisomer. The presence of TBAI (tetrabutylammonium iodide) was crucial to achieve the presented results, and it appears to hold the Ir (I) in a more stable anionic form, which is less prone to degradation under reaction conditions. For those who are afraid of working with large-scale hydrogenation reactions, authors say “the reactor operates at >98% liquid filled with the hydrogen distributed throughout the 45 pipes and downflow tubes resulting in a steady venting of nitrogen-diluted hydrogen over time. It is for

these reasons that the continuous process is viewed as a low risk process in spite of its operation at high pressure.” It is also important to note that authors could show the linear scale-up capability of continuous-flow process going from 48-L reactors up to 360-L reactors for production scale, leading to the desired product in 95% isolated yield.

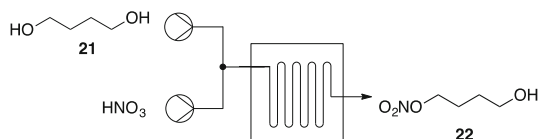
In 2009, one of the first FDA-approved examples of a continuous-flow process applied to active pharmaceutical ingredients (API) synthesis was presented by DSM [24] researchers on the nitration reaction toward the production of naproxinod, an anti-inflammatory drug (Scheme 6).

The task faced by DSM researchers was difficult since they had to develop a safe and highly efficient nitration process, where they should selectively nitrate only one hydroxyl group and still handle the very hazardous nitrated product. After several rounds of optimization tuning the conditions for the reaction, researchers have found the exact nitric acid concentration needed (65%), so it could be taken for scale-up. The operation unit has a total volume around 150 mL and process capability of 312 kg day⁻¹ working under GMP conditions. During the pilot plant campaign, 500 kg of qualified product (**22**) could be produced under the conditions developed.

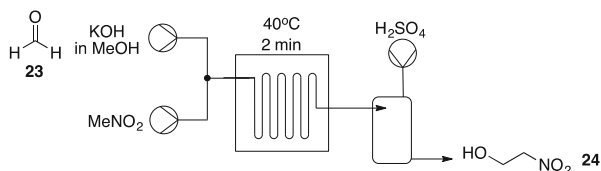
Researchers from Lonza and Novartis [25] have worked together in order to overcome a problem related to an early-stage starting material from aliskiren API synthesis, nitroethane. This reagent is required in kg amounts, since it is used in an organo-catalytic reaction between nitroethene and isovaleric aldehyde to form 2(*R*)-isopropyl-4-nitro-1-aldehyde, which is subsequently reduced by sodium borohydride to furnish the desired 2(*R*)-isopropyl-4-nitro-propan-1-ol. Since lower nitroalkanes are potentially explosive, a continuous-flow process was developed for the production of nitroethanol (**24**) in high yields (95%) and very short residence times, which after dehydration can afford nitroethane (Scheme 7).

An API developed by Merck [26] as an allosteric Akt inhibitor used for cancer treatment had one step optimized under continuous-flow conditions in order to ensure the production of kilogram quantities for clinical trials. During reaction optimization under batch conditions and gram scale, the design process worked as expected, but under larger scales the formylation reaction did not behave as under gram scale. Researchers have observed that the reaction solution turned into a thick gel, a phenomenon that had not been observed in gram-scale experiments.

Scheme 6 DSM continuous-flow nitration process



Scheme 7 Nitroethanol continuous-flow synthesis developed for aliskiren production



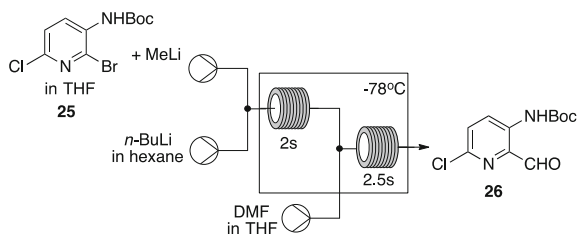
The batch temperature had to be raised to -45°C , and the agitator manually manipulated until the mixture was sufficiently mobile to allow stirring to continue automatically. The final yield was not affected but raised concerns about a possible scale-up. With these results in hands, authors have decided to develop a continuous-flow protocol in order to overcome the reaction media instability observed under batch conditions (Scheme 8).

The continuous-flow process developed was performed mixing amine (**25**) and MeLi. This solution was fed into a stainless steel tube reactor with an internal diameter of 6.35 mm and kept at -78°C using a dry ice-acetone bath. The amide stream was mixed with *n*-BuLi to form the dianion in a first residence tube, and the dianion was then combined with the DMF/THF feed solution in order to obtain the desired formylated product in 65% yield and purity equal to those obtained under batch conditions. It is important to note the very short residence times operated in this process, which uses flow rates up to 175 mL min^{-1} , allowing the production of 1 kg of the aldehyde (**26**) after just 1 h.

Since their discovery in the beginning of twenty-first century, click reactions [27, 28] have emerged as an important tool for organic chemists seeking for the construction of 1,2,3-triazole moiety for biological evaluation. The reaction takes place by reacting an organic azide, which can be generated in situ, followed by a coupling reaction with an acetylene partner catalyzed by copper. When alkyl azides are needed, the in situ generation of the required azide still suffers from the long reaction times and high temperatures needed to afford the desired product.

Aiming to develop a straightforward methodology to perform continuous-flow click reactions, researchers from Pfizer and coworkers [29] have worked on the construction of a copper flow reactor for the synthesis of substituted 1,2,3-triazoles. The idea behind their strategy was to use a copper coil to avoid adding a homogeneous catalyst to the reaction system. Reactions were optimized by the DOE (design of experiments) software, and a 5-min residence time was established as standard residence time for this transformation. Under the optimized conditions, 30 different substituted 1,2,3-triazoles could be synthesized at different scales with yields ranging from 20 to 92%. The substituted 1,2,3-triazole (**27**) was used as an example of preparative scale capability of the designed reactor (Fig. 1).

Another interesting work presented by researchers from Eli Lilly [20] has shown an improved process for the preparation of an imidazole intermediate through continuous-flow approach. They worked with ketoamide (**43**), which differs from



Scheme 8 Formylation process developed by Merck in order to avoid problems during scale-up under batch conditions

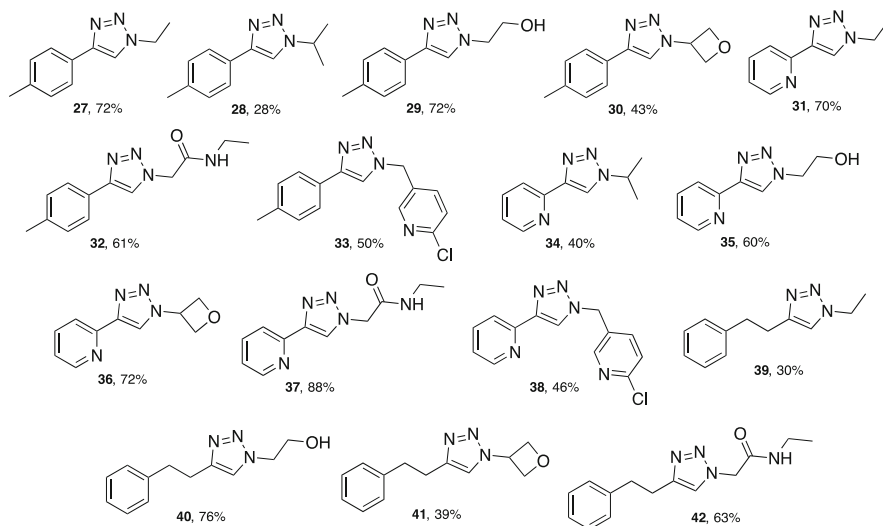
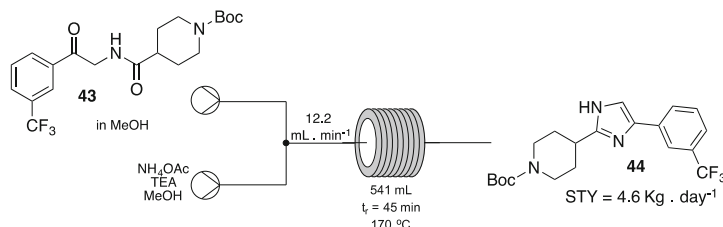


Fig. 1 Selected examples for the continuous-flow click reaction using copper coil



Scheme 9 Ketoamide strategy toward the synthesis of imidazole (**44**)

the desired substrate by a fluorine atom bounded to the aromatic ring at position 4. High T/P conditions were used to screen the best conditions for the imidazole formation, leading to the desired product with a residence time of 45 min at 170°C (Scheme 9).

Unfortunately, when applying the optimized process to the desired substrate, much lower yields and by-products were obtained as shown in Fig. 2. In addition to the desired imidazole product (**45**) and the deprotected product (**46**), significant amounts of aniline (**47**) and dimer (**48**) could also be found. It is important to note that for product qualification, the amount of aniline side product must be reduced to ppm level.

To overcome these problems and based on the initial optimization, researchers have performed a series of studies concluding that working with ketoamide (**49**) would lead to a faster reaction, avoiding some degradation pathways due to the prolonged exposure to high temperatures.

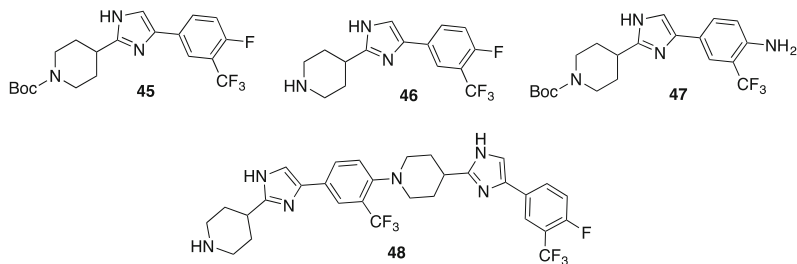
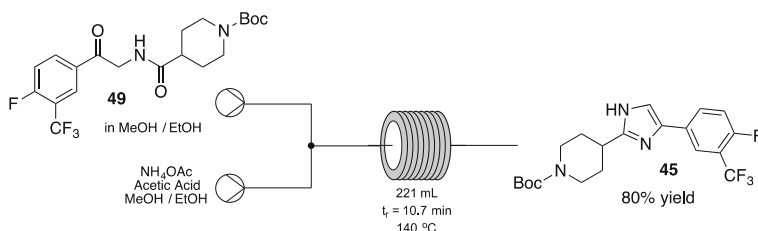


Fig. 2 Product and side products obtained under process conditions



Scheme 10 Optimized continuous-flow protocol for imidazole (**45**) formation starting from ketoamide (**49**)

After several rounds of optimization using a similar system as presented on Scheme 10, starting from ketoamide (**49**), authors have found that the best reaction conditions would lead to the desired product (**45**) in 80% yield, at 140°C, with a residence time of 10.7 min. Aniline impurity was reduced by the addition of acetic acid to the reaction media. Under these conditions, aniline concentration was found to be <50 ppm. The results obtained for this continuous-flow experiment represented a great improvement on reaction time (from 18 h batch to 10 min CF), with the same yield.

One of the several applications where continuous-flow processing can be very successful is on handling hazardous reactions. Researchers from Bristol-Myers Squibb [21] presented an interesting example on the synthesis of an intermediate for brivanib alaninate, where an oxidation reaction mediated by hydrogen peroxide and catalyzed by methylsulfonic acid (MSA) was a key step.

The first step for this reaction optimization was finding reaction conditions where the starting material has good solubility (20% water/THF) and reaction temperatures are below thermal runaway values ($T \sim 10^\circ\text{C}$). Moreover, identifying the number of MSA equivalents needed for reaction completion was important to reduce reaction time and improve product isolation, since neutral conditions were required for product stability.

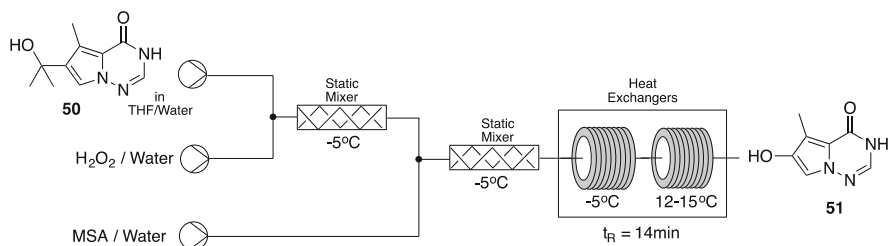
The total reaction time was less than 20 min, consisting of three different feeds (Feed A, starting material (**50**) in water/THF; Feed B, H_2O_2 /water; Feed C, MSA/water). First, a solution of starting material (**50**) in THF/water mixture was combined with H_2O_2 /water mixture through a static mixer at -5°C and then mixed

with feed C on another static mixer. Further residence time for reaction completion was provided with two heat exchangers at different temperatures, as shown on Scheme 11. This reaction setup was taken all the way to commercial scale, being able to process 44.8 kg of product per day.

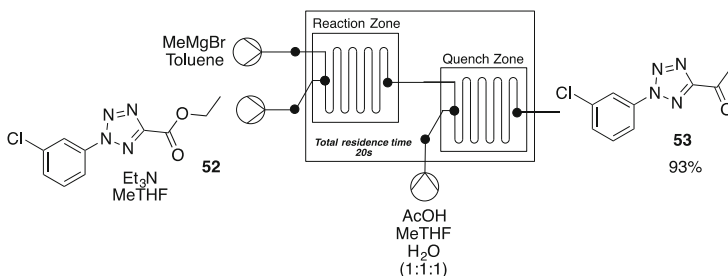
Developments of Grignard type protocols under continuous-flow conditions are always a major concern due to precipitation risks; depending on the substrates, fast and highly exothermic reactions can occur. Facing these challenges, researchers from AstraZeneca [30] have worked on the development of a continuous-flow protocol for manufacturing purpose where the Grignard reaction could be performed under controlled conditions.

Since the conditions optimized using a batch setup have shown that the use of 2 eqv of MeMgBr in relation to ketone was necessary for reaction completion with a final quench in acidic media, another issue had to be addressed when using continuous-flow technology, which was a more rapid reaction quench to avoid the formation of tertiary alcohol as a by-product (Scheme 12).

To achieve the desired results, authors have used an ART PR37 reactor with a total flow rate of 25 mL min⁻¹, allowing the conversion of 580 g of ester (**52**) under scale-up conditions, maintaining a very short residence time, of about 20 s. Unfortunately, precipitation has occurred despite all efforts to adapt the reaction conditions for running the Grignard reaction. A cleaning cycle was implemented using the quench solution to black-flush the reaction system when the pressure was above 5 bar. Every 45 min, the manufacturing system was stopped, and a cleaning cycle



Scheme 11 Lab scale continuous-flow process for the synthesis of an intermediate (**51**) from brivanib alaninate synthesis



Scheme 12 Grignard reaction under continuous-flow conditions

was performed. As a result of this scale-up, the formation of the undesired by-product was suppressed below 1% by the continuous-flow protocol, and the amount of MeMgBr used could also be reduced to less than 2 eqv.

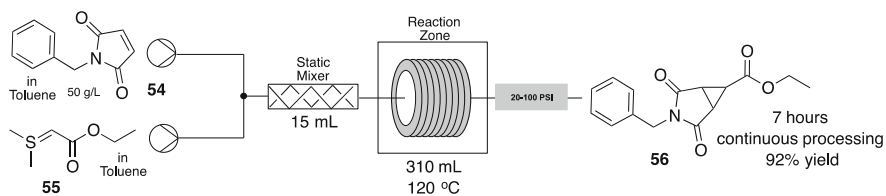
Researchers from Boehringer Ingelheim Pharmaceuticals [31] have developed an interesting continuous-flow multikilogram protocol for the cyclopropanation of *N*-benzyl maleimide (**54**), overcoming a series of problems found under batch conditions, mostly related to undesirable side products. All reaction optimization and kinetic analysis have been performed under batch conditions, and the best results translated to continuous-flow environment (Scheme 13).

The continuous manufacturing setup is presented on Scheme 13, where reagents are mixed through a T-mixer followed by a static mixer unit before entering the reaction zone. The reaction takes place inside a tube-in-tube reactor, where the outer tube was used as a jacket in order to keep the reaction temperature constant. When translating the reaction from batch to continuous-flow, further optimization was needed to ensure the right amount of excess EDSA (**55**) needed for reaction completion, as well as the best reaction temperature and residence time. Lab scale continuous-flow experiments were done before the scale-up in order to optimize the variables cited above.

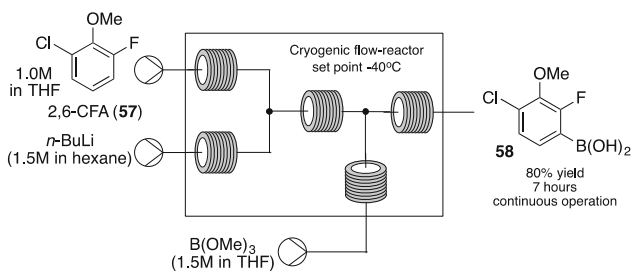
Under manufacturing conditions, a solution of (**54**) (50 g L^{-1}) was processed continuously for 7 h with a residence time of 2 min, leading to 92% yield and 3.3 kg of the final product (**56**). With the development of this process, authors could considerably reduce the cost due to higher reaction yield compared to batch process, and the robustness of this flow process was demonstrated for the synthesis of the product (**56**) on a multikilogram scale.

An interesting example on how continuous-flow process can lead to a better management of reaction parameters in order to avoid undesired products was presented by Dow Chemical researchers and coworkers [32]. In this work, a fluorine-directed lithiation was performed under cryogenic conditions, where careful control of the cryogenic cooling device was essential for achieving the desired results, avoiding the formation of benzyne, which leads to side products through a highly exothermic reaction pathway (Scheme 14).

The key point assessed by the authors was to control reaction temperatures at the different reaction/precooling zones in order to avoid degrading or side products formation. One example is the Li 2,6-CFA intermediate obtained after fluorine-directed lithiation of (**57**), which can degrade fast at temperatures above -26°C . In order to overcome these problems, a cryogenic cooling device was developed, where



Scheme 13 Large-scale cyclopropanation reaction under continuous-flow conditions



Scheme 14 Cryogenic continuous-flow reactor for fluorine-directed lithiation

thermocouples at different points at the reaction setup directly control the power output, maintaining the reaction temperature at the desired value. After subsequent optimizations, researchers have also identified that mixing during the fluorine-directed lithiation step was also crucial for a better reaction outcome. Authors have changed the outlet mixing tube from 2.44 to 4.0 mm ID so that a series of stirrer bars could be introduced into the tubing and a stepper motor used to stir the bars.

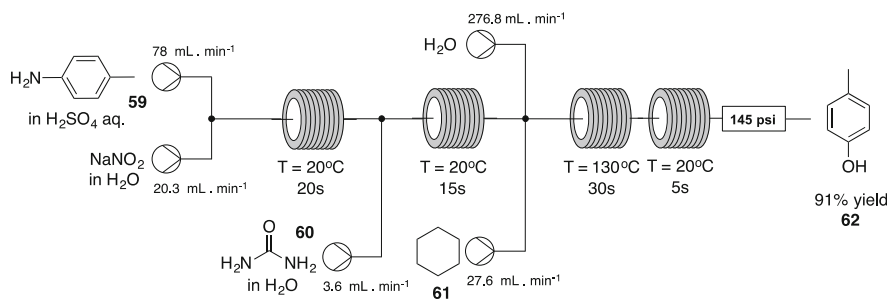
As a result of the optimization work, the final reaction setup could be designed to operate continuously for 7 h at 40°C, leading to the final product (**58**) in 80% yield.

The next two examples detailed below were not developed by the industry but represent very interesting transformations on multi-gram scale at university laboratory facilities. In both cases, important building blocks are synthesized starting from cheap materials in a very efficient process using hazardous chemical reactions.

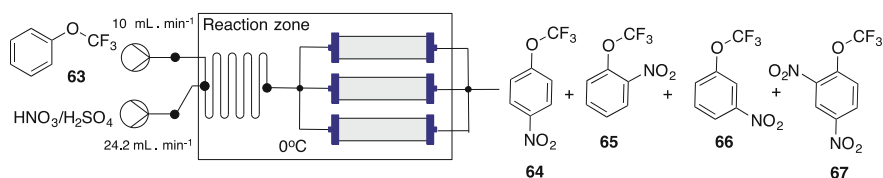
The first example performs a fully continuous-flow diazotization-hydrolysis protocol for the preparation of *p*-cresol [33], used on the synthesis of many active pharmaceutical ingredients. The major concern about adopting such strategy is the highly explosive diazonium salt intermediate, which could decompose under high temperatures. In this way, working on continuous-flow conditions could enhance safety by a better control of reaction parameters.

The synthetic route adopted by authors was the diazotization of *p*-toluidine (**59**) followed by hydrolysis of diazonium salt, leading to the desired product *p*-cresol (**62**) in very short residence times and excellent yields. Several rounds of optimization were done, and a complete analysis of impurities and process control were taken in order to reach the final process presented on Scheme 15.

The diazotization reaction was taken by reacting *p*-toluidine (**59**) with a sodium nitrite solution for 20-s residence time, followed by quenching with urea (**60**) solution for additional 15 s. In order to hydrolyze the diazonium salt, water and an organic solvent were introduced in the next step at high temperatures. Initially, authors have used toluene as an organic solvent, but nitration of toluene was observed as an issue on reaction selectivity. In order to overcome this problem, cyclohexane was chosen as a reaction cosolvent. After introduction of water and



Scheme 15 Fully continuous-flow diazotization-hydrolysis cascade toward the synthesis of *p*-cresol



Scheme 16 Continuous-flow scale-up of trifluoromethoxy benzene (**63**) nitration

cyclohexane, hydrolysis was performed at high temperatures for 30-s residence time, and the product (**61**) could be purified from the final solution by distillation, with 91% yield, and the process stability was observed during a long-time experiment (3 h).

Recently, a group of researchers from the Chinese Academy of Sciences reported a continuous-flow scale-up of trifluoromethoxy benzene (**63**) nitration [34]. Nitration of trifluoromethoxy benzene (**63**) has several issues related to side products that could be obtained, such as *p*-nitro (**64**), *o*-nitro (**65**), *m*-nitro (**66**), and di-nitro (**67**) products. Under batch conditions, solutions to overcome the loss of selectivity toward the desired product include low reaction temperatures (-10°C), diluted reaction media, and addition of the nitration solution for an extended period (28 h). The continuous-flow strategy envisioned by the authors features a microchannel mixing device followed by a series of packed bed reactors filled with small quartz beads in order to enhance mixing and the reaction carried out at 0°C (Scheme 16).

The optimized reaction conditions allowed researchers to achieve very good selectivity toward the desired *p*-nitro product, reducing the amount of undesired product to 1.42% in total. The starting material and the nitration solution were mixed into a microchannel mixing device, which takes the reaction mixture to four tubular reactors with 6 mm ID, filled with quartz beads, with a total residence time of 2.4 min and temperatures below -2°C . Under these conditions, 91.08% of *p*-nitro (**64**) could be obtained with conversions on 99% range. The optimized reaction leads to a selectivity of 98.1% toward the desired product.

3 Conclusions and Perspectives

Continuous manufacturing, also branded as flow chemistry, is an emerging technique that enables those working in research and development to rapidly screen reactions using continuous-flow reactors, leading to the identification of reaction conditions that are suitable for use at a production level. Various case studies have demonstrated that the technology is more cost effective. As a result, the technology can provide a paradigm enabling the development of a new patentable process, which can renew industry perspective.

References

1. Plutschack MB, Pieber B, Gilmore K, Seeberger PH (2017) *Chem Rev.* <https://doi.org/10.1021/acs.chemrev.7b00183>
2. Gutmann B, Cantillo D, Kappe CO (2015) *Angew Chem Int Ed* 54:6688
3. Porta R, Benaglia M, Puglisi A (2016) *Org Process Res Dev* 20:2
4. Movsisyan M, Delbeke EIP, Berton J, Battilocchio C, Ley SV, Stevens CV (2016) *Chem Soc Rev* 45:4892
5. Vaccaro L, Lanari D, Marrocchi A, Strappaveccia G (2014) *Green Chem* 16:3680
6. Pastre JC, Browne DL, Ley SV (2013) *Chem Soc Rev* 42:8849
7. Newman SG, Jensen KF (2013) *Green Chem* 15:1456
8. Hessel V, Kralisch D, Kockmann N, Noel T, Wang Q (2013) *ChemSusChem* 6:746
9. Baxendale IR, Brocken L, Mallia CJ (2013) *Green Processing Synth* 2:211
10. Razzaq T, Kappe CO (2010) *Chem Asian J* 5:1274
11. Fanelli F, Parisi G, Degennaro L, Luisi R (2017) *Beilstein J Org Chem* 13:520
12. Britton J, Raston CL (2017) *Chem Soc Rev* 46:1250
13. Kobayashi S (2016) *Chem Asian J* 11:425
14. Wiles C, Watts P (2014) *Green Chem* 16:55
15. Longstreet AR, Opalka SM, Campbell BS, Gupton BF, McQuade DT (2013) *Beilstein J Org Chem* 9:2570
16. Adamo A, Beingsner RL, Behnam M, Chen J, Jamison TF, Jensen KF, Monbaliu JC, Myerson AS, Revalor EM, Snead DR, Stelzer T, Weeranoppanant N, Wong SY, Zhang P (2016) *Science* 352:61
17. Mascia S, Heider PL, Zhang H, Lakerveld R, Benyahia B, Barton PI, Braatz RD, Cooney CL, Evans JMB, Jamison TF, Jensen KF, Myerson AS, Trout BL (2013) *Angew Chem Int Ed* 52:12359–12363
18. Heider PL, Born SC, Basak S, Benyahia B, Lakerveld R, Zhang H, Hogan R, Buchbinder L, Wolfe A, Mascia S, Evans JMB, Jamison TF, Jensen KF (2014) *Org Process Res Dev* 18:402
19. Cole KP, Groh JMC, Johnson MD, Burcham CL, Campbell BM, Diseroad WD, Heller MR, Howell JR, Kallman NJ, Koenig TM, May SA, Miller RD, Mitchell D, Myers DP, Myers SS, Phillips JL, Polster CS, White TD, Cashman J, Hurley D, Moylan R, Sheehan P, Spencer RD, Desmond K, Desmond P, Gowran O (2017) *Science* 356:1144
20. May SA, Johnson MD, Braden TM, Calvin JR, Haeberle BD, Jines AR, Miller RD, Plocharczyk EF, Renner GA, Richey RN, Schmid CR, Vaid RK, Yu H (2012) *Org Process Res Dev* 16:982
21. LaPorte TL, Spangler L, Hamedy M, Lobben P, Chan SH, Muslehiddinoglu J, Wang SSY (2014) *Org Process Res Dev* 18:1492

22. Marsini MA, Buono FG, Lorenz JC, Yang B-S, Reeves JT, Sidhu K, Sarvestani M, Tan Z, Zhang Y, Li N, Lee H, Brazzillo J, Nummy LJ, Chung JC, Luvaga IK, Narayanan BA, Wei X, Song JJ, Roschangar F, Yee NK, Senanayake CH (2017) *Green Chem* 19:1454
23. May SA, Johnson MD, Buser JY, Campbell AN, Frank SA, Haeberle BD, Hoffman PC, Lambertus GR, McFarland AD, Moher ED, White TD, Hurley DD, Corrigan AP, Gowran O, Kerrigan NG, Kissane MG, Lynch RR, Sheehan P, Spencer RD, Pulley SR, Stout JR (2016) *Org Process Res Dev* 20:1870
24. Braune S, Pçchlauer P, Reintjens R, Steinhofers S, Winter M, Lobet O, Guidat R, Woehl P, Guerneur C (2009) *Chim Oggi* 27:26
25. Roberge DM, Noti C, Irle E, Eyholzer M, Rittiner B, Penn G, Sedelmeier G, Schenkel B (2014) *J Flow Chem* 4:26
26. Grongsaard P, Bulger PG, Wallace DJ, Tan L, Chen Q, Dolman SJ, Nyrop J, Hoernner RS, Weisel M, Arredondo J, Itoh T, Xie C, Wen X, Zhao D, Muzzio DJ, Bassan EM, Shultz CS (2012) *Org Process Res Dev* 16:1069
27. Kolb HC, Finn MG, Sharpless KB (2001) *Angew Chem Int Ed* 40:2004
28. Rostovtsev VV, Green LG, Fokin VV, Sharpless KB (2002) *Angew Chem Int Ed* 41:2596
29. Bogdana AR, Sachb NW (2009) *Adv Synth Catal* 351:849
30. Odille FGJ, Stenemyr A, Pontén F (2014) *Org Process Res Dev* 18:1545
31. Buono FG, Eriksson MC, Yang B-S, Kapadia SR, Lee H, Brazzillo J, Lorenz JC, Nummy L, Busacca CA, Yee N, Senanayake C (2014) *Org Process Res Dev* 18:1527
32. Newby JA, Blaylock DW, Witt PM, Turner RM, Heider PL, Harji BH, Browne DL, Ley SV (2014) *Org Process Res Dev* 18:1221
33. Yu Z, Ye X, Xu Q, Xie X, Dong H, Su W (2017) *Org Process Res Dev* 21:1644
34. Wen Z, Jiao F, Yang M, Zhao S, Zhou F, Chen G (2017) *Org Process Res Dev*

Index

A

- Acetamidobenzenes, 286
- 2-Acetamido-5-bromo-4-methylpyridine, 276
- Acrylamide cyclization, 120
- Active pharmaceutical ingredients (APIs), heterocyclic, 1–3, 24, 78, 320
- Acyl azides, 54, 78, 117, 287–289, 378, 379
- N*-Acyliminium species, 192
- 2-Adamantanone, 230
- Adenosine, 89
- Akt inhibitor, 380
- Akt kinase inhibitor, 49
- Aliskiren, 376, 377, 380
- Alkenes, 13, 190
 - Heck-type cross dehydrogenative coupling, 365
 - oxidative functionalisation, 216
- 2-(2-Alkenyloxymethyl)-naphthalene-1-carbonitriles, 199
- Alkylations, 13, 25, 39, 88, 223, 266, 278, 282, 296, 324
 - metal-free, 199
- 3-Alkyl pyrazole, nitration, 358
- Alkylpyrazoles, 275
- Alkynylation, 240
- Alkynyl pyrimidines, 194
- Allergies, 42
- Alpidem, 26, 280
- Alzheimer's disease, 35, 243
- Amination, 11, 22, 281–296, 308
 - Buchwald-Hartwig, 172, 283
 - reductive, 40, 215, 324, 379
- Amino acids, 48, 59, 71, 128, 226, 230
- 2-Aminoadamantane-2-carboxylic acid, 229, 230
- 4-Amino-3-alkylpyrazoles, 275
- 2-Aminobenzoxazoles, 94
- 2-Amino-4-chloro-6-hydroxypyrimidine, 273
- 5-Amino-4-cyano-[1,2,3]-triazoles, 145
- Aminoimidazo[1,2-*a*]pyrimidines, 141
- Aminonitriles, 127
- Aminopeptidase (IRAP) inhibitors, 153
- Aminopyrimidines, 9, 141, 274, 285, 290
- 2-Aminoquinazolines, 333
- Amitriptyline, 352
- Amoxapine, 88
- β -Amyloid cleaving enzyme (BACE), 35,
- Analgesics, 39, 40, 75
- 4-Androstene-3,17-dione, 356
- Anesthetics, 39, 75
- Antibiotics, 15, 20, 63, 65
- Antihyperglycemic drugs, 81
- Antiparasitic agents, 15, 63
- Anti-seizure compounds, 34, 72
- Antiviral active compounds, 12, 57
- Anxiolytics, 26
- AR-A2, 73
- Arenes, hydroxylation, 296
 - lithiation, 349
- Artemether, 18
- Artemisinin acid, 19, 121, 365, 367
- Artemisinin, 15–19, 121, 218, 219, 367, 368
- Artemotil, 19
- Arylacetaldehyde derivatives, anti-Markovnikov, 365
- Aryl boronic acids/esters, 298
- Arylbromide, 346
- Aryl carbamates, 346
- Arylcyclopropyl boronates, 336
- Aryl halides, 347

AS-136A, 13
Ascaridole, 113, 367
Atazanavir, 57, 257
ATR kinase inhibitor, 4
Atropine, 48
Attention deficit hyperactivity disorder (ADHD), 36
AZD3293, 243
AZD9291 (osimertinib), 9
Azepane, 175
3H-Azepinones, 220
Azides, 156, 286
Azido-Schmidt ring expansion, 221
Aziridination, 200
Aziridines, 117, 200
 tricyclic, 121
2H-Azirines, 123, 190, 200
Azlactones, 230
Azoles, 295
Azomethine ylide, 190

B

BACE1 inhibitor, 330
Baeyer-Villiger oxidation, 207
Bassianolide, 20
Baylis-Hillman reaction, 195, 204, 205
BCP modulators, 91
Beauvericin, 20
Benadryl, 376
Benzaldehyde, 88, 148, 205, 271, 273, 292, 307, 354
Benzazoles, 170
Benzimidazoles, 39, 50, 51, 170, 177
 2-chloro-substituted, 177, 333
Benzoazepin, 224
Benzocyclobutanes, Diels-Alder cyclization, 334
2-Benzofuranylboronic acid, 253
Benzo[*h*]-1,6-naphthyridine-5(6*H*)-ones, 119
Benzotetramisole, 208
Benzothiazoles, 95, 170
Benzotriazoles, amination-reduction-diazotation, 282
Benzoxazoles, 94, 113, 170, 301
N-Benzylmaleimide, cyclopropanation, 223, 385
Benzyne, 282, 297, 310, 344, 346, 385
Bicyclo[3.2.1]octanoids, 221
Biginelli reaction, 94, 136, 151, 173, 204
Bipolar mania, 24
Boron trifluoride etherate, 361
Borrerine, 20

Borreverine, 226
Borylation, 255, 297, 349, 350
Boscalid, 65, 345
Bouguer-Lambert-Beer law, 106
Brivanib alaninate, 51, 383
Bromination, 75, 90, 339, 369
5-Bromo-*N*-benzyl indole, 278
3-Bromo-imidazo[1,2- α]pyridine, 369
2-Bromo-4-methylnicotinonitrile, 61
8-Bromo-6-nitro-1*H*-quinolin-2-one, 276
Bromophenyllithium, 344
8-Bromoquinolin-2-one, 276, 358
Bucherer-Bergs hydantoin, 141
Buchwald-Hartwig amination, 283, 289
Buchwald-Hartwig cross-couplings, 177
Buclizine, 42
Bupivacaine, 39
Butane-2,3-diacetal, 203
Butanedione, 204
N-*tert*-Butoxycarbonyl-5-ethoxycarbonyl-4-perhydroazepinone, 362

C

C-B bonds, 297
C-N bonds, 272
C-O bonds, 296
C(sp²)-C(sp) bond formation, 240
C(sp²)-C(sp³) bond formation, 263
Cages, 206
Camphorsulfonic acid, 204
Canagliflozin, 81
Capecitabine, 4
e-Caprolactam, 175
Carbocaine, 39
 β -Carbolines, 115
Carboxamides, 30
Cardiovascular diseases, 38, 74
Cariprazine, 24
Carvone, 216
Casein, inhibitors, 280
Catalysis, heterogeneous, 246
 homogeneous, 253
Catharanthine, 117
CCR1 antagonist, 78, 378
CCR8, 93, 327
Celecoxib, 96
Central nervous system, 67
Chan-Lam amination, 289, 294
Chemokine receptors, 93
Chemotherapeutic agents, 4, 49
Chloroarenes, dimethylamination, 284
Chloroazines, 283

- 5-Chloroindole, 301
5-Chloro-2-(methylamino)benzophenone, 29
Chloropyridines, 177, 282
 amination, 285
Chromenes, 149, 167
CI-972, 273
Cinnarizine, 42
Ciprofloxacin, 21, 285
Citronellal, 193
CKI, 90
Codeine, 75
Condensation, 161
Continuous flow, 103, 133, 187
Copper, 12, 34, 105, 143, 156, 245, 271, 293, 323, 334, 365, 381
Copper tube flow reactor (CTFR), 293
Corey-Chaykovsky epoxidation, 216
Coronaridine, 117
Coumarin, 98
p-Cresol, 386
Crizotinib, 96
Cross-coupling, 8, 39, 58, 125, 177, 237, 288, 349, 360
6-Cyano-2,2-dimethylchromene, 196
 α -Cyanooxepoxides, 216
Cyanohydrins, 195
Cyanopyridines, 126
Cycle time, 321
Cyclization, 110, 119
Cyclizine, 42
Cycloadditions, 34, 115, 121, 165, 188, 219, 282, 333, 360
Cyclodehydration, 200
Cycloheptenone, 216
4-Cyclohexylpyrrolo[1,2-*a*]quinoxaline, 117
Cyclopentenones, 123
Cyclopropanation, 67, 223, 385
- D**
DAAO inhibitor, 67
Daclatasvir, 62, 138
Dantrolene, 80
Debus–Radziszewski synthesis, 136
Decoration, 125
Deketalization, 140
3-Demethoxyerythratidinone, 198
Deoxynucleosides, 14
Depression, 30, 67
DHPM, 94
Diabetes, 81
Diaminopyrazoles, 331
Diaryl alkynes, 241
Diaryl amines, 291, 292
Diaryl ether, 296
Diarylmethanes, 271
1,4-Diaryltriazaoles, 143, 144
Diazabicyclo[3.1.0]hexanes, 116
Diazald, 189, 335, 361
Diazepam, 28, 230
Diazoalkanes, 360
Diazoketones, Wolff rearrangement 124
Diazomethane, 189, 335, 360
Diazonium reagents, 343
Diazo reagents, 343
 α -Diazosulfoxides, lactone-derived, 222
Diazo transfer, 222
Dibromobenzene lithiation, 344
Didehydroazepines, 220
Diethylaminosulfur trifluoride (DAST), 369
N,N-Diethyl-4-(3-fluorophenylpiperidin-4-ylidene)methyl)benzamide, 33
2,6-Difluorobenzylazide, 34
Difluoromethyl diazomethane, 190
Dihydroartemisinic acid, 16, 121
Dihydroartemisinin, 16
3,4-Dihydro-5*H*-benzo[*e*][1,4]diazepin-5-one, 215
Dihydroisoquinolines, 214
1,3-Dihydro-oxazines, 153
Dihydropyridine, 147, 149
Dihydropyridinones, 209
3,4-Dihydropyrimidin-2(1*H*)-ones, 151, 152, 204
Dihydropyrimidinones, 94, 173
Dihydropyrroles, 190, 191, 211
Dihydroquinazolinones, 153, 154
8,14-Dihydrothebaine, 75
Dimethoxybenzophenone (DMBP), 199
2-(Dimethylamino)pyridine, 178
Dimethylbarbituric acid, 193
Diphenhydramine hydrochloride, 230, 376
Diphenylphosphoryl azide, 287
3,5-Dipromopyridine, monopropynylation, 243
Disulfides, 113
Dodecylbenzenesulfonyl azide, 222
Dopamine D2 and D3 receptor partial agonist, 24
Doravirine, 58
Dumetorine, 86
- E**
Edoxudine, 14
Efavirenz, 12, 60, 213
Emerging technologies, 319

Enniatin C, 20
Epoxidation, 207, 216, 217
 Corey-Chaykovsky, 216
Eribulin mesylate, 52
2-Ethoxyquinazoline, 179
Ethyl diazoacetate, 221, 361
Ethyl(dimethylsulfuranylidene) acetate, 223
Ethyl isocynoacetate, 145
Ethyl nicotinate, 214
7-Ethyltryptophol, 79
Ethyne, Sonogashira coupling, 244
Etodolac, 79
Evacetrapib, 379
Exothermic reactions, 343

F

Fanetizole, 43, 141
Fast reactions, 343
Fenofibrate, 88
Finkelstein reaction, 294
Fischer indole synthesis, 140
Flash chemistry, 193, 300, 309, 343, 356
Flow chemistry, 1, 161, 319
Flow reactor, 103
Fluorine-containing heterocycles, 129
4-Fluoro-3,5-dimethyl-1*H*-pyrazole, 369
3-Fluoropentane-2,4-dione, 369
5-Fluoropicolinic acid, 35
4-Fluoropyrazoles, 138
5-Fluorouracil, 5
Fluoxetine hydrochloride, 230
Frogs, poison/toxins, 82
Functionalization, 237
Fungicides, 65
Furofuran, 220
4*H*-Furo[3,2-*b*]pyrrole-5-carboxylic acid, 67

G

GABA antagonists, 280
Galocitabine, 5
GDC-0944, 259
Gemcitabine monophosphate, 5
Glutamate subtype 5 receptor negative
 allosteric modulator (mGlu5 NAM), 146
Glycopeptides, 126
Goldberg amidation, 294
Goniofufrone, 122
Gould–Jacobs cyclization, 167, 334
Grignard reagents, 88, 230, 344, 352–355, 363,
 384

Groebke–Blackburn–Bienaymé reaction, 141
Grossamide, 44, 225
Guanidines, cyclic, 94

H

Halogenation, 343, 369
2-Halovinylithium, 350
Hantzsch dihydropyridine, 148
Hantzsch pyrrole synthesis, 136
Hantzsch thiazole synthesis, 140, 173
Hazardous reagents, 343
Heck–Cassar reaction, 240
Heck coupling, cross-dehydrogenative, 261
Hemetsberger–Knittel indole
 synthesis, 289, 331
Hennoxazole A, 202
Hepatitis C virus translation inhibitor, 94
Heteroarenes, 237–311
High-temperature chemistry, 161, 163,
 176, 332
Histriocotoxins, 82
HIV/AIDS, 12, 57
 protease inhibitor, 257
 replication inhibitors, 151
5HT, 338
5HT1B antagonist, 30
Hydantoin, 141
Hydrocodone (dihydrocodeinone), 75
Hydroxyalkyl azides, 221
Hydroxymorphinone, 40, 365
2-Hydroxy-1,4-naphthoquinone, 208
4-(4-Hydroxyphenyl)cyclohexan-1-one, 64
4-Hydroxypyridine, etherification, 296
Hydroxypyrrrolotriazine, 51
Hydroxyquinolines, 167
Hydroxytetrahydrofurans, 218
Hypertension, 38, 74

I

Iloperidone, 25
Imatinib, 7–9, 284, 290
Imidazo[1,2-*a*]arenes, 279
Imidazoles, 62, 85, 98, 116, 137, 141, 381, 383
 1*H*-4-substituted, 138
Imidazolidinones, 170
Imidazolines, 200, 201
Imidazo[1,2-*a*]pyridine-2-carboxamides, 22
Imidazo[1,2-*a*]pyridines, 26, 27, 281
Imidazo[1,2-*b*]pyridazines, 90, 280
Iminium ether salts, 221

Indoles, 95, 113, 124, 128, 262, 271, 289, 305, 331, 365
2-(1*H*-Indol-3-yl)thiazoles, 140
Inflammation, 43, 78, 92, 140, 210
Integrated flow/systems, 319, 324
Iodoindoles, 264, 306
Iodothiophene, 240
Ionic liquids, 137, 278
 1,3-dialkylimidazolium-based, 137
Iridium (III), 105
Isatins, 222
Isoborreverine, 20, 226
Isocyanates, 8, 24, 78, 93, 287, 288, 379
Isonitriles, 155, 156
Isonitrosoacetanilide, 222
Isoprene, 195
Isopropyl-4-nitro-propan-1-ol, 380
Isoxazolidine, 83, 227

J

JAK2 kinase inhibitor, 53

K

Ketoamides, 124, 381–383
 β -Ketoesters, 145, 146, 361, 362
Kondrat'eva reaction, 168
Kumada-Corriu coupling, 258

L

Lactams, 124, 215
 β -Lactams, 124, 189, 207, 208
 γ -Lactams, 48
Lactones, 207, 217, 218
Lamivudine, 61
Lead optimization, 319
Lennox-Gastaut syndrome, 164
Levomilnacipran, 67
Levulinic acid, 214
Lidocaine, 230, 376
Light source, 103
Linezolid, 65, 66
Lithiation, 12, 60, 72, 83, 88, 256, 270, 298, 311, 344, 385
Lithiation-zincation-Negishi coupling, 259
LLM-105, 277
LOPHTOR (flow-through photochemical microreactor), 338
LY2886721, 35
 γ -Lycorane, 228

M

Malaria, 15, 63, 121, 147, 192, 218, 365, 367
Maleimides, 115
 cyclopropanation, 223
Marcaine, 39
Meclinetant, 68
Mepivacaine, 39
Metal photosensitizers, 103
1-Methylazepane, 175
2-Methylbenzimidazole, 163
3-Methyl-4-nitropyrazole, 275
Methylphenidate, 36
O-Methyl siphonazole A, 202
Methyltetrazoles, 361
Micardis, 38
Microwave-assisted, continuous flow organic synthesis (MACOS), 331
Minisci epoxidation, 207, 216
Mizoroki-Heck coupling, 261
Morpholines, 173
Multicomponent reactions (MCR), 133, 280
Multi-jet oscillating disk reactor (MJOD), 207
Multistep continuous processes, 1, 3, 49
Mur ligase inhibitor, 22

N

Naproxinod, 380
Naropin, 39
NBI-75043, 72, 353
Neostenine, 121, 197
Neurodegenerative diseases, 35
Nevirapine, 61, 151
Nitration, 273, 343, 356
Nitrile ylides, 123, 190
Nitro amino esters, 215
Nitropyridine, 277
N-Nitroso pyrazolines, 190
Noroxymorphone, 40, 77
NS5A inhibitors, 138
Nucleophilic aromatic substitution (SNAr), 177
Nucleophilic substitution, 278
Nucleosides, 88

O

Olanzapine, 25, 283
 δ -Opioid receptor agonist, 33
Organometallic reagents, 343
Osimertinib, 9
Oxadiazoles, 146, 170, 172, 279, 325
Oxazinones, 167
Oxaziridines, 125

Oxazoles, 168, 202
Oxazolidinones, 170
Oxazolines, 201
Oxidation, aerobic, 112, 121
Oxomaritidine, 10, 224
Oxygenations, 112, 121, 343, 363
Oxytocin, oxidative photosynthesis, 114
OZ439, 63, 147, 192

P

Palladium, 40, 46, 74, 127, 248–258, 269, 289, 297, 300, 328, 349, 360, 365
PARP-1 inhibitor, 54
Pauciflorol F, 203, 347
Pauson-Khand reaction, 123
Pentane-2,4-dione, 369
Peptoids, 154
Perhydrohistrionicotoxin, 83, 227
Pericyclic reactions, 164
Phenanthrenes, 124
6(*5H*)-Phenanthridinones, 119
Phenyl iodine(III) dicyclohexanecarboxylate, 117
Phosgene, 362
Photoaziridination, 118
Photocycloadditions, 115–122, 197
Photodecarboxylation, 199
Photoredox catalysis, 103, 129
 cyclization, 153
 cycloadditions, 115
 visible light, 108
Photosensitizers, 15, 104, 113, 114, 117
 metal, 104
 organic, 103
Picolinic acids, 363
Picolinoyl chloride, 39
Piperazination, 284
Piperazines, 22, 42, 173, 285
Piperidines, 37, 173, 177, 214
Piperidones, 34, 220, 362
PNP inhibitor, 273
Povarov reaction, 149
Pressure, high, 39, 142, 161, 240, 296, 363, 379
Prexasertib, 55, 286, 377
Process windows, 161
Propargylic alcohols, 12, 13, 213, 230, 355, 356
Propiolamide, 34
Prozac, 376
Pseudotabersonine, 117
Pseudovincadifformine, 117
Pummerer rearrangement, 356
Pyranonaphthoquinones, 208

Pyrazine-2-carboxamide, 23
Pyrazines, 56, 177, 277
 2-chloro-substituted, 177
Pyrazofurin, 96
Pyrazoles, 96, 139, 170, 171, 294, 323
 nitration, 275, 356
1-Pyrazoline, 361
Pyridazinone, 153
Pyridines, 332
Pyrimidines, 75, 194, 273, 283
Pyrimidin-4-ol, 362
Pyrimidinones, 34, 94, 151, 167, 173
Pyrimidones, 334
Pyrrole-3-carboxylic acids, 136
Pyrroles, 110, 121, 136, 170, 198, 271
Pyrrolidines, 170
 photoredox synthesis, 111
 substituted, 190
Pyrrolizidines, 192, 199
Pyrrolo[1,2-*a*]azepine, 121
Pyrrolo[2,3-*g*][1,3]benzothiazoles, 95
Pyrroloquinoxaline, 153

Q

Quinazolines, 2-chlorosubstituted, 177
Quinodimethanes, 193
Quinolines, 173, 177, 214, 266, 282, 299, 369
 2-chloro-substituted, 177
Quinolones, 167
Quinoxalines, 153, 177, 214
 2-chlorosubstituted, 177

R

Radziszewski reaction, 137
Rearrangements, 117, 124, 273, 286–288, 309, 346
 Curtius-type, 117
 Fries, 346
 Pummerer, 356
 Schmidt and Beckmann, 124
Regitz diazo transfer, 222
Ribociclib, 11
Rimonabant, 96
Ritalin, 36
(*S*)-Rolipram, 45, 210
Ropivacaine, 39
Roskamp reaction, 361
Rosuvastatin, 74
Rufinamide, 34, 72, 145, 164
Ruppert's reagent, 369
Ruthenium (II), 105, 110, 127, 211

S

Salicylic acid, 273
Sandmeyer reaction, 222, 307, 360
Scaffold decoration, 125
Schizophrenia, 24, 25, 67
Sedatives, 26
Segmented flow, 76, 142, 242, 262, 297, 322, 325
Serotonin-norepinephrine reuptake inhibitor, 67
Sildenafil, 96, 274, 275, 360
Singlet oxygen, 16, 112, 216, 366
Siphenazole, 85
Skraup reaction, 173
Sparteine, 350
Spirocyclisation, 212, 229
Spiro-oxindole dihydroquinazolinones, 153
Spiropiperidines, 227
Squaramide, 208
Stimulants, 36
Stop-flow micro-tubing reactor (SFMT), 244
Structural activity relationships (SAR), 321
Sulfonamides, 216, 218, 309, 327, 361
 cyclic, 216, 218
Suzuki coupling, 54, 129
Suzuki cross-coupling, 39, 58
Suzuki-Miyaura coupling (SMC), 244–257, 289, 298, 349
Swern oxidation, 356, 357
SWIFT (Synthesis with integrated flow technology), 324

T

T-cell tyrosine phosphatase (TCPTP), 327
Telmisartan, 38
Temperature, high, 161, 176, 332
Testosterone, 356
Tetrahydrobenzo[4,5]cyclohepta[1,2-*c*]pyrrol-1(2*H*)-one, 110
Tetrahydrofurans, 111, 112, 219
 photoredox synthesis, 111, 120
Tetrahydroindolizine, 110
Tetrahydroisoquinolines, 167
Tetrahydro-1,3-isoxazines, 205
Tetrahydro-2*H*-pyran, 369
Tetrahydropyrazolo[3,4-*b*]quinolin-5(6*H*)-one, 205
Tetrahydropyridines, 150
Tetrahydroquinolines, 120, 149
Tetrazoles, 165, 166, 361
Thebaine, 75

Thiazoles, 94, 140, 151, 173, 323
5-(Thiazol-2-yl)-3,4-dihydropyrimidin-2(1*H*)-one, 151
Thieno[3,2-*c*]quinolin-4(5*H*)-ones, 119
Thioamide, 94
Thiophenes, 25, 81, 170, 253, 262, 273, 298, 304, 347
Thiophenols, 309
Thioureas, 31, 44, 141, 151, 284, 293
Thioamide, 115
Tramadol, 354
Triazoles, 142–146, 166, 192, 193, 323, 381
Triazolopyridines, 282
Tricyclo-1,4-benzoxazines, photoredox synthesis, 113
Trifluoromethoxy benzene, nitration, 387
Trifluoromethylation, 129
Trifluoromethyl diazomethane, 190
2-(Trifluoromethyl)-2*H*-[1,3]oxazino[2,3-*a*]isoquinolines, 152
Trimethyl-tetrahydroisobenzofuran-1,3-dione, 195
Trioxolane, 147
Tropine, 48
Tungsten, 127, 217
Tyrosine kinase inhibitor, 7

U

Ullmann amination, 293
Ullmann coupling, 288
Ullmann diaryl ether synthesis, 296
Ultrasonication, 73, 245, 253, 260, 283, 292
UV light, 103, 110, 125, 252, 338

V

Valium, 376
Vildagliptin, 81
Vinyl azides, 116, 122, 123, 190, 288
Visible light, 103, 110, 338

W

Wolff rearrangement, 124, 222
Wolff-Staudinger cascade reaction, 189

Z

Zolpidem, 26–28, 280